



University
of Glasgow

Olijnyk, Daria (2011) *Pubertal mouse mammary gland development - transcriptome analysis and the investigation of Fbln2 expression and function*. PhD thesis.

<http://theses.gla.ac.uk/2996/>

Copyright and moral rights for this thesis are retained by the author

A copy can be downloaded for personal non-commercial research or study, without prior permission or charge

This thesis cannot be reproduced or quoted extensively from without first obtaining permission in writing from the Author

The content must not be changed in any way or sold commercially in any format or medium without the formal permission of the Author

When referring to this work, full bibliographic details including the author, title, awarding institution and date of the thesis must be given

**Pubertal Mouse Mammary Gland Development-
Transcriptome Analysis and the Investigation of
Fbln2 Expression and Function**

Daria Olijnyk (B.Sc, MRes)

Thesis submitted to the University of Glasgow in fulfilment of the
requirements for the degree of Doctor of Philosophy

June 2011

Institute of Cancer Sciences
College of Medical, Veterinary and Life Sciences
University of Glasgow

For my parents, Bogusława and Bogusław Olijnyk and grandmother,
Anna Bandurak

Abstract

Mouse mammary gland morphogenesis at puberty is a complex developmental process, regulated by systemic hormones, local growth factors and dependent on the epithelial/epithelial and epithelial/stromal interactions. TEBs which invade the fat pad are important in laying down the epithelial framework of the gland at this time point. The objective of this thesis was to use a combination of 'pathway-' and 'candidate gene analysis' of the transcriptome of isolated TEBs and ducts and associated stroma, combined with detailed analyses of selected proteins, to further define the key proteins and processes involved at puberty. Using GeneChip® Mouse Exon 1.0 ST Arrays we identified the epithelial-, epithelial-stromal- and stromal transcriptomes of TEBs and ducts and defined the major functional pathways/biological processes in each compartment. By ranking the transcripts according to their expression levels and known functions in other systems, we identified genes of potential importance for pubertal mammary morphogenesis. We focused our study on *Upk3a* and *Fbln2* and their protein products. *Upk3a* could only be detected at mRNA level and thus further analysis was based on *Fbln2*. We demonstrated that *Fbln2 V1* and *Fbln2* protein are predominantly expressed in the epithelium and stroma of TEBs. Using hormone primed mice we demonstrated that *Fbln2* expression and localisation in the mouse mammary gland is positively regulated by E2 and P. Furthermore, by a combination of further *in silico* analysis, *in vitro* functional assays, IHC and IF we identified *Vcan*, *Lama1*, *Fbn1*, *ColVIa3*, *ColIVa1*, *ColXVIIIa1*, *Eln*, *Per*, *Acan*, *Nid*, *Itgb3* and *Itga5* as potential binding partners of *Fbln2* in mammary gland. Finally, we reported lack of an obvious mammary phenotype in *Fbln2* KO^{-/-} mice at puberty but demonstrated that this may be attributed to the over-compensation by *Fbln1*.

This thesis demonstrates the benefit of DNA microarray analysis in studying pubertal development of mouse mammary gland. It identifies *Fbln2* as a potential pubertal mammary regulator which by interacting with various ECM proteins at different sites of mammary milieu may contribute to an array of structural and migratory functions during mammary morphogenesis. These data substantially add to the understanding of the development of mammary gland at puberty and reveal many potential avenues for further investigations.

Table of Contents

1	Introduction.....	22
1.1	Overview of mouse mammary gland development	22
1.1.1	Embryonic development of mouse mammary gland.....	23
1.1.2	Postnatal development of mouse mammary gland.....	27
1.2	Mouse mammary gland morphogenesis at puberty	30
1.2.1	The morphology and characteristics of pubertal mouse mammary gland	31
1.2.1.1	Epithelium	31
1.2.1.1.1	TEBs.....	33
1.2.1.1.2	Ducts.....	35
1.2.1.2	Fat pad	37
1.2.1.2.1	Adipose tissue	38
1.2.1.2.2	Fibroblasts	39
1.2.1.2.3	Migratory cells of the immune system	39
1.2.1.2.4	ECM	40
1.2.2	Motility in the mouse mammary gland at puberty	42
1.2.2.1	TEBs.....	42
1.2.2.1.1	Forward movement.....	43
1.2.2.1.2	Bifurcation	44
1.2.2.1.3	Turning	47
1.2.2.2	Ducts.....	48
1.2.3	Regulation of ductal morphogenesis at puberty	49
1.2.3.1	Epithelial-epithelial communication	49
1.2.3.2	Epithelial-stromal interactions	51
1.2.3.2.1	Hormonal control of pubertal mouse mammary gland morphogenesis	51
1.2.3.2.2	Local growth control of pubertal mouse mammary gland development	57
1.2.3.2.3	Transcriptional control of pubertal mouse mammary gland development	63
1.2.3.2.4	Immune response cells and cytokines in the regulation of pubertal mammary gland development	68
1.2.3.2.5	The role of other stromal components in regulation of pubertal mammary morphogenesis	74
1.2.3.2.6	Axonal guidance proteins	78
1.2.3.2.7	Other regulators of pubertal mouse mammary gland morphogenesis	80
1.2.4	Summary.....	80
1.3	Microarray analysis of gene expression to study pubertal mouse mammary gland development	81
2	Materials and methods	90
2.1	Materials	90
2.1.1	Reagents and materials	90
2.1.2	Solutions and Buffers	95
2.1.3	Electric equipment.....	97
2.2	Methodology.....	98
2.2.1	Sample Collection	98
2.2.1.1	Mouse husbandry.....	98
2.2.1.2	Dissection of mouse mammary glands	99
2.2.1.3	Dissection of other mouse organs and tissues	101

2.2.1.4	Collection of mouse mammary gland tissue strips	101
2.2.1.5	Collection of isolated epithelium.....	101
2.2.2	Cell culture.....	103
2.2.2.1	Cell lines and Cell maintenance	103
2.2.2.2	Cell Counting	104
2.2.2.3	Plasmid information and plasmid DNA purification	104
2.2.2.4	Transfections	106
2.2.2.4.1	Optimisation of transfections	106
2.2.2.4.2	Fbln2 over-expression in HC11 cells.....	108
2.2.2.5	Wound Healing Assay	108
2.2.2.6	Adhesion Assays	109
2.2.2.6.1	Adhesion of pRc/CMV-Fbln2 transfected HC11 cells to plastic surface	109
2.2.2.6.2	Adhesion of pRc/CMV-Fbln2 transfected HC11 cells to ECM proteins	109
2.2.3	Protein work	110
2.2.3.1	Protein extraction from the cell lines	110
2.2.3.2	Protein extraction from the frozen tissues	111
2.2.3.3	Protein Quantification	111
2.2.3.4	Concentration of Protein Extracts.....	112
2.2.3.5	Electrophoresis and Western blotting.....	112
2.2.4	RNA and DNA.....	116
2.2.4.1	Preparation of total RNA.....	116
2.2.4.1.1	Preparation of collected frozen tissue for RNA extraction	116
2.2.4.1.2	Preparation of isolated mammary gland epithelium for RNA extraction	116
2.2.4.1.3	Extraction of RNA from frozen tissue and isolated epithelium	117
2.2.4.1.4	Extraction of RNA from cell lines.....	117
2.2.4.2	DNase I treatment	118
2.2.4.3	RNA purification, concentration and on column DNase I digestion	118
2.2.4.4	Quantification of the nucleic acid (RNA or DNA).....	118
2.2.4.5	Quality assessment of RNA	119
2.2.4.6	cDNA Synthesis - Reverse transcription polymerase chain reaction (RT-PCR)	119
2.2.4.7	Standard PCR	120
2.2.4.8	DNA Agarose Gel Electrophoresis.....	121
2.2.4.9	Q RT PCR.....	121
2.2.4.10	DNA Sequencing.....	124
2.2.4.11	Restriction Digestion	126
2.2.5	Microarray analysis of pubertal gene expression	126
2.2.5.1	Collection of the experimental material	126
2.2.5.2	Extraction, purification, concentration, quantification and quality assessment of RNA	127
2.2.5.3	Microarray data generation workflow.....	127
2.2.5.3.1	Reduction of ribosomal RNA (rRNA)	127
2.2.5.3.2	Synthesis of double stranded cDNA (ds cDNA)	129
2.2.5.3.3	Synthesis of cRNA	129
2.2.5.3.4	Synthesis of ss cDNA.....	129
2.2.5.3.5	Fragmentation and terminal labelling of ss cDNA.....	130
2.2.5.3.6	Hybridisation of ss cDNA to microarray chips.....	130
2.2.5.3.7	Washing, staining and scanning of the arrays.....	130

2.2.5.3.8	Signal detection and calculation of the cell intensity data (.CEL file)	131
2.2.5.4	Background correction, normalisation and probe set summarisation	131
2.2.5.5	Gene expression analysis at the gene level - The identification of 'up-regulated gene sets'	133
2.2.5.5.1	TEB and duct epithelium 'up-regulated gene sets'	133
2.2.5.5.2	TEB and duct epithelial-stromal 'up-regulated gene sets'	134
2.2.5.5.3	Epithelium-free Fat pad 'up-regulated gene set'	135
2.2.5.6	Gene expression analysis on the gene level - The identification of 'expressed gene sets'	135
2.2.5.6.1	TEB- and duct-only epithelium 'expressed gene sets'	135
2.2.5.6.2	TEB- and duct-only stroma 'expressed gene sets'	136
2.2.5.7	Expression Analysis at the exon level	137
2.2.5.8	Microarray data quality assessment	138
2.2.5.9	'Functional' analysis of identified genes	139
2.2.5.9.1	Ingenuity Pathway Analysis (IPA)	139
2.2.5.9.2	EMT signature	140
2.2.5.9.3	Literature Search	140
2.2.5.9.4	Oestrogen responsive genes	140
2.2.6	Tissue processing and staining	142
2.2.6.1	Preparation of mouse mammary gland wholemounts stained with carmine	142
2.2.6.2	Tissue fixation, paraffin wax embedding and sectioning	142
2.2.6.3	Preparation of paraffin embedded tissue sections for IHC and IF	143
2.2.6.4	IHC on paraffin embedded tissue sections	143
2.2.6.5	IF on paraffin embedded tissue sections	144
2.2.6.6	Haematoxylin and Eosin (H&Eo) staining	146
2.2.6.7	Elastica van Gieson (EVG) staining	146
2.2.7	In vivo hormonal treatment of mouse mammary glands	147
2.2.7.1	Priming of mice with hormone pellets	147
2.2.7.2	Mammary gland morphology assessment and tissue processing	148
2.2.8	Visualisation and imaging	148
2.2.8.1	Fluorescence microscopy	148
2.2.8.2	Confocal microscopy	149
2.2.8.3	Light microscopy	149
3	Pubertal transcriptome of mouse mammary gland - Microarray analysis	150
3.1	Introduction	150
3.2	Results	150
3.2.1	Collection of biological material	153
3.2.2	Characterisation of pubertal development stages in WT and TG mice	156
3.2.3	Experimental set up for microarray analysis	156
3.2.4	RNA hybridisation to GeneChip® Mouse Exon 1.0 ST Arrays	160
3.2.5	Microarray data quality control	162
3.2.6	Bioinformatic analysis of the pubertal mouse mammary gland transcriptome	167
3.2.6.1	<i>Gene expression analysis - Identification of the 'up-regulated gene sets'</i>	167
3.2.6.1.1	TEB and duct epithelium 'up-regulated gene sets'	167
3.2.6.1.2	TEB and duct epithelium-stroma 'up-regulated gene sets'	168

3.2.6.1.3	Epithelium-free Fat pad ‘up-regulated gene set’	172
3.2.6.2	<i>Gene expression analysis - Identification of the ‘expressed gene sets’</i>	172
3.2.6.2.1	TEB- and duct epithelium-only ‘expressed gene sets’	172
3.2.6.2.2	TEB- and duct stroma-only ‘expressed gene sets’	173
3.2.6.3	Identification and classification of new, potential regulators of pubertal mouse mammary gland morphogenesis - candidate gene approach	173
3.2.6.4	Comparison analysis of biological functions over-represented in the epithelial and stromal transcriptomes of TEBs and ducts. (Pathway analysis)	178
3.2.6.4.1	Molecular and Cellular Functions: Identification of the top 5 over-represented categories	183
3.2.6.4.2	Physiological System Development and Function - Identification of the top 5 over-represented categories	185
3.2.6.5	‘Cellular Movement’ during pubertal mouse mammary gland morphogenesis - Comparison of transcriptomes from TEBs and ducts....	188
3.2.6.6	‘Nervous System Development and Function’ during mouse mammary gland morphogenesis - Comparison of transcriptomes from TEBs and ducts	193
3.2.6.7	‘Embryonic Development’ during pubertal mouse mammary gland morphogenesis - Comparison of transcriptomes from TEBs and ducts	194
3.2.7	Summary.....	196
3.3	Discussion	197
3.3.1	Identification of pubertal signature of mouse mammary gland - Main concept behind the analysis	199
3.3.2	Identification and classification of new potential regulators of mouse mammary gland morphogenesis at puberty	200
3.3.2.1	Comments on the methodology used	201
3.3.2.2	Comments on the results	205
3.3.2.3	Further analyses	206
3.3.3	Identification and comparison of functional characteristics of the epithelial and stromal transcriptomes of TEBs and ducts.....	208
3.3.3.1	Comments on methodology used	208
3.3.3.2	Comments on results	210
3.3.3.2.1	Characterisation of the TEB and duct transcriptomes using ‘expressed gene sets’	211
3.3.3.2.2	Characterisation of TEB and duct transcriptomes based on the ‘up-regulated gene sets’	216
3.3.3.3	Association of pubertal development with embryogenesis ...	219
3.3.3.4	Association of pubertal development with EMT	220
3.3.3.5	Association of pubertal transcriptome with nervous system ..	221
3.3.3.6	Further analyses	222
3.3.4	Summary.....	223
4	Identification of new potential regulators of pubertal mouse mammary gland morphogenesis: Uroplakin 3a and Fibulin 2.....	226
4.1	Introduction	226
4.2	Results.....	226
4.2.1	UROPLAKIN 3A	226
4.2.1.1	Introduction	226
4.2.1.2	Validation of Upk3a expression in pubertal mouse mammary gland	228

4.2.2	FIBULIN 2	233
4.2.2.1	Introduction	233
4.2.2.2	Validation of Fbln2 expression during pubertal mouse mammary gland development.	237
4.2.2.3	Localisation of Fbln2 in the pubertal mouse mammary gland	241
4.2.2.4	Fbln2 expression across the different stages of mouse mammary gland development.	244
4.2.2.5	Localisation of Fbln2 expression using a preliminary <i>in vitro</i> model of TEB explant culture	253
4.2.2.6	Fbln2 splice variants and their pubertal expression pattern.	255
4.2.2.7	Characterisation of the additional, 150 kDa and 135 kDa proteins, detected by the routine anti-Fbln2 antibody.....	260
4.2.2.8	The impact of systemic hormones on the regulation of Fbln2 expression in mouse mammary gland.	266
4.2.2.9	Investigation of Fbln2 functions in non malignant mouse mammary epithelial cells <i>in vitro</i> by the over-expression of Fbln2 in HC11 cells	270
4.2.2.9.1	Optimisation of transfection	270
4.2.2.9.2	The effect of Fbln2 on the migratory properties of HC11 cells	272
4.2.2.9.3	The effect of Fbln2 on the adhesiveness of HC11 cells	272
4.2.2.10	Fbln2 binding partners and their expression during pubertal mouse mammary gland development.	274
4.2.2.10.1	Fibronectin and Fbln2 co localisation study.	277
4.2.2.10.2	Elastin and Fbln2 co-localisation study	279
4.2.2.11	Fbln2 is not essential for pre-pubertal and pubertal mouse mammary gland development.	282
4.2.2.12	Summary	285
4.3	Discussion	289
4.3.1	Uroplakin 3a.....	290
4.3.2	Fibulin 2	292
4.3.2.1	Localisation of Fbln2 in pubertal mouse mammary gland	293
4.3.2.2	The characteristics of Fbln2 expression in mammary gland..	299
4.3.2.3	Hormonal regulation of Fbln2 expression	302
4.3.2.4	Potential functions of Fbln2 in pubertal mouse mammary gland	304
4.3.2.4.1	Structural function	304
4.3.2.4.2	Migratory function	307
4.3.2.5	Summary	311
5	Final conclusions and future work	312
5.1	Final Conclusions	312
5.2	Future directions	313
5.2.1	Further analysis of TEB and duct transcriptomes to study mouse mammary gland development at puberty	313
5.2.2	Further analysis of TEB and duct transcriptomes to study breast cancer	315
5.2.3	The use of microRNA profiling to study pubertal development of mouse mammary gland.....	316
5.2.4	Further investigation into the role of Upk3a and Fbln2 in pubertal morphogenesis of mouse mammary gland.....	317
6	Appendices.....	320
7	Bibliography.....	322

List of Figures

Figure 1-1 Overview of mouse mammary gland embryogenesis.	25
Figure 1-2 Overview of the postnatal mouse mammary gland development.	28
Figure 1-3 Morphology of pubertal mouse mammary gland.	32
Figure 1-4 Structure of TEB with duct and surrounding stroma.	34
Figure 1-5 Branching morphogenesis in pubertal mouse mammary gland.....	45
Figure 2-1 Dissection of the 4-th (inguinal) mouse mammary gland.	100
Figure 2-2 7 weeks old 4-th mouse mammary glands.	102
Figure 2-3 Histograms showing comparison analysis of amplification curves of Q RT PCR product amplified from two distinct samples.....	125
Figure 2-4 GeneChip® WTr Sense 1µg Total RNA Target Labelling Assay Manual - Schematic representation of the experimental steps.	128
Figure 3-1 Microarray data analysis paradigm.....	151
Figure 3-2 Isolated pubertal epithelium.	154
Figure 3-3 Whole mouse mammary glands.....	155
Figure 3-4 Wholemounds of different stages of pubertal mouse mammary gland development.	157
Figure 3-5 Assessment of hybridisation efficiency.....	161
Figure 3-6 Microarray data quality controls.	163
Figure 3-7 Validation of microarray gene expression profiling by RT PCR analysis.	166
Figure 3-8 Identification of TEB- and duct-associated stromal genes.	174
Figure 3-9 Identification of TEB epithelial gene set.....	176
Figure 3-10 Literature search based analysis of the 65 TEB epithelial gene set.	177
Figure 3-11 Selective, Ingenuity Pathway Analysis (IPA)-based functional comparison analysis of the identified pubertal gene sets.	189
Figure 4-1 Upk3a expression profiling in the pubertal mouse mammary gland by microarray analysis.....	229
Figure 4-2 Validation of <i>Upk3a</i> mRNA expression in the pubertal mouse mammary gland by Q RT PCR.....	230
Figure 4-3 Validation of Upk3a protein expression in the pubertal mouse mammary gland.....	232
Figure 4-4 The overview of domain models for Fbln2 (<i>M. musculus</i> and <i>H. sapiens</i> and Fbln1C (<i>M. musculus</i>).	234
Figure 4-5 Fbln2 expression profiling in the pubertal mouse mammary gland by microarray analysis.....	238
Figure 4-6 Validation of Fbln2 expression in pubertal mouse mammary gland..	240
Figure 4-7 Localisation of Fbln2 expression in pubertal mouse mammary gland by IHC.....	242
Figure 4-8 Localisation of Fbln2 expression in the pubertal TEBs and ducts by IHC.....	243
Figure 4-9 Localisation of Fbln2 expression in the pubertal epithelium of TEBs and ducts by IF.....	245
Figure 4-10 Localisation of Fbln2 expression in the pubertal TEB by IF.	246
Figure 4-11 3D reconstruction of pubertal TEBs and ducts stained with anti-Fbln2 antibody.	247
Figure 4-12 <i>Fbln2</i> mRNA expression throughout different stages of mouse mammary gland development by Q RT PCR.	248
Figure 4-13 Fbln2 protein expression and localisation during virgin mouse mammary gland development by IHC.	250

Figure 4-14 Fbln2 protein expression and localisation in the mouse mammary gland during pregnancy time points by IHC.....	251
Figure 4-15 Fbln2 protein expression and localisation in the mouse mammary gland during lactation and involution by IHC.....	252
Figure 4-16 Fbln2 protein expression in the stromal capsule throughout the developmental time points of mouse mammary gland morphogenesis by IHC. .	254
Figure 4-17 Preliminary analysis of the morphological characteristics of explant culture outgrowths by ICH.	256
Figure 4-18 Preliminary investigation of Fbln2 expression in the outgrowths of TEB explants by ICH.	257
Figure 4-19 The expression of Fbln2 splice variants in the pubertal mouse mammary gland.....	259
Figure 4-20 Fbln2 expression profiling in the mouse cell lines and identification of Fbln2 V2 expression in Eph4 cells.	262
Figure 4-21 Comparison of Fbln2 expression pattern detected using different antibodies.	264
Figure 4-22 Comparison of Fbln2 expression pattern detected using different lysis buffers.	265
Figure 4-23 Hormonal regulation of <i>Fbln2</i> expression at the mRNA level by Q RT PCR.	268
Figure 4-24 Hormonal regulation of Fbln2 expression on protein level by IHC. .	269
Figure 4-25 <i>In vitro</i> over-expression of Fbln2 in HC11 cells.....	271
Figure 4-26 The effect of Fbln2 on the regulation of HC11 cells migration using a wound healing assay.	273
Figure 4-27 Effect of Fbln2 on the regulation of adhesive properties of HC11 cells using adhesion assays.	275
Figure 4-28 Potential binding partners for Fbln2 in the mouse mammary gland and their pubertal gene expression level.	276
Figure 4-29 Co-localisation of Fbln2 and Fn expression in the pubertal mouse mammary gland using IF.....	280
Figure 4-30 Localisation of Eln expression in pubertal mouse mammary gland using Elastica van Gieson staining.	281
Figure 4-31 Comparison of Fbln2 expression in Fbln2 WT and Fbln2 KO ^{-/-} pubertal mouse mammary glands by IHC.	283
Figure 4-32 Wholemout analysis of pre-pubertal and pubertal Fbln2 KO ^{-/-} mouse mammary gland.	284
Figure 4-33 Comparison of TEB histology in WT and Fbln2 KO ^{-/-} pubertal mouse mammary glands by H&E staining.....	286
Figure 4-34 The up-regulation and spatial localisation of Fbln1 in the epithelium of Fbln2 KO ^{-/-} pubertal mouse mammary glands.	287
Figure 4-35 Localisation of Fbln2 expression in pubertal TEB by IHC.....	295
Figure 4-36 Wholemouts collected from hormone primed TG mice.	303

List of Tables

Table 1-1 List of pubertal regulators of mouse mammary gland and the effect they exert on TEB motility or ductal branching.....	82
Table 1-2 Summary of the microarray studies carried out on the pubertal mouse mammary glands, to date, and their main characteristics.	89
Table 2-1 List of reagents and materials.....	94
Table 2-2 List of solutions and buffers.	96
Table 2-3 List of electric equipment.	97
Table 2-4 Primary and secondary antibodies used for Western Blotting.	115
Table 2-5 Primers used in Standard PCR.	122
Table 2-6 Probes and primers used in Q RT PCR.	122
Table 2-7 Primers used in sequencing.	122
Table 2-8 EMT signature genes.	141
Table 2-9 Primary antibodies used for staining of paraffin embedded tissue sections using IHC and IF methods.	145
Table 3-1 Description of RNA samples used for microarray analysis of pubertal gene expression.....	159
Table 3-2 List of reference genes known to be associated with TEB and duct environments and the level of their up-regulation in the generated in this study gene lists.....	165
Table 3-3 Number of genes up-regulated in each transcriptome.	169
Table 3-4 Top 20 genes over-expressed in isolated TEBs, ducts, Post-LN and Pre-LN strips.	170
Table 3-5 Categorisation of 65 TEB epithelial genes based on molecular and biological function.	179
Table 3-6 Comparison of the top 5 cellular and molecular functions over-represented in the epithelial and stromal data sets of TEBs and ducts.	184
Table 3-7 Comparison of the top 5 categories associated with the physiological system development and function shown to be over-represented in the epithelial and stromal data sets of TEBs and ducts.....	186
Table 3-8 List of EMT core signature genes also identified as differentially expressed in TEB environment.	192
Table 4-1 List of Fbln2 binding partners up-regulated during pubertal mouse mammary gland development.	278
Table 4-2 List of Fbln2 binding partners shown to exhibit an unaltered expression level during pubertal mouse mammary gland development.	278

List of Appendices

Appendix 1 Fbln2 V1 expression vector.	320
Appendix 2 List of genes over-expressed in TEB and duct epithelium.....	320
Appendix 3 List of genes over-expressed in Post- and Pre-LN mouse mammary gland tissue strips.	320
Appendix 4 List of genes over-expressed in the epithelium free mammary Fat pad.....	320
Appendix 5 List of genes expressed in TEB-only and duct-only epithelium.	320
Appendix 6 List of genes expressed in TEB-only and duct-only stroma.....	320
Appendix 7 List of genes associated with the identified 'Molecular and Cellular Function' categories.	320
Appendix 8 List of genes associated with the identified 'Physiological System Development and Function' categories.	320
Appendix 9 List of functional sub-group associated with 'Cellular Movement", 'Nervous System Development and Function' and 'Embryonic Development' and their associated genes.	320
Appendix 10 List of presentations prepared on the data from this thesis	321

List of Supplementary Material

Supplementary DVD

Abbreviations

2D	2 dimensional
Aa	Aminoacid
Acan	Aggrecan
ADAM	A Disintegrin And Metalloprotease
ADAMTS	ADAM metallopeptidase with thrombospondin type 1 motif
ADI	Average difference intensity
Aldh1a3	Aldehyde dehydrogenase family 1, subfamily A3
AMU	Asymmetric membrane units
AP-1	Activator protein 1
Ap1m2	Adaptor protein complex AP1, mu 2 subunit
AP-2	Activator protein 2
AP-2 γ	Activating enhancer binding protein 2 gamma
Areg	Amphiregulin
ATF	Activating transcription factor
BASP	Brain acid-soluble protein 1
Bax	Bcl2-associated X protein
Bcl-2	B-cell leukaemia 2
Bim	Bcl2-like 11
BL	Basal lamina
Blc-x	Chemokine ligand 13
BM	Basement membrane
BMP4	Bone morphogenic protein 4
BSA	Bovine serum albumin
Bst1	Bone marrow stromal cell antigen 1
BTC	Betacellulin
Btk	Brutton agammaglabulinemia tyrosine kinase
<i>C. elegans</i>	<i>Caenorhabditis elegans</i>
C/EBP	CCAAT-enhancer binding protein
Calciol	1,25- dihydroxyvitamin D3
Cbrd1	Cytochrome b reductase 1
Ccl3	Chemokine (C-C motif) ligand 3
Ccnd1	Cyclin D1
Ccr2	Chemokine (C-C motif) receptor 2
Cd10	Common acute lymphoblastic leukemia antigen
Cd14	Cd 14 antigen
Cd2	Cd 2 antigen
Cd22	Cd 22 antigen
Cd4	Cd 4 antigen
CITED1	Cbp/p300 - interacting transactivator with Glu/Asp-rich carboxy-terminal domain 1
cJUN	Oncogenes Jun
c-Met	Met proto-oncogene
CMV	cytomegalovirus
c-myc	Myelocytomatosis oncogene
Coll	Collagen type I
CollIV	Collagen type IV
CollVal	Collagen IV alpha I
ColVIaIII	Collagen VI alpha III
ColXVIIIaI	Collagen XVIII alpha

Cp	Crossing point
CSF-1	Colony stimulating factor 1
CSF-1R	CSF-1 receptor
Cxadr	Coxsackie virus and adenovirus receptor
<i>D. melanogaster</i>	<i>Drosophila melanogaster</i>
DAB+	3,3-Diaminobenzidine tetrahydrochloride chromogen
DAPI	4,6-diamidino-2-phenylindole dihydrochloride
Dhh	Hedgehog
Dkk1	Dickkopf 1
Dlg7	Disk large homologue 7
DMEM	Dulbecco's Modified Eagle medium
DMEM/F12	Dulbecco's Modified Eagle Medium: Nutrient Mixture F-12
DMSO	Dimethyl sulfoxide
DNA	Deoxyribonucleic acid
dNTPs	Deoxy nucleotide-5'-triphosphate
dPBS	Phosphate Buffered Saline
DTT	Dithiothreitol
E	Embryonic day
<i>E. coli</i>	<i>Escherichia coli</i>
E2	Oestrogen
ECM	Extracellular matrix
Ecm1	Extracellular matrix protein 1
Ect2	Ect2 oncogene
EDTA	Ethylenediaminetetraacetic acid
EFNB2	Ephrin receptor B2
EGF	Epidermal growth factor
EGFP	Enhanced green fluorescent protein
Elf4	E74-like factor 4
Eln	Elastin
Emb	Embigin
EMT	Epithelial to mesenchymal transition
Eo	Eosin
EPG	Epigen
Eph	Ephrin
EPHB4	Ephrin receptor B4
EPR	Epiregulin
ER	Oestrogen receptor
ErbB2	Erythroblastic leukemia viral oncogene homolog 2
ErbB3	Erythroblastic leukemia viral oncogene homolog 3
ErbB4	V-erb-a erythroblastic leukemia viral oncogene homolog 4
ERGDB	Oestrogen response gene database
ER β	Oestrogen receptor beta
ER α	Oestrogen receptor alpha
EVG	Elastica van Gieson
Fap	Fibroblast activation protein
Fbln1	Fibulin 1
Fbln2	Fibulin 2
Fbn1	Fibrillin 1
FBS	Fetal bovine serum
FC	Fold change
FDR	False discovery rate

Fgf	Fibroblast growth factor
Fgf10	Fibroblast growth factor 10
FGFR	Fibroblast growth factor receptor
Fgfr2b	Fibroblast growth factor 2b receptor
Flk-1	Kinase insert domain protein receptor
Flt-1	FMS-like tyrosine kinase 1
Fn	Fibronectin
Fos	FBJ osteosarcoma
FSH	Follicle stimulating hormone
FU	Fluorescence unit
G	Glucocorticoid
<i>G. gallus</i>	<i>Gallus gallus</i>
GATA3	GATA binding protein 3
GCOS	GeneChip® Operating Software
GFP	Green fluorescent protein
GH	Growth hormone
GHR	Growth hormone receptor
GnRH	Gonadotrophin-releasing hormone
GON-1	Abnormal GONad Development
Gpc3	Glypican 3
GR	Glucocorticoid receptor
Gsn	Gelsolin
H	Haematoxylin
<i>H. sapiens</i>	<i>Homo sapiens</i>
HFC	Highest fold change
HGF	Hepatocyte growth factor
HIN-1	High in normal 1
HRP	Horseradish peroxidase
IF	Immunofluorescence
IGF-1	Insulin growth factor 1
IGFR	Insulin growth factor receptor
IHC	Immunohistochemistry
IKB	Ingenuity knowledge base
IL18	Interleukin 18
IL5	Interleukin 5
IL6	Interleukin 6
IL8	Interleukin 8
Irf	Interferon regulatory factor
IRS1	Insulin receptor substrates 1
IRS2	Insulin receptor substrates 2
Itga5	Integrin α 5
Itgb3	Integrin β 3
Kcnk1	Potassium channel, subfamily K, member 1
Klk8	Kallikrein-related peptidase 8
KO	Knock out
Krt18	Keratin 18
Lad	Ladinin
Lama1	Laminin
LB	Luria Bertani Broth
LBP	Lipopolysaccharide binding protein
Lef-1	Lymphocyte enhancer factor factor-1
LFC	Limit fold change
LH	Gonadotrophins-luteinising hormone

LIF	Leukaemia inhibitory factor
LN	Lymph node
LOX	Lysyl oxidase
Lrp5	Low density lipoprotein receptor-related protein 5
Lrp6	Low density lipoprotein receptor-related protein 6
Ltf	Lactotransferrin
<i>M. musculus</i>	<i>Mus musculus</i>
MEC	Mammary epithelial cells
MED1	Mediator complex subunit 1
MFC	Minimum fold change
MFGE8	Secreted milk fat globule - EGF factor 8
MMP	Matrix metalloprotease
MMTV	Mouse mammary tumour virus
Msx1	Homeobox msh-like 1
Msx2	Homeobox msh-like 2
MTA1	Mediator complex subunit 1
Na	Cysteine rich domain of N-terminus of Fbln2
Nb	Cysteine free domain of N-terminus of Fbln2
Ndrg1	N-myc downstream regulated gene 1
Neo1	Neogenin 1
Nid	Nidogen
Nrg3	Neuregulin 3
Ntn1	Netrin 1
OD	Optical density
P	Progesterone
P190-B	Rho GTPase activating protein 5
p53	Tumour suppressor p53
PAGE	Polyacrylamide gel electrophoresis
PCA	Principal component analysis
Per	Perlacan
PI-MEC	Parity induced mammary epithelial cells
PM	Perfect match
PR	Progesterone receptor
PRAI	PR activity indicator
PRL	Prolactin
PRLR	Prolactin receptor
PTH	Parathyroid hormone
PTHrP	Lymphocyte differentiation parathyroid hormone-related protein
Pygo-2	Pygopus 2
RGD	Arg-Gly-Asp attachment site
RIN	RNA integrity number
RMA	Robust Multichip Analysis
RNA	Ribonucleic acid
RPMI-1640	Roswell park memorial institute 1640 medium
RT	Room temperature
S.E.M.	Standard error of the mean
SAPE	Streptavidin Phycoerythrin
SD	Standard deviation
Sema3B	Semaphorin 3B
S-GAG	Sulphate-rich glycosaminoglycans
SGP-2	Serum gp70 production 2
SHBG	Sex hormone binding globulin

Sirpa	Signal regulatory protein α
Slp1	Synaptotagmin-like 1
SLRP	Small Leucine-Rich Proteoglycan
SMA	Smooth muscle α -actin
Smad	Sma/Mad-related protein
Sp1	Trans-acting transcription factor 1
SPARC	Secreted Protein Acidic and Rich in cysteine
Sprr1A	Small proline rich protein 1A
SRC	Steroid-receptor co-activator
Ss	Single stranded
STAT3	Signal transducer and activator of transcription 3
Stc2	Stanniocalcin 2
TBS	Tris buffered saline
Tbx3	T-box transcription factor 3
TEB	Terminal end bud
Tek	Endothelial-specific receptor tyrosine kinase
TG	Transgenic GFP expressing C57BL/6 mice
TGF- β	Transforming growth factor β
Tm	Melting temperature
Tn	Tenascin-C
TNF α	Tumour necrosis factor alpha
Trim-29	Tripartite motif-containing 29
tTG2	Tissue transglutaminase 2
U	Units
Upk3a	Uroplakin 3a
V	Volts
Vcan	Versican
VDR	Vitamin D3 receptor
VEGF	Vascular endothelial growth factor
Vtn	Vitronectin
WAP	Whey acidic protein
Wnt	Wingless-related
WT	Wild type C57BL/6 mice
WTr	Whole transcript

Acknowledgements

First and foremost, I would like to sincerely thank my supervisors, Prof. B. A. Gusterson, Dr. J. S. Morris and Dr. T. Stein for their invaluable guidance, help and support both at professional and personal level throughout my PhD. I feel very lucky to have had supervisors who perfectly balanced challenge with understanding. I would also like to take this moment to further thank Prof. B. A. Gusterson for his kindness, support and continuous enthusiasm which inspired me and helped to overcome difficulties.

I would also like to thank all members of Dr. Stein, Dr. Hamilton and Dr. West lab, past and present, for their help, patience, kindness and optimism that made my PhD such a pleasant experience. A special thanks to Marie-Anne for teaching me the methodology; Emilio for entertainment at lunch times; Alex, Clare, John and especially Rod for performing most of the IHC and IF and my amazing friends Camille for sharing her knowledge, optimism, supporting me and being a great listener and Juanma whose scientific expertise, help, advice, unconditional support and friendship were invaluable for me both in and out of the lab. I could not have wished for nicer people to work with.

I am grateful to all staff at the Biological Services Central facilities at Gilmorehill Campus and the Veterinary Research Facility and Beatson Institute for Cancer Research on the Gartcube Estate, especially David McLaughlin, Davina Graham and Stephen Bell for their help with mouse husbandry. I am also indebted to Dr. Pawel Herzyk, Jing Wang and Dr. Daniel Crowther for their help with microarray analysis. Thank you to Dr. Tomoko Iwata for allowing me to use her microscope, Dr. Jane Plumb for letting me use her laboratory space at the Beatson Institute for Cancer Research and Dr. Kurt Anderson and Dr. Tom Gilbey for their help with microscopy. Finally, I would like to stress my gratitude for our collaborators, Dr. Mon Li-Chu of Thomas Jefferson University for providing us with anti-Fbln2 and anti-Fbln1 antibodies and helpful discussions about Fbln2 project and Dr. T Tsuda and Jennifer Joyce of Wilmington Nemours/Alfred I. DuPont Hospital for Children for collecting and processing of Fbln2 KO^{-/-} mouse mammary glands.

I would like to thank my family, especially my parents, Bogusława and Bogusław Olijnyk and grandmother - Anna Bandurak, to whom this thesis is dedicated, for their unconditional support, love and optimism during this PhD and throughout my life. A special thanks to my boyfriend, Adam for his invaluable patience, understanding, support and belief in me, especially during the write-up period. I would like to thank my lovely friends both in Glasgow and in Poland, in particular Milica, Linda, Juanma, Camille and Marta for their motivation and loving support throughout the PhD and making my life in Glasgow very enjoyable.

Finally, I am grateful to Breakthrough Breast Cancer and the Institute of Cancer Sciences at Glasgow University for funding and the opportunity to carry out this research.

Author's declaration

I am the sole author of this thesis. The work presented here is entirely my own, unless otherwise stated.

1 Introduction

1.1 Overview of mouse mammary gland development

The mammary gland is an epidermis derived organ that develops as a result of reciprocal epithelial-mesenchymal interactions and its primary function is to provide milk [1]. The mammary gland is exclusively present in mammals and it is the only organ where the majority of development occurs postnatally, with the onset at puberty. The mammary gland consists of an epithelial ductal tree which is surrounded by fat pad. The ductal tree forms a branched network of ducts that transport milk to the nipple to feed the new born. Mice have five pairs of mammary glands located to both thoracic (near forelimb) (3 pairs) and inguinal (next to hindlimb) (2 pairs) body regions. There is a gradient of differentiation between the murine glands, with the first being the least and fifth, the most differentiated [2]. The mammary glands initially develop in both female and male embryos. Sexual dimorphism arises as a result of androgen production by the testis and becomes apparent from embryonic day 14 (E14) [3].

During embryogenesis and puberty the mammary gland undergoes a series of complex and dynamic morphological changes that result in epithelial invasion of the surrounding fat pad and development of a ductal network. During pregnancy alveolar structures establish. During lactation milk is produced and released and after the pups are weaned a regression to the mature virgin-like state, by a process called involution, takes place. Both the wide array of developmental stages and postnatal development make the mammary gland a valuable model to delineate general mechanisms of morphogenesis. Processes involved in the formation of embryonic mammary placodes are similar to these that orchestrate formation of other skin appendages, such as teeth and feathers [4]. Hallmarks of puberty include extensive elongation of ducts and secondary branching making the mammary gland a good model to study branching morphogenesis and cell/tissue migration or invasion. During pregnancy, on the other hand, the mammary gland can be used to study not only branching morphogenesis but also cellular proliferation, since elevated cell proliferation and formation of additional tertiary ductal side branches, terminating in alveolar buds are characteristic of this developmental stage. Involution is a perfect system to

study cell death by apoptosis as the post-lactational regression is the most dramatic example of physiologically regulated apoptosis in adult tissue. Finally, an understanding of the biological processes implicated in mammary morphogenesis may assist our understanding of cancer as similar processes of proliferation, apoptosis and invasion occur in both.

Female mouse mammary gland morphology during the embryonic and postnatal development (pre-puberty, puberty, adulthood, pregnancy, lactation and involution) and its main regulatory cues are discussed below. Detailed analysis of pubertal mouse mammary development and its regulation, which this thesis focuses on, is presented in 1.2.

1.1.1 Embryonic development of mouse mammary gland

Mammary gland development begins at E10 with the formation of the milk/mammary lines. Milk lines arise from ectoderm and stretch between the anterior and posterior limb buds, on the ventral side of the embryo. The columnar, multilayered cells within the milk line are delineated by the expression of Wnt pathway members including Wnt 10a and Wnt 6. At E11.5 the mammary lines resolve into mammary placodes - lens-shaped epidermal structures consisting of several layers of large columnar cells which are not uniformly orientated and are likely to derive from epidermal cells that migrate along the milk lines [5]. There are five pairs of mammary placodes in the mouse embryo. The development of individual pairs is not simultaneous and occurs in a distinct order [5] [6] [3]. Subsequently each mammary placode invaginates into the underlying mesenchyme to form a mammary bud [7]. From E12 to E14 the mammary buds submerge beneath the skin [5]. This is accompanied by two processes: formation of an epidermal-like cell stalk connecting the mammary bud to the skin and formation of the condensed primary mammary mesenchyme and embryonic fat pad [7]. Primary mesenchyme consists of multiple layers of fibroblasts [8]. It surrounds the basal lamina (BL) (laminin and heparan sulphate proteoglycans) of the stalk and ball of a mammary bud [9]. The fat pad, on the other hand, forms distally to the mammary bud and consists of loosely positioned preadipocytes [8]. At E16 mammary buds elongate to form mammary sprouts which invade primary mesenchyme and grow into the embryonic fat pad,

where they undergo branching to create a primary ductal tree with a lumen which opens on the surface of the skin. The ductal opening is surrounded by a nipple sheath which is formed by epidermal invagination [3] [10]. By E18.5 the rudimentary mammary tree consists of one short primary duct and about 10-15 initial branches. The rudimentary tree grows very slowly until puberty when the next cycle of extensive branching and elongation occurs (reviewed in [3]). It forms a scaffold on which further postnatal developmental changes will occur. An overview of female embryonic mouse mammary gland development is demonstrated in **Figure 1-1**.

Embryonic development of mouse mammary glands is fully dependent on the continuous communication between the ectoderm and mesenchyme of the developing mammary rudiment [11] [12], as shown by Sakakura *et al.* (1987), where mouse mammary epithelial explants fail to form buds when removed from its mesenchymal environment [7]. If recombined with mammary epithelial mesenchyme, epithelial explants from elsewhere in the embryo develop into mammary epithelium. The importance of primary mesenchyme in governing mammary cellular fate is also highlighted by the fact that the recombination experiments are only successful at E14-E17 - when the primary mesenchyme is formed [13]. The E17 mammary epithelium shows different morphological responses to the mammary mesenchyme and mammary fat pad. When grafted to an E14-E17 fat pad, normal ductal development can be seen, but when combined with E12-E17 mammary mesenchyme, ductal hyperplasia, characterised by frequent branching and lack of ductal elongation occurs [8]. Sustained epithelial-mesenchymal interactions direct and regulate expansion of placodes, formation of mammary buds and development of the rudimentary ductal tree.

The canonical pathways which signal from epithelium to mesenchyme and orchestrate different stages of embryonic mammary morphogenesis include wingless-related (Wnt), fibroblast growth factor (Fgf), T-lymphocyte differentiation parathyroid hormone-related protein signalling (PTHrP) and Insulin growth factor 1/Rho GTPase activating protein 5 (IGF-1/p190-B) pathways. Proteins associated with Wnt and FGF signalling are known to be essential for the milk line specification and placode formation. Deficiency of t-box transcription factor 3 (Tbx3) which can be induced by Wnt signalling results

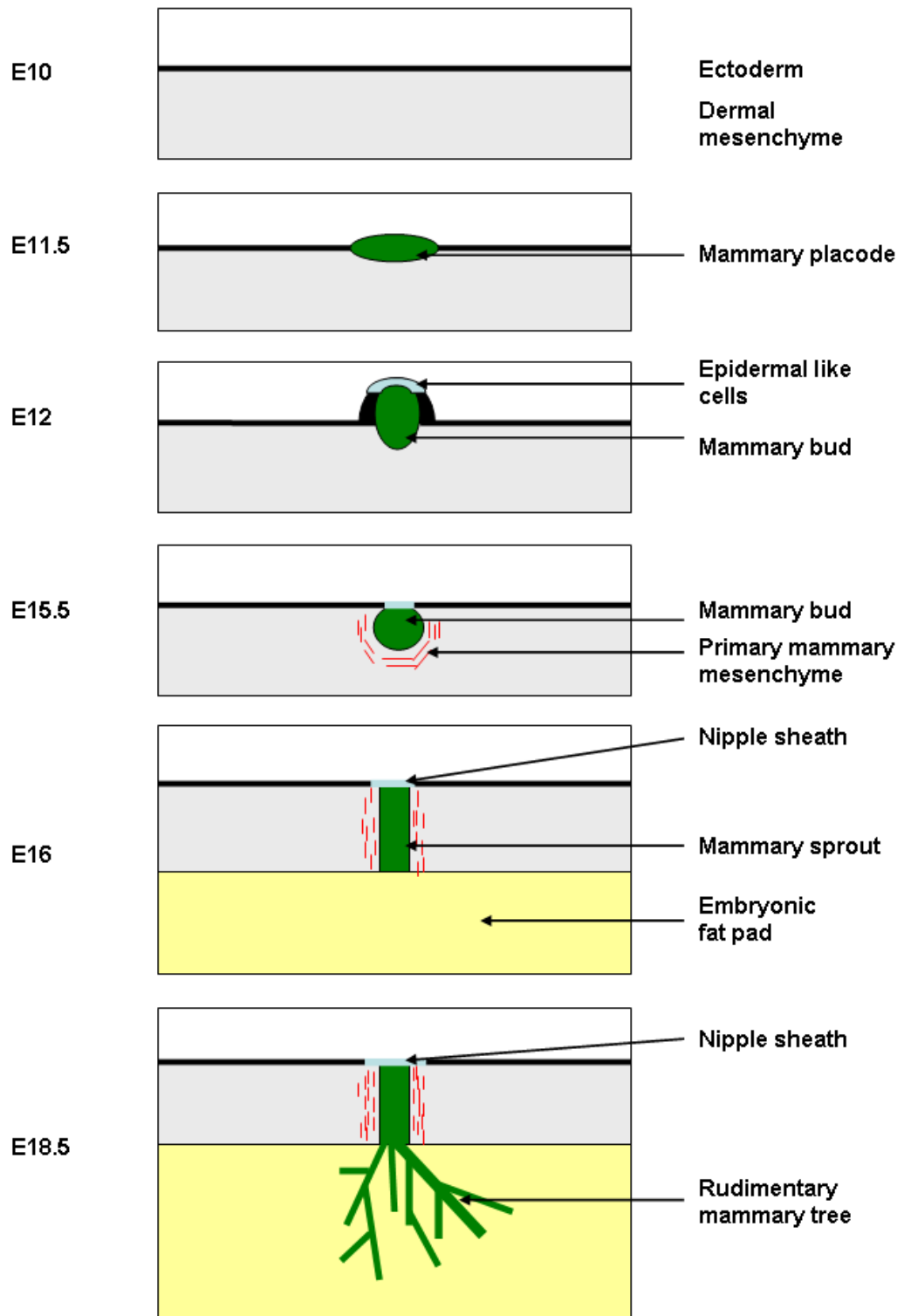


Figure 1-1 Overview of mouse mammary gland embryogenesis.

The embryonic development of mouse mammary gland starts with the formation of a mammary placode at E11.5. By E12 a mammary bud is apparent as a swelling on the surface of the ectoderm. By E15 the mammary bud invaginates and mammary mesenchyme condenses to form primary mammary mesenchyme. The mammary bud elongates to form a mammary sprout which further elongates to invade the underlying fat pad (E16). Finally at E18.5 the mammary sprout has branched to form a rudimentary mammary tree. The newly formed mammary tree is composed of a primary duct with a lumen opening into the nipple and multiple branched secondary ducts.

in complete loss of placodes [14] while loss of lymphocyte enhancer factor factor-1 (Lef1), a Wnt target gene, leads to loss of two pairs of placodes and the underdevelopment of the remaining ones [15]. In addition to its role in mammary line and placode formation, Wnt signalling also contributes to mammary bud formation. The decrease in mammary bud size is associated with the loss of Wnt modifier - pygopus 2 (Pygo2) or Wnt coreceptors low density lipoprotein receptor-related protein 5 (Lrp5) and Lrp6 expression [16] [17] [18]. Furthermore, loss of Lrp6 or Pygo2 expression also impairs the formation of the primary ductal system [17] [16]. Finally, blocking of Wnt signalling at E14.5 with its inhibitor dickkopf 1(Dkk1) results in suppression of mammary bud formation [19]. Fibroblast growth factor 10 (Fgf10) is expressed at E10.5-E11, when it localises directly underneath the forming mammary line suggesting a function in early mammary line specification. Fgf10 and fibroblast growth factor 2b receptor (Fgfr2b) are also necessary for the development of mammary buds as their deficiency results in the failure of all but mammary bud number 4 to develop [20]. On the other hand, expression of transcription factor GATA binding protein 3 (GATA3), which is implicated in regulation of T lymphocyte differentiation in response to parasitic infections, is essential for both placode and nipple sheath formation [21]. PTHrP signalling is essential for full differentiation of mammary mesenchyme (essential for determining of epithelial cell fate), formation of the nipple sheath and further ductal morphogenesis [10] [22]. The downstream target of PTHrP, bone morphogenic protein 4 (BMP4) also plays a role in regulation of embryonic mammary ductal morphogenesis [23]. Finally, disruption of the IGF-1/p190-B pathway by knock out (KO) of p190-B (inhibits Rho activity) or insulin receptor substrates 1 or 2 (IRS1 and 2) expression, results in formation of small mammary buds and disorganisation of the mammary mesenchyme [24]. Some of the other molecules which are critical for embryonic mammogenesis include: v-erb-a erythroblastic leukemia viral oncogene homolog 4 (ErbB4) ligand - neuregulin 3 (Nrg3) [25], homeobox msh-like 2 (Msx2) and Msx1 the double KO^{-/-} of which results in the formation of small placodes which fail to transform into mammary buds [26].

1.1.2 Postnatal development of mouse mammary gland

The majority of mammary gland morphogenesis occurs postnatally. It begins during puberty with ductal proliferation, carries on through adulthood with oestrus cycle induced early alveolar development and is completed with the cycles of proliferation, differentiation and cell death with each pregnancy, lactation and involution. The summary of the subsequent stages of postnatal mouse mammary gland development is shown in **Figure 1-2**.

At birth, the mammary gland consists of a rudimentary ductal tree which is similar to that seen at the E18.5 (**Figure 1-1**). During the first few weeks of postnatal life, up until the onset of puberty, the mammary rudiment grows allometrically. At the onset of puberty (~3-4 weeks) increased levels of gonadotrophins and oestrogen in the serum trigger formation of terminal end buds (TEBs), which in turn drive ductal elongation. The ductal tree expands via ductal elongation and branching up until week ~10-12 (adulthood) when the ductal system becomes fully developed. Detailed overview of pubertal mammary gland morphogenesis is discussed in **Section 1.2**.

At ~10-12 weeks of age, depending on the mouse strain, the edges of the fat pad are reached, TEBs start regressing into terminal end ducts and ductal outgrowth ceases. In response to ovarian hormones, secreted with each oestrus cycle, mature ductal epithelium further undergoes cycles of proliferation, differentiation and involution that results in formation of small ductal branches and lateral buds [27]. Lateral buds then turn either into lateral branches or form alveolar buds. Lateral branches are characterised by the presence of a cap cell layer at its growing tip (as seen in TEBs). Alveolar buds are comprised of a single epithelial cell layer enclosing a hollow lumen [28]. During pregnancy-induced growth, alveolar buds progress into fully differentiated units capable of milk secretion called alveoli. Although the secretion of milk occurs during lactation the expression of milk proteins can already be observed during the oestrus cycle in murine adult virgin mammary glands [29].

Pregnancy is further characterised by extended epithelial differentiation. In mice gestation lasts for 19-21 days. Its onset is defined by two events: extensive proliferation and branching of the ductal epithelium and formation of alveolar

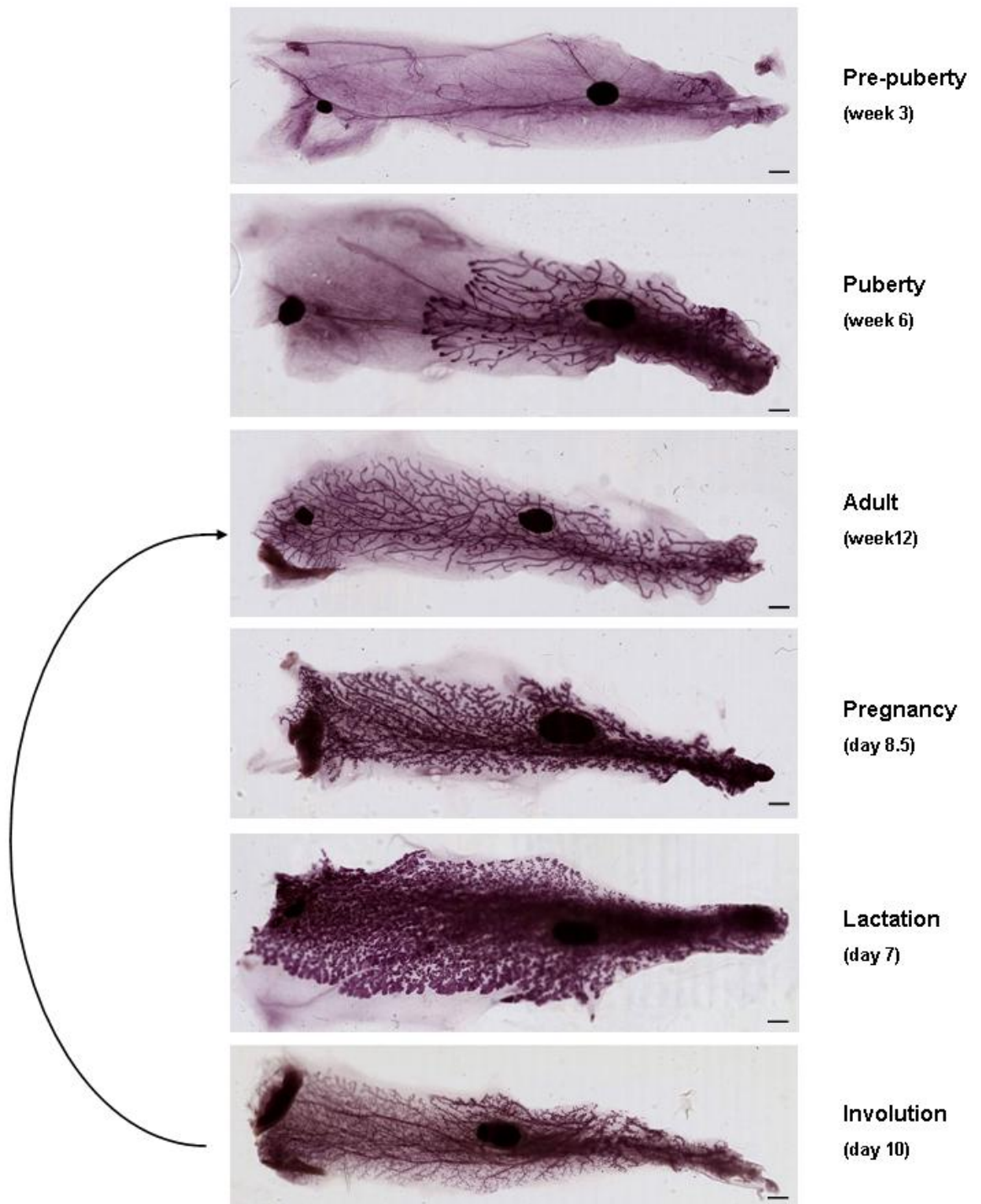


Figure 1-2 Overview of the postnatal mouse mammary gland development.

Figure shows the representative stages of mouse mammary gland morphogenesis. At pre-puberty, the mammary gland consists of a rudimentary tree that contains TEB-like structures and is similar to that seen at E18.5. Onset of puberty initiates TEBs formation and bifurcation, ductal elongation and branching, which collectively form a ductal tree. Upon reaching adulthood, most TEBs regress and ductal expansion ceases. Mature ductal epithelium undergoes estrus cycle dependent cycles of proliferation, differentiation and involution which gives rise to tertiary branching and development of lateral buds. With the onset of pregnancy, the rate of proliferation increases and lateral buds develop into alveoli. At parturition and during lactation, the whole gland is filled with alveoli that produce milk proteins and lipid which are secreted and transported through the ducts to feed the pups. Upon weaning, the alveoli regress and the gland undergoes remodelling in the process called involution, which returns the gland to a morphological state similar, but not identical, to that seen in mature virgin mice (adulthood).

buds, as seen in murine adult virgin mammary glands. Towards the middle part of pregnancy, alveolar buds cleave and further differentiate to form individual alveoli (lobuloalveolar phase of mammary gland morphogenesis). Alveoli synthesise and secrete milk from late pregnancy and throughout lactation. As for epithelial ducts and virgin alveolar buds, the alveoli are formed by the luminal (innermost cells enclosing the lumen) and myoepithelial cells (outermost cells). Here, however, the myoepithelial cells are less continuous. This enables the direct contact of luminal cells with the basement membrane (BM), which is critical for full differentiation and milk secretion [30]. Alveoli are suggested to originate from the lobule-limited progenitor cells [31] (reviewed in [32]). By gestation day 18, the alveolar epithelial cells enlarge and produce milk proteins (whey acidic protein (WAP) and α -lactalbumin, β -casein) and lipids in preparation for lactation [33]. At the final stages of pregnancy, alveoli occupy the majority of the fat pad. Secretion of milk proteins and lipids to the alveolar lumen starts one day prior to parturition. The main regulators of gestation include progesterone (P) and prolactin (PRL). Presence of progesterone receptors (PRs) is critical for mediating ductal outgrowth and lobuloalveolar differentiation (reviewed in [34]). Furthermore, P suppresses active milk secretion. The absence of alveoli is also associated with lack of prolactin receptor (PRLR) expression [35].

At parturition, the luminal epithelium becomes flattened due to the engorgement of alveoli and firstly colostrum and then milk and lipids are secreted to the lumen. PRL acts on luminal epithelial cells to sustain milk secretion [36]. In response to oxytocin, the surrounding myoepithelial cells contract to force milk out of the alveoli into the ducts, towards the nipple. This process of milk secretion is referred to as lactation and can occur for up to 3 weeks. It is stimulated by suckling pups which cause the release of oxytocin [28].

After natural or forced weaning (pup removal) and in response to milk stasis, the mammary gland enters a phase of dramatic cell death and tissue remodelling, called involution. At this time point, the expression of genes encoding milk proteins decreases to basal level. The expression of genes associated with processes such as apoptosis (e.g. serum gp70 production 2 (SGP-2), signal transducer and activator of transcription 3 (STAT3)), regulation of proliferation and differentiation (e.g. tumour suppressor p53 (p53),

myelocytomatosis oncogene (c-myc), transforming growth factor β (TGF- β) [37] increases. Inflammation/acute phase response proteins also increase at this time (e.g. CD 14 antigen (CD14), lipopolysaccharide binding protein (LBP)) [38] [39] (reviewed in [40]). Initially, during the first 2-3 days the process is reversible and lactation can be reintroduced upon suckling [41].

Apoptosis of the alveolar secretory luminal cells commences just within hours after weaning and by day 3 it becomes irreversible [42]. The alveoli collapse into clusters of epithelial cells and the fat pad is thought to become refilled with adipocytes. The collapsed apoptotic epithelium is cleared mainly by neighbouring epithelial cells which recognise and engulf them into the specialised vesicles called the efferosomes [43] [44]. By day 4 of involution the clearance of apoptotic cells is completed and the epithelial, stromal and BM-associated rearrangements occur [44] [37]. Involution lasts for 14-21 days approximately and at its conclusion, the mammary gland resembles a pre-pregnant mature mammary gland. In comparison to the virgin gland, however, the involuted gland is more differentiated and contains the occasional remaining alveoli [28].

1.2 Mouse mammary gland morphogenesis at puberty

The onset of puberty can be defined by three pubertal events: vaginal opening, first vaginal cornification and onset of cyclicity. The vaginal opening, first oestrus and the following increase in the production and secretion of gonadotrophins and oestrogen (E2) are the most frequently used measurements of puberty in mice. The timing of all three pubertal events depends on the strain of mice [45]. Generally, the onset of puberty arises at 3-4 weeks of age. In some mice, however, it can occur several weeks after vaginal cornification [46]. In C57BL/6 mice the vaginal opening, first vaginal cornification and first oestrus occur at approximately 4, 6 and 8 weeks of age respectively [45]. The murine oestrus cycle lasts for 4-5 days and comprises of four phases: proestrus, oestrus (ovulation), metoestrus and dioestrus. Each of these stages are characterised by distinct changes in vaginal cytology and mammary gland morphology. As described by Bronson *et al.* (1975), in virgin mice, proestrus is associated with appearance of small TEBs at the ducts located at the periphery of the gland

(similar structures can be seen at pre-puberty) and large, blunt projections on the main ducts at the nipple region. At oestrus, the mammary ducts become dilated and TEBs elongate. Epithelial growth regresses during metoestrus when ducts decrease in width and their endings collapse giving rise to the very open network of narrow, thread-like ducts seen in dioestrus [47]. At each subsequent oestrus cycle, a slight burst of proliferation and growth of mammary epithelium can be noted [48].

Morphologically, the pubertal mouse mammary gland consists of two compartments: epithelial and stromal (fat pad). In addition each mammary gland has one or two lymph nodes (LN), blood vessels and nerves [49]. The epithelial compartment of the pubertal mouse mammary gland consists of TEBs and ducts. TEBs, which are situated at the ends of ducts, promote and direct the outgrowth of the ductal tree into the surrounding fat pad [50]. TEBs migrate forward and bifurcate while ductal epithelium elongates behind them thus producing secondary branches and a ductal network. Epithelial expansion peaks between ~ 4-7 weeks of age and takes place until the whole fat pad is filled (~10-12 weeks of age), when TEBs regress and the extensive mitotic activity, ductal outgrowth and branching cease, with only minor proliferative activity noted in response to the oestrus cycle [51]. The structure of pubertal mouse mammary gland is illustrated in **Figure 1-3**.

1.2.1 The morphology and characteristics of pubertal mouse mammary gland

1.2.1.1 Epithelium

Although both TEBs and ducts are essential for pubertal outgrowth their role is very different. These differences are reflected in their morphology, the character of their surrounding stroma, the mechanisms underlying branching morphogenesis, outgrowth and its regulation.

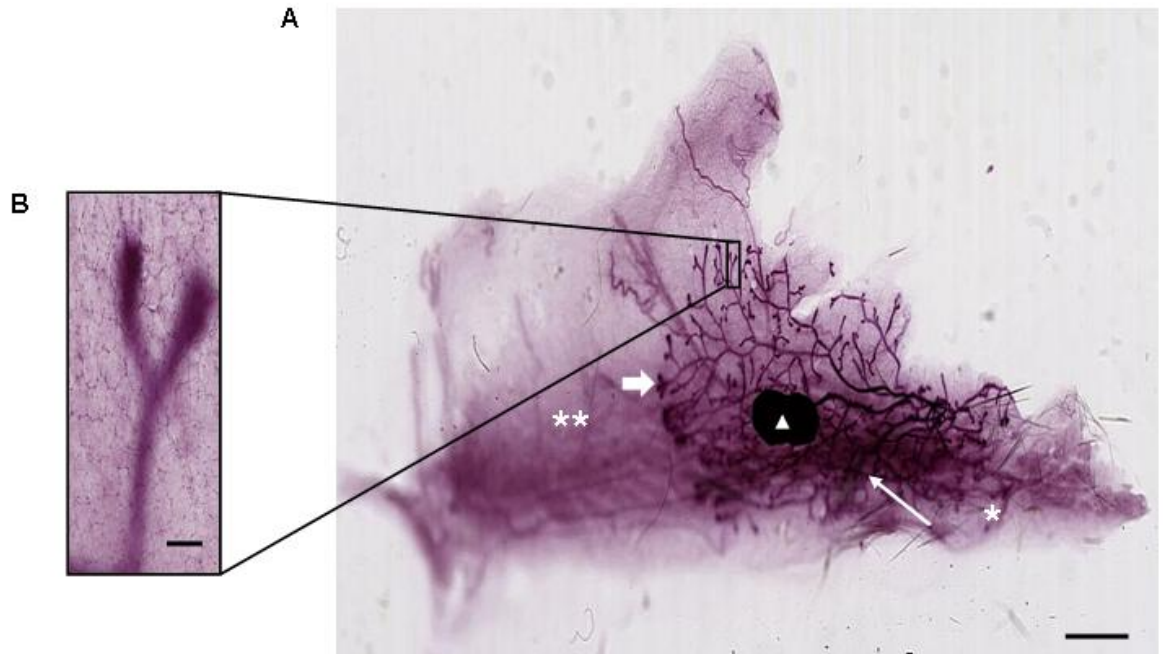


Figure 1-3 Morphology of pubertal mouse mammary gland.

Carmine alum stained wholemount of a pubertal C57BL/6 mouse mammary gland (6 week old).

(A) The asterisk denotes the nipple region; double asterisk represents the Fat pad; the thin arrow shows ducts; thick arrow denotes TEBs while arrowhead the LN. Scale bar is 2.5 mm. **(B)** Magnified image of two TEBs and a duct. Scale bar is 100 μ m.

1.2.1.1.1 *TEBs*

TEBs are bulbous epithelial structures which range in size from 0.1 to 0.5mm [52]. They are mainly present at puberty, when they drive directional outgrowth of the ductal tree, at the rate of approximately 0.5mm/day [53]. Similar structures can be seen between late gestation and week 1 of pre-puberty where they appear in response to maternal hormones. The decrease in maternal hormones stops mitosis in the TEB-like structures, until the onset of cyclicity at puberty when cellular proliferation begins again [7] [54]. TEBs consist of two types of epithelial cells: inner body cells and outer cap cells (**Figure 1-4 B and C**). Cap cells are enveloped by a BM that belongs to the extracellular matrix (ECM), and this will be discussed in 1.2.1.2.4

Cap cells are exclusively present in TEBs [55] and TEB-like structures where they form either a single or double layered envelope all around the body of the TEB. The number of cap cells is proportional to the size of TEB [54]. At the apical side, they are adjacent to the BM while at the lateral side, although slightly separated, they flank the bulk of the TEB. Cap cells located at the tip of TEB are characterised by loose organisation, presence of multiple intercellular spaces, and a lack of specialised cell junctions for adhesion or communication. As shown by Williams and Daniel (1983) they can be easily detached from the underlying bulk of the TEB and overlaying BM when treated with testicular hyaluronidase [53]. The nuclei of cap cells are round or oval with diffuse chromatin while their cytoplasm comprises of multiple free ribosomes, a moderate number of mitochondria, some rough endoplasmic reticulum and lipid droplets. Highly organised cytoskeletal elements are lacking.

Cap cells exhibit poor apical-basal polarity evidenced by sporadic secretion of hyaluronate and laminin (Lama1) (BM molecules) to their interior surfaces [56]. At the tip of the TEB cap cells have a columnar shape. As the contour of TEB is followed to its lateral sides and neck, however, the columnar cells progressively transform into cuboidal (lateral) and spindle shaped (neck) cells. The spindle shaped cells exhibit the characteristics of myoepithelial cells (outer cell layer in ducts) suggesting that the myoepithelium of the subtending ducts originates from cap cells. In addition, it is suggested that individual cap cells are able to

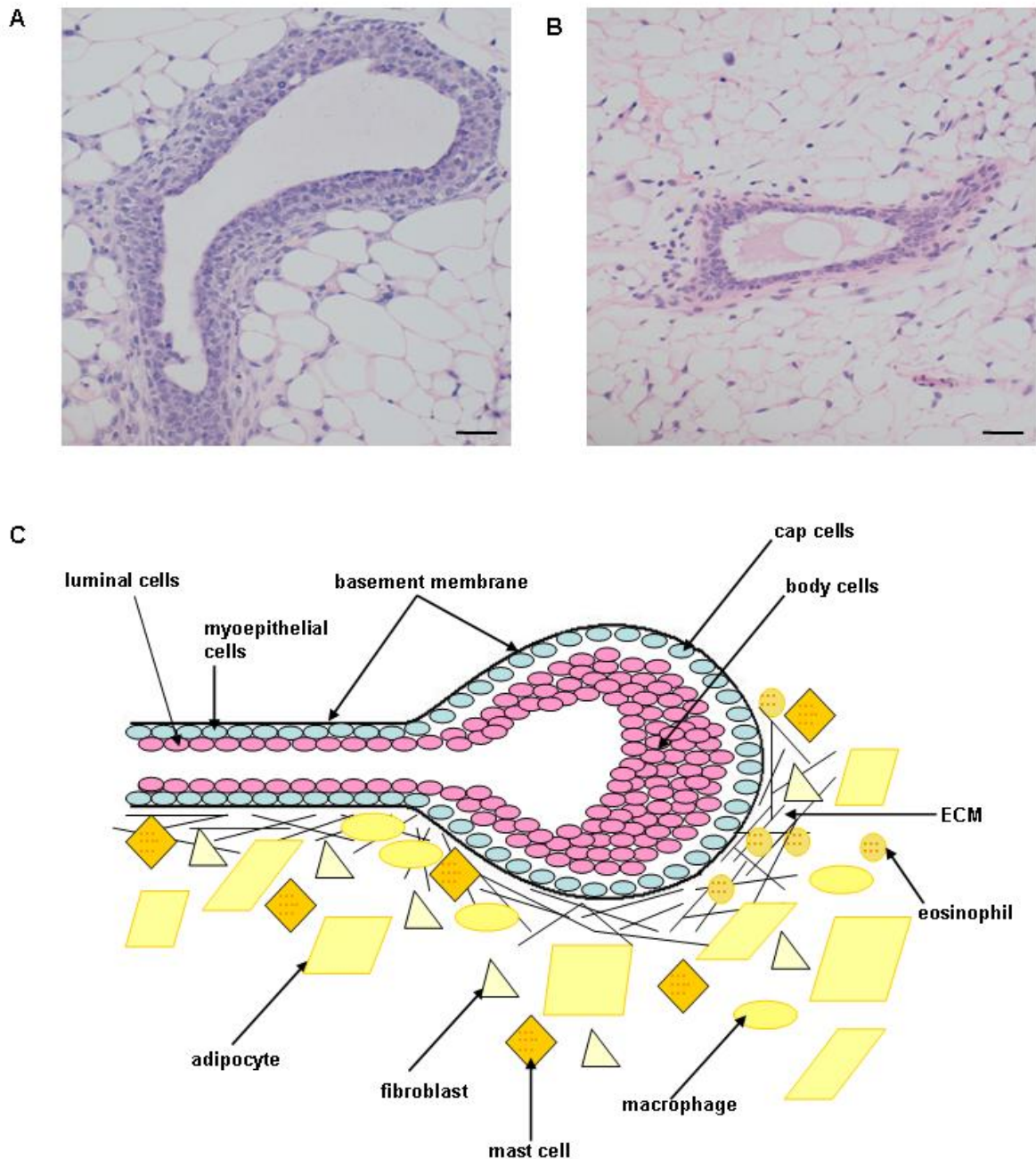


Figure 1-4 Structure of TEB with duct and surrounding stroma.

(A) (B) H&E stained section through (A) TEB and (B) duct. (C) Diagram representing structural characteristics of epithelial and stromal compartments of TEB and duct. TEB consists of a single layer of outer cap cells and multiple layered inner body cells. Cap cells give rise to myoepithelial cells of ducts, while body cells most likely differentiate into the ductal luminal cells. Both TEBs and ducts are surrounded by a BM. The stromal environment of TEBs and ducts consists of adipocytes, fibroblasts and mast cells. In addition, macrophages and eosinophils can be also seen in the stroma around TEB. The ECM provides a link between the epithelial and stromal cells. Scale bars are 50 μ m.

break away and migrate to deeper regions of the body of TEB. Cap cells stained using their molecular markers: P-cadherin (Cdh3) (adhesion molecule specific for cap cells) [57] and Lama1 (BM component synthesised in epithelium) [58] translocated to the body cell layers, where they gradually lost the expression of cap cell markers in favour of acquiring a luminal identity. Similar observations were confirmed using phase-contrast time-lapse microcinematography of freshly isolated TEBs [53]. Together these events suggest that cap cells contribute to the body cells and therefore are likely to be progenitors of the luminal epithelial cells of ducts. Furthermore, due to their presence at the tips of migrating TEBs, but not ductal tips of mature adult epithelium [59] it is likely that cap cells play a pivotal role in directing and patterning of ductal outgrowth.

The main bulk of the TEB, however, is formed by tightly compacted and multilayered body cells (6-10 layers). Morphologically, body cells are similar to ductal luminal cells and they are proposed to be their progenitors. Body cells tend to be polarised and possess tight cell-cell junctions characterised by the expression of E-cadherins (Cdh1) [53] [57]. The outer layers, although, in some places separated by an intercellular space, are in contact with cap cells while the inner most layer of body cells surrounds the lumen of the TEB. Inner layers of body cells are characterised by a high apoptotic rate that can be detected by TUNEL assay and positive B-cell leukaemia 2 (Bcl-2), chemokine ligand 13 (Bcl-x) and Bcl-2-associated X protein (Bax) expression (apoptotic checkpoint proteins) while the outermost body cells layers are more proliferative. Apoptosis is p53-independent and most probably leads to lumen formation. Each TEB contains reciprocal zones of apoptotic and proliferative cells which, although dispersed throughout the TEB, tend to appear in close proximity to each other [60]. The observed rate of apoptosis (11.3 %) is higher than that calculated for any other stage of mouse mammary development (apoptosis detected for involution is 4.5%) or that detected during kidney morphogenesis (3%) [61].

1.2.1.1.2 Ducts

Ducts account for the majority of the mammary epithelium at puberty where they form a branched ductal tree that serves as a scaffold on which secretory alveoli develop during pregnancy. In comparison to TEBs, however, ductal

epithelium is relatively growth quiescent [62]. Ducts are composed of an inner luminal and outer myoepithelial layer. Myoepithelial cells are surrounded by BM (Figure 1-4 A and C). Myoepithelial cells form a thin monolayer of basally arranged cuboidal cells. They are likely to play a part in signal transition between the BM and the internally located luminal epithelium. Cytologically, myoepithelial cells are characterised by desmosomes, hemidesmosomes, myofilaments, irregular nuclei with marked heterochromatin, peripheral cytoplasmic caveoli and ragged basal borders. Luminal epithelial cells, on the other hand, exhibit short, blunt microvilli on their apical surface and display well-developed cell-cell junctions [63]. Generally they form a monolayer but in some regions 1-3 layer thick wall of ductal epithelium around the hollow lumen can be seen. The layer closest to the lumen exhibits a higher apoptosis rate than that seen in the more outer cell layers which is consistent with a role of apoptosis in lumen formation [61] [60]. In addition, the ductal lumen may originate from the lumen of the advancing TEBs. One of the markers of luminal epithelial cells is keratin 18 (Krt18) [64] while the smooth muscle α -actin (SMA) marks the myoepithelial cells [65].

Both TEBs and ducts, i.e. the entire pubertal mammary epithelial tree contain stem cells which further persist through the subsequent stages of mammary morphogenesis and are capable of reconstructing a complete and functional gland when transplanted into cleared mammary fat pad of recipient host [66] [67] [68]. Mammary stem cells are defined as undifferentiated, pluripotent, relatively quiescent and long lived cells. As shown by the experiments based on the serial transplantation of mammary epithelium from the MMTV infected mice to the fat pads of recipient host, the mammary stem cells are capable of producing 5-8 transplant generations before senescing [68]. Furthermore, they exhibit the capacity to self maintain and proliferate - it is suggested that when transplanted, a stem cell initially divides symmetrically to repopulate the gland but any of their subsequent divisions, if and when they happen, are most probably asymmetric (with the template DNA strand being retained) (reviewed in [32]). Moreover, apart from the 'mother' stem cells that act as initial progenitors that give rise to cellular make up of mammary gland, as firstly demonstrated by transplantation studies using limiting dilution of mammary epithelial cells, the following generations of the 'daughter' mammary stem cells

produce two distinct lineage-limited progenitor cells: duct-limited and lobule-limited (also called - the parity induced mammary epithelial cells- PI-MEC) progenitors. Duct-limited progenitors produce oestrogen receptor (ER)^{+/-} and PR^{+/-} luminal cells and cap cells but are unable to produce progeny capable of sustaining epithelial growth at pregnancy and during alveologenesis, while the lobule-limited progenitors give rise to ER^{+/-} and PR^{+/-} luminal epithelial and myoepithelial cells, but are incapable of generating cap cells and thus can not give rise to ductal tree [31]. Both progenitor cell types are therefore essential to create mouse mammary gland in its entirety.

1.2.1.2 Fat pad

Fat pad (stroma) is a crucial component of the mouse mammary gland. Not only does it provide the structural scaffold for the ductal epithelial tree but it also regulates its morphogenesis. Numerous studies in which pre-pubertal fat pads were cleared from their endogenous epithelium and engrafted with exogenous epithelium demonstrated its magnificent role in sustaining and directing epithelial cell fate and promoting growth [69] [66]. As demonstrated by Daniel *et al.* (1968), transplantation of a small fragment of ductal epithelium into the cleared fat pad results in reconstitution of the whole ductal tree. In this experiment epithelial growth is induced at puberty and the mature ductal tree is formed within 10-12 weeks after transplantation [59]. This phenomenon was further elucidated by Kordon *et al.* (1998) who suggested the capability of the cleared fat pad (mature) to allow growth of the whole mammary gland from a single pluripotent mammary stem cell [68] which in 2006 has been demonstrated to be true by Shackleton *et al.* [70]. Furthermore, it has also been shown that testicular cells, when mixed with mammary epithelial cells (MECs) and transplanted into denuded fat pad, acquire an epithelial cell fate and contribute to ductal outgrowth [71]. Similar results were also obtained firstly with murine fetal and adult neural stem cells combined with equal numbers of MECs and engrafted into the clear fat pad [72] and secondly with the MECs mixed with human embryonic carcinoma cells (NTERA2cl) which, when inoculated into denuded fat pad, reprogrammed to normal MECs and contributed progeny to the resulting functional mammary outgrowths [73]. It is worth noting, however, that no outgrowths could be seen if the exogenous implants were not mixed with MECs upon the transplantation. Recently, it was also shown that mammary

morphogenesis can be induced and promoted by transplantation of mouse stem cells which are undergoing hematopoietic differentiation into the receptive cleared murine mammary fat pads [74]. This phenomenon of cell fate regulation by the stromal environment can be also seen in reverse experiments where mammary embryonic epithelium cotransplanted into salivary gland mesenchyme and grafted under the renal capsule of a host mouse, formed structures that resembled salivary glands [75].

This ability to impose and regulate cell fate is attributed to stem cell niche - a milieu, which based on current knowledge, includes the stromal environment, pluripotent cells, lineage-specific progenitors and fully differentiated cells which all contribute and signal together to support, maintain and control the stem cell/progenitor fate (reviewed in [32]).

Pubertal mouse mammary stroma is very heterogeneous in its composition. Adipose tissue is the most abundant mesenchymal cell type followed by fibroblasts, ECM, immune cells, endothelial and neural cells (**Figure 1-4 C**) [76].

1.2.1.2.1 Adipose tissue

There are two types of adipose tissue: brown adipocytes which are energy dissipating cells and white adipocytes which store energy [77]. Brown adipocytes, as opposed to white ones, are highly innervated and functionally controlled by the sympathetic nervous system [78]. They contain numerous well developed mitochondria and multilocular lipid inclusions whereas white adipocytes consist of a single, large inclusion and a low number of mitochondria [79]. Both are present throughout pubertal mouse mammary development. Brown adipocytes are most prevalent during pre-puberty where they surround the ductal tree (between the nipple and lymph node) but their structural contribution to mammary stroma decreases as the mice age and prior to adulthood they are undetectable [80]. White adipocytes, on the other hand, are present throughout mammary development where they are known to secrete a range of hormones, cytokines and growth factors, such as leptin, adiponectin, hepatocyte growth factor (HGF), collagen type VI (ColVI), interleukin 6 (IL-6) and tumour necrosis factor alpha (TNF α) and metabolise androgen to E2 [81].

1.2.1.2.2 Fibroblasts

The second most abundant type of stromal cells present in pubertal mouse mammary glands are fibroblasts - principal components of all connective tissues. Fibroblasts are spindle shaped. They are embedded within the ECM which they synthesise and maintain. They secrete collagen type I (Coll), III and V, fibronectin (Fn) and matrix metalloproteases (MMPs) which are essential for ECM maintenance; Lama1 and ColIV for BM formation. They are also involved in wound healing, regulation of inflammation and epithelial morphogenesis via secretion of growth factors (reviewed in [82]).

1.2.1.2.3 Migratory cells of the immune system

Migratory cells of the immune and haemopoietic system such as macrophages, eosinophils and mast cells are other crucial components of the mammary stroma. Macrophages and eosinophils detected by the marker protein F4/80 are associated with morphogenesis of numerous tissues. Initially, expression of macrophages in the mouse mammary gland can be detected at 2.5 weeks of age where they gather around the rudimental ductal tree. At puberty, however, macrophages cluster at the neck of TEBs where they support epithelial development, angiogenesis and matrix remodelling. The macrophages secrete trophic factors which are thought to play a role in Coll assembly and organisation into fibrillar bundles, which in turn are suggested as a part of the mechanism which directs the shape of TEBs and provides a framework for their outgrowth [83]. Furthermore, macrophages also intersperse among the adipocytes where they are involved in the phagocytosis of dying tissue [84]. Some macrophages also locate inside TEBs within the population of body cells that are proximal to the lumen. The recruitment of macrophages to the TEB is paralleled by the appearance of eosinophils which localise at the tips of TEBs. Initial recruitment of macrophages to the pre-pubertal mammary gland is regulated by colony stimulating factor 1 (CSF-1) [85]. It is expressed by the developing ducts and secreted as biologically active cell surface protein while the CSF-1 receptor (CSF-1R) is exclusively expressed on the macrophages [86] [85]. Specialised recruitment of macrophages to the TEBs, on the other hand, depends on the chemo-attractant action of chemokine C10 the expression of which depends on

the eosinophil recruitment around TEBs [87]. The recruitment of eosinophils, in turn, is regulated by interleukin 5 (IL-5) and eotaxin. IL-5 mobilizes eosinophils and their progenitors from the bone marrow while eotaxin directs their homing around TEBs [88] [87]. Similar spatial localisation and regulatory dependency suggest that macrophages and eosinophils could act synergistically [87].

Recently, further examination of immune response cells in pubertal mouse mammary gland morphogenesis identified mast cells in the stromal microenvironment [89]. Mast cells are produced in the bone marrow and released into the blood stream to be delivered into tissues, where they mature i.e. acquire a granular phenotype. The granules consist of histamine, proteoglycans, growth factors, proteases and many other factors which are secreted into the surrounding microenvironment through the process of degranulation. Mast cells are normally present around blood vessels, nerves, epithelial cells and muscle cells [90]. In the mammary gland, a few (scattered around the stroma) mast cells can be detected during pre-puberty. Peak of their activity, however, occurs at puberty when most mast cells gather in the stroma surrounding the BM of TEBs and ducts, the stroma ahead of the advancing TEB and around blood vessels. Some mast cells can be also seen at the periphery of the LN [89].

1.2.1.2.4 ECM

Stromal cells surrounding mammary epithelium are embedded in cell-secreted interstitial ECM. ECM can be divided into two compartments: BM and fibrous connective tissue (reviewed in [91]). BM can be also referred to as basal lamina (BL). The two names are often used interchangeably; BM refers to an ECM structure visualised by light microscopy while BL is visualised only by electron microscopy. BM is a highly organised outermost component of TEB and ducts that lies directly outside cap cells and myoepithelial cells respectively. It consists of three layers. Namely, lamina lucida interna, formed by periodically arranged stalks, lamina densa and anionic globular lamina externa. (reviewed in [91]). Lamina lucida interna and -externa contain high levels of proteoglycans which facilitate the attachment of lamina densa to both epithelial cell surface and collagen fibres which are part of the ECM fibrous connective tissue. There are

two types of proteoglycans: hyaluronate - present at the tip of the advancing bud and sulphate-rich glycosaminoglycans (S-GAGs) which are present towards the neck of the bud where ductal morphogenesis takes place [50]. S-GAGs are linear polysaccharides which consist of repeating hexuronic acid and hexosamine and are generally associated with cellular differentiation, tissue stabilisation and collagen fibrillogenesis [92]. The affinity of BM to ECM proteins also differs with the spatial location.

As shown by Williams and Daniel (1983), when TEBs were teased away from the surrounding stroma the anterior part of BM was free of stromal adhesions while the neck region was still attached to ECM fibres and adipocytes. Furthermore, transmission electron microscopy carried out by the same research group, on the TEBs that were surgically removed from fat pad, demonstrated heterogeneity in the thickness of BM and the composition of its associated ECM depending on whether the tip or neck of TEBs was studied. BM at the anterior side was 104nm thick and its associated stromal cells appeared undifferentiated and mesenchyme derived. In contrast, at the neck of TEB, BM consisted of multiple folded layers (14 times thicker) and its associated stromal environment exhibited cytoplasmic specialisation [53]. In the ducts, BM was 130nm thick [53] and synthesised by myoepithelial cells while around TEBs, it was synthesised by cap cells and fibroblasts [93] [50] [94]. Major constituents of BM are Lama1, CollIV, nidogens (Nid) and perlacan (Per) (reviewed in [91]).

The second type of mammary ECM, the fibrous connective tissue, is characterised by the absence of epithelial cells and presence of fibroblasts and immune cells. It is rich in collagen content. Some of its other components include Fn, fibrillar collagens, tenascin-C (Tn), elastin fibres (Eln), Small Leucine-Rich Proteoglycan (SLRP) such as decorin and biglycan type I [95] and Secreted Protein Acidic and Rich in cysteine (SPARC) [95] (reviewed [91]). These proteins are then cross linked via covalent chemical bonds to organise, stabilise and regulate the tension of the ECM scaffold. The cross linking is catalysed by lysyl oxidase (LOX) and tissue transglutaminase 2 (tTG2) [96] [97]. The composition of the fibrous connective ECM also varies depending on its spatial location in the growing mammary gland. It is denser at the neck region of TEBs or around the ducts and looser at the tips of TEBs. ECM interacts with the cytoskeleton of epithelial cells via integrins.

ECM not only anchors the epithelial cells and provides them with physical support, but is also essential for signal transmission between stromal and epithelial cells which is a prerequisite to normal mammary gland development. As demonstrated by Emerman *et al.* (1977), mammary epithelial cells collected from pregnant or lactating glands failed to synthesise milk proteins in response to lactogenic hormones when cultured on a plastic substrate, but did so when cultured on floating collagen membranes [98].

Fibrous connective ECM is also capable of cleaving, binding and sequestering signalling molecules. Some of these molecules that can bind to ECM include: Amphiregulin (Areg), IGF-like binding proteins, TGF- β , Wnts and FGFs. Binding of TGF- β to ECM is facilitated by transglutaminase while growth factors and cytokines bind to ECM through GAGs [99] [50]. GAGs are thought to act as “glue” that enables the attachment of secreted molecules to BM or fibrillar matrix [50]. Most of these molecules are then released and activated as a result of ECM remodelling by enzymes, mostly MMPs (reviewed in [100] [91]). Some molecules, such as TGF- β , however, can be also released from ECM by altering its mechanical tension [101].

1.2.2 Motility in the mouse mammary gland at puberty

1.2.2.1 TEBs

TEBs serve as the driving force of ductal development during puberty. These highly motile structures pattern the open architecture of the mammary gland by driving the linear forward growth and undergoing dichotomous bifurcation, hence giving rise to the major branches of the ductal tree and preferentially directing ductal outgrowth into the epithelium-free fat pad. The motile behaviour of TEBs is dynamic and highly receptive to the surrounding environment. As shown by Hinck and Silberstein (2005), introduction of a plastic obstacle into the fat pad that surrounds advancing ducts alters normal ductal architecture. Not only do the ducts change their migratory path in an attempt to avoid the obstacle, but they still manage to recreate the normal ductal spacing pattern similar to that seen in the unaffected part of the gland [102].

1.2.2.1.1 Forward movement

Motility of TEBs encompasses three behaviours: forward movement, bifurcation and turning. There are two different hypotheses for the mechanism of forward movement. It is suggested that TEBs either pull themselves forward or push forward [102]. The first theory, however, is unlikely as no cellular extensions (filopodia) or actin protrusions (lamelliopodia) which are usually associated with the leading edge of single or groups of collectively migrating cells have been demonstrated on the TEB's surface to date. The second hypothesis, on the other hand, is supported by the electron microscopy demonstration of adipocytes' imprints on the BL that surrounds the tip of advancing TEBs [102]. It is speculated that this forward movement of TEBs results from the increased cell mass, produced by intensive mitosis in both cap and body cells of TEBs [102] [62]. The level of mitotic activity translates into the size of TEBs and depends on the phase of oestrus cycle. The highest mitotic activity of TEB can be seen during the transition from proestrus to late oestrus when TEBs reach their maximum size, acquire an elongated shape and the border between epithelium and surrounding stroma becomes indistinct and straddled by the multiple replicating cells [103] and it is likely that forward outgrowth occurs at this time point. At metoestrus and dioestrus TEBs have a low mitotic index and small size. This shrinkage of TEBs could potentially be attributed to the migration of cells out of the bud to form a new segment of duct [103]. It is also likely that TEBs push forward using the pressure generated during reshaping of the TEB into the dimensions of a duct. This phenomenon takes place at the neck of the TEB and is characterised by the addition of new cells into the subtending ducts, extensive ECM remodelling and Coll deposition at the flanks and neck of the TEB which, taken together create a girdle to contain and direct the pressure and hence contribute to the elongation [53].

The forward movement of TEBs may also result from the unusual composition of its BM. BM surrounding the tip of TEBs is rich in hyaluronan while that enclosing the neck region is associated with collagens [50] [53]. Both the documented association of hyaluronic acid with cell mobility during embryogenesis and the observation that during microdissection or enzymatic digestion the tip of TEB separates much easier from the surrounding stroma than its neck suggest that

hyaluronan may facilitate forward movement by reducing friction and epithelial-stromal adhesion during cellular migration [104] [53].

Recent experiments carried out using 3D Matrigel cultures of mammary epithelial organoids suggested collective cell migration and cellular rearrangements as two possible mechanisms facilitating the forward movement of TEBs [105]. This type of cellular migration has been already described for neuronal precursors in the zebra fish lateral line, epithelial cells during dorsal closure and migrating border cells in *Drosophila melanogaster* [106] [107] [108]. Collective cell migration is characterised by coherent movement of a group of cells where cells at the front show cellular extensions or protrusions projected in the direction of movement. In the cultured TEB-like organoids, however, the leading edge of cells, although lacking cellular protrusions, remained adherent as demonstrated by positive Cdh1 and Cdh3 staining and showed presence of dynamic cellular rearrangements [105]. It must, however, be stressed that organoids *in vitro* are not a good model of TEBs *in vivo*. Thus, it is crucial to develop appropriate *in vitro* models to aid the study of TEBs migration and the first step towards this goal would be to isolate and maintain pubertal mammary glands *in vitro*. During the course of the work for this thesis, pilot experiments were carried out to maintain TEB explants in culture (4.1.2.5).

1.2.2.1.2 Bifurcation

Bifurcation of TEBs is a defining morphogenetic event in the patterning of ductal branching during puberty (**Figure 1-5**). The appearance of a cleft creates an indent in the epithelium which in turn marks the site where the primary branching will occur and from which two new TEBs will elongate. Newly formed TEBs continue to invade stroma and give rise to two subtending primary ducts. The exact mechanism underlying TEB bifurcation, however, has not yet been elucidated.



Figure 1-5 Branching morphogenesis in pubertal mouse mammary gland.

High-magnification carmine alum-stained wholemount (6 weeks) showing a fragment of duct with lateral branches forming (arrow and arrow head) and a bifurcating TEB (asterisk). Scale bar is 200 μ m.

The few existing studies suggest the importance of the BM and ECM composition in driving the process [50] [109]. Silberstein (2001) proposed the formation of a cleft in the distal surface of the TEB to result from highly localised presence of S-GAG and Coll in this region. According to this model, the focal induction of S-GAG in the BM of TEB, followed by the deposition of Coll in the surrounding ECM would retard the growth advancement at the induction point and, on the other hand, promote the directional elongation of newly bifurcated lobes [56].

Further insights into the process of TEB bifurcation were delivered using 3D culture of EpH4. EpH4 cells derive from normal mammary epithelium of a mid-pregnant mouse and when embedded in the cavities of Coll gel and cultured under specified conditions, they form hollow epithelial tubes of defined geometry. Upon the addition of epidermal growth factor (EGF) or HGF, these tubules are able to undergo branching morphogenesis similar to that seen during TEB bifurcation or ductal branching *in vivo*. Parts of these tubules are also shown to express vimentin [110], one of the main markers used to identify a mesenchymal phenotype. In these experiments the sites of vimentin expression were identified by real time imaging of the expression of green fluorescent protein (GFP) under the control of a vimentin promoter. Cells present at subsequent bifurcation/branching sites were shown to acquire an invasive mesenchymal phenotype, suggesting that cells are instructed to branch depending on their spatial location and ability to attain the invasive phenotype. Furthermore, it was also demonstrated that an increase in tubule length resulted in increased magnitude of branching and curved tubules branched preferentially from the convex side of the curve, suggesting that the magnitude and position of bifurcation/branching is dependent on the initial geometry of the tubule. Further analysis revealed that the observed bifurcation/branching did not coincide with increased epithelial proliferation or enhanced signalling by growth factor receptors. The bifurcation/branching position, however, was determined by the concentration gradient of stromal inhibitory morphogens, such as TGF- β , as their concentration was shown to be lowest in the position where bifurcation/branching was induced [110]. Taken together, these results suggest that an epithelial-to-mesenchymal (EMT)-like transition event is required at the branch points for bifurcation/branching to occur and TEB (or duct) geometry,

length and stromal composition are likely to control the position of bifurcation/branching.

EMT can be identified during certain other events that require epithelial remodelling and multilayering, such as embryogenesis, organ development, tissue regeneration and cancer progression and metastasis. It is characterised by a series of biochemical changes that enable polarised epithelial cells which normally interact with BM to acquire a mesenchymal phenotype, consistent with enhanced migratory capacity, invasiveness, increased resistance to apoptosis and elevated production of ECM components. The completion of EMT is marked by ECM degradation and the detachment of the mesenchymal-like cells away from the epithelial cell layer [111].

Epithelial bifurcation is also essential for the formation of lungs, kidneys or salivary glands [112].

1.2.2.1.3 Turning

Another area which has not yet been extensively researched is the mechanism underlying the coordinated, directional turning of TEBs and spatial patterning of ductal branches in response to other approaching epithelial branches. No clear explanation for this phenomenon has been proposed to date. However, the stromal environment surrounding the tips of TEBs may act as a source of chemo-attractants or inhibitors which could govern the direction of the outgrowth. In fact, various guiding molecules such as cytokines (CSF-1 or eotaxin) or axonal guidance proteins (small proline rich protein 1A - Sprr1A, semaphorin 3B - Sema3B or brain abundant membrane attached signal protein - BASP) have been reported in this region [87] [113]. Moreover, when EpH4 cells were cultured on Coll matrices to form epithelial tubules in response to FGF or HGF (See 1.2.2.1.2), an increase in the local concentration of the inhibitor - TGF- β by decreasing the distance between tubules, ceased the growth/branching when the distance between epithelial tubules was $\leq 75\mu\text{m}$ [110]. Although highly speculative, the asymmetric deposition and remodelling of S-GAG and Coll may control the turning of TEB as the extended synthesis and deposition of Coll on one side of the end bud might channel its extension in the opposite direction.

Asymmetric mitosis has also been considered as a potential effector of directional outgrowth. No obvious correlation, however, was observed between mitosis and turning when mitotic patterns were examined [102].

In conclusion, although numerous suggestions have been made to unravel the mechanism underlying the motility of TEBs, in the absence of solid scientific evidence, all these questions still remain to be elucidated.

1.2.2.2 Ducts

Motile behaviour exhibited by ducts at puberty is limited to branching morphogenesis. There are two types of branch-point that form on the ductal scaffold during this time point - secondary (lateral branching) and tertiary branching. The former process is fundamental for epithelial tree formation and occurs throughout the whole of puberty until the entire fat pad is filled with an extensive system of branched ducts. Tertiary branching, on the other hand, takes place after the margins of mammary fat pad are met. It occurs in response to recurrent oestrus cycles and gives rise to a much less pronounced form of epithelial growth - short tertiary branches ending with initial alveolar buds.

Secondary branches originate from primary ducts. The formation of lateral branches can be seen in **Figure 1-5**. Secondary branches most probably bud out from the basal myoepithelial cell layer and while keeping the BM intact invade the surrounding stroma, but the exact mechanism underlying this phenomenon is still to be elucidated [114]. Newly formed secondary branches have end buds which, like TEBs on primary ducts, are characterised by cap cells and smooth-surfaced BM. In this case, the cap cells may form by reverse differentiation of ductal basal myoepithelium, although the lack of scientific evidence means the involvement of other underlying epithelial cells in this process can not be excluded.

The branching mechanism has been shown to be fairly conserved between organs (salivary gland, lung, kidney, pancreas, and mammary glands) and species (*Drosophila Melanogaster*) hence it is likely that, for example, cell migration, cell rearrangement and change of cell shape, as suggested for *D. melanogaster* [115] [116], could be the underlying events of ductal branching in mouse

mammary gland too [112]. It is likely therefore, that the research on branching morphogenesis in other systems may be the key facilitator for its understanding in mammary gland development. Finally, as previously discussed in 1.2.2.1.2 it is suggested that the EMT-like transition event is required at the branch points for branching to occur and the ductal geometry, ductal length and stromal composition are likely to control the position of branching [110].

1.2.3 Regulation of ductal morphogenesis at puberty

Normal pubertal morphogenesis of mouse mammary gland, i.e. ductal outgrowth, branching morphogenesis and patterning of the open architecture of the ductal tree depends fully on the correct regulation of TEB motility, bifurcation and patterning and lateral ductal branching. The nature of these regulatory signals is very complex. For normal pubertal development to occur, both proper communication between the epithelial cells and cross-talk between epithelial and stromal compartments needs to be maintained. Epithelial-epithelial cross-talk encompasses cell-cell interactions within the TEB. The communication between epithelium and stroma, on the other hand, is multifactorial. It occurs through the ECM and encompasses hormonal and local growth factor signalling and other stroma-derived signalling.

1.2.3.1 Epithelial-epithelial communication

Maintenance of cellular integrity within TEB is essential for normal ductal outgrowth. As demonstrated by experiments which disrupt cellular adhesion protein function, e.g. cadherins (Cdh), Netrin-1 (Ntn1) or its receptor Neogenin (Neo1), erythroblastic leukemia viral oncogene homolog 2 (ErbB2) or erythroblastic leukemia viral oncogene homolog 3 (ErbB3), deregulation of cellular communication between epithelial cells compromises ductal elongation [57] [117] [118] [119].

Cadherins

Cadherins are an integral part of adherent junctions and desmosomes which contribute to joining cells together physically. There are at least two types of cadherins expressed in the TEB - E-cadherin and P-cadherin. The former is

expressed by the body cells while the latter is synthesised in the cap cells. As demonstrated by Daniel *et al.* (1995), using slow-release implants containing function blocking antibody surgically inserted ahead of advancing ducts, lack of E-cadherin resulted in significantly disrupted adhesion between body cells. This was followed by an abrupt decline in DNA synthesis and disruption of ductal elongation. The observed phenotype was reversible upon withdrawal of the function blocking antibodies. Similar experiments, designed to ablate the expression of P-cadherin in cap cells resulted in much less disruption of cellular morphology and a much smaller decline in DNA synthesis than following E-cadherin depletion. No aberrant phenotype could be seen, suggesting that although tissue integrity is essential for ductal outgrowth either the modest perturbation in TEB structure can be accommodated or other molecules compensate for the loss of cadherin expression [57].

Netrin 1 and Neogenin 1

Disorganisation of TEB structure and retarded ductal elongation was caused by a homozygous loss-of-function mutation in either *Ntn1* or its receptor, *Neo1*. Although, initially identified as guidance cues for developing neurons, this family of proteins has recently been identified in TEBs at puberty [120] [117]. *Ntn1* was expressed by body cells and secreted to its cell membranes and ECM while *Neo1* was expressed in a complementary pattern by the overlaying cap cells. In TEBs, loss of function of either gene resulted in significantly disrupted adhesion between the cap and body cell layers, followed by the appearance of large spaces below the cap cell region which were filled with dissociated cap cells. Breaks in BM were also seen. However, the rate of DNA synthesis stayed constant. These observations highlight the crucial role of *Ntn1* and *Neo1* signalling in mediating cellular contact between cap and body cells which in turn is essential for maintenance of TEB integrity, but has no obvious effect on the outgrowth of the ductal tree, as suggested by the normal ductal elongation seen in either *Neo1* or *Ntn1* KO^{-/-} mice [117].

Erythroblastic leukemia viral oncogene homolog 2 and 3

Similar loss of adhesion between the cap and body cells of TEB was also demonstrated in mouse mammary gland harbouring homozygous loss-of-function

mutations in either *ErbB2* or *ErbB3* - orphan receptors which form heterodimers with epidermal growth factor receptor (EGFR), ErbB3 and ErbB4 allowing them to respond to EGF- and Nrg1 - like growth factors. In both mice, TEBs were small and disorganised, with exaggerated spaces between the two cellular compartments and ductal elongation was significantly reduced [118] [119]. The *ErbB3* KO^{-/-} mice, however, showed an additional increase in the number of TEBs and lateral branches [119]. Thus, suggesting presence of divergent roles of ErbB2 or ErbB3 in controlling ductal morphogenesis.

1.2.3.2 Epithelial-stromal interactions

The second prerequisite for normal ductal morphogenesis during puberty is an uninterrupted cross-talk between epithelial-stromal compartments. This ability of stromal cells to communicate and signal to the outgrowing epithelium is an underlying mechanism for the morphogenic effect which hormonal and local growth factor signalling and other stroma-derived signals exert on the epithelium.

1.2.3.2.1 *Hormonal control of pubertal mouse mammary gland morphogenesis*

Oestrogen and Progesterone

The two main sex hormones at puberty are oestrogen (E) and progesterone (P). E is produced from androgens during the process of aromatization catalysed by an enzyme called aromatase. Aromatase can be found in many tissues including gonads, brain, adipose tissue, placenta, endometrium skin or bone. There are three major members of the E family: estradiol (E2), estrone and estriol. E2 is the most potent one and is responsible for most E mediated signalling in women [121]. Most of the circulating E2 is produced by the ovaries. Other tissue such as the adrenal cortex, however, can also serve as a minor source. P is the major naturally occurring member of the progesterone family, and like E2, is mainly produced by the ovaries and secondly by the adrenal cortex. During pregnancy the placenta synthesises P. Since both hormones are mainly synthesised in the ovaries the hallmark for their production is the onset of puberty - the time when

the ovaries develop. At puberty, increased production of gonadotrophin-releasing hormone (GnRH) by the hypothalamus stimulates the production of gonadotrophins- luteinising hormone (LH) and follicle stimulating hormone (FSH) in the pituitary gland. The gonadotrophins stimulate pubertal development of ovaries which in turn produce E2 and P. From then onwards levels of both hormones fluctuate depending on the levels of FSH and LH, i.e. the phase of oestrus cycle, causing changes in reproductive organs (vagina, uterus, and mammary glands). The normal oestrus cycle of the laboratory mouse lasts for 4-6 days and it can be divided into four stages (proestrus, oestrus, metoestrus and dioestrus). Together, proestrus and oestrus contribute to the follicular phase while metoestrus and dioestrus constitute the luteal phase. The follicular phase is characterised by an increase in FSH levels which in turn stimulate aromatase production and thus E2 synthesis. Increased E2 suppresses further release of FSH while promoting LH synthesis and hence ovulation. Increased LH stimulates the synthesis of P and luteotrophic hormone (LTH) and initiates the onset of the luteal phase [47]. In return, P decreases the expression of aromatase and thus negatively regulates E2 levels [122]. If mating takes place at this time point, the rising level of LTH activates the corpus luteum which in conjunction with P prepares the uterus to receive the fertilised egg. In the absence of pregnancy, titers of gonadal hormones decrease terminating the luteal phase and allowing reabsorption of the endometrium and succession of a new cycle [47]. Mammary glands, like the uterus and vagina, undergo a series of anabolic and catabolic changes during the oestrus cycle (**See 1.2**).

Since the E2 and P driven onset of puberty parallels TEB formation and ductal morphogenesis of mouse mammary gland, E2 was suggested as the main regulator of this process. The role of E2 in mouse mammary gland development has been studied since 1900 when it was demonstrated that ovariectomy causes cessation of mouse mammary gland development and exogenous E2 can restore it (reviewed in [123]). Classical endocrine ablation-replacement experiments carried out by Lyons (1958) and Nandi (1958) showed that mouse mammary glands underdeveloped due to simultaneous ovariectomy, hypophysectomy and adrenalectomy respond to combined treatment with E2 and growth hormone (GH) by restoring normal ductal morphogenesis. GH on its own induced only mild stimulation and pure E2 none at all [124] [125]. Taken together, these results

established the endocrine basis for ductal outgrowth that stands today. Since then, it has been shown that E2 triggers the development of TEBs, stimulates DNA synthesis in the mammary epithelium (mostly in TEBs) and proliferation of stromal cells [126] [127] [128]. It has also been demonstrated that E2 signals through oestrogen receptor alpha (ER α) and its ablation results in formation of underdeveloped mammary glands comprising a truncated ductal rudiment which lacked TEBs [129]. The rudimentary ductal structure was comparable to that seen in wild type newborn mice. Further autoradiographic experiments, demonstrated that murine mammary ER α localises to mammary epithelium of TEBs and ducts (except for cap cells) and stroma surrounding TEBs. However, co-transplantation of ER α KO^{-/-} embryonic mammary epithelium with wild type stroma showed that stromal not epithelial, ER α is essential for normal ductal elongation as only wild type stroma supported epithelial outgrowth [130] [131] [132]. In contrast, other experiments based on tissue grafts collected from hormone stimulated adult mice indicated that both stromal and epithelial ERs were essential for normal pubertal outgrowth. Most recently, however, a newly engineered ER α KO^{-/-} mouse model showed that ER α expression was not completely ablated in the early ER α KO^{-/-} mouse models and in fact, it is the epithelial rather than stromal ER α that is essential for ductal outgrowth during puberty [133]. Moreover, despite its role in mediating cellular proliferation, most of the proliferating cells lacked ER α expression suggesting a paracrine manner of E2 signalling in which E2 promotes ductal outgrowth by signalling through epithelial ER α to promote proliferation in adjacent cells. EGF and Areg which are a locally produced growth factor are likely to act as the downstream effector of E2 in inducing cellular proliferation, whereas TGF- β could be responsible for the proliferative quiescence of ER α expressing cells (See 1.2.3.2.2) [134]. In 1996, a second oestrogen receptor, ER β was identified. Although to a much lesser extent, ER β was also expressed in the pubertal mouse mammary. Its ablation (ER β KO^{-/-} mice), however, did not alter normal pubertal outgrowth, suggesting that it is dispensable for pubertal mouse mammary gland development. Double KO, ER α / β KO^{-/-} mice showed a mammary phenotype which was similar to that seen for ER α mice [131].

In contrast to E2, P is mainly declared as non essential for pubertal mouse mammary development. More recent evidence showed that P orchestrates

morphological changes associated with both pre-pregnancy where it is involved in preparation of the uterus for egg implantation after fertilization, and pregnancy when it is essential for maintaining the placenta and inhibition of uterine contractility [47]. In the mammary gland, the action of P is mediated through PR. There are two isoforms of PR in mammary gland: PR-A and PR-B. PRs localise to both epithelium and stroma. Selective PR-A $KO^{-/-}$, PR-B $KO^{-/-}$ mice and general PR $KO^{-/-}$ mice show that the exclusive interaction of P with stromally localised PR-B regulates tertiary side branching in virgin mice and lobuloalveolar development in pregnant mice [135] [136] [137] [138]. Evidence for a role of P in proliferation, however, is not straightforward. Administration of P to ovariectomised mice increases DNA synthesis in epithelial cells of TEBs and ducts which suggests P may play an intermediate role in regulating pubertal morphogenesis, possibly by mediating DNA synthesis [139]. However, since E2 promotes the expression of PR-A, the regulation of this mitogenic effect would have to be PR independent [140]. Furthermore, when administered with IGF-1 to ovariectomised IGF-1 $KO^{-/-}$ mice, P enhances the action of IGF-1 and promotes ductal outgrowth during puberty by producing duct extension and branching equivalent to that seen with IGF-1 plus E2, but without an increase in the number of TEBs (See 1.2.3.2.2). No such effect on the ductal epithelium can be noted with P or IGF-1 acting independently [141]. This finding may explain the very rapid epithelial outgrowth during puberty when oestrus cycle P and E2 acting together with IGF-1 could stimulate this outgrowth.

Glucocorticoid

Other systemic hormones such as glucocorticoids (G), GH or parathyroid hormone (PTH) have also been implicated in pubertal mouse mammary development. Glucocorticoids are adrenal hormones which were initially described as essential for inducing the expression of milk proteins during lactation [142]. They function by binding to glucocorticoid receptors (GRs) and stimulate target gene transcription either by direct binding to DNA or by protein-protein interactions. GR $KO^{-/-}$ results in postnatal lethality as mice die shortly after birth due to respiratory failure [143]. Further experiments, demonstrated that the GR $KO^{-/-}$ anlagen can be rescued from these mice when transplanted into the cleared fat pad of wild type mice where it produces abnormal mouse mammary glands, characterised by multiple layers of luminal epithelial cells along some of the

ducts, increased periductal stroma and a much higher rate of ductal outgrowth than that seen in the wild type epithelium. Furthermore, mice which were genetically engineered to express a mutated form of GR that lacked the ability to bind DNA but maintained the receptor-protein binding function, also exhibited reduced side branching and the presence of some TEBs in the adult gland [144]. Together these results provide strong evidence for the role of G signalling, through GR, in regulating normal mouse mammary gland morphogenesis at puberty [145].

Growth hormone

GH is a pituitary hormone which binds to growth hormone receptors (GHRs) expressed in both epithelial and stromal compartments of virgin mouse mammary glands [146]. Research devoted to understanding the role of GH in pubertal mammary morphogenesis dates back to the early 1990s. In 1993 it was demonstrated that the implantation of GH release pellets into pubertal mammary glands of E2 treated hypophysectomised, ovariectomised rats stimulated an increase in TEB number [147]. Since the exogenous E2 alone failed to rescue this pubertal phenotype it was hypothesised that the GH driven phenotype arose independently of E2 signalling [148]. The importance of GH for normal pubertal mouse mammary gland development was further elucidated using GHR KO^{-/-} mice. Loss of GHR produces severe retardation of ductal outgrowth and side branching impairment. Furthermore, tissue recombination experiments, in which GHR KO^{-/-} epithelium was grafted into the cleared fat pads of wild type mice revealed that epithelial GHR is dispensable for normal pubertal morphogenesis [149]. These findings suggest that GH in conjunction with stromal GHR acts independently or synergistically with E2 and is necessary for the regulation of normal pubertal mouse mammary gland morphogenesis. In fact, GH is now considered as the second most important driver of pubertal morphogenesis after E2.

Parathyroid hormone

Although initially associated with mammary gland embryogenesis both PTH and PTHrP are implicated in pubertal mouse mammary gland development. PTH is secreted by the parathyroid gland while PTHrP is produced by numerous adult

and embryonic tissues including mammary glands where PTHrP expression is concentrated in the cap cells of TEBs and myoepithelial cells. The cognate receptors are located in the surrounding stroma which suggests paracrine signalling is important. In 1995 mice over-expressing either PTH or PTHrP under the control of a *Krt14* promoter showed severe impairment of ductal elongation and branching at puberty [150]. More recently mice engineered to over-express PTHrP under the control of a *Krt14* promoter in a tetracycline-regulated manner showed that this phenotype depended on the timing of PTHrP over-expression. When transiently over-expressed in prenatal mice, PTHrP impaired branching whereas the decreased rate of ductal elongation was seen exclusively in response to PTHrP over-expression at puberty. In addition, the defect in ductal elongation was associated with a failure to decrease apoptosis of epithelial cells in TEB and increase the proliferation in response to E2 and P [151]. Unfortunately the PTHrP KO^{-/-} mouse model failed to provide further insights into the impact of PTHrP on pubertal morphogenesis due to its embryonic lethality [22].

Vitamin D

Although, endocrine glands determine the hormonal milieu for pubertal mouse mammary gland development additional systemic factors such as vitamin D3 are also involved in the orchestration of this process. Vitamin D3 can be either produced in skin of vertebrates after the exposure to ultraviolet B (UVB) light from the sun or artificial sources or occurs naturally in a small range of food (fatty fish, eggs, meat). Upon ingestion, vitamin D3 gets converted to its hormonally active form - 1,25- dihydroxyvitamin D3 (calcitriol) which interacts with the vitamin D3 receptor (VDR). VDR is a nuclear steroid hormone receptor which localises to pubertal stroma and epithelium of TEBs and subtending ducts. The expression of VDR in TEBs is much higher in mitotically quiescent than proliferating cells. VDR KO^{-/-} mice display enhanced development of mammary glands during puberty after supplementation with dietary Ca²⁺ to regulate fertility, serum E2 and neonatal growth. This pubertal phenotype is characterised by extensive ductal elongation and branching and an increase in the number of TEBs. Further growth enhancement is seen on exposure of VDR KO^{-/-} mice to ovarian hormones *in vivo* or during whole mammary gland organ culture [152]. Collectively, these results suggest that vitamin D3 signals through

VDR to oppose E2 driven proliferation and to maintain cellular differentiation, hence participating in negative regulation of pubertal outgrowth of mouse mammary gland [153].

1.2.3.2.2 Local growth control of pubertal mouse mammary gland development

Although systemic hormones play a central role in pubertal mouse mammary gland morphogenesis (See 1.2.3.2.1) this observation was challenged by the discovery that proliferating cells in TEBs and ducts are in fact those that lack expression of steroid hormone receptors and that the receptor-expressing cells are often those adjacent to these cells. This suggested that systemic hormones regulate cellular proliferation in a paracrine manner using local mediators. Since some of the locally produced growth factors were able to mediate the effect of some of the hormones, they were thought to play the role of local mediators of hormone signalling. Further evidence for this was that the expression of these growth factors could rescue several of the mammary phenotypes seen in the steroid mouse models while their ablation produced mammary phenotypes that were similar to these seen in steroid mouse models. Since then, mammary gland growth factors that signal via their receptors have been demonstrated to play a pivotal role in pubertal mouse mammary gland morphogenesis by acting both as a part of and independently of systemic hormone signalling.

There are four main families of growth factors and their receptors that regulate pubertal mouse mammary gland development. These include: FGFs and FGF receptors (FGFRs); HGF and its receptor - met proto-oncogene (*c-Met*); IGFs and IGF receptors (IGFRs) and EGF-related proteins and their EGFRs (also called ErbB family of proteins and ErbB receptors). All of these receptors belong to the receptor tyrosine kinase superfamily (reviewed in [154]).

Fibroblast growth factors

The FGF ligand family consists of 18 members. These can be further subdivided into six subfamilies called FGF1, FGF4, FGF7, FGF8, FGF9 and FGF19. Each FGF ligand binds to a specific FGFR. The receptors are encoded by four different

genes which are alternatively spliced to produce at least seven FGFRs (reviewed in [154]). Initially, FGFs and FGFRs were established as critical during mouse mammary gland embryogenesis (See 1.1.1). Subsequent research, however, revealed that FGF1, FGF2, FGF4, FGF7 and FGF10 as well as receptors FGFR1 and FGFR2 were also expressed in mouse mammary gland during puberty (reviewed in [155]). Conditional over-expression of FGF3 in the mouse mammary epithelium during puberty resulted in cessation of ductal elongation. Ductal epithelium was expanded, multilayered and full of cysts (severe epithelial hyperplasia). The phenotype was proposed to arise from the imbalance between mitogenic and apoptotic signals [156]. The pubertal phenotype of mammary glands lacking FGF3 (FGF3 KO^{-/-} mice), however, has not yet been elucidated due to the severe lethality of these mice [157].

Other members of the family have also been shown, mainly through genetically engineered mice, to have impact on mammary development. Mice over-expressing FGF4 under the control of the WAP promoter which initiates WAP-FGF4 expression at the onset of puberty (~ 4 weeks) showed decreased apoptosis within TEBs which in turn led to the inhibition of ductal elongation after a week of FGF4 expression. TEBs were present in normal numbers but exhibited impaired morphology. The decrease in apoptotic index was attributed to the increase in Bcl2 which serves as an anti-apoptotic factor [158]. More recently, Parsa *et al.* (2008) demonstrated high expression of FGF10 and its receptor FGFR2IIIb in the stroma and epithelium of pubertal mouse mammary gland respectively. Induced, by using a transactivator/tetracycline promoter (mice homozygous for FGFR null allele die at midgestation), reduction of pubertal FGFR2IIIb triggered a 40% reduction in ductal outgrowth compared to wild type controls and complete loss of TEBs. The phenotype was reversible upon removal of doxycycline [159]. A related study, based on the novel mosaic mouse model for FGFR2IIIb expression, confirmed expression of FGFR2IIIb in TEB and duct epithelium and was first to identify the advancing tip of TEB as a main site of epithelial FGFR2IIIb expression whilst demonstrating its lack of function in mature ducts. In TEBs, the FGFR2IIIb null cells were at a competitive disadvantage to their heterozygous counterparts showing decreased cellular proliferation followed by growth retardation, whereas null cells present in the duct did not alter their cellular activity [160].

FGF ligands and their receptors regulate tracheal branching in *Drosophila melanogaster* and lung sac development in mice. As seen in *Drosophila* mutants *breathless* (encodes *FGFR* homologue) and *branchless* (encodes *FGF* homologue), alteration of either of these genes results in complete ablation of tracheal branching. Similarly, the ablation of *FGF10* in mice (*FGF10* KO^{-/-} mice) strikingly inhibits branching in the lung, demonstrating the critical role of this growth factor in the bifurcation of buds during lung morphogenesis [161]. The signalling mechanism of bifurcation in the mammary gland has not been yet elucidated, however, since primary branching shows evolutionary conservation between species it is likely that FGF ligands and receptors take part in TEB bifurcation.

Hepatocyte growth factor

HGF (also known as scatter factor) and its receptor c-Met are also expressed and regulated during pubertal morphogenesis of mouse mammary gland. HGF is expressed by mesenchymal cells while c-Met is produced by the epithelium [162]. KO of either HGF or c-Met have not been studied due to their prenatal lethality resulting from liver and placental defects. Insight into the role of HGF in pubertal morphogenesis, however, has been gained using mammary gland organ culture, cell culture and transplantation experiments. In organ culture, branching morphogenesis of ductal epithelium was promoted on addition of exogenous HGF, but abolished when antisense nucleotides which blocked endogenous HGF expression were used [162]. In transplant experiments where retrovirally infected epithelial cells were transplanted into clear fat pads, the over-expression of HGF in the mammary gland epithelium resulted in an increase in the size of TEBs and the number of ductal branch points compared to controls [163]. Furthermore, HGF was also able to promote proliferation of epithelial cells and production of tubular/ductal morphology when epithelial cells, co-cultured with mammary fibroblasts or supplemented with fibroblast conditioned medium were grown in collagen gels using a minimally supplemented serum-free medium. Treatment of epithelial cultures with HGF neutralizing antibody reversed this morphogenic effect. Treatment of mammary fibroblasts with E2 increased the production of HGF [164] and more recently, it was demonstrated that together HGF and EGF act synergistically to enhance proliferation, scatter and invasion of HC11 cells (non-tumourigenic mammary epithelial cells) in culture [165]. Thus HGF is capable of regulating pubertal mammary gland

development by acting downstream from E2 and potentially cooperating with EGF to mediate cellular proliferation.

Insulin like growth factor 1

IGF-1 is a local mediator of GH signalling. GH increased *IGF-1* mRNA levels within the mammary glands of hypophysectomised rats [166] and this effect was further enhanced by the presence of E2 [167]. Given the pivotal role of GH in pubertal mouse mammary gland morphogenesis, it was not surprising that IGF-1 also emerged as an important player in pubertal development. In fact, IGF-1 signalling was demonstrated to be potent enough to substitute for GH and mimic GH-induced mammary morphogenesis [167].

Early studies of IGF-1 function, carried out using hypophysectomised, castrated, sexually immature male rats, demonstrated that when administered with E2, IGF-1 induced development of TEBs [168]. On its own, IGF-1 exhibited a smaller although still significant effect on pubertal mouse mammary gland morphogenesis. With E2, however, the morphogenic effect of IGF-1 was significantly enhanced and similar to that seen when E2 and GH were administered [167]. More recently, IGF-1 was shown to be expressed in the epithelium and stroma of the pubertal mouse mammary gland [169]. Loss of IGF-1 expression (IGF-1 KO^{-/-} mice) was associated with impaired TEB development and limited ductal outgrowth with fewer branches than wild type controls. This phenotype was reversible upon administration of exogenous IGF-1 or IGF-1 with E2. No stimulatory effect was seen, however, when a combination of GH and E2 was administered to mice, indicating that the morphogenic effect of GH is fully mediated by IGF-1 [170]. Similarly, embryonic mammary buds rescued from prenatally lethal IGF-1R KO^{-/-} mice and grafted into cleared fat pads of wild type hosts, showed limited ductal branching and decreased size, number and proliferative index of TEBs [171]. IGF-1 also permits the morphogenic action of P in the mammary gland (See 1.2.3.2.1). In addition, the reduction in ductal branching, but not elongation seen in IGF-1R KO^{-/-} mice means it is likely IGF-1 may play a role in governing TEB bifurcation. This hypothesis, however, is still to be proven. Collectively, these studies suggest that IGF-1 in conjunction with IGF-1R acts downstream of GH and when administered with E2 is responsible for TEB formation and ductal morphogenesis during pubertal mouse mammary gland

development. Furthermore, IGF-1 acting independently of E2 can promote pubertal morphogenesis to some extent, but as for GH, E2 is required for a full effect.

EGF-related ligands and receptors

There are four types of EGF receptors: EGFR, ErbB2, ErbB3 and ErbB4. Peptides in the EGF family are produced as transmembrane precursors that, upon cleavage, bind and activate EGF receptors. Some of the proteases that are known to facilitate this cleavage include A Disintegrin and Metalloprotease (ADAM) and MMP families [172] [173]. EGF-like ligands are characterised by the presence of a six-cysteine residue motif, the EGF domain, and depending on their receptor specificity can be divided into three groups. Group one binds EGFR and consists of: EGF, Areg, TGF- α and epigen (EPG); group two binds either EGFR or ErbB4 and consists of betacellulin (BTC), heparin-binding EGF (HB-EGF) and epiregulin (EPR) while the third group binds ErbB3 or ErbB4 - Nrg-1 and Nrg-2 or just ErbB4 - Nrg-3 and Nrg-4 [174]. Some of these EGF-family ligands (EGF and Areg) and ErbB receptors - (EGFR and ErbB2) are expressed in and are essential for normal pubertal mouse mammary development.

The EGFR is strongly expressed in the epithelium and adjacent stroma of TEBs. Some expression is also noted in ductal myoepithelium and its surrounding stroma [175]. As demonstrated in *waved-2* mutant mice which express a truncated form of EGFR (lacks the functional tyrosine kinase domain) under the control of a mammary gland specific promoter (the mouse mammary tumour virus (MMTV) promoter), impairment of EGFR leads to a significant inhibition of ductal morphogenesis with reduced outgrowth and branching [176]. A similar phenotype was also seen with complete EGFR loss. Since EGFR KO^{-/-} mice are not viable, their mammary glands have to be transplanted into a wild type host to study epithelial morphogenesis. EGFR null mammary glands show severe cessation of ductal outgrowth but when transplanted into the wild type stroma, the pubertal phenotype of EGFR KO epithelium can be rescued. However, this is not true for reciprocal experiments. Thus, it was suggested that signalling through stromal EGFR is critical for normal pubertal ductal morphogenesis while the epithelial EGFR is not essential for this process [177].

The importance of EGFR signalling was further highlighted when EGF-like ligands (EGF and Areg) were shown to be capable of promoting ductal outgrowth at puberty and to act as a downstream effector of E2 signalling. Coleman *et al.* (1988) showed that the administration of EGF rescued the mammary gland phenotype seen in ovariectomised mice. The delivery of EGF via slow-release pellets stimulated formation of new TEBs, restored normal TEB histomorphology and the reappearance of cap cells, reinitiated DNA synthesis in epithelial cells and led to an increase in ductal diameter [175]. In contrast, a neutralising antibody to EGF inhibited the stimulatory effect of E2 on TEBs [178] suggesting mitogenic and morphogenic properties of EGF, an ability to substitute for E2 and serve as a downstream effector of E2 signalling in mouse mammary gland.

The most profound defect in pubertal ductal morphogenesis has been seen in Areg KO^{-/-} mouse mammary glands. Targeted loss of Areg resulted in stunted ductal outgrowth, but the formation, shape and morphology of TEBs in Areg KO^{-/-} glands remained unaffected. In contrast, implantation of Areg-secreting pellets, promoted ductal outgrowth in the pubertal mouse mammary gland [179]. When compared with other EGF-like ligands, Areg exhibited the highest pubertal expression. In the mammary gland, Areg expression is mainly associated with the epithelium of advancing TEBs but lower expression, can be also demonstrated in the ductal epithelium and its surrounding stroma [180]. In ovariectomised mice, Areg expression becomes strongly up-regulated after E2 treatment. The lack of Areg expression in ER α KO^{-/-} mammary glands demonstrated that the induction of Areg occurred through the ER α . Furthermore, as Areg KO^{-/-} epithelium engrafted into the cleared fat pad of the wild type host failed to rescue ductal outgrowth it was concluded that epithelial Areg expression is required to induce proliferation of mammary epithelium. Further research on mice containing mammary epithelium that was mosaic for wild type and Areg KO^{-/-} cells, revealed that when in close vicinity to wild type cells, Areg KO^{-/-} cells were able to proliferate and contribute to ductal outgrowth, suggesting a paracrine mechanism of Areg signalling [181]. Areg, like other EGF-like ligands is expressed as an inactive precursor which must be shed from the cell surface. *In vitro* cleavage of Areg by ADAM17 has been previously demonstrated [182]. *In vivo*, unprocessed Areg was found in the mammary glands obtained from ADAM17 KO^{-/-} mice, showing ADAM17 also mediates the cleavage of Areg in mammary glands

and its absence leads to a pubertal phenotype which is similar to that seen in *Areg* KO^{-/-} mice [183]. Collectively these data suggest that *Areg* acts downstream of E2 in the epithelial compartment, where it is released by ADAM17 to act in a paracrine manner on stromal EGFR to promote normal ductal morphogenesis at puberty.

The role of ErbB2 in pubertal mouse mammary gland development has already been mentioned since a loss-of-function mutation in *ErbB2* affects cell-cell adhesion causing severe alteration in TEB morphology and a delay in ductal outgrowth (See 1.2.3.1) [118]. Similarly, mammary-specific ablation of ErbB2 through MMTV-Cre-mediated recombination resulted in a defect in ductal elongation and reduced branching [184]. In order to respond to growth factors, ErbB2 has to form a heterodimer with EGFR, ErbB3 or ErbB4. The pivotal role of EGFR in pubertal morphogenesis has already been described. Furthermore, ErbB3 has also been demonstrated to be crucial for ductal outgrowth during puberty. When transplanted to the fat pads of wild type hosts, embryonic mammary buds of ErbB3 KO^{-/-} mice showed increased impaired ductal elongation and increase in the number TEB and lateral branches [119]. ErbB4, on the other hand, exerts pro-differentiation and anti-proliferative effects on mammary epithelium [185]. Its expression is lowest during periods of epithelial outgrowth, such as puberty (reviewed in [186]) and its loss (*ErbB4* KO^{-/-} mice) does not impact ductal morphogenesis at puberty [187].

1.2.3.2.3 Transcriptional control of pubertal mouse mammary gland development

Correct transcriptional regulation of gene expression is a very important prerequisite of normal organ, tissue or cell morphogenesis. Since systemic hormones are pivotal in regulating pubertal mouse mammary gland morphogenesis the main group of associated transcription factors are nuclear hormone receptors, such as ER, PR, GR and VDR. Each of these receptors utilises a common mechanism of action. Classically, upon activation by the hormonal ligand, nuclear hormone receptors undergo a conformational change and working in synergy with specific co-activators and co-repressors bind to the hormone response element of a gene and so regulate its transcription. In some cases,

however, other non-genomic mechanisms of action can be used. Specific co-activators can exert their function on particular downstream target genes of the individual receptor to determine a specific response to the hormone [188].

Steroid receptor co-activator family

SRC-1 and SRC-3 belong to the steroid-receptor co-activator (SRC) family and illustrate how these unique tissue specific responses to hormones occur. SRC proteins function as co-factors for steroid hormone receptors such as P, E2 and thyroid hormone receptor. SRC-1 KO^{-/-} mice exhibited reduced ductal branching and ductal outgrowth at puberty. Their ability to respond to E2 or P treatment was also impaired compared to their wild type counterparts [189]. Similar cessation of ductal outgrowth was also seen in SRC-3 deficient (SRC-3 KO^{-/-}) mouse mammary glands. In this case, however, the observed mammary phenotype was secondary to other associated defects, such as dwarfism, delayed puberty and reduced female reproductive function, since the E2 treatment rescued the mammary phenotype but not the other observed defects [190]. More recently, bigenic PRAI-SRC-1 KO^{-/-} and PRAI-SRC-3 KO^{-/-} mice were generated to compare the role of SRC family members on PR activity in the mammary gland and uterus by crossing PR activity indicator (PRAI) mice with SRC-1 KO^{-/-} or SRC-3 KO^{-/-} mice. PRAI was linked to GFP to monitor its activity. Loss of SRC-1 impaired the E2- and P-induced activation of PR in the uterus but not in mammary glands. In contrast ablation of SRC-3 impaired the activation of PR by E2 and P in the mammary gland but not in the uterus. Together, these results reveal SRC-3 as a primary co-activator of PR in the mammary gland and show SRC-1 to be its primary co-activator in uterus [191]. The absence of a pubertal mammary phenotype in SRC-3 KO^{-/-} mice can be explained by the minimal role that PR plays in pubertal mouse mammary gland development. The distinct pubertal mammary phenotype in SRC-1 mice, on the other hand, is probably due to the requirement for SRC-1 in ER activation and function. Furthermore, SRC-2 appears to be an indispensable co-regulator of both uterine and mammary gland responses to P as demonstrated by a mouse model in which SRC-2 function is abrogated only in PR expressing cells. The absence of SRC-2 in uterus impaired embryo implantation while lack of SRC-2 in mammary gland resulted in defective branching morphogenesis [192].

Cbp/p300 -interacting transactivator with Glu/Asp-rich carboxy-terminal domain

1

Another co-activator of ER that is crucial for pubertal mouse mammary gland development is the Cbp/p300 - interacting transactivator with Glu/Asp-rich carboxy-terminal domain 1 (CITED1). Loss of CITED1 (CITED1 KO^{-/-} mice) in mammary glands caused reduced ductal outgrowth and aberrant ductal patterning. Ducts appeared dilated and spatial patterning of subtending branches was lost [193]. This phenotype probably arose due to altered transcription of some ER target genes, such as Areg, EGFR/ErbB2 or stanniocalcin 2 (Stc2). Synergistic interaction between these two proteins during pubertal mouse mammary gland morphogenesis is supported by the observation that both CITED1 and ER α localise to the same mammary epithelial cells [194].

The activator protein 1

The activator protein 1 (AP-1) is also involved in E2 signalling at puberty either acting as a co-regulator for ER or as a downstream target. AP-1 is a transcription factor composed of dimers of the oncogenes Jun (cJun), FBJ osteosarcoma (Fos) or other factors such as activating transcription factor (ATF) proteins. Early experiments targeting cJun in AP-1 KO^{-/-} mice resulted in their embryonic lethality so mammary gland development was not examined in these mice. More recently, a bi-transgenic mouse model, has been generated, expressing an inducible AP-1 inhibitor (Tam67) under the control of the MMTV promoter such that AP-1 could be inhibited in a controlled manner. If inhibited at puberty, AP-1 deficiency resulted in reduced size of the ductal tree by decreasing cellular proliferation but increasing apoptosis which reflected onto pubertal morphogenesis by suppressing primary ductal branching and decreasing TEB formation. Inhibition of AP-1 also suppressed the expression of both AP-1 dependent genes, such as vimentin, fibronectin or TIMP-1 and AP-1 dependent growth regulatory genes (cyclin D1 and c-myc) and reduced the ability of the mammary gland to respond to E2 and P treatment [195].

Mediator complex subunit 1

Mediator complex subunit 1 (MED1) is another co-activator of nuclear hormone receptors. It may act as a main bridge for direct communication between the transcriptional activator and general transcription machinery (especially RNA Polymerase II) and facilitate nuclear receptor-mediated gene transcription [196]. The interaction between receptor and MED1 is mediated through the LxxLL motif that is present in MED1. In MED1 LxxLL motif mutant knockin mice, disruption of the LxxLL motif resulted in severe defects in pubertal mouse mammary gland development manifested by decreased ductal outgrowth and side branching and decreased cellular proliferation. Furthermore, aberration of normal LxxLL function down-regulated the expression of ER α -regulated genes (cyclin D1, PR) and, as seen in AP-1 KO^{-/-} mice, reduced the ability of the mammary gland to respond to E2 stimulation and diminished E2-regulated ductal outgrowth. Together, these results show that MED1 is important for pubertal mouse mammary gland morphogenesis. Loss of its function decreased cellular proliferation and down-regulated E2 signalling, both of which resulted in delayed development of the mammary tree at puberty [197].

Metastasis-associated protein 1

Metastasis-associated protein 1 (MTA1) is an ER co-modulator which causes inappropriate mammary gland development if deregulated during puberty. Transgenic mice over-expressing MTA1 under the control of the MMTV promoter displayed increased proliferation of ductal epithelium leading to extensive side branching and precocious differentiation of mammary glands. The mammary glands of these pubertal transgenic mice strongly resembled those in wild type mid-pregnant mice. A similar phenotype could also be seen in mammary glands collected from ovariectomised female mice, suggesting that an E2-independent mechanism might cause these morphological changes. MTA1 over-expression also deregulated pubertal β -casein, β -catenin and cyclin D1 expression, decreased PR-B expression and increased PR-A expression [198].

CCAAT-enhancer binding proteins

CCAAT-enhancer binding proteins (C/EBPs) belong to the family of leucine zipper DNA binding transcription factors. There are six members, called C/EBP α to C/EBP ζ which promote the expression of certain genes by interaction with the CCAAT box motif on their promoter. C/EBP α , C/EBP β and C/EBP δ are differentially expressed in mouse mammary gland (reviewed in [199]) but only C/EBP β , to date, is important for pubertal mammary morphogenesis. C/EBP β KO^{-/-} mice showed disrupted ductal morphogenesis that was characterised by reduced outgrowth and branching [200]. This disruption persisted until adulthood, when enlarged ducts and a reduced number of side branches could be noted [201]. In tissue transplantation experiments, a pubertal phenotype arose mostly due to the absence of C/EBP β in the mammary epithelium, although partly induced by an ovarian defect. When wild type epithelium was grafted into the empty fat pad of C/EBP β KO^{-/-} mice normal mammary epithelial outgrowth was seen. In contrast, C/EBP β KO^{-/-} epithelium grafted into the empty fat pad of a wild type host failed to develop. The mechanism by which C/EBP β regulates pubertal ductal morphogenesis has yet to be elucidated. However, since E2 partially rescues the pubertal phenotype, C/EBP β may act downstream of hormone signalling cascades and compromised E2 signalling may be partially responsible for the observed pubertal phenotype [200].

GATA binding protein 3

GATA-3 is one of the six highly conserved transcription factors that belong to the GATA family. In mammary gland morphogenesis, GATA-3 expression marks the formation of the embryonic placode, which makes it the earliest transcription factor that is expressed. Its expression persists throughout the whole of mammary development. At puberty, GATA-3 is the most highly expressed transcription factor in the mammary epithelium, where it localises to the ductal luminal cells and the body cells of TEBs. Conditional deletion of GATA-3 impaired TEB formation and hence severely compromised ductal morphogenesis. Furthermore, its prolonged loss led to large numbers of undifferentiated luminal cells and compromised cellular attachment to the BM which in the long term led to caspase-activated cell death [202]. GATA-3 is therefore important for normal

mouse mammary gland development by maintaining differentiation of luminal epithelial cells.

Activating enhancer binding protein 2 gamma

Another transcription factor pivotal for normal mouse mammary gland development at puberty is the activating enhancer binding protein 2 gamma (AP-2 γ). AP-2 γ regulates gene expression during embryogenesis. In the mammary gland, AP-2 γ localises to cap and body cells of TEB. Mice lacking AP-2 γ (AP-2 γ KO^{-/-} mice) displayed reduced proliferation within the cells of TEB leading to impaired ductal branching and elongation. Although these mice expressed ER, normal mammary development could not be restored by adding of exogenous E2, suggesting AP-2 γ may regulate ductal outgrowth by acting downstream of ovarian hormones [203].

1.2.3.2.4 Immune response cells and cytokines in the regulation of pubertal mammary gland development

Although, it has been comprehensively documented that the combined activities of stroma/epithelium expressed systemic hormones and locally acting growth factors are pivotal for normal mammary epithelial morphogenesis at puberty, a number of mouse models with uncompromised hormonal signalling have still demonstrated abnormalities in pubertal mammary morphology. This suggests that other molecular players may be involved in normal mammary gland morphogenesis.

Both positive and negative signalling is crucial for regulating epithelial outgrowth and maintenance of ductal tree open architecture. The growth-promoting signalling factors within pubertal mouse mammary gland development have been well researched and the key players have been described in this section. In contrast, the mechanisms by which mammary epithelial outgrowth ceases, as a response to ductal patterning or reaching the end of the fat pad, are much less clear. To date, the best candidate for an inhibitory factor that regulates epithelial outgrowth at puberty and consequently ductal patterning is TGF- β .

Transforming growth factor beta family

TGF- β proteins belong to the superfamily of multifunctional secreted cytokines that comprises TGF- β (TGF- β 1, TGF- β 2 and TGF- β 3), BMPs, activins, inhibins, nodals, myostatin and others [204]. Members of the TGF- β superfamily signal through their heteromeric type I and type II serine/threonine kinase receptors. TGF- β binding to the type II receptor results in the recruitment of a type I receptor to the complex. The receptor type II further facilitates phosphorylation of the receptor type I on the serine and threonine residues which results in its activation and hence initiation of signalling to the downstream components of the pathway, mainly Sma/Mad-related (Smad) proteins. Several copies of Smads aggregate to form complexes which translocate to the nucleus to regulate gene transcription [205]. TGF- β mediated cellular processes are very diverse and include: cell division, differentiation, proliferation, migration, adhesion, morphogenesis and programmed cell death. Five of the TGF- β family members: TGF- β transcripts, inhibins, activins, nodal and BMPs are expressed in the mammary gland.

Transforming growth factor beta

TGF- β transcripts show overlapping expression within epithelium of TEBs and ducts. TGF- β 1 and TGF- β 3 mostly localise to body cells of TEBs and luminal and myoepithelial cells of ducts with higher TGF- β levels in the former than the latter. Some TGF- β 3 expression further associates with cap cells and myoepithelial cells while the additional expression of TGF- β 1 can be also denoted in stroma that surrounds epithelium, where it forms a complex with ECM around ducts that are rather growth quiescent at puberty (in contrast to TEBs). TGF- β 2 expression although weak is detectable over both the epithelial and stromal compartments of pubertal mammary gland. In contrast, no TGF- β peptides could be seen in the stroma at the front of advancing TEBs [206]. In fact, TEBs were shown to regress upon the administration of TGF- β 1, TGF- β 2 or TGF- β 3 releasing pellets. The growth inhibited mammary epithelium was histologically normal and the inhibitory effect was fully reversible [206] [207]. The administration of exogenous TGF- β 1, however, had an impact on the morphology of stroma surrounding the tip of TEBs. As demonstrated by Silberstein G. B. et al. (1990), an epithelium-dependent fibrous connective

tissue cap, that consisted of S-GAGs, Coll and chondroitin sulfate which was indistinguishable from that seen on the flanks of TEBs and ducts was identified in front of the manipulated TEBs [208].

A marked suppression of TEB outgrowth and lateral branching resulting in the impairment of normal ductal patterning and duct hypoplasia has also been demonstrated in mouse models engineered to over-express TGF- β 1, using simian TGF- β 1 mutated to produce a constitutively active product under the control of the MMTV promoter/enhancer [209]. The inhibitory effect of TGF- β on mammary epithelium was further confirmed when endogenous TGF- β levels in mammary gland were manipulated. Mice carrying a function-ablating dominant-negative mutation in TGF- β receptor type II, expressed under the control of a metallothionein-derived promoter, showed a dramatic increase in lateral branching of ductal epithelium that overrode normal ductal spacing. Furthermore, TGF- β receptor type II localised to stroma, suggesting a paracrine manner of TGF- β signalling [210]. In contrast, a decrease of TGF- β 1 expression, in TGF- β 1 KO^{+/-} mice, which expressed only 10-30 % of TGF- β 1 protein levels, caused accelerated ductal development and cellular proliferation at puberty. Tissue transplantation experiments showed this TGF- β 1-deficient phenotype was intrinsic to the epithelium. Further analysis, based on the use of antibodies raised against the latent (active) form of TGF- β 1 revealed that TGF- β 1 expression in these mice was modulated by the oestrus cycle. Together with the increased epithelial proliferation seen on administration of E2 and P to ovariectomised TGF- β 1 KO^{+/-} mice, this suggested a role for ovarian hormones in the expression of TGF- β 1 which in turn regulates the proliferative response to hormones [211].

Investigation of the effect of complete loss of TGF- β 1 on pubertal mammary gland morphogenesis has been difficult due to the early lethality of TGF- β 1 KO^{-/-} mice which die from a gross inflammatory response before reaching 3 weeks of age [212]. Recently, however, this pathological phenotype has been rescued by immunocompromising the mice. TGF- β 1 KO^{-/-} mice exhibited fairly normal ductal outgrowth at puberty. When transplanted to wild type recipients, however, TGF- β 1 KO^{-/-} epithelium exhibited a much higher rate of outgrowth than that seen for TGF- β 1 epithelium. Thus, two opposing roles of TGF- β 1 in pubertal mouse mammary gland morphogenesis can be suggested: autocrine inhibition of ductal

outgrowth and endocrine/paracrine stimulation of ductal morphogenesis [213]. The autocrine nature of TGF- β 1 signalling is confirmed by co-localisation of TGF- β 1 and phosphorylated Smad 2/3 (downstream target of activated TGF- β) to the same cells. Since, nuclear Smad co-localised with ER α , and ER α positive cells do not proliferate, it was further investigated whether TGF- β 1 could inhibit the proliferative capacity of these cells. In fact, the number of proliferating, ER α positive cells increased in mature ducts of TGF- β 1 KO^{-/-} glands (especially during oestrus) and was significantly reduced in mouse models over-expressing active TGF- β 1. At puberty, however, no evidence for TGF- β 1-regulated proliferation of ER α positive cells was denoted [214]. Thus, although TGF- β 1 appears to act in an autocrine manner to inhibit the proliferative index of ER α expressing cells, in mature mammary glands, at puberty this regulatory effect appears to be independent of TGF- β 1 expression. TGF- β 1 has been recently shown to regulate spacing of ductal branching. Using an *in vitro* 3D assay to reconstruct ductal structures characteristic of mammary epithelium, local, low gradients of TGF- β 1 were demonstrated to control the positional milieu of ductal lateral branching [110]. Collectively, these results provide evidence for the role of TGF- β in regulating TEB outgrowth and lateral ductal branching. TGF- β seems to act through its type II receptor in both an autocrine and paracrine manner and as recently suggested, HGF is likely to play a role in TGF- β paracrine signalling. HGF stimulates ductal branching morphogenesis *in vitro* and its expression is significantly increased in mutant TGF- β receptor transgenic mice [215] [210]. Thus inhibition of epithelial outgrowth may be a result of HGF inhibition by TGF- β .

Inhibins and Activins

Inhibins and activins also regulate mouse mammary gland development at puberty. Activins function as dimers of two subunits: β A and β B. There are three types of activins that have been identified to date, namely activin A (β A β A), activin B (β B β B) and activin AB (β A β B). The inhibin family, on the other hand, consists of two members who share a common α subunit: inhibin A (α β A) and inhibin B (α β B). Inactivation of the activin/inhibin gene β B and thus loss of activin B, activin AB, inhibin B or a combination of the three affects ductal architecture during puberty. Ductal elongation was incomplete and TEBs showed abnormal morphology and failed to regress upon reaching the end of the fat pad

persisting up until postpartum. This mammary phenotype, however, could be rescued by transplantation of β B-deficient epithelium into the cleared fat pads of wild type hosts, suggesting stromal regulation of β B-dependent epithelial morphogenesis at puberty [216].

Nodal

Nodal is a potent embryonic regulator which is also crucial for normal mouse mammary gland morphogenesis. It is expressed in ductal epithelium at puberty and transgenic mice, carrying lacZ floxed nodal alleles that display 25% decreased expression of *Nodal*, exhibited impaired ductal branching at puberty. Furthermore, when administered into the mammary gland in the form of slow-release pellets, nodal influenced both the direction and development of branching [217].

Bone morphogenic proteins

BMP2 and BMP4 are also expressed during pubertal mouse mammary gland morphogenesis [218]. BMP-4 potentiated the mitogenic activity exerted by several growth factors on mammary epithelium. When added in combination with suboptimal concentrations of FGF2, FGF7, FGF10, EGF or HGF, growth factor induced proliferation of epithelial cells in low density *in vitro* culture was significantly enhanced confirming its potential role in ductal morphogenesis [219].

Macrophages and Eosinophils

The formation and outgrowth of TEBs during puberty is closely paralleled by the homing of macrophages and eosinophils to the mammary gland where they localise to the extracellular regions of TEBs (See 1.2.1.2.3). Because of their spatial location and timing of expression, many research groups have focused on their role in puberty and demonstrated that both macrophages and eosinophils are essential for the normal outgrowth of the ductal tree. As demonstrated by Gouon-Evans *et al.* (2002), mice depleted of a hematopoietic system, by gamma irradiation, showed significant curtailment of pubertal morphogenesis with complete absence of TEBs and therefore an arrest of ductal outgrowth. This

phenotype, however, could be rescued by bone marrow transplantation that replaced the population of leukocytes [85].

The critical role of macrophages during puberty was further highlighted by analysis of CSF-1 null mice (osteopetrotic mice which are deficient in CSF-1 due to a naturally occurring inactivating mutation). These mice showed impaired formation and outgrowth of TEBs and defective ductal branching [220] [85]. This TEB-associated phenotype has, more recently, been suggested to result from the impaired Coll fibrillogenesis which is at least partly promoted by macrophages (and thus reduced in CSF-1 null mice) and provides a framework for TEBs elongation [83].

Macrophages contribute to ECM remodelling during wound healing and produce ECM components, such as Fn or thrombospondin 1 as well as ECM degrading proteases such as MMP-7 which degrades collagen. Given the importance of ECM remodelling during ductal outgrowth, the association of macrophages with Coll fibrillogenesis and the dramatic phenotype of CSF-1 null or hematopoietic system depleted mice it is very likely that the ECM remodelling is the way that macrophages take part in regulation of mouse mammary ductal morphogenesis at puberty.

Mammary gland branching and TEB formation are also reduced in mice homozygous for a null mutation in eotaxin, i.e. deficient in eosinophils [85].

Mast cells

Another immune system response element that has been recently discovered to localise to TEB stroma during puberty are mast cells [89]. Previously, mast cells were thought only to contribute to allergy, inflammatory disease or cancer development. However, using two transgenic mice models - Kit^{+/W-sh} and Kit^{W-sh/W-sh}, Lilla *et al.* (2009) showed that mast cells are also required for normal mammary development [89]. Complete or partial ubiquitous deficiency of mast cells was seen in transgenic mice which were either heterozygous or homozygous for a spontaneous inversion mutation in the regulatory region of the c-kit proto-oncogene, which is located at the white spotting (W) locus and encodes a putative tyrosine kinase receptor [221] [222]. Wholemout analysis showed no

abnormal phenotype in pre-pubertal mouse mammary glands. At puberty (5 weeks), however, the mammary glands collected from mast cell deficient mice ($\text{Kit}^{\text{W-sh/W-sh}}$) showed a significantly reduced number of TEBs and ducts than their wild type counterparts while $\text{Kit}^{+/W-sh}$ mice showed an intermediate phenotype. These phenotypes persisted until adulthood, where the reduced ductal length and number of duct ends were still present. The observed growth impairment was independent of macrophage or eosinophil recruitment (mast cells serve as key recruiters of leukocytes) as no differences in the amount of these cells could be seen in the $\text{Kit}^{\text{W-sh}}$ mutant mice. These phenotypes most likely resulted from decreased cellular proliferation noted in TEBs and ducts in these mice [85] [89]. In addition, treatment of 3 week old female CD1 outbred mice with cromolyn sodium for 2 weeks revealed that degranulation is critical for mast cells to affect ductal mouse mammary gland morphogenesis, because of essential mediators (such as serine protease) of TEB outgrowth within the mast cells' granules. As demonstrated by the wholemounts, TEB formation and ductal outgrowth were significantly inhibited in response to the treatment [89].

1.2.3.2.5 The role of other stromal components in regulation of pubertal mammary morphogenesis

Further insight into the mechanisms regulating pubertal morphogenesis was gained when the growth-promoting potential of the TEB stroma and its associated cells was researched in more detail. Not only immune response cells, but all types of stromal cells found in close proximity to outgrowing mammary epithelium, namely adipocytes, fibroblasts and ECM, play a dynamic and essential role in promoting and regulation this outgrowth.

Adipocytes

Experiments based on FAT-ATTAC mice, designed to facilitate inducible and reversible loss of adipocytes (induced by dimerisation of caspase 8 fusion protein and thus apoptosis), showed that the absence of adipocytes resulted in failure of TEBs to redevelop at puberty and impaired ductal elongation and branching [223]. In this mouse model, in which adipocytes can be reversibly ablated at any point during the mouse's life span a significant reduction in ductal branching,

number of TEBs and changes in proliferation and apoptosis associated with TEB epithelium were seen when adipocytes were ablated (both white and brown) in 2 week old mice [224]. The dynamic and growth promoting character of mammary fat pad, however, is not only due to the morphogenic activity of its resident cells, but also depends on extensive DNA synthesis. As shown by Berger *et al.* (1983), extensive DNA synthesis was detected in the stroma surrounding the invading TEB while far less DNA synthesis was detectable around growth-terminated ducts in the adult gland [225].

ECM

BM and the fibrous connective tissue of ECM are also essential for TEB maintenance, pubertal outgrowth *in vivo* and epithelial mammary tubulogenesis *in vitro*. ECM and its components provide a scaffold for epithelial cells, play an active role in regulating cellular shape, proliferation and polarity and are essential in mediating the cross-talk between epithelial and stromal compartments. ECM remodelling is believed to be pivotal in enabling the epithelial invasion of the fat pad during pubertal mammary morphogenesis.

ECM signalling

There are many studies that show uninterrupted ECM signalling and normal ECM composition to be important in normal pubertal development. Both Streuli (1998) and Klinowska (1999) used antibody mediated ablation of β -integrin, the main mechanotransducer that relays ECM cues, to demonstrate reversibly inhibited TEB development *in vivo* and blocked tubulogenesis *in vitro* [226] [227]. Mammary epithelial cells cultured on Lama1-Coll based ECM showed increased cell growth, inhibition of lumen formation and loss of cellular polarity when the structural characteristics of ECM, such as its stiffness, were altered [228]. Disruption of Coll/Lama1 signalling in pubertal mouse mammary glands of mice lacking their exclusive receptor ($\alpha 2$ integrin subunit $KO^{-/-}$ mice) resulted in reduced branching of the epithelial tree [229]. In contrast, mouse mammary gland explants formed branched “spikes” when minced, 3D cultured in Coll gels and stimulated with any of the growth factors [230]. Moreover, the impairment in Coll fibrillogenesis has been shown to delay the outgrowth of TEB [83] *in vivo*.

Taken together, these results indicate that Coll is an important regulator of epithelial outgrowth and branching during puberty.

Compromised branching morphogenesis has also been noted with Fn deficiency in the salivary gland. *Ex vivo* down-regulation of Fn expression using siRNA, anti-Fn antibody or anti- β 1 integrin subunit antibody (α 5 β 1 integrin serves as Fn receptor) blocked cleft formation and branching in the salivary gland [231]. The similarity between salivary gland and mammary gland branching morphogenesis suggests that Fn may also be involved in the latter. In fact, recent experiments based on conditional KO of Fn in mammary epithelium (Cre-loxP-mediated gene KO technology) showed Fn deletion to cause a moderate retardation of pubertal mammary morphogenesis manifested by delayed ductal outgrowth and decreased branching [232]. Disruption of Tn-C in mice did not produce any visible abnormalities [233], while the functions of the remaining mammary gland ECM-associated molecules, Lama1, Per, Nid, SLRP, SPARC, Eln and other fibrillar collagens are yet to be elucidated in pubertal mouse mammary gland development.

ECM remodelling

ECM remodelling is essential for normal development of the mouse mammary gland. Degradation and remodelling of ECM at puberty provide a permissive environment for ductal elongation and branching facilitated by proteases. There are two main types of matrix degrading proteases that are activated during mammary gland remodelling. These are MMPs and a serine protease called plasmin. MMPs are synthesised as zymogens and their activity is regulated mostly by transcription and the action of their endogenous inhibitors, the tissue inhibitors of metalloproteases (TIMPs). Plasmin is also activated from its precursor, plasminogen and is involved in the degradation of fibrin and laminin and activation of pro-MMP3, -MMP9 and -MMP13 precursors (reviewed in [234]). Mouse mammary glands treated with the broad spectrum MMP inhibitor, GM6001 displayed arrested ductal outgrowth and impaired branching [235]. Five MMPs can be identified in the normal mouse mammary gland at puberty: MMP2, MMP3, MMP9, MMP11 and MMP14.

Mice lacking MMP2 (MMP2 KO^{-/-} mice) were characterised by delayed ductal outgrowth, increased number of apoptotic cells in TEB but an elevated number of secondary branches. The phenotype, however, does not persist for long, as by late puberty, normal ductal morphogenesis is restored.

The mammary glands of MMP3 deficient mice (MMP3 KO^{-/-}), on the other hand, displayed a ductal tree that is thinner and characterised by a lower number of side branches than that seen in the wild type control. The rate of ductal invasion as well as the number and size of TEBs in these mice, however, were normal [235]. The opposite phenotype, ducts with supernumerary side branches, could be seen in transgenic mice expressing an autoactivated form of MMP3 controlled by the WAP promoter [236]. Similarly, an increased number of epithelial branching compared to wild type littermates could also be detected in mice expressing activated MMP3 under the regulation of a MMTV promoter [237]. It should be noted, however, that the normal MMP3 expression is associated with the stromal compartment of the pubertal mouse mammary gland while these two studies were designed to express MMP3 in epithelium using MMTV or WAP promoters [235]. None-the-less, it appears that MMP2 stimulates TEB migration whilst also inhibiting lateral branch formation and MMP3 directs spatial localisation of branch points.

In addition, MMP9 may also stimulate epithelial branching *in vitro*. Using a 3D primary culture model of rat mammary epithelial organoids that were grown on reconstituted BM, it was shown that TNF-stimulated secretion of activated MMP9 coincided with increased proliferation and branching morphogenesis of epithelial cells. This effect was blocked by adding MMP9 neutralizing antibody [238]. The effect of MMP9 on epithelial branching morphogenesis *in vivo*, however, is yet to be elucidated. Using a similar culture system Simian *et al.* (2001) showed that the addition of plasmin or plasminogen to primary mammary organoid cultures mediated branching morphogenesis whereas the MMP inhibitor, galardin blocked this morphogenic effect. Thus, plasmin stimulated epithelial branching morphogenesis in culture by MMP activation rather than by direct ECM degradation [230].

The endogenous expression of TIMPs during pubertal mouse mammary gland development is differentially regulated. At pre-puberty, TIMP1 and TIMP2 are

minimally expressed but show significantly high expression at both puberty and adulthood while TIMP3 and TIMP4 are highly expressed at pre-puberty and remain abundant at puberty. All TIMPs are produced by mammary epithelial cells and fibroblasts except for TIMP2 which is exclusively synthesised by epithelial cells. Implanting TIMP1 releasing pellets into the outgrowing mouse mammary gland led to decreased proliferation in TEBs which then resulted in attenuated ductal expansion. In contrast, transgenic mice generated to reduce TIMP1 levels by using TIMP1 antisense RNA expression under the control of the MMTV promoter displayed augmented mammary ductal expansion and an increase in the number of ducts as well as disruption of BM integrity [239]. Moreover, the complete loss of TIMP1 in TIMP1 KO^{-/-} mice produced morphologically altered TEBs that were bigger than those seen in wild type controls [235].

In addition, the enzymatic degradation of hyaluronate *in situ* disrupted the cellular organisation of TEBs [52] [50], whilst S-GAG-degrading enzymes, β -glucuronidase and N-acetylglucosaminidase, strongly localised to cap cells of TEB and myoepithelial ductal cells [102]. This suggests that correct regulation of polysaccharides turnover in BM and within the fibrous ECM (some ECM molecules possess the ability to bind S-GAGs) is also important for normal ductal morphogenesis. Collectively, these results demonstrate that proteases and their inhibitors are critical in regulating ductal elongation and branching during normal pubertal mouse mammary gland morphogenesis, at least in part, by regulating BM integrity.

Finally, ECM mediated regulation of pubertal outgrowth can also be executed by regulating the morphogenic activity of growth factors and cytokines which are known to commonly bind to ECM (reviewed in [100] [91]).

1.2.3.2.6 Axonal guidance proteins

Microarray experiments have shown that axonal guidance proteins, expressed in neural growth cones and previously thought to function only in neuronal guidance, can also play a key role in regulating mouse mammary gland development at puberty.

Netrin 1 and Neogenin 1

As previously discussed in 1.2.3.1, Ntn-1 and Neo-1 appear to play important roles other than just guiding neurons and axons during nervous system development, although, their role in pubertal mammary gland morphogenesis is most likely to be associated with adhesion rather than guidance.

Ephrin family of receptor tyrosine kinases and their ligands

Another group of axonal guidance proteins involved in embryonic development and morphogenesis of many adult organs including pubertal mouse mammary gland development is the ephrin (Eph) family of receptor tyrosine kinases and their ligands [240]. Both the Eph receptor B4 (EPHB4) and its cognate ligand ephrin B2 (EFNB2) are expressed in the ductal epithelium of pubertal mouse mammary gland. EPHB4 localises predominantly to the myoepithelial cells while the expression of EFNB2 is associated with luminal epithelial cells. Their expression commences with the onset of ductal elongation at puberty and appears to be further differentially regulated during the oestrus cycle. Furthermore, mammary gland associated expression of both the receptor and ligand is abolished in ovariectomised mice but can be restored with E2 treatment [241]. Over-expression of the EPHB4 receptor under the control of the MMTV-LTR promoter resulted in delayed epithelial morphogenesis at puberty manifested by delayed ductal outgrowth and reduced secondary and tertiary branching when compared to the wild type controls [242]. Thus, EFNB2 signalling via EPHB4 is regulated in an oestrogen dependent manner and this interaction is important for normal epithelial outgrowth and ductal patterning at puberty.

Brain acid-soluble protein 1, Small proline rich protein 1A and Semaphorins

Further insights into the role of axonal guidance proteins during pubertal mouse mammary gland morphogenesis were gained from the microarray study by Morris *et al.* (2006) who demonstrated high expression of BASP1 and Sppr1A, Sema(s): Sema3B, 3C, 4A, 4F and their receptors- plexins and neuropilins in the epithelium of TEBs [113]. However, the effect that these proteins exert on mouse mammary gland development has yet to be elucidated *in vivo*.

1.2.3.2.7 Other regulators of pubertal mouse mammary gland morphogenesis

Other proteins which have been shown through KO models to regulate mouse mammary gland development include actin binding protein - gelsolin (Gsn) [243]; pro-apoptotic factor - Bcl2-like 11 (Bim) [244]; secreted milk fat globule - EGF factor 8 (MFGE8) [245] and Crk splice variant II [246].

Gelsolin

Mice with a targeted deletion of Gsn (Gsn KO^{-/-} mice) displayed inhibited ductal elongation. The ductal tree resembled a rudimentary structure up until week 9 when TEBs become evident and ductal outgrowth begun. Cellular proliferation in TEBs was also diminished when compared to their age-matched wild type controls. Transplantation of Gsn null epithelium into the fat pad of wild type mice, however, resulted in the restoration of normal ductal morphogenesis, suggesting that stromal Gsn is required for pubertal mouse mammary development [243].

Pro-apoptotic factor-Bim, Crk splice variant II, Secreted milk fat globule-EGF factor 8

Delayed ductal outgrowth paralleled by the increased deposition of Coll at the front of TEBs was also shown in Crk II over-expressing mice [246]. Deficiency of Bim, on the other hand, prevented induction of apoptosis and proper lumen formation in TEB and ducts at puberty [244] while loss of MFGE8 led to a severe reduction in ductal branching and formation of thin and poorly developed TEBs [245].

1.2.4 Summary

Pubertal mouse mammary gland morphogenesis is a complex process that involves ductal elongation, TEB bifurcation and ductal branching and epithelial patterning. Its regulation is facilitated by a wide range of factors that are expressed in the epithelium and stroma, including hormones and growth factors; ECM molecules and proteases with their inhibitors; immune cells and other

stromal cells. The cross talk between epithelial and epithelial-stromal cells provides global and directional cues for this development. A summarised list of pubertal regulators of mouse mammary gland and the effect they exert on TEB motility or ductal branching can be seen in **Table 1-1**.

1.3 Microarray analysis of gene expression to study pubertal mouse mammary gland development

In order to fully understand regulatory mechanisms that control organ development an understanding of the genome, the products it encodes and the way they interact to produce the complex living organism is crucial. Since protein based research is often less sensitive, more difficult and time consuming, gene expression profiling emerged as an effective way of studying genetic make-up of cells. Gene expression analysis can be performed either on an individual gene basis, using techniques such as northern blot or reverse transcription polymerase chain reaction (RT-PCR), or more efficiently, on the whole genome level using DNA microarrays. Both northern blotting and RT-PCR require the design of primers and probes for each individual gene, making the process of analysis of multiple genes timely and rather expensive. Thus, since the completion of the human genome project and sequencing projects in other species that identified many genes of unknown function, DNA microarray has become a very popular tool for transcriptome analysis. In fact it has revolutionised the whole area of genomic research.

The DNA microarray technique is based on one of the most fundamental biological laws which is a high hybridisation affinity between two complementary strands of nucleic acids. In microarray technology, single stranded DNA sequences, in the form of either cDNA fragments (~ 100 nucleotides) or synthesised oligonucleotides (most commonly 25 nucleotides) that represent specific genomic coding sequences, called probes, are immobilised (spotted) or directly synthesised onto the solid surface of an array [247]. The surfaces most commonly used to produce microarrays are nitrocellulose or charged nylon membranes or coated glass slides. Once extracted from the biological material, purified RNA is converted into single stranded cDNA, labelled using either fluorescent dye or more rarely a

Effect on motility	Overexpression of protein/ gene	Deficiency/Function impairment of protein/gene
TEB		
Reduced ductal elongation	PTH [150], PTHR [150], FGF3 [156], FGF4 [158], TIMP-1 [239], EPBHB4 [242], TGF- β [209] [206]	E-cadh [57], ErbB2 [118], ErbB3 [119], ER α [129], GHR [149], FGFR2IIIb [159], Areg [179], IGF-1 [170], EGFR [176], ADAM17 [183], SRC-1 [189], SRC-3 [190], MED-1 [197], CITED-1 [194], C/EBP β [201], AP-2 γ [203], Fn [232], MMP-2 [235], TIMP-1 [239], Gsn [243], Activin B [216], Activin AB [216], Inhibin B [216], Macrophages [85], Eosinophils [85], Adipocytes [223], Fibroblasts [248], Crkl [246]
Increased ductal elongation	IGF-1 with P [141], Areg [179]	GR [144], VDR [152], TGF- β [211]
Disorganisation of TEB morphology and structure	FGF4 [158]	ErbB2 [118], ErbB3 [119], MFGE8 [249], Ntn1 [117], Neo1 [117], IGF-1 [170], Inhibin B [216], Activin AB [216], Activin A [216]
Decrease in TEB formation	TGF- β [206] [209], EGF [175], Itgb [226]	GATA-3 [202], CSF-1 [85] [220], Eotaxin [85], Mast cells [89], AP-1 [195], IGF-1R [171], VDR [152]
Absence of TEBs		ER α [129], FGFR2IIIb [159], Adipocytes [223], Macrophages [85], Eosinophils [85]
Decrease in TEB size		ErbB2 [118], ErbB3 [119], IGF-1R [171]
Increase in TEB size	HGF [163]	TIMP-1 [235]
Aberrant ductal patterning	TGF- β [209], Nodal [217]	CITED-1 [194]
Reduced branching	PTH [150], PTHrP [150], TGF- β [209], EPBHB4 [242]	GR [144], GHR [144], IGF-1 [170], IGF-1R [171], EGFR [176], SRC-1 [189], SRC-3 [190], SRC-2 [192], AP-1 [195], MED-1 [197], C/EBP β [201], AP-2 γ [203], Nodal [217], CSF-1 [220] [85], Eotaxin [85], Adipocytes [223], α 2 integrin subunit [229], Fn [232], MMP-3 [235], MFGE8 [245]
Increased branching	IGF-1 with P [141], MMP-3 [236] [237], HGF [162] [163], MMP-9 [238], MTA-1 [198], Nodal [217]	ErbB2 [118], ErbB3 [119], VDR [152], TGF- β [210], MMP-2 [235]

Table 1-1 List of pubertal regulators of mouse mammary gland and the effect they exert on TEB motility or ductal branching.

radioactive isotope and hybridised to the array chip [250]. Upon hybridisation the array is scanned to detect the location of hybridisation sites to determine which gene is expressed in the sample of interest. The intensity of the signal detected at each hybridisation site further translates into the level of gene expression, enabling the researcher to determine whether the gene is expressed and at what magnitude. Fluorescence data can then be normalised, verified and analysed by a variety of methods.

Currently there are 5 main types of DNA microarray platforms that differ in the type of solid surface, the length of probe and the method of manufacture, namely: printed arrays, *in situ* synthesised arrays, high density bead arrays, electronic arrays and liquid bead suspension arrays (reviewed in [251]). Printed arrays are the first microarrays that were used in research laboratories. They are made of glass slides printed with DNA probes (cDNA or 25-80 nt long oligonucleotides) [252]. For *in situ* synthesised arrays, the oligonucleotides are directly synthesised on the quartz surface using photochemistry. Multiple probe sets are used per individual gene to improve sensitivity, specificity and statistical accuracy [253]. The length of probes depends on the manufacturer; Affymetrix GeneChips contain 25 nt long probes, Agilent ~ 60 nt probes and Roche NimbleGen 60-100 nt long probes (reviewed in [251]). Furthermore, the recently developed Affymetrix GeneChip Exon arrays allow the analysis of gene expression at the exon as well as the whole transcript level. High density bead array technology, on the other hand, is based on the sequence tagged beads randomly assorted on silicon slides [254]. In electronic microarrays, the hybridisation and immobilisation of the DNA onto the array surface is facilitated by an electric field and streptavidin-biotin bonds respectively. The NanoChip 400 is one of the platforms that operate using this system [255]. Finally, the most advanced microarray technology, the liquid-bead suspension arrays are 3D arrays that utilise microspheres as a solid support for the application of probes and flow cytometry for bead and target detection (reviewed in [251]). Affymetrix GeneChip Exon arrays are the arrays of choice in this study. They accommodate oligonucleotide sequences that translate into 17500 well-annotated transcripts and every exon of each transcript is represented by four probe-sets (each consisting of 3-4 25 nt long probes) (For further details on the platform and microarray data generation workflow see 3.2.1.3 and 2.2.5.3 respectively).

The main advantage of microarray technology is the quick and reproducible analysis of literally thousands of genes in one experiment. This increases the efficiency with which potential trends in cellular functions, regulatory mechanisms and pathways can be identified. The high sensitivity of microarrays minimises the amount of starting material that is required to carry out the analysis, while the high-throughput nature of the data provides an overview of the transcriptome which is useful for selection of potentially important gene targets. As with every technique, microarray analysis also has limitations and they include: i) quality of RNA - degraded mRNA can produce false microarray data, and ii) occurrence of discrepancies between mRNA and protein expression levels.

Microarray based gene expression profiling has been used to study mouse mammary gland development in the past. To date, most of these studies are time course microarray experiments that utilise whole mammary glands obtained from various stages of development, ranging from pre-puberty up to involution. There are only six published microarray studies, however, that address pubertal mouse mammary gland development. Four of these: Morris *et al.* (2006) [113], Kouros-Mehr *et al.* (2006) [256], McBryan *et al.* (2007) [194] and Deroo *et al.* (2009) [257] focus directly on puberty. The two former ones use isolated TEB and ducts and compare gene expression in TEBs with the gene expression elsewhere in the gland whereas the latter two compare gene expression in whole mouse mammary glands collected at different pubertal time points. The two remaining microarray studies by Master *et al.* (2002) [258] and Howlin *et al.* (2006) [193] present gene expression analysis across the whole development of mouse mammary gland, including puberty.

The study by Morris *et al.* (2006) was carried out to identify new genes associated with migration of TEBs and ductal differentiation at puberty [113]. It used a novel digestion-based technique to isolate TEBs and ducts from their surrounding stroma [259]. After digestion with type II collagenase isolated epithelial structures were collected under a dissecting microscope and when the sufficient amount of isolates was obtained, RNA extraction was performed. The gene expression profile of isolated TEBs and ducts was then compared using *in situ* synthesised, oligonucleotide microarrays (Affymetrix). To confirm the results and ensure that the removal of epithelium from its natural environment

did not alter gene expression, the RNA expression was additionally compared between whole mammary gland strips. Pairs of mammary glands were collected from 5-6 week old mice. One of the mammary glands was whole mounted and stained with carmine alum to assess the position of the TEB advancement front. Based on this morphology, the contralateral gland from the same mouse was then cut transversely into four tissue strips: Pre-LN (ductal epithelium and stroma), LN (epithelium and stroma of ducts and LN), Post-LN (TEB and ducts epithelium and stroma) and Fat pad (epithelium free stroma). 91 genes were shown to be expressed more highly in TEB than duct epithelium. Functional analysis of this gene set revealed that the majority of these genes (57%) were associated with DNA replication, cell division or cell cycle regulation. More interestingly, however, this was the first study that highlighted expression of axonal guidance proteins in TEBs at puberty. Three genes in particular: *BASP-1*, *Sprr1A* and *Sema3B* were associated with TEB epithelium. However, TEB associated expression of a number of other semaphorins (*Sema3C*, *4A*, *4F* and *4d*) along with their receptors, *Plexins A2*, *A3*, *B2* and *D1* and *Neuropilins 1* and *2* were also detectable [113]. This was consistent with the findings of the proteomic study that was previously published by the same research group [259] which led to the conclusion that axonal growth cone associated proteins are likely to regulate the migration of TEBs at puberty.

Kouros-Mehr and Werb, on the other hand, used β -actin-GFP reporter mice (5 week old) to surgically microdissect TEB, mature ducts and epithelium-free stromal compartments [256]. These mice show ubiquitous expression of GFP in their mammary glands which enables their visualisation and facilitates precise dissection of TEB or duct microenvironments (epithelium and its proximal stroma) and epithelium free stroma. RNA was extracted from the different microenvironments and the transcriptomes of TEB and mature duct microenvironments were compared with epithelium free stroma to identify novel genes involved in the regulation of mouse mammary branching morphogenesis. This microarray study was performed using long-oligonucleotide (80 nt long) *in situ* synthesised arrays (Operon) and it identified 1074 genes exclusively expressed in the TEB microenvironment and 222 genes in the mature duct microenvironment. A further 385 genes were up-regulated in both the TEB and duct microenvironments when compared to empty Fat pad. Some of the main

gene families identified within these gene sets and further verified using *in situ* hybridisation included: Wnt (*Wnt-2*, *5a*, *7b*, *Dsh-3*, *Frizzled-1* and *Frizzeld-2*) and hedgehog (*Dhh*), ephrin (*Ephrin-B1* and *A2*) family members and EMT molecules (*Twist-1*, *Twist-2* and *Snail*) [256]. This suggested that the Wnt family members which have also shown a similar expression pattern in the developing lung [260] [261]; *Dhh*, which is likely to act as an activator of hedgehog signalling which is important for mammary gland development [262]; ephrins, which belong to axonal guidance proteins [263], and Twist and Snail transcription factors, which are the markers of mesenchymal phenotype [264], all may play a potential key role in the orchestration of mouse mammary gland morphogenesis.

McBryan *et al.* (2007) carried out an expression microarray time course analysis on the whole mouse mammary glands to assess gene expression changes associated with the onset of puberty. Five representative stages of pubertal development were chosen (V3, V4, V5, V6 and V7). As shown by wholemound analysis, TEBs were absent from the 3 week old mammary glands, present at 4, 5 and 6 weeks and had regressed by the week 7. Gene expression analysis was carried out using Affymetrix MOE430A arrays and a pubertal gene set consisting of 930 unique transcripts was identified. Further analysis showed Wnt-, TGF- β and oestrogen signalling pathways members to be enriched at puberty and highlighted biological functions such as growth factor activity, cell growth, fatty acid metabolism, proteolysis and peptidolysis as over-represented in mouse mammary gland transcriptome at puberty. Moreover, the pubertal gene set was further analysed to identify genes that were expressed or repressed specifically upon the presence or absence of TEBs, i.e. 'TEB profile' genes. As a result, 15 expressed and 9 repressed 'TEB profile' genes were found and the 'apoptosis' and 'cell cycle regulation' were identified as the main biological functions associated with TEB associated genes [194].

The latest microarray analysis carried out using biological material obtained from pubertal mouse mammary glands was published by Deroo B. J. *et al.* (2009) [257]. The main focus of this study was the identification of an E2-responsive pubertal gene set. Thus, mice were ovariectomised at pre-puberty and treated with 17- β estradiol hormone pellets from 2 to 28 days. RNA was extracted from whole mammary glands collected at 2, 5, 7, 14 and 28 days after implantation and global gene expression was analysed using *in situ* synthesised

oligonucleotide microarrays (Agilent). This showed that the observed gene expression changes mimicked those that appear at puberty in normal mice. Both overlapping and distinct gene profiles were identified at different time points, i.e. at varying extents of ductal elongation. The most common functional categories associated with the E2 regulated genes that were over-expressed included: cell proliferation, immune response and metabolism/catabolism while the carbohydrate-metabolism associated genes were down-regulated in response to E2. Collectively, this analysis confirmed that E2 has a crucial role in ductal outgrowth of the mouse mammary gland at puberty and identified pubertal genes whose expression is regulated by E2 signalling [257].

Some further insights into the pubertal transcriptome of mouse mammary gland were also provided by the two time course experiments: the early study of Master *et al.* (2002) [258] and more recent microarray analysis carried out by Howlin *et al.* (2006) [193]. Although the former study performed microarray analysis on 12 time points that were chosen across the whole mouse mammary development it focused mainly on pre-puberty. The most important finding was that brown adipose tissue is a component of pre-pubertal stroma and that the mammary gland functions in adaptive thermogenesis [258]. The study carried out by Howlin *et al.* (2006) consisted of two separate microarray analyses. The initial study compared gene expression across the whole development of mouse mammary gland and the main finding was the role of CITED1 in mouse mammary gland development at puberty. The importance of CITED1 in pubertal morphogenesis has previously been discussed in 1.2.3.2.3.

A summary of the microarray studies carried out to examine the transcriptome of pubertal mouse mammary gland and their main characteristics is shown in **Table 1-2**.

At the beginning of the work for this thesis, in November 2006, it had been demonstrated in our laboratory that it was possible to isolate TEBs and ducts that could be rapidly processed to generate high quality RNA. The Morris *et al.* (2006) paper had limitations in terms of the restricted transcriptome represented on these early microarray chips and the methods available for analysis [113]. It was therefore decided that one objective of this thesis would be to use novel exon *in situ* synthesised, oligonucleotide microarrays, which

provide a much wider gene range and also enable the differential examination of gene expression at the exon level, use wild type mice to collect isolated TEB and duct epithelium and GFP mice to accurately microdissect TEBs and ducts contained within the stroma and to carry out their in depth analysis. In addition to elucidating the signalling pathways and biological processes that were differentially over-represented in the TEB and duct epithelium and surrounding stroma it was also hypothesised that this approach would identify new genes of interest that could be followed up at a functional level. As a result, we identified new genes expressed in both epithelial compartments of TEBs and ducts and the main biological functions and processes that these genes are involved in. Furthermore, with our study we also added to the understanding of pubertal mouse mammary morphogenesis by carrying out, a completely novel identification of the gene expression signature of TEB and duct associated stroma (See Chapter 3).

Study	Biological material used	Main findings	Ref
Morris <i>et al.</i> (2006)	Enzymatically isolated epithelium of TEBs and ducts Pre-LN, Post-LN and Fat pad tissue strips	Association of axonal guidance proteins with TEB migration at puberty	[113]
Kouros-Mehr <i>et al.</i> (2006)	Microdissected microenvironments of TEBs, mature ducts and epithelium-free stroma	Association of Wnt, hedgehog, ephrin family members and EMT markers with branching morphogenesis at puberty	[256]
McBryan <i>et al.</i> (2007)	Whole mouse mammary glands collected at 5 pubertal time points (V3, V4, V5, V6 and V7)	Association of Wnt, TGF- β and oestrogen signalling pathway members with epithelial outgrowth at puberty	[194]
Deroo <i>et al.</i> (2009)	Pubertal whole mammary glands collected from ovariectomised 17- β estradiol treated mice	Identification oestrogen-response genes at puberty and characterisation of common functional categories	[257]
Master S. R. <i>et al.</i> (2002)	Whole mammary glands collected throughout whole mammary gland development	Overview of gene expression pattern	[258]
Howlin J. <i>et al.</i> (2006)	Whole mammary glands collected throughout whole mammary gland development, Whole mammary gland collected from CITED1 null heterozygous and homozygous mice.	Identification of CITED1 as a key regulator of pubertal mammary development, Involvement of CITED1 in the regulation of E2 and TGF- β response genes	[193]

Table 1-2 Summary of the microarray studies carried out on the pubertal mouse mammary glands, to date, and their main characteristics.

2 Materials and methods

2.1 Materials

2.1.1 Reagents and materials

Animal husbandry	
Beekay Rat and Mouse diet No 1	B & K Universal Ltd., Hull, UK
M3 cages	North Kent Plastic Cages Ltd., Kent, UK
Wood chips	The Andersons, Inc; Maumee, Ohio, USA
Sample collection	
Collagenase type II	Sigma Aldrich Company Ltd., Dorset, UK
Fetal Bovine Serum (FBS) (0.1%)	Sigma Aldrich Company Ltd., Dorset, UK
Gridded contact dish	Nalge Nunc International, Hereford, UK
Histobond [®] + glass slides	Paul Marienfeld GmbH & Co. KG; Landa-Königshofen, Germany
Leibovitz L15 medium	Invitrogen Ltd.; Paisley, UK
Neutral buffered formalin (10%)	Genta Medical; York, UK
RNaseZap	Applied Biosystems/Ambion; Austin, USA
Scalpel blades	Swann-Morton, Ltd.; Sheffield, England
Surgical instruments	John Weiss International; Milton Keynes, UK
Trizol [®] Reagent	Invitrogen Ltd., Paisley, UK
Cell culture and Explant Culture	
75 cm ² tissue culture filter flasks	Corning Incorporated, Corning, USA
Dulbecco's Modified Eagle medium (DMEM)	Invitrogen Ltd., Paisley UK
Dulbecco's Modified Eagle Medium: Nutrient Mixture F-12 (DMEM/F12)	Invitrogen Ltd., Paisley UK
Epidermal growth factor (EGF)	PeproTech EC Ltd., London, UK
FBS (10%)	Sigma Aldrich Company Ltd., Dorset, UK
Fibronectin	Sigma Aldrich Company Ltd., Dorset, UK
Haemocytometer	Superior, Marienfeld, Germany
Insulin	Sigma Aldrich Company Ltd., Dorset, UK
Lab-Tek-II Chamber Slide [™] System	Nalge Nunc International Corp., Naperville, USA
Leukaemia Inhibitory factor (LIF)	Donated by Dr. J. Mounthford
L-glutamine	Invitrogen Ltd., Paisley UK
Phosphate Buffered Saline (dPBS)	Invitrogen Ltd., Paisley UK
Roswell park memorial institute 1640 (RPMI-1640) medium	Invitrogen Ltd., Paisley UK

Trypsin-EDTA Solution (0.25%)	Sigma Aldrich Company Ltd., Dorset, UK
Cloning	
Ampicillin	Sigma Aldrich Company Ltd., Dorset, UK
Bacterial culture dishes	Sterilin Ltd. UK, Aberbargoet, UK
Competent DH5 α E. coli cells	Invitrogen Ltd., Paisley, UK
Ethylenediaminetetraacetic acid (EDTA) (2mM)	Sigma Aldrich Company Ltd., Dorset, UK
HiSpeed [®] Plasmid Maxi kit	Qiagen Ltd., Crawley, UK
Luria Bertani (LB) Broth	Sigma Aldrich Company Ltd., Dorset, UK
Microbiological spreader	Microspec, Ellesmere Port, UK
NaCl	VWR International Ltd., Dublin, Ireland
pcDNA3	Invitrogen Ltd., Paisley UK
pEGFP	Clontech-Takara Bio Europe, Saint-Germain-en-Laye, France
pRc/CMV-Fbln2	Donated by Dr. Mon-Li Chu, Thomas Jefferson University, Philadelphia, USA
QIAprep Miniprep kit	Qiagen Ltd., Crawley, UK
S.O.C. medium	Invitrogen Ltd., Paisley UK
Tryptone	ForMedium [™] , Norfolk, UK
Yeast extract	Sigma Aldrich Company Ltd., Dorset, UK
Cell transfections and Adhesion assays	
10 cm cell culture plate	Corning Incorporated, Corning, USA
12 well tissue culture plate	Corning Incorporated, Corning, USA
25 cm ² tissue flask	Corning Incorporated, Corning, USA
DharmaFECT [®] Duo Transfection Reagent	Thermo Fisher Scientific Inc., Surrey, UK
Extracellular Matrix (ECM) Cell Adhesion Array Kit	Millipore Ltd, Livingstone, UK
Lipofectamine [™] 2000 Transfection Reagent	Invitrogen Ltd., Paisley UK
Opti-MEM [®] I Reduced Serum Medium	Invitrogen Ltd., Paisley UK
Protein work	
Amersham ECL Western blotting detection reagents and analysis system	GE Healthcare UK Limited, Little Chalfont, UK
Anti-Actin (C-20) antibody	Santa Cruz Biotechnology Inc., Santa Cruz, USA
Anti-C-terminus of Fbln2 antibody	Santa Cruz Biotechnology Inc., Santa Cruz, USA
Anti-Fbln2 antibody	Donated by Dr. Mon Li Chu (Thomas Jefferson University, Philadelphia, USA)
Anti-goat (HRP-labelled) rabbit polyclonal antibody	Dako UK Ltd., Eli, UK
Anti-mouse (HRP-labelled) rabbit polyclonal antibody	Dako UK Ltd., Eli, UK

Anti-N-terminus of Fbln2 antibody	Santa Cruz Biotechnology Inc., Santa Cruz, USA
Anti-rabbit (HRP-labelled) donkey polyclonal antibody	GE Healthcare UK Limited, Little Chalfont, UK
Anti-Upk3a (AU1) antibody	Donated by Dr. T. Sun (New York University Medical School, New York, USA)
BCA™ Protein Assay Kit	Thermo Fisher Scientific Inc., Surrey, UK
Bis-Tris-HCl buffered (pH 6.4) (4-12%) gel	Invitrogen Ltd., Paisley UK
Bovine Serum Albumin (BSA)	Thermo Fisher Scientific Inc., Surrey, UK
Cell lifters	Corning Incorporated, Corning, USA
Dithiothreitol (DTT)	Sigma Aldrich Company Ltd., Dorset, UK
Glycine	Sigma Aldrich Company Ltd., Dorset, UK
Marvel Original dried skimmed milk	Premier International Foods Ltd., Susson, UK
Methanol	Thermo Fisher Scientific Inc., Surrey, UK
Microcon® Centrifugal Filter Device equipped in the Ultracel YM-3 membrane	Millipore Ltd, Livingstone, UK
Novex NuPage™ Electrophoresis system	Invitrogen Ltd., Paisley UK
Novex XCell II™ Blot module	Invitrogen Ltd., Paisley UK
Novex® Sharp Pre-stained Protein Standards	Invitrogen Ltd., Paisley UK
NP-40	Sigma Aldrich Company Ltd., Dorset, UK
NuPage LDS sample buffer (4x)	Invitrogen Ltd., Paisley UK
NuPage MES SDS running buffer (20X)	Invitrogen Ltd., Paisley UK
NuPage transfer buffer (20X)	Invitrogen Ltd., Paisley UK
Phosphatase inhibitor cocktail 2	Sigma Aldrich Company Ltd., Dorset, UK
Ponceau S stain	Sigma Aldrich Company Ltd., Dorset, UK
Protease inhibitor cocktail tablets	Roche Diagnostics Ltd., Burgess Hill, UK
Sodium deoxycholate	Sigma Aldrich Company Ltd., Dorset, UK
Sodium dodecyl sulfate (SDS)	Sigma Aldrich Company Ltd., Dorset, UK
TRIS (TRIZMA base)	Thermo Fisher Scientific Inc., Surrey, UK
NuPage Tris-Acetate polyacrylamide gel (3-8%)	Invitrogen Ltd., Paisley UK
NuPage Tris-Acetate SDS Running Buffer (20X)	Invitrogen Ltd., Paisley UK
Tween-20	Sigma Aldrich Company Ltd., Dorset, UK
Urea	Sigma Aldrich Company Ltd., Dorset, UK
Whatman® Protran® Nitrocellulose Transfer Membrane (0.2 µm)	Sigma Aldrich Company Ltd., Dorset, UK
RNA and DNA	
0.5 ml microcentrifuge tube	Thermo Fisher Scientific Inc., Surrey, UK
Acetylated BSA (10µg/µl)	Promega Corporation, Madison, USA
Agilent RNA 6000 Nano Kit	Agilent Technologies. Inc. UK, UK
Dimethyl sulfoxide (DMSO)	Sigma Aldrich Company Ltd., UK
DNA-free™ Kit	Applied Biosystems/Ambion; Austin, USA

dNTPs mix (10mM)	Invitrogen Ltd., Paisley UK
Electrophoresis grade agarose	Invitrogen Ltd., Paisley UK
Ethidium bromide (10mg/ml)	Sigma Aldrich Company Ltd., Dorset, UK
GoTag [®] DNA Polymerase (5U/μl)	Promega Corporation, Madison, USA
Green GoTag [®] Flexi Buffer (5X)	Promega Corporation, Madison, USA
J Buffer (1X)	Promega Corporation, Madison, USA
LightCycler [®] 480 96 Well Plates	Roche Applied Science, Mannheim, Germany
LightCycler [®] 480 Probes Master (2X)	Roche Applied Science, Mannheim, Germany
LightCycler [®] 480 Sealing Foil	Roche Applied Science, Mannheim, Germany
MgCl ₂ (25mM)	Promega Corporation, Madison, USA
Oligo dT primer (0.5 μg/μl)	Invitrogen Ltd., Paisley UK
Random primer (1 μg/μl or 100 ng/μl)	Invitrogen Ltd., Paisley UK
Reaction Buffer (cDNA synthesis)	Roche Diagnostics Ltd., Burgess Hill, UK
RNase OUT (40U/μl)	Invitrogen Ltd., Paisley UK
RNase-free 1.5 microcentrifuge tube	Applied Biosystems/Ambion; Austin, USA
RNase-free H ₂ O	Applied Biosystems/Ambion; Austin, USA
RNeasy [®] Micro Kit	Qiagen Ltd., Crawley, UK
RNeasy [®] Mini Kit	Qiagen Ltd., Crawley, UK
Sma I enzyme (10U/μl)	Promega Corporation, Madison, USA
Transcriptor Reverse Transcriptase (20 U/μl)	Roche Diagnostics Ltd., Burgess Hill, UK
Microarray analysis of pubertal gene expression	
Biotinylated LNA RiboMinus probes (100 pmol/μL)	Invitrogen Ltd., Paisley, UK
GeneChip [®] Hybridisation, Wash and Stain Kit	Affymetrix UK Ltd., High Wycombe, UK
GeneChip [®] IVT cRNA Cleanup Kit	Affymetrix UK Ltd., High Wycombe, UK
GeneChip [®] Mouse Exon 1.0 ST Array	Affymetrix UK Ltd., High Wycombe, UK
GeneChip [®] Whole Transcript (WTr) Sense 1 μg Total RNA Target Labelling Assay	Affymetrix UK Ltd., High Wycombe, UK
GeneChip [®] WTr cDNA Synthesis Kit	Affymetrix UK Ltd., High Wycombe, UK
GeneChip [®] WTr Terminal Labelling Kit	Affymetrix UK Ltd., High Wycombe, UK
RiboMinus Human/Mouse Transcriptome Isolation Kit	Affymetrix UK Ltd., High Wycombe, UK
Streptavidin coated RiboMinus Magnetic Beads	Invitrogen Ltd., Paisley, UK
T7 RNA Polymerase GeneChip [®] WTr cDNA Amplification Kit	Affymetrix UK Ltd., High Wycombe, UK
Tissue processing and staining	
3,3-Diaminobenzidine tetrahydrochloride (DAB) +	Dako UK Ltd., Eli, UK

Chromogen	
Acetic Acid (analytical grade)	VWR International Ltd., Dublin, Ireland
Acid Alcohol (1%)	Sigma Aldrich Company Ltd., UK
Alexa Fluor 488 dye	Invitrogen Ltd., Paisley, UK
Alexa Fluor 594 dye	Invitrogen Ltd., Paisley, UK
Anhydrous MgSO ₄	Thermo Fisher Scientific Inc., Surrey, UK
Antibody Diluent	Dako UK Ltd., Eli, UK
Anti-Fbln1 antibody	Donated by Dr. Mon-Li Chu, Thomas Jefferson University, Philadelphia, USA
Anti-Fibronectin (ab2413) antibody	Abcam Inc; Cambridge, USA
BD Microlance™ 3 needle	Becton Dickinson UK Ltd., Oxford, UK
Carmine	Sigma Aldrich Company Ltd., UK
Chloroform (analytical grade)	Thermo Fisher Scientific Inc., Surrey, UK
Coplin Jar	Raymond A. Lamb Ltd., Eastbourne, UK
Elastica van Gieson (EVG) kit	Merck KGaA; Darmstadt, Germany
Eosin (1%)	CellPath Ltd.; Newtown, UK
Ethanol (analytical grade)	Hayman Ltd., Witham, UK
Haematoxylin Z	CellPath Ltd.; Newtown, UK
Horse Serum (2.5%)	Vector Laboratories Ltd.; Peterborough, UK
Image-iT™ FX Signal Enhancer	Invitrogen Ltd., Paisley, UK
KAl(SO ₄) ₂	Sigma Aldrich Company Ltd., UK
NaHCO ₃	Sigma Aldrich Company Ltd., UK
Pertex	CellPath Ltd., Newtown, UK
ProLong® Gold antifade reagent with 4,6-diamidino-2-phenylindole dihydrochloride (DAPI)	Invitrogen Ltd., Paisley, UK
Superfrost® Plus slides	Thermo Fisher Scientific Inc., Surrey, UK
Thymol	Sigma Aldrich Company Ltd., UK
Twin Frost Microscope Slide	Raymond A. Lamb Ltd., Eastbourne, UK
Weigert's solution A	Merck KGaA; Darmstadt, Germany
Weigert's solution B	Merck KGaA; Darmstadt, Germany
Xylene	Genta Environmental Ltd., York, UK
<i>In vivo</i> hormonal treatment of mouse mammary glands	
21 day release oestrogen (E2) (0.72mg/pellet) pellet	Innovative Research of America, Sarasota, Florida, USA
21 day release oestrogen-progesterone (E2+P) (0.1mg/pellet, 10 mg/pellet) pellet	Innovative Research of America, Sarasota, Florida, USA
21 day release placebo (10.01 mg/pellet) pellet	Innovative Research of America, Sarasota, Florida, USA
Biogel®P Suretech surgical gloves	Marigold Industrial Ltd., Broxbourne, UK
Polyamide 6 blue monofilament non-absorbable suture 5-0 Ethicon	Johnson & Johnson; Langhorne, PA, USA

Table 2-1 List of reagents and materials.

2.1.2 Solutions and Buffers

Name of solution	Method of preparation
Cell culture	
EDTA-PBS buffer (2mM)	2mM EDTA in dPBS, sterilized by filtration
Cloning	
LB-Agar (1.5%)	10g of Tryptone, 5g of yeast extract and 10g NaCl and 15g of Agar in 1L of dH ₂ O, sterilised by autoclaving, pH 7.5
Protein work	
2.5% BSA blocking solution	2.5% BSA in 1X TBS Tween-20 wash buffer
3% milk blocking solution	3% Marvel Original dried skimmed milk in 1X TBS Tween-20 wash buffer
EDTA buffer	10mM EDTA, protease inhibitor and phosphatase inhibitor cocktail in TBS
NP-40 buffer	50mM TRIS pH 7.5, 150mM NaCl, 5mM EDTA, 1% NP-40, protease inhibitor and phosphatase inhibitor cocktail in dH ₂ O
RIPA buffer	25mM TRIS pH 8, 150mM NaCl, 1% NP-40, 1% sodium deoxycholate, 0.1% SDS, protease inhibitor and phosphatase inhibitor cocktail in dH ₂ O
Stripping buffer pH 2.2	5M Glycine, 0.1% SDS, 1% (v/v) Tween-20, pH 2.2 in dH ₂ O
Tris Buffered Saline (TBS) buffer (10X)	50mM Tris-HCl, 150mM NaCl, pH 7.4 in dH ₂ O
TBS Tween-20 wash buffer (1X)	1X TBS, 0.1% (v/v) Tween-20 in dH ₂ O
Transfer buffer (western blotting) (1X)	1X NuPage transfer buffer, 10% methanol in dH ₂ O
Urea buffer	6M Urea, protease inhibitor and phosphatase inhibitor cocktail in TBS
Tissue processing and staining	
1 mM EDTA buffer (pH 8)	1mM EDTA disodium salt, 4.5mM TRIS, pH 8 in dH ₂ O
Carmine dye	2mM Carmine, 5mM KAl(SO ₄) ₂ in dH ₂ O, boil for 20 min, filter and add crystal of Thymol (preservative)
Carnoy's fixative	6 parts of 100 % (v/v) ethanol, 3 parts of chloroform and 1 part of acetic acid
Scott's tap water	81.14mM anhydrous MgSO ₄ , 41.66mM NaHCO ₃ in dH ₂ O
TBS buffer pH 7.6 (10X)	50mM Tris-HCl, 150mM NaCl, pH 7.6 in dH ₂ O

TBS Tween-20 buffer pH 7.6 (1X)	1X TBS, 0.1% (v/v) Tween-20 detergent in dH ₂ O
Weigert's A&B solution	Weigert's solution A (Alcoholic Haematoxylin Solution) and Weigert's solution B (Hydrochloric Acid Iron(III) Nitrate Solution) mixed 1:1

Table 2-2 List of solutions and buffers.

2.1.3 Electric equipment

Agilent 2100 bioanalyser	Agilent Technologies. Inc. UK, South Queensferry, UK
Biometra T 3000 Thermocycler	Thistle Scientific Ltd., Glasgow, UK
C-28 centrifuge	Boeckel and Co; Hamburg, Germany
CKX41 microscope	Olympus UK Ltd., Surrey, UK
Dissecting microscope	Olympus UK Ltd., Surrey, UK
Dynatech MR7000 Plate Reader	Primera Scientific LLC, Princeton, NJ, USA
Electrisaver E30 Thermostat heated chamber	RS Components Ltd., Corby, UK
Fluororber vaporiser	The Harvard Apparatus, Kent, UK
Fujifilm Fla-5000	Raytek Scientific Ltd., Sheffield, UK
Galaxy S tissue culture incubator	New Brunswick Scientific, Cambridge, UK
Intelligent Dark Box LAS-3000	Fujifilm UK Ltd., Manchester, UK
Labophot-2 light microscope	Nikon UK Ltd.; Kingston upon Thymes, UK
Leica ASP300 tissue processor	Leica Microsystems Ltd.; Milton Keynes, UK
Leica DMD108 Digital Microimaging Network	Leica Microsystems Ltd.; UK
Leica EG1150C cold plate	Leica Microsystems Ltd.; Milton Keynes, UK
Leica EG1150H heated paraffin dispensing module	Leica Microsystems Ltd.; Milton Keynes, UK
Leica TCS SP2 confocal microscope	Leica Microsystems Ltd.; UK
Leitz 1512 microtome	Leica Microsystems Ltd.; Milton Keynes, UK
LightCycler [®] 480 Instrument	Roche Applied Science, Germany
Mikro-Dismembrator	B. Braun Biotech International GmbH, Melsungen, Germany
NanoDrop ND 1000 Spectrophotometer	NanoDrop Technologies, USA
NanoZoomer Digital Pathology scanner	Hamamatsu; Bridgewater, USA
ND-1000 Spectrophotometer	NanoDrop Technologies, USA
IX51 inverted microscope	Olympus UK Ltd., Southend-on-Sea, UK
Shaking incubator Certomat [®] BS-1	B. Braun Biotech International, Allentown, USA
Stemi SV6 fluorescent dissecting microscope	Carl Zeiss Ltd., Welwyn Garden City, UK
Water bath	Thermo Fisher Scientific Inc., Surrey, UK

Table 2-3 List of electric equipment.

2.2 Methodology

2.2.1 Sample Collection

2.2.1.1 Mouse husbandry

Wild type C57BL/6 (WT), transgenic EGFP expressing C57/BL6 (TG) and Fibulin 2-null C57BL/6 (*Fbln2* KO^{-/-}) mice were used for the purpose of this research. The WT mice were supplied by Harlan UK Limited Breeding Laboratories while the TG colony was derived from a breeding pair kindly donated by Prof. Cathrin Briskin (EPFL/ISREC, Lausanne, Switzerland). TG animals were of C57BL/6 background and constitutively expressed the EGFP transgene under the control of a CAG promoter (combination of β -actin promoter and hCMV enhancer) [265]. Males heterozygous for EGFP expression were mated with WT female mice in order to establish our own colony of transgenic mice. WT and EGFP heterozygous female littermates were used for further experiments. The male offspring were culled before weaning unless needed for breeding purposes. The mice were accommodated and bred at the Biological Services Central Facilities at Gilmorehill Campus and the Veterinary Research Facility on the Garscube Estate, Glasgow.

Animals were kept in conventional M3 cages bedded with wood chips and paper nesting material. Each of the cages was equipped *ad lib* with food; Beekay Rat and Mouse diet No 1 and *ad lib* tap water containers. Mice were housed in a temperature-controlled environment at $21 \pm 1^\circ\text{C}$ with humidity of 45% to 55% on a 12-hour (h) light, 12-h dark exposure cycle. All WT mice were allowed a 7 day acclimatisation period after their arrival on site prior to being used for experiments. The transgenic founder breeders were screened for the presence of pathogens upon their arrival.

Fbln2 KO^{-/-} mice were initially generated by Dr. Chu (Thomas Jefferson University, Philadelphia, USA) [266] but bred and kindly made available for mammary gland collection by Dr. Tsuda (Nemours/Alfred I. DuPont Hospital for Children, Wilmington, USA). Tissue collection for wholemounting and paraffin

embedding was carried out in Nemours/Alfred I. DuPont Hospital for Children in Wilmington in USA by Mrs. Joyce.

2.2.1.2 Dissection of mouse mammary glands

The weight and age of the animals was recorded prior to culling. Surgical instruments were sterilized by autoclaving prior to performing the dissections. Mammary tissue was obtained from both left and right fourth inguinal glands of WT and TG females. Tissue was collected at the following stages of development: virgin (between 2 and 12 weeks old), pregnancy (day 3, 8.5, 12.5, 14.5 17.5), lactation (day 1 and 7) and forced involution (day 1, 2, 3, 4, 10 and 20). The first day of pregnancy was denoted by the appearance of a vaginal plug (counted as day 0.5). The collection of mammary glands from pregnant, lactating and involuting mice was performed by Marie-Anne Pringle. Mice were euthanized by a schedule 1 method of killing, either cervical dislocation or rising concentration of carbon dioxide. Death was confirmed by checking for absence of heart beat, respiration and paw withdrawal due to pinching the toe. The cadaver was placed on a corkboard in dorsal recumbent position and secured to the board using metal pins. 70% ethanol (v/v) was applied to the body and a midline inverted Y incision into the skin was performed using blunt scissors. The incision began halfway between the fourth and fifth nipples and continued rostrally to the thorax and laterally to each thigh. The skin flaps with mammary glands attached were then pulled away from the peritoneum and secured to the corkboard (**Figure 2-1**). Mammary tissue was gently excised using dissecting scissors and forceps. Glands to be used for isolation of epithelium were chilled on ice in Leibovitz L15 medium. Glands to be used for microarray studies and protein or RNA extraction had their lymph nodes removed prior to being snap frozen in liquid nitrogen. Glands to be used for immunohistochemistry (IHC) or immunofluorescence (IF) were transferred to 10% Neutral Buffered Formalin upon removal. Glands to be used for tissue imaging, tissue strips collection or organ culture were gently dissected out and immediately used for further applications. Glands to be used for carmine alum stained wholemount analysis were spread out on microscope slides and placed in Carnoy's fixative.

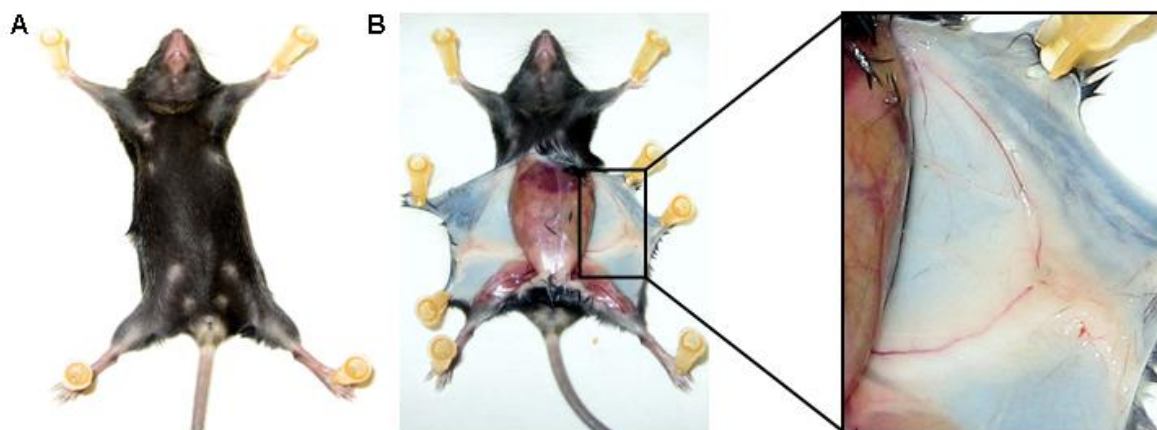


Figure 2-1 Dissection of the 4-th (inguinal) mouse mammary gland.

(A) The image illustrates a mouse carcass secured to the corkboard in the recumbent position, ventral side up. **(B)** Image demonstrates carcass with 4-th mammary gland exposed by incision. Insert shows a higher magnification of the left mammary gland.

2.2.1.3 Dissection of other mouse organs and tissues

All tissues and organs used in this research were excised from adult WT or TG mice at the Veterinary Research Facility, Garscube Estate, Glasgow, UK. Surgical instruments were sterilised by autoclaving prior to performing the dissection. Animals were weighed and euthanized by cervical dislocation. Collected organs of interest were either fixed in 10% Neutral Buffered Formalin or snap frozen in liquid nitrogen depending on their further application.

2.2.1.4 Collection of mouse mammary gland tissue strips

Pre-pubertal and pubertal mouse mammary gland can be divided into the following sections: pre lymph node (Pre-LN), post lymph node (Post-LN) and empty fat pad (Fat pad). The Pre-LN tissue strip contains ductal epithelium and stroma, the Post-LN tissue strip consists of TEBs, duct epithelium and surrounding stroma while Fat pad consists of epithelium-free stroma (**Figure 2-2 A**). Mammary gland tissue strips were collected from 7 week old TG mice. Mice were transferred to the Beatson Animal Facility (Beatson Institute for Cancer Research, Glasgow, UK) immediately before commencing the experiments where they were culled by cervical dislocation. Glands were excised as described above in the designated area of Dr. Tomoko Iwata's laboratory (Beatson Institute of Cancer Research, Glasgow, UK). The 4-th mammary gland was gently spread onto a HistoBond[®]+ glass slide, visualised using Stemi V6 fluorescent dissecting microscope and imaged (**Figure 2-2 B**). Tissue strips were cut using sterile scalpel blades under the fluorescent dissecting microscope (**See 2.2.8.1**) and snap frozen in liquid nitrogen. Collected tissue was used for microarray analysis or RNA and protein extraction. All work surfaces and instruments used in the collection of tissue strips for use in RNA extraction were cleaned using RNaseZap prior to commencing work.

2.2.1.5 Collection of isolated epithelium

Two types of epithelial structures, TEBs and ducts, were extracted from the mammary tissue dissected from WT mice, aged between 6-8 weeks as described above. 20 glands were removed for each experiment and chilled in Leibovitz L-15 medium. Collected tissue was coarsely minced using surgical non-sterile

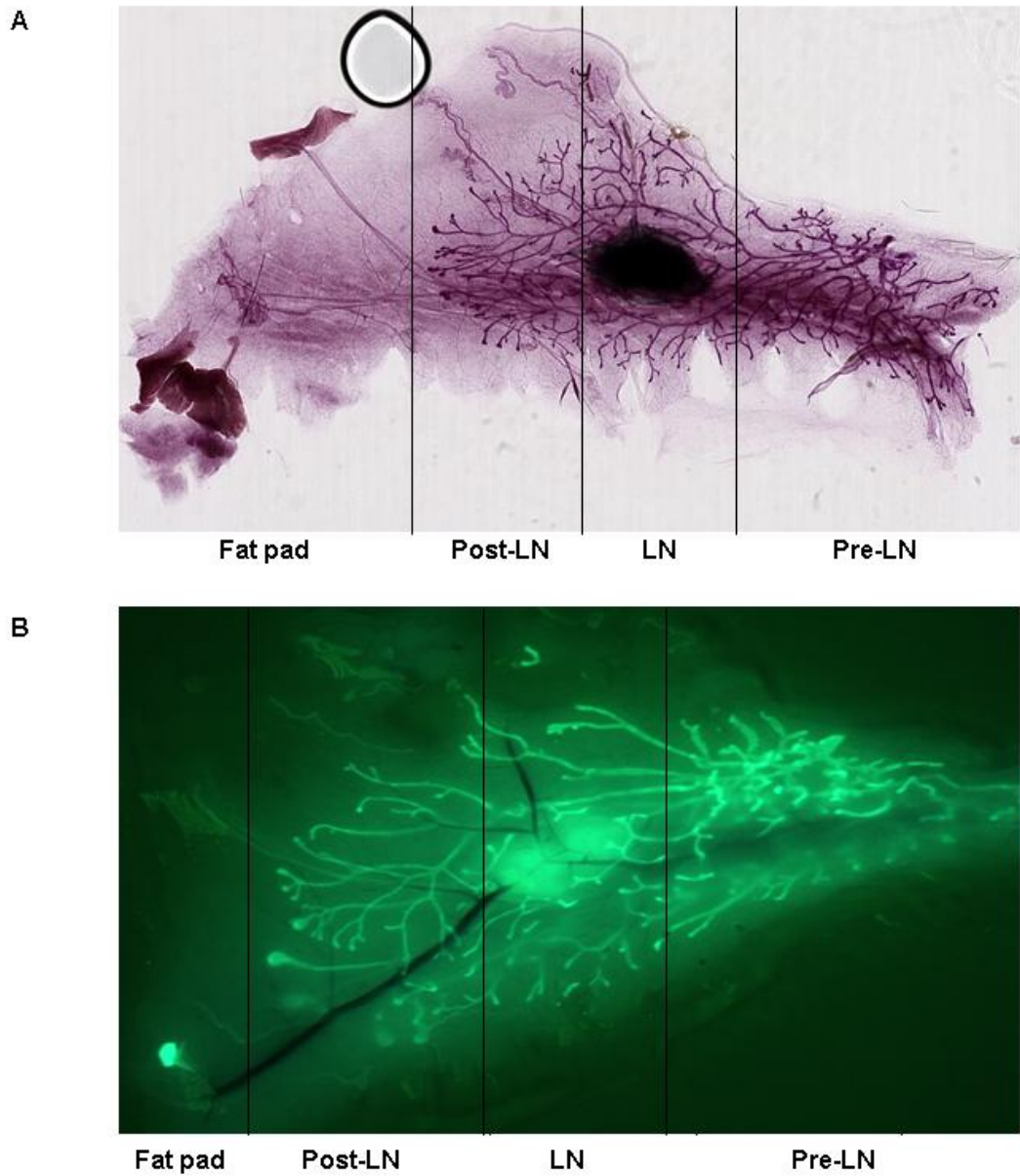


Figure 2-2 7 weeks old 4-th mouse mammary glands.

(A) Mouse mammary gland wholemount stained with Carmine stain, collected from WT mice **(B)** Mammary gland collected from TG mice imaged with a fluorescent dissecting microscope.

scalpel blades and subjected to 1mg/ml (w/v) collagenase type II digestion in Leibovitz L-15 medium. The enzymatic reaction was carried out at 37°C for 35 min using a shaking incubator Certomat® BS-1 at max speed. The tissue soup was then shaken by hand to encourage the release of the epithelial structures from the tissue. The obtained suspension was split between two universals, diluted in fresh, ice-cold Leibovitz L-15 medium supplemented with 0.1% FBS to inhibit the collagenase activity and centrifuged for 5 min at room temperature (RT) at 250rcf using a C-28 centrifuge. The resulting supernatants were then gently aspirated and pellets gently resuspended in 1 ml of Leibovitz L-15 medium and combined prior to being transferred into a gridded contact dish. The released TEBs and ducts were visualised by means of a dissecting microscope and manually collected using a 10µl Gilson pipette. Isolated epithelial structures were stored in 50-100µl volume of TRIzol® Reagent at -80°C prior to extraction of RNA or fixed in 10% Neutral Buffered Formalin to be used in IHC or IF.

2.2.2 Cell culture

2.2.2.1 Cell lines and Cell maintenance

Cell lines used in this study comprised three mouse non-tumourigenic cell lines: EpH4 and HC11, derived from mouse mammary epithelium, and NIH3T3 derived from mouse embryonic fibroblasts. NIH3T3 were kindly supplied by Dr. Iglesias while EpH4 and HC11 cells were kindly supplied by Prof. Birchmeier (Max-Delbrück-Centrum für Molekulare Medizin, Berlin, Germany) and Dr. Allan (formerly Hannah Research Institute, Glasgow, UK) respectively.

Unless stated otherwise, all cells were routinely grown in 75cm² tissue culture filter flasks in a Galaxy S tissue culture incubator at 37°C in a humidified atmosphere with 5% CO₂. Growth conditions applied to each cell line were as follows: EpH4 cells - DMEM, 10% FBS, 2mM L-glutamine; HC11 cells - RPMI-1640, 10% FBS, 2mM L-glutamine, 5µl/ml insulin, 10ng/ml EGF and NIH3T3 cells - DMEM, 10% FBS, 2mM L-glutamine. All cell culture maintenance and *in vitro* experiments were performed under sterile conditions.

For maintenance purposes, all cells were grown until nearly confluent. They were then washed twice with sterile dPBS (1X), detached from the tissue culture

flask via enzymatic proteolysis facilitated by incubation with 0.25% Trypsin-EDTA Solution for 2 min at 37°C and passaged into the fresh tissue culture flask by splitting 1:7 for NIH3T3, 1:12 for EpH4 and 1:5 for HC11 cells.

2.2.2.2 Cell Counting

Cells were then counted using a haemocytometer as follows: 10µl of cell suspension was applied to the upper and lower chambers of the haemocytometer, the number of cells per 1mm² square was counted in 3 different areas and the mean number of cells was calculated. The number of cells in 1ml of medium was calculated by multiplying mean number of cells with 10⁴.

2.2.2.3 Plasmid information and plasmid DNA purification

Plasmid Information

The eukaryotic expression vectors used in this study were pEGFP, pcDNA3 and pRc/CMV-Fbln2 (**Appendix 1**). pEGFP encoded Enhanced Green Fluorescent Protein (EGFP) under the control of a cytomegalovirus (CMV) promoter while pcDNA3 is an empty vector and hence was used as a negative transfection control. pRc/CMV-Fbln2 contains variant 1 (V1) of the mouse *Fbln2* gene (NM_007992) under the control of a CMV promoter.

Preparation of LB Agar plates

1.5% LB-Agar was prepared (**See Solutions and Buffers**) and autoclaved. The mix was then preheated in the microwave, left to cool down and then supplemented with 100µg/ml of Ampicillin. Finally it was poured onto bacterial culture dishes, allowed to solidify and stored upside down at 4°C.

Purification of plasmid DNA

pRc/CMV-Fbln2 was obtained as DNA blotted onto filter paper. DNA was eluted from the filter paper by placing the area of filter paper containing the plasmid in a 1.5ml Eppendorf tube and incubating in 50µl of dH₂O for 30 min at RT,

followed by centrifugation for 3 min at 13,000rcf. 1µl of eluted plasmid DNA was then transformed into 50µl of competent DH5α E. coli cells. Transformation was performed by incubating the cells with the DNA on ice for 20 min, heat shocking for 90 sec at 42°C to facilitate plasmid entry and returning to ice for a further 2 min. Transformed cells were then incubated with 250µl of S.O.C. medium for 45 min at 37°C with agitation at 220rpm using a Certomat® BS-1 shaking incubator to assist cell recovery. Finally, 50µl of the transformation mix was transferred onto prepared LB-Agar (1.5%) plates containing 100µg/ml of Ampicillin, spread using a sterile disposable microbiological spreader and incubated upside down overnight at 37°C. After the incubation period the plate was investigated for the presence of single bacterial colonies. Four colonies were picked and each one was transferred to 10ml of LB medium supplemented with 100µg/ml of Ampicillin and cultured overnight at 37°C with agitation at 220rpm using Certomat® BS-1 shaking incubator. 100µl of each culture were kept at 4°C. Obtained bacterial cultures were then centrifuged at 5,000rcf at 4°C for 15 min. Supernatant was removed and plasmid DNA was retrieved from the bacteria and purified using QIAprep Miniprep kit as per manufacturer's instructions. Briefly, bacteria were lysed under alkaline conditions. The lysate was neutralised and adjusted to high salt binding conditions and cleared from the cell debris by centrifugation. Plasmid DNA was then selectively bound to a QIAprep silica-based membrane, washed to remove endonucleases and salts and eluted in RNase-free H₂O (low salt conditions).

The DNA was quantified using a NanoDrop ND-1000 Spectrophotometer (See 2.2.4.4).

Each plasmid preparation was checked using restriction digestion (See 2.2.4.11).

Once the correct clone was identified by restriction digestion, 25µg of plasmid DNA was sent for sequencing to confirm the sequence of the insert (See 2.2.4.10). Six primers were designed (See 2.2.4.7) (Table 2-5) to amplify the full sequence of Fbln2 V1 publicly available at the Nucleotide Database of the National Centre for Biotechnology Information (NCBI) (<http://www.ncbi.nlm.nih.gov/>) (NM_007992). Sequencing results were visualised and examined using Chromas Lite 2.01 (Technelysium Pty Ltd) and

compared to the publicly available Fbln2 V1 GeneBank nucleotide sequence using Basic Local Alignment Search Tool (BLAST), blastn algorithm (<http://blast.ncbi.nlm.nih.gov/>) to assess the degree of similarity.

Once the correct clone was identified, the aliquot of bacteria set aside before DNA purification, was transferred to a flask containing 150ml of LB medium supplemented with 100µg/ml of Ampicillin and grown overnight at 37°C with agitation at 220rpm. Bacterial cultures were then centrifuged at 5,000rcf at 4°C for 15 min. Supernatant was removed and plasmid DNA was extracted from the bacteria and purified using HiSpeed® Plasmid Maxi kit as per manufacturer's instructions. Briefly, bacteria were lysed under alkaline conditions and the DNA, proteins and cell debris were precipitated from the lysate. Lysate was filtered through the Anion Exchange Resin under the appropriate low salt and pH conditions to facilitate DNA binding to the Resin. Resin was then washed to remove the remains of RNA, proteins and low molecular weight impurities. Plasmid DNA was eluted in high salt buffer, concentrated and desalted via isopropanol precipitation and finally eluted in RNase-free H₂O.

Purified DNA from the pEGFP and pcDNA3 was kindly supplied by Dr. Camille Huser.

2.2.2.4 Transfections

Transfections were performed on HC11 cells using 3 different plasmids: pEGFP, pcDNA3 and pRc/CMV-Fbln2 and a liposomal transfection reagent.

2.2.2.4.1 *Optimisation of transfections*

The optimisation of transfection efficiency and toxicity was performed for DharmaFECT® Duo Transfection Reagent and Lipofectamine™ 2000 in order to find optimal transfection conditions for HC11 cells. All optimisation experiments were performed using the pEGFP. HC11 cells were plated in growth medium in 6 well tissue culture plates at the same density per well 24-48h before transfection. Cells at the time of transfection were 60-80% confluent.

Optimisation of Transfections using Lipofectamine™ Transfection Reagent

Optimisation of the transfection protocol for Lipofectamine™ was performed as follows: 4µg of DNA of pEGFP and varying volumes of Lipofectamine™ transfection reagent (2µl, 4µl, 6µl, 10µl and 12µl) were diluted in 250µl of Opti-MEM® I Reduced Serum Medium by gentle mixing. All mixes were incubated at RT for 5 min. Diluted pEGFP DNA samples were then added to each of the diluted transfection reagent mixes and incubated at RT for a further 20 min in order to facilitate generation of the DNA-liposomes complexes. Finally 500µl of complexes were added directly to each well containing HC11 cells and fresh standard cell culture medium. Cells were then returned to incubator. After 5h the culture medium was changed. Cells were then further incubated to be tested for the transgene expression by fluorescence microscopy (See 2.2.8.1).

Optimisation of Transfections using DharmaFECT® Duo Transfection Reagent

Optimisation of the transfection protocol for DharmaFECT® Duo Transfection Reagent was performed as follows: 100µl of 20µg/ml of pEGFP was mixed with 100µl of serum free culture medium. Increasing volumes of DharmaFECT® Duo Transfection Reagent (2µl, 4µl and 6µl) were each diluted in 200µl of serum free culture medium and incubated at RT for 5 min. The DNA dilutions were then added to the transfection reagent mixes and incubated at RT for an additional 20 min. Finally, 1.6ml of fresh standard cell culture medium was added to each mix and the diluted complexes were added to each well containing HC11 cells. Cells were then tested for transgene expression after 48h of incubation.

The efficiency of transfections, i.e. estimation of the EGFP transgene expression levels was performed using an inverted fluorescent microscope. Each well was visualised and imaged at x400 magnification (See 2.2.8.1). The number of EGFP expressing cells was counted at 3 chosen random fields within the well and the mean number of cells and standard errors of the mean (S.E.M.) were calculated.

2.2.2.4.2 *Fbln2* over-expression in HC11 cells

Fbln2 was over-expressed by transfecting HC11 cells with pRc/CMV-*Fbln2* using Lipofectamine[™] transfection reagent for 48h. The plasmid DNA to transfection reagent ratio was 1:1 and it was adjusted for the size of each tissue culture plate or dish. PcDNA3 DNA was used as a negative control in all experiments.

The experimental procedure was carried out as described above (See 2.2.2.4.1). Transfected HC11 cells were then incubated for 48h prior to being collected in RIPA buffer (See Solutions and Buffers) for protein extraction or used for further applications. Transgene expression was determined by Western blotting.

2.2.2.5 Wound Healing Assay

HC11 cells were plated in 6 well cell culture plates at equal density per well and transfected in triplicates with either pRc/CMV-*Fbln2* or pcDNA3 using Lipofectamine[™] transfection reagent as described above (See 2.2.2.4.1). 48h after the transfections, when cells had become confluent, a double cross was marked on the surface of each well using a sterile 200 μ l pipette tip. As *Fbln2* is an ECM molecule, the culture medium was collected from each well, spun down at RT for 5 min at 1,100rcf to discard floating cells, mixed with fresh culture medium and placed back on the cells. Two areas around the double cross were selected for each well to be imaged over time. Images were acquired straight after performing the scratch, i.e. at 0 h and after 4, 7, 11, 24 and 36h. The width of the gap was measured in triplicate for each selected area at x400 magnification (See 2.2.8.3). The experiment was repeated 3 times. Mean values and S.E.M. were calculated for each well, and the percentage of gap closure over time in each well was plotted. Upon completion of the assay, cells were collected in RIPA buffer for protein extraction to determine transgene expression by Western blotting.

2.2.2.6 Adhesion Assays

2.2.2.6.1 *Adhesion of pRc/CMV-Fbln2 transfected HC11 cells to plastic surface*

HC11 were plated in 75cm² tissue culture flasks prior to being transfected with either pRc/CMV-Fbln2 or pcDNA3 with Lipofectamine™ transfection reagent as described above (See 2.2.2.4.1). 48h after transfection, the cells were washed twice with sterile dPBS (1x), detached from the tissue culture flask by incubation with filtered 2mM EDTA-PBS buffer (See Solutions and Buffers) for 10 min at RT, resuspended, centrifuged at 150rcf for 3 min at RT, washed twice in filtered 2mM EDTA-PBS buffer and resuspended in 2ml of DMEM. Cells were then counted (See 2.2.2.2) and plated at a final concentration of 1.5x10⁶ cells/ml in 96-well tissue culture plate in quintuplicates at 100µl/well and incubated for 2h. Adherent cells were then washed, stained and quantified using the methodology and reagents from the ECM Cell Adhesion Array Kit as described below (See 2.2.2.6.2).

2.2.2.6.2 *Adhesion of pRc/CMV-Fbln2 transfected HC11 cells to ECM proteins*

Influence of Fbln2 over-expression on the adhesiveness of HC11 cells to human ECM proteins, such as Coll, CollI, CollIV, Fn, Lama1, Tnc and vitronectin (Vtn) was studied using ECM Cell Adhesion Array Kit. The ECM Cell Adhesion Array Kit utilises colorimetric detection of the amount of experimental cells adherent to wells coated with seven human ECM proteins in a 96-well cell culture plate. BSA-coated wells are used as a negative control. The main experimental steps of the assay include: plating of the cells at a given constant density per well, cell attachment, washing, staining and determination of the relative cell attachment via absorbance reading.

Determination of the optimal cell density was performed using untransfected HC11 cells at three different concentrations (0.5x10⁶ cells/ml, 1x10⁶ cells/ml and 2x10⁶ cells/ml) and the relative cell attachment was determined according to the manufacturer's instructions. Briefly, HC11 cells were plated in 75cm²

tissue culture flasks and cultured until confluent. Cells were then detached from the flask using filtered 2mM EDTA-PBS buffer (See 2.2.2.6.1), counted (See 2.2.2.2) and plated at the final concentration in the supplied strips in 100µl/well and incubated for 2h. Each strip was rehydrated with 200µl of dPBS for 10 min prior to being used for the experiment. After incubation, culture medium was aspirated from the wells and cells were washed three times with 200µl/well of supplied Assay Buffer to remove unattached cells. The remaining attached cells were then stained for 5 min with 100µl/well of the supplied Cell Stain Solution, washed three times with deionised H₂O to remove excess staining solution and allowed to air dry. Finally, the stain was released from the cells and solubilized by the addition of 100µl of supplied Extraction Buffer to each well and incubating the plate at RT for 15 min while shaking. The amount of released stain was directly proportional to the amount of attached cells and it was determined using absorbance readings at 560nm.

The amount of Fbln2 over-expressing HC11 cells adherent to different ECM proteins was determined as follows: HC11 cells were plated in 75cm² cell culture flasks prior to being transfected with either pRc/CMV-Fbln2 or pcDNA3 as described above (See 2.2.2.4). 48h after transfection, both cell lines were washed twice with sterile dPBS (1x), detached from the flask using filtered 2mM EDTA-PBS, washed, resuspended in DMEM and counted as described above. Both cell lines were then resuspended in DMEM to a final concentration of 1.5x10⁶ cells/ml, plated in triplicates, incubated, washed, stained and analysed following the experimental steps described above. The mean amount of cells and S.E.M. for each condition were calculated and plotted.

2.2.3 Protein work

2.2.3.1 Protein extraction from the cell lines

Protein extracts were collected from untransfected cell lines grown to sub-confluency in either 6 well plates or 10cm cell culture dishes. Protein extraction from transfected cells was performed upon completion of transfections or wound healing assays.

Cells were washed twice with dPBS and incubated on ice with either 0.25ml/per well (6 well tissue culture plate) or 0.5ml/plate (10cm tissue culture) of ice cold RIPA lysis buffer until the cells were lysed, i.e. the buffer became viscous due to the nucleic acid release and the cell membranes appeared digested when viewed under an Olympus CKX41 microscope at x400 magnification. The cell lysates were then scraped off from the tissue culture dishes or plates using cell lifters, transferred to 1.5 Eppendorf tubes and incubated on ice for a further 15 min with occasional mixing. The cell lysate was finally centrifuged at 4°C for 20 min 25,000rcf to separate the fraction of extracted proteins (supernatant) from cell debris (pellet). The supernatant, i.e. protein lysate was then quantified (See 2.2.3.3), concentrated, used for Western Blotting or stored at -80°C.

2.2.3.2 Protein extraction from the frozen tissues

Frozen tissues were pooled or individually crushed in liquid nitrogen using a mortar and pestle cooled on dry ice. The obtained tissue powder was transferred to a Down's Homogeniser chilled on dry ice and resuspended in 0.5ml of ice cold NP-40, RIPA, EDTA or Urea lysis buffers (See Solutions and Buffers). Homogenised samples were transferred to ice chilled 1.5ml microcentrifuge tubes and placed on dry ice. The obtained tissue lysates were then defrosted, incubated on ice for 30 min to facilitate further cell lysis and centrifuged at 25,000rcf at 4°C for 20 min to separate out the fraction of extracted proteins from the cell debris. The resulting supernatant was retained, quantified, concentrated, used in Western blotting or stored at -80°C.

2.2.3.3 Protein Quantification

The concentration of proteins was determined with the BCA™ Protein Assay Kit that utilises the ability of proteins in alkaline medium to facilitate Cu^{2+} to Cu^{1+} reduction (Biuret reaction). Briefly, 10 μl of each sample (diluted 1:5) was plated in the 96 well tissue culture plate along with equal volumes of eight BSA protein standards (0, 25, 125, 250, 500, 750, 1000 and 1500 $\mu\text{g}/\text{ml}$). Each sample and protein standard was plated in duplicate and triplicate respectively and mixed with 200 μl of BCA reagent (prepared by mixing Reagent A and Reagent B in a 50:1 ratio). The plate was then incubated at RT for 30-40 min. The absorbance of each well was read at 570nm using a Dynatech MR7000 Plate Reader and

Revelation Version 3.04 software (Revelation UK, London, UK). Finally, the absorbance readings of BSA standards were used to plot a standard curve and calculation of sample protein concentration was based on a linear line of best fit using Microsoft Excel[®].

2.2.3.4 Concentration of Protein Extracts

Cellular protein extracts of a concentration too low to be used for further applications were concentrated using a Microcon[®] Centrifugal Filter Device with Ultracel YM-3 membrane according to the manufacturer's instructions. The Ultracel YM-3 membrane has a cut off of 3kDa. Briefly, a maximal volume of 0.5ml of protein extract was transferred into the sample reservoir assembled with the collection vial and sealed with the attached cap. The column was then centrifuged at 14,000rcf for 40 min at RT with the cap strap aligned to the centre of the rotor. The reservoir was then removed from the column, placed upside down in the new collection vial and spun at 1,000rcf for 3 min to retain the concentrate. The concentration of the resulting extract was once more determined by the BCA[™] Protein Assay Kit.

2.2.3.5 Electrophoresis and Western blotting

One dimensional electrophoresis under denaturing conditions and in the presence of 0.1% SDS was performed to enable separation of the proteins according to their molecular weight. The separation and blotting of proteins was carried out using the Novex NuPage[™] Electrophoresis system.

Sample preparation

Prior to SDS polyacrylamide gel electrophoresis (PAGE), 25-50 μ g of each protein extract was mixed with 0.33 volumes of 4xNuPage LDS sample buffer and 0.1 volume of 1M DTT. The mix was incubated at 70°C for 10 min to facilitate protein denaturation.

SDS polyacrylamide gel electrophoresis

The prepared protein samples were resolved on either 4-12% Bis-Tris-HCl buffered (pH6.4) gels in the presence of 1xNuPage MES SDS running buffer or 3-8% Tris-Acetate polyacrylamide gels in the presence of 1X Tris-Acetate SDS Running Buffer. Molecular weight markers, Novex® Sharp Pre-stained Protein Standards, were separated alongside the samples. The choice of polyacrylamide gel type was dependent on the molecular weight of the protein of interest and the level of resolution required. 500µl of NuPage Antioxidant was added to the inner chamber of the gel apparatus. 4-12% Bis-Tris gels were electrophoresed at a constant voltage of 200V for approximately 45 min, while the 3-8% Tris-Acetate polyacrylamide gels were run for 60 min at a constant voltage of 150V.

Protein Transfer

Upon completion of electrophoresis, proteins were transferred from the SDS polyacrylamide gel onto Whatman® Protran® Nitrocellulose Transfer Membrane (0.2µm) using a Novex XCell II™ Blot module, protein transfer buffer (**See Solutions and Buffers**), sponges and filter papers. Filter papers, transfer membrane and sponges were pre-soaked in protein transfer buffer and protein transfer was carried out at a constant voltage of 30V for 60 min.

Membrane Blocking and Incubation with Antibodies

After protein transfer the nitrocellulose membrane was removed from the module and briefly stained with Ponceau S stain (0.1% Ponceau S (w/v) in 5% acetic acid (v/v)) to determine the efficiency of the transfer. 1xTBS Tween-20 wash buffer (**See Solutions and Buffers**) was used to remove the stain. The blot was incubated for 40 min at RT in 3% Marvel Original dried skimmed milk blocking solution (**See Solutions and Buffers**) or 2.5% BSA blocking solutions (**See Solutions and Buffers**). It was then incubated for 2h at RT or overnight at 4°C with primary antibody, washed three times with 1xTBS Tween-20 wash buffer for 10 min, incubated for 1h at RT with horseradish peroxidase (HRP)-labelled secondary antibody and finally washed three more times with 1xTBS Tween-20 wash buffer for 10 min. All of the above incubations and washes were performed using horizontal or oscillating shakers. Both primary and secondary antibodies

were diluted in 1xTBS Tween-20 wash buffer to the final working concentrations shown in **(Table 2-4)**.

Signal Detection

The HRP activity of the secondary antibodies allow antigen detection to be carried out using chemiluminescence, i.e. emission of light resulting from dissipation of energy from the product of chemical reaction. In this system, HRP catalyses oxidation of luminol in the presence of phenol (chemical enhancer) in alkaline conditions.

Signal detection was performed using the Amersham ECL Western blotting detection reagents and analysis system as per manufacture's instructions. The membrane was incubated with the prepared detection mix (equal volume of detection solution 1 and 2) for 1 min at RT. Excess solution was removed from the membrane prior to and after the incubation. The membrane was then wrapped in Saran wrap and the chemiluminescence signal was detected using an Intelligent Dark Box LAS-3000 equipped with a cooled to -30°C charge coupled device, camera and FO.85 Fujinon Lens. Images were acquired and analysed using LAS-3000 v.2.2 software (Fujifilm UK Ltd., UK) after 4-20 min of exposure under standard sensitivity. Densitometry was performed using MacBiophotonics ImageJ (<http://rsb.info.nih.gov/ij/>).

Stripping for re-probing of membranes

In order to be re-used, the membranes were transferred into 1xTBS Tween-20 wash buffer immediately after performing the signal detection step of Western blotting and stored at 4°C for up to 48h. When needed, membranes were briefly rinsed twice in 1xTBS Tween-20 wash buffer, washed for 5 min in 1xTBS Tween-20 wash buffer and stripped of attached primary and secondary antibodies by two separate 10 min incubations in stripping buffer (pH2.2) (**See Solutions and Buffers**), rinsing in-between. Membranes were then finally washed using 1xTBS Tween-20 wash buffer three times for 5 min to fully remove detached antibodies and eliminate the remains of stripping buffer. All washes and incubations were performed at RT, using an oscillating shaker. Stripped membranes were then

Primary antibody and Source	Blocking solution	Final concentration
Anti-Upk3a (AU1) Mouse monoclonal, donated by Dr. T. Sun (New York University Medical School, New York, US)	2.5% BSA	1: 1000
Anti-Fbln2 Rabbit polyclonal, donated by Dr. Mon Li Chu (Thomas Jefferson University, Philadelphia, US)	3% milk	1:5000
Anti-Actin (C-20) Goat polyclonal, Santa Cruz Biotechnology Inc., Santa Cruz, USA	3% milk	1:1000
Anti-N-terminus of Fbln2 Rabbit polyclonal, Santa Cruz Biotechnology Inc., USA	3% milk	1:400
Anti-C-terminus of Fbln2 Goat polyclonal, Santa Cruz Biotechnology Inc., USA	3% milk	1:200
Secondary antibody and Source	Blocking solution	Final concentration
Anti-goat (HRP-labelled) Rabbit polyclonal, Dako UK Ltd., Eli, UK	3% milk	1:3000
Anti-rabbit (HRP-labelled) Donkey polyclonal, GE Healthcare UK Ltd., UK	3% milk	1:5000
Anti-Mouse (HRP-labelled) Rabbit polyclonal, Dako UK Ltd	3% milk	1:3000

Table 2-4 Primary and secondary antibodies used for Western Blotting.

blocked and re-probed with primary and secondary antibodies and used to detect other proteins of interest as described above.

2.2.4 RNA and DNA

2.2.4.1 Preparation of total RNA

To prevent contamination by environmental RNases, all instruments and working surfaces were cleaned using RNaseZap and RNase-free 1.5 microcentrifuge tubes were used as standard throughout the experimental procedure.

2.2.4.1.1 Preparation of collected frozen tissue for RNA extraction

Frozen tissues were pooled or individually crushed in liquid nitrogen using a pestle and mortar previously cooled on dry ice. The obtained tissue powder was transferred to a liquid nitrogen chilled polytetrafluoroethylene capsule and further homogenised using a Mikro-Dismembrator for 20 sec at 15,000rpm. According to the amount of starting material, the homogenate was resuspended in 1-3ml of TRIzol[®] reagent transferred to 1.5ml tubes and stored at -80°C until all samples were ready for further processing.

Once all samples were collected, they were thawed on ice, mixed by vortexing and incubated at RT for 5 min in order to facilitate the complete dissociation of nucleoprotein complexes.

2.2.4.1.2 Preparation of isolated mammary gland epithelium for RNA extraction

Isolated TEBs and ducts (See 2.2.1.5) previously collected in TRIzol[®] reagent and stored at -80°C were thawed on ice and mixed by vortexing. All TEBs were pooled together in a final volume of 1ml of TRIzol[®] reagent. The ducts were pooled in the same way. Samples were then incubated at RT for 5 min.

2.2.4.1.3 Extraction of RNA from frozen tissue and isolated epithelium

Extraction of RNA was performed as follows: 0.2ml of chloroform was added per 1ml of TRIzol[®] reagent to each sample. Tubes were manually shaken for 15 sec, incubated for 2-3 min at RT and centrifuged at 12,000rcf for 15 min at 4°C in order to separate the mixture into the three phases: a lower red phase that contained phenol-chloroform, intermediate phase containing DNA and proteins and an upper aqueous transparent phase containing RNA. The latter colourless phase was transferred to a new tube and the RNA was precipitated by mixing with 0.5ml of isopropanol and incubated for 10 min at RT. The precipitated RNA was then sedimented by centrifugation at 12,000rcf for 10 min at 4°C. The RNA pellet was washed by adding 1ml of 75% (v/v) ethanol (RT) and vortexing. Finally, the RNA pellet was retained by centrifugation at 7,500rcf for 5 min at 4°C, careful removal of the supernatant and air drying. The RNA obtained from frozen tissue was then resuspended in 10-40µl of RNase-free H₂O. The RNA extracted from isolated mammary gland epithelium was resuspended in 10µl of RNase-free H₂O. All RNA extracted from TEBs was then combined and all RNA obtained from the ducts was combined. Extracted RNA was quantified (See 2.2.4.4) and quality assessed (See 2.2.4.5), snap frozen and stored at - 80°C until used for further applications.

2.2.4.1.4 Extraction of RNA from cell lines

RNA extraction from cell lines was performed using an RNeasy[®] Mini Kit as per manufacturer's instructions. Briefly, once grown close to confluency the cells were washed twice with dPBS (1x) and lysed using 0.6ml RLT Buffer. The obtained cell lysates were transferred in 1.5ml Eppendorf tubes, homogenised by pipetting, mixed with 1 volume of 70% of ethanol (aids RNA binding to the membrane) and transferred onto RNeasy spin column. Membrane bound RNA was washed and residual ethanol was removed. RNA was then eluted in 20-30µl of RNA-free H₂O. Eluted RNA was quantified, subjected to DNase I digestion (See 2.2.4.2), snap-frozen, and stored at - 80°C until used for further applications.

2.2.4.2 DNase I treatment

All RNA to be used for cDNA production (RT-PCR) was subjected to DNase I treatment using a DNA-free™ Kit as per manufacturer's instructions to eliminate DNA contamination. Briefly, 0.1 volume of 10xDNase I Buffer and 1µl of DNase I (2U/µl) were incubated with the RNA for 20 min at 37°C. 0.1 volume of DNase Inactivation Reagent was then incubated with the reaction mix for 2 min at RT. The purified RNA was then retained by centrifugation at 9,300rcf for 1.5 min, snap frozen and stored at - 80°C until used for further applications.

2.2.4.3 RNA purification, concentration and on column DNase I digestion

All RNA extracted for use in microarray experiments was purified, DNase I on column digested and concentrated using an RNeasy® Micro Kit, as per manufacturer's instructions. The RNeasy® Micro Kit is used to purify small amounts of RNA and remove genomic contaminants as well as RNAs < 200 nucleotides, including 5.8S rRNA, 5S RNA and tRNA. Briefly, RNA was bound to an RNeasy silica-based membrane using the appropriate binding conditions of a high-salt buffer supplemented with ethanol. Membrane bound RNA was then DNase I digested with RNase-Free DNase, washed on the column and eluted in 13µl of RNA-free H₂O. The eluted, purified and concentrated RNA was quantified (See 2.2.4.4) and its quality assessed (See 2.2.4.5) prior to snap freezing and storing at - 80°C until used for further applications.

2.2.4.4 Quantification of the nucleic acid (RNA or DNA)

Both concentration as well as purity of the extracted nucleic acid was estimated using a NanoDrop ND-1000 Spectrophotometer. Based on the absorbance at 260/280 nm the concentration of 1µl of extraction product was calculated using ND-1000 U3.3.0 software (NanoDrop Technologies, USA). RNase-free water was used as a blank control. The ratio of the readings at 260nm and 280nm was used to estimate the purity of nucleic acid.

2.2.4.5 Quality assessment of RNA

The quality and integrity of RNA was assessed using an Agilent 2100 bioanalyser and Agilent RNA 6000 Nano Kit, as per manufacturer's instructions. The Agilent RNA kit consists of RNA chips containing a set of interconnected micro channels that are used to electrophoretically separate RNA fragments according to their size. The assessment of total RNA quality is based on the calculation of 28S rRNA to 18S rRNA ratio and the estimation of integrity of the total RNA sample, i.e. RNA integrity number (RIN). RIN is estimated taking into consideration the entire electrophoretic trace of the RNA sample.

2.2.4.6 cDNA Synthesis - Reverse transcription polymerase chain reaction (RT-PCR)

The process of RT-PCR is catalysed by reverse transcriptase and involves the synthesis of single stranded cDNA from RNA template. Obtained cDNAs can then be used in further applications that require the direct comparison of samples as the amounts of cDNA produced are linear.

Briefly, 1µg/µl or 100ng/µl of isolated, DNase I treated RNA of interest was transferred to 0.5ml microcentrifuge tubes, mixed with 1µl of either oligo dT primers (0.5µg/µl) (used to produce full length cDNA to be send for sequencing) or random primers (used to produce fragments of cDNA to be used for Quantitative Real Time Polymerase Chain Reaction (Q RT PCR)) and supplemented with dH₂O to a final volume of 13µl. To denature the RNA, the reaction mix was incubated at 65°C for 5 min and chilled on ice. Each sample was then supplemented with 7.6µl of the reaction master mix, containing the following (final concentrations are shown): 1xReaction Buffer, 1mM dNTPs mix (10mM), 1U/µl of RNase OUT (40U/µl), 0.03% of DMSO and 0.5U/µl of Transcriptor Reverse Transcriptase (20U/µl). The resulting mix was incubated at 25°C for 10 min, followed by 50°C for 30 min, to allow primer annealing, and 85°C for 5 min to inactivate Transcriptor Reverse Transcriptase. In each reaction run, a negative control that lacked reverse transcriptase (-RT) was prepared along with the samples of interest to measure the presence of any DNA contamination.

2.2.4.7 Standard PCR

Primer Design

Design of the primers was performed either using Primer3 software developed at the Whitehead Institute for Biomedical Research (<http://frodo.wi.mit.edu/>) (Rozen S., Skaletsky H. J., 2000) or manually using either Ensemble Genome Browser (<http://www.ensembl.org/index.html>) or the Gene database at the National Centre for Biotechnology Information (NCBI) (National Library of Medicine, Bethesda, USA) available at: <http://www.ncbi.nlm.nih.gov/> to view the gene sequence and BLAST algorithm (<http://blast.ncbi.nlm.nih.gov/Blast.cgi>) to ensure that the designed primers were sequence specific. The characteristics of the designed primers, such as melting temperature (T_m), likely presence of secondary structure or probability to form primer-dimer complexes were examined either by Primer 3 software or using the DNA calculator application available from Sigma-Aldrich® (<http://www.sigma-genosys.com/calc/DNACalc.asp>). A list of primers used for PCR is shown in **Table 2-5**.

PCR conditions

All the reactions were prepared in a final volume of 50 μ l in 0.5ml PCR tubes. Each reaction contained the following: 2 μ l of cDNA template, 1xGreen GoTag® Flexi Buffer (5x), 1mM MgCl₂ (25mM), 0.2mM dNTPs mix, 1 μ M of forward (10 μ M) and 1 μ M of reverse primers (10 μ M) (**Table 2-5**), 0.025U/ μ l GoTag® DNA Polymerase (5U/ μ l) and dH₂O. For each PCR run, a control reaction that lacked template cDNA was prepared to ensure that no contamination was present. The cycling was performed using a Biometra T 3000 Thermocycler under the following conditions: initial denaturation at 95°C for 2 min followed by multiple cycles of 95°C for 15 sec (denaturation), 60°C for 30 sec (annealing), 72°C for 1min/1kb of amplicon (extension) and a final step of extension at 72°C for 10 min. The number of cycles employed in each PCR varied from 28 to 30 depending on the abundance of transcript.

2.2.4.8 DNA Agarose Gel Electrophoresis

PCR products were separated by size using agarose gel electrophoresis with 1% or 1.5% agarose gels and 0.5xTAE running buffer (Tris-acetate-EDTA, pH8.5). Agarose gels were prepared by diluting electrophoresis grade agarose in 0.5X TAE buffer and adding 1-2 μ l of intercalating dye ethidium bromide (10mg/ml) to the gel to facilitate visualisation of amplicons. 10-20 μ l of each PCR product was then mixed with 0.4 volumes of 5xGreen GoTag[®] Flexi Buffer and loaded into each well of the gel and electrophoresis was carried out at 90-110V. Gels were examined using Fujifilm Fla-5000 and FLA5000 Image Reader software v. 2.0 (Fujifilm UK Ltd., Sheffield, UK). Images were manipulated using Advanced Image Data Analyser v. 4.13 (Aida) (Fujifilm UK Ltd., UK) or Adobe Photoshop CS2 (Adobe Photoshop Systems Inc., Mountain View, US). Either a 100bp or 1kb DNA ladder was used as a size marker.

2.2.4.9 Q RT PCR

Real time PCR is a quantitative method used to determine transcript expression levels using cDNA synthesised from the sample of interest as template for gene amplification via PCR. For the purposes of this project a hydrolysis probe-based system was chosen for the detection and quantification of amplicons. Each hydrolysis probe is sequence specific, with labelled probes, designed to anneal to template cDNA flanked by the two primer sites. Hydrolysis probes contain a fluorescent reporter dye at their 5' end and a quencher label at their 3' end. The 3' end of each probe is phosphorylated, hence it can not be extended during the PCR. When the probe is not annealed, fluorescence is suppressed by the close proximity of the quencher and is undetectable. During the annealing process of the PCR the probe hybridises to the template before the primers due to its lower T_m. FastStart Taq DNA Polymerase cleaves the probe due to its 5'-3' exonuclease activity, while extending the primer, hence releasing the dye, whose fluorescent emission can then be measured. The fluorescent signal increases exponentially with each PCR cycle until the reagents are used up.

Transcript name	Species	Forward primer	Reverse primer	Amplicon size (bp)	T _m (°C)
Upk3a	mouse	tctgtgcatgtttgatagctca	gaagcttgctggagaacacc	710	63,63
Fbln2 V1	mouse	cctgcaaagacaatggacc	tcgtccacgtctgtgcattc	394	66,67
Fbln2 V2	mouse	cctgcaaagacaatggacc	tcgtccacgtctgtgcattc	256	66,67

Table 2-5 Primers used in Standard PCR.

T_m stands for melting temperature.

Transcript name	Species	Forward primer	Reverse primer	Probe sequence	Amplicon position (bp)
Fbln2 V1	M.m.	tgttggtggggacacagcta	ccatcaaactcgtcttggt	ctgcttcc	2202-2296
Fbln2	M.m.	tctgtcccagaggtgatct	ctgcacaacaggtctcgattag	ctccacca	1402-1462
Fbln2 V1	H.s.	caggtggcctctaaccacat	ttgcaggttcattgtcttt	tgccactg	2124-2193
Fbln2	H.s.	Agctgcaccacggagagt	cctctgtgccagtgaca	tggtgatg	4732-4803
Ect2	M.m.	cgacatgtagccaacacat	ttgtatttacttcaaggattct	tgtggctg	2371-2456
Upk3a	M.m.	Ttctgctcgtgggttc	cattccccatcagaactgc	tcctcagc	740-811
Upk3a	H.s.	ccctgcccttcttctacttg	atcagaactccccatgtcca	cctcagcc	656-729
Fbn2	M.m.	gcctgtcctgtcagaggttc	caccatcggagaccat	ctgtgcct	1331-1394
Emb	M.m.	tgggtaatgaaaccgcaca	gtggcacgacaccagtagg	ggagga	804-945
Dlg7	M.m.	gttgcgacattgttggat	aaaccgactggcaaacg	ggatgctg	264-330
Itih2	M.m.	aagagcaaagggcaagacg	tcacctctgtgttgaagttctc	aggagcag	553-626
β actin	M.m.	aaggccaaccgtgaaaagat	gtggtacgaccagaggcatac	tgctgtcc	416-525
β actin	H.s.	Attggcaatgagcggttc	tgaaggtagttcgtggatgc	cttccagc	832-922
Krt18	M.m.	agatgacaccaatcacacaag	ctccagaccttgacttctc	agctggag	600-709
Krt18	H.s.	tgatgacaccaatcacacga	ggcttgtaggccttttacttcc	agctggag	682-793
Ltf	M.m.	Gggcaagtgcggttagtt	ccattgctttggaggattt	tgccagag	1294-1353
Sema3B	M.m.	Ttcttctccgcgagtcc	gccaccaggtcattcct	ggaagcag	939-1034
Sprr1A	M.m.	cctgaagacctgatcaccaga	aggcaatgggactcataagc	ggctgctg	504-566

Table 2-6 Probes and primers used in Q RT PCR.

For species, M.m. stands for *Mus musculus* while H.s. stands for *Homo sapiens*. Amplicon position refers to the position of amplicon on mRNA with regards to the 5' end of the genes which corresponds to transcription start site on DNA.

Name of the primer	Primer sequence	Primer annealing site (bp)	T _m (°C)
Fbln2 V1 684	gtaacttctcggatgctgagg	684	64
Fbln2 V1 1607	caaggagggtgagacctgtg	1607	65
Fbln2 V1 2060	atagaggtgccccacaagttg	2060	64
Fbln2 V1 3192	gcatacctgcacagacatcg	3192	64
Fbln2 V1 3488	tcacggaatgtcaaactca	3488	64
T7 promoter	taatacgaactcactataggg		51
Upk3a	gaagcttgctggagaacacc	714	63

Table 2-7 Primers used in sequencing.

For Fbln2 and Upk3a based primers the start of primer annealing site refers to the position on cDNA. Primer annealing site on T7 promoter refers to the position on the plasmid (pRc/CMV-Fbln2). T_m stands for melting temperature.

Probe and primers design for Q RT PCR

The selection of hydrolysis probes and the design of the primers were performed using ProbeFinder software (Roche Applied Science, Germany) (www.roche-applied-science.com). ProbeFinder software uses transcript information deposited in NCBI Reference Sequence Database to find the optimal set of probe and primers for each transcript of interest. Primers were selected to be on either side of exon-exon splice junctions to eliminate false positive signals from DNA contamination. A list of the primers and probes used is shown in **Table 2-6**.

All primer sequences were designed to have a melting temperature (T_m) of 60°C and flank probe hybridisation sites. All primers were purchased from Sigma Aldrich Company Ltd., Dorset, UK.

Q RT PCR Conditions

Q RT PCR for each sample was performed as follows: 1µl of template cDNA was added in triplicate to the wells of LightCycler® 480 96 Well Plates. A negative control that lacked reverse transcriptase (-RT) during cDNA preparation was included on each plate to measure the presence of any residual, contaminating DNA and estimate the level of background noise. Each well was then supplemented with the following reaction mix: 0.1µM of probe (2µM), 0.36µM of the forward (7.2µM) and 0.36µM of the reverse (7.2µM) primers (**See Table 2-6**), 1xLightCycler® 480 Probes Master (2x) and H₂O to a final reaction volume of 20µl. The stock 2xLightCycler® 480 Probes Master contained dNTPs (10mM), 6.4mM MgCl₂ and FastStart Taq DNA Polymerase which is a thermostable polymerase only activated at high temperatures.

The Prepared 96-well plate was then sealed using LightCycler® 480 Sealing Foil and centrifuged at RT at 850rcf for 2 min. The PCR was carried out using a LightCycler® 480 Instrument as follows: 1 cycle at 95°C for 10 min to activate the FastStart Taq DNA Polymerase, 40-50 cycles at 95°C for 15 sec followed by 60°C for 30 sec to perform primer and probe annealing and cDNA amplification and 1 cycle at 40°C for 30 sec to cool down.

The cDNA of each sample was amplified using probes and primers designed to amplify the gene of interest and house keeping genes: *β-actin* or *Krt18*. The raw data for each sample was then analysed using LightCycler® 480 software v.1.5 (Roche Applied Science, Germany), measuring the level of detected fluorescence over each PCR cycle and plotting an amplification curve for each sample. Every reaction profile consisted of three phases: lag phase (background phase), exponential log phase and plateau phase (**Figure 2-3 A**). The fluorescence values of the log phase only were retained for analysis.

Relative Gene Expression Analysis

The fluorescence signal was analysed as follows: PCR cycles from the beginning up to 5 cycles before the beginning of the log phase, showing irregular fluorescence were excluded (**Figure 2-3 A**); the noise band was set to eliminate background noise (**Figure 2-3 B**); 6 fit points were selected to calculate the fitted log-line of the exponential portion of each amplification curve and the threshold line was manually fitted in the middle of the calculated log-line and the crossing point (Cp) values (cycle number at which given sample crosses given fluorescence threshold) were calculated for each sample along with the standard deviation (SD) (**Figure 2-3 C**).

Cp values obtained for individual samples amplified, using both primers of interest and house keeping primers, were used to calculate the relative concentration of transcripts. Calculations were performed with Microsoft Excel® using the $2^{-\Delta\Delta C_p}$ method as follows: the difference in Cp (ΔC_p) between the transcript of interest and a house keeping gene was calculated for each sample. The difference in ΔC_p ($\Delta\Delta C_p$) between compared samples was then calculated and the relative gene expression (expression fold change) was calculated between the compared samples by setting $\Delta\Delta C_p$ of the reference sample to 0 and following $2^{-\Delta\Delta C_p}$ equation.

2.2.4.10 DNA Sequencing

Sequencing of linear DNA or plasmid DNA was performed via the GATC Biotech sequencing service (<http://www.gatc-biotech.com/en/home.html>) using

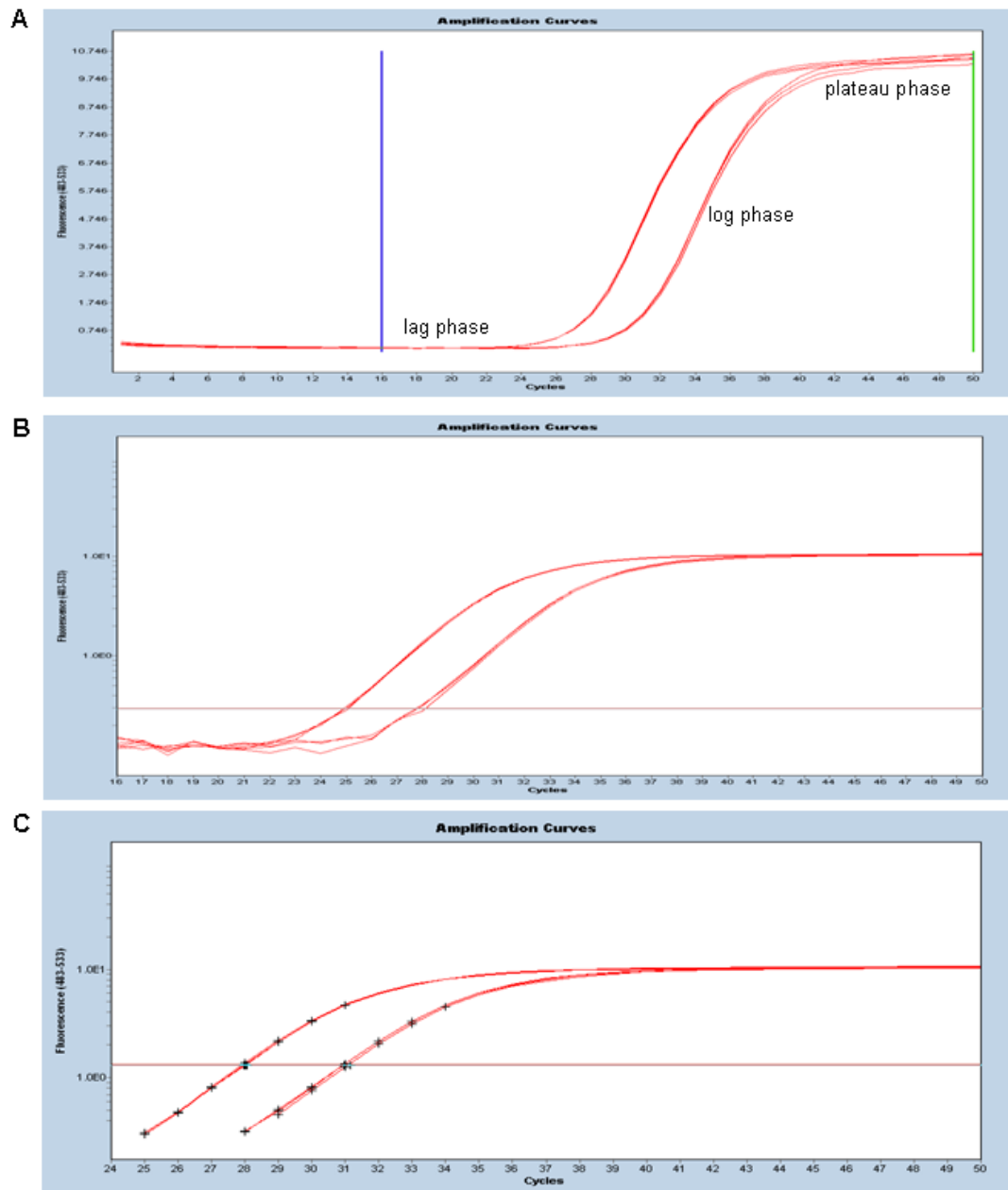


Figure 2-3 Histograms showing comparison analysis of amplification curves of Q RT PCR product amplified from two distinct samples.

Y axis shows level of detected fluorescence. X axis shows number of PCR cycles **(A)** Amplification curves showing lag, log and plateau phases. Setting of the cut off band for exclusion of signal generated during initial PCR cycles **(B)** Setting of the background noise band cut off **(C)** Selection of fit points and calculation of Cp values. Cp value for each sample corresponds to number of PCR cycles calculated at the crossing point of amplification curve with purple horizontal line. Figures were exported from LightCycler® 480 software v.1.5.

30ng/ μ l subjected DNA and 10pmol/ μ l of forward primer. Obtained chromatograms were visualised using Chromas Lite v.2.01 software (Technelysium Pty Ltd., Tewantin, Australia). A list of primers used in sequencing is shown in **Table 2-7**.

2.2.4.11 Restriction Digestion

Restriction digestion was performed using Sma I enzyme to identify the correct clones of pRc/CMV-Fbln2 DNA (**See 2.2.2.3**). 1 μ g/ μ l of plasmid DNA, 1xJ Buffer (10mM Tris-HCl, 7mM MgCl₂, 50mM KCl, 1mM DTT, pH7.5), 0.1 μ g/ μ l of acetylated BSA (10 μ g/ μ l) and 0.25U/ μ l of Sma I enzyme (10U/ μ l) were mixed with dH₂O to a final volume of 20 μ l. The reaction mix was then incubated at 25°C for 4h. The differently sized restriction digestion products were resolved and visualised via electrophoresis, using 1% agarose gel (**See 2.2.4.8**).

2.2.5 Microarray analysis of pubertal gene expression

Gene expression profiling was performed on the isolated pubertal epithelium of TEBs and ducts, pubertal mammary gland tissue strips (Pre-LN, Post-LN and Fat pad) and whole adult mouse mammary glands (negative control for pubertal gene expression) collected from female mice. Biological material was then processed to extract good quality RNA. RNA was converted to single strand (ss) cDNA which was then hybridised to microarray chips. Obtained data was normalised, assessed in terms of its quality and analysed.

2.2.5.1 Collection of the experimental material

All experimental material was obtained from both left and right 4th mammary glands collected from pubertal or adult virgin WT or TG female mice. The excision of mammary glands from WT and TG mice was performed at the Biological Services Central Facilities at Gilmorehill Campus, Glasgow and at the Beatson Institute for Cancer Research in Glasgow respectively, following the methodology described before (**See 2.2.1.2**).

WT females were used for isolation and collection of the mammary gland epithelial structures, i.e. TEBs and ducts (**See 2.2.1.5**) and whole mammary

glands (See 2.2.1.2). Epithelium was collected into 100µl of TRIzol[®] reagent and stored at -80°C until subjected to RNA extraction. Whole mammary glands were subjected to central LN removal upon dissection, snap freezing in liquid nitrogen and storing at -80°C until RNA extraction. TG mice were used to collect the tissue strips (See 2.2.1.4) which were snap frozen in liquid nitrogen upon collection and stored at -80°C until RNA extraction.

2.2.5.2 Extraction, purification, concentration, quantification and quality assessment of RNA

RNA was extracted from isolated epithelium stored in TRIzol[®] reagent, mammary gland tissue strips and whole mammary glands stored at -80°C, as described previously (See 2.2.4.1.1-2.2.4.1.3). Extracted RNA was quantified using the NanoDrop ND-1000 Spectrophotometer (See 2.2.4.4), purified, subjected to on-column DNase I treatment, combined and concentrated using an RNeasy[®] Mikro Kit (See 2.2.4.3). The RNA was then re-quantified as described above and its quality assessed using the Agilent 2100 bioanalyser (See 2.2.4.5).

2.2.5.3 Microarray data generation workflow

Samples of extracted and purified RNA were used as a matrix to generate single strand, sense, biotin labelled cDNAs that were hybridised to GeneChip[®] Mouse Exon 1.0 ST Arrays, following GeneChip[®] Whole Transcript (WTr) Sense 1µg Total RNA Target Labelling Assay Manual (Affymetrix UK Ltd., High Wycombe, UK) (Figure 2-4) and using appropriate Affymetrix kits. All of the experimental procedures described in sections 2.2.5.3.1-2.2.5.3.8 were performed at the Henry Wellcome Functional Genomics Facility by Mrs. Wang.

Briefly, 1.5µg of each total RNA resuspended in a maximum volume of 3.2µl of RNase-free H₂O was mixed with 2µl of supplied, freshly diluted Poly-A RNA controls (4 different transcripts) mix.

2.2.5.3.1 Reduction of ribosomal RNA (rRNA)

Total RNA/Poly-A RNA controls mix was then subjected to reduction of 28S and 18S ribosomal RNA (rRNA) populations using a RiboMinus Human/Mouse

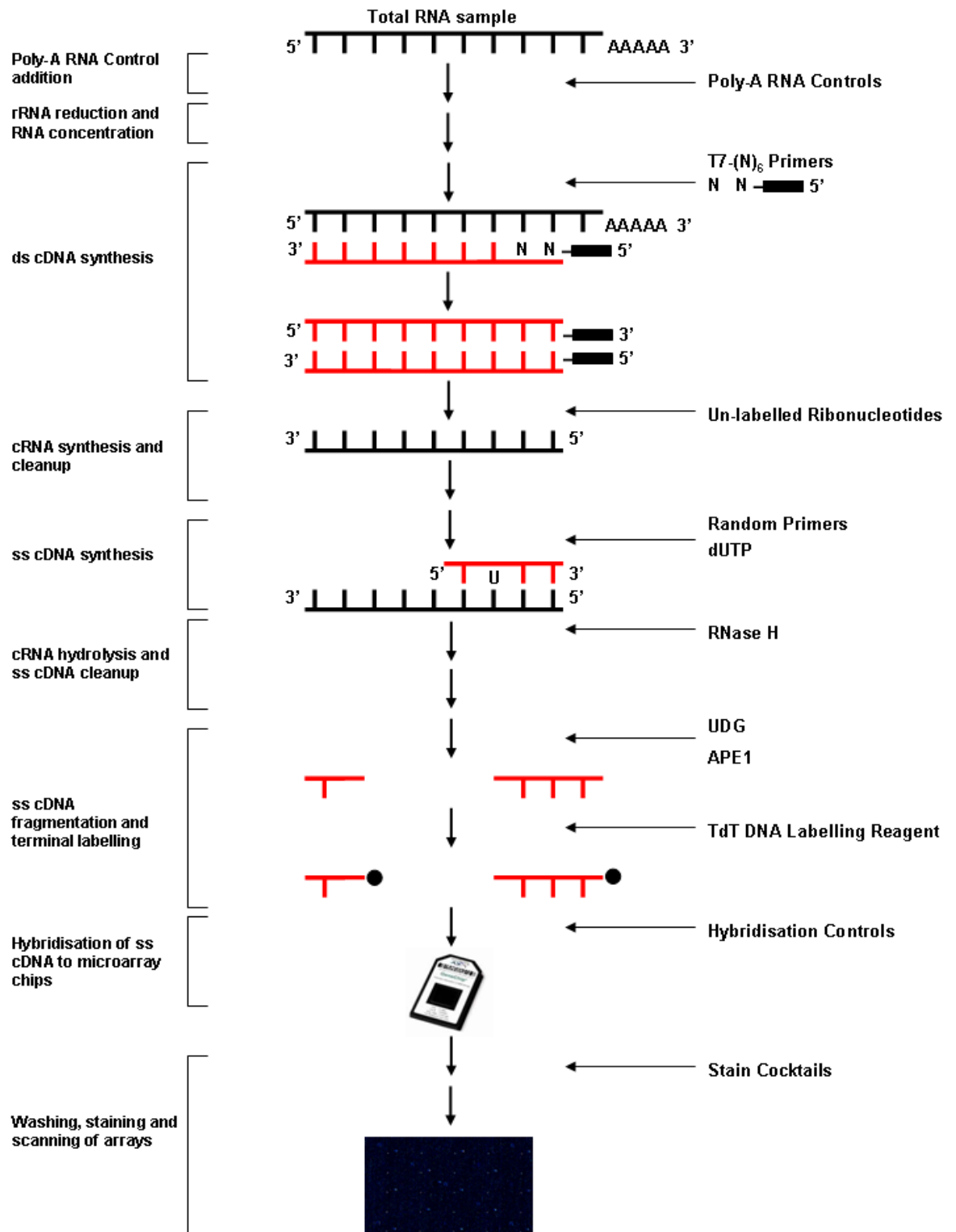


Figure 2-4 GeneChip® WTr Sense 1µg Total RNA Target Labelling Assay Manual – Schematic representation of the experimental steps.

Transcriptome Isolation Kit which facilitates hybridisation of four biotinylated LNA RiboMinus probes (100pmol/ μ L) to abundant 18S and 28S rRNA species in the total RNA of interest, in the presence of betaine to increase hybridisation stringency. Probe bound rRNAs were then removed from the hybridisation mix using streptavidin coated RiboMinus Magnetic Beads and supernatant containing rRNA-Reduced Total RNA/Poly-A RNA Controls Mix was concentrated using GeneChip[®] IVT cRNA Cleanup Kit. The quality of recovered RNA was analysed with the Agilent 2100 bioanalyser (See 2.2.4.5).

2.2.5.3.2 Synthesis of double stranded cDNA (ds cDNA)

rRNA-reduced total RNA/Poly-A RNA Controls Mix was then used as a template for the synthesis of the ds cDNA using GeneChip[®] WTr cDNA Synthesis Kit. First-strand cDNA synthesis was performed using random primers tagged with T7promoter sequence (500ng/ μ l), SuperScript II reverse transcriptase, dNTPs (10mM), DTT (0.1M) and 5x1st Strand Buffer. Second-strand cDNA synthesis was carried out using MgCl₂ (17.5mM), dNTPs (10mM) and DNA Polymerase I to facilitate the synthesis and RNase H to degrade the mRNA hybridised to the first-strand DNA.

2.2.5.3.3 Synthesis of cRNA

Obtained ds cDNA was subsequently used as a template for antisense cRNA production. cRNA synthesis was facilitated by T7 RNA Polymerase using a GeneChip[®] WTr cDNA Amplification Kit. cRNA was then purified by means of a GeneChip[®] Sample Cleanup Module and quantified using a NanoDrop ND-1000 Spectrophotometer (See 2.2.4.4).

2.2.5.3.4 Synthesis of ss cDNA

Purified cRNA was reverse transcribed by means of a GeneChip[®] WTr cDNA Synthesis Kit using random primers (3 μ g/ μ l), SuperScript II reverse transcriptase, DTT (0.1M), dNTP+dUTP (10mM) and 5x1st Strand Buffer. ss cDNA containing incorporated dUTP was then hydrolyzed from cRNA-cDNA hetero-duplexes by

means of RNase H, purified using the GeneChip[®] WTr cDNA Synthesis Kit and the GeneChip[®] Sample Cleanup Module as per manufacturer's instructions and quantified using a NanoDrop ND-1000 Spectrophotometer (See 2.2.4.4).

2.2.5.3.5 Fragmentation and terminal labelling of ss cDNA

The ss cDNA was then subjected to fragmentation and labelling using a GeneChip[®] WT Terminal Labelling Kit. Fragmentation was facilitated by the combination of uracil DNA glycosidase (UDG) (10U/ μ l) and apurinic/apyrimidinic endonuclease 1 (APE 1) (1000U/ μ l) which recognise exogenous dUTP residues. The efficiency of fragmentation, i.e. the size range of obtained ss cDNA fragments, was profiled using an Agilent 2100 bioanalyser (See 2.2.4.5).

The labelling of DNA was performed by terminal deoxynucleotidyl transferase using an Affymetrix[®] DNA labelling reagent covalently linked to biotin.

2.2.5.3.6 Hybridisation of ss cDNA to microarray chips

Fragmented and biotin labelled ss cDNA was hybridised to GeneChip[®] Mouse Exon 1.0 ST chips using a GeneChip[®] Hybridisation, Wash and Stain Kit. Internal hybridisation quality controls such as bioB, bioC, bioD, cre and oligonucleotide B2 were hybridised to the chips alongside the target cDNA in the presence of 7% DMSO and 2xHybridisation Mix. Biotinylated oligonucleotide B2 hybridises to features around the edge, inside and in the corners of the chip and the signal that it emits is used to align the grid of the array (See 2.2.5.3.8). BioB, bioC, bioD and cre are probe sets for prokaryotic genes. Pre-prepared at varied concentrations, ss cDNAs of BioB, bioC, bioD and cre serve as internal hybridisation controls (See 2.2.5.8). Array hybridisation was performed by 16h long incubation in 45°C in a hybridisation oven with agitation at 60rpm.

2.2.5.3.7 Washing, staining and scanning of the arrays

Hybridised arrays were washed, stained and scanned using a GeneChip[®] Hybridisation, Wash and Stain Kit. Staining of the arrays was performed by using

Streptavidin Phycoerythrin (SAPE) that binds to biotin on hybridised cDNA. SAPE signal was amplified by using anti-streptavidin biotinylated antibody and anti-biotin SAPE conjugated antibody. The amplified signal intensity emitted by SAPE was detected and measured during scanning of the arrays. All above procedures were performed with a GeneChip® Fluidics Station 450/250 and GeneChip® Scanner 3000 7G, operated by GeneChip® Operating Software (GCOS) (Affymetrix UK Ltd., UK). All samples were washed, stained and scanned together to reduce technical variability.

2.2.5.3.8 Signal detection and calculation of the cell intensity data (.CEL file)

Signal intensity emitted by SAPE bound to each probe was detected by the scanner and imaged using GCOS which displays a picture of each scanned array (.DAT file) and superimposes the grid on the image. The main grid and sub-grids are generated using an Alignment Algorithm which uses check board images of oligonucleotide B2 positive hybridisation controls located at the corners of the array to superimpose the grid on the scanned image and align it so that each square in the grid delineates a probe cell.

A Cell Intensity Algorithm was then used to compute a single intensity value for each probe cell using fluorescence intensity values from each pixel on the array to calculate the cell intensity data (.CEL file).

2.2.5.4 Background correction, normalisation and probe set summarisation

The .CEL file was further analysed using a Robust Multichip Analysis (RMA) algorithm, a multi-chip approach that consists of three steps: background correction, normalisation and data summarisation.

The RMA algorithm was computed using either Expression Console™ software v.1.0 (Affymetrix UK Ltd., UK), Partek® Genomics™ Suite (Partek Incorporated, St Louis, US) or XRAY Excel® Array Analysis v.2.5 (Biotique Systems Inc. Reno, USA). All analyses were performed at the core level, i.e. only taking into

consideration probe sets mapped to BLAST alignments of mRNA with annotated full length gene coding sequences.

Background correction of intensities of perfect match (PM) probes was used to remove systematic effects that could not be explained by biological variation within each individual chip. It uses only information contained on the given chip and it is based on the model $O = S + N$, where O stands for overall intensity; S stands for signal and is assumed to be exponentially distributed (α); N means background noise which is assumed to be normally distributed ($\mu \sigma^2$) [267]

Normalisation was used to remove the non-biological variation throughout all microarray chips used for the experiment. In this experiment non parametric quantile normalisation was used, which is based on the assumption that there is a common pattern of distribution of intensities across the microarray chips [268]. For each input array, for each probe expression value the ' i^{th} ' percentile probe expression value is replaced by the average of all ' i^{th} ' percentile points across all of the arrays. When all the probe scores are sorted, a master distribution of intensity is created and the distribution of intensity for each probe is mathematically fitted to the master distribution of intensity.

Summarisation of the probe intensity levels across each microarray chip obtained summarised expression values (.CHP files) for each transcript ID or exon cluster ID. This was performed using Median Polish which takes into consideration probe and chip effects, predicting transcript ID or exon cluster ID expression and combining the information across the chips. Median Polish is an algorithm that takes \log_2 of the probes' signal intensity and fits a robust linear model.

In summary, the process of computing the expression data using RMA provides final signal intensity data which can be interpreted as

$$E = S(N(B(X)))$$

Where E is the final intensity data of either the transcript ID or exon cluster ID, S is Median Polish summarization, N is quantile normalisation, B is the RMA background correction process and X is the raw intensity of probes across the whole array.

2.2.5.5 Gene expression analysis at the gene level - The identification of 'up-regulated gene sets'

This section and the following section 2.2.5.6 should be read in conjunction with Figure 3-1 (p.151).

Gene expression analysis at the gene level was performed using transcript IDs. The 'up-regulated gene sets' - list of genes are up-regulated above the set level in one environment when compared to the other environment. 'Up-regulated gene sets' were identified for the epithelial transcriptomes of TEBs and ducts (See 2.2.5.5.1), epithelial-stromal transcriptomes of TEBs and ducts (See 2.2.5.5.2) and the epithelium-free Fat pad (See 2.2.5.5.3).

2.2.5.5.1 TEB and duct epithelium 'up-regulated gene sets'

Transcripts whose expression was higher in the epithelium of TEBs than in ducts or higher in ducts than in TEBs were identified using signal intensity data obtained from isolated epithelium of TEBs and ducts. Differentially expressed transcripts were identified using a 5% Limit Fold Change (5% LFC) Model [269] and the transcript ID expression data obtained using the RMA algorithm (Expression Console™ software v.1.0).

The 5% LFC Model was calculated as follows: First, signal intensity data for all transcripts obtained from duplicate TEB samples (T1 and T2) and duplicate duct samples (D1 and D2) were evaluated to exclude transcripts characterised by too low an expression intensity (background expression), i.e. average difference intensity (ADI). As recommended, to reduce background noise the ADI threshold was set to 20 and transcript IDs with ADIs equal to or lower than 20 were set to 20 across all experiments (T1, T2, D1, D2) and therefore eliminated [269]. ADIs of each transcript were then compared between the replicates of individual samples (T1 vs T2 and T2 vs T1) and (D1 vs D2 and D2 vs D1) to exclude transcripts of expression level variation between replicates greater or equal to 2. ADIs of the remaining transcripts were then used to calculate the mean ADI for TEBs and mean ADI for ducts. The mean ADI for each transcript over-expressed in either TEBs or ducts was computed using the expression data of T1

and T2 or D1 and D2 respectively. Non-annotated internal Affymetrix controls, as enlisted by Affymetrix UK Ltd were subtracted from the 2 transcript IDs lists. The mean ADI values for the TEB and duct associated transcripts were then utilised to calculate the highest fold change (HFC), i.e. a maximum change in gene expression between the compared samples. The HFC for the TEB associated transcripts was obtained by calculating the ratio of the mean ADI in TEBs to mean ADI in ducts for each transcript. The HFC for each ducts-associated transcript was obtained by calculating the ratio of the mean duct ADI to mean TEB ADI for the given transcript. The remaining transcripts in each data set (TEB or duct) were then sorted according to their mean ADI, divided into 200 gene rich bins and sorted within each bin, descending according to HFC. The top 5% of transcripts within each bin were considered as significantly over-expressed. Finally gene rank was assigned to each transcript. Gene rank was calculated by multiplying HFC by ADI therefore incorporating both the magnitude of fold change (FC) and expression value.

All of the above calculations were performed using Microsoft Excel. Transcript IDs were annotated using the NetAffx Analysis Centre tool developed by Affymetrix.

2.2.5.5.2 TEB and duct epithelial-stromal ‘up-regulated gene sets’

To compare transcripts of epithelial genes within a stromal environment rather than in isolation, mammary gland tissue strips were analysed using transcript ID signal intensity data. Expression levels of each transcript were compared between Pre-LN and Post-LN of mammary gland tissue strips and transcripts whose expression was differentially expressed between TEBs and duct environments were identified. The RMA algorithm, statistical analysis and identification of significantly differentially expressed transcripts were performed using Partek[®] Genomics[™] Suite. Bioinformatic analysis of the data sets was performed at the core level, using 2-Way Alternative Splice Paired ANOVA. Transcripts of at least 1.5 fold change in expression and with p-value<0.05 were considered as significantly differentially expressed.

2.2.5.5.3 Epithelium-free Fat pad ‘up-regulated gene set’

To identify genes differentially expressed in the epithelium-free Fat pad of the pubertal mouse mammary gland the expression levels (signal intensity data) of each transcript ID were compared between the Fat pad and Post-LN tissue strips data sets. Gene expression analysis was performed using Partek® Genomics™ Suite as described above (2.2.5.5.4). Transcripts of at least 1.5 fold change in expression and with $p\text{-value} < 0.05$ were considered as significantly differentially expressed.

2.2.5.6 Gene expression analysis on the gene level – The identification of ‘expressed gene sets’

The ‘expressed gene sets’ are defined as lists of genes expressed ≥ 1.1 fold change cut off in one environment when compared to the other environment

2.2.5.6.1 TEB- and duct-only epithelium ‘expressed gene sets’

Genes expressed in the epithelium of TEB and ducts were identified using signal intensity data obtained from the microarrays performed on the epithelium of isolated TEBs and ducts. Signal intensity data was obtained using RMA performed by Expression Console™ software v 1.0. All transcript IDs corresponding to non-annotated internal Affymetrix controls were excluded from the data sets as described above. ADIs lower than 20 were set to 20. The signal intensity levels of each transcript ID were compared in multiple ways between replicates in the TEB and duct data sets (T1 vs D1) (T1 vs D2) (T2 vs D1) and (T2 vs D2) to calculate the minimum change in gene expression between the compared data sets, i.e. MFC. All transcript IDs with a FC equal to 1 across all four comparisons were excluded from the analysis. The remaining transcript IDs were divided into genes expressed only in either TEBs or ducts. All transcripts with a MFC increase of 1.1 in the TEBs compared to ducts were considered to be only expressed in TEBs, while the ones with a MFC decrease in expression of 1.1 were considered as only expressed in the ducts.

All of the above calculations were performed using Microsoft Excel. Transcripts IDs were annotated using the NetAffx Analysis Centre tool developed by Affymetrix.

2.2.5.6.2 TEB- and duct-only stroma 'expressed gene sets'

Transcripts expressed in the stroma surrounding TEBs and the stroma around ducts were identified using signal intensity data obtained from the mammary gland tissue strips and isolated epithelium. For the purpose of this analysis RMA was performed using Expression Console™ software v 1.0 and the obtained signal intensity data sets were used to identify TEB-only stroma- or duct-only stroma-associated transcripts.

Transcript ID expression levels obtained from the Post-LN, isolated epithelium of TEBs and ducts data sets were compared and used to identify stromal genes around TEBs and ducts in the Post-LN strip. Stroma expressed transcripts were identified by subtracting all transcript IDs whose expression was associated with epithelium of TEBs or ducts from the list of Post-LN transcript IDs, as follows. Transcript IDs corresponding to non-annotated internal Affymetrix controls were excluded from the data sets, as described above. ADIs lower than 20 were set to 20 and any transcripts with an ADI value of 20 across all replicate data sets within each experimental condition (Post-LN 1, Post-LN 2, Post-LN 3) (T1, T2) (D1, D2) were eliminated to reduce background noise. Expression levels of each transcript ID were compared in multiple ways between replicates for Post-LN and TEB data sets (Post-LN 1 vs T1, Post-LN 2 vs T1, Post-LN 3 vs T1, Post-LN 1 vs T2, Post-LN 2 vs T2, Post-LN 3 vs T2) and Post-LN and duct data sets (Post-LN 1 vs D1, Post-LN 2 vs D1, Post-LN 3 vs D1, Post-LN 1 vs D2, Post-LN 2 vs D2, Post-LN 3 vs D2) to calculate the minimum change in gene expression between compared data sets, i.e. MFC. Expression ratios of each transcript ID between Post-LN and TEB data sets and Post-LN and duct data sets were examined and used to exclude the transcript IDs expressed in epithelium from the Post-LN data set. All transcripts with a minimum of 1.1 FC increase in the Post-LN data set in comparison to their expression in TEBs or ducts were considered as stromal. The epithelial expression marker, *cytokeratin 14 (CK14)* expression level was used to identify the FC cut off between epithelial and stromal genes. *CK14* expression

was 2.6 and 2.7 times lower in the Post-LN data set than in TEB and duct data sets respectively and thus a FC cut off of 1.1 ought to minimise the number of the epithelial genes falsely identified as stromal.

Transcript ID expression levels obtained from the Pre-LN, isolated duct epithelium and TEB epithelium data sets were compared and used to identify the stromal genes expressed around ducts and occasional TEBs in the Pre-LN strips. Stroma expressed transcript IDs were identified by subtracting all transcript IDs whose expression was shown to be associated with the epithelium of ducts or TEBs from the list of Pre-LN transcript IDs, as described above.

Finally the lists of transcript IDs expressed in the Post-LN strip stroma and Pre-LN strip stroma were compared using GeneVenn List Diagram (University of Southern Mississippi, <http://mcbc.usm.edu/genevenn/genevenn.htm>) to exclude the common transcript IDs and identify those associated with only the stroma around either TEBs in Post-LN tissue strips or ducts in Pre-LN tissue strips.

All of the above calculations were performed using Microsoft Excel. Transcript IDs were annotated using the NetAffx Analysis Centre tool developed by Affymetrix.

2.2.5.7 Expression Analysis at the exon level

Gene expression analysis at the exon level was performed for isolated TEBs and ducts using exon cluster ID signal intensity data. Gene expression analysis at the exon level was performed to analyse alternative splicing and differential expression of each exon within a gene throughout the data sets.

After converting probe cell signal intensity data into exon cluster ID signal intensity data using the RMA algorithm, expression analysis was performed by comparing Pre-LN, Post-LN and mammary fat pad tissue strip data sets with isolated TEB and isolated duct data sets, to identify transcript IDs which had alternative splice variants differentially expressed in TEB and duct environments. The RMA algorithm, statistical analysis and identification of significantly differentially expressed transcripts and alternatively expressed

splice variants were performed using XRAY Excel[®] Array Analysis v.2.5 Microsoft[®] Excel[®] add-in. Bioinformatic analysis of the data sets was performed at the core level, using a Nested Mix Model ANOVA and the Benjamini and Hochberg False Discovery Rate (FDR) Multiple Test Correction. Probe sets not significantly expressed above background, i.e. of a p-value \geq 0.05 derived using the Fisher Test were excluded from the analysis. Whole transcripts and splice variants of at least 2 fold change in expression and p-value $<$ 0.05 were considered to be significantly differentially expressed.

2.2.5.8 Microarray data quality assessment

Quality and reliability of the data generated during microarray analysis was assessed using six different quality assessment metrics:

- Visual assessment of microarray chips.
- Quality of hybridisation was estimated by investigating the probe set signal intensity values for prokaryotic internal hybridisation controls (bioB, bioC, bioD, cre) throughout the arrays. The signal intensities were graphed using Expression Console[™] software v 1.0.
- The degree of similarity between the replicates of each biological sample and the variation between different biological samples was investigated and graphed using PCA (Principal Component Analysis). PCA is a method designed to capture the variation in the datasets by reducing the dimensionality of the data to capture the most important features. PCA analysis was performed using Partek[®] Genomics[™] Suite.
- Reliability of the generated gene lists was verified by screening these lists for the presence of previously published genes known to be associated with epithelium of TEBs, epithelium of ducts, stroma of TEBs and stroma of ducts.
- The accuracy of the generated data was assessed by comparing lists of genes found to be over-expressed in TEB epithelium, duct epithelium and Post-LN tissue strip to ensure that epithelial genes expressed in isolated

TEB and duct were also present in Post-LN strip but no ductal genes were present in TEB and vice versa. The comparison was computed using GeneVenn List Diagram (University of Southern Mississippi, <http://mcbc.usm.edu/genevenn/genevenn.htm>).

- Finally, the observed over-expression of chosen genes in given compartments was verified using Q RT PCR.

2.2.5.9 'Functional' analysis of identified genes

Further analysis of identified gene lists was performed to gather more information about the biological functions and characteristics of the data sets of interest as well as individually selected genes.

2.2.5.9.1 *Ingenuity Pathway Analysis (IPA)*

The groups of genes whose expression was characteristic of either epithelial or stromal environment of TEBs or ducts were analysed to identify the over-represented molecular, cellular functions and processes. The analysis was performed using IPA v 8.0 (Ingenuity Systems Inc., Redwood, US). IPA uses its own data repository, Ingenuity Knowledge Base (IKB), to assess biological functions that are most significantly represented in the analysed data. Data sets are screened for the presence of mapped (identified within IKB), function/pathway eligible molecules, i.e. genes that have at least one functional annotation in IKB and the over-represented functions are identified and ranked according to the p-values. P-values are calculated with a right-tailed Fisher's Exact Test and Benjamini-Hochberg False Discovery Rate multiple testing correction. This takes into account the following parameters: the number of function eligible genes that are known in IKB to comply with a particular functional category, the total number of molecules in the IKB with potential to be associated with the functional category of interest, the total number of molecules in IKB database and the total number of function eligible molecules in IKB data set.

2.2.5.9.2 EMT signature

Gene sets shown to be differentially expressed in the TEB environment were further screened for the presence of EMT signature genes. The EMT signature, used in this study, consists of the EMT core signature genes identified by Taube *et al.* (2010) (87 and 159 genes up- and down-regulated respectively in breast cancer cells when manipulated to undergo EMT) [270] and 10 other mesenchymal markers which were absent from this signature but previously shown by other research groups as associated with EMT (9 genes up- and 1 down-regulated in response to EMT). The EMT signature genes are listed in **Table 2-8**.

2.2.5.9.3 Literature Search

Genes were also studied on an individual basis using a literature search approach to identify those not previously associated with mammary gland biology but exhibiting related biological functions. The main search engines used to gather information comprised of: PubMed (<http://www.ncbi.nlm.nih.gov/pubmed>) and AceView (<http://www.ncbi.nlm.nih.gov/IEB/Research/Acembly/index.html>) applications developed by NCBI, GeneCards[®] (<http://www.genecards.org/index.shtml>) (Crown Human Genomics Centre, Bioinformatics Unit of the Weizmann Institute of Science in Rehovot, Israel) and Google Scholar (<http://scholar.google.co.uk/>).

2.2.5.9.4 Oestrogen responsive genes

Oestrogen responsive genes were identified using the Estrogen Responsive Gene Database v.2 (ERGDB), an integrated knowledge database which includes genes whose expression levels have experimentally been proven to be either up-regulated or down-regulated by E2 [271].

	EMT Signature Genes	Ref
Up-regulated in response to EMT	Fbln5, Grem1, Col3a1, Col1a2, Dcn, Cdh2, Enpp2, Postn, Rgs4, C5orf13, Prrx1, Fbn1, Srgn, Spock1, Prr16, Dlc1, Bin1, Rgl1, Igfbp4, Pvr13, Cdh11, Olfml3, Mmp2, Myl9, Col5a2, Ctgf, Plekhc1, Zeb1, Ror1, Ptger2, Chn1, Pmp22, Tram2, Tagln, Tnfaip6, Creb3l1, Ugdh, Has2, Dnajb4, Cdkn2c, Ccdc92, Wnt5a, Igfbp3, Ppm1d, Filip1l, Pdgfc, Tbx3, Xylt1, Fap, Dpt, Stc1, Krt81, Mmp1, Hs3st2, Lmcd1, N-Pac, Sept6, Nr2f1, Sccpdh, Mlph, Ltbp2, Tpm1, Ankrd25, Ddr2, Sema5a, Tgfb1i1, Pcolce, Stard13, Nid1, Sync1, Enox1, Fstl1, Vim, Mme, C10orf56, Ltbp1, Nrp1, Thy1, Nebl, Tns3, Ecm1, Fbln1, Tuba1a, Copz2, Cybrd1, Ppap2b, Ptx3, Fads2, Bgn, Tshz1, Zbtb38	[270]
	Twist	[272]
	Snail3	[273]
	Slug	[274]
	ZEB2	[275]
	Gsc	[276]
	FOXC1	[277]
	TCF3, Ctnnb1	[278]
	FOXC2	[279]
Down-regulated in response to EMT	C20orf19, Snx10, Tp73l, Kcnk1, Bdkrb2, Anxa8, Anxa8l1, Loc728113, Rhbdf2, Loc653562, Slc6a10p, Slc6a8, Krt18, Cds1, Thbd, Nefm, Rps6ka1, Smpdl3b, Abca12, Rhod, Krt14, Prkch, Zbed2, C10orf10, Lrrc1, Stap2, Jup, Il4r, Perp, Fgfbp1, Myo1d, Fat2, Wwc1, Fzd3, Znf165, Snca, Kiaa1815, Prss8, Sh2d3a, Gnal, Bik, Cdh3, Kiaa0888, Krt5, Gjb3, Kiaa0040, Celsr2, F11r, Nup62cl, Serpinb1, Spint2, Polr3g, Elmo3, Il1rn, Tspan1, Ifi30, Pls1, Loc729884, Tmprss11e, C1orf116, Alox15b, Col17a1, Rtel1, Tnfrsf6b, Lad1, Ptpn3, Mst1r, Epha1, E2f5, Krt6b, Stac, Itgb4, C6orf105, Gls2, Anxa3, Dst, Arhgap25, Dsc2, Slc6a8, Lsr, Cldn1, Flj20366, Cyp4f11, Ccnd2, Fgfr2, Ablim1, Xdh, Camk2b, Dsg3, Naip, Ocln, Krt17, Saa1, Saa2, Prrg4, Ank3, C10orf116, Tmprss4, Cst6, Ndr1, S100a8, Coro1a, Klk5, Exph5, Irx4, Irf6, Hook1, Artn, Flj12684, Slc2a9, Klk8, Tmem40, Trim29, Hbegf, Aldh1a3, Rbm35b, Myo5c, Cyp27b1, Il1b, Nmu, Krt16, Cdh1, Jag2, Vsnl1, Rln2, Ctsl2, Syk, Saa1, Epb41l4b, Rnf128, St14, Leprel1, Pi3, Ap1m2, Ckmt1a, Ckmt1b, Grhl2, Arhgap8, Loc553158, Igfbp2, Il18, Ca9, S100a14, Ca2, Krt15, Eva1, Tmem30b, S100a7, Klk7, Lgals7, Fst, Cxadr, Sipi, Rbm35a, Rab25, Uchl1, Klk10, Tacstd1, Serpinb2, Sprr1a, Fgfr3, Sprr1b	[270]
	E-cad	[280]

Table 2-8 EMT signature genes.

The EMT signature consists of the EMT core signature genes identified by Taube *et al.* (2010) (87 and 159 genes up- and down-regulated respectively in breast cancer cells when manipulated to undergo EMT) [270] and 10 other mesenchymal markers which were absent from this signature but previously shown by other research groups as associated with EMT (9 genes up- and 1 down-regulated in response to EMT).

2.2.6 Tissue processing and staining

2.2.6.1 Preparation of mouse mammary gland wholemounts stained with carmine

Immediately after dissecting from WT or Fbln2 KO^{-/-} mice, the fourth inguinal mammary glands were placed individually on a Twin Frost Microscope Slide. The tissue was spread out using metal BD Microlance™ 3 needles, the slide was placed into a Coplin Jar containing Carnoy's fixative (**See Solutions and Buffers**) and fixed for 3h on an orbital shaker at RT. The gland was then hydrated through decreasing concentrations of ethanol [40 min in 70% (v/v), 50% (v/v), 30% (v/v) ethanol], followed by distilled water, and stained overnight with Carmine dye (**See Solutions and Buffers**). The gland was then de-hydrated by serially placing the tissue for 40 min in dH₂O and increasing concentrations of ethanol [30% (v/v), 50% (v/v), 70% (v/v) and 100% (v/v)] to remove excess H₂O. The wholemount was finally placed in xylene for at least 12h to remove all traces of alcohol. The tissue was mounted using Pertex mounting medium, cover slipped and stored.

2.2.6.2 Tissue fixation, paraffin wax embedding and sectioning

Excised glands were fixed in 10% Neutral Buffered Formalin for 4-24h prior to being transferred into a plastic cassette, processed and paraffin wax embedded using a Leica ASP300 tissue processor as follows: tissue was de-hydrated through a graded concentration of ethanol (50 min in 50% (v/v), 50 min in 80% (v/v) ethanol and 1h in 100% ethanol (v/v)) and placed in xylene for 2h at 37°C, under vacuum conditions, transferred into paraffin wax for 4h and stored at -60°C overnight.

Paraffin wax embedded tissue was then placed at the bottom of chilled metal grids and additional wax was used to embed it into paraffin wax blocks using a Leica EG1150H heated paraffin dispensing module. Paraffin tissue blocks were left to solidify for 30 min on Leica EG1150C cold plate, chilled to -5°C and stored at RT until required.

Sectioning of paraffin wax blocks was performed using a Leitz 1512 microtome. 3-4 μ m sections were routinely cut but 10 μ m were used for 3D structure reconstruction experiments

Paraffin sections were cut and placed on the surface of a 40°C water bath, a metal blade was used to separate them and Superfrost® Plus electrostatically charged slides were used to pick the sections up from the water bath. Slides with paraffin embedded tissue sections were left to dry for 1h at 62°C.

2.2.6.3 Preparation of paraffin embedded tissue sections for IHC and IF

Paraffin embedded tissue sections were deparaffinized, rehydrated and subjected to antigen retrieval prior to being used in IHC or IF staining.

Slides were deparaffinized by submerging in xylene 3 times for 5 min, and rehydrated in decreasing concentrations of ethanol (100% (v/v) twice for 3 min, 70% (v/v) for 3 min) and running tap water for at least 2 min. Tissue sections were then pre-treated with 3% (v/v) hydrogen peroxide for 10 min to quench endogenous peroxidases, rinsed in running tap water and subjected to antigen retrieval to unmask epitopes that can be masked during the fixation process due to the cross linkage by formalin. Antigen retrieval was performed using 1mM EDTA buffer (pH8) (**See Solutions and Buffers**) as follows: 1L of 1mM EDTA buffer (pH8) was brought to boiling in a microwave pressure cooker, slides were added to the boiling EDTA buffer and heated in the microwave at full pressure for a further 7 min, of which 4 min were precisely timed for slides to be held at the retrieval pressure. Slides were placed in running tap water for 10 min to cool down prior to being used for IHC or IF staining.

2.2.6.4 IHC on paraffin embedded tissue sections

All incubations were performed at RT using a humidity chamber as follows: after antigen retrieval, slides were incubated in TBS-Tween 20 pH7.6 (**See Solutions and Buffers**) for 5 min. Excess wash buffer was drained off and tissue sections were blocked with pre-diluted 2.5% Horse Serum for 20 min to prevent non-specific binding. Tissue sections were then incubated with the primary antibody of interest (**Table 2-9**) for 30 min and rinsed again with TBS-Tween 20 three

times for 5 min. Primary antibodies were diluted to their final concentrations (**Table 2-9**) using Antibody Diluent. Washed tissue sections were then incubated for 30 min with the appropriate secondary antibody diluted 1:500 in Antibody Diluent, washed using TBS-Tween 20 three times for 5 min and incubated in diluted (1 drop in 1ml of Antibody Diluent) DAB + Chromogen for 4 min. Secondary antibodies were conjugated with HRP that catalyzes oxidation of DAB. The oxidation product can be seen in the form of a brown stain. Stained tissue sections were then washed under running tap water for at least 5 min, counterstained with haematoxylin (**See 2.2.6.6**), de-hydrated through increasing concentrations of ethanol (1 min in 30 % (v/v), 50 % (v/v), 70 % (v/v) ethanol), dipped in xylene for 40 sec and mounted using Pertex mounting medium and cover slips. Stained tissue sections were visualised and imaged (**See 2.2.8.3**) and stored at RT.

Negative control (lacking primary antibody) and positive control (tissue known to express protein of interest) were used in each staining run.

2.2.6.5 IF on paraffin embedded tissue sections

All incubations were performed at RT using a humidity chamber as follows: after antigen retrieval, tissue sections were rinsed in TBS-Tween 20 pH7.6. Excess TBS was drained off and tissue sections were incubated with Image-iT™ FX Signal Enhancer for 30 min to block the unspecific background staining that can result from tissue autofluorescence. Sections were then washed with TBS-Tween 20 to remove the remaining Image-iT™ FX Signal Enhancer, blocked with pre-diluted 2.5% Horse Serum for 15 min, rinsed with TBS-Tween 20 and incubated with the primary antibody of interest for 30 min (**Table 2-9**). Primary antibodies were diluted to their final concentrations (**Table 2-9**) using Antibody Diluent. After the incubation, tissue sections were washed twice for 5 min with TBS-Tween 20 and incubated for 20 min in darkness with fluorescent secondary antibody diluted 1:1000 in Antibody Diluent. Secondary antibodies were conjugated to either Alexa Fluor 488 dye (green) or Alexa Fluor 594 dye (red) to allow visualisation. Tissue sections were finally washed twice for 5 min with TBS-Tween 20 and mounted using ProLong® Gold antifade reagent with DAPI to stain the nuclei. A cover slip was applied onto each slide and sealed with nail varnish

Primary antibody and Source	Final concentration for ICH	Final concentration for IF
Anti-Upk3a (AU1) Mouse monoclonal, donated by Dr. T. Sun	1:100	
Anti-Fbln2 Rabbit polyclonal, donated by Dr. Mon Li Chu	1:10 000	1:15 000
Anti-Fbln1 Rabbit polyclonal, donated by Dr. Mon Li Chu	1:1 000	
Fibronectin (ab2413) Rabbit polyclonal, Abcam Inc; Cambridge, USA		1:1 000

Table 2-9 Primary antibodies used for staining of paraffin embedded tissue sections using IHC and IF methods.

after 24h. Tissue sections were visualised, imaged (See 2.2.8.2) and stored at 4°C in darkness.

Negative control (lacking primary antibody) and positive control (tissue known to express protein of interest) were used in each staining run.

2.2.6.6 Haematoxylin and Eosin (H&Eo) staining

Every fifth section cut from paraffin embedded tissue blocks was stained with haematoxylin Z which stains negatively charged organelles such as nuclei (blue) and 1% eosin which stains positively charged cell compartments such as cytoplasm (pink) to study the morphology of the specimen. Staining of tissue sections with H&E was performed as follows: slides were immersed in xylene 3 times for 5 min and 99% ethanol 3 times for 20 sec and rinsed in water. After incubation in haematoxylin for 2 min slides were washed under running tap water, dipped in 1% Acid Alcohol (HCl), rinsed again in running tap water, dipped in Scott's Tap Water (See Solutions and Buffers) for 30 sec and rinsed before examining under a light microscope to assess the intensity of haematoxylin staining. If the staining intensity was optimal, slides were transferred to eosin for 2 min and rinsed thoroughly using running tap water. Stained tissue sections were then de-hydrated through increasing concentrations of ethanol (1 min in 30% (v/v), 50% (v/v), 70% (v/v) ethanol), immersed in xylene for 40 sec, mounted using Pertex mounting medium, cover slipped, examined under a microscope (See 2.2.8.3) and stored.

2.2.6.7 Elastica van Gieson (EVG) staining

EVG staining was performed using the EVG kit as per manufacturer's instructions. Briefly, tissue section were immersed in xylene 3 times for 5 min, re-hydrated by dipping in 99% ethanol 3 times for 20 sec and rinsed with water. Tissue sections were then placed in Elastin according to Weigert's resorcin-fuchsin solution for 10 min, rinsed under running tap water, immersed in Weigert's A&B solution (See Solutions and Buffers) for 5 min, rinsed again and placed in Picrofuchsin solution according to van Gieson for 2 min and 70% (v/v) ethanol for 1 min. Stained sections were then de-hydrated through increasing concentrations of ethanol (1 min in 30% (v/v), 50% (v/v), 70% (v/v) ethanol),

immersed in xylene for 40 sec, mounted using Pertex mounting medium, cover slipped, examined under a microscope (See 2.2.8.3) and stored.

2.2.7 *In vivo* hormonal treatment of mouse mammary glands

Hormonal treatment (priming) was performed using female TG and WT mice to study the regulation of Fbln2 by systemic hormones (E2 and P) in pubertal mouse mammary gland *in vivo*.

2.2.7.1 Priming of mice with hormone pellets

Hormones were administered to animals in the form of subcutaneous pellets to deliver standardized, continuous release of the active ingredient in the animal over a given period of time. For the purpose of this study, 21 day release oestrogen (E2) (0.72mg/pellet), oestrogen-progesterone (E2+P) (0.1mg/pellet, 10mg/pellet) or placebo (10.01mg/pellet) hormone pellets were implanted in 3.5 week old pubertal TG mice.

Pellet implantation was performed on a single mouse at a time. After being weighed, the animal was anaesthetised in an induction chamber via ISoFlo[®] isoflurane (Abbot Laboratories Ltd., Kent, UK) inhalation, marked by ear punching and shaved at the back of the neck. The animal was then transferred to the surgical table, covered with a sterile cloth and anaesthesia maintained using a slow gas rate delivered through a mask placed over its nose. The anaesthesia was monitored by pinching the toe of the animal and checking for lack of paw withdrawal. The exposed skin at the back of the neck was sterilized with 70% ethanol and an incision through the skin was made using sharp sterile scissors. The skin at the top part of the incision was then lifted with sterile forceps and, using the tip of a second pair of blunt-ended sterile forceps to separate the skin from the body wall, a pocket was created for the pellet. The hormone pellet was then gently placed in the created pocket and the skin on either site of the incision was sutured using Polyamide 6 blue monofilament non-absorbable suture 5-0 Ethicon. The implanted mouse was transferred to an Electrisaver E30 thermostat heated chamber to recover from anaesthesia and then placed back into the breeding cage (See 2.2.1.1). Animal vital signs were closely monitored throughout the surgical procedure, recovery process and

thereafter. All animal work was carried out under personal licence PIL 60/11179 and project licence PPL 60/3712.

All of the surgical instruments used for mice priming were sterilized by autoclaving prior to performing the surgery. Surgical procedures were carried out in surgical gowns using Biogel[®]P Suretech surgical gloves at the Biological Services at Veterinary Research Facility in Garscube Estate in Glasgow under the supervision of a named veterinary surgeon residing at the facility or the facility manager. Isoflurane was administered in contained conditions at all times, using a calibrated thermostatically controlled Veterinary Fluosorber vaporiser, induction chamber, suitable circuit and scavenging system.

Implanted mice were primed with hormones for 7 days prior to being culled to collect the mammary glands and use them for further applications.

2.2.7.2 Mammary gland morphology assessment and tissue processing

The excision of mammary glands (See 2.2.1.2) was performed at the Beatson Institute for Cancer Research, Glasgow, UK. Mice were culled by cervical dislocation to ensure minimal tissue deterioration. Both left and right 4th inguinal mammary glands were collected. Upon dissection, mammary glands were spread onto HistoBond[®]+ glass slides, visualised using a fluorescent dissecting microscope and imaged at x80 magnification (See 2.2.8.1). Glands were then either snap frozen in liquid nitrogen or fixed in 10% Neutral Buffered Formalin to be used in further applications.

2.2.8 Visualisation and imaging

2.2.8.1 Fluorescence microscopy

Mammary glands excised from TG mice were visualised using a Stemi SV6 fluorescent dissecting microscope and imaged with Axio Vision release 4.6.3 software (Carl Zeiss Ltd., UK)

To monitor the efficiency of transfections, an Olympus IX51 inverted microscope equipped with U-MNIBA3 filter for the detection of 470-495nm wave length

(green narrow) was used for visualisation while image acquisition was carried out using F-view Soft Imaging System (Olympus UK Ltd., UK) and Cell^P Imaging software (Olympus UK Ltd., UK).

2.2.8.2 Confocal microscopy

Tissue sections stained using IF methods were examined using a Leica TCS SP2 confocal microscope with x63 oil immersion lens and imaged using Leica Confocal Software (Leica Microsystems Ltd.; UK). Multiple images were captured for each tissue section using 360nm (DAPI) and 488nm filters (green fluorescence).

3D tissue structure reconstruction was performed using Volocity® 3D Imaging Software (PerkinElmer; Massachusetts, USA) using Z-stag data obtained via confocal microscopy. Z-stags were captured every 0.7-0.8µm. Confocal microscopy and 3D structure reconstruction was performed at the Beatson Institute for Cancer Research.

2.2.8.3 Light microscopy

Wound healing experiments were monitored using an Olympus IX51 inverted microscope. F-view Soft Imaging System and Cell^P Imaging software were used to acquire images and calculate the percentage of wound closure.

Most of the tissue sections stained using IHC and the wholemounts were examined using a Labophot-2 light microscope and imaged and scanned using a NanoZoomer Digital Pathology scanner at x200 magnification. The obtained images were then manipulated and analysed using Digital Image Hub (SlidePath; Dublin, Ireland). Remaining tissue sections stained using IHC, EVG stain or H&E were examined and imaged using Leica DMD108 Digital Microimaging Network.

3 Pubertal transcriptome of mouse mammary gland - Microarray analysis

3.1 Introduction

One of the aims of this project was to study the pubertal transcriptome of the mouse mammary gland and to identify individual genes and biological functions/pathways that may be associated with TEB motility. Mouse mammary gland development during puberty, i.e. from 4 to 10 weeks of age, is a complex process of epithelial expansion into the surrounding stroma and differentiation. During this time TEBs provide the driving force for the invasion of the ductal tree into the empty fat pad. The whole process is tightly regulated by a multitude of cues, including systemic hormones and interactions between epithelial and stromal cells.

3.2 Results

This chapter should be read in conjunction with **Figure 3-1** (p.151) which provides a paradigm of microarray data analysis carried out in this project.

To study pubertal mouse mammary gland development different types of biological material were collected (isolated epithelium, mammary gland tissue strips and whole mouse mammary glands) (**See 3.2.1**) and the microarray analysis of TEB and duct epithelial and stromal transcriptomes was performed. And since TEBs are the driving force of ductal morphogenesis, this study focused on:

- Identification of genes associated with TEBs and ducts transcriptomes (**See 3.2.6.1 and 3.2.6.2**).
- Identification and classification of new, potential regulators of pubertal mouse mammary gland morphogenesis - (Candidate gene approach) (**See 3.2.6.3**).

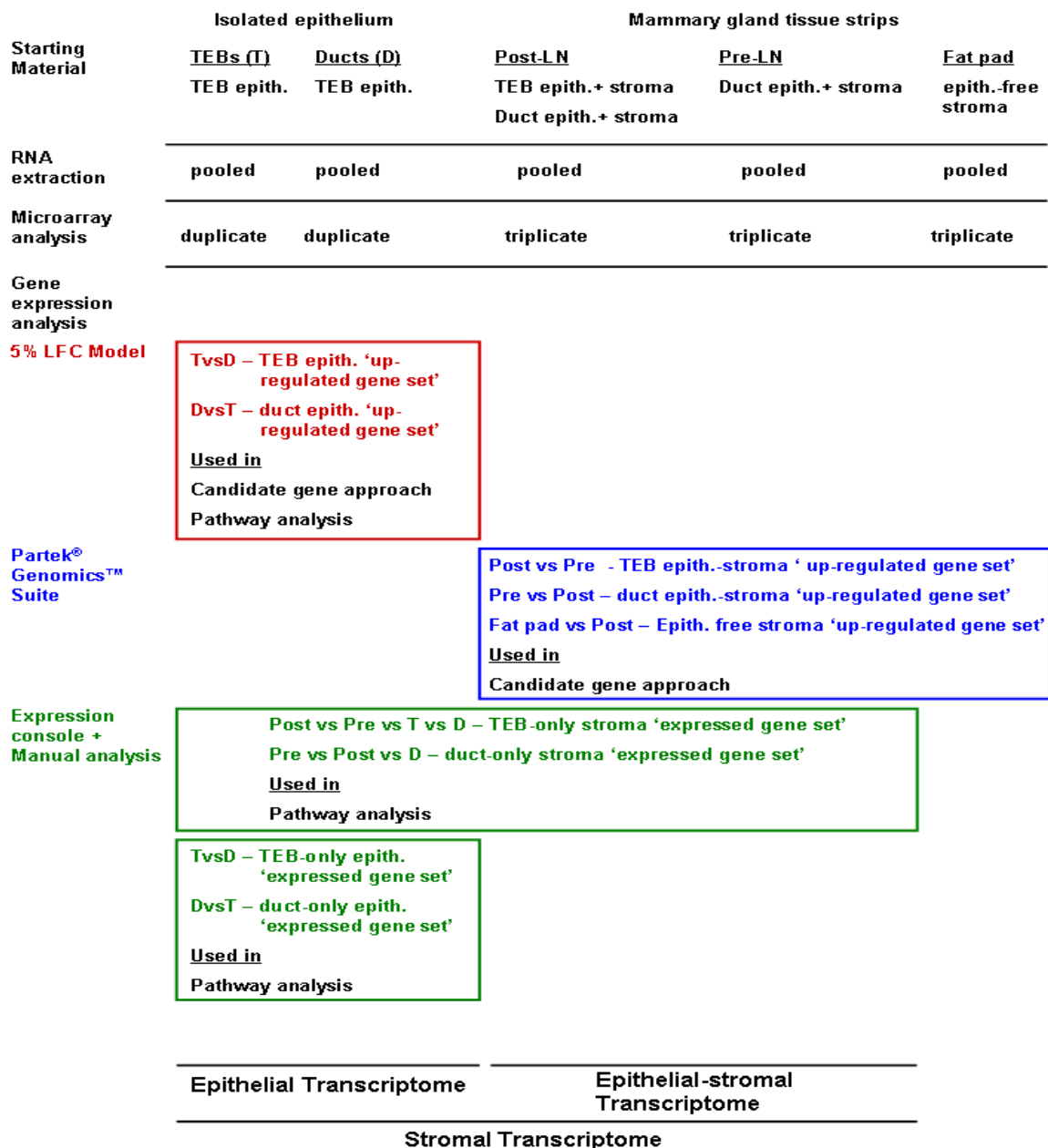


Figure 3-1 Microarray data analysis paradigm.

Gene expression analysis was performed on RNA obtained from isolated TEBs (T), ducts (D), mammary gland tissue strips (Pre-LN, Post-LN and Fat pad). Gene expression analysis was performed using 5% LFC Model to identify TEB and duct epithelium ‘up-regulated gene sets’ (See 2.2.5.5.1) and these were then used for ‘candidate gene approach analysis’ and ‘pathway analysis’. Gene expression analysis was performed using Partek® Genomic™ Suite to identify TEB and duct stromal-epithelial ‘up-regulated genes sets’ (See 2.2.5.5.2) and these were then used for ‘candidate gene approach analysis’. Finally Expression Console and manual analysis was used to compare gene expression in Post-LN, Pre-LN, isolated TEB- and isolated duct epithelium to identify TEB-only and duct-only stroma ‘expressed gene sets’ (See 2.2.5.6.2). Isolated TEB- and isolated duct epithelium gene expression was also compared to identify TEB- and duct-only epithelium ‘expressed gene sets’ (See 2.2.5.6.1). TEB- and duct-only epithelium and stroma ‘expressed gene sets’ were then used in ‘pathway analysis’. The ‘expressed gene set’ is defined as list of genes expressed ≥ 1.1 fold change cut off in one environment when compared to other environment. The ‘up-regulated gene set’ is defined as a list of genes up-regulated above the set level, in one environment when compared to other environment. TEB and duct epithelium ‘up-regulated gene sets’ and ‘expressed gene sets’ were used to study the epithelial transcriptome of TEBs and ducts. TEB and duct epithelial-stromal ‘up-regulated gene sets’ were used to study the epithelial-stromal transcriptomes of TEBs and ducts. TEB- and duct-only stroma ‘expressed gene sets’ were used to study the stromal transcriptomes of TEBs and ducts.

- Identification and comparison of functional characteristics of the epithelial and stromal transcriptomes of TEBs and ducts - (Pathway analysis) (See 3.2.6.4 - 3.2.6.7).

As a result, the different types of transcriptomes, the epithelial-, stromal- and epithelial-stromal transcriptomes, were identified in this project to study gene expression in TEBs and ducts. This allowed us to gain further insights into the function of epithelium and stroma in ductal morphogenesis and to study stromal-epithelial interactions during epithelial outgrowth at puberty. In addition, the Fat pad transcriptome was identified to study the gene expression in the distal, epithelium-free Fat pad at puberty.

Each of these transcriptomes was represented using either of the two different types of gene sets, the 'up-regulated gene sets' or 'expressed gene sets'.

The 'up-regulated gene sets', defined as lists of genes up-regulated above the set level in one environment when compared to the other environment, were identified to study epithelial and epithelial-stromal transcriptomes of TEBs and ducts and the epithelium free Fat pad (See 2.2.5.5).

The 'expressed gene sets', defined as lists of genes expressed ≥ 1.1 fold change cut off in one environment when compared to the other environment, were identified to study stromal transcriptomes of TEBs and ducts and epithelial transcriptomes of TEBs and ducts as the analysis used to select the stroma associated genes (manual screening of the raw gene expression data from the isolated epithelium and tissue strips) did not allow calculation of FCs but only enabled presence or absence of gene expression to be determined (See 2.2.5.6).

The TEB epithelium 'up-regulated gene set' (TEBs vs ducts) and Post-LN 'up-regulated gene set' (Post-LN vs Pre-LN strips) were used for candidate gene approach.

The degree of potential hormonal regulation of gene expression during puberty, based on the number of oestrogen responsive genes, as defined by ERGDB, within the generated gene list, was also established.

The TEB- and duct epithelium ‘up-regulated gene sets’ (TEBs vs ducts) (ducts vs TEBs), TEB- and duct-only epithelium ‘expressed gene sets’ (TEBs vs ducts) (ducts vs TEBs) and TEB- and duct-only stroma ‘expressed gene sets’ (TEBs vs ducts) (ducts vs TEBs) were used in pathway analysis.

3.2.1 Collection of biological material

Gene expression profiling of ductal outgrowth in pubertal mouse mammary gland was performed using the following biological material:

- Isolated epithelium of TEBs and ducts (**Figure 3-2 A, 3-2B and 3-2C**),
- Mammary gland tissue strips containing either ductal epithelium and surrounding stroma (Pre-LN); ducts and TEBs’ epithelium and surrounding stroma (Post-LN) or epithelium free stroma (Fat pad) (**Figure 3-3 A**)
- Whole adult virgin mammary glands (**Figure 3-3 B**).

TEBs, ducts and whole adult glands were isolated from WT mice. Mammary gland tissue strips were collected from TG mice.

In WT mice visualisation of mammary gland epithelium is only possible with whole mounts fixed and stained for example with carmine alum. However, fixation of the tissue prior to imaging makes it unsuitable for use in further molecular applications. In TG mice, the mammary ductal tree is easily visible under UV light and so the stage of development, presence and size of TEBs can be easily assessed allowing increased precision in setting boundaries between the Pre-LN, Post-LN and Fat pad tissue strips.

Microarray analysis of isolated TEBs and ducts was performed to characterise the specific epithelial transcriptomes. Microarray analysis of mammary gland tissue strips further permitted the study of epithelial-stromal interactions in the pubertal mammary gland. Gene expression analysis of both epithelial structures and tissue strips was used for the identification and characterisation of the stromal transcriptome around TEBs and ducts during puberty. Adult glands served as negative controls.

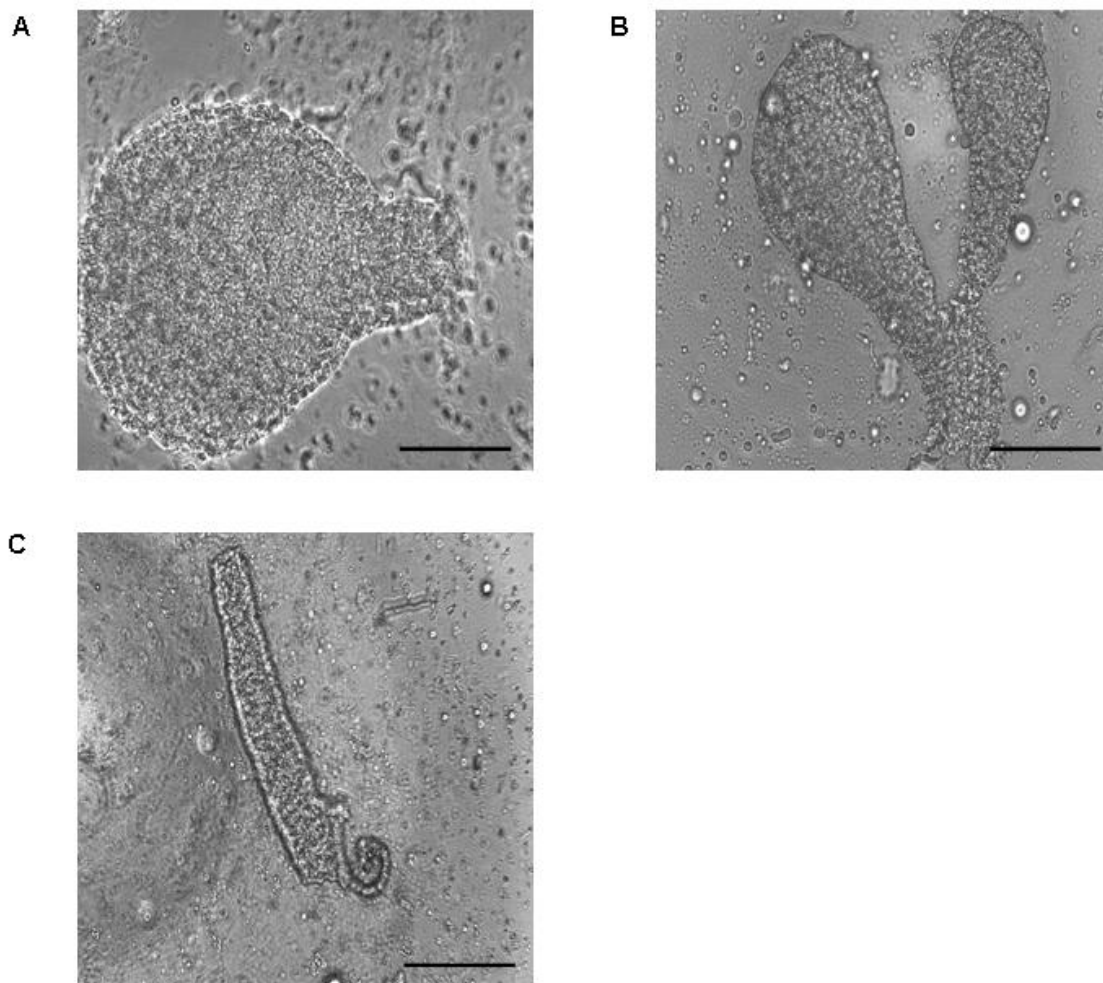


Figure 3-2 Isolated pubertal epithelium.

Phase contrast microscopic images showing (A) (B) TEBs and (C) a duct isolated from pubertal mouse mammary gland following collagenase II treatment. Mammary glands were collected from 6-7 week old WT female mice. Photographs were taken using an Olympus IX51 microscope. Scale bars are 50 μ m.

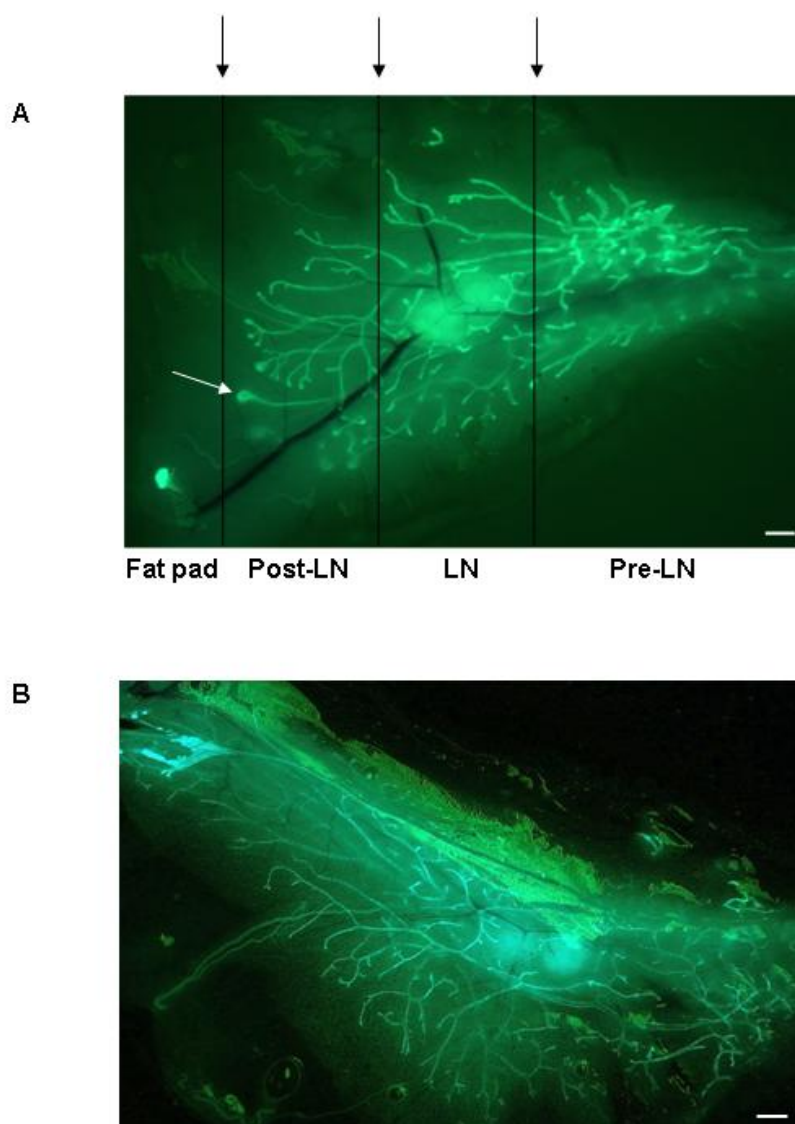


Figure 3-3 Whole mouse mammary glands.

Fluorescent microscopic images showing **(A)** Mouse mammary gland tissue strips collected from a 7 week TG. The ductal epithelium and the central LN are clearly visible and the vertical black lines (black arrows) illustrate where cuts were made to divide the gland into tissue strips. White arrow denotes TEB. **(B)** Whole adult mouse mammary gland obtained from 12 week old TG female mouse. Both photographs were taken using Stemi SV6 fluorescence dissecting microscope. Scale bars are 1mm.

3.2.2 Characterisation of pubertal development stages in WT and TG mice

Prior to the collection of biological material, mammary glands obtained from 29 WT and 23 TG mice were used to study the time course of the morphological changes during puberty in each mouse strain to ensure their comparability. Mammary glands were collected from 4, 5, 6, 7, 9 and 12 week old TG mice and visualised using a fluorescence dissecting microscope (**Figure 3-4 A**). Mammary glands from 5, 6 and 7 week old WT mice were wholemounted and stained with carmine alum (**Figure 3-4 B**). All mice were weighed at gland collection.

The length of the ductal tree as well as the size and number of TEBs were compared between collected glands. Mammary glands obtained from 4 week old mice were characterised by an undeveloped, rudimentary ductal tree. Numerous TEBs and significant outgrowth of the ductal tree was noticeable at 5-8 weeks of age, with the most prominent TEBs observed at 6-7 weeks of age. Upon reaching 9 weeks of age most of the mammary fat pad was filled with ductal epithelium and very few small TEBs were visible. At 12 weeks of age, the whole mouse mammary gland fat pad was filled with a ductal tree and hardly any TEBs were present. Furthermore, mammary glands collected from mice that weighed 16-18 g had the largest and most numerous TEBs. The extent of ductal outgrowth at given developmental stages was comparable between WT and TG mouse mammary glands.

Based on the above conclusions, mammary glands were collected from TG mice weighing 16-18g and aged 7 weeks to obtain tissue strips or WT mice aged 6-7 weeks to collect isolated TEBs and ducts. Adult mammary glands, collected at 12 weeks of age, which do not contain TEBs, were used as negative controls.

3.2.3 Experimental set up for microarray analysis

1145 TEBs and 1111 ducts were isolated from mammary glands collected from 300 WT mice. 12 Pre-LN, 12-Post-LN and 12 Fat pad mammary gland strips were collected from 6 TG mice and 6 whole mammary glands were obtained from 3 WT adult mice.

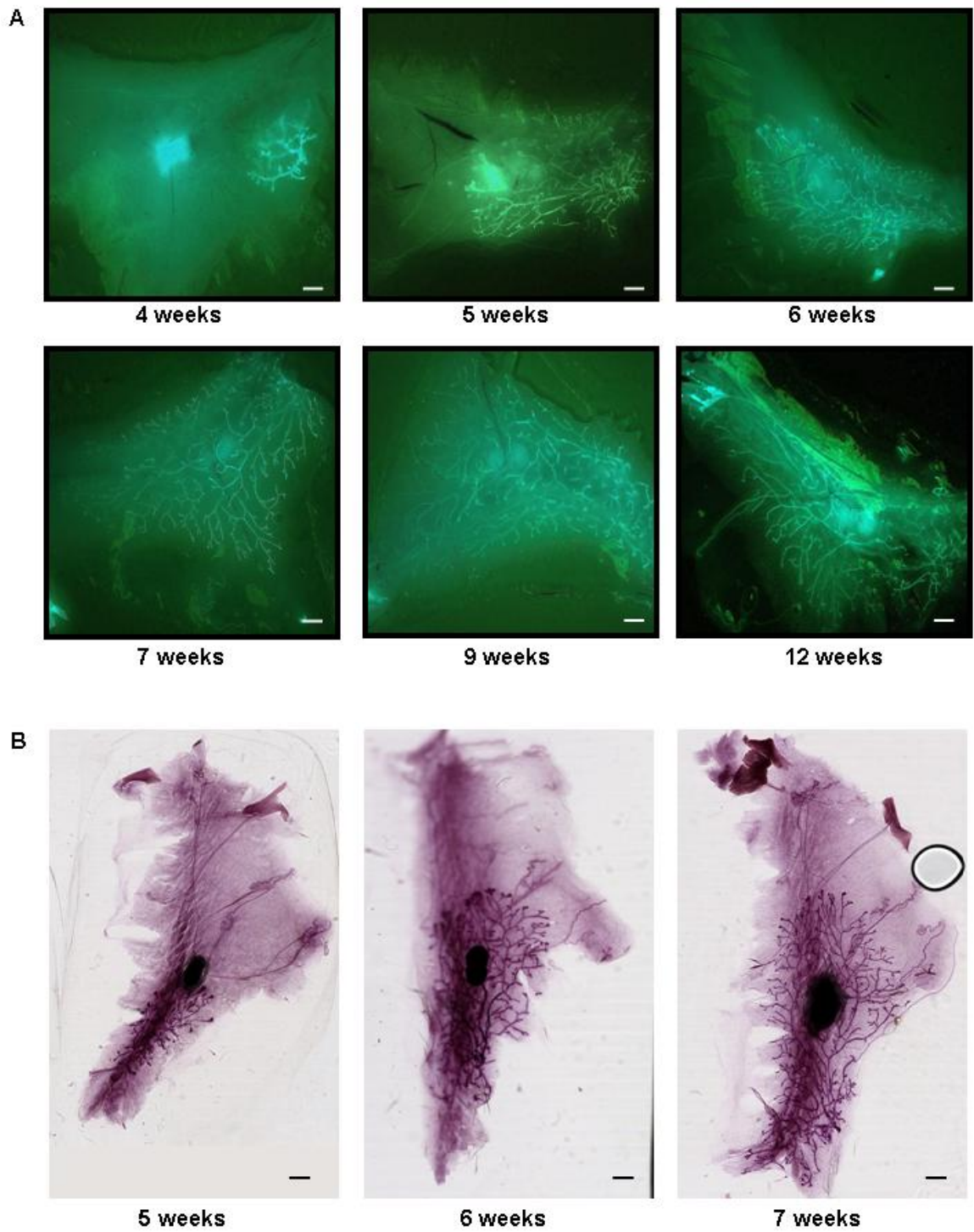


Figure 3-4 Wholemounts of different stages of pubertal mouse mammary gland development.

(A) Wholemounts collected from TG mice. **(B)** Carmine stained wholemounts obtained from WT mice. Scale bars are 1mm.

The collected biological material was pooled as shown in **Table 3-1** and 16 samples of RNA were extracted, purified and hybridised to GeneChip® Mouse Exon 1.0 ST arrays (**Figure 2-4**) (p. 106).

Isolated TEBs and isolated ducts were pooled prior to extracting RNA to ensure that a sufficient amount of RNA, 1.5 µg per microarray chip, was obtained. This experimental design also allowed the production of RNA samples representative of a 300 mice population, not biased by mouse to mouse biological variation. For both TEBs and ducts the amount of extracted RNA was only sufficient to be divided into 2 samples, generating technical duplicates. Prior to RNA extraction, mammary gland tissue strips were paired to enable a more comprehensive comparison of data between tissue strips and to ensure sufficient yield of extracted RNA and to minimise biological variation.

Animal breeding, excision and handling of biological material and experimental conditions for preparation of RNA samples were maintained as similarly as possible to minimize data discrepancy that could occur due to technical variation. This included extraction of RNA from mammary gland tissue strips at the same time and within a very short time from the RNA extraction from pooled TEBs and ducts and adult mammary glands, using the same batches of reagents and equipment.

The GeneChip® Mouse Exon 1.0 ST microarray platform was chosen for this project as it allows the investigation of the level of transcription at both whole transcript and exon levels. Each GeneChip® Mouse Exon 1.0 ST array contains only PM probes and accommodates oligonucleotide sequences that translate into 17,500 well-annotated transcript IDs based on publicly available, empirically obtained annotations of the mouse genome sequence built in 2004. A single array consists of over 4.5 million probes (25 oligonucleotide long sequences complementary to each corresponding sequence from the genome) which are synthesised *in situ*. A set of four distinctive, perfect match probes makes a probe set and usually four probe sets make up an exon cluster, i.e. a number of probes of nucleotide sequences unique for each exon. Multiple exon clusters can be grouped into over 80,000 transcript clusters, i.e. groups of putative alternatively spliced gene isoforms and each gene is annotated by a transcript ID.

RNA sample number	RNA sample source (See collection of experimental material)	Characteristics	Replicate type
1, 2	Isolated TEBs	RNA extracted from pooled TEBs was divided into 2 samples	Technical duplicate
3, 4	Isolated ducts	RNA extracted from pooled ducts was divided into 2 samples	Technical duplicate
5, 6, 7	Pre-LN mammary gland strips	Each RNA sample (replicate) contained RNA extracted from a pair of mice. The same pair of mice was used for replicates 5,8,11, second pair for replicates 6,9,12 and third pair for 7,10,13	Biological triplicate
8, 9, 10	Post-LN mammary gland strips		Biological triplicate
11, 12, 13	Fat pad mammary gland strips		Biological triplicate
14, 15, 16	Whole mammary glands		Each RNA sample (replicate) was extracted from an individual mouse (both glands)

Table 3-1 Description of RNA samples used for microarray analysis of pubertal gene expression. Isolated epithelium of TEBs and ducts was collected from 6-7 week old WT mice. Mammary gland tissue strips were collected from 7 week old TG mice. Whole mammary glands were collected from 12 week old WT mice.

3.2.4 RNA hybridisation to GeneChip[®] Mouse Exon 1.0 ST Arrays

All RNA samples were subjected to quality and integrity assessment using an Agilent 2100 bioanalyser (See 2.2.4.5). Quality assessment was based on the calculation of 28S rRNA to 18S rRNA ratio which ideally should be 2:1. RNA integrity number (RIN) was estimated taking into consideration the entire electrophoretic trace of the RNA sample. RINs were within the acceptable range for all of the RNA samples, i.e. between 6-10 as recommended by Qiagen Ltd.: for RNA samples obtained from TEBs and ducts they were 6.2; for RNA samples obtained from mammary gland tissue strips they varied between 7.7 and 9.0; and for RNA of adult glands they were between 8.4-8.8. Thus, all 16 RNA samples were able to be hybridised to the GeneChip[®] Mouse Exon 1.0 ST Arrays using appropriate Affymetrix kits (See 2.2.5.3). Efficiency and performance was monitored throughout the procedure by performing quality assessment after 28S and 18S rRNA reduction (See 2.2.5.3.1) and before and after ss cDNA fragmentation (See 2.2.5.3.5). Representative electrophoretograms, shown in **Figure 3-5**, illustrate that high quality of all samples was maintained throughout the experimental steps. The trace for total RNA showed low background noise between the clear 28S and 18S peaks and minimal low molecular weight contamination (**Figure 3-5 A**). The trace obtained after rRNA reduction, which was performed to minimise the background, increase specificity and sensitivity of the array and increase efficiency of cDNA synthesis, showed successful reduction of 28S and 18S peaks from 20 and 27 fluorescence units (FU) respectively to 2 and 3 FU respectively (**Figure 3-5 B**). Electrophoretograms of ss cDNA before and after fragmentation demonstrated successful elimination of large ss cDNA fragments in favour of accumulation of smaller size range of ss cDNA fragments (**Figure 3-5 C and D**). Successfully fragmented ss cDNAs were hybridised to the microarray chips. Arrays were washed, stained and scanned and the obtained .CEL files normalised, background corrected and summarised (See 2.2.5.4). Technical variability was minimised by processing all the samples together.

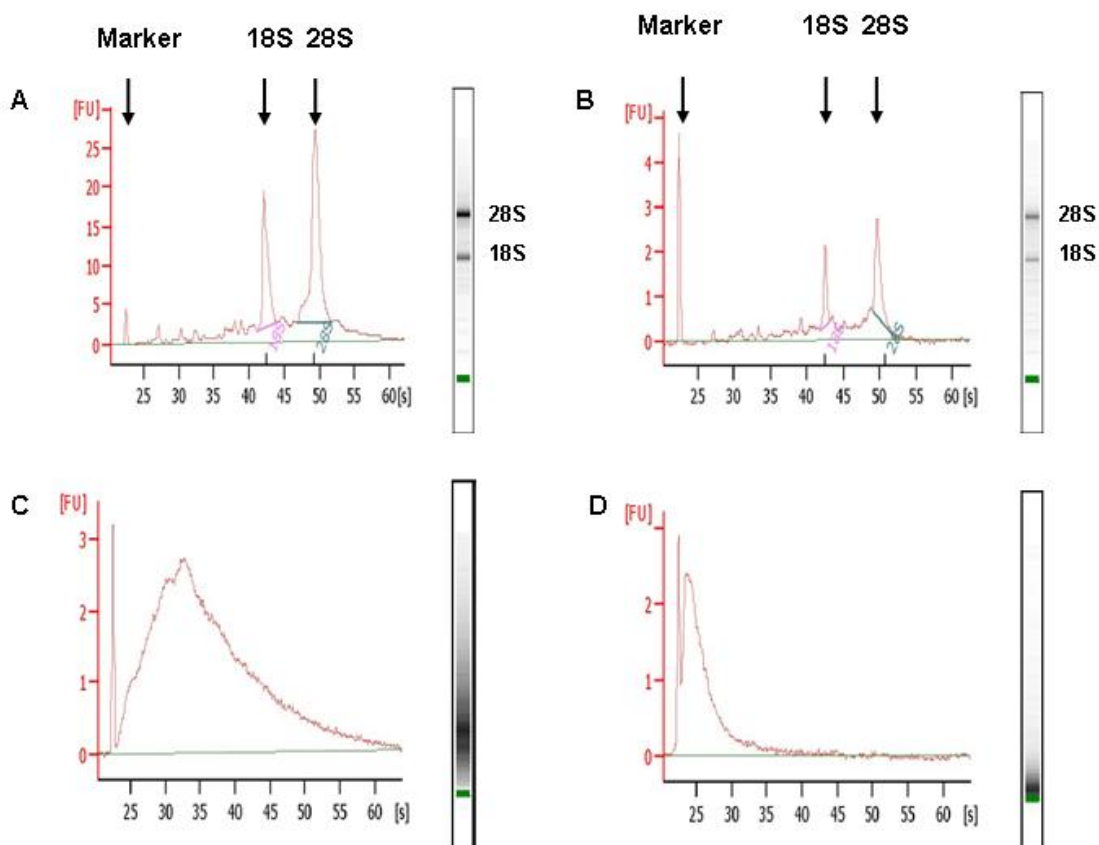


Figure 3-5 Assessment of hybridisation efficiency.

Representative electrophoretograms showing RNA quality **(A)** after RNA extraction, **(B)** after rRNA reduction and cDNA quality **(C)** before cDNA fragmentation and **(D)** after cDNA fragmentation. **(A)** **(B)** Show good quality of the total and rRNA reduced RNA. The three visible peaks stand for the molecular weight marker, 18S rRNA and 28S rRNA. **(C)** **(D)** Demonstrate successful reduction in size of cDNA fragments. The two visible peaks stand for the molecular weight marker and a pool of cDNA fragments. **(A)** **(B)** Agarose gel separation of the total RNA and **(C)** **(D)** total cDNA are shown on the right hand side of each electrophoretogram.

3.2.5 Microarray data quality control

A number of quality control measures were performed throughout the experimental stages of the microarray analysis to monitor and ensure good quality of the generated data (See 2.2.5.8). Visual inspection of the scanned arrays did not show any irregularities. Furthermore, the quality check of RNA hybridisation, performed by investigating the signal intensity of a probe set for prokaryotic internal hybridisation controls (bioB, bioC, bioD and cre) showed the cre control, which was hybridised to the array at the highest concentration, to be characterised by highest signal intensity, followed by bioD, bioC and bioB (Figure 3-6 A), thus, showing the expected rank order of spikes. Comparison of sample replicates at the whole genome level, performed after data normalisation, background correction and summarisation using PCA, showed all replicates of each biological sample to cluster together apart from the replicates of the isolated ducts, which showed higher variability. Although the two replicates failed to cluster precisely, the discrepancy was deemed slight enough that neither of them was considered an outlier. The variability between the replicates of each biological sample was therefore concluded to be minimal. Replicates of different biological samples, on the other hand, clustered away from each other. This was mostly apparent when comparing the clustering of replicates of isolated epithelium (TEBs and ducts) with replicates of tissue strips and whole virgin glands. Samples of TEBs and ducts were shown to cluster in the same area of the plot indicating similar pattern of gene expression. Samples of tissue strips and whole adult virgin glands were also shown to cluster together but at a distance from the TEBs and ducts clusters indicating, as expected, dissimilarity in gene expression between the two groups of samples and possibly reflected differences in sample preparation. Together this confirmed a reproducibility and reliability of the generated data (Figure 3-6 B and C).

Final data quality control that was carried out after the analysis of the microarray data, using a list of genes previously published as associated with either epithelial or stromal compartments of TEBs or ducts, revealed presence of these genes within the appropriate gene lists generated in this study thus ensuring the reliability of our data. The list of reference genes screened for in

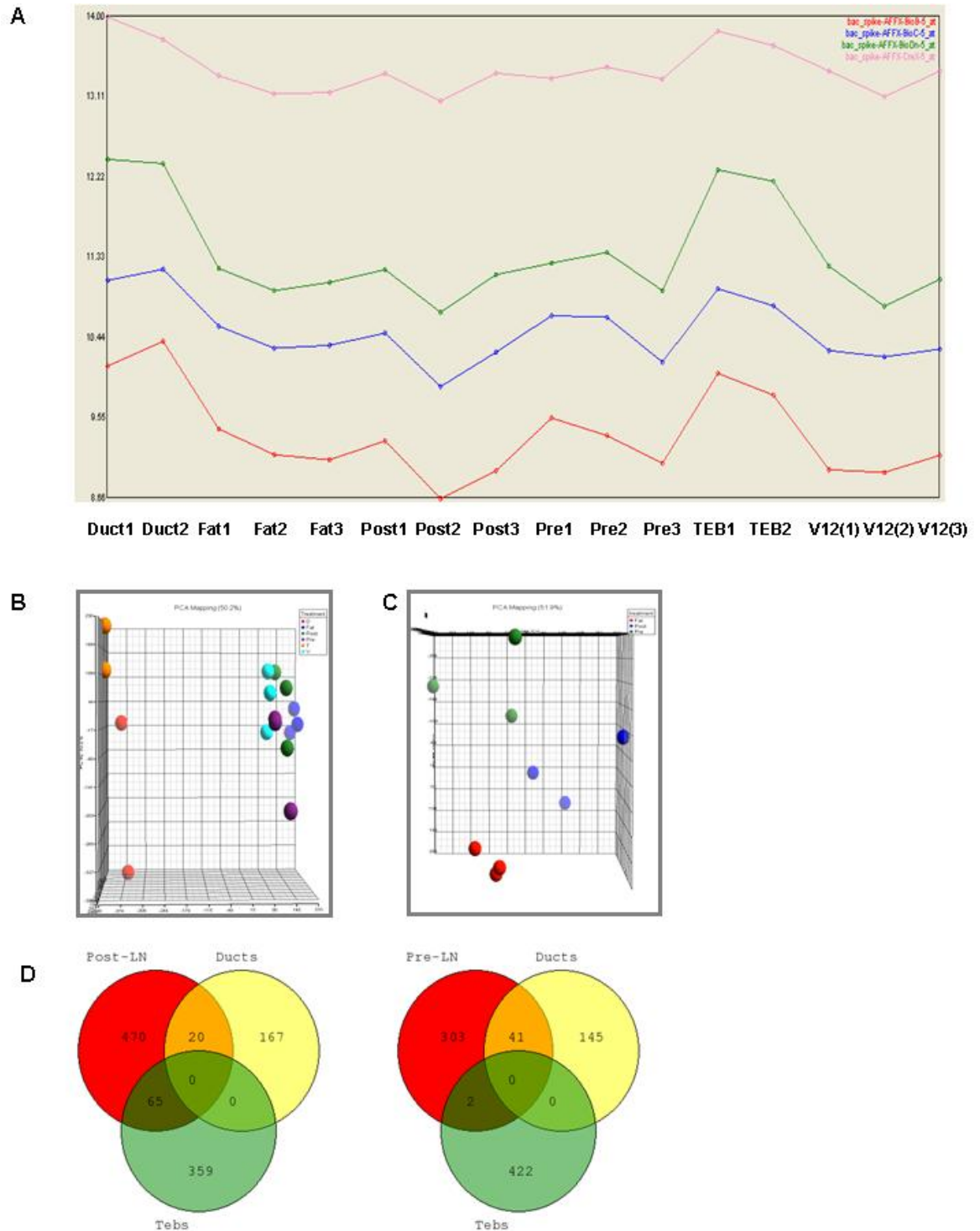


Figure 3-6 Microarray data quality controls.

(A) Quality check of RNA hybridisation. Figure illustrates the intensity of the hybridisation signal (Y axis) of Cre, bioD, bio C and bioB internal hybridisation controls across all the microarray chips (X axis). (B) (C) PCA based comparisons of clustering patterns of samples replicates. (B) Image shows TEBs (yellow) and ducts (red) replicates clustering together but away from Post-LN (green), Pre-LN (violet), Fat pad (blue) mammary gland tissue strips and whole adult gland (light blue) replicates. (C) Image illustrates close clustering of replicates of each tissue strip. Each tissue strip is represented as follows: Pre-LN (green), Post-LN (blue) and Fat pad (red). (D) Venn diagram comparison of lists of genes found to be differentially expressed in isolated TEB vs duct and Post-LN vs Pre-LN tissue strips. Red, yellow and green circles illustrate genes associated with Post-LN (right) or Pre-LN (left) strips, isolated ducts and isolated TEBs respectively. Common parts between the circles represent genes that are commonly over-expressed in the compared gene lists.

each compartment, their calculated FC and rank numbers are shown in **Table 3-2**.

Furthermore, Venn diagram comparisons of lists of genes found to be differentially expressed in TEB epithelium vs duct epithelium and Post-LN vs Pre-LN tissue strips identified 20 genes commonly up-regulated in both Post-LN (Post-LN vs Pre-LN) and duct epithelium (Ducts vs TEBs) gene lists and 65 genes commonly up-regulated in both Post-LN (Post-LN vs Pre-LN) and TEB epithelium (TEBs vs Ducts). This was expected as Post-LN strips contain TEB as well as ductal epithelium. Furthermore, 41 and 2 of the over-expressed genes in ducts (Ducts vs TEBs) and TEBs (TEBs vs Ducts) respectively were shown to be also up-regulated in Pre-LN when compared to Post-LN (**Figure 3-6 D**). This was also expected as although the Pre-LN strip contains mostly ductal epithelium it may contain a very low number of TEBs.

Finally, to confirm the reproducibility of the microarray data, the expression levels of a selected set of genes was confirmed using QRT PCR analysis. Genes that were chosen for validation included some that had never been associated with mammary gland development previously, such as *embigin (Emb)* and *Disk large homolog 7 (Dlg7)*, and others that had: *Sema3B* [113] and *lactotransferrin (Ltf)* [113]. Expression of the genes was validated using RNA extracted from Post-LN and Pre-LN strips collected from three animals, different from those used for the microarray study. Tissue strips were used to avoid using valuable RNA obtained from TEBs and ducts. Gene expression levels were normalised against the expression levels of the epithelial marker *Ktr18* to measure the abundance of gene expression in relation to the amount of epithelium present. As seen in **Figure 3-7 A** expression of *Emb*, *Dlg7* and *Sema3B* was higher in the Post-LN strip than Pre-LN strip while expression of *Ltf* was up-regulated in Pre-LN strip compared to Post-LN. Those findings reflect the microarray analysis results which showed over-expression of *Emb*, *Dlg7* and *Sema3B* in isolated TEB epithelium and Post-LN strip and up-regulation of *Ltf* in isolated duct epithelium and Pre-LN strip (**Figure 3-7 B**). The up-regulation of all genes but *Dlg7* was identified as statistically significant.

Together, all quality control measures that were carried out were deemed satisfactory.

Tissue Compartment	Gene Symbols	FC From TEB-Duct or Post-LN-Pre-LN analysis	Rank number From TEB-Duct or Post-LN-Pre-LN analysis	Literature reference
TEB epithelium	Sema3B	3.6	69	[113]
	Pcp4	2.4	25	[113]
	Itih2	5.12	23	[113]
	Wnt5a	3.09	32	[256]
	Cited1	2.02	89	[194]
Duct epithelium	Btn1a1	3.5	60	[113]
	Lalba	4.25	24	[113]
	Ltf	11.5	3	[113]
TEB stroma	Plexin C1	2.44	70	[113]

Table 3-2 List of reference genes known to be associated with TEB and duct environments and the level of their up-regulation in the generated in this study gene lists.

FC and Rank number for epithelium and stroma expressed genes were calculated using 5% LFC Model (See 3.2.6.1.1) and Partek[®] Genomic[™] Suite software (See 3.2.6.1.2) respectively.

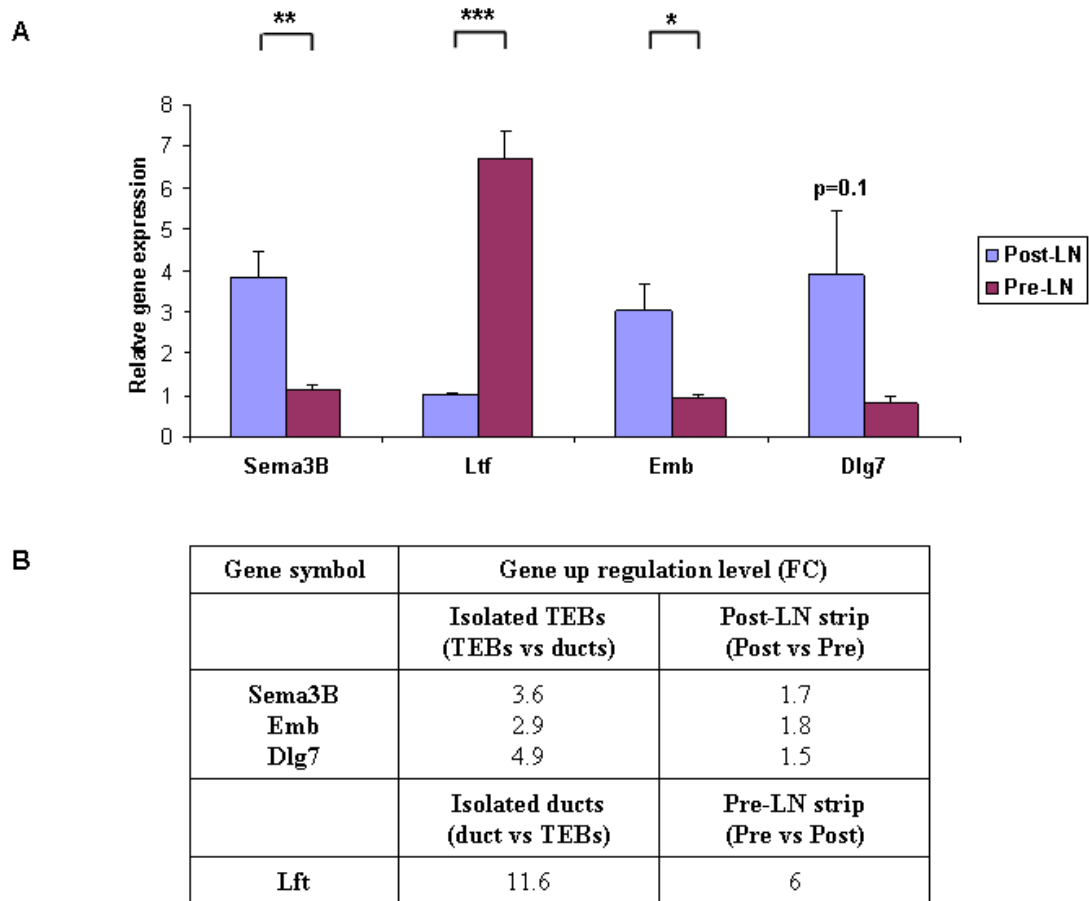


Figure 3-7 Validation of microarray gene expression profiling by RT PCR analysis.

(A) RT PCR. The graph illustrates mean expression levels of *Sema3B*, *Ltf*, *Emb* and *Dlg7* in Post-LN strip relative to Pre-LN strip. *Krt18* expression was used as an internal control for normalisation. Error bars are S.E.M. (*) denotes statistical significance, (*) $p \leq 0.05$ (**) $p \leq 0.01$ (***) $p \leq 0.001$, $n=3$

(B) Microarray analysis. The table shows the levels of *Sema3B*, *Emb* and *Dlg7* up-regulation in the isolated TEBs (TEBs vs ducts) and Post-LN strip (Post-LN vs Pre-LN) and *Ltf* up-regulation level in the isolated ducts (ducts vs TEBs) and Pre-LN strip (Pre-LN vs Post-LN). All FCs are statistically significant.

3.2.6 Bioinformatic analysis of the pubertal mouse mammary gland transcriptome

The bioinformatic analysis carried out in this project included three areas that are listed below and should be read in conjunction with **Figure 3-1** (p.151) which provides an overview of the paradigm for data analysis adopted in this study.

- Identification of genes associated with TEBs and ducts transcriptomes (See 3.2.6.1 and 3.2.6.2).
- Identification and classification of new, potential regulators of pubertal mouse mammary gland morphogenesis - (Candidate gene approach) (See 3.2.6.3).
- Identification and comparison of functional characteristics of the epithelial and stromal transcriptomes of TEBs and ducts - (Pathway analysis) (See 3.2.6.4 - 3.2.6.7).

3.2.6.1 Gene expression analysis - Identification of the ‘up-regulated gene sets’

Briefly, the ‘up-regulated gene sets’ are defined as lists of genes up-regulated above the set level, in one environment when compared to the other environment.

3.2.6.1.1 TEB and duct epithelium ‘up-regulated gene sets’

Due to the low yield of RNA, obtained from isolated TEBs and ducts, microarray analysis had to be performed in duplicate rather than triplicate which caused analysis limitations. Given that statistical tests can not be applied in analyses consisting of fewer than three samples, we employed the 5% LFC Model which is used for data analyses in the absence of large numbers of experimental replicates [269]. The 5% LFC Model aids identification of the significantly expressed genes by calculating the rank number (RN) based on the absolute

expression levels of transcripts across the compared conditions, ‘binning’ them across their absolute expression levels and selecting the first 5% of the transcripts in each bin with the highest FC (HFC). Selected genes are ranked according to both FC and expression level and the most significantly over-expressed genes are identified (**See 2.2.5.5.1**). The 5% benchmark is based on the finding brought by the survey of numerous publications on microarray analysis that shows that regardless of the gene selection method used, in general less than 5% of the total gene number show differential expression [269].

Initially 23,239 transcript IDs, i.e. genes, were employed in the analysis from which 3,038 were excluded after Average Difference Intensity (ADI) adjustment. A high level of variation in expression levels between the replicates resulted in further elimination of 1,425 transcript IDs in order to minimise false positive results. The remaining 18,777 genes (92.2%) were divided into transcripts up-regulated in TEBs or ducts. 11,738 and 7,039 genes were shown to be over-expressed in TEBs and ducts respectively. All non-annotated, internal Affymetrix controls, as defined by Affymetrix UK Ltd, were subtracted from the lists. To identify the top 5% of TEB and duct up-regulated genes, the transcripts over-expressed in TEBs were ‘binned’ into 58 bins that contained 200 genes and one that consisted of 137 genes while the transcripts over-expressed in ducts were divided into 39 bins that were 200 genes rich and one that consisted of 37 genes (**See 2.2.5.5.1**). The gene expression analysis aided identification of 425 and 186 genes over-expressed in isolated TEBs and ducts respectively (**Table 3-3**). The ranked top 20 genes from each gene list and their FC are shown in **Table 3-4**. Full gene lists are shown in **Appendix 2**.

3.2.6.1.2 TEB and duct epithelium-stroma ‘up-regulated gene sets’

The combined stromal-epithelial transcriptome of TEBs and ducts was identified using RNA extracted from Pre-LN and Post-LN mammary gland tissue strips. The yield of RNA obtained in each RNA extraction was sufficient to perform gene expression analysis in triplicate using Partek[®] Genomics[™] Suite software (**See 2.2.5.5.2**). Comparison of Post-LN vs Pre-LN gene expression aided the identification of 565 and 361 genes over-expressed in Post-LN strip (epithelial-stromal signature of TEBs) and Pre-LN strip (epithelial-stromal ductal

Transcriptome Type	Data comparison type		
	TEBs - ducts	Post-LN - Pre-LN	Post-LN - Fat pad
Isolated TEBs	425		
Isolated ducts	186		
Post-LN strip		565	670
Pre-LN strip		361	
Fat pad strip			688

Table 3-3 Number of genes up-regulated in each transcriptome.

Transcriptomes of the isolated epithelium were identified by comparing gene expression levels across TEB and duct data sets. Genes up-regulated in Post-LN, Pre-LN and Fat pad mammary gland tissue strips were identified by comparing gene expression levels across Post-LN, Pre-LN and Fat pad data sets. Up-regulation of all identified genes was statistically significant, i.e. $p \leq 0.05$ for genes over-expressed in Pre-LN and Post-LN and within the 5% LFC Model for genes over-expressed in TEBs and ducts isolated epithelium.

Table 3-4 Top 20 genes over-expressed in isolated TEBs, ducts, Post-LN and Pre-LN strips.
 FC(s) of gene expression were calculated from TEBs vs ducts and Post-LN vs Pre-LN gene expression comparisons. All FC(s) were statistically significant, i.e. $p \leq 0.05$ for genes over-expressed in Pre-LN and Post-LN and within the 5% LFC Model for genes over-expressed in TEBs and ducts isolated epithelium.

Gene symbol	FC	Gene name	Gene bank symbol
Isolated epithelium of TEBs			
Upk3a	10.7	Uroplakin 3a	NM_023478
Fbg	5.4	Fibrinogen	NM_181849
N/A	4.9	RIKEN cDNA 2810417H13 gene,	NM_026515
Hist1h1b	2.6	Histone cluster 1, H1b	NM_020034
Ccna2	5.3	Cyclin A2	NM_009828
Hist1h2ab	6.5	Histone cluster 1, H2ab	NM_175660
Serpinb11	8.45	Serine (or cysteine) peptidase inhibitor, clade B, member 11	NM_025867
Plk1	5.7	Polo-like kinase 1	NM_011121
Mt2	2.3	Metallothionein	NM_008630
Rrm1	3.1	Ribonucleotide reductase M1	NM_009103
Ccnb2	6.2	Cyclin B2	NM_007630
Crispld2	4.4	Cysteine-rich secretory protein LCCL domain containing	NM_030209
Uhrf1	4.8	Ubiquitin-like, containing PHD and RING finger domains 1	NM_010931
Racgap1	4.6	RAC GTPase-activating protein 1	NM_012025
Top2a	5.1	Topoisomerase (DNA) II alpha	NM_011623
Ccnd1	2.1	Cyclin D1	NM_007631
Tubb5	1.8	Tubulin beta 5	NM_011655
Plrg1	1.9	Pleiotropic regulator 1	NM_016784
Gsta4	2.6	Glutathione S-transferase alpha 4	NM_010357
Kif2C	6.4	Kinesin family member 2C	NM_134471
Isolated epithelium of ducts			
AY036118	4.6	cDNA sequence AY036118	N/A
Dub2a	6.9	Deubiquitinating enzyme 2a	NM_010089
Ltf	11.5	Lactotransferrin	NM_008522
Indo	2.5	Indoleamine-pyrrole 2,3 dioxygenase	NM_008324
Dmbt1	2.5	Deleted in malignant brain tumours 1	NM_007769
Cst3	1.4	Cystatin C	NM_009976
Slc7a2	3.1	Solute carrier family, member 2	NM_007514
Clca2	2.9	Chloride channel calcium activated 1	NM_009899
Tph1	9.6	Tryptophan hydroxylase 1	NM_009414
Cd79a	2.3	CD79A antigen	NM_007655
Slc 5a5	2.5	Solute carrier family 5	NM_053248
Pcgf1	2.6	Polycomb group ring finger 1	NM_197992
Ly6d	1.4	Lymphocyte antigen 6 complex, locus D	NM_010742
Cp	3.3	Ceruloplasmin	NM_007752
Agtr1a	3.0	Angiotensin II receptor, type 1a	NM_177322
Abp1	2.9	Amiloride binding protein 1	NM_029638
Trf	2.2	Transferrin	NM_133977
Atp6v1b1	2.6	ATPase H ⁺ transporting lysosomal V1 subunit B1	NM_134157
Tmem86a	2.1	Transmembrane protein 86A	NM_026436
Krt17	2.2	Keratin 17	NM_010663
Post-LN strip			
N/A	5.1	RIKEN cDNA 2810417H13 gene	NM_026515
Cxcl13	4.5	Chemokine (C-X-C motif) ligand 13	NM_018866
Ifit1	3.9	Interferon-induced protein with tetratricopeptide repeats	NM_008331
C6	3.9	Complement component 6	NM_016704
Gm11428	3.7	Predicted gene 11428	NM_001081957
Il1r2	3.7	Interleukin 1 receptor type II	NM_010555
Lyve1	3.6	Lymphatic vessel endothelial hyaluronan	NM_053247

Tlr8	3.6	receptor 1	NM_133212
Cd86	3.5	Toll-like receptor 8	NM_019388
Mgl1	3.5	CD86 antigen	NM_010796
Fcna	3.3	Macrophage galactose N-acetyl-galactosamine specific lectin	NM_007995
Tlr7	3.3	Ficolin A	NM_133211
Agt	3.2	Toll-like receptor 7	NM_007428
Akr1c14	3.2	Angiotensinogen	NM_134072
Cd163	3.2	Aldo-keto reductase family 1, member C14	NM_053094
H19	3.2	CD163 antigen	NM_001592
Ms4a6b	3.1	H19 fetal liver mRNA	NM_027209
Itgam	3.1	Membrane-spanning 4-domains, subfamily A, member 6B	NM_008401
Plek	3.1	Integrin alpha M	AK038804
Emr1	3.1	Pleckstrin	NM_010130
		EGF-like module containing, mucin-like, hormone receptor-like sequence 1	
Pre-LN strip			
Ucp1	31.3	Uncoupling protein1	NM_009463
Fabp3	8.4	Fatty acid binding protein 3	NM_010174
Slc27a2	7.3	Solute carrier family 27	NM_011978
Otop1	7.2	Otopetrin 1	NM_172709
Ltf	6.0	Lactotransferrin	NM_008522
N/A	6.0	RIKEN cDNA 5439419D17 gene	NM_175166
Cpt1b	6.0	Carnitine palmitoyltransferase 1b	NM_009948
Chi3l1	5.6	Chitinase 3-like 1	NM_007695
Acot11	4.2	Acyl-CoA thioesterase 11	NM_025590
Cidea	3.8	Cell-death-inducing DNA fragmentation factor, alpha subunit-like effector	NM_007702
Dio2	3.8	Deiodinase, iodothyronine, type II	NM_007703
Elov3	3.5	Elongation of very long chain fatty acids (FEN1/Elo2, SUR4/elo3, yeast)-like 3	NM_053248
Slc5a5	3.5	Solute carrier family 5	NM_053248
Indo	3.4	Indoleamine-pyrrole 2,3 dioxygenase	NM_008324
Muc13	3.3	Mucin 13	NM_010739
Scg3	3.2	Secretogranin III	NM_009130
Slpi	3.1	Secretory leukocyte peptidase inhibitor	NM_011414
Tspan8	3.0	Tertraspanin 8	NM_146010
Lgr5	2.9	Leucine rich repeat containing G protein coupled receptor 5	NM_010195
Ppara	2.8	Peroxisome proliferator activated receptor alpha	NM_011144

transcriptome) respectively (See Table 3-3). All of the above gene lists were created using $FC \geq 1.5$ and $p \leq 0.05$ cut off. The top 20 genes up-regulated in TEB and ductal stromal-epithelial signatures along with their FC are shown in Table 3-4. Full lists of the above identified genes are shown in Appendix 3.

3.2.6.1.3 Epithelium-free Fat pad ‘up-regulated gene set’

The Fat pad transcriptome was identified using RNA obtained from Fat pad, Pre-LN and Post-LN mammary gland tissue strips. The yield of RNA obtained in each RNA extraction was sufficient to perform gene expression analysis in triplicate using Partek® Genomics™ Suite software (See 2.2.5.5.3). Gene expression was compared between Fat pad and Post-LN and 688 genes were found as over-expressed in Fat pad compared to Post-LN strip (Table 3-3). Gene list was created using $FC \geq 1.5$ and $p \leq 0.05$ cut off. Full lists of the above identified genes are shown in Appendix 4.

3.2.6.2 Gene expression analysis - Identification of the ‘expressed gene sets’

Briefly, the ‘expressed gene sets’ are defined as lists of genes expressed ≥ 1.1 fold change cut off in one environment when compared to the other environment.

3.2.6.2.1 TEB- and duct epithelium-only ‘expressed gene sets’

6,577 non-annotated internal Affymetrix controls were excluded from both data sets that initially consisted of 23,239 genes. The remaining 16,661 genes were further reduced by 11,020 genes that were considered to be expressed to the same level in the TEBs and ducts. A TEB-only expressed transcriptome was identified after subtraction of genes expressed in the ducts from the TEB data set. Genes only expressed in the ducts were identified by removing the TEB expressed genes from the ductal data set (See 2.2.5.6.1). This resulted in a set of 5,641 genes, which included 1,646 TEB associated genes ($FC \geq 1.1$) and 3,982 duct associated genes ($FC \leq 0.9$). The full list of genes identified to be expressed specifically either in the epithelium of TEBs or ducts is shown in Appendix 5.

3.2.6.2.2 TEB- and duct stroma-only ‘expressed gene sets’

Stromal genes expressed around the epithelium of TEBs and ducts were identified by comparing Post-LN and Pre-LN expressed genes with the gene sets of isolated TEBs and ducts. Genes expressed in the epithelium of TEBs and ducts were subtracted from the Post-LN and Pre-LN gene data sets to remove the epithelium associated genes. Then the list of genes remaining in the Post-LN data set was compared with the Pre-LN data set (See 2.2.5.6.2). The Post-LN strip consists of the epithelium and stroma of TEBs and ducts while the Pre-LN strip predominantly consists of ductal epithelium and stroma. In addition both tissue strips contain stroma distant from the epithelial structures, i.e. distal stroma. The comparison of epithelium-free Post-LN and Pre-LN gene sets therefore permits the identification of stromal genes associated with TEBs in the Post-LN tissue strip and ducts in the Pre-LN strip after exclusion of stromal genes common to both environments (stromal genes expressed around both the epithelium of TEBs as well as ducts and genes of the distal stroma).

Both, Post-LN and Pre-LN gene lists initially consisted of 23,239 genes, which was reduced to 16,661 genes after exclusion of 6,577 transcript IDs corresponding to non-annotated internal Affymetrix controls. Further elimination of 14,071 TEB and 537 duct epithelium expressed genes from the Post-LN data set and 14,219 duct and 756 TEBs epithelium expressed genes from the Pre-LN data set led to the identification of the 2,053 Post-LN expressed and 1,687 Pre-LN expressed stromal genes. A Venn diagram based comparison of these stromal transcript IDs revealed the presence of 579 TEB- and 213 duct stroma-only associated genes (Figure 3-8). The full list of above identified stromal genes is shown in Appendix 6.

3.2.6.3 Identification and classification of new, potential regulators of pubertal mouse mammary gland morphogenesis – candidate gene approach

The main search for new genes, potentially involved in the orchestration of ductal tree outgrowth during puberty, was carried out using the list of genes identified to be over-expressed in the epithelium of TEBs. TEBs were chosen as a focus of the study due to the key role they play in governing directional ductal

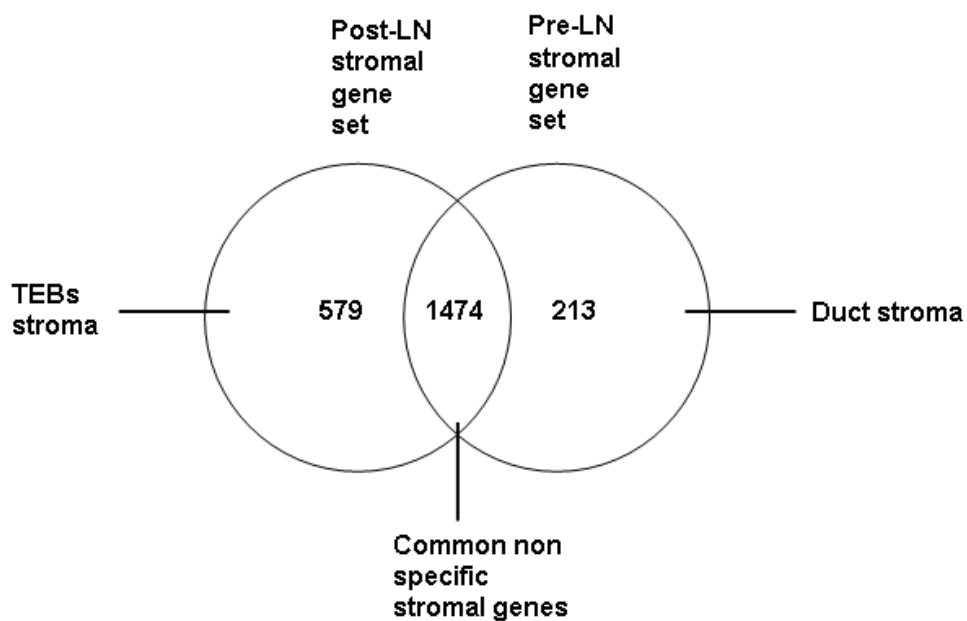


Figure 3-8 Identification of TEB- and duct-associated stromal genes.

The Venn diagram shows identification of 579 and 213 genes expressed only in the stroma of TEBs or ducts respectively. Common non-specific stromal genes (1,474) are represented by the eclipse. The list of stromal genes was created by subtracting the epithelium expressed genes of TEBs and ducts from the Post-LN and Pre-LN gene data sets and comparing lists of genes remaining in the Post-LN data set with Pre-LN data set. Full list of identified genes is deposited in **Appendix 6**.

outgrowth during puberty. The list of new genes that could potentially be involved in regulation of pubertal mammary morphogenesis was obtained by comparing the list of genes up-regulated in isolated TEBs (TEBs vs ducts) with genes up-regulated in Post-LN strips (Post-LN vs Pre-LN) and identifying the common gene set. The common gene set therefore contained transcripts whose expression was significantly up-regulated in both the epithelium of isolated TEBs and epithelium or stroma of TEBs placed within their natural environment, i.e. surrounded by stroma. This type of analysis also ensured that the up-regulated genes included in the final epithelial gene set were not influenced by any of the technical issues that could arise during the enzymatic isolation, collection or storage of the isolated TEBs.

The Venn diagram comparison of 425 and 565 genes over-expressed in TEBs and Post-LN strips respectively revealed the presence of 65 common genes (**Figure 3-9**). The molecular function of each gene and its involvement in other biological processes that share similarities with pubertal mammary gland development was researched using information deposited in publicly available databases and published scientific papers, and the potential significance in pubertal mammary gland morphogenesis was evaluated. Classification of the genes according to their main molecular functions identified 11 functional categories. The majority of genes (58.5%) encoded proteins that exhibited molecular functions connected with cell cycle and cellular proliferation, 15.3% were functionally implicated in cellular adhesion, 13.8% in cell death, 9.2% in intracellular transport and 7.7% in DNA repair. The remaining genes encoded proteins involved in signal transduction (6.1%), metabolism (6.1%), regulation of transcription (6.1%) and immune response (4.6%). A further 6.1% and 1.5% of the genes encoded structural proteins and growth factors respectively. The remaining 2 genes (3%) were left uncategorised due to unknown function (**Figure 3-10 A**).

Furthermore, of particular interest was also each gene's involvement in other biological processes that share similarities with mammary gland development (**See 2.2.5.9.3**). The biological processes of interest included: cellular migration, lung and kidney morphogenesis or cancer, embryonic and branching morphogenesis, axonal guidance. Their association with pubertal mouse mammary gland will be discussed in **3.3.2.1**. Literature available on each gene was also searched for previously documented evidence of a role in mammary

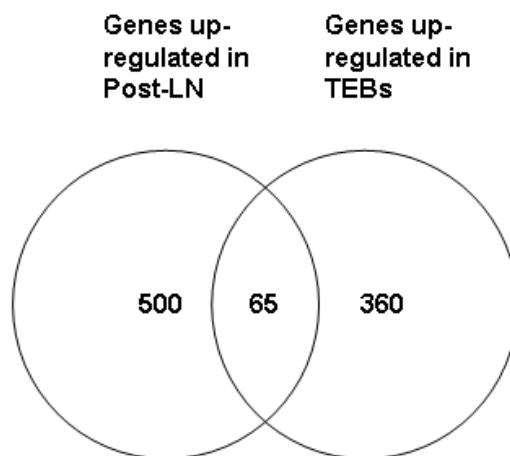
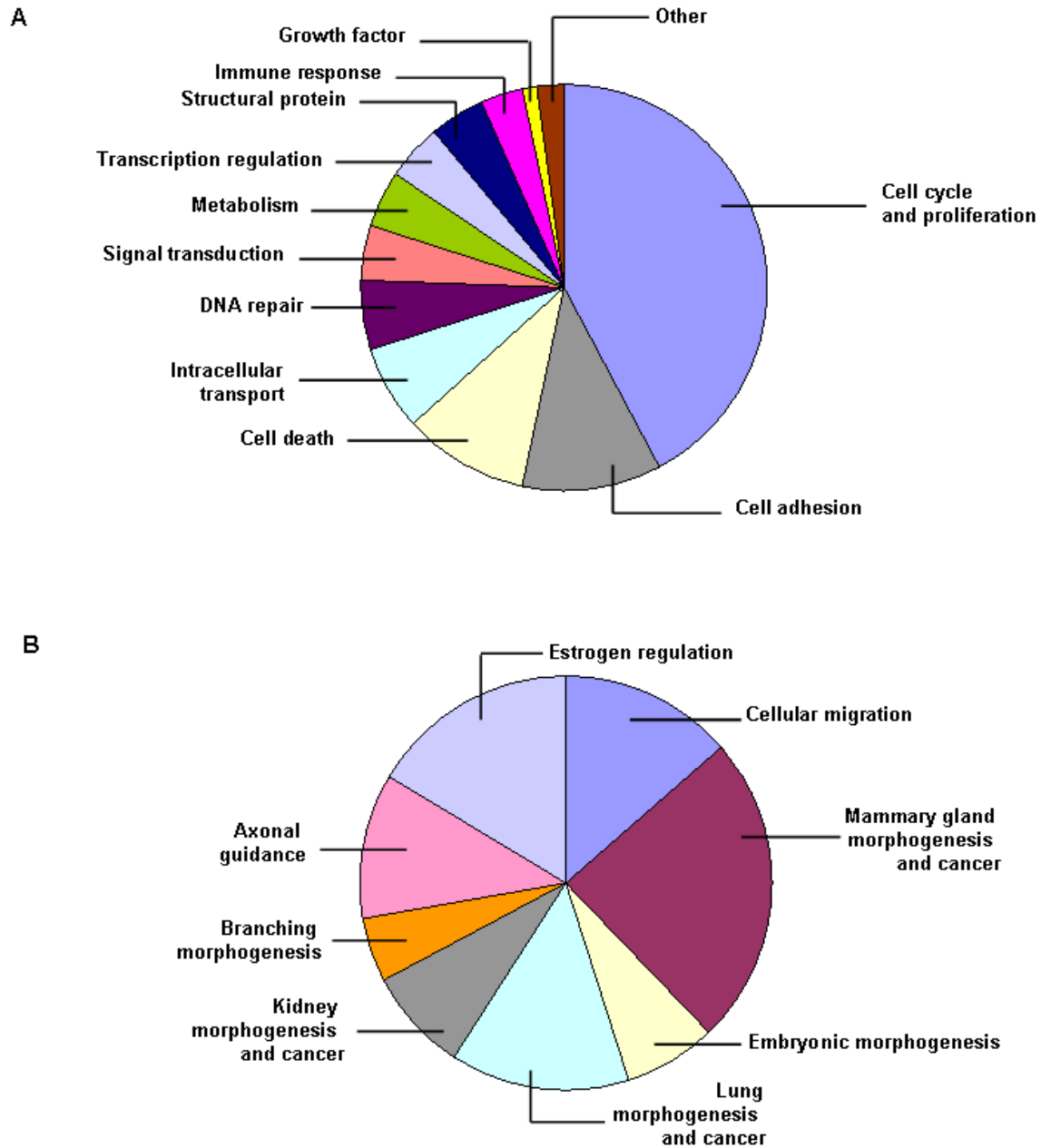


Figure 3-9 Identification of TEB epithelial gene set.

The Venn diagram shows the identification of 65 genes common to gene lists of 425 up-regulated genes in isolated TEBs (TEBs vs ducts) and 565 up-regulated genes in Post-LN strip. Full list of identified genes is shown in **Table 3.5**.



gland development or breast cancer. Furthermore, since E2 is one of the main hormonal cues regulating pubertal morphogenesis potential oestrogen responsiveness based on ERGDB, a database which includes genes whose expression has been experimentally shown to be up-regulated or down-regulated by E2 (See 2.2.5.9.4), was noted for each gene. Literature searches for all genes except *Lama1* and *Ect2 oncogene (Ect2)* were focused on information obtained from *M. musculus* and *H. sapiens*. Functional information on *Ect2* was based on *D. melanogaster* and *C. elegans* while the functional information on *Lama1* was obtained from *G. gallus*. As a result, it was revealed that 52% of identified genes were previously recognized to be associated with mammary gland morphogenesis and breast cancer. A further 30.7% and 16.9% were known to be involved in lung and kidney morphogenesis and cancer respectively while 15.3%, 29.2%, 13.8% and 24.6% were known to be implicated in embryogenesis, cellular migration, branching morphogenesis and axonal guidance respectively. Finally, 35.4% of examined genes were identified to be oestrogen responsive as defined by ERGDB (Figure 3-10 B).

The list of genes included in each molecular function and the type of biological functions they comply with are shown in Table 3-5.

3.2.6.4 Comparison analysis of biological functions over-represented in the epithelial and stromal transcriptomes of TEBs and ducts. (Pathway analysis)

IPA was used to perform a global characterisation of the biological functions over-represented within the following gene sets. See Figure 3-1 (p.151) for the overview.

- the TEB and duct epithelium ‘up-regulated gene sets’
- the TEB-only and duct-only epithelium ‘expressed gene sets’
- the TEB-only and duct-only stroma ‘expressed gene sets’

Table 3-5 Categorisation of 65 TEB epithelial genes based on molecular and biological function.

TEB epithelial gene set comprised genes identified as commonly up-regulated in both isolated TEBs (TEB vs duct) and Post-LN tissue strips (Post-LN vs Pre-LN). All genes except *Ect2* were assigned a molecular and biological function using information obtained from a literature search based on *M. musculus* and *H. sapiens*. Some biological functions of *Ect2* were studied using *C. elegans* (*).

Gene Symbol	Gene Name	Biological Function							Reference	
		Migration	Morphogenesis/Cancer					Axonal Guidance		Oestrogen
			Mammary Gland	Embryonic	Lung	Kidney	Branching			
Molecular Function: Cell Cycle (mitosis, meiosis, replication) and Cellular Proliferation										
Anln	Anilin	x	x		x	x		x	x	[281] [282] [283]
Asf1B	Asf1 anti-silencing function 1 homolog B									
AurkB	Aurora kinase B		x		x				x	[284] [285]
Birc5	Baculoviral IAP repeat-containing 5	x	x		x				x	[286] [287] [288]
Bub1	Budding uninhibited by benzimidazoles 1 homolog		x		x					[289] [290] [291]
Bub1B	Budding uninhibited by benzimidazoles 1 homolog beta				x				x	[292]
Ccna2	Cyclin A2		x							[293]
Ccnb2	Cyclin B2									
Cenpa	Centromere protein A		x						x	[294]
Dlg7	Disk large homolog 7		x			x	x			[295] [296] [297]
Dna2L	DNA2 DNA replication helicase 2-like		x						x	[298]
Ect2	Ect 2 oncogene	x(*)			x			x		[299] [300] [301] [302]
Fbxo5	F-box protein 5		x							[303]
Figl1	Fidgetin-like 1			x	x					[304] [305] [306]
H2afx	H2A Histone family member X		x						x	[307]
Hells	Helicase, lymphoid specific									
Hist1H2ab	Histone cluster, H2ab								x	
Incep	Inner centromere protein		x		x					[308] [284] [285]
Kif11	Kinesin family member 11	x	x		x			x	x	[309] [310] [311] [312]
Kif23	Kinesin family member 23									
Kif2C	Kinesin family member 2C	x							x	[313]
Mcm3	Minichromosome maintenance deficient 3		x		x	x			x	[314] [315] [316]
Mcm5	Minichromosome maintenance deficient 5								x	
Ncaph	Non-SMC condensing I complex, subunit H									
Nusap1	Nuclear and spindle associated protein 1								x	
Pbk	PDZ binding kinase		x		x	x			x	[317] [318] [319]
Plk1	Polo-like kinase 1	x	x						x	[320]

Prc1	Protein regulator of cytokinesis 1		x						x	[321]
Racgap1	Rac CTPase-activating protein 1	x	x	x		x			x	[322] [323] [324] [325] [326]
Sgol2	Shugoshin-like 2 (<i>S. Pombe</i>)									
Skp2	S-phase kinase-associated protein 2	x	x		x				x	[327] [328] [329] [330]
Smc4	Structural maintenance of chromosomes 4									
Stil	Scl/Tal1 interrupting locus			x					x	[331]
Tk1	Thymidine kinase 1		x						x	[332]
Top2a	Topoisomerase (DNA)II alpha		x						x	[333] [334]
Tpx2	Microtubule-associated protein homolog (<i>X. Laevis</i>)								x	[335]
Uhrf1	Ubiquitin-like, containing PHD and RING finger domains		x		x	x			x	[336] [337] [338]
Zwilch	Kinetochore associated, homolog (<i>D. Melanogaster</i>)									
Molecular Function: Cell Adhesion										
Dlg7	Disk large homolog		x			x	x			[295] [296] [297]
Emb	Embigin	x	x	x		x	x			[339] [340] [341]
Fbln2	Fibulin 2	x	x	x		x				[342] [343] [344]
Fbn2	Fibrillin 2	x		x	x	x	x			[345] [346] [347]
Fgb	Fibrinogen	x	x		x	x			x	[348] [349] [350]
Lama1	Laminin	x	x	x					x	[351] [227]
Ppp2r2b	Protein phosphatase 2 regulatory subunit		x							[352]
Reln	Reelin	x	x				x	x		[353] [354]
Vcan	Versican	x	x		x	x	x	x		[355] [356] [357]
Wnt5a	Wingless-related MMTV integration site 5a	x	x	x	x		x	x	x	[358] [261] [359]
Molecular Function: Cell Death (apoptosis, ubiquitin proteasome pathway)										
Atad2	ATPase family, AAA domain containing 2		x		x				x	[360]
Birc5	Baculoviral IAP repeat-containing 5	x	x		x				x	[287] [286] [288]
Bub1	Budding uninhibited by benzimidazoles 1 homolog		x		x					[292]
Ccna2	Cyclin A2		x							[293]
Fbxo5	F-box protein 5		x							[303]
Figl1	Fidgetin-like 1			x	x					[304] [305] [306]
Ppp2r2b	Protein phosphatase 2 regulatory subunit		x							[352]
Skp2	S-phase kinase-associated protein 2	x	x		x				x	[327] [328] [329] [330]
Tk1	Thymidine kinase 1		x						x	[332]
Molecular Function: Intracellular Transport										
Kif11	Kinesin family member 11	x	x		x				x	[309] [310] [311] [312]
Kif23	Kinesin family member 23									
Kif2C	Kinesin family member 2C	x							x	[313]
Racgap1	Rac CTPase-activating protein 1	x	x	x		x			x	[322] [323] [325] [324]

Thus, epithelial transcriptomes of TEBs and ducts were represented by two gene sets each, i.e. an 'up-regulated gene set' and 'expressed gene set' while their stroma associated signatures were represented by the 'expressed gene set' only. 'Pathway analysis' of these gene sets was performed to depict and compare the functional characteristics between epithelial and stromal transcriptomes of TEBs and ducts.

Each data set was screened for the presence of mapped, function eligible genes, which were then assigned to different functional categories depending on their molecular and cellular function or their role in development and function of physiological systems. The over-represented biological functions were ranked according to the calculated p-values (See 2.2.5.9.1).

The following numbers of genes were shown to be mapped and allocated a function according to IKD: within the 'up-regulated gene sets' of the TEB and duct epithelium respectively, 422 and 186 were mapped and 355 (83%) and 148 (79%) were allocated a function. With the 'expressed gene sets' of TEB and duct epithelium respectively, 1374 and 3470 genes were mapped and 1198 (72%) and 2810 (70%) genes were allocated a function. Finally the stroma 'expressed gene sets' of TEB and duct consisted of 568 and 211 mapped genes respectively, of which 443 (76.5%) and 149 (70%) were allocated a function.

'Pathway analysis' revealed clear differences between biological functions over-represented in the data sets of the TEBs and ducts environments. Differences in the biological functions were prominent in both of the studied functional categories, i.e. molecular and cellular function and physiological systems development and function. The top 5 molecular and cellular functions and the top 5 functions associated with physiological systems development and function that were over-represented in the data sets along with the number of genes complying with each category are shown in Table 3-6 and Table 3-7 respectively.

3.2.6.4.1 Molecular and Cellular Functions: Identification of the top 5 over-represented categories

Genes up-regulated in TEB and duct epithelium ('up-regulated gene sets')

Briefly, as seen in **Table 3-6**, the set of genes up-regulated in TEB epithelium was functionally mostly associated with cell cycle and cell proliferation ('Cell Cycle', 'Cellular Assembly and Organisation', 'Cellular Growth and Proliferation') and 'DNA Replication, Recombination and Repair'. The duct epithelium up-regulated gene set was rather associated with cellular signalling ('Cell-to-Cell Signalling and Interaction', 'Cell Signalling'), 'Molecular Transport' or 'Cell Death' than 'Cell Proliferation'. Both of the above mentioned gene sets also contained genes functionally associated with 'Cellular Movement' which was interestingly ranked higher in the ductal data set (#2) with 24.3% of genes than in the TEB data set (#4) with 6% of genes.

Genes expressed in the TEB- and duct-only epithelium ('expressed gene sets')

More prominent differences between the epithelial transcriptomes of TEBs and ducts were revealed when the IPA results for the entire expressed transcriptomes of TEB- or duct-only epithelium were compared. The most apparent difference was seen in terms of 'Cellular Movement' which was the most over-represented function in the TEBs data set (27.8% of genes) but was absent from the top 5 functions associated with the ductal data set. The remaining four top functional categories of the TEB data set were associated with cellular proliferation and signalling ('Cellular Growth and Proliferation', 'Cell-to-Cell Signalling and Interaction', 'Cellular Signalling') and 'Molecular Transport' which made it comparable to the functional profile of the TEB 'up-regulated gene set'. In contrast, the duct-only 'expressed gene set' was shown to share fewer similarities with the duct 'up-regulated gene set' and represented a more regulatory profile ('DNA Replication, Recombination and Repair', 'RNA Post-Transcriptional Modification', 'Cellular Assembly and Organisation') than the TEB-only 'expressed gene set'. 'Cell Cycle' and 'Molecular Transport' were the two remaining biological functions over-represented in the duct-only 'expressed gene set'.

TEBs		DUCTS	
Molecular and Cellular Function	Number of genes (% of function eligible)	Molecular and Cellular Function	Number of genes (% of function eligible)
GENES UP-REGUATED IN THE ISOLATED EPITHELIUM 'UP-REGULATED GENE SETS'			
Cell Cycle	137 (38.6%)	Cell-to-Cell Signalling and Interaction	45 (30.4%)
Cellular Assembly and Organisation	82 (23%)	Cellular Movement	36 (24.3%)
DNA Replication, Recombination and Repair	122 (34%)	Cell Death	55 (37.1%)
Cellular Movement	22 (6%)	Cell Signalling	39 (26.3%)
Cellular Growth and Proliferation	126 (35.5%)	Molecular Transport	52 (35%)
GENES EXPRESSED IN THE ISOLATED EPITHELIUM 'EXPRESSED GENE SETS'			
Cellular Movement	333 (27.8%)	DNA Replication, Recombination and Repair	332 (11.8%)
Cell-to-Cell Signalling and Interaction	334 (27.9%)	Cell Cycle	416 (14.8%)
Cellular Growth and Proliferation	414 (34.5%)	RNA Post-Transcriptional Modification	113 (4%)
Cell Signalling	232 (19.3%)	Cellular Assembly and Organisation	151 (5.3%)
Molecular Transport	209 (17.4%)	Molecular Transport	103 (3.6%)
GENES EXPRESSED IN THE STROMA 'EXPRESSED GENE SETS'			
Cell Death	148 (33.4%)	Lipid Metabolism	22 (14.7%)
Cell Morphology	76 (17.1%)	Small Molecule Biochemistry	42 (28.9%)
Cellular Growth and Proliferation	141 (31.8%)	Carbohydrate Metabolism	15 (10%)
Cellular Movement	96 (20.5%)	Cellular Compromise	7 (4.7%)
Cell-to-Cell Signalling and Interaction	105 (23.7%)	Cell Morphology	11 (7.4%)

Table 3-6 Comparison of the top 5 cellular and molecular functions over-represented in the epithelial and stromal data sets of TEBs and ducts.

The top 5 functions were identified using IPA. The over-representation of each functional category within the data set was shown to be statistically significant ($p \leq 0.05$). Functional analysis was performed on the three gene sets: genes up-regulated in the isolated epithelium of TEBs and ducts (**3.2.6.1.1**), genes expressed in the isolated epithelium of TEBs and ducts (**3.2.6.2.1**) and genes expressed in the stroma of TEBs and ducts (**3.2.6.2.2**). Only genes mapped and function eligible according to the IKD were used for the analysis. Number of genes and the calculation of the percentage of genes were based on the number of genes associated with the given function and the number of function eligible genes within the studied data set. The list of genes belonging to each functional category and the calculated p-values are shown in **Appendix 7**.

Genes expressed in TEB- and duct-only stroma ('expressed gene sets')

The biggest differences between the TEB and duct transcriptomes were identified in the stromal compartments. The stroma of the TEB-only, similarly to the epithelium, was characterised as a very dynamic and motile environment ('Cell Morphology', 'Cellular Growth and Proliferation', 'Cell Death', 'Cell-to-Cell Signalling and Interaction', 'Cellular Movement'). On the other hand, the stromal transcriptome of the ducts was mostly involved in sustaining the ductal epithelium by being involved in metabolic processes ('Lipid Metabolism', 'Small Molecule Biochemistry' or 'Carbohydrate Metabolism'), 'Cellular Compromise' and 'Cell Morphology'.

3.2.6.4.2 Physiological System Development and Function - Identification of the top 5 over- represented categories

Functional differences between TEB and duct epithelial and stromal data sets were also noticeable with regards to their involvement in physiological system development and function. Only 1.1%-6.5%, 1.8%-2.9% and 0.7%-8.7% genes, however, were assigned to the top 5 functions in the TEB epithelium 'up-regulated genes set', duct-only epithelium 'expressed gene set' and duct-only stroma 'expressed gene set' respectively.

Genes up-regulated in TEB and duct epithelium ('up-regulated gene sets')

As seen in the **Table 3-7** most of the genes identified to be up-regulated in the TEB epithelium were involved in maintenance of tissue morphology and embryonic development. Furthermore, they were also found to play roles in regulating the function and development of connective tissue and cardiovascular, skeletal and muscle systems. Genes up-regulated in the duct epithelium were also shown to play roles in the 'Development and Function of the Cardiovascular System' and to be functionally associated with 'Tissue Morphology and Development'. In addition, genes over-expressed in the duct epithelium were involved in 'Haematological System Development and Function' and 'Immune Cell Trafficking'.

TEBs		DUCTS	
Physiological System Development and Function	Number of genes (% of function eligible)	Physiological System Development and Function	Number of genes (% of function eligible)
GENES UP-REGULATED IN THE ISOLATED EPITHELIUM 'UP-REGULATED GENE SETS'			
Tissue Morphology	12 (3.4%)	Haematological System Development and Function	51 (34.4%)
Embryonic Development	23 (6.5%)	Tissue Morphology	34 (23%)
Cardiovascular System Development and Function	4 (1.1%)	Immune Cell Trafficking	35 (23.6%)
Connective Tissue Development and Function	29 (8.1%)	Cardiovascular System Development and Function	21 (14.2%)
Skeletal and Muscular System Development and Function	4 (1.1%)	Tissue Development	23 (15.5%)
GENES EXPRESSED IN THE ISOLATED EPITHELIUM 'EXPRESSED GENE SETS'			
Immune Response	339 (28.3%)	Connective Tissue Development and Function	83 (2.9%)
Immune and Lymphatic System Development and Function	301 (25.1%)	Embryonic Development	65 (2.3%)
Tissue Morphology	245 (20.4%)	Tumour Morphology	53 (1.8%)
Haematological System Development and Function	348 (29%)	Cardiovascular System Development and Function	57 (2%)
Tissue Development	309 (25.8%)	Organ Development	57 (2%)
GENES EXPRESSED IN THE STROMA 'EXPRESSED GENE SETS'			
Organismal Survival	74 (16.7%)	Skeletal and Muscular System Development and Function	13 (8.7%)
Haematological System Development and Function	102 (23%)	Tissue Development	10 (6.7%)
Cardiovascular System Development and Function	51 (11.5%)	Organismal Development	9 (6%)
Tissue Morphology	75 (16.9%)	Auditory and Vestibular System Development and Function	1 (0.7%)
Tissue Development	88 (19.8%)	Cardiovascular System Development and Function	6 (4%)

Table 3-7 Comparison of the top 5 categories associated with the physiological system development and function shown to be over-represented in the epithelial and stromal data sets of TEBs and ducts.

For the legend see **Table 3-5**. The list of genes belonging to each functional category and the calculated p-values are shown in **Appendix 8**.

Genes expressed in the TEB- and duct-only epithelium ('expressed gene sets')

The top functional categories over-represented in the epithelium of TEB- and duct-only 'expressed gene sets' were different to these seen in the TEB and duct epithelium 'up-regulated gene sets'. Although, 'Tissue Morphology' and 'Tissue Development' were still within the functional categories over-represented in the TEB-only epithelium 'expressed gene set', here the highest ranked functions were 'Immune Response' (28.3% of genes) and 'Immune System Development and Function' (25.1% of genes). In contrast to the analysis based on the up-regulated epithelial genes, this analysis indicated that the 'Haematological System Development and Function' was associated with the TEBs. Furthermore, functional categories, such as 'Embryonic Development', 'Cardiovascular- and Connective Tissue Development and Function' were also shown to be associated with ducts instead of TEBs, contradicting the results of the above presented analysis. The two remaining functional categories for the duct-only epithelium expressed gene data set were 'Tumour Morphology' and 'Organ Development'.

Genes expressed in the TEB- and duct-only stroma ('expressed gene sets')

Finally, functional analysis of genes expressed in the stroma failed to reveal any new functional characteristics of the TEB-only stroma, apart from implicating it in 'Organism survival'. It confirmed, however, the contribution of TEB associated genes (epithelial as well as stromal) to the regulation of tissue morphology and development and their involvement in the development and function of haematological and cardiovascular systems. Analysis of the duct-only stroma 'expressed gene set', however, implicated this transcriptome in both - the previously mentioned functional categories ('Skeletal- and Cardiovascular System Development and Function', 'Tissue Development') and new ones, such as - 'Organism Development', 'Auditory and Vestibular System Development and Function'.

All functional categories found to be over-represented in this analysis were statistically significant. The list of genes implicated in each cellular/molecular process-based category and physiological system development and function based categories, alongside with the p-values calculated for each category are shown in **Appendix 7** and **Appendix 8** respectively.

3.2.6.5 ‘Cellular Movement’ during pubertal mouse mammary gland morphogenesis – Comparison of transcriptomes from TEBs and ducts

The association of TEB and duct transcriptomes with the three key biological functions: ‘Cellular Movement’, ‘Nervous System Development and Function’ and ‘Embryonic Development’ were chosen to be discussed in more detail (See 3.2.6.5, 3.2.6.6 and 3.2.6.7) (Figure 3-11).

One of the main events which characterises pubertal mouse mammary gland development is the expansion of the ductal tree. This ductal morphogenesis consists of ductal elongation mediated by TEBs outgrowth, branching and directional turning, and secondary ductal branching. None of these processes are yet fully characterised but based on their motile character they are likely to be associated with the expression of genes functionally involved in migratory processes, cellular movement or cellular invasion.

Hence, to explore this hypothesis, the information obtained from IPA (See 3.2.6.4) was used to examine the level and expression pattern of genes associated with ‘Cellular Movement’ during pubertal mouse mammary gland development. Genes identified as associated with the ‘Cellular Movement’ according to the IKD, were compared throughout all six gene sets (TEB or duct epithelium ‘up-regulated gene sets’, TEB- or duct-only epithelium ‘expressed gene sets’, TEB- or duct-only stroma ‘expressed gene sets’). Furthermore, based on the emerging evidence which shows the association of EMT, which is a process in which the adherent epithelial cells shed their epithelial characteristics in favour of acquiring mesenchymal properties, with promoting cellular migration during embryonic development or cellular invasion during tumour metastasis formation (reviewed in [373]), the gene sets shown to be differentially expressed in TEB environment were manually screened for the presence of EMT signature genes. The EMT signature consists of EMT core signature genes plus 10 additional key mesenchymal markers (See 2.2.5.9.2). The EMT core signature

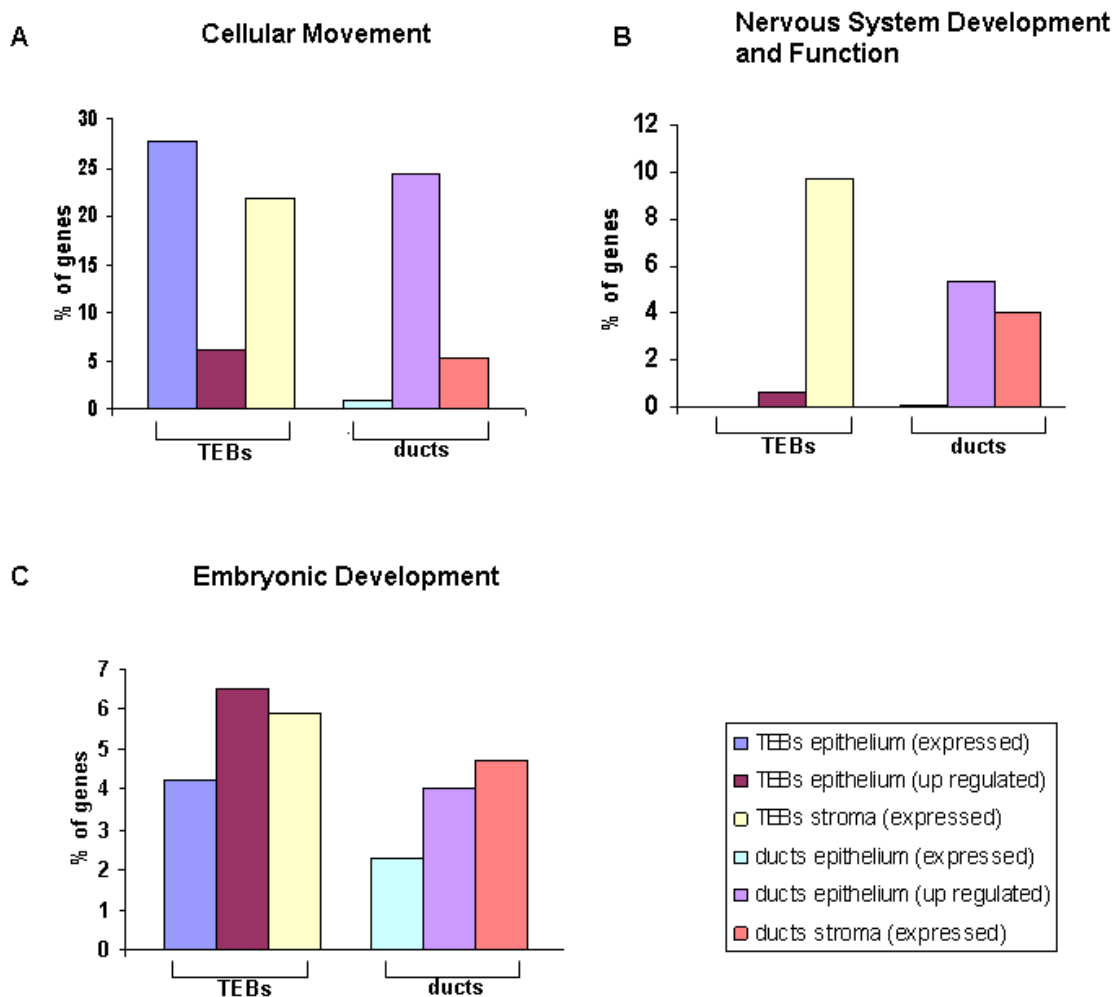


Figure 3-11 Selective, Ingenuity Pathway Analysis (IPA)-based functional comparison analysis of the identified pubertal gene sets.

IPA analysis was performed as described in 3.2.1.5 and the following functional categories were selected for the comparison analysis: **(A)** Cellular Movement **(B)** Nervous System Development and Function **(C)** Embryonic Development. The association of each functional category within the data set was shown to be statistically significantly ($p \leq 0.05$). Comparison analysis was performed using three gene sets: genes up-regulated in the isolated epithelium of TEBs and ducts (3.2.6.1.1), genes expressed in the isolated epithelium of TEBs and ducts (3.2.6.2.1) and genes expressed in the stroma of TEBs and ducts (3.2.6.2.2). Only genes mapped and 'function eligible' according to the IKD were used for the analysis. The calculation of the percentages of genes associated with each category was based on the number of genes associated with the given function and the overall number of function eligible genes within the studied data set. The full list of subcategories identified within each functional category, genes belonging to each subcategory and the calculated p-values are shown in **Appendix 9**.

was developed by Taube *at al.* (2010) and it consists of 87 and 159 genes that were found up-regulated and down-regulated respectively as a response to inducing EMT in breast cancer cells *in vitro* [270] (See Table 2-8). Based on the fact that a mesenchymal genotype can be characterised by both the up-regulation of mesenchymal and down-regulation of epithelial markers both the TEB up- and down-regulated (i.e. duct up-regulated) gene lists were screened.

The presence of mesenchymal markers (up-regulated in response to EMT) amongst the TEB down-regulated genes and the presence of epithelial markers (down-regulated in response to EMT) in the TEB up-regulated genes was also assessed. This served as a negative control.

Terminal end buds

In general, most genes associated with ‘Cellular Movement’ were identified within the TEB gene sets. 27.8%, 21.7% and 6.2% of epithelium ‘expressed-’, stroma ‘expressed-’ and epithelium ‘up-regulated gene sets’ respectively were shown to be functionally implicated in ‘Cellular Movement’ (Figure 3-11 A). Some of the functional sub categories represented in the gene set expressed in the TEB-only epithelium were ‘cellular movement or migration of eukaryotic cells, -immune response cells, -cell lines (normal, embryonic, tumour)’; ‘infiltration or chemotaxis of eukaryotic cells, ‘-immune response cells’ and ‘invasion of eukaryotic cells, -cell lines (normal and tumour)’. Some of the genes expressed in the TEB-only stroma were shown to be involved in the ‘movement of eukaryotic cells, -cell lines (normal and tumour)’; ‘migration of normal cells, -cell lines (normal and tumour), -immune response cells’; ‘cell movement of central nervous system cells, -immune response cells, -tumour cell lines’; ‘invasion of normal cells and neuroglia’ and ‘chemotaxis of eukaryotic cells, -bone and nervous tissue cell lines’. Genes up-regulated in the TEBs epithelium, on the other hand, were shown to be mostly implicated in the ‘chemorepulsion of neuritis’ and ‘chemotaxis of bone marrow-derived macrophages’.

The screening of TEB environment up-and down-regulated genes lists for the presence of EMT signature genes revealed presence of 3 and 11 EMT up-regulated markers within TEB epithelium (TEBs vs ducts) and TEB epithelium-stroma (Post-LN vs Pre-LN) up-regulated genes respectively which accounted for

3 % and 11% of EMT signature genes respectively. As for the EMT down-regulated markers, 8 (5%) and 16 (10%) of them could be seen in TEB epithelium (ducts vs TEBs) and TEB epithelium-stroma (Pre-LN vs Post-LN) down-regulated genes respectively. Furthermore, 17 out of the 31 EMT marker genes found to be differentially expressed in TEB environment, have not yet been described or studied in mouse mammary gland before. These genes are: *Col1a2*, *Col5a2*, *Extracellular matrix protein 1(Ecm1)*, *Fibroblast activation protein (Fap)*, *Fibulin 1 (Fbln1)*, *Fibrillin 1 (Fbn1)*, *Cytochrome b reductase 1 (Cybrd1)*, *Adaptor protein complex AP1, mu 2 subunit (Ap1m2)*, *Coxsackie virus and adenovirus receptor (Cxadr)*, *Potassium channel, subfamily K, member 1(Kcnk1)*, *Kallikrein-related peptidase 8 (Klk8)*, *Ladinin (Lad1)*, *Tripartite motif-containing 29 (Trim29)*, *Aldehyde dehydrogenase family 1, subfamily A3 (Aldh1a3)*, *N-myc downstream regulated gene 1 (Ndr g1)* and *Synaptotagmin-like 1 (Slp1)*.

The negative experimental control, however, revealed that 4 (4%) and 3 (3%) of EMT up-regulated genes (mesenchymal markers) were down-regulated in TEB epithelium (ducts vs TEBs) and TEB epithelium-stroma (Pre-LN vs Post-LN) respectively and 6 (3.7%) and 5 (3%) of EMT down-regulated genes (epithelial markers) were up-regulated in TEB epithelium (TEBs vs ducts) and TEB epithelium-stroma (Post-LN vs Pre-LN) respectively.

Full list of identified genes can be seen in **Table 3-7**.

Ducts

Looking at the gene expression for ducts, 24.3%, 5.3% and 0.9% of genes belonging to the epithelium ‘up-regulated-’, stroma ‘expressed-’, epithelium ‘expressed gene sets’ respectively were shown to be functionally involved in processes associated with ‘Cellular Movement’ (**Figure 3-11 A**). Genes up-regulated in duct epithelium were shown to be associated with the following subcategories: ‘cell movement of immune response cells’, ‘-cell lines (normal and tumour)’; ‘cell rolling’ or ‘infiltration of immune response cells’; ‘chemotaxis of immune response cells and fibroblasts’; ‘migration of immune response cells, -cell lines (normal and tumour), -astrocytes’ and ‘invasion of normal cells, -cell lines (normal and tumour)’. Subcategories for the stroma

EMT up-regulated markers up-regulated in	
Isolated TEB epithelium	TEB epithelium and stroma
Cytochrome b reductase 1 (Cybrd1) Hyaluronan synthase 1 (Has2) Wingless-related MMTV integration site 5a (Wnt5a)	Collagen type1, alpha 2 (Col1a2) Collagen type 5, alpha 2(Col5a2) Discorin domain receptor family member 2 (Ddr2) Extracellular matrix protein 1 (ECM1) Fibroblast activation protein (FAP) Fibulin 1 (Fbln1) Fibrillin 1 (Fbn1) Olfactomedin-like 3 (Olfml3) Procollagen C-endopeptidase enhancer protein (Pcolce) Paired related homeobox 1 (Prrx1) Wingless-related MMTV integration site 5a (Wnt5a)
EMT down-regulated markers down-regulated in	
Isolated TEB epithelium	TEB epithelium and stroma
Annexin A8 (Anxa8) Aldehyde dehydrogenase family 1 subfamily 3a (Aldh1a3) Interleukin 1 beta (Il1b) Keratin 14 (Krt14) Keratin 15 (Krt 15) Keratin 17 (Krt17) N-myc downstream regulated gene 1 (Ndrgr1) Stomatin-like 1 (Slp1)	Annexin A8 (Anxa8) Adaptor protein complex AP-1, mu 2 subunit (Ap1m2) BCL-2 interacting killer (BIK) Coxsackie virus and adenovirus receptor (Cxadr) Interferon regulatory factor 6 (Irf6) Potassium channel, subfamily K, member 1 (Kcnk1) Kallikrein related-peptidase 8 (Klk8) Keratin 17 (Krt17) Keratin 18 (Krt18) Keratin 5 (Krt5) Ladinin (Lad1) Prostatin (Prss8) Tripartite motif-containing 29 (Trim29) Stomatin-like 1 (Slp1)
EMT up-regulated markers down-regulated in (negative control)	
Isolated TEB epithelium	TEB epithelium and stroma
Latent transforming growth factor beta binding protein 1 (Ltbp1) Latent transforming growth factor beta binding protein 2 (Ltbp2) Membrane metallo endopeptidase (Mme) Pentraxin related gene (Ptx3)	Coiled-coil domain containing 92 (Ccdc92) Latent transforming growth factor beta binding protein 2 (Ltbp2) Melanophilin (Mlph)
EMT down-regulated markers up-regulated in (negative control)	
Isolated TEBs	TEB epithelium and stroma
Cyclin D2 (Ccnd2) Desmocollin 2 (Dsc2) Insulin-like growth factor binding protein 2 (Igf2) Keratin 5b (Krt6b) Rnf128 S100 calcium binding protein A14 (S110a14)	Annexin A3 (Anxa3) Gho GTPase activating protein 25 (Arhgap25) Coronin, actin binding protein 1A (Coro1a) Interferon gamma inducible protein 30 (Ifi30) Interleukin 80 (Il80)

Table 3-8 List of EMT core signature genes also identified as differentially expressed in TEB environment.

EMT signature consists of the EMT core signature genes plus the 10 additional key mesenchymal markers (**See Table 2-8**). EMT signature consists of the up-regulated as well as down-regulated in response to EMT genes thus both the TEB up-regulated (TEBs vs ducts) (Post-LN vs Pre-LN) and down-regulated (ducts vs TEBs) (Pre-LN vs Post-LN) gene lists were screened. Genes that have not been studied in mouse mammary gland before are highlighted in grey. Screening for EMT up-regulated markers identified as down-regulated in TEB environment and the EMT down-regulated markers identified as up-regulated in TEB environment was used as a negative control.

expressed genes around ducts only included: ‘cell movement of microtubules, - epithelial cells’; ‘migration of muscle cells, -gonadal cell lines, -hepatic stellate cells, -proepicardial cells’; ‘invasion of hybrid cells, -smooth muscle cells’ and ‘chemotaxis of keratinocytes’. Finally, all of the ‘Cellular Movement’ associated genes expressed in the duct-only epithelium were functionally connected with ‘cytokinesis’.

In summary, the following gene sets were identified as exhibiting the most motile character: TEB-only epithelium ‘expressed gene set’, duct epithelium ‘up-regulated gene set’, TEB-only stroma ‘expressed gene set’ and duct-only stroma ‘expressed gene set’.

The full list of detailed functional categories, calculated p-values and genes complying with each category are shown in **Appendix 9 A**.

3.2.6.6 ‘Nervous System Development and Function’ during mouse mammary gland morphogenesis – Comparison of transcriptomes from TEBs and ducts

Several genes previously recorded to be associated with nervous system development or function, i.e. axonal guidance or axonal growth cones development, were recently suggested to be involved in a ductal morphogenesis of the mouse mammary gland [113] [259].

Based on those observations, we performed a detailed functional analysis of the ‘Nervous System Development and Function’ associated genes in the transcriptomes of TEBs and ducts.

The study was based on the information obtained from the IPA and the comparison analysis was performed as described in **3.2.6.4**. As presented in **Figure 3-11 B**, the majority of nervous system associated genes were expressed within the stroma of TEBs (9.7%), duct epithelium up-regulated genes (5.4%) and the duct-only stroma (4%). In contrast, very few nervous system associated genes were expressed within the TEB epithelium ‘up-regulated gene set’ (0.9%) and duct epithelium ‘expressed gene set’ (0.1%).

Terminal end buds

Thus, the clearest reference in pubertal mouse mammary gland gene expression to the pattern of gene expression characteristic for the nervous system development and function was seen in the stroma of the TEBs. In contrast, the epithelium of TEBs expressed only a single gene, implicated in chemorepulsion of sympathetic neurites (*Sema3B*). Some of the TEB-only stroma associated functional subcategories included: 'outgrowth of neurites', '-sensory axons'; 'myelination'; 'activation, chemorepulsion or stimulation of neurons'; 'migration or survival of astrocytes' and 'chemotaxis of neuronal tissue cell lines'.

Ducts

Although fewer 'Nervous System Development and Function' associated genes, were found in the ductal genes sets, they were expressed almost equally between epithelium and stroma. Some of the functional subcategories were as follows: 'survival, migration of astrocytes'; 'activation and stimulation of neurons' (duct epithelium up-regulated genes), 'maturation of synaptic vesicles' (duct-only epithelium expressed genes) and 'axogenesis of neurons' and 'communication of nervous tissue cell lines' (duct-only stroma expressed genes).

The full list of detailed functional categories, calculated p-values and genes complying with each category are shown in **Appendix 9 B**.

3.2.6.7 'Embryonic Development' during pubertal mouse mammary gland morphogenesis – Comparison of transcriptomes from TEBs and ducts

Embryonic development is known to be fully dependent on the presence of reciprocal signalling between the epithelial and mesenchymal environments [374]. Furthermore, stromal-epithelial interactions are vital for normal post natal ductal outgrowth and branching of the mouse mammary gland [126] and play an important role in creating a permissive environment for initiation and promotion of carcinogenesis (reviewed in [375]).

Given the great importance of stromal-epithelial cross-talk during both mouse mammary morphogenesis and embryonic development, the TEB and ductal gene sets were also screened for the presence of genes, identified in the IKD as implicated in ‘Embryonic Development’ (as described in 3.2.6.4). IPA based, comparison analysis identified ‘Embryonic Development’ associated genes in all of the examined genes sets, i.e. both epithelial and stromal compartments of TEBs and ducts. The direct comparison of TEB and duct environments showed a slightly stronger association of TEB data sets with ‘Embryonic Development’ than duct data sets. Furthermore, both epithelial and stromal compartments of TEBs or ducts contained a similar percentage of genes known to be involved in embryonic development.

Terminal end buds

Amongst TEB gene sets, 4.2%, 6.5% and 5.9% of epithelium expressed, epithelium up-regulated and stroma expressed genes respectively were shown to be functionally associated with the embryonic development (Figure 3-11 C). Some of the functional subcategories identified to be associated with the TEBs gene sets were as follows: ‘remodelling or patterning of the tissue (epithelium expressed genes)’, ‘formation of embryoblast and mesenchyme’; ‘survival of embryonic cells’; ‘patterning of nervous tissue’ (epithelium up-regulated genes) and ‘development of embryo’.

Ducts

As for ducts gene sets, 2.3%, 4% and 4.7% of epithelium expressed, epithelium up-regulated and stroma expressed genes respectively were previously implicated in ‘Embryonic Development’ (Figure 3-11 C). The following examples of functional subcategories were associated with identified genes: ‘survival or cell death of embryonic cells’; ‘growth of embryo and blastocyst’; ‘folding of embryonic tissue’; ‘proliferation of morula’ (epithelium expressed genes); ‘formation of forelimb bud’, ‘morphology of branchial arch’ (stroma expressed genes) while all of the ‘Embryonic Development’ associated genes identified in the ductal epithelium ‘up-regulated gene set’ were shown to be functionally implicated in ‘branching morphogenesis of carcinoma, -thyroid tumour, and kidney cell lines’.

The full list of detailed functional categories, calculated p-values and genes complying with each category are shown in **Appendix 9 C**.

3.2.7 Summary

This study was performed to carry out detailed microarray analysis of the mouse mammary gland pubertal transcriptome. As a result, 6 individual gene sets, containing genes expressed or up-regulated in the epithelium or stroma of the TEBs or ducts were identified. Furthermore, 65 genes were selected as potential new regulators of pubertal mouse mammary gland morphogenesis, based on their association with the epithelium of TEBs. A literature search allowed classification of these genes according to their main biological function and involvement in other biological processes known to share similarities with mammary gland morphogenesis, i.e. lung, kidney morphogenesis and cancer, cellular migration, embryonic and branching morphogenesis and axonal guidance. Further ‘functional’ analysis was performed on the epithelial and stromal gene sets using IPA to identify the top biological functions over-represented in each gene set. Epithelial and stromal gene sets were also screened and compared for the presence of ‘Cellular Movement’, ‘Nervous System Development and Function’ and ‘Embryonic Development’ associated genes and the main associated functional categories were identified. Finally, TEB environment up-regulated and down-regulated genes were screened for the presence of EMT-associated genes.

3.3 Discussion

Gene expression profiling using DNA microarrays is one of the most successful tool for the analysis of global gene expression. Although it does have its drawbacks, such as decreased sensitivity of signal detection if the gene expressing cells comprise a small subset of cells within the tested tissue, and requirement for good quality RNA, it is the only method that allows simultaneous analysis of the expression levels for large numbers of genes. Since the completion of the human genome project and sequencing projects in other species, DNA microarrays aid quick and comprehensive analysis and comparison of multiple transcriptomes. This high throughput overview of the transcriptome can then be used to either identify the differentially expressed genes or over-represented trends in cellular functions, regulatory mechanisms and pathways which taken together provide clues about the studied system and can serve as a scaffold for further investigations.

The principal aim of this part of the project was to use oligonucleotide microarrays to study gene expression during ductal outgrowth of pubertal mouse mammary gland to investigate its underlying mechanisms. The main morphological characteristic of the mouse mammary gland at this stage is the presence of TEBs at the tips of the growing ducts. TEBs are only seen at puberty and generally regress upon adulthood when ductal epithelium reaches the edge of the fat pad. They are highly motile, and based on their localisation, they are thought to drive forward ductal outgrowth, promote primary branching by undergoing dichotomous bifurcation and turning and regulate spatial patterning of the ductal tree (reviewed in 1.2.2.1). Thus, it seems that a good understanding of TEB biology is fundamental to understanding the mechanisms that underlie and regulate the phenomenon of ductal morphogenesis. Despite that the function of individual genes in TEB formation and ductal outgrowth have been studied using several mouse models (for example: over-expression of FGF4 or ErbB2 deficiency was shown to cause disorganisation of TEB morphology and structure [158] [118]) (Table 1-1) or *in vitro* experiments, such as 3D Matrigel gel cultures of mammary epithelial organoids [105], our current knowledge of TEB associated gene expression is limited to two microarray studies, carried out by Morris *et al.* (2006) [259] and Kouros-Mehr *et al.* (2006) [256]. Although, to

date, there are six microarray analyses that have been carried out to provide insights into the pubertal transcriptome, these are the only two that used isolated epithelium of TEBs and ducts, with the former using enzymatic digestion and the latter microdissection to isolate the epithelium. McBryan *et al.* (2007) [194]; Deroo *et al.* (2009) [257]; Howlin *et al.* (2006) [193] and Master *et al.* (2002) [258] used whole mouse mammary glands which although useful for comparing general gene expression patterns between samples, are limited in their detection of genes that are weakly expressed or present only within a minor population of cells, as for TEBs in the whole mammary gland.

Given the importance of TEBs in pubertal mouse mammary gland morphogenesis and the currently limited understanding of the biology behind the TEB driven ductal patterning at puberty, this project was devised to present a comprehensive study of the TEB transcriptome. The experimental methodology that we used was based on that previously developed in our laboratory and published by Morris *et al.* (2006) using an enzyme-based technique for TEB and duct isolation. It uses collagenase II to digest collagen and mechanical force to further separate the epithelium from the stroma and as demonstrated in that early study is an efficient way to isolate the individual epithelial structures without compromising the quality of their RNA content [113]. Collagen fibres are major components of the fibrous ECM in the mouse mammary gland. They anchor the epithelial cells and provide them with physical support and thus, when digested, the epithelium can be easily separated from its surrounding stroma. It is worth noting, however, that the composition of the fibrous connective ECM and thus the amount of deposited collagen varies depending on its spatial location. It is denser at the neck region of TEBs or around the ducts and looser at the tips and flanks of TEBs [53]. Therefore, while it is fairly easy to isolate a clear TEB, it is often seen that the ductal epithelium requires longer exposure to enzyme to be successfully isolated from the stroma. The Morris *et al.* (2006) study, however, had limitations in terms of the restricted transcriptome represented on these early microarray chips - MG-U74Av2 chips from Affymetrix (10, 043 annotated transcripts) and the methods available for data analyses at the time.

In our study, we used Affymetrix exon *in situ* synthesised oligonucleotide microarrays, which provide 17,500 well annotated transcript IDs and enable the

differential examination of gene expression at the exon level. Along with manual analysis, we used several types of bioinformatic software to facilitate a comprehensive analysis of the obtained microarray data. Although, similarly to Morris *et al.* (2006), we used WT mice to collect isolated TEB and duct epithelium, we employed TG mice instead of their WT counterparts to collect mammary tissue strips. TG mice express EGFP under the control of a CAG promoter (combination of β -actin promoter and hCMV enhancer) [265]. Due to differences in cell density, EGFP expression is stronger in epithelium than in stroma, which facilitates the visualisation of the ductal tree under UV and thus enables more accurate assessment of tissue strip boundaries and hence more reliable comparison of microarray data. We used the RNA extracted from mammary tissue strips, Pre-LN (ductal epithelium and stroma) and Post-LN (TEB and duct epithelium and stroma) to validate gene expression patterns obtained from the isolated epithelium [113]. Both TEB and ducts are embedded in mammary stroma which not only provides physical support, but also serves as a signalling source which is a prerequisite for normal TEB formation and ductal outgrowth. It is, therefore, important to ensure that the removal of epithelium from its natural environment does not alter gene expression. In addition, Post- and Pre-LN tissue strips were used to identify the stroma associated genes around TEBs and ducts respectively.

3.3.1 Identification of pubertal signature of mouse mammary gland - Main concept behind the analysis

We compared gene expression levels between TEBs and ducts and identified genome wide epithelium- (See 3.2.6.1.1 and 3.2.6.2.1), epithelium-stroma- (See 3.2.6.1.2) and stroma associated (See 3.2.6.2.2) signatures of TEBs and ducts and thus presented the most comprehensive study of these structures to date. Reciprocal cross-talk between epithelial and stromal compartments is one of the prerequisites for normal ductal morphogenesis at puberty; however, most studies trying to decipher epithelial or stromal gene expression have mostly used IHC, IF or *in situ* hybridisation on mouse mammary gland tissue sections [152] [256] which is time consuming and can only investigate a restricted number of pre-chosen genes. More recently microarray analysis has been utilised to investigate TEB and duct associated gene expression. While both Kouros-Mehr *et*

al. (2006) and Morris *et al.* (2006) successfully isolated and studied epithelial-stromal environments of TEBs and ducts, and Morris *et al.* (2006) further succeeded in the isolation and comparison of their epithelial transcriptomes, the characterisation of stromal transcriptomes has proven a bigger challenge and has not been previously reported. Our study therefore not only adds to the understanding of epithelial transcriptomes, but also identifies and characterises stromal signatures of TEB and ducts so providing detailed gene expression analysis of both epithelium and stroma of TEBs and ducts.

We used various microarray analysis tools to identify different types of gene sets (either the 'up-regulated gene sets' or the 'expressed gene sets') and thus produced an extensive array of gene expression data that could be used to unravel and study the characteristics of each signature.

Given the large amount of collected data, this project was mainly focused on:

- Identification of new potential regulators of mouse mammary gland morphogenesis at puberty.
- Identification and comparison of functional characteristics of the epithelial and stromal transcriptomes of TEBs and ducts.

The overview of the experimental design of microarray analyses carried out in this project can be seen in **Figure 3-1** (p.151). The entire expression database (.CEL and .CHP files) however, is made available in a **Supplementary DVD**.

3.3.2 Identification and classification of new potential regulators of mouse mammary gland morphogenesis at puberty

Numerous studies have identified stromal and epithelial genes that could orchestrate ductal morphogenesis to date (reviewed in **1.2.3**). Some of the most recent findings include: the essential role of Reelin (Reln) signalling in normal extension and expansion of the ductal tree [353] and the requirement for Crkl expression in normal ductal elongation at puberty [246]. Here, we further contribute to this research by utilizing microarray gene expression analysis to search for new pubertal regulators of ductal outgrowth. Since this produced a

vast amount of gene expression data we focused our search solely on TEBs. It is important to note, however, that although when compared to TEBs, ducts are considered growth quiescent, they do give rise to secondary branching and thus play an important role in pubertal patterning of the ductal tree [114]. It may therefore be of benefit to repeat these analyses using the duct ‘up-regulated gene set’.

3.3.2.1 Comments on the methodology used

We looked at two sets of TEB ‘up-regulated gene sets’: the TEB epithelium- and TEB epithelial-stromal ‘up-regulated gene sets’. These were identified using isolated epithelium and whole mammary tissue strips respectively (For the summary of experimental concept see **Figure 3-1**). We used the whole mammary tissue strips to ensure that the observed changes in gene expression were real and did not arise as a result of the isolation procedure or errors in data analysis. Although an original study by Morris *et al.* (2006) [113] had indicated this was not the case, it is possible that any potential difference in the handling or preparation of biological material might affect gene expression which in turn might influence the results. Although enzymatic digestion proved an excellent tool for the isolation of stroma-free TEBs and ducts, its efficiency posed a major limitation. Based on personal observations, only 2 TEB and 2 ducts on average, that were not contaminated by the remains of stroma, could be retrieved from each mouse mammary gland. The limited number, along with the small size of these structures (the size of TEBs ranges from 0.1 to 0.5 mm [52] and is thought to be affected by the phase of oestrus cycle [47]) mean that a large number of mice (~150) would be needed to collect the minimal amount of RNA (1.5µg) required for each GeneChip[®] Mouse Exon 1.0 ST microarray chip. In this project, therefore, to limit the use of animals we collected fewer epithelial structures and therefore attained only enough RNA to carry out the gene expression analysis of isolated epithelium in duplicate instead of triplicate.

Since conventional statistical significance can only be assessed with a minimum of three replicates, in this project we employed an alternative method for microarray analysis - a 5% LFC Model (**See 2.2.5.5.1**). Briefly, FC for each gene is evaluated across the entire range of absolute expression levels for any number of experimental conditions and replicates. Genes are then systematically binned

across the entire range of expression values and the top 5% of genes with HFC in each bin are considered as significantly differentially expressed. The selected genes are then ranked by a calculation that combines the FC and absolute expression and the degree of importance for each gene is assigned. Compared to standard bioinformatical approaches, which select differentially expressed genes by setting a FC cut off and using p-value as a measure of statistical significance, the 5% LFC Model selects the differentially expressed genes on the basis of their FC and expression levels.

In conventional analysis most of the inherent error in calculated gene expression results from two issues: at low expression intensities, genes tend to show a greater error in their measured expression levels and thus may falsely reach any given FC cut-off, while at higher intensities where fewer errors in measured gene expression levels are observed, genes whose expression is significantly changed might be missed [269]. By selecting differentially expressed genes on the basis of both their FC and expression levels to minimise their inherent errors, the 5% LFC Model enables confident analysis of microarray data, particularly where no standard measurement of inherent error can be used due to insufficient replicates.

Despite its potential, however, there has only been one documented use of the 5% LFC Model in microarray analysis since 2002, when it was first developed [376]. To ensure its experimental reliability we used whole mammary tissue strips and conventional microarray analysis to validate the data analysed using LFC Model. When collected from six animals, tissue strips provided enough RNA for the microarray analysis to be carried out in triplicate; hence gene expression profiling could be performed using standard parameters, such as FC and p-value and standard software, such as Partek[®] Genomics[™] Suite software (See 2.2.5.5.2). This served as good control to assess the performance and validate the reliability of the generated data. It is important to note, however, that both the FC cut-off (Partek[®] Genomics[™] Suite software) and X% (LFC Model) use arbitrary parameters and thus although set within their common range in this project (1.5 and 3.0 for FC and 5%-10% for LFC) the parameters may sometimes be inappropriate. Additional measures of data quality control are therefore necessary to validate the results of microarray analysis. Here, we performed a number of quality control measures throughout the experimental stages of the

microarray analysis and successfully confirmed the quality of our data (**Figure 3-6**) (**Figure 3-7**) (**Table 3-2**).

We identified a list of 65 genes with enriched expression in the epithelium of TEBs (**See 3.2.6.3**) (**Table 3-5**). These genes were chosen as initial gene targets due to their association with both the epithelium of isolated TEBs and Post-LN strip, which ensured a high level of stringency in our analysis. The remaining 360 TEB epithelium up-regulated genes, however, can be seen in **Appendix 2**. It is tempting to speculate that most of these TEB associated genes may be functionally involved in the regulation of TEB motility and ductal patterning. However, the term 'TEB motility' still needs to be clearly defined and is quite complex in reality. Despite being at the centre of mammary gland associated research since the early 1970's, only a few suggestions have been made to explain the enigma of TEB movement (**See 1.2.3**) to date. For example: motile activities of TEBs may be explained by three actions: forward movement, bifurcation and turning; forward movement may be driven by the increased cell mass that results from intensive mitosis (as demonstrated by high mitotic rate and thymidine-labelling index [377] [126] [102] in the cells of TEB); guiding molecules (CFS-1 or eotaxin) [87] and growth factors (TGF- β) [110] may be implicated in TEB turning; and BM and ECM composition may be important for TEB bifurcation [50] [56] [109]. More recently, microarray technology has provided data on gene expression function in TEBs that confirmed that most of the genes up-regulated in TEB environment associate with DNA replication, cell division or cell-cycle regulation as well as axonal guidance, actin remodelling, ECM interaction, nucleotide synthesis, protease activity, apoptosis and cellular adhesion [113] [256]. Here, we performed a literature search on the 65 TEB epithelium-associated genes to further characterise their functional groups and thus contribute to the scientific understanding of the enigma of TEB motility.

Since no clear criteria could be used to select potential regulators of TEB motility, we took each gene in turn and searched the literature for an association with other biological processes that are known to share similarities with pubertal mouse mammary development, and could therefore serve as candidate regulators of ductal outgrowth. The processes that we focused on were: embryogenesis, branching morphogenesis, lung- kidney- development or cancer, migration and axonal guidance.

Embryogenesis and pubertal mouse mammary gland development both depend on uninterrupted cross-talk between endodermal or ectodermal/epithelial and mesenchymal/stromal cells [11] [12]. For example, during mammary gland embryogenesis, at day E16 mammary buds elongate to form mammary sprouts which invade primary mesenchyme to grow into the embryonic fat pad where they undergo branching to create a primary ductal tree. At puberty (~3 to ~10 weeks) the ductal tree elongates and branches by epithelial invasion of surrounding stroma with forward movement, primary branching and turning being driven by TEBs. This forward movement of TEBs most likely occurs due to cell rearrangement and collective migration [105] (See 1.2.2.1.1) as recently also demonstrated for nephron formation during kidney morphogenesis of zebrafish (*Danio rerio*) using *in vivo* cell imaging [378]. It is worth noting, however, that in nephron formation, full epithelial polarisation of pronephric cells is preserved [378] whereas TEB-like organoids are multilayered and only partially polarised [105]. Branching morphogenesis in kidneys and lungs shares further similarities with mammary glands, including the dependence on epithelial-stromal cross talk in which MMPs are thought to be crucial, (reviewed in [379]) and the regulatory role of FGF family members (reviewed in [379]). As is the case for primary branch formation of mouse mammary gland, most of the renal tubular branches (~75%) that form during murine kidney development *in vitro* also result from bifurcation [380]. Not only are the fundamentals of branching morphogenesis hypothesised to be similar for different organs but they are also similar across a range of organisms. For example, *Sprouty* is a gene involved in both mammalian kidney branching [381] and tracheal branching morphogenesis in *Drosophila m.* [382]. Similar extrapolations can be applied to the basic aspects of migration. Cellular migration is essential for organism development and although fundamental to a diverse spectrum of processes such as organogenesis, wound healing or immune response it is conducted in different ways with some cells migrating as individuals (germ [383] and immune [384] cells) and others collectively as tightly or loosely associated groups (neural crest formation, wound healing [385], epithelial organogenesis [105] [378] [386]). Regardless of the process, some common features of migration include: a degree of polarity, active use of the cytoskeleton (actin, myosin) and dynamic interactions between migratory cells and their surrounding environment (reviewed in [387]). As is the case for single cell migration, collective cell

migration may also be involved in tissue invasion during tumorigenesis [388] [389]. Other processes that drive cancer progression in mammary gland, kidney or lung and which can assist our understanding of normal organogenesis of these organs include epithelial-mesenchymal interactions and ECM remodelling. In a comparison of genetic similarities between embryonic lung development and lung carcinoma MYC, Hedgehog, Rb and Wnt pathways were highlighted in both the normal lung development and tumorigenesis [390]. Finally, axonal guidance molecules (*Spr1A*, *Sema3B*, *BASP1*) which act on axonal growth cones and govern neuronal migration during nervous system development have also been detected in the TEB environment during mammary gland outgrowth at puberty [113] and thus may be important in directing its epithelial outgrowth, as recently shown for *Reln* - originally identified as crucial for neuronal migration [353].

The similarities between these biological processes and pubertal mouse mammary gland development highlighted above, suggest that molecular regulators may also be conserved across different organs/biological processes. A few of such proteins have indeed been identified. For example, *Fgf2br* is essential both for the development of mammary buds during embryogenesis and maintenance of TEBs at puberty [20] [159]; *p190B-RhoGAP* is necessary for the development of embryonic mammary bud and TEB migration at puberty [24] [391]; both *Ntn1* and *Neo1* although initially identified as axonal growth guidance cues are also essential for the maintenance of TEB integrity and normal ductal morphogenesis at puberty [120] [117]; *TGF- β* is a potent inhibitor of branching morphogenesis in mammary gland, kidney and lung (reviewed in [379]) while the increased levels of *MMP2* and *MMP14* are seen at the tips of both the uterine and mammary branches *in vivo* [235] [392].

3.3.2.2 Comments on the results

Firstly, we found that the majority (58.5%) of the 65 TEB epithelium enriched genes were associated with proliferation or cell-cycle activity which is consistent with the previous observations of *Morris et al.* (2006) [113]; *Kouros-Mehr et al.* (2006) [256] and *McBryan et al.* [194]. Also in agreement with the two latter studies, we showed that 15.3%, 13.8%, 9.2%, 6.1%, 6.1% and 6.1% of these genes encoded proteins that are implicated in cellular adhesion, cell death,

intracellular transport, regulation of transcription, structural proteins and metabolism respectively. A previously unreported finding, however, was that DNA repair (7.7%), signal transduction (6.1%) and immune response (4.6%) were significantly over-represented within the TEB epithelium associated genes (**Figure 3-10 A**) (**Table 3-5**). Secondly, we identified genes that have previously been associated with normal lung (19) and kidney (10) morphogenesis/cancer and others that are known to be implicated in cellular migration (19), nervous system development (16), embryogenesis (10) and branching morphogenesis (9) providing a wide array of candidate genes with potential as regulators of ductal pubertal development (**Figure 3-10 B**) (**Table 3-5**). Together, the strong association of TEB transcriptome with proliferation and cell cycle associated genes supports the hypothesis that the forward movement of TEBs may result from the increased cell mass, caused by intensive mitosis in both cap and body cells [102]. While the identification of immune response- and cellular adhesion-linked genes as associated with TEB transcriptome may further highlight the importance of immune response for ductal outgrowth (Reviewed in 1.2.3.2.4) and the possibility of collective cell migration to serve as a mode for TEB elongation [105]. Finally, the strong link between the TEB transcriptome and the lung-, kidney-, nervous system-, branching morphogenesis, embryonic development or cellular migration associated genes supports the idea that the degree of conservation can be noted during the morphogenesis of different organs and for different developmental processes and further highlights the potential of these systems/processes to provide information on the TEB driven mammary morphogenesis at puberty.

Finally, based on these findings, we identified *Fbln2* as a candidate regulator of ductal morphogenesis at puberty and investigated its expression and function in mammary gland as discussed in detail in **Chapter 4**.

3.3.2.3 Further analyses

Other genes that share this potential and could be investigated in the future include *Emb* or *Fbn2*. *Emb* is a cell adhesion molecule that is expressed in the uterine bud of the developing kidney [341], mammary gland cancer- and embryonic cell lines [339] [340] and involuting mouse mammary gland [340] and is thought to be implicated in regulating cell-ECM interactions during

development [340], branching morphogenesis during kidney development [341] and migration of adipose tissue macrophages [393]. Fbn2 which also belongs to the family of cell adhesion molecules, is associated with epithelial-mesenchymal interactions during lung and kidney embryogenesis [346] [347]. It may also be involved in branching morphogenesis in lungs, since treatment with Fbn2 antisense oligodeoxynucleotide leads to smaller lungs with only a rudimentary epithelial tree [346]. Its heparin- and integrin-binding sites also suggested a role in cellular migration [394].

When screening for other potential regulators of mouse mammary gland development at puberty, in future it may be beneficial to include branching morphogenesis of salivary gland (reviewed in [379] [395]) or embryonic development of other skin appendages such as hair follicles and teeth respectively (reviewed in [396]) since there is considerable molecular conservation of branching morphogenesis between epithelial organs and similarities between embryonic development and pubertal morphogenesis of mouse mammary gland. Despite this, however, it must be noted, that several organ-specific cues can be distinguished for each biological process. For example, i) embryonic branching in lung and kidney is accompanied by an outgrowth of the whole organ whereas the dimensions of the mammary gland stroma in which epithelial branching occurs do not change or ii) epithelial branching in mammalian lungs and kidney takes place prenatally and adopts a rather conventional pattern in lungs (almost identical between the individuals) while most of the mammary gland development takes place after birth and appears non-stereotyped as its epithelial patterning depends on the milieu. Hence, using our comparative approach, any new genes identified as likely to serve an important role in pubertal mouse mammary gland development would be those conserved in various systems rather than specific to mammary morphogenesis. Furthermore, although genes up-regulated in TEB are an obvious primary target when studying the genomics behind TEB driven mammary morphogenesis, the TEB down-regulated (i.e. ducts up-regulated) genes may be equally important. Although no down-regulated genes have been described as essential for ductal morphogenesis as yet, this phenomenon has been reported in other systems. Down-regulation of *Hox-A7*, a gene involved in ECM regulation and cell migration during lineage commitment or maturation seems to be

essential for early HL-60 monocytic differentiation. As demonstrated *in vitro* using bone marrow stromal-like matrix sustained expression of *Hox-A7* impaired cellular migration and adhesion to fibronectin and thus impaired monocytic differentiation [397]. Finally, it is also important to mention that not only the differentially expressed (i.e. up- or down-regulated) genes but also the genes that are globally expressed in the pubertal mammary epithelium may play a role in its morphogenesis. In fact, an example of such gene has previously been reported by Howlin *et al.* who showed that *CITED1*, which expression level is similar for the TEB and duct epithelium, is essential for pubertal outgrowth [193]. A comparison analysis of the pubertal and adult (V12) mouse mammary gland transcriptomes would therefore be needed in the future to further decipher this phenomenon.

Other ways to search for candidate genes rather than looking for those showing similar cellular/biological functions are: i) by selecting on their level of over-expression (we used this approach to identify *Upk3a* as a second target gene as discussed in detail in **Chapter 4**); ii) by chromosomal location or iii) by association with canonical pathways which are already known to be involved in the studied system.

3.3.3 Identification and comparison of functional characteristics of the epithelial and stromal transcriptomes of TEBs and ducts

Since little is known about differences in gene expression between the TEB and duct environments, especially between their epithelial and stromal compartments, as a third part of this project, we identified an array of biological functions that characterise each compartment.

3.3.3.1 Comments on methodology used

We identified four ‘expressed gene sets’, namely: TEB-only stroma-, duct-only stroma- and TEB-only epithelium-, duct- only epithelium- in addition to two ‘up-regulated gene sets’, namely: TEB epithelium- and duct epithelium-. The ‘up-regulated gene sets’ were used to compare the epithelial gene expression only,

as discussed above. ‘The expressed gene sets’, on the other hand, were used to find differences in gene expression between stroma and epithelium. This is because the analysis used to select the stroma associated genes (manual screening of the raw gene expression data from the isolated epithelium and tissue strips (See 3.2.6.2.2)) did not allow calculation of FCs but only enabled presence or absence of gene expression to be determined. To provide a suitable comparison we also identified epithelium expressed gene sets (See 3.2.6.2.1). For summary of experimental concept see Table 2-5.

When using gene lists to elucidate the general trends in biological processes or pathways there are different sets of criteria that can be used. Firstly, rather than using the most highly expressed genes, it may be argued that a gene set consisting of the widest range of representative genes may be of more relevance to understand the biological system in question. Genes with large changes in expression values may not necessarily make the strongest contribution to biological processes and thus should not be prioritised over those that show less pronounced expression levels. Furthermore, it is not necessary for all genes within a given pathway or biological process to be highly differentially expressed in order for the pathway to be important. Thus, the ‘expressed gene sets’, although initially used in this study because of the limitation of the methodology used for data analysis, actually provided a comprehensive and unbiased analysis since they include genes with a range of expression levels from the most highly expressed to those with expression only slightly altered.

In contrast, the ‘up-regulated gene sets’ used in ‘pathway analysis’ helped to focus the analysis. By incorporating genes expressed over a certain level and thus excluding genes whose expression oscillated around the baseline level (of FC 1.1) and thus may have been associated with the specific environment just due to chance, the risk of non specificity in identified profiles was reduced. Moreover, since some biological processes, e.g. EMT require both the up-regulation of mesenchymal genes (*Twist* [272], *Snail 3* [273], *Slug* [274]) and down-regulation of the epithelial markers (*E-cad* [280], *Spr1a* [270]), only the use of the ‘up-regulated gene sets’ together with the corresponding ‘down-regulated gene set’ will fully unravel such mechanisms. This analysis could not be executed using the ‘expressed gene sets’.

Therefore in this study, we used both the ‘expressed gene sets’ and ‘up-regulated gene sets’ to provide a comprehensive novel analysis of the general trends and differences in the functional characteristics of TEB and duct epithelium and stroma (‘expressed gene sets’). We also compared the biological processes associated with the genes identified as significantly up-regulated in TEB and duct epithelium (‘up-regulated gene sets’). In addition to that, since we used both gene sets to functionally characterise the TEB and duct epithelium we enabled the comparison of the potential differences in generated data when using different gene list.

3.3.3.2 Comments on results

Since the motility of TEBs and ducts at puberty is very different we originally hypothesised that their gene expression would reflect different patterns of biological behaviour and indeed this was the case, as outlined below.

‘Pathway analysis’ on the basis on microarray data is a valuable tool to establish the biological changes that occur in biological systems and has as such been widely used. However, it is also important to bear in mind its limitations. Firstly, it is based on mRNA expression only. Secondly, the association of genes with given processes is established depending on the information deposited in the manually created knowledge data base (See 3.3.3.5). Some of the genes selected by IPA as indicative of the given functional category are non specific and can often be found to associate with a range of different cellular functions and systems. It is therefore, important to note that this type of analysis may be biased and not fully representative of functional processes activated *in vivo* and thus should be interpreted with caution and only used as a starting point for further investigation.

3.3.3.2.1 *Characterisation of the TEB and duct transcriptomes using ‘expressed gene sets’*

Terminal end bud epithelium

Comparison of the ‘expressed gene sets’ showed both the epithelium and stroma of TEBs to be strongly associated with ‘Cellular Movement’ (27.8% and 20.5% of genes respectively) and ‘Cell-Cell Signalling and Interaction’ (27.9% and 23.7% of genes respectively) (Table 3-5). Thus, suggesting not only a high but also a comparable level of the motility associated genes in both milieus. In general, this finding would not be surprising as it is in agreement with the emerging idea of both the epithelial and stromal compartments of TEB being necessary for ductal outgrowth but playing different role in its regulation (reviewed in 1.2.3.2). Here, however, the link between TEB transcriptome and ‘Cellular Migration’ was mostly attributed to the presence of genes associated with the regulation of immune cell motility.

As shown by IPA results, the sub-groups within the ‘Cellular Movement’ category that were common for the epithelium and stroma of TEB included both positive and negative regulation of e.g. ‘the movement or migration of the immune system components’ (eosinophils, mononuclear lymphocytes, phagocytes, leukocytes and monocytes) or ‘-nervous system components’ (dendric cells). This association with immune cell motility was further seen in the TEB epithelium exclusive sub-categories, which consisted of both positive and negative regulation of the ‘movement/migration of neutrophils, -macrophages, -T lymphocytes, -antigen presenting cells, -bone marrow cells’; ‘chemotaxis of blood cells, -dendric cells, -leukocytes’ and ‘homing of phagocytes, -lymphocytes, -blood cells’ and ‘migration and chemotaxis of tumour cell lines’ (Appendix 9 A).

This striking association of TEB epithelium with the immune response gene signature was further supported in our analysis by an association of the epithelium expressed gene set with ‘Immune Response’ (28.3%), ‘Immune and Lymphatic System Development and Function’ (25.1%) and ‘Haematological System Development and Function’ (29%). Together, these results are in

agreement with the emerging importance of innate immune response for pubertal mammary morphogenesis.

As reviewed in **Chapter 1 (1.2.1.2.3 and 1.2.3.2.4)**, the formation and outgrowth of TEBs during puberty is closely paralleled and dependent on the accumulation of macrophages, eosinophils and mast cells in the stroma around TEBs (macrophages, eosinophils) and ducts (mast cells) [85] [89]. Furthermore, inflammatory cells (neutrophils, eosinophils, macrophages and plasma cells) and acute-phase response genes, such as *CD14*, *lipopolysaccharide-binding protein (Lbp)* and *STAT3* associate with early involution of mouse mammary gland suggesting a wound healing-like process to be a part of the early response to weaning [38]. The recruitment of haemopoietic cells may be regulated by the signalling cues expressed in mammary epithelium (reviewed in [87]). As demonstrated for macrophages, the growth factor which regulates their motility (CSF-1) [398] is expressed in mammary epithelial cells [87] and when ablated (null mutation in *CSF-1* - *Csf1^{OP}/Csf1^{OP}* mice [220]) or dysfunctional (loss of CSF-1 receptor - *CSF-1R KO^{-/-}* mice [399]) a reduced macrophage density in mammary gland can be seen. Furthermore, a high expression of the cytokines *IL-6*, *IL-8* and *High in normal 1 (HIN-1)* have been reported in human breast epithelial cells [400] [401].

Here, we report that, as suggested by the results of IPA, epithelial transcriptome of TEBs may also encode proteins involved in positive regulation of ‘proliferation/activation/accumulation of mononuclear leukocytes (*Cd 2 antigen - Cd2*, *Cd 22 antigen - Cd22*), -T lymphocytes (*Cd 4 antigen - Cd4*) and -B lymphocytes’ (*Bone marrow stromal cell antigen 1 - Bst1*, *Bruton agammaglobulinemia tyrosine kinase - Btk*) and ‘adhesion of neutrophils’ (*Chemokine (C-C motif) ligand 3 - Ccl3*). It is important to note, however, that not all of these genes are specific to the identified process. While *Cd4* and *Bst1* serve as markers of T and B cells respectively, *Btk* expression have been associated with both the B cell maturation and mast cell activation. *Ccl3* has been associated with neutrophils and T-lymphocytes. Thus, although these data are in agreement with our ‘Cellular Migration’ results which also suggested the high abundance of genes associated with the immune system components and their motility within the epithelium of TEBs (which in fact is higher than that seen for the stroma) it is important to note that some of these genes may not be

specific to the immune response. The other possibility is that because of the direct proximity of haemopoietic cells and mammary epithelium and as seen for macrophages, potential association of immune cells with Coll fibres which are deposited around the flanks of TEBs [83], some immune cells may have been isolated with mammary epithelium.

Nevertheless, if confirmed, these data may not only further highlight the importance of the immune response in pubertal mammary morphogenesis but also support and add to the understanding of the emerging role of mammary epithelium in controlling the homing of migrating hematopoietic cells into adjacent stroma. Furthermore, since macrophages have also been shown to localise to the inside of the body of TEBs [87], it may be that the immune system components other than macrophages also associate with mammary epithelium but additional research should be carried out to validate these possibilities. T and B lymphocyte markers and neutrophil associated genes have been suggested as TEB epithelium expressed by both the results of 'Immune Response' and 'Cellular migration' groupings. Furthermore, these immune system components have previously been reported as involved in wound healing and shown to infiltrate the mammary gland during pregnancy (B lymphocytes) [402] and involution (neutrophils) [38] but have not yet been reported in the pubertal mouse mammary gland. In fact, a previous study, using leukocyte lineage markers (B220, CD3 and Gr1) demonstrated that while present in the mammary lymph node, no T-, B lymphocytes or neutrophils could be seen in the vicinity of its pubertal epithelium [87]. Despite this, since wound healing has previously been linked to mammary involution and several traits characteristic of wound repair are seen in pubertal mammary morphogenesis (epithelial growth, stromal reorganisation and immune cell infiltration) the repeated identification of T-, B lymphocyte or neutrophil associated genes in pubertal mouse mammary gland should be investigated further.

Terminal end bud stroma

A similar association with the immune system was detected by IPA, in the TEB-only stroma 'expressed gene set', where 'Haematological System Development and Function' ranked to the top 5 over-represented processes and encompassed the 23% of TEB stroma and IPA eligible genes (Table 3-7). This was also

consistent with the results of the analysis, discussed above, that showed an association of TEB stroma with the migratory signature of immune system components. Most of the sub-categories associated with the stroma expressed genes were similar to these identified for the TEB epithelium gene set. Some of the stroma-exclusive categories, however, included positive regulation of ‘proliferation of natural killer T lymphocytes (NKTL)’ (*E74-like factor 4 - Elf4*, *Interleukin 18 - Il18*), ‘recruitment/quantity of phagocytes (*Glypican 3 - Gpc3*) and -Langerhans cells’ (*Signal regulatory protein a - Sirpa*, *Interferon regulatory factor - Irf*). The Langerhans cells are dendritic cells of the epidermis which are similar in morphology and function to macrophages. They capture, uptake and process antigens while the NTKL and phagocytes mark cells for destruction by apoptosis and ingest antigens respectively. As mentioned before, it is important to note, however, that neither *Elf4* nor *Il18* are exclusive to NKTL cells but can also be associated with T-lymphocytes while *Gpc3* is a membrane associated proteoglycan which has also been suggested to play role in cell division in many cell types. *Sirpa*, furthermore, may also be involved in phagocytosis, mast- and dendritic cells activation. Thus, the association of TEB stroma with these immune cells should be taken with caution. Nonetheless, if confirmed, these results may add to the understanding of the role of phagocytosis (as suggested for macrophages [84] [87]) in contributing to stroma remodelling at the tip of the advancing TEB at puberty.

As previously mentioned, the stromal transcriptome of TEBs has also been suggested to associate with ‘Cellular Movement’ (Table 3-6). While it was partially suggested as being involved in regulating the ‘motility of immune system- and nervous system components’ (See the first paragraph of this section) some of the other genes within the stroma of TEBs additionally appeared to be associated with ‘movement/chemotaxis of cancer cell lines’ and ‘invasion of neuroglia’ (provides support and protection for growing neurons). Given the emerging similarities between TEB outgrowth and breast cancer progression and neuronal development further investigation of these genes in ductal morphogenesis may prove beneficial.

Finally, as proposed by IPA, association of TEB stroma with ‘Cardiovascular System Development and Function’ (11.5%) (Table 3-7) may be suggestive of the presence of dynamic cardiovascular morphogenesis at puberty. To date, there

has only been one published study that looked into vessel development during mouse mammary gland development at puberty. It has reported, however, that no morphological evidence for active vascular development in pubertal mouse mammary gland can be seen, identifying embryogenesis, pregnancy and lactation as the highly angiogenic time points [403]. Our data further suggested that the epithelial transcriptome of ducts may also contain the angiogenesis associated genes (**Table 3-7**) and that TEB epithelium expresses high levels of *Vascular endothelial growth factor (VEGF)*, which is a known stimulator of angiogenesis. Thus, if confirmed, these results could shine a new light on the area of vascular development during mammary gland morphogenesis and the role of TEBs in angiogenesis. Further research will be necessary to validate these possibilities.

Some of the other processes identified in TEB stroma included ‘Cell Death’ (33.4%), ‘Tissue Morphology’ (16.9%) and ‘Tissue Development’ (19.8%). These are in agreement with TEB stroma being an actively remodelling milieu (**Table 3-6**) (**Table 3-7**).

Duct epithelium

In contrast to the TEB environment, neither the migratory nor the immune system associated gene signatures could be identified in the duct ‘expressed gene sets’. Furthermore, as compared to TEBs, where both the epithelial and stromal compartments shared fairly similar functional characteristics, substantial differences were detected in the functional roles of ductal epithelial and stromal transcriptomes. Our analysis suggested that the processes that are highest in the ductal epithelial transcriptome are ‘Embryonic Development’ (2.3%) (**See 3.3.3.3**) and ‘Connective Tissue Development and Function’ (2.9%) (**Table 3-7**). It is important to note, however, that the association of ductal transcriptome with these categories is based on a very low percentage of genes and thus may not be fully reliable. Furthermore, all sub-categories within the ‘Connective Tissue Development and Function’ group were associated with fibroblasts which may also indicate the contamination of ductal epithelium with stroma during the isolation procedure.

The rest of the duct-only epithelium ‘expressed gene set’ was suggested to associate mostly with non-specialised mechanisms essential for cell survival, replication and regulation of gene expression. Namely, ‘Cell Cycle’ (14.8%), DNA- or RNA-processing associated applications (11.8% and 4% respectively) or organogenesis - ‘Cellular Assembly and Organisation’ (Table 3-6). These suggest that, although lower than in TEBs, considerable levels of cellular proliferation are sustained in ductal epithelium.

Duct stroma

The transcriptome associated with ductal stroma was mainly linked to ‘Lipid Metabolism’ (14.7%), ‘Carbohydrate Metabolism’ (15%) and ‘Small Molecule Biochemistry’ (28.9%) (Table 3-6) and thus indicated an intense metabolic activity. Lipid and carbohydrate metabolism has been reported in lactating mouse mammary glands in experiments dating back to 1950 [404] while the metabolism of brown adipose tissue (fatty acid metabolism) has been studied in 2002 by Master *et al.* using the pre-pubertal mouse mammary glands [258]. More recently the expression of genes associated with ‘Lipid Metabolism’ and ‘Carbohydrate Metabolism’ was demonstrated to decrease during puberty in normal mice [258] or in response to estradiol in ovariectomised mice [257]. To our knowledge, however, a detailed biochemical study of metabolic changes accompanying pubertal mouse mammary gland morphogenesis has not yet been performed. Here, we identified the ductal stroma as the place of highest metabolic activity in pubertal mouse mammary gland and identified the list of associated genes (Appendix 7) which may provide a foundation for further investigations.

3.3.3.2.2 Characterisation of TEB and duct transcriptomes based on the ‘up-regulated gene sets’

Terminal end bud epithelium

The suggested differences between TEBs and ducts were further highlighted by comparing the epithelium ‘up-regulated gene sets’. As was the case for TEB epithelium-only ‘expressed gene set’ the mRNAs up-regulated in the epithelium

of TEBs were mainly associated with cell survival and proliferation ('Cell cycle' (38.6%), DNA Replication, Recombination and Repair (34%) and Cellular Growth and Proliferation' (35.5%)), which is consistent with the results of Morris *et al.* (2006) and Kouros-Mehr *et al.* (2006) [256], as well as 'Cellular Movement' (6%) (Table 3-6). As opposed to the 'expressed gene set', which was suggested to be closely associated with movement of immune- and nervous system components, the up-regulated genes of TEB epithelium were mainly associated with 'promoting the cytokinesis' and 'chemorepulsion of neurites' (*Sema3A*, *Sema3B*). 'Embryonic Development' (See 3.3.3.3) which was not seen in the 'expressed gene set', 'Connective Tissue Development and Function' and 'Skeletal and Muscular Development and Function' were also over-represented (Table 3-7). The sub-groups in 'Skeletal and Muscular Development and Function' category were mostly associated with fibroblasts (which again may indicate stromal contamination) and promoting the 'cell cycle progression in muscle cells'.

Duct epithelium

Whereas the top functional characteristics of TEB epithelium 'expressed-' and TEB epithelium 'up-regulated gene sets' were reasonably comparable this was not the case for the ductal gene sets, where only one category, the 'Molecular Transport' was common to both analyses (Table 3-6). The most striking result from this analysis was that 'Cellular Movement' associated genes were the second highest functional group within the duct epithelium 'up-regulated gene set' (Table 3-6). Furthermore, a wide array of functional sub-categories associated with cellular motility (immune cell, nervous system component, smooth muscle cell, cancer cell line, kidney morphogenesis) were over-represented within the ductal epithelial transcriptome while the TEBs were suggested to associate mostly with immune cell migration (expressed genes), axonal guidance and cytokinesis (up-regulated genes). This was further surprising as the 'Cellular Movement' signature appeared to be stronger in duct- rather than TEB up-regulated transcriptomes. Over all, these results suggest that ductal epithelium may play a bigger role in regulating pubertal morphogenesis in mammary gland than previously anticipated. Another possibility is that the duct epithelium 'up-regulated genes' that were functionally classified under the 'Cellular Migration' category rather than being the makers of motile behaviour they are common regulators of various processes and thus *in vivo* they may not

function to drive cellular migration in ductal epithelium. Further examination of individual genes involved in each category should be performed to validate these possibilities (**Appendix 9 A**).

The suggested presence of immune system-associated genes in the duct epithelium 'up-regulated gene set', as demonstrated by the contribution of the 34.4% of genes to the 'Haematological System Development and Function' and 26.3% to 'Immune Cell Trafficking' (**Table 3-7**) is in agreement with the previously discussed association of duct-only expressed genes with the immune response components (**See above**). While many of the functional sub-groups within the immune system category were similar to those identified for TEB environment (e.g. positive regulation of the 'recruitment/activation of neutrophils, -phagocytes, -lymphocytes, -mast cells') the 'change of shape of basophils' (*Ccl3*, *Chemokine (C-C motif) receptor 2 - Ccr2*) was specific to this gene set. *Ccl3* is a chemokine. Although, as seen for many other genes, mentioned in analysis, it is not entirely basophile specific (eosinophils, neutrophils), it has been shown to promote the chemotaxis of granulocytes. Thus, its expression by ductal epithelium may support the role of mammary epithelium in the recruitment of haemopoietic cells to the proximal mammary stroma. The expression of *Ccr2* in ductal epithelium, however, is less clear (it has been previously shown to be expressed by mammary epithelium during inflammation [405]).

Granulocytes may either act to induce an inflammatory reaction (mostly allergy) or ingest foreign particles. If confirmed, the association of mammary epithelium with phagocytes may suggest a possible role of phagocytosis in lumen formation. Pubertal epithelium and especially TEBs show very substantial apoptotic rate (11.3 %) which is higher than that calculated for any other stage of mouse mammary development (apoptosis detected for involution is 4.5%) [61]. It must be noted, however, that the association of immune cells with lumen formation has only been suggested by one study. Gouon-Evans *et al.* (2002) reported that macrophages which engulf apoptotic epithelial cells can be seen in the proximal area of lumen within the TEBs [87]. To date, it has been further proposed that lumen formation in pubertal epithelium is dependent on caspase-mediated apoptosis and Bcl2-like 11 (BIM) expression, which may induce the detachment of cells from its matrix, termed anoikis (as previously seen during involution) and

thus mark cells for degradation [244] [406]. This can be further supported by the recent finding showing that the body cells of TEBs lack matrix attachment [244]. The down-regulation or loss of BIM *in vitro* or in BIM KO^{-/-} mice, however, although prevented apoptotic clearance of cells did not abrogate but only delayed lumen formation in both systems, thus suggesting presence of alternative mechanisms for lumen formation and clearing [244]. Hence, further research into its possible mechanisms should be warranted.

In summary, the functional characteristics of TEBs and ducts appeared quite different depending on the type of gene sets used for the analysis. This suggests that both types of analysis ought to be completed for a comprehensive picture of gene expression patterns and the use of ‘pathway analysis’ to aid functional characterisation of transcriptomes should be taken with a lot of caution.

3.3.3.3 Association of pubertal development with embryogenesis

Similarities between embryonic development and pubertal mouse mammary gland development have already been discussed in 3.3.2 with some of the embryogenesis associated genes suggested as potential regulators of mammary gland morphogenesis at puberty. For that analysis, however, we hypothesised that it is the TEB transcriptome that would contain the embryonic development associated genes. The identification of the duct-only epithelium ‘expressed gene set’ as that most associated with this process suggested, however, that the morphogenic potential of embryogenesis associated genes should perhaps be assessed with respect to the ductal transcriptome rather than the TEB one. The embryonic signature identified within the duct-only epithelium ‘expressed gene set’, however, associated with embryonic cell lines, which is general and did not hint towards any specific assumptions. What stands out, however, and may provide the foundation for further research is the association of ductal epithelium ‘up-regulated gene set’ with the positive regulation of ‘branching morphogenesis’ (kidney, carcinoma, thyroid and kidney cell lines) and the association of duct-only stroma ‘expressed gene set’ with promoting the ‘morphogenesis of forelimb bud, branchial arch and cardiovascular system’. Some, although fewer, ‘Embryonic development’ related genes, and thus not complying with top 5 categories, could be also seen in the TEB transcriptome. As for the duct-only epithelium expressed genes, however, the link of TEB gene sets

with the ‘Embryonic Development’ is fairly general (**Appendix 9 C**). In summary, these suggest that both TEB and duct transcriptomes associate with the ‘Embryonic Development’ gene signature and as mammary gland is the only organ where the majority of development occurs postnatally these results reflect the highly morphogenic character of its development at puberty.

3.3.3.4 Association of pubertal development with EMT

Although, initially reported as fundamental for cellular migration during embryonic development, recent evidence, although highly controversial, has linked EMT with cellular invasion during tumour progression and metastasis formation (reviewed in [373] [407]). Not only do epithelial breast cancer cell lines express mesenchymal markers *in vitro* [270], but using different mouse models of breast cancer with genetically marked epithelial and mesenchymal cells, the presence of some EMT markers has been demonstrated in breast cancer cells *in vivo* [408] [409]. Since there are parallels between embryonic development, cancer progression and mammary gland outgrowth, i.e. epithelial invasion of surrounding stroma and poor polarity seen in the cap cells of TEBs (further discussed in 5.2.2) [56], it is tempting to speculate that EMT may serve as a mechanism underlying ductal outgrowth and that cap cells may serve as sites of this transition (they lack cell-cell junctions, show poor apical basal polarity and localise to the outer layer of TEBs).

In fact, this possibility has already been addressed by two studies. Kouros-Mehr *et al.* (2006) found that *Snail-1* and *Twist-1*, mesenchymal markers of EMT, were enriched in the TEB microenvironment when compared to its ductal counterpart [256] while Nelson *et al.* (2006), using epithelial tubules formed by EpH4 cells in 3D culture, demonstrated that an EMT-like transition event is required at the branch points for branching to occur [110].

Since the mesenchymal genotype can be characterised by both the up-regulation of mesenchymal- and the down-regulation of epithelial markers (The list of EMT markers can be seen in **Table 2-8**) in this project we further examined this issue by screening the TEB environment up- and down-regulated (i.e. duct environment up-regulated) gene sets for the presence of EMT signature genes. We looked at 256 EMT markers and thus performed the most comprehensive

analysis of the EMT response in pubertal mouse mammary gland development to date. We found that 13% of mesenchymal markers were up-regulated in TEB while 12% of epithelial markers were down-regulated in TEB environment (up-regulated in ducts) highlighting the potential for TEB outgrowth to be promoted by EMT. However, our negative control showed that a further 6.25% of the epithelial makers were up-regulated in TEB compartment while a 6.8% of the mesenchymal markers were seen in the TEB down-regulated milieu (**Table 3-7**). Moreover, as further revealed by literature search, performed on the individual EMT associated genes differentially expressed in TEB transcriptome but not yet described or studied in mammary, i.e. 17 out of 31 EMT marker genes (*Col1a2*, *Col5a2*, *Ecm1*, *Fap*, *Fbln1*, *Fbn1*, *Cybrd1*, *Ap1m2*, *Cxadr*, *Kcnk1*, *Klk8*, *Lad1*, *Trim29*, *Aldh1a3*, *Ndr1* and *Slp1*) some of these markers were non specific.

In summary, these results may suggest the individual EMT associated genes with the potential to be important for pubertal morphogenesis. For example, *Prrx1*, a member of homeobox gene family that is one of the mesenchymal markers found to be over-expressed in TEBs, has previously been shown to be critical for tooth morphogenesis [410]. Furthermore, homeobox genes in general have been associated with normal embryonic and postnatal mouse mammary gland development and carcinogenesis [411]. However, due to the lack of specificity of some genes in the EMT signature and a relatively high number of the negative control genes within the TEB transcriptome these results do not allow to make final conclusions about the involvement of EMT in pubertal mammary morphogenesis, but also they do not rule it out.

3.3.3.5 Association of pubertal transcriptome with nervous system

The ‘Nervous System Development and Function’ was not identified amongst the top functions over-expressed in pubertal transcriptome. The known association of axonal guidance proteins with ductal outgrowth at puberty (**See 3.3.2.1**), however, prompted us to further screen the TEB and duct gene sets for the presence of the nervous system associated genes. In contrast to previous findings (**3.3.2.1**) which associated axonal guidance molecules with the epithelium of TEBs, our results suggested that, in fact, it is primarily the stroma of TEBs that shows this association. The stroma contained 43 genes involved in processes such as ‘outgrowth of neurites (projections from the cell body of a neuron), -sensory

axons'; 'survival/quantity of astrocytes (glial cells in brain or spinal cord), - neurites' or 'myelination' (formation of myelin sheath around axon or neuron). Fewer, but still a significant number of nervous system associated genes could be identified in both the epithelium and stroma of ducts and these appeared to be involved in 'migration/survival of astrocytes'; 'stimulation/activation of neurons' (epithelium) and 'axogenesis and branching of axons' (stroma). The TEB epithelium in comparison, had a transcriptome least associated with the nervous system, with only one gene - *Sema3B*, linked to chemorepulsion of neurites (**Appendix 9 B**). To fully appreciate the strength of these results, however, it is important to note that, to date, several genes identified as associated with neuronal development have been also implicated in angiogenesis. *Neuropilin 1* and *2* have been characterised as receptors for both semaphorins in axonal guidance and VEGF for angiogenesis (reviewed in [412]). Thus, it is possible that this neuronal signature may be indicative of vascular- rather than neuronal development. Further examination of individual genes identified within these subcategories should be warranted. Nonetheless, if confirmed, these results may provide further positive evidence that the axonal guidance/nervous system development gene signature is associated with pubertal mouse mammary development, highlight mammary stroma as its source and potentially provide new gene targets which could be studied in the future to help to further unravel the link between mammary and axonal development.

3.3.3.6 Further analyses

In general IPA is a powerful and desirable tool for post-analysis of microarray data and frequently appears as software of choice in published gene expression studies [413] [414] [415]. It is, however, based on a manually created database which although curated by PhD trained scientists, updated quarterly and based on information mined from 32 top peer-reviewed journals, is man-made and may therefore be prone to bias and not always up to date with the literature. In addition, genes can only be assigned a specific function based on the information deposited in the database. Thus, since IPA depends on its own comprehensive but biased knowledge database, the results may be limited and influenced by its content. Furthermore, it is important to note that some of the genes used by IPA as indicative of the given functional category are non specific and can often be found to associate with a range of different cells and

processes. Some of the other non specific genes not mentioned in this discussion include *Endothelial-specific receptor tyrosine kinase (Tek)* or *Cyclin D1 (Ccdn1)*. *Tek* is normally associated with endothelial cells, but in our analysis defined a positive regulator of the ‘quantity of antigen presenting cells’ while *Ccdn1* is generally abundant throughout cell cycle but defined here as a maker of the ‘chemotaxis of bone marrow derived macrophages’. This may introduce additional bias into the analysis. Having said that, it is also important to note that many genes, such as *Cd4*, *Bst1*, *Elf4* which are specific markers of T lymphocytes, B lymphocytes and NKTLs respectively have also been found in our analysis. It must be stressed, therefore, that the results of IPA analysis and any other ‘pathway analysis’, may be used to sketch the general picture that could highlight and suggest the potential avenues for further investigation, but has the potential to be biased and thus should be interpreted with caution.

Furthermore, since this study was based entirely on RNA data and not all RNA undergoes translation or protein products from RNA may at times locate to sites different from their RNA matrices (as seen for extracellular proteins) it is important to note that the proteins transcribed from epithelial mRNA might localise to the stroma rather than the epithelium. The converse is also true as seen for some of the BM components, such as *Lama1*, which, although synthesised in stromal fibroblasts is detectable as protein in BM [82]. Thus, although transcriptomics might be used for initial studies, protein analysis is needed to fully decipher the characteristics of organ morphogenesis.

In addition, it is important to note that all the results presented in this chapter were based on the up-regulated or expressed genes only. Hence, it may be beneficial to repeat the ‘pathway analysis’ for TEB and duct epithelium up-regulated genes using both the up- and down-regulated gene sets simultaneously.

3.3.4 Summary

In summary, our work has shown that microarray analysis can be used both to identify potential new regulators (e.g. *Fbln2*, *Upk3a*) and provide clues that may help to characterise complex processes and their drivers associated with mouse mammary gland development at puberty. We identified the genome wide

epithelium-, epithelial-stromal- and stroma-associated signatures of TEBs and ducts and compared the biological functions and processes associated with each transcriptome. As a result, not only did we add to the understanding of the epithelial transcriptomes of TEBs and ducts but also provided insights into the characteristics of their stromal gene expression and thus presented the most comprehensive gene expression analysis of TEBs and ducts to date.

We highlighted the association of TEB transcriptome with kidney and lung morphogenesis/cancer, cellular migration, nervous system, embryonic development and branching morphogenesis associated gene signatures and suggested that these genes could provide new pubertal regulators of mammary morphogenesis.

We suggested that the stroma and epithelium of TEBs associates with similar processes and these are mainly 'Cellular Migration', 'Immune System Development and Function' and 'Embryonic Development' whereas the epithelial and stromal signatures of ducts may differ considerably. We suggested that the ductal epithelial transcriptome associates with 'Embryonic Development'- and immune system (especially the migration of immune system components) gene signatures while ductal stroma appears as a place of high metabolic activity. Thus, suggesting that mammary epithelium may express cues that promote the infiltration of haemopoietic cells into epithelium adjacent stroma and proposed that an active angiogenesis may occur in mammary gland at puberty. In addition, we presented the most comprehensive analysis of the EMT response associated genes in pubertal mouse mammary gland development, to date, but were not able to draw final conclusions from our data on its involvement in controlling TEB outgrowth. We addressed the potential association of the pubertal mammary transcriptome with neuronal development gene signature and suggested that the TEB stroma and duct epithelium may comprise the highest number of axonal guidance genes.

Finally, we identified the potential presence of many cell types, including neutrophils, T-, B-lymphocytes and NTKLs; and genes, such as: *Emb*, *Fbn2*, *Fap* or *Slit1* that have not previously been linked to pubertal mouse mammary gland but may be potentially important for its morphogenesis. These pose many

questions that still need to be answered and may suggest many potential avenues of investigation that could guide future work.

4 Identification of new potential regulators of pubertal mouse mammary gland morphogenesis: Uroplakin 3a and Fibulin 2

4.1 Introduction

One of the main focuses of the microarray analysis performed in this study was the identification of new genes with potential to regulate pubertal mouse mammary gland development (See 3.2.6.3). These were selected from the list of 65 TEB epithelium up-regulated genes based on two criteria such as: i) FC level ii) association with biological processes known to share similarities with pubertal mouse mammary gland morphogenesis (See 3.2.6.3) (Table 3-5). Two genes *Uroplakin 3a* (*Upk3a*) and *Fibulin 2* (*Fbln2*) were identified and selected for further investigation.

4.2 Results

4.2.1 UROPLAKIN 3A

4.2.1.1 Introduction

Upk3a was selected as a candidate regulator of pubertal mouse mammary gland development because it was identified as the most over-expressed gene within the 65-gene list. In fact, as shown by 5% LFC Model-based microarray analysis, *Upk3a* was identified as the most up-regulated gene (10.74 fold up-regulated) in the epithelium of isolated TEBs (TEBs vs ducts) (Table 3-4).

To date, *Upk3a* has only been detected and functionally associated with normal or impaired bladder development. It encodes a membrane protein consisting of 287 amino acids (aa) and is characterised by a molecular mass of 47 kDa from which ~ 29 kDa and ~ 18 kDa account for apoprotein and complex glycans respectively. The mature *Upk3a* protein consists of a 189 aa long N-terminal domain that encloses all potential N-glycosylation sites and a 52 aa long C-

terminal, cytoplasmic domain within which multiple phosphorylation sites are contained. The remaining ~ 46 aa make up a single transmembrane domain.

Upk3a belongs to the uroplakin family, which consists of four additional proteins: Upk1a (27 kDa), Upk1b (28 kDa), Upk2 (15 kDa) and Upk3b (35 kDa) [416] [417]. The cytoplasmic domain is exclusive to Upk3a and was postulated to enable the interaction of Upk3a with the cell cytoskeleton [418]. N- and C-terminal domains of Upk3a are joined by a single transmembrane domain [418] [419]. All five uroplakins are known to be integral, structural components of a differentiated bladder urothelium. The two dimensional (2D) crystals of hexagonally packed 16 nm uroplakin particles have been shown to assemble as plaques and are called asymmetric membrane units (AMU). Plaques line the apical side of terminally differentiated mammalian urothelial umbrella cells, called superficial cells [420] [421]. Urothelial plaques are postulated to function as a permeability barrier and serve as a means for stabilizing the luminal bladder surface during contractions and expansion [422]. In the urothelium, uroplakins exist and function as heterodimers (1a/2 and 1b/3) [423] [424]. This conformation enables them to exit from the endoplasmic reticulum and is a prerequisite to reach the cell surface [425]. Formation of Upk3a/Upk1b heterodimer triggers a conformational change in Upk3a and protein maturation. The 43 kDa immature, endoplasmic reticulum form of Upk3a gets converted to the 47 kDa glycosylated, mature and stable protein (Golgi form).

Gene targeted ablation of *Upk3a* confirmed its functional association and vital role in normal plaque formation [422]. Examination of bladder structure and function in Upk3a deficient mice revealed a reduced size of the urothelial plaques causing increased urothelial permeability, increased proliferation of umbrella cells, presence of retrograde flow of urine from the bladder into the ureters (vesicoureteral reflux), accumulation of urine in the renal pelvis (hydronephrosis), abnormal voiding patterns and an increase in spontaneous contractions and pressure in the bladder [422] [420] [426] [427]. Furthermore, Matsumoto *et al.* (2008) showed that loss of Upk3a expression is associated with the occurrence of transitional cell carcinoma, a highly aggressive, invasive bladder cancer [428]. In contrast, Lai *et al.* (2010), however, identified Upk3a as a novel promising marker for the detection of bladder carcinoma from urine [429].

Given the lack of an established, precise biological function and its exclusivity in association with the urothelium derived structures, such as renal pelvis, urethra, urinary bladder and prostate urethra [430] when all other human tissues with an exception for ovarian Brenner tumour, which however, is thought to be of urothelial origin, have to date been demonstrated as negative for *Upk3a* expression [431], *Upk3a* emerged as an interesting target for mouse mammary gland associated research. Our aim was to confirm the up-regulation of *Upk3a* expression in the mouse mammary gland during puberty, determine its precise localisation in TEBs and identify its role in normal mouse mammary gland development at puberty.

4.2.1.2 Validation of *Upk3a* expression in pubertal mouse mammary gland.

The association of *Upk3a* with the TEB transcriptome was further supported by microarray comparison analysis of Post-LN and Pre-LN data sets (Partek[®] Genomics™ Suite software) (See 2.2.5.5.2) where *Upk3a* was shown to be 3.01 fold over-expressed in the Post-LN strip - ranking (#) to position 21 (p-value < 0.001) (Figure 4-1 A).

The TEB associated increase of *Upk3a* expression was also seen very clearly when the level of absolute gene expression was compared across all microarray replicates. The expression level was shown to be uniform across the replicates of each biological sample except for one 12 week old virgin replicate. The highest expression level of *Upk3a* was noted in the isolated epithelium of TEBs. The isolated ductal epithelium and Post-LN strips showed the second highest *Upk3a* expression level (10.74- and 11.1- fold lower than isolated TEB epithelium respectively). *Upk3a* expression in Pre-LN strips was 3.01 and 3.1 fold lower than that seen in Post-LN strips and isolated ducts respectively. The lowest *Upk3a* expression, however, was noted in the Fat pad with the *Upk3a* gene expression level similar to the one detected in the negative control - adult (V12) mammary glands (Figure 4-1 B).

Further validation of TEBs-associated pattern of *Upk3a* expression in the mouse mammary gland was performed using Q RT PCR. As seen in Figure 4-2 A, *Upk3a* mRNA levels displayed a 4-fold increase in expression levels in the Post-LN strips

A

Type of comparison	Fold change	Rank number
TEBs vs ducts	10.74	1
Post-LN vs Pre-LN	3.01	21

B

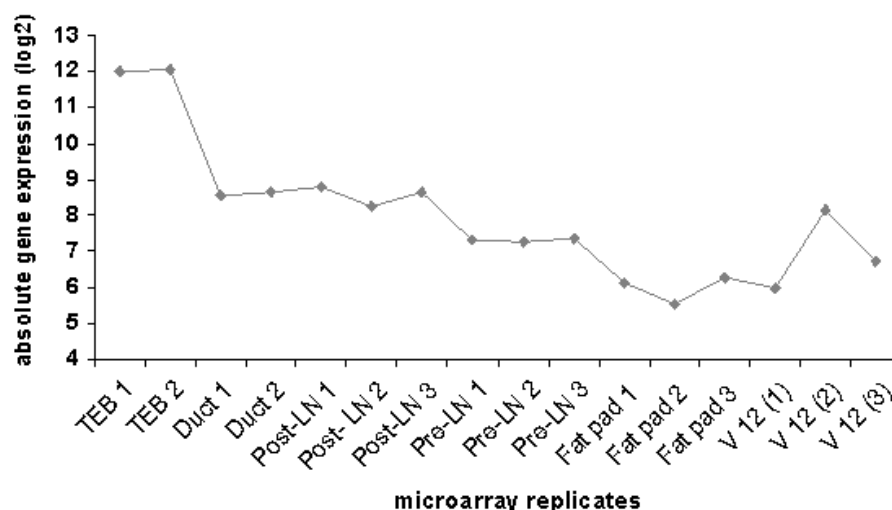


Figure 4-1 *Upk3a* expression profiling in the pubertal mouse mammary gland by microarray analysis.

(A) Level of *Upk3a* up-regulation in the TEBs (TEBs vs ducts) and Post-LN strips (Post-LN vs Pre-LN). Microarray analysis of TEB and duct data sets were performed using 5% LFC Model (See 2.2.5.5.1), while the Post-LN and Pre-LN data sets were compared using Partek® Genomics™ Suite software (See 2.2.5.5.2). Rank number was assigned based on the FC level. Calculated FCs were statistically significant i.e. $p\text{-value} \leq 0.05$ for genes over-expressed in Post-LN and within 5% LFC Model for genes over-expressed in the TEBs isolated epithelium. (B) Absolute *Upk3a* expression levels for all microarray replicates. Absolute gene expression in each microarray replicate was calculated using Expression Console™. RMA was performed prior to gene expression analysis and the gene expression is denoted as log2 value.

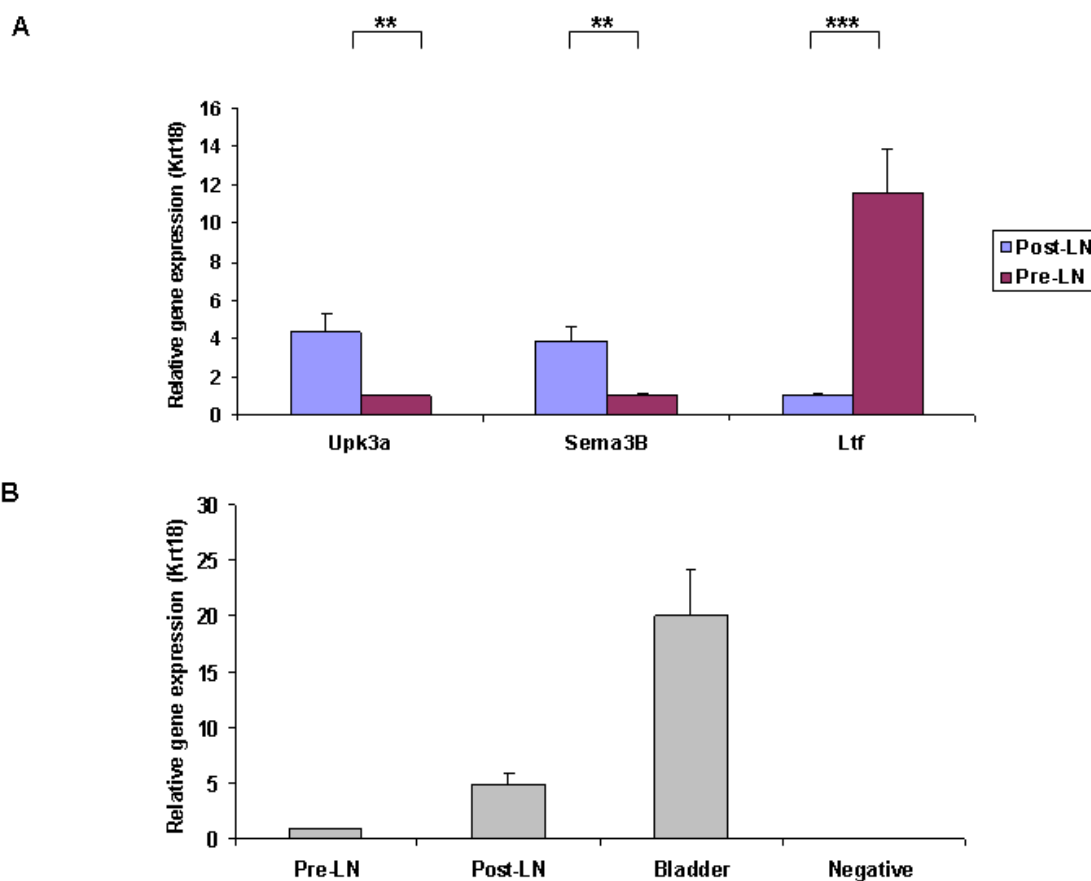


Figure 4-2 Validation of *Upk3a* mRNA expression in the pubertal mouse mammary gland by Q RT PCR.

(A) Mean expression level of *Upk3a*, *Sema3B* and *Ltf* mRNA in the Post-LN strips relative to Pre-LN tissue strips. *Sema3B* and *Ltf* served as controls. *Krt18* expression was used as an internal control for normalisation. Error bars are S.E.M. (*) denotes statistical significance, (*) p-value \leq 0.05 (**) p-value \leq 0.01 (***) p-value \leq 0.001, n=3

(B) Representative illustration of the mean expression level of *Upk3a* in Post-LN strip and bladder relative to Pre-LN strip. The cDNA produced from bladder RNA without addition of Reverse Transcriptase (RT) served as a negative expression control. *Krt18* expression was used as an internal control. Error bars are S.E.M. calculated between the technical replicates, n=1.

in comparison to the Pre-LN mouse mammary gland tissue strips. Expression levels of *Sema3B* and *Ltf* that are known to be expressed in the TEB and duct epithelium respectively were used as experimental controls. Due to the prevalent association of *Upk3a* expression with the TEB epithelium, the *Upk3a* expression was measured by normalising the calculated gene expression level against that of *Krt18*. In addition mouse bladder was used as a positive control. *Krt18* is a marker of both epithelial cells and urothelial umbrella cells [432] [433]. The calculated expression of *Upk3a* in the Post-LN mouse mammary gland tissue strip, although higher than that in the Pre-LN strip, was 17-fold lower than in the mouse bladder (**Figure 4-2 B**).

Despite the presence of *Upk3a* mRNA in pubertal mouse mammary gland and its TEB-associated expression pattern, its expression in the mammary epithelium could not be confirmed at the protein level. Western blot analysis of protein extracts from Post-LN and Pre-LN mouse mammary gland tissue strips showed a lack of *Upk3a* expression in the mammary gland although the protein was present in murine bladder (positive control) (**Figure 4-3 A**). The antibody used in this study (AU1) is an *Upk3a* specific mouse IgG1 monoclonal antibody that recognizes an unspecified epitope residing within the extracellular domain [419]. *Upk3a* in the bladder protein extract was detected on the western blot as bands of between 43-47 kDa which corresponded to the size of the immature (Endoplasmic reticulum) or mature (Golgi) forms of *Upk3a*. These bands were absent from the Post-LN and Pre-LN blots. The lack of *Upk3a* protein expression in the pubertal mouse mammary glands was further confirmed using IHC. Paraffin wax embedded tissue sections of mammary gland and bladder, collected from 6 week old mouse were stained with AU1. In the bladder the umbrella cell region stained very strongly and uniformly for *Upk3a* (**Figure 4-3 D**). Although faint staining was also visible in the apical side of the mammary gland luminal epithelium (**Figure 4-3 B**) the same staining pattern was present in the negative control section (no primary antibody) and it was therefore considered as non specific secondary antibody reactivity (**Figure 4-3 C**).

In order to ensure that the discrepancy between the mRNA and protein levels of *Upk3a* in the mouse mammary gland was not attributed to a tissue specific alteration in the gene sequence affecting the epitope recognised by the AU1 antibody, full length *Upk3a* cDNA was synthesised from pubertal mammary gland

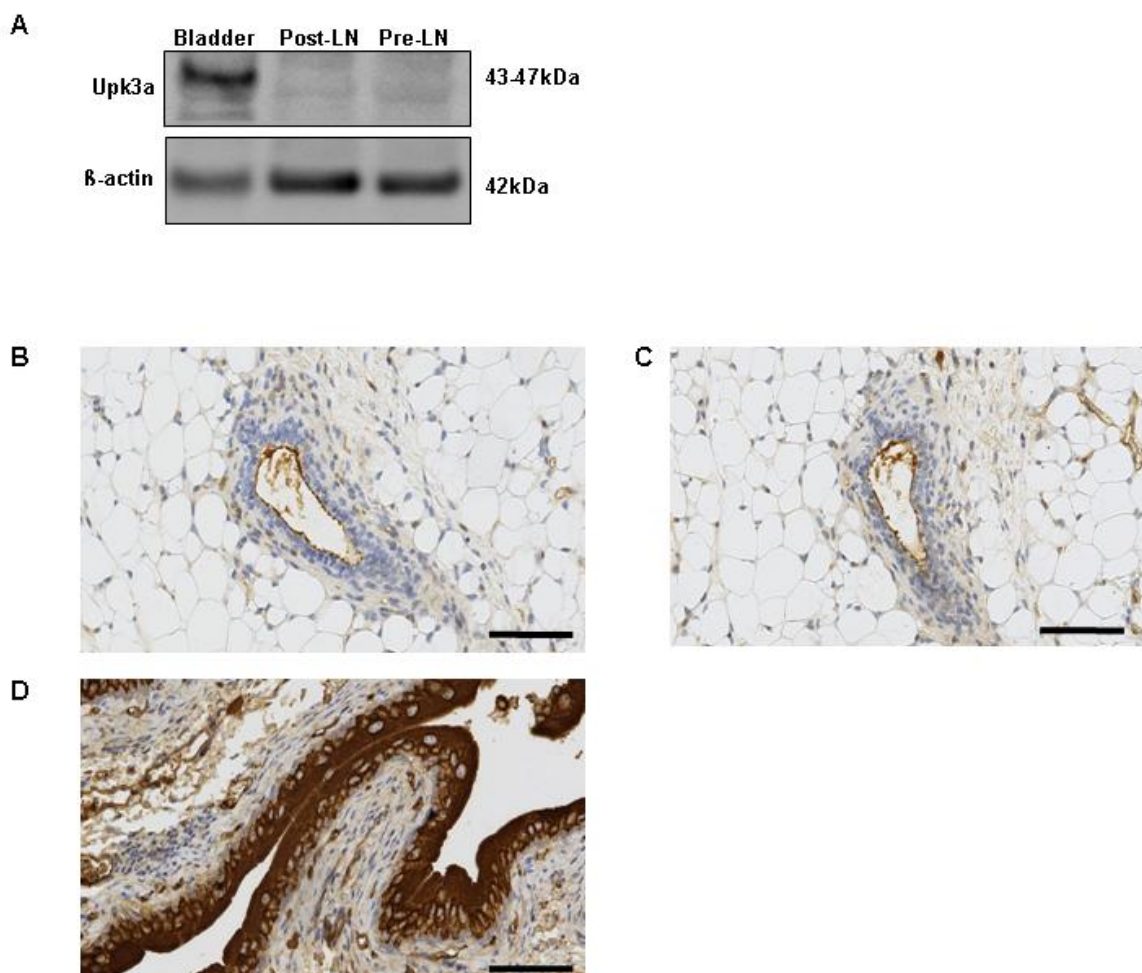


Figure 4-3 Validation of Upk3a protein expression in the pubertal mouse mammary gland.

(A) Western Blotting. Representative analysis of Upk3a expression in the bladder (positive control), Post-LN strip and Pre-LN strip. Upk3a protein (47kDa) was identified using mouse monoclonal AU1 antibody. β -actin was used as loading control. n=2

(B) (C) (D) IHC. **(B) (C)** Longitudinal sections through a 6 week old mouse mammary gland, showing fragment of representative epithelium and **(D)** mouse bladder showing part of urothelium. **(B) (D)** were stained using AU1 antibody. **(C)** serves as negative control (no primary antibody). **(D)** serves as positive control. Upk3a staining was prominent in urothelial umbrella cell region. Staining seen on the apical border of luminal epithelial cells in the mouse mammary gland was unspecific as it is also visible in the negative control. Secondary antibody was horseradish peroxidase conjugated. At least 3 animals were examined. Scale bars are 100 μ m.

Pre-LN and Post-LN tissue strips and urinary bladder and sequenced. The length of cDNA obtained from all three sites was equal and there were no major differences in the nucleotide sequence or nucleotide rearrangements between the sequences.

In summary, although Upk3a had potential to be a pubertal, TEB-associated regulator of mammary gland morphogenesis its expression could only be detected at the mRNA level.

4.2.2 FIBULIN 2

4.2.2.1 Introduction

Fbln2 was selected as a candidate regulator of pubertal mouse mammary gland development because it was identified within the 65 TEB epithelium up-regulated genes and has previously been reported to associate with other biological processes known to share similarities with ductal morphogenesis, such as cell adhesion and migration, embryonic development and kidney morphogenesis (Table 3-5).

Fbln2 belongs to the highly conserved, ancient family of ECM glycoproteins. The family name originates from the word *fibula* which in Latin means ‘clasp’ or ‘buckle’ and refers to their ability to act as a linker for other proteins. The Fibulin family incorporates six known members (Fbln1-Fbln6), all of which are characterised by the presence of a series of EGF-like motifs, followed by the carboxy-terminal fibulin-type module. The closest relative to Fbln2 is Fbln1C which shares 43 % aa sequence identity (Figure 4-4 A).

Fbln2 cDNA was originally cloned from mouse fibroblasts in 1993 [434] and the gene was located to the mouse chromosome 6 band D-E [435]. *Fbln2* was shown to exist as two alternatively spliced variants: V1 and V2, consisting of 18 and 17 exons respectively. Based on the cDNA sequence, *Fbln2* V1 was predicted to comprise a 3633 bp-long open reading frame as well as a 50bp and 664bp long 5’ and 3’ untranslated regions respectively. At the protein level, Fbln2 translated into a 26-residue long signal peptide and a 1195-residues long mature protein.

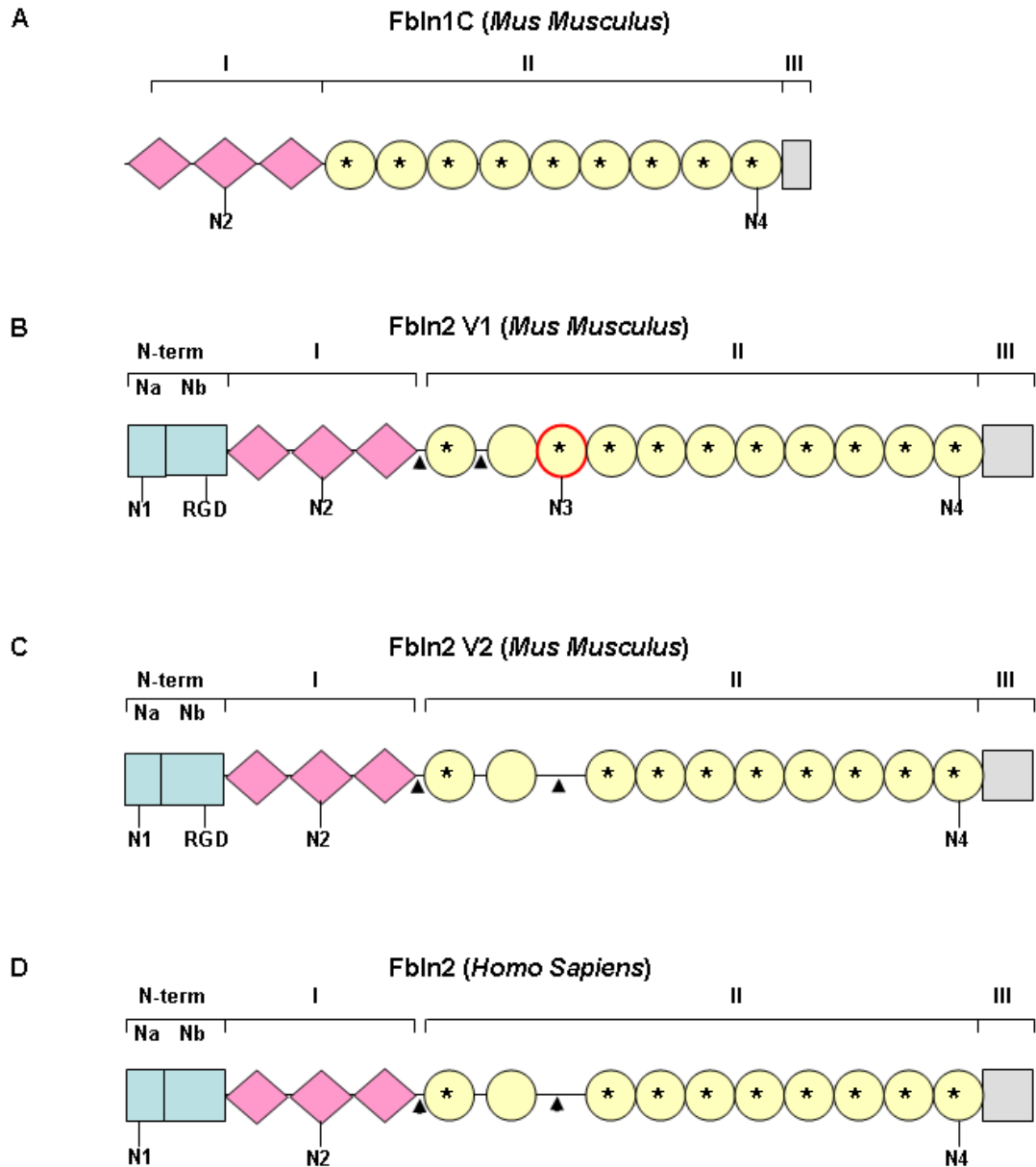


Figure 4-4 The overview of domain models for Fbln2 (*M. musculus* and *H. sapiens* and Fbln1C (*M. musculus*).

Names of domains are indicated on the top of each diagram. Blue boxes at the left hand side denote the N-terminus domain (N-term). The N-term domain consists of Na and Nb subdomains. Pink diamonds in domain I indicated three motifs related to anaphylatoxins. Yellow circles in domain II denote EGF-like repeats and those with asterisk in the middle possess Ca^{2+} binding consensus sequence. The first EGF-like repeat is linked to domain I and the second EGF-like repeat with aa linkers (arrow head). The yellow circle with red outline represents exon 9. The gray box at the right hand side denotes the C-terminal domain (III) Annotation seen at the bottom of each diagram indicate positions of the potential N-glycosylation sites (N1, N2, N3 and N4) and the position of RGD consensus (RGD).

(A) Murine Fbln1C. Fbln1 C is the closest relative to Fbln2 with 43% aa identity. It lacks the N-terminal domain, has 9 EGF-like repeats and its C-terminal domain is shorter **(B)** Murine Fbln2 V1 (top model) and **(C)** Fbln2 V2 (bottom model). Fbln2 V2 lacks EGF-like domain 3 which is encoded by exon 9. Potential glycosylation site 2 (N2) is also absent **(D)** The human Fbln2 lacks exon 9 and thus does not encode EGF-like repeat 3. Potential glycosylation site 2 (N2) and the RGD consensus sequence are absent.

Fbln2 V1 (195 kDa) consists of four domains (N, I, II and III). The N-terminus (N-domain) is unique to Fbln2. It incorporates two sub domains spanning over 408 aa residues. The first sub domain is cysteine rich (Na) and the second is cysteine free (Nb). Domain I consists of three anaphylatoxin-like motifs (each ~ 40 aa long and containing six cysteines) and is connected to the domain II via a 50 aa long link. Domain II consists of 11 EGF-like repeats, 10 of which contain consensus motifs for Ca^{2+} binding that are hypothesized to regulate protein-protein interactions [434] [436]. In general EGF-like repeats are postulated to participate in the interactions of ECM proteins with cellular receptors [437] as well as play a role in the stabilization of protein structure due to the presence of multiple disulfide bridges which in conjunction with other copies of Fbln2 protein facilitate the formation of rod-like structures [438]. Recombinant Fbln2 incorporates three disulfide bridges and is produced and secreted by human cell clones as a disulfide-bonded trimer. The final, domain III (C-terminal) of Fbln2 V1 is composed of a single globular module. Furthermore, as indicated by the aa sequence prediction study, there are four potential N-linked glycosylation sites at the aa positions 179, 497, 737 and 1072 and a single Arg-Gly-Asp (RGD) attachment site, indicative of adhesive properties, at position 395-397 (**Figure 4-4 B**).

Fbln2 V2 shares all of the above sequence characteristics but for the presence of exon 9 which encodes the EGF-like domain 3 (709-755 aa) and contains a single potential N-linked glycosylation site (aa 737) (**Figure 4-4 C**).

Fbln2 shows a high degree of interspecies conservation as the human protein shares around 90% aa identity with the domains Na, I, II and III and 62% with the domain Nb of the murine counterpart. The human gene thus far characterised lacks the EGF-like repeat on exon 9, hence encodes only the shorter (V2) *Fbln2* isoform and fails to contain the predicted RGD domain, which results in a substantial difference in cell adhesion activity and RGD-dependent integrin receptor binding between the two species [435] (**Figure 4-4 D**).

The promoter region of *Fbln2* has been shown to contain the trans-acting transcription factor 1 (Sp1)-, activator protein 2 (AP-2)- and CCAAT enhancer binding protein (C/EBP) binding sites [439]. The Sp1 consensus sequence is involved in gene expression in early development and confers high promoter

activity while the AP-2 and C/EBP transcription factors are known to regulate gene expression during embryogenesis and differentiation respectively.

Expression of *Fbln2* is detected mostly at the BMs and stroma of many mouse embryonic and adult tissues. During embryogenesis it is prominently expressed at embryonic sites of EMT during cardiac valvuloseptal formation [343] or precartilage formation [440]. In adulthood it is still associated with the valves and septa of heart [343], endothelial cells (EC) of the aortic arch and coronary blood vessels [441] and it can further be seen in skin (epidermal cell layer, dermis and adipose tissue), keratinocytes of hair follicles, epithelial cell layer and Bowman's and Descemet's membranes and stroma of cornea and surrounding the extracellular spaces around the muscle fibres in the skeletal and heart muscles. A lower level of *Fbln2* mRNA expression has also been detected in the lung, liver, kidney, brain, spleen and testis [434].

Based on *in vitro* studies the function of *Fbln2* may be in forming intramolecular bridges which link and stabilize the organisation of supramolecular ECM structures, i.e. basement membranes, elastic fibres and fibronectin matrix [442] [443] [444]. Furthermore, *Fbln2* co-localises and interacts with *Fbn1* in the bundles of microfibrils that appear to intersect the lamina densa of kidney glomeruli and perichondrium [344]. The timing of expression, tissue localisation and spatial localisation within the tissues also suggest that it may promote either proliferation or differentiation or migration of mesenchymal cells during organogenesis and endorse structural stability during adulthood. The detection of *Fbln2* expression in testis [445] and ovaries [435] in connection with the recently discovered involvement of *Fbln2* in the sequestering of sex hormone binding globulin (SHBG) within the stroma of uterus and thus regulating the access of SHBG to target cells [446], suggest functional association of *Fbln2* with the female and male reproduction systems. Finally, since it is over-expressed during wound repair processes, *Fbln2* may also be involved in tissue remodelling [447] [448]. In contrast to the *in vitro* studies, however, an *in vivo* *Fbln2* KO^{-/-} based study did not confirm the need for *Fbln2* in elastogenesis, development and fertility as the *Fbln2*-null mice were shown to be viable, fertile and lacking any gross anatomical abnormalities or dysfunction in assembly of elastic fibres [266]. Very recently, however, the generation of double KO mice for *Fbln2* and *Fbln5* shone a new light onto *Fbln2* function, demonstrating that both of the

proteins function cooperatively to redirect the assembly of elastic fibres to form the internal elastic lamina in blood vessels during postnatal development [449].

Finally, the dysfunction of *Fbln2* has been associated with some pathological conditions. Deposition of *Fbln2* in elastic fibres was demonstrated in solar elastosis, a skin condition caused by sun damage [450]. In tumourigenesis, *Fbln2* has been identified to have opposing functions. On the one hand, it was found amongst the metastasis-associated genes in adenocarcinomas [451], was over-expressed in a HER2/Neu -driven mouse model of breast cancer [452] and was associated with poor prognosis and metastatic potential of primary solid tumours of different types [451]. On the other hand, however it was identified as frequently methylated in breast tumors [453] and down-regulated in breast cancer cell lines and primary breast tumours [342].

Given the association of *Fbln2* with organogenesis, tissue remodelling and tumourigenesis and its documented involvement in the regulation of cell adhesion and migration in different biological systems, together with the up to date lack of reported *Fbln2* expression and association with mouse mammary gland development, *Fbln2* arose as a promising novel target in the study of pubertal regulators of mouse mammary gland morphogenesis. Thus, we aimed to confirm and examine the *Fbln2* expression pattern during normal mouse mammary gland development, with a focus on puberty. Furthermore, we set out to study the role of *Fbln2* in pubertal morphogenesis by examining the morphology of the ductal tree in *Fbln2* KO^{-/-} mice, exploring the expression patterns of its binding partners, estimating the influence of systemic hormones on its expression *in vivo* and investigating its role in the regulation of cell migration and adhesion *in vitro*. Finally, we set out to establish a TEB explant culture model to facilitate the study *Fbln2* expression *in vitro*.

4.2.2.2 Validation of *Fbln2* expression during pubertal mouse mammary gland development.

Fbln2 was amongst the 65 genes commonly up-regulated in the epithelium of TEBs (TEBs vs ducts) (5% LFC Model) (See 3.2.6.1.1) and Post-LN strip (Post-LN vs Pre-LN) (Partek[®] Genomics[™] Suite software) (See 3.2.6.1.2) by 2.16 fold (# 182) and 1.75 fold (# 285) (p-value<0.001) respectively (Figure 4-5 A). The

A

Type of comparison	Fold change	Rank number
TEBs vs ducts	2.16	182
Post-LN vs Pre-LN	1.75	285

B

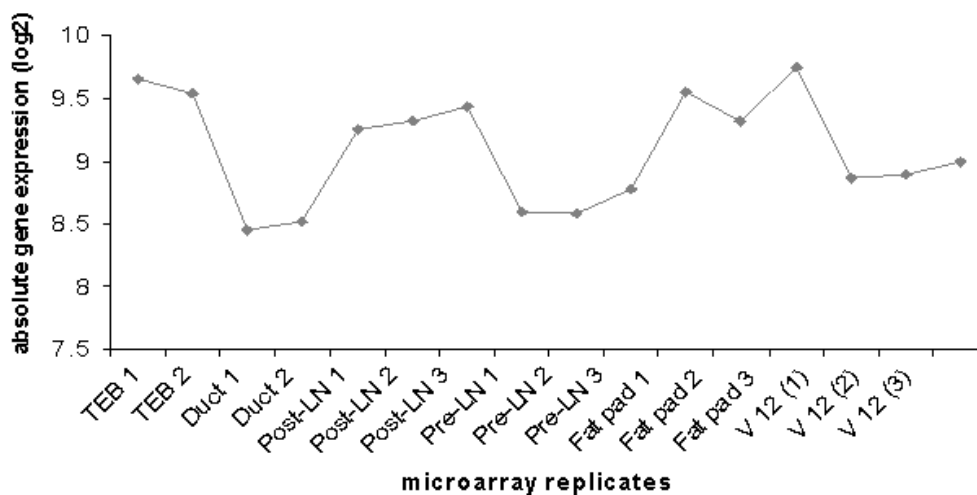


Figure 4-5 *Fbln2* expression profiling in the pubertal mouse mammary gland by microarray analysis.

(A) Level of *Fbln2* up-regulation in the TEBs (TEBs vs ducts) and Post-LN strips (Post-LN vs Pre-LN). Microarray analysis of TEB and duct data sets were performed using 5% LFC Model (**See 2.2.5.5.1**), while the Post-LN and Pre-LN data sets were compared using Partek® Genomics™ Suite software (**See 2.2.5.5.2**). Rank number was assigned based on the FC level. Calculated FCs were statistically significant i.e. $p\text{-value} \leq 0.05$ for genes over-expressed in Post-LN and within 5% LFC Model for genes over-expressed in isolated epithelium of TEBs. **(B)** Absolute *Fbln2* expression levels throughout all microarray replicates. Absolute gene expression in each microarray replicate was calculated using Expression Console™. RMA was performed prior to gene expression analysis and the gene expression is denoted as log2 value.

increase of *Fbln2* expression in association with TEBs was confirmed when the level of absolute gene expression was compared across all replicates used in the microarray experiment. The comparison of absolute gene expression also revealed the expression of *Fbln2* within the empty Fat pad. The Fat pad was excised at a significant distance from the epithelium to prevent its contamination with epithelium and its associated stroma. The absolute level of *Fbln2* expression was highest in isolated TEBs, Fat pad and Post-LN strips with Fat pad showing similar and Post-LN -1.2 fold lower gene expression levels than isolated TEBs. Some variability between the replicates could be seen for the Fat pad strips. The absolute level of *Fbln2* expression was lower in the remaining samples, with isolated duct epithelium, Pre-LN strip and V12 showing 2.16, 1.9 and 1.6 fold lower expression than that calculated in the isolated TEB epithelium respectively (**Figure 4-5 B**).

Expression of *Fbln2* within the epithelium of TEBs was further confirmed by Q RT PCR analysis of total RNA extracts collected from isolated TEBs and ducts and Post-LN and Pre-LN mammary gland tissue strips. The Fat pad associated expression of *Fbln2* was not taken into consideration in these as well as most of the subsequent experiments since at the time of the study *Fbln2* was thought to be mostly expressed in the epithelium and only low expression was thought to be associated with stroma (absolute gene expression profiling and some of the protein localisation studies were performed as one of the last analyses). As seen in **Figure 4-6 A and B** *Fbln2* expression was 3.4 fold higher in both, isolated TEBs compared to ducts, and Post-LN strip compared to Pre-LN. Expression levels of *Sprr1A* and *Ltf*, genes previously associated with TEB and duct epithelium respectively were used as experimental controls. As only the epithelium associated expression of *Fbln2* was taken into consideration in this experiment, *Krt18* (an epithelial marker) instead of β -actin (expressed ubiquitously in the tissue) was used for normalisation. *Krt18* aids the normalisation of the calculated gene levels to the amount of epithelium. It is worth noting, however, that Post-LN and Pre-LN strips consist of both epithelium and its associated stroma, which as suggested by the high absolute expression of *Fbln2* in Fat pad (**Figure 4-5 B**) and further demonstrated in succeeding experiments (**Figure 4-7**), also expresses *Fbln2*. Therefore despite using *Krt18* normalisation to examine

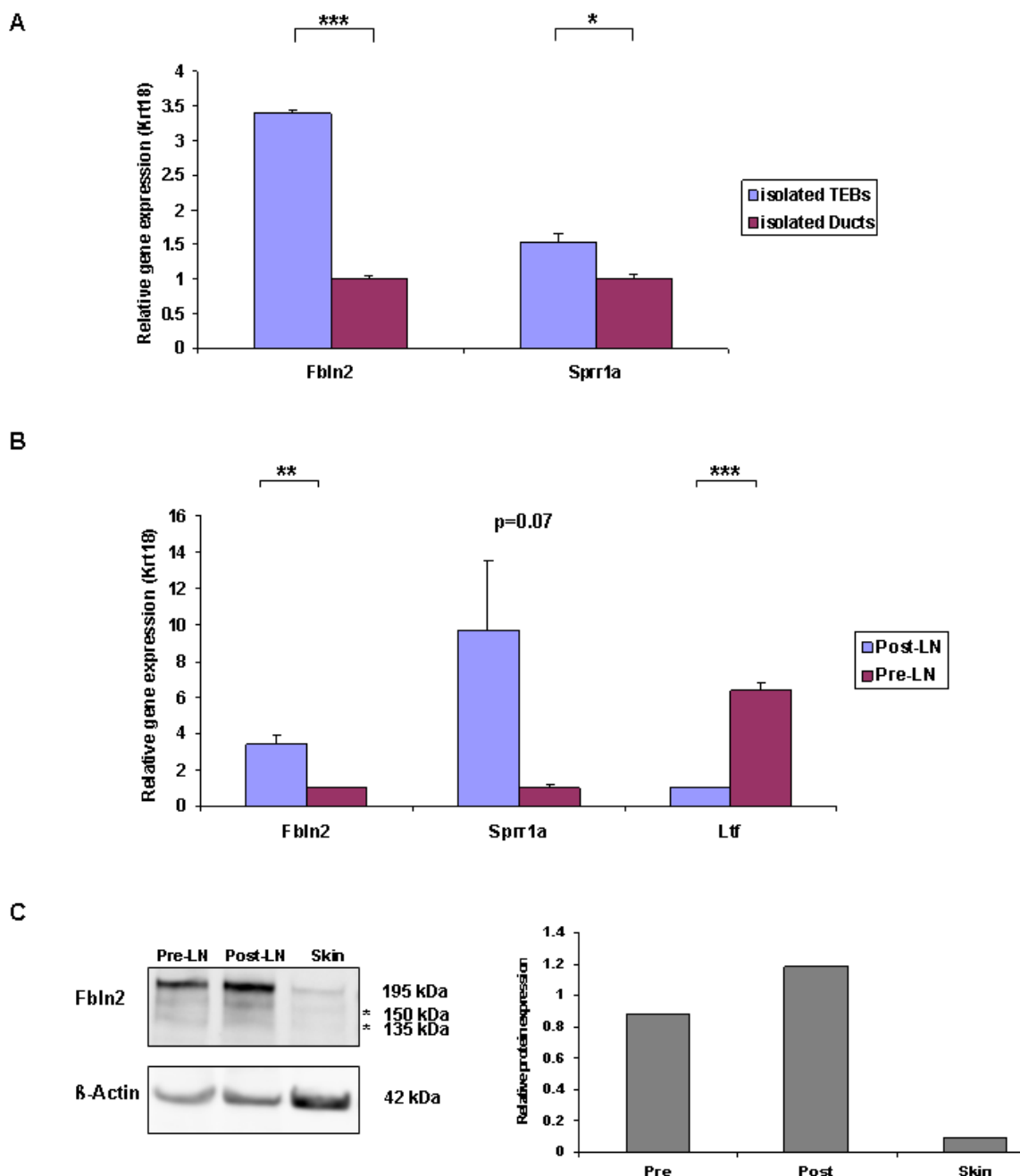


Figure 4-6 Validation of Fbln2 expression in pubertal mouse mammary gland.

(A) (B) Q RT PCR. **(A)** Mean expression level of *Fbln2* and *Sprr1a* mRNA in isolated TEBs relative to isolated ducts and **(B)** *Fbln2*, *Sprr1a* and *Ltf* mRNA in the Post-LN strips relative to Pre-LN tissue strips. *Sprr1a* and *Ltf* served as controls for TEBs and ducts respectively. *Krt18* expression was used as an internal control for normalisation. In **(A)** n =pooled from 300 mice and error bars denote technical variability. In **(B)** error bars are S.E.M. and (*) denotes statistical significance, (*) p -value \leq 0.05 (**) p -value \leq 0.01 (***) p -value \leq 0.001, n =3

(C) Western Blotting. Representative analysis of Fbln2 expression in the Pre-LN strips, Post-LN strips and skin (positive control). Fbln2 protein (195 kDa) was identified using rabbit polyclonal anti-Fbln2 antibody. Asterisks (*) denote two additional, uncharacterised bands of a lower molecular weight (150 kDa, 135 kDa). β -actin was used as loading control. n =3. Densitometry was carried out to calculate relative expression of Fbln2 protein normalised to β -actin protein levels for the same set of samples.

epithelial gene expression, some of the detected signal might be attributed to the stromal compartment.

Pubertal expression of *Fbln2* (195 kDa) was further confirmed at the protein level by Western Blotting using protein lysates, extracted with RIPA buffer from murine skin and Post-, Pre-LN tissue strips and blotted under denaturing conditions (**Figure 4-6 C**). The level of *Fbln2* expression was 1.6 and 6.2 fold higher in the Post-LN strip than the Pre-LN strip and skin respectively (positive expression control) as revealed in densitometry analysis. Previously reported, uncharacterised bands of the mobility below the predicted protein (150 kDa and 135 kDa) (denoted by asterisks in **Figure 4-6 C**) were also present.

4.2.2.3 Localisation of *Fbln2* in the pubertal mouse mammary gland

To assess the localisation of *Fbln2* within the pubertal mouse mammary gland, 6 week old mammary glands were fixed in 10 % Neutral Buffered Formalin, paraffin wax embedded and sectioned. Chosen sections were H&E stained to assess tissue morphology and ensure the presence of TEB and duct epithelium. Positively evaluated tissue sections were stained with routine anti-*Fbln2* antibody using IHC and IF. Haematoxylin and DAPI were used as nuclear counterstains for IHC and IF respectively. The obtained results were consistent with the *Fbln2* expression profile determined by microarray analysis.

As seen in **Figure 4-7**, *Fbln2* expression was localised to both the epithelium and the stroma of pubertal mouse mammary gland. Stromal expression was restricted to the proximal zone surrounding the TEB and duct epithelium, with the former appearing stronger; and the distal capsule located at the very edge of the Fat pad. While *Fbln2* was present in the stroma surrounding both TEBs and ducts its epithelial expression was almost exclusively associated with TEBs. As seen by IHC on transverse sections through the isolated TEBs and TEBs surrounded by the stroma (Post-LN strip) most *Fbln2* expression was localised to the cap cells (the outermost cell layer in TEBs) (**Figure 4-8 A**). The additional expression of *Fbln2* in the TEBs was present in the body cells (**Figure 4-8 A**). In comparison to the TEBs, ductal epithelial expression of *Fbln2* was very weak (**Figure 4-8 B**).

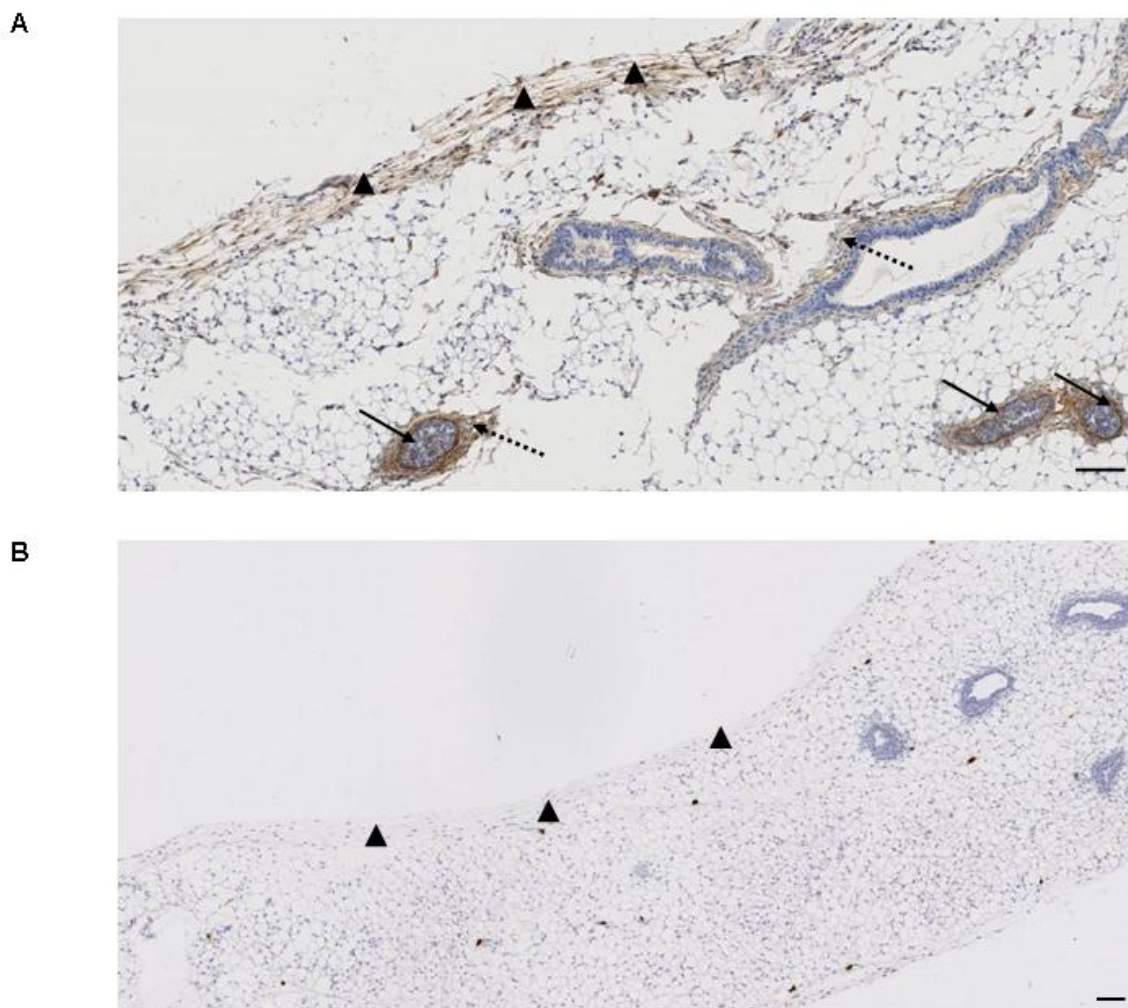


Figure 4-7 Localisation of Fbln2 expression in pubertal mouse mammary gland by IHC.

(A) Longitudinal section through 6 week old mouse mammary gland stained with rabbit polyclonal anti-Fbln2 antibody and horse radish peroxidase conjugated secondary antibody (brown). Haematoxylin (blue) was used to stain nuclei. Fbln2 expression was associated with epithelium of TEBs (arrow), stroma around TEBs and ducts (dotted arrow), stromal capsule around the edge of the fat pad (arrow head). **(B)** negative (no primary antibody) control. Scale bars are 100 μ m.

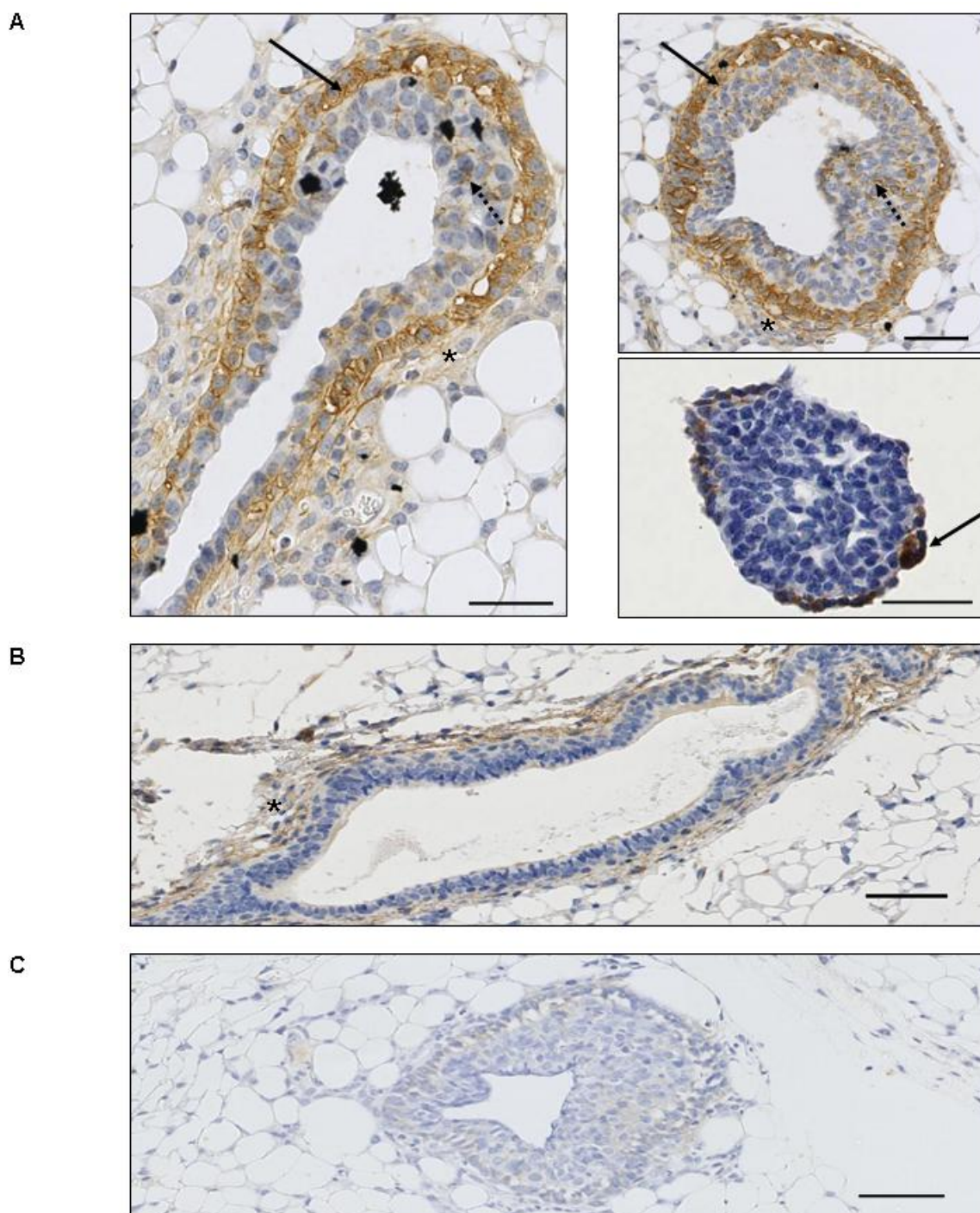


Figure 4-8 Localisation of Fbln2 expression in the pubertal TEBs and ducts by IHC.

(A) Longitudinal (left) and transverse (top right) sections through a TEB and its surrounding stroma (left) and transverse section through an enzymatically isolated TEB (bottom right) **(B)** Longitudinal section through a duct and its surrounding stroma. **(C)** Negative (no primary antibody) control. Staining in **(A)** **(B)** was performed using anti-Fbln2 antibody (brown). Haematoxylin was used to stain nuclei (blue). In **(A)** most Fbln2 expression was associated with the outer cell layer of TEBs (cap cells) (arrow). Some expression was also detectable within body cells (dotted arrow) and the stroma around TEB (asterisk). Fbln2 expression seemed to localise to the cell membranes, cytoplasm and extracellular spaces. **(B)** In the duct, Fbln2 expression was weak and mostly associated with the stroma around ductal epithelium (asterisk). Scale bars are 50 µm.

A similar pattern of expression was observed when longitudinal sections through the TEBs and ducts were stained for *Fbln2* using IF (**Figure 4-9**). *Fbln2* expression was almost absent from ductal epithelium (**Figure 4-9 C**), but was present abundantly in the cap cell- and at a lower level in body cell-region of TEBs (transverse and longitudinal sections) (**Figure 4-9 A-B**). In the cap cells, *Fbln2* staining appeared membrane bound, cytoplasmic and extracellular (**Figure 4-10 A**) while within the body cells it was present in cytoplasm or between the cells and was not uniformly expressed across all body cells (**Figure 4-10 B**). Some *Fbln2* positive staining could also be seen in the BM region (**Figure 4-10 A**). The expression of *Fbln2* in cap cell membranes and low cytoplasmic expression in ductal epithelium were further demonstrated when 3D reconstruction was performed on the series of transverse sections through pubertal mouse mammary gland (**Figure 4-11**).

The observed staining pattern was specific to *Fbln2*-antibody binding as demonstrated by the absence of staining in the epithelium of the negative (no primary antibody) controls (**Figure 4-8 C**) (**Figure 4-9 D**). Positive *Fbln2* expression was also noted in the blood vessels throughout mammary gland tissue (in all IHC and IF sections) (data not shown).

IHC and IF of pubertal mouse mammary glands demonstrated that *Fbln2* expression was stronger in the TEBs and their surrounding stroma than in the ducts, thus confirming our microarray, Q RT-PCR and Western blot results.

4.2.2.4 *Fbln2* expression across the different stages of mouse mammary gland development.

Post-natal mouse mammary gland morphogenesis can be divided into the following six distinct developmental stages: pre-puberty, puberty, adulthood, pregnancy, lactation and involution. Each of these stages is characterised by diverse events and regulated in a different manner. Therefore, the expression of *Fbln2* at the RNA level and its tissue localisation was investigated throughout the various developmental stages using whole tissue strips and whole mouse mammary glands (**Figure 4-12 A**). The experiments were performed using Q RT PCR and IHC. Relative to the Post-LN strip, the level of *Fbln2* expression was 3.6 fold up-regulated in whole mammary glands during pre-puberty but similar

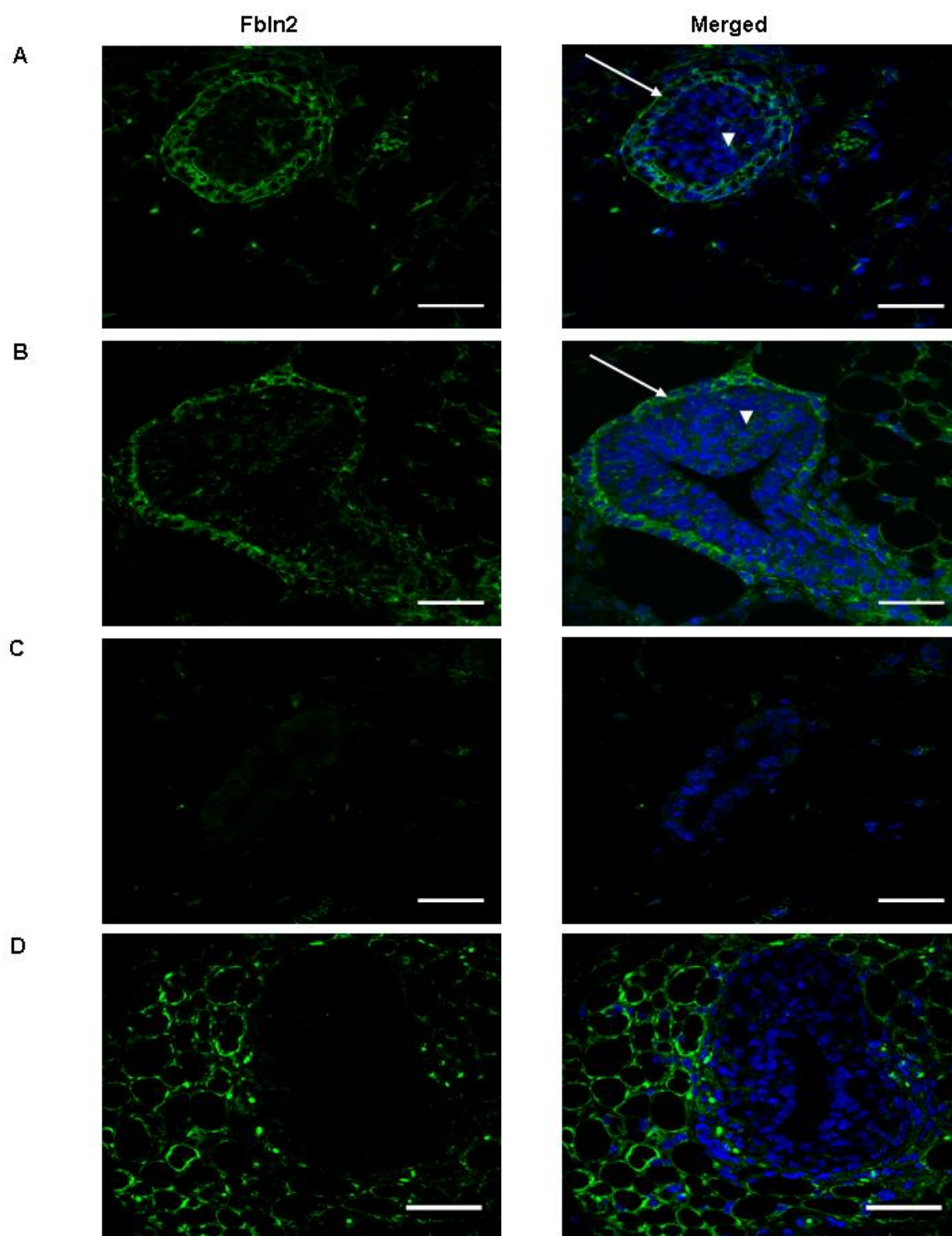


Figure 4-9 Localisation of Fbln2 expression in the pubertal epithelium of TEBs and ducts by IF.

(A) Transverse and (B) longitudinal sections through TEB and (C) longitudinal sections through duct of 6 week old mouse mammary glands are shown. (D) is a negative control (no primary antibody). Staining was performed using Alexa Fluor 488 conjugated anti-Fbln2 antibody (green) and nuclear DAPI (blue). Fbln2 expression was associated with cap cells (arrow) (A) (B). Weak staining could be seen in body cells (arrow head). Very weak Fbln2 staining could be detected in the duct (C) Images were captured by confocal microscopy. Scale bars are 50 μ m.

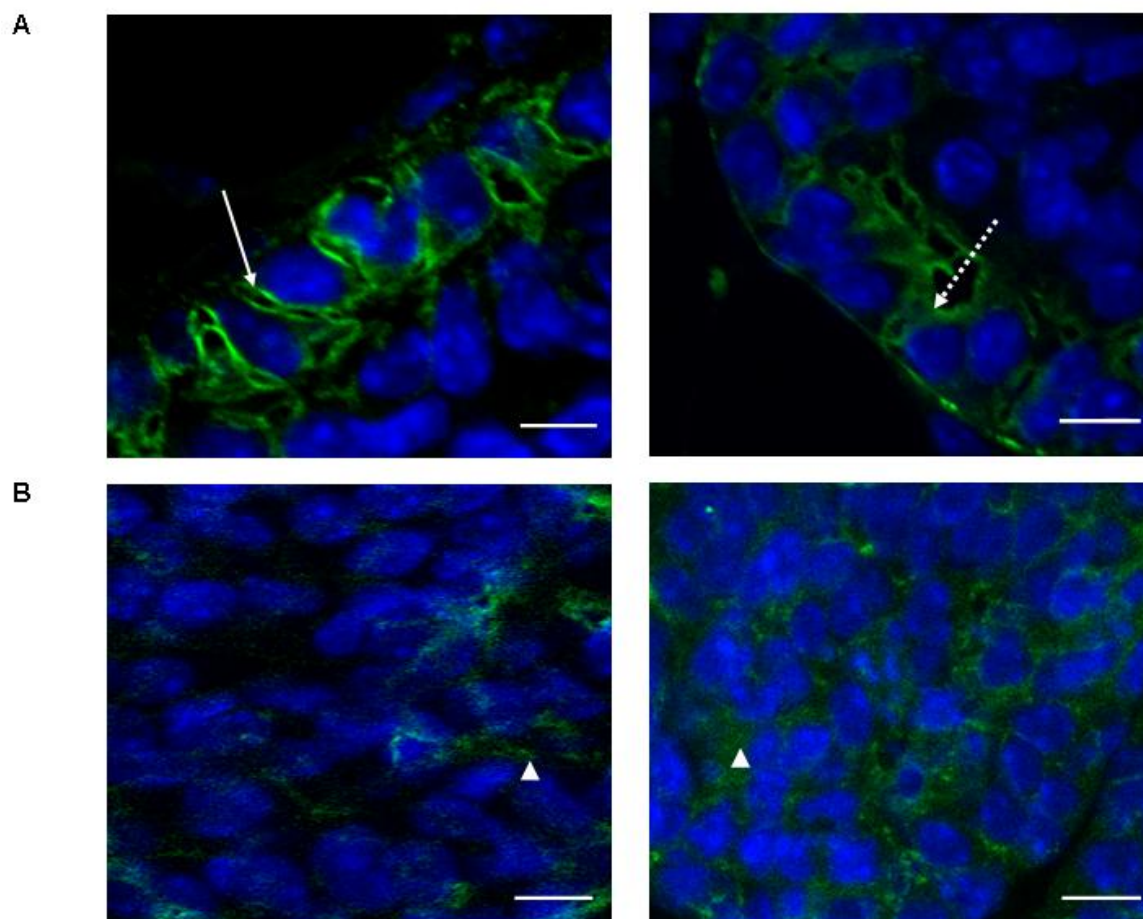


Figure 4-10 Localisation of Fbln2 expression in the pubertal TEB by IF.

Images show representative areas of the pubertal TEBs stained with anti-Fbln2 antibody that are shown in **Figure 4-9**. **(A)** Cap cells showing membrane (arrow) and cytoplasmic (dashed arrow) staining pattern **(B)** Body cells showing Fbln2 staining in the cytoplasm or extracellular spaces (arrow head). Images were acquired by confocal microscopy. Scale bars are 10 μm .

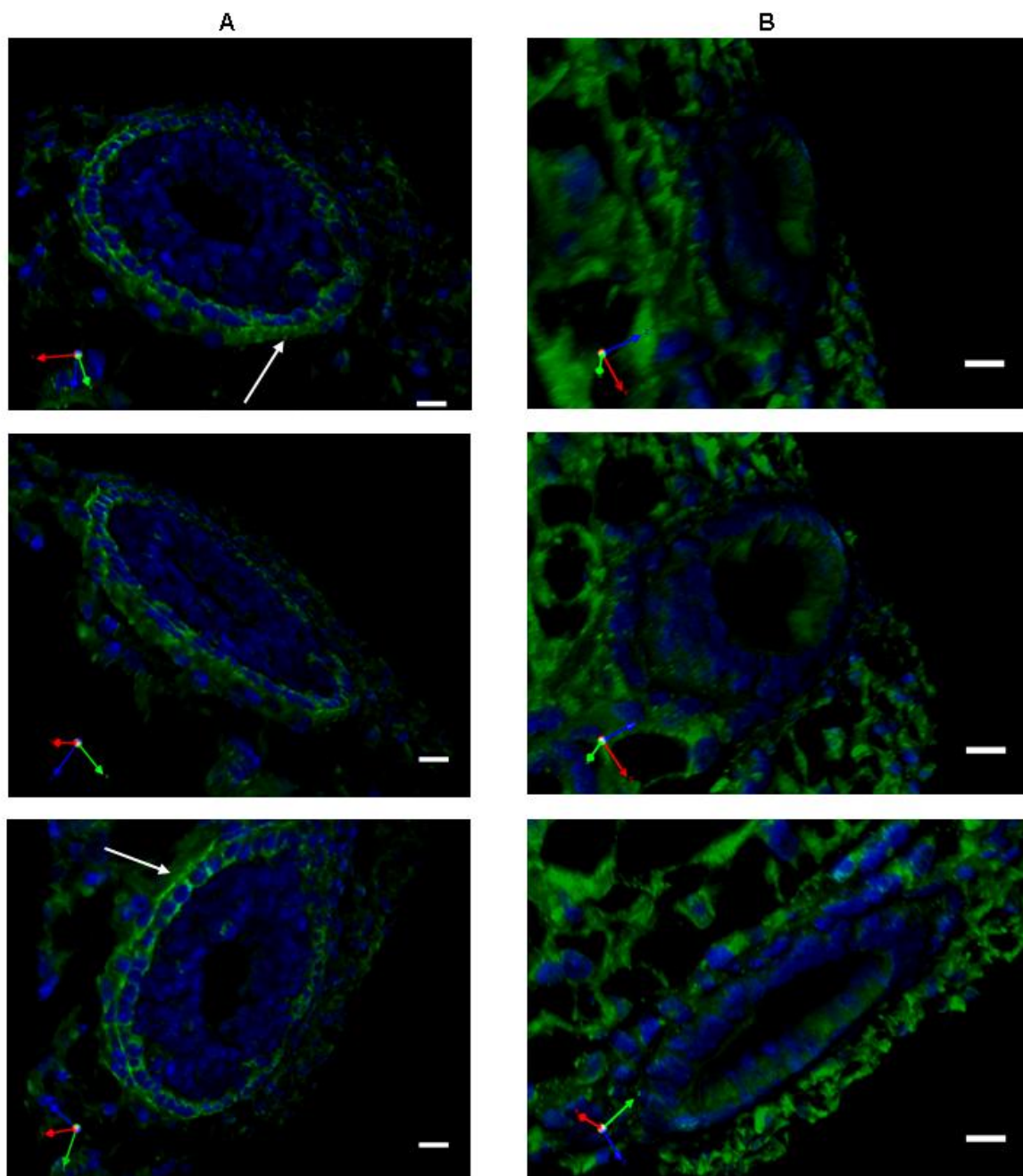


Figure 4-11 3D reconstruction of pubertal TEBs and ducts stained with anti-Fbln2 antibody. 3D reconstruction of the series of **(A)** transverse sections through the TEB and **(B)** longitudinal sections through the duct of a 6 week mouse mammary gland. 3D reconstruction was performed using Velocity software. Images were acquired every 0.7-0.8 μm . **(A)** Fbln2 staining in the TEB was restricted to cap cells and BM region (white arrow). Duct epithelium was negative for Fbln2 expression. Weak staining visible in **B** was nonspecific (**See Figure 4-9 D**). Images were captured by confocal microscopy. Scale bars are 20 μm .

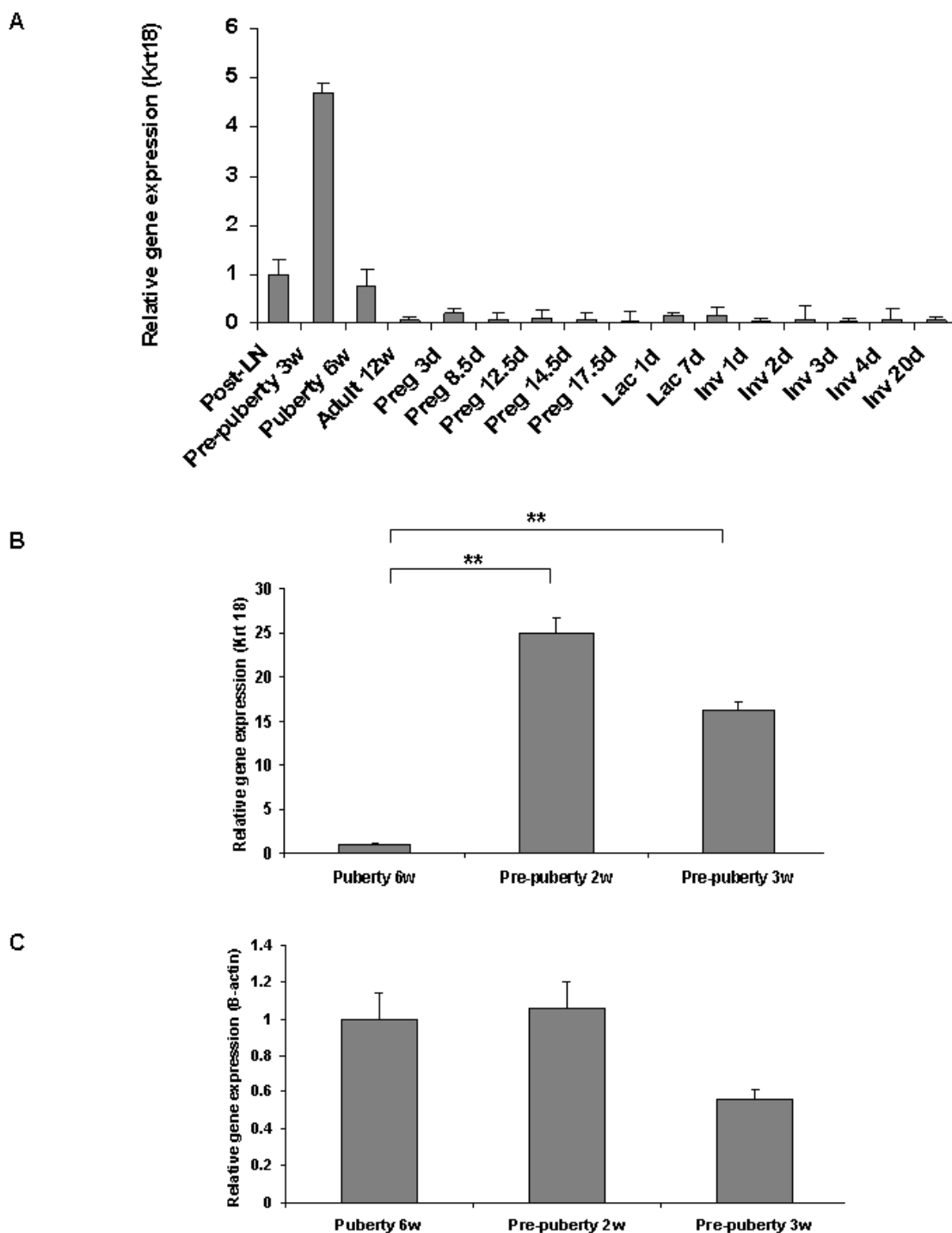


Figure 4-12 *Fbln2* mRNA expression throughout different stages of mouse mammary gland development by Q RT PCR.

(A) Mean expression levels of *Fbln2* in whole glands collected at pre-puberty, puberty, adulthood, pregnancy, lactation and involution. Post-LN strip served as a positive control. Expression levels were normalised against *Krt18*. Error bars denote technical variability, $n=1$, as only 1 animal was used per time point but experiments were repeated 3 times.

(B) (C) Mean expression levels of *Fbln2* in whole glands collected at pre-puberty (2 and 3 weeks) relative to puberty 6 weeks. Expression levels were normalised against *Krt 18* (B) and β -actin (C). Error bars are S.E.M, (*) denotes statistical significance (**) $p \leq 0.01$, $n=3$. Experiments were done in triplicates for each sample.

during puberty, which served as a good experimental control. Furthermore, moderate *Fbln2* expression (although significantly lower than in the Post-LN strip) was also noted in the following samples: pregnancy day 3, lactation days 1 and 7. However, this experiment was performed on samples collected from a single set of animals, hence detected expression levels might not be fully representative. Since *Fbln2* was expressed at the protein level in both epithelium and stroma of the pubertal mouse mammary gland, *Fbln2* RNA expression profiling was repeated at chosen time points (pre-puberty, puberty) to compare the levels of *Fbln2* expression relative to the amount of epithelium or to the total number of cells. This was calculated by normalising the gene expression to *Krt18* and β -*actin* expression levels respectively. Initially only *Krt18* was used for normalisation, but with the expression of *Fbln2* in stroma noted on IHC, IF and absolute gene expression profiling, data was re-normalised against β -*actin* since its expression is ubiquitous. This showed that the level of *Fbln2* expression varied depending on whether its expression was normalised to the amount of epithelium or to the total number of cells. When normalised to *Krt18*, pre-pubertal *Fbln2* expression at 2 and 3 weeks was on average 25 and 16 fold higher than its pubertal (6 weeks) expression respectively (**Figure 4-12 B**) and all of these FCs were statistically significant. In contrast when normalised to β -*actin*, *Fbln2* expression levels were similar between all of the three time points, with only the pre-puberty week 3 sample showing slightly lower expression (**Figure 4-12 C**). None of these FCs, however, reached statistical significance.

A similar pattern of *Fbln2* expression was observed at the protein level. In concordance with the mRNA expression profile, IHC stained sections of the mouse mammary gland developmental stages demonstrated positive *Fbln2* expression during pre-puberty, puberty, adulthood and early pregnancy (**Figure 4-13, 4-14**). In discrepancy with the mRNA data, however, no *Fbln2* expression was detected during lactation (**Figure 4-15 A**). In the pre-pubertal and pubertal mammary gland *Fbln2* localised to the epithelium (cap cells and body cells) and stroma around TEB-like structure and TEBs respectively (**Figure 4-13 A-C**). During puberty, protein expression was also detectable in the duct epithelium and stroma, as discussed in 4.1.2.3 (**Figure 4-13 C**). This ductal expression pattern, although very diminished, was further detectable in the 12 week old

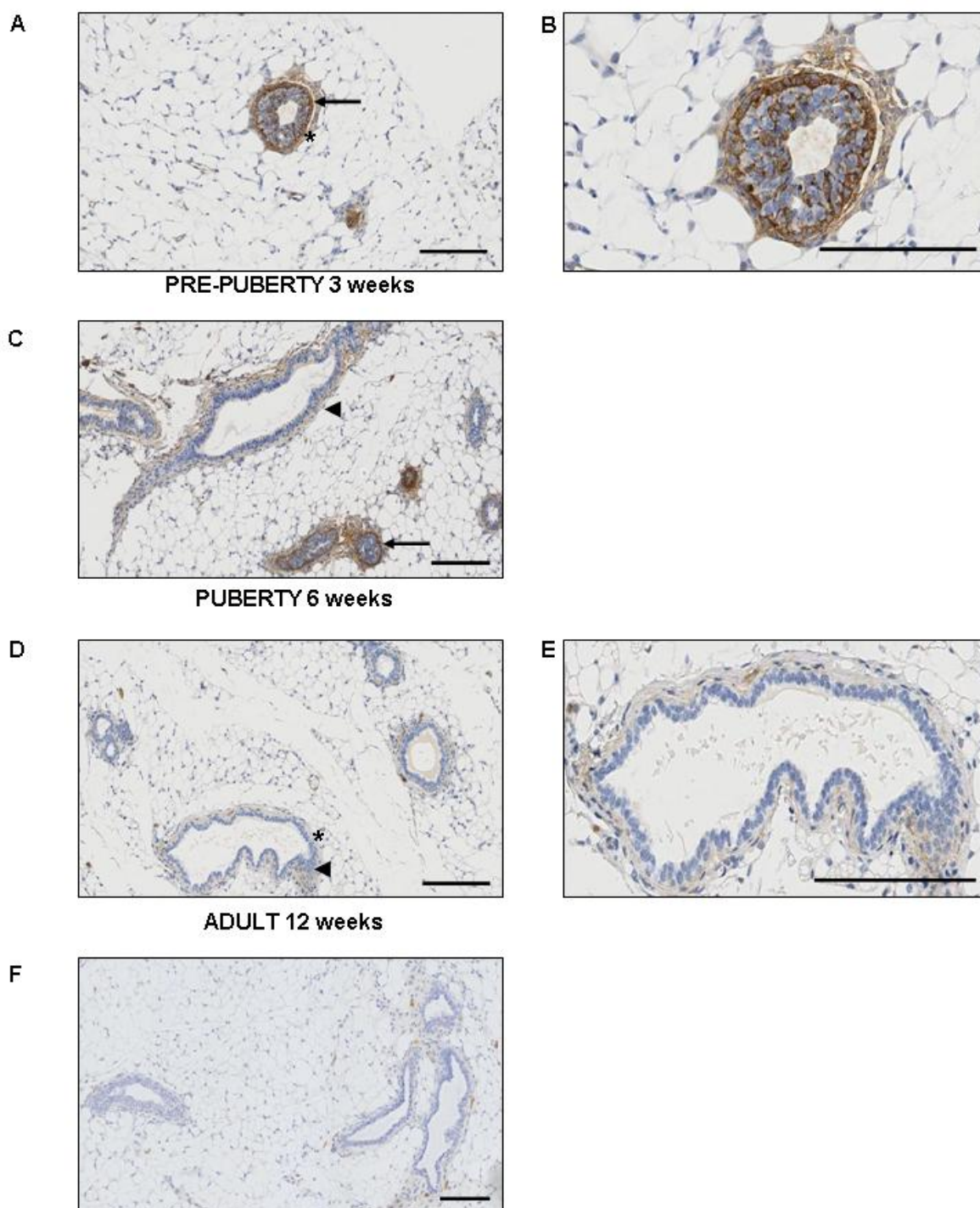


Figure 4-13 Fbln2 protein expression and localisation during virgin mouse mammary gland development by IHC.

Longitudinal and transverse sections through (A) (B) 3, (C) 6 and (D) (E) 12 weeks old mouse mammary glands showing representative fragments of epithelium stained with anti-Fbln2 antibody (brown). Nuclei were stained with haematoxylin (blue). (B) and (E) are higher magnification images of the areas highlighted by asterisks in images A and D respectively. (F) shows a negative (no primary antibody) control. Fbln2 expression was localised to the TEBs (black arrows) (A) (C) and in much lesser extend to the pubertal ducts (black arrow heads) (C). In the adult mammary gland some weak Fbln2 expression was associated with the stroma around ducts (arrow head) (D). Scale bars are 200 μm . At least 3 animals (6 glands) were examined per developmental stage.

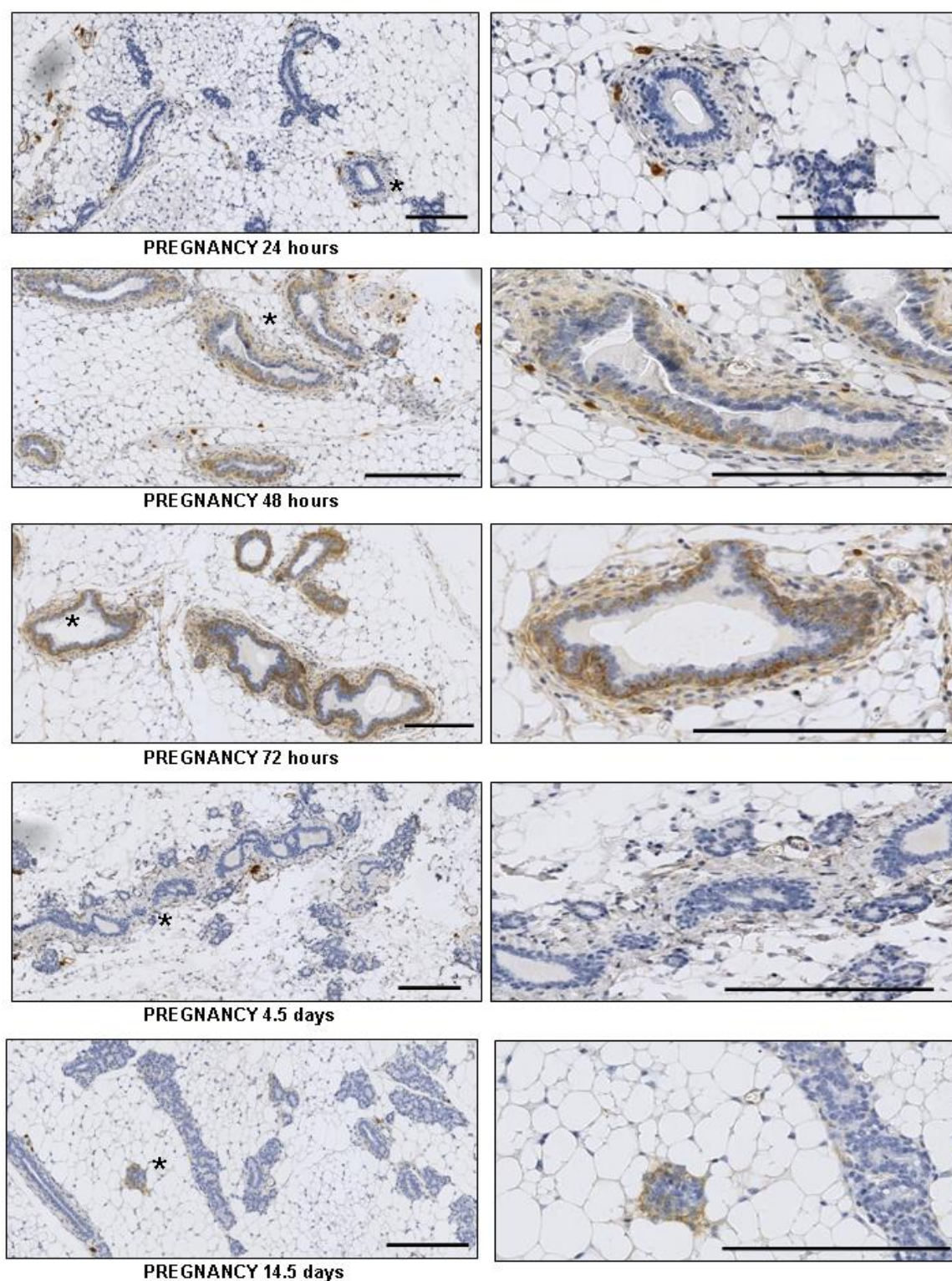


Figure 4-14 Fbln2 protein expression and localisation in the mouse mammary gland during pregnancy time points by IHC.

Longitudinal sections through mammary glands collected from pregnant mice (left) and magnified fragments of representative epithelium (right) (highlighted by asterisk on the left) stained with anti-Fbln2 antibody (brown). Nuclei were stained with Haematoxylin (blue). Fbln2 expression switched on 48h after conception, increased by 72h and disappeared by pregnancy day 4.5. Some Fbln2 positive staining could be seen at 14.5 days. Scale bars are 200 μ m. At least 3 animals (6 glands) were examined per developmental stage.

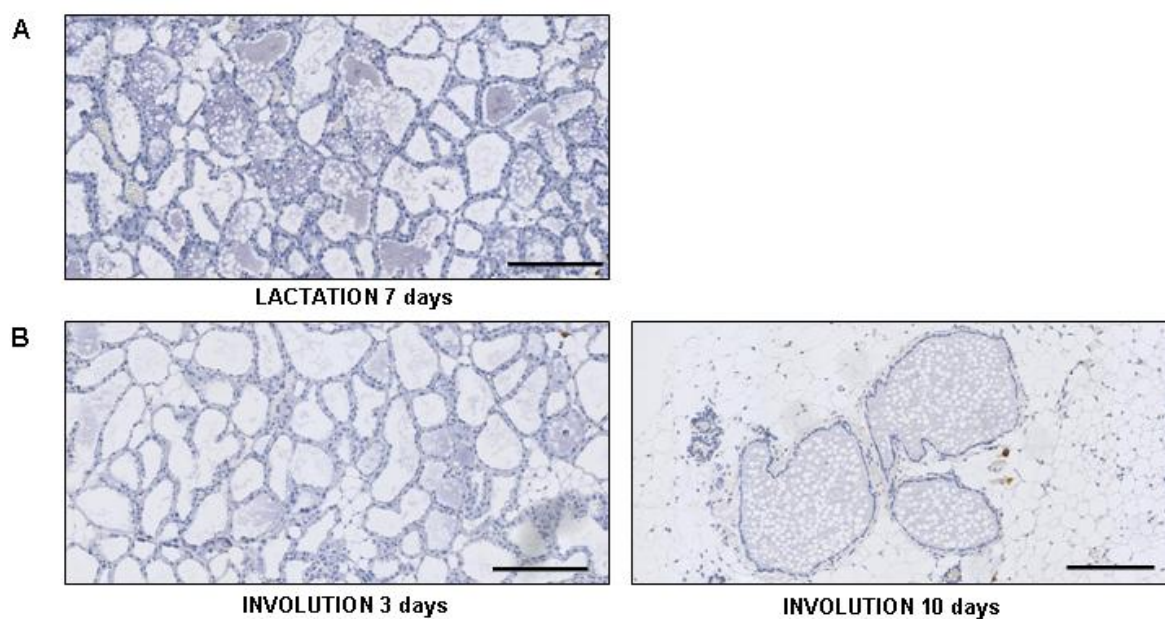


Figure 4-15 Fbln2 protein expression and localisation in the mouse mammary gland during lactation and involution by IHC.

Longitudinal sections through **(A)** lactating and **(B)** involuting mouse mammary glands showing representative fragments of epithelium stained with anti-Fbln2 antibody (brown). Nuclei were stained with Haematoxylin (blue). No Fbln2 expression could be detected. Scale bars are 200 μm . At least 3 animals (6 glands) were examined per developmental stage.

adult mammary glands (**Figure 4-13 D and E**). Prominent Fbln2 expression, comparable to that in the pre-pubertal or pubertal TEBs was detectable during early pregnancy, with the onset at 48h, a peak at 72h and disappearance by day 4.5 (**Figure 4-14**). At these time points, Fbln2 appeared localised exclusively to the cell membranes and cytoplasm of the outer most, presumably myoepithelial layer of the ductal epithelium and the stroma around it (as seen at puberty).

The expression of Fbln2 in the distal stromal capsule was very prominent at pre-puberty (3 weeks), puberty (6 weeks) and pregnancy 72h; largely reduced by the onset of adulthood and pregnancy day 14.5 and absent from involution day 7 and lactation day 3 (**Figure 4-16 A-G**).

All of the observed staining was specific to Fbln2-antibody binding as demonstrated by the lack of staining in the negative (no primary antibody) controls (**Figure 4-13 F**) (**Figure 4-16 H**).

4.2.2.5 Localisation of Fbln2 expression using a preliminary *in vitro* model of TEB explant culture

The confocal images and light microscopy suggested that the Fbln2 was present in the cytoplasm, on the membrane and possibly in the extracellular spaces in TEBs at puberty. In order to analyse the localisation more precisely we decided to attempt to culture TEBs as explants, with the assumption that the cap cells and the body cells would migrate out from the explant as a monolayer or multilayer and thus be more amenable to study. Consideration was given to using TEBs embedded in Matrigel, but this would have involved histological sectioning. The methodology was based on that used previously for keratinocyte explant cultures [454] with modifications which were thought might help to maintain the cells. Briefly, TEBs were isolated as previously described (**2.2.1.5**) and plated out on fibronectin (10ug/ml) coated chamber slides, with a thin film of culture medium (Dulbecco's Modified Eagle Medium: Nutrient Mixture F-12 (DMEM/F12) supplemented with 2mM L-glutamine and Leukaemia Inhibitory Factor (LIF) (1000U/ml). LIF was used in an attempt to prevent differentiation. Fibronectin was used to improve attachment. Explants were cultured in Galaxy S tissue culture incubator at 37°C in a humidified atmosphere with 5% CO₂.

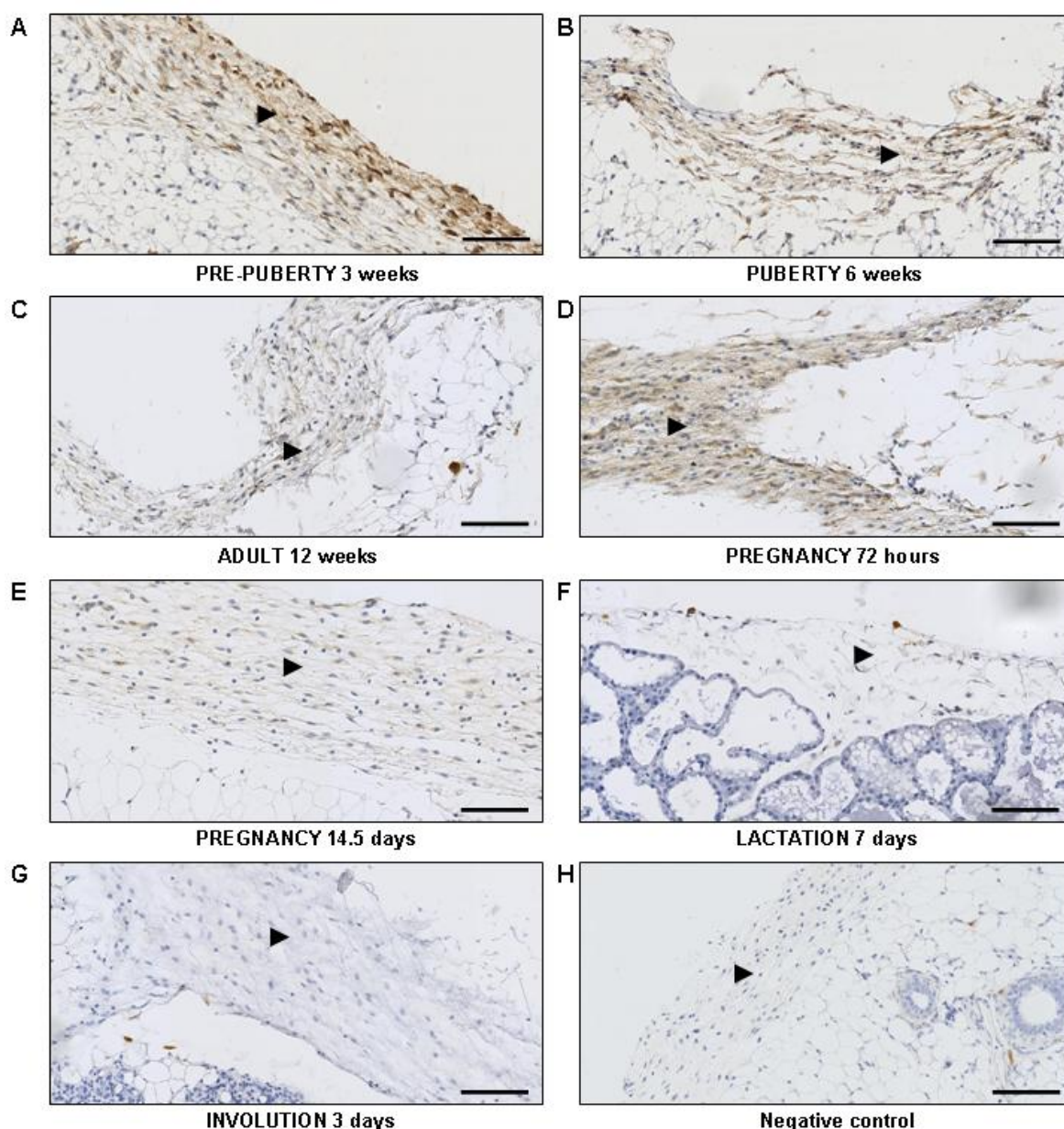


Figure 4-16 Fbln2 protein expression in the stromal capsule throughout the developmental time points of mouse mammary gland morphogenesis by IHC.

Sections through mouse mammary glands collected at different time points during mammary morphogenesis showing representative fragments of stromal capsule (arrow head) stained with anti-Fbln2 antibody (brown). Nuclei are stained with Haematoxylin (blue). Strong Fbln2 expression could be seen at pre-puberty (3 weeks) **(A)**, puberty (6 weeks) **(B)** and pregnancy 72h **(D)**. Weaker Fbln2 expression could be noted in adulthood (12 weeks) **(C)** and pregnancy 14.5d **(E)**. No Fbln2 staining could be seen in lactation day 7 **(F)**, involution day 3 **(G)** and negative (no primary antibody) control **(H)**. Scale bars are 100 μm . At least 3 animals were examined for each time point.

After 24h, explants attached and further medium was added to a level of 2mm, with care not to disturb the explants. Cells spread out from the periphery of the explant over the next 4 days and the cultures were then terminated by fixation in absolute alcohol. A pavement of epithelial cells formed around the explant (**Figure 4-17**). Cell division was seen in the outgrowths, but the majority of the outgrowth was through migration and cell spreading. The preliminary IHC analysis of outgrowths demonstrated: i) positive Ktr18 staining in all of the cells within the outgrowth, suggesting their epithelial origin (**Figure 4-17 A**); ii) positive Krt14 staining in some of the cells, confirming their epithelial origin (**Figure 4-17 B**); iii) positive SMA staining seen in the cells at the periphery of the outgrowths, suggesting their myoepithelial/cap cell character (**Figure 4-17 C**). On the basis of this preliminary characterisation of the epithelial nature of the outgrowths we stained the cultures with routine anti-Fbln2 antibody. Explants showed positive Fbln2 expression which localised to the cytoplasm, cell membranes and cellular processes that protruded from some cells and resembled cob-web-like structure which seems to run around, above and between cells like intracellular glue (**Figure 4-18**). The cytoplasmic and cell-membrane associated expression of Fbln2 is consistent with the sites of its expression in the epithelium of TEB *in vivo* (**Figure 4-10**). No double labelling was performed, but there was no correlation between the distribution of the CK14 and SMA positive cells and the Fbln2 expression. This was a very preliminary study, but enabled us to localise the Fbln2 *in vitro* and to confirm the localisation of the protein and its apparent secretion into the extracellular compartment. Clearly this explant system also has limitations, with lack of stroma, the all important immune system and loss of the *in vivo* 3D cellular organisation, but may have some role in studies of body and cap cells if further characterised.

4.2.2.6 Fbln2 splice variants and their pubertal expression pattern.

As mentioned previously, there are two alternative splice variants of *Fbln2* gene, known as *Fbln2 V1* and *Fbln2 V2*. The former includes 18 exons while the latter lacks the sequence for exon 9 and hence consists of 17 exons (**Figure 4-19 A**). The distribution pattern of the two splice variants appears tissue specific. As shown by Grässel *et al.* (1990), using PCR and exon 9 flanking primers to amplify the cDNA of Fbln2, *Fbln2 V1* is predominantly expressed in the heart while *Fbln2*

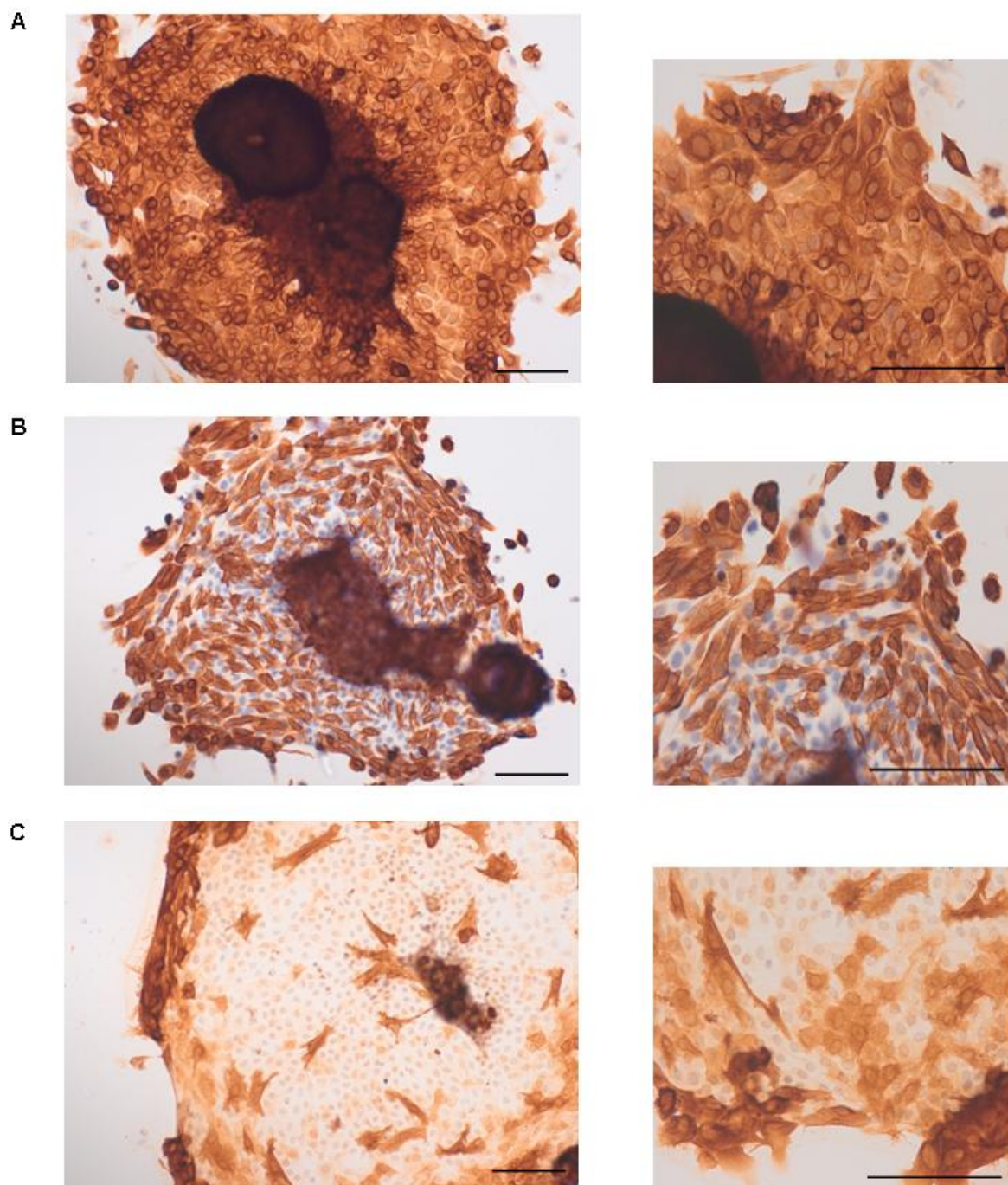


Figure 4-17 Preliminary analysis of the morphological characteristics of explant culture outgrowths by ICH.

TEB explant outgrowths stained with **(A)** anti-Krt18, **(B)** anti-Krt14 and **(C)** anti-SMA antibodies. **(A)** **(B)** Positive Krt18 (uniform) and Krt14 (some cells) staining suggests the epithelial character of outgrowths. **(C)** Positive SMA staining, seen at the periphery of the outgrowths, suggests a myoepithelial/cap cell character of these cells. At least 3 TEB outgrowths were stained with each antibody and examined. Scale bars are 100 μ m.

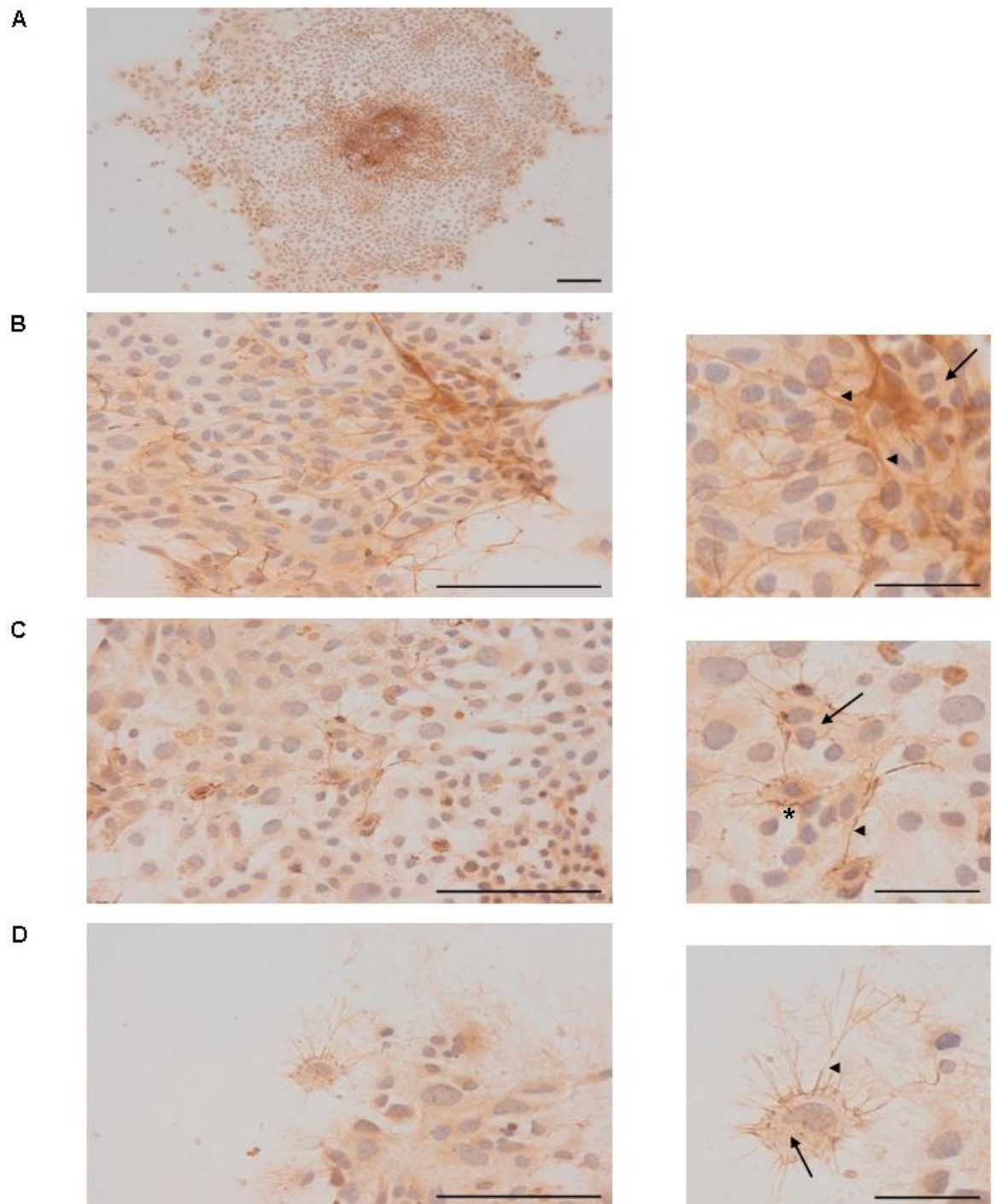


Figure 4-18 Preliminary investigation of Fbln2 expression in the outgrowths of TEB explants by ICH.

(A) Image of TEB explant outgrowth **(B) (C) (D)** Representative fragments of TEB explant shown in **A**. Fbln2 expression appeared to be associated with the cytoplasm (arrow), cell membranes (asterisk) and cellular processes of some cells within the outgrowths. At least 3 TEB outgrowths were stained with anti-Fbln2 antibody and examined. Scale bars are 100µm (right) and 25µm (left).

V2 is more abundant in the kidney. The NIH3T3 cell line expresses only full length *Fbln2*, i.e. *Fbln2 V1* [439].

In this project, two distinct methods of splice variant detection were used to analyse the mammary gland specific pattern of *Fbln2 V1* and *Fbln2 V2* expression. Firstly, the expression of each exon was analysed and compared between the isolated TEBs and ducts using the XRAY Excel® Array based microarray analysis (See 2.2.5.7). Secondly, the cDNA produced from the RNA extracted from the Post-LN, Pre-LN tissue strips and isolated TEBs and ducts was PCR amplified as described by Grässel *et al.* [439] and resolved by using agarose gel electrophoresis. Primer location is demonstrated in **Figure 4-19 A**.

Fbln2 exon expression analysis showed a comparable exon expression pattern between the isolated TEBs and ducts. As demonstrated in **Figure 4-19 B**, the two lines indicating mean expression of *Fbln2* in TEBs (blue line) and ducts (red line) were roughly parallel and where present, the divergence from this parallel co-localisation (exons that are contained within the two vertical lines) was too small to be significant. Thus, a lack of variation in alternative RNA splicing between TEBs and ducts was demonstrated. A more detailed, probe set based gene expression analysis of the probe set number 9 which is complimentary to the DNA fragment between nucleotide positions 91209637-91209763, thus corresponding to exon 9 of *Fbln2* gene (91209624-91209764) confirmed the above mentioned finding (**Figure 4-19 C**). No significant difference in the expression pattern was seen either when the 9th probe set was compared to other probe sets which suggested that exon 9 was expressed at a similar level to the remaining exons or when the 9th probe set was compared between TEB and duct samples, suggesting a similar level of exon 9 expression in both samples (**Figure 4-19 C**). Given that exon 9 is only present in *Fbln2 V1* it would suggest this isoform is prevalent in both the TEB and duct samples.

PCR based analysis further revealed the presence of both *V1* and *V2 Fbln2* splice variants in the Post-LN and Pre-LN mammary tissue strips and isolated TEBs and ducts. As seen in **Figure 4-19 D**, the corresponding electrophoresis gels presented two amplification bands of 394 and 254 bp consistent with the size predicted for *V1* and *V2 Fbln2* variants respectively. The *V1* splice isoform of *Fbln2* appeared stronger in the Post-LN strips and isolated TEBs and ducts which

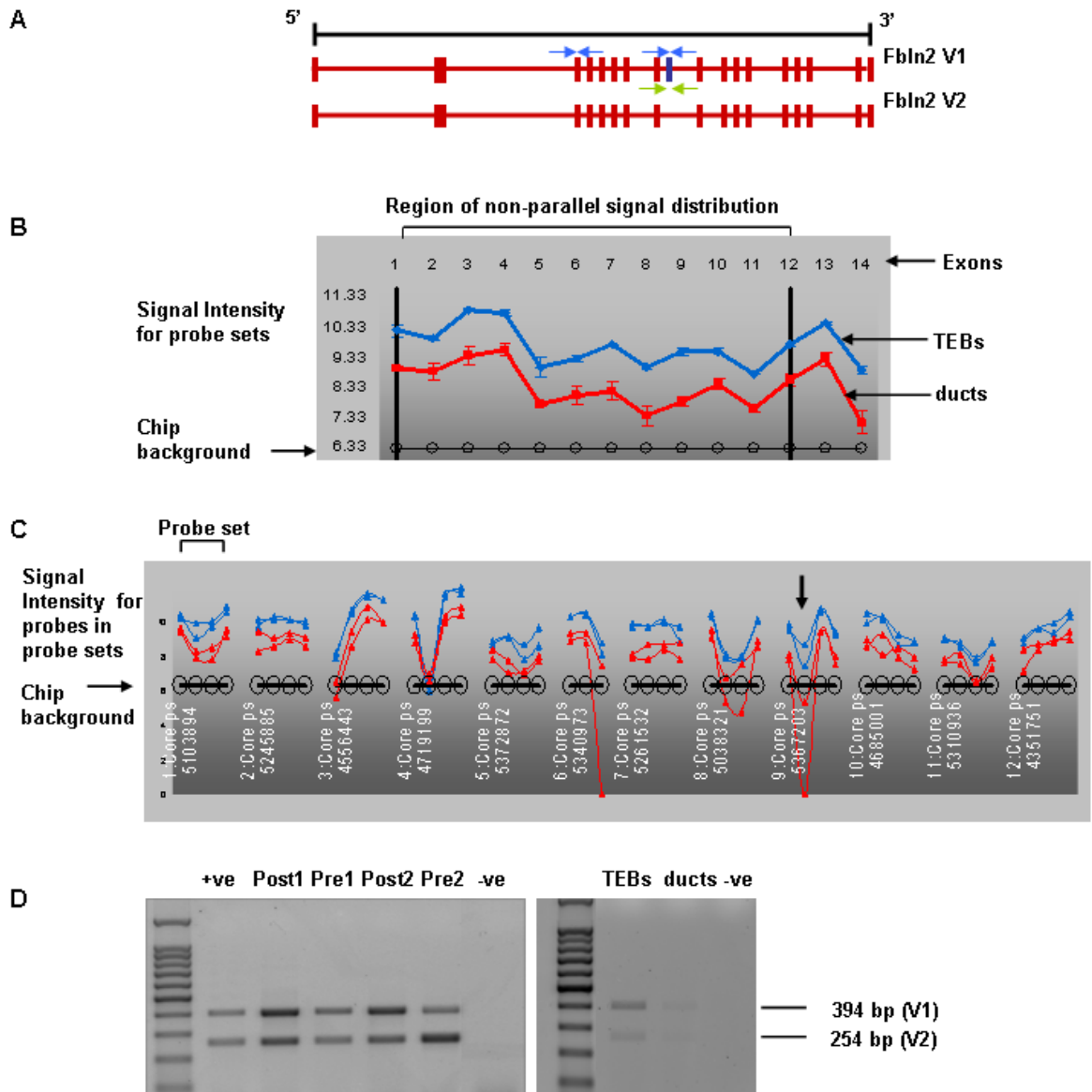


Figure 4-19 The expression of Fbln2 splice variants in the pubertal mouse mammary gland. **(A)** Graphical comparison of Fbln2 V1 and Fbln2 V2 genomic DNA organisation. Red boxes indicate common exons. Blue box denotes exon 9 (exclusive for Fbln2 V1). The approximate locations of primer annealing sites are denoted with arrows. Green arrows show primers used for PCR experiments. Blue arrows show primers used in Q RT PCR experiments. **(B) (C)** Comparison of *Fbln2* expression in isolated TEBs (blue) and duct (red). Analysis shown at **(B)** the exon level and **(C)** probe set level. Each probe set represents a different exon cluster and there is one exon cluster per exon. Comparison was carried out using XRAY Excel® Array Analysis v.2.5 Microsoft® Excel® add-in. Probe set number 9 was designed against a fragment of DNA located in exon 9 (absent from *Fbln2* V2). Although 12 exons showed non parallel expression level between TEB and duct samples (denoted by two vertical black lines) the differences in expression were not significant enough to indicate differences in alternative splicing between the samples. Error bars indicate standard deviation at each **(B)** probe set or **(C)** probe. **(D)** PCR. Electropherogram illustrating presence of Fbln2 V1 (394 bp) and V2 (254 bp) splice variants expression in Post-LN and Pre-LN strips and isolated TEBs and ducts. +ve contains cDNA from mouse kidney (positive control). -ve are PCR quality controls (-RT). Tissue strips were collected from two individual mice. Fbln2 V1 seems to be prevalent in Post-LN strip and isolated TEBs or ducts samples. V1:V2 ratio in Pre-LN strip is inconclusive, n=pooled from 300 mice for the isolated TEBs and ducts for tissue strips 1 animal was used for each Pre-LN and Post-LN strips. Experiment was repeated 4 times with similar results.

was consistent with the exon expression data. No difference in band strength, however, was seen for the V1/V2 ratio in the Pre-LN strips. The observed expression pattern of Fbln2 splice variants was representative of mammary gland tissue strips collected from 4 individual mice and isolated TEBs and ducts pooled from 300 mice. cDNA synthesized from kidney RNA served as a positive control.

4.2.2.7 Characterisation of the additional, 150 kDa and 135 kDa proteins, detected by the routine anti-Fbln2 antibody.

Although the molecular weight of the mature, monomeric Fbln2 protein is 195 kDa, two major, additional bands of a molecular weight of 150 kDa and 135 kDa were detectable using the anti-Fbln2 antibody throughout most of the Western blotting experiments. Bands of similar molecular weight have also been reported by other research groups (using the same antibody) and speculated to arise as a result of proteolytic cleavage, but their true nature has not yet been elucidated [434] [455].

To investigate the identity of the two bands further and check for differences in their expression in different components of mouse mammary gland, experiments were designed to test the following hypotheses: (1) 195 kDa band stands for Fbln2 V1 while 150 kDa or 135 kDa denotes Fbln2 V2; (2) both bands (135 kDa and 150 kDa) arise due to the N- or C-terminus targeted proteolytic cleavage; (3) the proteolytic cleavage pattern could vary depending on the stromal environment of proteases present.

HYPOTHESIS 1: The first hypothesis resulted from molecular mass prediction studies carried out for Fbln2 V1 and V2. The mass of the V1 isoform was predicted as 131 kDa, revealing that the remaining 64 kDa of the mature protein is attributed to post-translational modifications, such as N-glycosylation. Fbln2 V2 was predicted to weigh 126 kDa. However, since there are 4 potential N-glycosylation sites in the Fbln2 V1 sequence and one of them is located within exon 9 which is absent from its V2 counterpart, it is likely that the actual size difference between the V1 and V2 isoforms is much greater than 5 kDa, and thus the V2 isoform of Fbln2 could in fact weigh 150 kDa. To test this hypothesis, we used protein extracts from NIH3T3 (mouse fibroblasts), EpH4 and HC11 (mouse mammary epithelial) cell lines. These cell lines were chosen on the basis of

cDNA profiling by PCR as described in 4.2.2.6 which showed that NIH3T3 express both Fbln2 V1 and Fbln2 V2 isoforms, EpH4 express only the Fbln2 V2 isoform while HC11 show no Fbln2 at all and thus when studied collectively they serve a good system to investigate the identity of Fbln2 bands. As seen on the representative gels in **Figure 4-20 A**, the amplification bands of 394 (V1) and 254 (V2) bp were seen in the NIH3T3 cell line while only the lower weight one of 254 bp (V2) was detectable in the EpH4 amplicon. No amplicons were produced from HC11 cDNA. Q RT PCR further confirmed these results (**Figure 4-20 B**). By using two sets of primers, designed to amplify the common region of V1 and V2 isoforms or Fbln2 V2 exclusively (designed against cDNA fragment spanning exon 8 and 10) the exact same pattern of Fbln2 splice variant expression, as demonstrated by cDNA profiling by PCR, was seen. Primer location is demonstrated in **Figure 4-19 A**. On the basis of these findings, Fbln2 protein expression was compared between EpH4, NIH3T3 and HC11 cells. The Western blot, however, showed no major differences in the Fbln2 banding pattern between the protein extracts from the EpH4 and NIH3T3 cells, as all three main bands (195 kDa, 150 kDa, and 135 kDa) were visible. There was no loss of 195 kDa (putative V1) either (**Figure 4-20 C**). The only slight difference was visible when the mobility of the top two bands was compared between lanes. In the EpH4 cells protein extracts the top band, corresponding to the mature Fbln2 protein showed a slightly lower molecular weight than that seen in NIH3T3 cells at 195 kDa. The middle band, on the other hand, appeared to migrate slower, corresponding to a higher molecular weight than its NIH3T3 counterpart. All of the bands detected were specific for Fbln2-anti-Fbln2 antibody binding as demonstrated by the lack of bands in the negative control (HC11 cells). Collectively, it was demonstrated that it is unlikely for either the 150 kDa band or the 135 kDa band to correspond to Fbln2 V2.

HYPOTHESIS 2: To test the second hypothesis, that both of the lower molecular weight bands arise due to N- or C-terminus targeted proteolytic cleavage, we initially aimed to use two additional, commercial antibodies, raised against N- or C-terminus of Fbln2 (**See Figure 4-4 B and C**). It was, however, not possible to test this hypothesis as the anti-C-terminus antibody could not be used due to problems with its optimisation (data not shown). As a result, we used the anti-N-terminus antibody only and thus tested for the presence of the potential

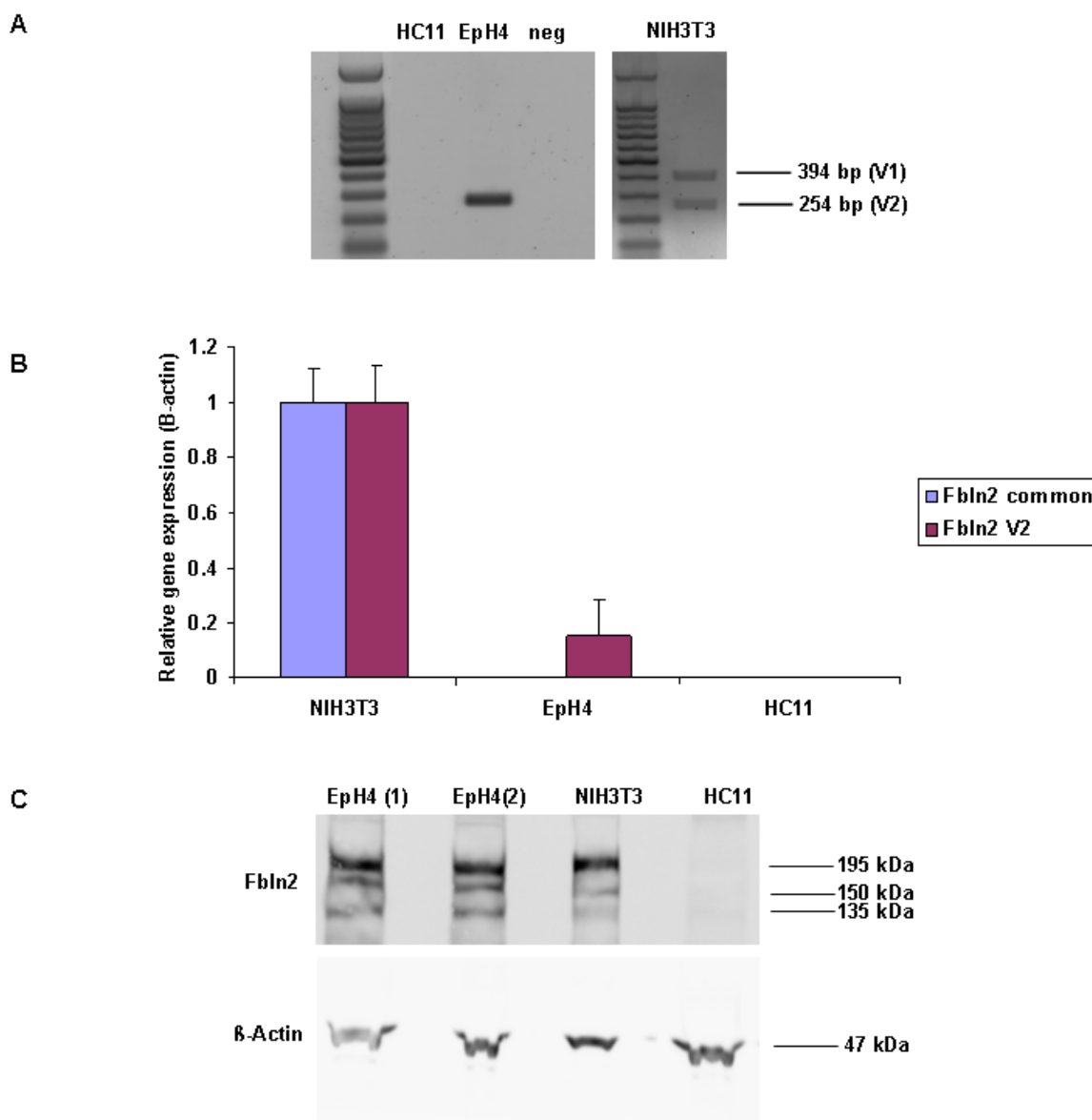


Figure 4-20 Fbln2 expression profiling in the mouse cell lines and identification of Fbln2 V2 expression in EpH4 cells.

(A) PCR. Electrophoretogram illustrating Fbln2 V2 (254 bp) expression in EpH4 cells. HC11 cells were used as a negative Fbln2 expression control. –RT was used as PCR quality control, n=1 (B) Q RT PCR. *Fbln2* and *Fbln2* V2 expression profiling in NIH3T3, EpH4 and HC11 cells. Total *Fbln2* expression was estimated using primers designed against the common region of *Fbln2* V1 and V2 splice variants. Expression of *Fbln2* V2 was identified using PCR primers designed to span exon 8 and 10 (*Fbln2* V2 lacks exon 9). β -actin expression was used as an internal control for normalisation. Graph shows exclusive *Fbln2* V2 expression in EpH4 cells and lack of *Fbln2* or *Fbln2* V1 expression in HC11 cells. NIH3T3 cells were used as positive control (express both splice variants). Error bars denote technical variability (S.E.M.), n=1 (C) Western blotting. Fbln2 (195 kDa) expression in the protein extracts collected from two different EpH4 cell cultures, NIH3T3 cells (positive control) and HC11 cells (negative control). Protein extracts were collected using RIPA buffer. Expression analysis was performed using anti-Fbln2 antibody. β -actin was used as loading control.

variation in proteolytic cleavage solely within the N-terminus of Fbln2. The N-terminus anti-Fbln2 antibody was used to detect Fbln2 expression in the NIH3T3 protein extracts (RIPA lysis buffer) and the resulting expression pattern was compared with that detected with the anti-Fbln2 antibody routinely used in this project (raised against the whole protein) [434]. As demonstrated in **Figure 4-21**, the largest two bands (195 kDa and 150 kDa) were detectable with both the full-length and N-terminus anti-Fbln2 antibodies. The discrepancies in the signal intensities seen between the two antibodies were most probably attributed to the difference in the protein-antibody binding affinities. The 135 kDa band, however, was absent from the blot incubated with the anti-N-terminus antibody indicating either the absence of protein's N-terminus within the sequence denoted by this band or the lack of cross-reactivity between the antibody and protein sequence in this instance. Nonetheless, this suggested that proteolytic cleavage could be responsible for the banding pattern. HC11 protein extract was used as negative control to ensure the antibody specificity.

HYPOTHESIS 3: This experiment was designed to test whether the banding pattern detected by the anti-Fbln2 antibody (full length) was dependent on the origin of mammary stroma, i.e. if it was TEB- or duct-associated, and at the same time to test whether the lysis buffer used for Fbln2 extraction had an effect. Protein extracts from Post-LN and Pre-LN strips were prepared using four lysis buffers to investigate the varied efficiency in Fbln2 solubilisation and were compared by Western blotting. The lysis buffers used in this experiment included: RIPA, NP-40, EDTA and Urea. Both RIPA and NP-40 belong to the group of detergent lysis buffers. EDTA and Urea buffers, on the other hand, do not contain detergents. EDTA buffer binds Ca^{2+} which is essential for the maintenance of the trimeric structure of Fbln2 while the Urea buffer causes the denaturation of proteins. Both the EDTA and Urea buffers were previously shown to solubilise 80% of Fbln2 [444]. Post- and Pre-LN tissue strips were selected as they contain the epithelium and stroma of both TEBs and ducts or only the ductal compartment respectively, hence enabling the comparison of TEB and duct environments. As seen in **Figure 4-22** there was no obvious difference between the banding patterns detected in the Post-LN and Pre-LN protein extracts. However, although the three main bands were detectable in NP-40, EDTA and Urea protein lysates there was some difference between the signal

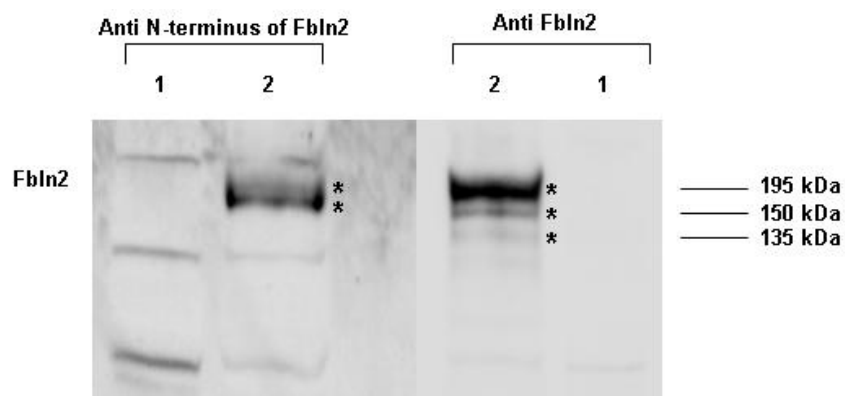


Figure 4-21 Comparison of Fbln2 expression pattern detected using different antibodies.

Western blotting showing Fbln2 expression in two mouse cell lines; HC11 (negative control) (lane 1) and NIH3T3 (lane 2). Expression analysis was performed with two antibodies raised against N-terminus of Fbln2 (left) and the whole protein (right). Protein extracts were collected using RIPA lysis buffer. Blot was cut in two to allow different antibody probing on the same blot. Experiment was performed using protein lysates extracted upon three different cell passages. Bands of interest are highlighted by asterisks.

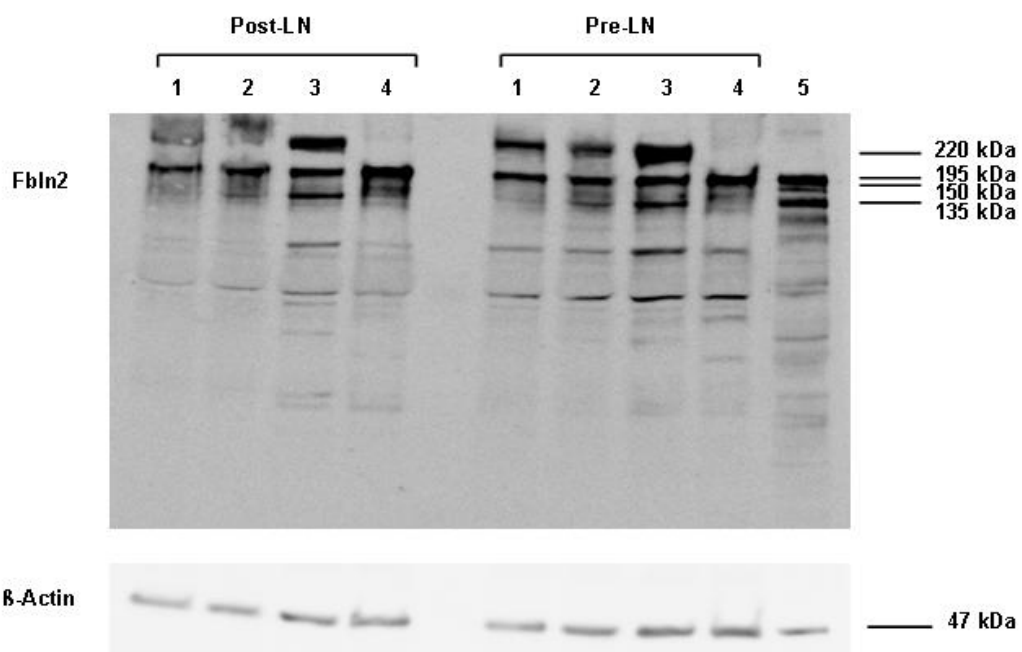


Figure 4-22 Comparison of Fbln2 expression pattern detected using different lysis buffers. Western blotting. Analysis of Fbln2 expression pattern in Post-LN (lanes 1-4 on the left) and Pre-LN strips (lanes 1-4 on the right) protein extracts prepared using following lysis buffers: RIPA (lane 1), NP-40 (lane 2), EDTA (lane 3) and Urea (lane 4). Protein extract collected from NIH3T3 (RIPA buffer) was used as a positive control (lane 5). Expression analysis was performed using anti-Fbln2 antibody. β -actin was used as loading control. n=1

intensities of the 150 kDa and 135 kDa bands. The 195 kDa was prominent in all the protein lysates. The 150 kDa band was the least visible in NP-40 and EDTA protein lysates while the 135 kDa band was the least detectable one in the Urea protein lysate. Although, the expression of all three bands that correspond to Fbln2 has previously been shown to be detectable in Post-LN and Pre-LN RIPA buffer protein extracts (See Figure 4-6 C), no evident expression of the 150 kDa and 135 kDa bands could be demonstrated in RIPA protein lysate used in this experiment. This could be due to the degradation of this protein extract. Furthermore, an additional ~220 kDa band was present in all of the lysates except for the Urea lysate. It is unclear what the ~220 kDa band corresponds to. NIH3T3 cells protein lysate extracted in RIPA buffer served as a positive control. The direct comparison of protein lysates was valid as demonstrated by uniform β -actin expression levels throughout the samples. Taken together, these results show that the observed cleavage pattern is uniform across the TEB and duct microenvironments which suggests that the processing of Fbln2 does not rely on any of the proteases that are exclusive to the either TEB or duct stroma. Secondly, as seen in Figure 4-22, different lysis buffers extract the 150 kDa and 135 kDa Fbln2 bands with different efficiencies and thus it may be beneficial to employ the identified optimal extraction conditions to further study each of these bands.

4.2.2.8 The impact of systemic hormones on the regulation of Fbln2 expression in mouse mammary gland.

Hormonal regulation of *Fbln2* has already been documented by Okada *et al.* (2003) and Gu *et al.* (2007) who demonstrated its stimulation by P in human endometrial stromal cells *in vitro* [456] and down-regulation by hydrocortisone in the bone marrow stroma *in vitro* respectively [457]. Taking this into consideration along with knowledge of the importance of systemic hormones in pubertal mouse mammary development, the impact of E2 and P on mouse mammary gland Fbln2 expression was examined. Hormone induced changes in Fbln2 expression and tissue localisation were assessed using mouse mammary glands collected from 4.5 week old mice primed for a week with E2, E2+P or placebo hormone pellets prior to gland excision.

As shown by the Q RT PCR, expression of *Fbln2* was highly up-regulated by both the E2 and E2+P hormonal treatments (**Figure 4-23**). The mean expression of *Fbln2* in the E2+P and E2 primed glands was 40.4 fold and 36.2 fold higher respectively than that calculated in the Pre-LN strip (negative control). Glands primed with placebo pellets showed a 7.1 fold up-regulation in *Fbln2* expression when compared with Pre-LN strip. Furthermore, a 3.5 fold up-regulation of *Fbln2* was calculated in the Post-LN strip when compared to Pre-LN strip and it was used as a positive control. When gene expression was compared only between the treated mammary glands, using the placebo as a reference, *Fbln2* was 4 fold and 3.6 fold up-regulated in the E2+P and E2 treated glands respectively. The difference in *Fbln2* expression was statistically significantly only when comparing placebo and E2+P treatments. The level of *Fbln2* over-expression in the E2 treated glands compared to placebo ones failed to reach statistical significance probably due to considerable biological variation and a low number of replicates (4 mice). It is possible, however, that the calculated FC(s) may differ slightly as at the time of commencing these experiments, prior to localisation studies, *Fbln2* was thought to be associated only with mammary epithelium and so levels of *Fbln2* were normalised using *Krt18* expression, i.e. the amount of epithelium instead of the total number of cells.

Thus, to confirm the Q RT PCR results, the impact of E2 and E2+P on *Fbln2* expression and spatial localisation was analysed at the protein level by IHC, using the routine anti-*Fbln2* antibody (**Figure 4-24**). The obtained results provided further insights into hormone induced changes in *Fbln2* expression and localisation in mouse mammary gland. In the placebo primed mice (control), the mammary gland associated expression of *Fbln2* was similar to that seen in pre-pubertal/pubertal mice (**Figure 4-24 A**). *Fbln2* was mostly localised to the epithelium and stroma of TEBs. Some *Fbln2* expression was also detectable in the ductal stroma and stromal capsule at the edge of Fat pad. The pattern of *Fbln2* expression in the mammary TEBs and ducts of the E2+P primed mice was similar to that seen in placebo. *Fbln2* was consistently localised to the epithelium and stroma of TEBs and on a much lower level to the stroma of ducts (**Figure 4-24 B**). What was different between the two treatments, however, was the significant increase in *Fbln2* expression at the stromal capsule at the edge of Fat pad (**Figure 4-24 A and B**). This stromal capsule-specific increase in *Fbln2*

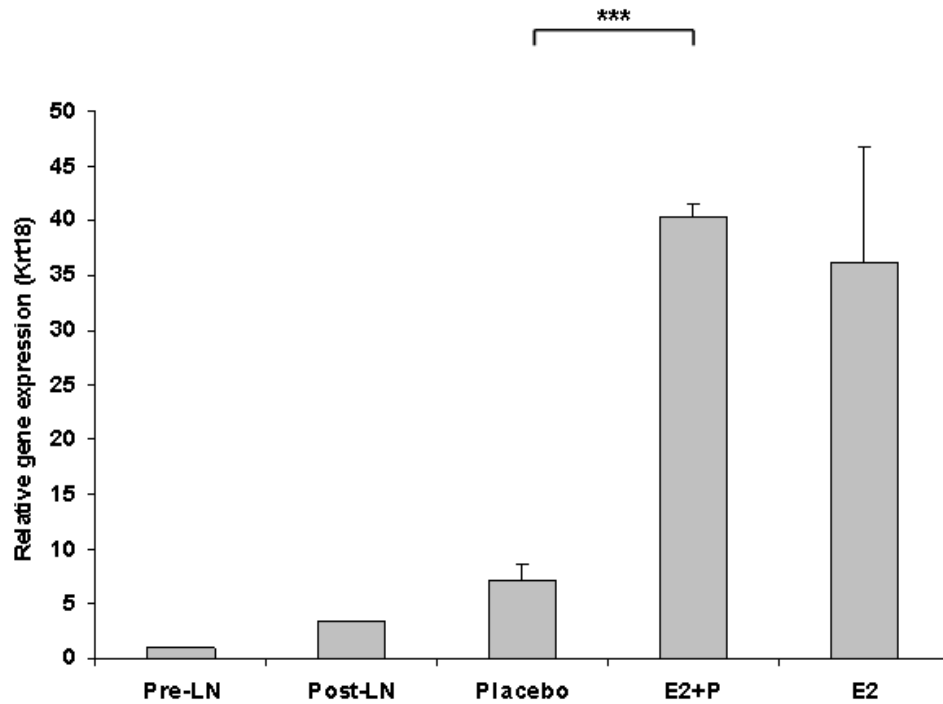


Figure 4-23 Hormonal regulation of *Fbln2* expression at the mRNA level by Q RT PCR.

Mean expression level of *Fbln2* in Post-LN tissue strip (6 weeks old) and hormone primed glands (4.5 weeks old) – placebo, oestrogen-progesterone (E2+P) and oestrogen (E2), relative to Pre-LN tissue strip (6 weeks old). Post-LN and placebo were used as positive controls. Pre-LN was used as negative control. *Krt18* expression was used as an internal control for normalisation. Error bars are S.E.M. (***) denotes statistical significance of $p\text{-value} \leq 0.001$, $n=1$ (Pre-LN and Post-LN) $n=3$ (placebo and E+P) $n=4$ (E). N stands for number of animals. Both glands were used from each animal.

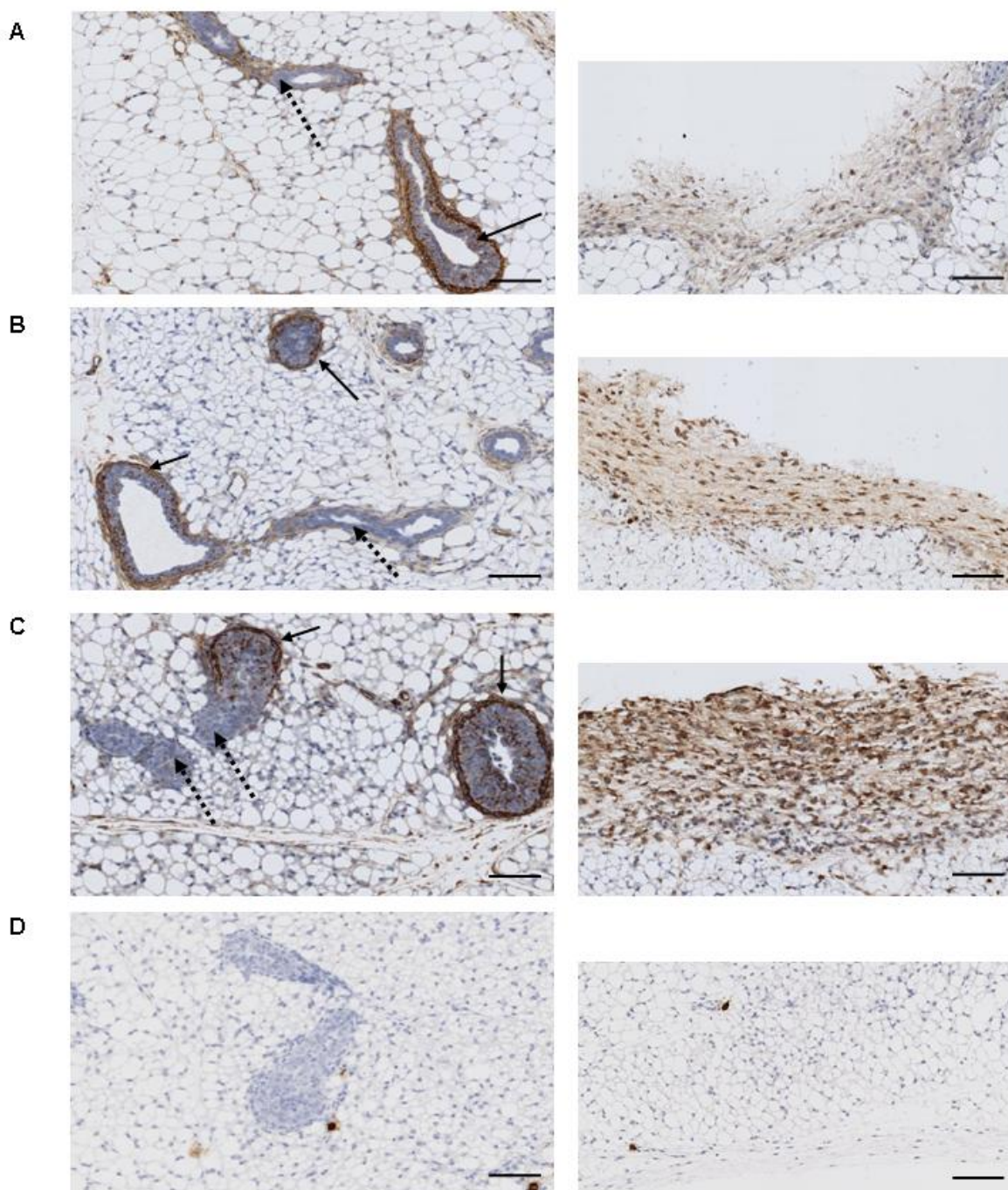


Figure 4-24 Hormonal regulation of Fbln2 expression on protein level by IHC.

(A) (B) (C) Sections through 4.5 week old mouse mammary glands obtained from mouse primed with **(A)** placebo, **(B)** E+P and **(C)** E hormone pellets for 1 week prior to tissue collection. Mammary glands were stained with anti-Fbln2 antibody (brown) and Haematoxylin (blue) to visualise nuclei. **(D)** Negative (no primary) antibody control. Images on the left show mammary epithelium. Images on the right show stromal capsule around the edge of Fat pad. **(A)** Placebo treated glands showed normal Fbln2 staining pattern – prevalent in TEB epithelium, weaker in duct epithelium and present in the stroma around epithelium and in the capsule around the edges. **(B)** E+P treated glands showed similar epithelial staining pattern to placebo treated glands. Higher Fbln2 staining, however, could be noted in the stromal capsule around the edge of the Fat pad. **(C)** E primed glands showed lack of Fbln2 expression in the ductal epithelium and its high abundance in the stromal capsule. Arrows denote TEBs and dotted arrows indicate ducts. At least 3 mice (6 mammary glands) were studied for each treatment. Scale bars are 100 µm.

expression was even more pronounced when the mammary glands obtained from the E2 treated animals were examined while the ductal localisation of Fbln2 seemed completely absent from these glands (**Figure 4-24 C**). All of the observed staining patterns were specific to Fbln2-antibody binding as demonstrated by the lack of the staining in the negative (no primary antibody) control (**Figure 4-24 D**).

4.2.2.9 Investigation of Fbln2 functions in non malignant mouse mammary epithelial cells *in vitro* by the over-expression of Fbln2 in HC11 cells.

As shown in this project, pubertal mammary expression of Fbln2 is mainly localised to the BM, outer membranes, cytoplasm of cap cells and most probably the cytoplasm and extracellular spaces between the body cells of mouse mammary TEBs. Given this specific epithelial localisation of Fbln2 and widely recognised importance of TEBs for promoting the directional outgrowth of the ductal tree, we examined the involvement of Fbln2 in cellular migration and adhesion *in vitro* using HC11 cells. The HC11 cell line originates from normal mammary epithelial cells [458] and, as demonstrated previously, lacks Fbln2 expression (both at the RNA and protein level) (**Figure 4-20**). It therefore provides a good system for studying the impact of Fbln2 over-expression on normal mouse mammary epithelium. Over-expression of Fbln2 was performed by transfecting the HC11 cells with a Fbln2 expressing plasmid (pRc/CMV-Fbln2) (**See 2.2.2.3**).

4.2.2.9.1 Optimisation of transfection

Optimal experimental conditions were established by transfecting equal amounts of HC11 cells with pEGFP reporter plasmid, using varied volumes of two different transfection reagents (Lipofectamine™ and DharmaFECT®) and DNA (in a transfection reagent to DNA ratio of 1:1) and examining the number and appearance of cells 24h after transfection, using a fluorescent microscope (**See 2.2.2.4.1**). As demonstrated in **Figure 4-25 A**, maximal transfection efficiency and minimal cell toxicity were achieved using 4 µl of Lipofectamine™ and 4µg of DNA, thus making it standard for all further experiments. A representative image

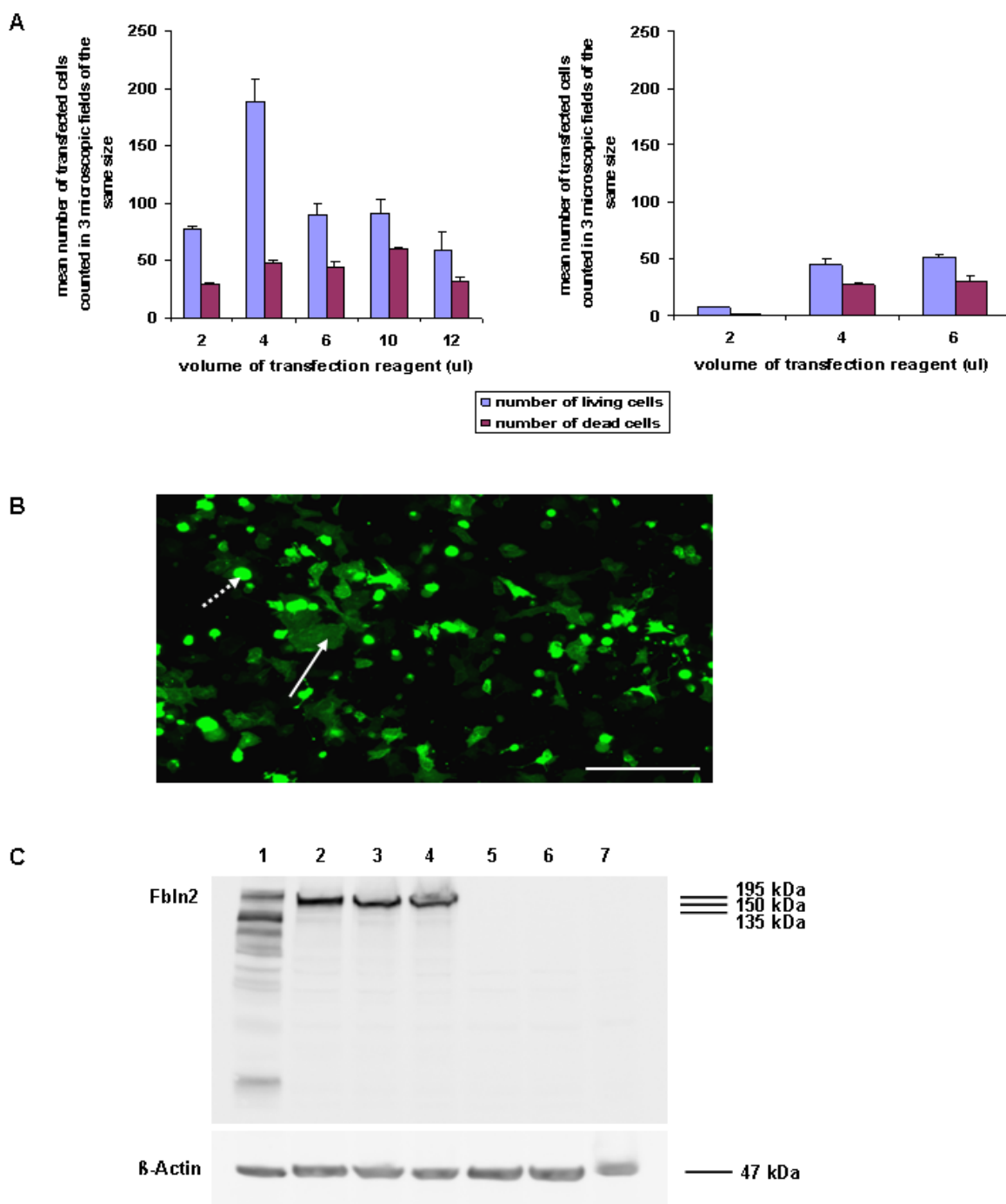


Figure 4-25 *In vitro* over-expression of Fbln2 in HC11 cells.

(A) Optimisation of transfection efficiency. Different volumes of transfection reagents, either Lipofectamine™(left) or DharmaFECT® Duo (right) Transfection Reagents were used to transfect equal amount of HC11 cells with pEGFP (transfection reagent to DNA ratio 1:1). Green fluorescent cells (living and dead) were counted. Error bars are S.E.M. Experiments were repeated 3 times **(B)** Representative image of HC11 cells transfected with pEGFP using optimal transfection conditions - 4µl of Lipofectamine™ Transfection Reagent and 4µg DNA – used for all subsequent transfections. Living cell is denoted with white arrow. Dead cell is highlighted with white dotted arrow. Scale bar is 500 µm **(C)** Western blot. Fbln2 (195 kDa) expression in HC11 cells transfected with pRc/CMV-Fbln2 (lanes 2-4) and pcDNA3 (negative control) (lanes 5-7). Fbln2 expression was analysed 24h after the transfections. Protein extract obtained from NIH3T3 cells (lane 1) was used as positive control. β-actin was used as a loading control. Experiments were repeated 3 times.

of cells transfected using the identified optimal conditions is shown in **Figure 4-25 B**. Once the optimal conditions were found, transient transfections were used to over-express Fbln2 V1 in HC11 cells. Western blotting confirmed the introduction of Fbln2 V1 into HC11 cells (**Figure 4-25 C**). All three bands corresponding to various Fbln2 fragments were seen on the blot (lane 2, 3 and 4). The largest, 195 kDa band, however, appeared much stronger than the two smaller ones (150 kDa, 135 kDa). The appearance of these bands was specific to Fbln2 V1-antibody binding detected by the anti-Fbln2 antibody as none of these bands were detected in the negative control (HC11 cells transfected with the empty vector, pcDNA3) (lane 5, 6 and 7). NIH3T3 cells (lane 1) were used as a positive control. No morphological changes could be seen in the transfected cells.

4.2.2.9.2 The effect of Fbln2 on the migratory properties of HC11 cells

Fbln2 over-expressing HC11 cells were used to assess the impact of Fbln2 on cell migration. Empty vector transfected HC11 cells were used as a negative control (**Figure 4-26 A**). The migratory properties of pRc/CMV-Fbln2 transfected HC11 cells were studied on confluent cells using a wound healing assay (scratch assay) (**See 2.2.2.5**). The percentage of wound closure was compared at each time point (4h, 7h, 11h, 24h and 36h) after creating the scratch for Fbln2 over-expressing- and control cells. There was no difference in the speed of wound closure between the two types of HC11 cells, suggesting that Fbln2 does not have an impact on the speed of cellular migration in HC11 cells under the given conditions (**Figure 4-26 B**).

4.2.2.9.3 The effect of Fbln2 on the adhesiveness of HC11 cells

The pRc/CMV-Fbln2 and empty vector transfected (control) HC11 cells were further used to investigate the impact of Fbln2 on regulating the adhesiveness of cells to plastic or ECM proteins coated surfaces (**See 2.2.2.6**). ECM molecules used in this assay included: Coll, ColIII, ColIV, Fn, Lama1, Tn and Vtn. Blank wells were coated with BSA and served as a negative control for the ECM substrates

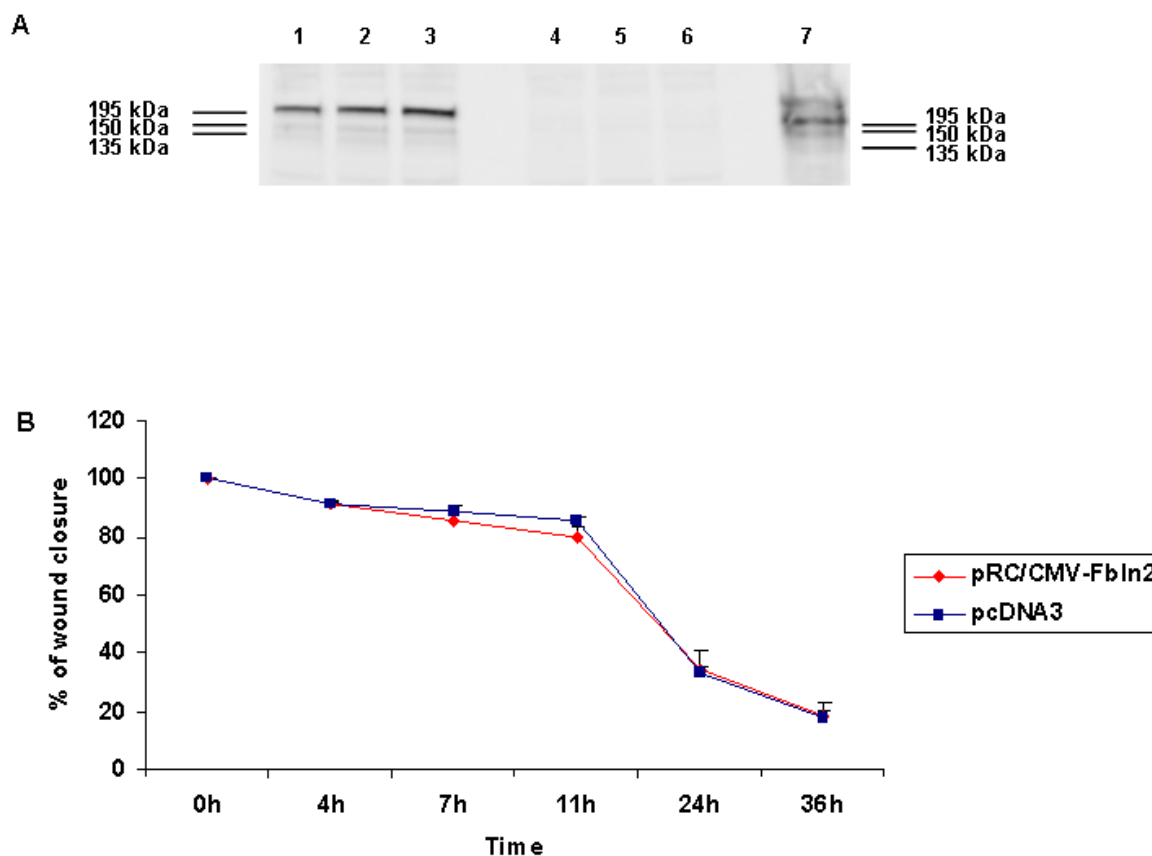


Figure 4-26 The effect of Fbln2 on the regulation of HC11 cells migration using a wound healing assay.

(A) Western blot showing the levels of Fbln2 expression in HC11 cells, used in wound healing assays. Protein extracts were prepared using RIPA buffer, at the conclusion of each assay. Fbln2 (195 kDa) expression in HC11 cells transfected with pRc/CMV-Fbln2 (lanes 1-3) and pcDNA3 (negative control) (lanes 4-6). Protein extract obtained from NIH3T3 cells (lane 7) was used as positive control. The same amount of protein (50 μ g) was loaded to each well. **(B)** Representative graph illustrates the speed of wound closure in HC11 cells transfected with pRC/CMV-Fbln2 (to express Fbln2 V1) or pcDNA3 (negative control). The assay was performed on confluent cells (48h after transfections). No difference in the speed of cell migration could be noted in Fbln2 expressing HC11 cells in comparison to empty vector transfected HC11 cells. Error bars are S.E.M. Experiments were performed 3 times.

(experimental noise) while the HC11 cells transfected with empty vector served as a negative control for Fbln2 expression. The adhesion assay was performed using HC11 cells plated at a density of 1.5×10^6 cells/well which was chosen to give optical density (OD) values within the optimal OD detection range (0.5-1), after optimisation of experimental conditions (**Figure 4-27 A**).

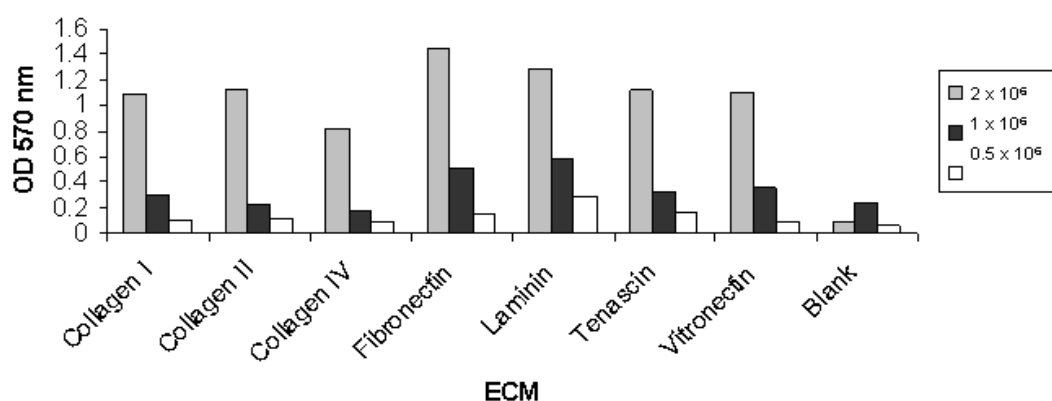
Fbln2 over-expression increased the adhesiveness of HC11 cells to four ECM proteins, i.e. increased OD significantly - Vtn (0.369), Tn (0.307), Fn (0.289) and Lama1 (0.239). Furthermore, these four ECM molecules appeared successful in stimulating the adhesion of HC11 cells as the ODs for both Fbln2 transfected- and control cells were distinguishably higher than these seen for the remaining three ECM molecules (Coll, ColIII and ColIV) where in general a much lower level of adhesiveness of HC11 cells, with no major difference between Fbln2 over-expressing- or control cells, was noted (**Figure 4-27 B**). Similarly, as seen in **Figure 4-27 C**, Fbln2 over-expression appeared to have no significant effect on the adhesion of HC11 cells to plastic surfaces. Dry wells (no cells added) were used as a negative control.

4.2.2.10 Fbln2 binding partners and their expression during pubertal mouse mammary gland development.

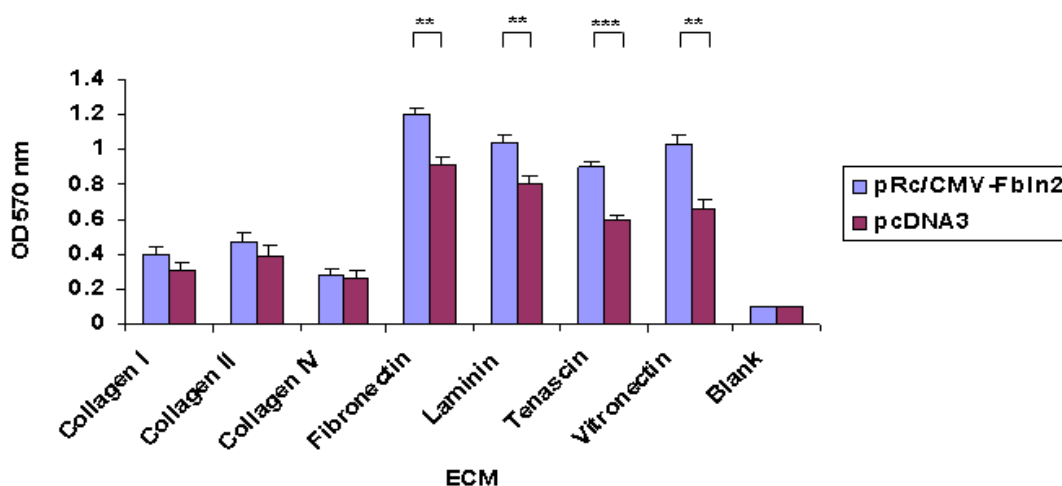
Based on the finding that Fbln2 interaction with some ECM proteins increases their adhesiveness to HC11 cells (**See 4.2.2.9.3**) and published evidence for the presence of an extensive array of protein-protein interactions between Fbln2 and some ECM proteins or cell membrane receptors, the pubertal mammary gland associated expression of Fbln2 binding partners was investigated.

Depending on the type of the biological or experimental system or studied protein function, different proteins have been reported to bind to Fbln2. None of these molecules, however, have yet been studied in association with Fbln2 in the mouse mammary gland. An up to date literature search identified 13 proteins as Fbln2 binding partners (**Figure 4-28**). 11 of these proteins were located to ECM, i.e. versican (Vcan), Lama1, Fbn1, collagen VIaIII (ColVIaIII), collagen IVaI (ColIVaI), collagen XVIIIaI (ColXVIIIaI), Eln, Fn, perlacan (Per), aggrecan (Acan), Nid. The remaining two, the integrin $\beta 3$ (Itgb3) and integrin $\alpha 5$ (Itga5) were previously shown to function as membrane receptors for Fbln2.

A



B



C

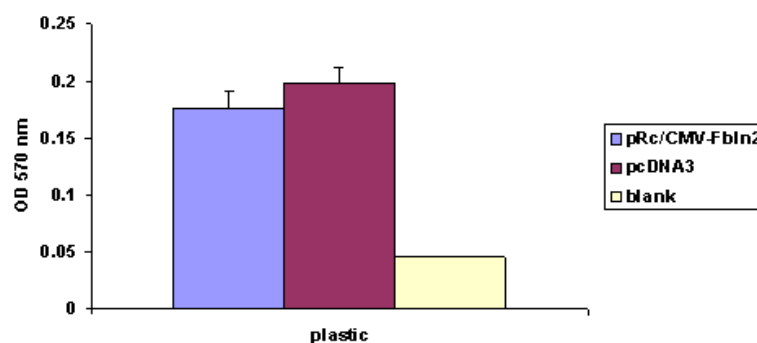


Figure 4-27 Effect of Fbln2 on the regulation of adhesive properties of HC11 cells using adhesion assays.

(A) (B) Cell adhesion to ECM proteins **(A)** Optimisation of assay sensitivity. Untransfected HC11 cells at 3 different cell/ml concentrations (0.5×10^6 , 1×10^6 and 2×10^6) were used. A concentration of 1.5×10^6 cells/ml was regarded as optimal and used in all subsequent adhesion assays. Data was calculated based on one transfection experiment. One well per condition was seeded **(B)** HC11 cells either transfected with pRc/CMV-Fbln2 (to express Fbln2 V1) or pcDNA3 (negative control) vectors for 24h – comparison of adhesiveness to ECM proteins. Blank wells were coated with BSA. Error bars denote technical variability (S.E.M), (**) denotes statistical significance p -value ≤ 0.01 , (***) p -value ≤ 0.001 . Data is based on one transfection experiment. Cells were seeded in triplicates for each condition. **(C)** Cell adhesion to plastic surfaces. HC11 cells either transfected with pRc/CMV-Fbln2 (to express Fbln2 V1) or pcDNA3 (negative control) vectors for 24h. Blank lacks any cells. Data is based on single experiment. Cells were seeded in triplicates for each experimental condition. Error bars are S.E.M. and denote technical variability.

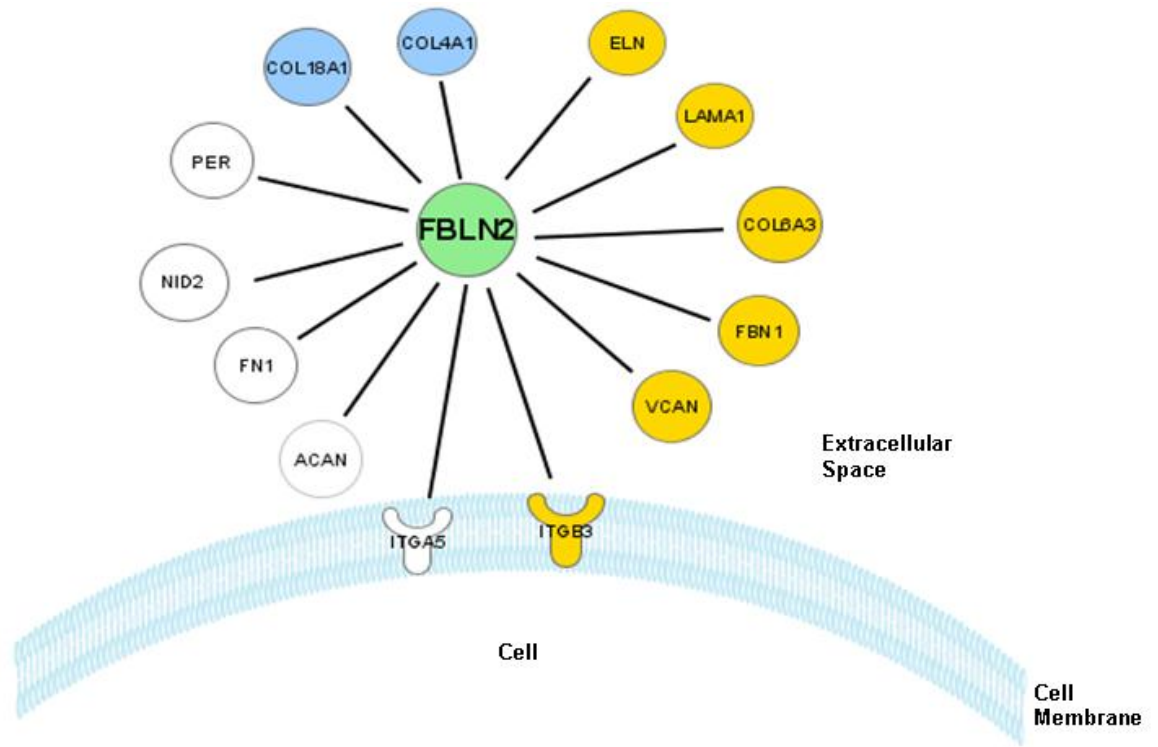


Figure 4-28 Potential binding partners for Fbln2 in the mouse mammary gland and their pubertal gene expression level.

Selection of Fbln2 binding partners and their cellular compartmentalization was based on a literature search. All 13 proteins were shown to interact with Fbln2 in different experimental systems. Pubertal gene expression was examined using Post-LN up-regulated gene set (Post-LN vs Pre-LN) (**See 3.2.6.1.2**) and TEB up-regulated gene set (TEBs vs ducts) (**See 3.2.6.1.1.**). Genes identified as up-regulated in Post-LN strips and TEBs are marked as yellow and blue circles respectively. White circles denote genes showing unaltered expression in the Post-LN and Pre-LN strips. A circle denotes an ECM protein while a T-like shape represents a transmembrane receptor. This image was created using IPA software.

In order to identify which of these proteins could potentially serve as Fbln2 binding partners in pubertal mouse mammary gland, expression of each of these factors was assessed in our microarray data set. Since Fbln2 appeared to be over-expressed in the epithelium and stroma of TEBs and the stromal capsule around the edge of the Fat pad, these tissue compartments were used to examine the level of pubertal expression for the known Fbln2 binding partners. The Post-LN up-regulated gene set (Post-LN vs Pre-LN) (See 3.2.6.1.2) and isolated TEBs up-regulated gene set (TEBs vs ducts) (See 3.2.6.1.1) were used to identify genes up-regulated in TEB stroma and epithelium and TEB epithelium respectively, while the empty Fat pad up-regulated gene set (See 3.2.6.1.3) was used to determine genes over-expressed in the distal Fat pad (stromal capsule). Nearly half of the examined genes (6/13) were shown to be up-regulated in the Post-LN strip, i.e. TEB epithelium and surrounding stroma. The highest up-regulation (2.64 fold) was noted for *Vcan*. A further two potential binding partners (*Col11a1*, *Col18a1*) were identified as over-expressed in the isolated epithelium of TEB. None of the molecules of interest, however, was shown to be significantly over-expressed in the empty Fat pad. The names of the classified genes and the levels of their up-regulation (FC values) are summarized in Table 4-1. The remaining 5 genes, that is *Fn*, *Per*, *Acan*, *Nid2* and *Itga5* did not differ in their expression level between the Post-LN and Pre-LN tissue strips (Table 4-2). *Fn*, *Per* and *Itga5* were expressed at a high level in both tissue compartments. *Acan* and *Nid2*, in contrast were minimally expressed during pubertal morphogenesis. A summary of the Fbln2 binding partners' pubertal expression pattern is shown in Figure 4-28.

4.2.2.10.1 Fibronectin and Fbln2 co localisation study.

The best documented binding partner for Fbln2 is Fn. It is associated with Fbln2 in the bone marrow stroma *in vivo* [459] and during skin regeneration [460] and shows binding in protein interaction studies *in vitro* [442]. Based on the existing documentation of Fbln2-Fn interaction *in vivo* and the evidence that of all binding partners, Fbln2 shows the strongest binding affinity to Fn (equal for both mouse and human proteins) [442], a potential interaction between Fbln2 and Fn during pubertal mouse mammary morphogenesis was investigated further. Although, Fn was not shown to be significantly over-expressed in the TEB

Gene name	Gene symbol	FC	Original Reference
GENES UP-REGULATED IN THE POST-LN STRIP			
Versican	Vcan	2.64	[461] [448]
Laminin	Lama1	1.88	[462]
Integrin beta 3	Itgb3	1.59	[463]
Fibrillin 1	Fbn1	1.54	[344]
Collagen 6a3	Col6a3	1.61	[442]
Elastin	Eln	1.75	[464] [443]
GENES UP-REGULATED IN THE ISOLATED TEBs			
Collagen 4a1	Col4a1	1.73	[442]
Collagen 18a1	Col18a1	1.87	[443]

Table 4-1 List of Fbln2 binding partners up-regulated during pubertal mouse mammary gland development.

Selection of Fbln2 binding partners was based on a literature search with reference given in column 4. Pubertal gene expression was examined using Post-LN up-regulated gene set (Post-LN vs Pre-LN) (**See 3.2.6.1.2**) and TEB up-regulated gene set (TEBs vs ducts) (**See 3.2.6.1.1**). All FCs were statistically significant.

Gene name	Gene symbol	Level of expression	Original Reference
Fibronectin	Fn1	High	[444] [442] [460] [459]
Perlecan	Per	High	[442]
Aggrecan	Acan	Low	[461]
Nidogen 2	Nid2	Low	[442]
Integrin alpha 5	Itga5	High	[463]

Table 4-2 List of Fbln2 binding partners shown to exhibit an unaltered expression level during pubertal mouse mammary gland development.

Selection of Fbln2 binding partners was based on a literature search. Firstly, pubertal gene expression was examined using Post-LN up-regulated gene set (Post-LN vs Pre-LN) (**See 3.2.6.1.2**) and TEB up-regulated gene set (TEBs vs ducts) (**See 3.2.6.1.1**). Secondly, each gene's expression level in the Post-LN and Pre-LN strip was compared using RMA normalised gene expression data. The expression level for each gene was denoted as low, medium or high.

epithelium or stroma (Post-LN) its expression was high in the Post-LN strip where Fbln2 was shown to be over-expressed. To examine the possibility of the two proteins interacting during the outgrowth of TEBs, IF was used to examine the co-localisation of the two proteins in the 6 week old mouse mammary gland. The co-localisation was performed using serial tissue sections since both antibodies used in this experiment were raised in the same host. As seen in the representative confocal images of mammary epithelium, shown in **Figure 4-29**, Fbln2 failed to co-localise with Fn. As previously demonstrated, Fbln2 was expressed in the epithelium and stroma of TEBs and to a much lower extent in the ductal epithelium (**Figure 4-29 A-B**) while Fn appeared to be exclusively localised to the stroma around ducts (**Figure 4-29 B**). The trace of Fn expression visible in the TEBs epithelium (**Figure 4-29 A**) is nonspecific, as it also appears to be present in the negative (no primary antibody) control (**Figure 4-29 C**).

4.2.2.10.2 Elastin and Fbln2 co-localisation study

Eln, after Fn is the second most investigated binding partner of Fbln2. *In vivo*, it is mostly present in blood vessels, lung and skin tissue where it interacts with Fbn1 to form elastic fibres which are critical for tissue elasticity [465]. Based on the recently suggested role of Fbln2 in elastic fibre assembly in internal elastic lamina of blood vessels [449] and significant up-regulation of *Eln* expression in TEB environment (**See Table 4-1**), preliminary experiments were carried out to assess the potential of Fbln2 and Eln interaction during pubertal mouse mammary morphogenesis. The localisation of Eln expression in 6 week old mouse mammary glands was carried out using EVG staining (**See 2.2.6.7**) and the obtained expression pattern was compared to that determined for Fbln2. As shown in representative light microscopy images, although mostly absent from the epithelium and stroma of TEB (a single Eln fibre can be seen in TEB stroma) (**Figure 4-30 A**), a positive Eln expression, as shown in positive staining control (**Figure 4-30 C**), could be seen in the distal stromal capsule (**Figure 4-30 B**) of pubertal mouse mammary gland. Since Fbln2 is seen to localise to this region it may be that the two proteins interact during pubertal mammary morphogenesis but further investigation is needed to assess this possibility.

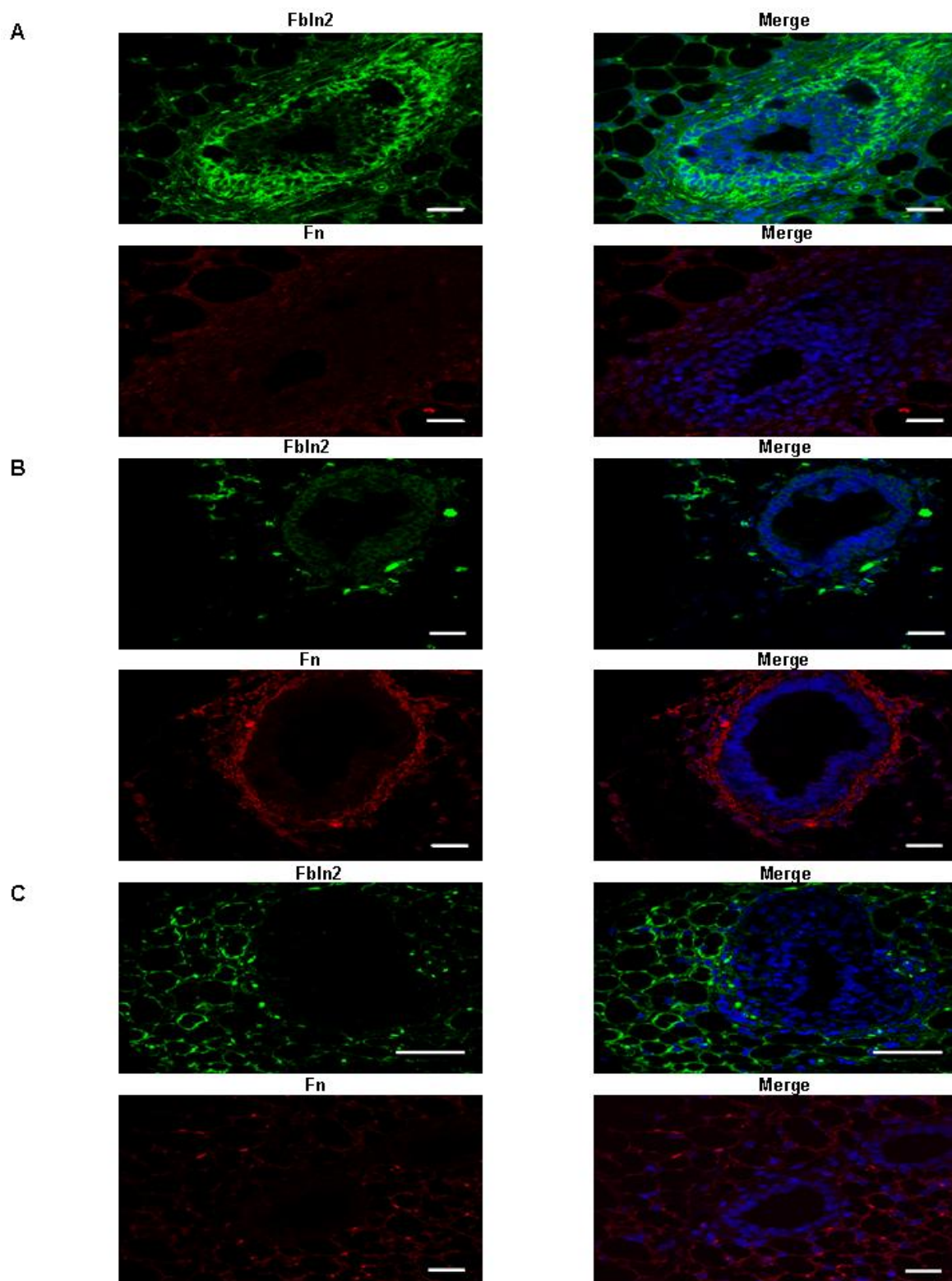


Figure 4-29 Co-localisation of Fbln2 and Fn expression in the pubertal mouse mammary gland using IF.

Transverse sections through a 6 week mouse mammary gland showing (A) TEB and (B) duct stained with anti-Fbln2 (green) or anti-Fn (red) antibodies and nuclear DAPI (blue). (C) shows negative (no primary antibody) controls. Fbln2 and Fn did not co-localise in the epithelium or its surrounding stroma in pubertal mouse mammary gland. Images were acquired using confocal microscopy. Scale bars are 50 μm .

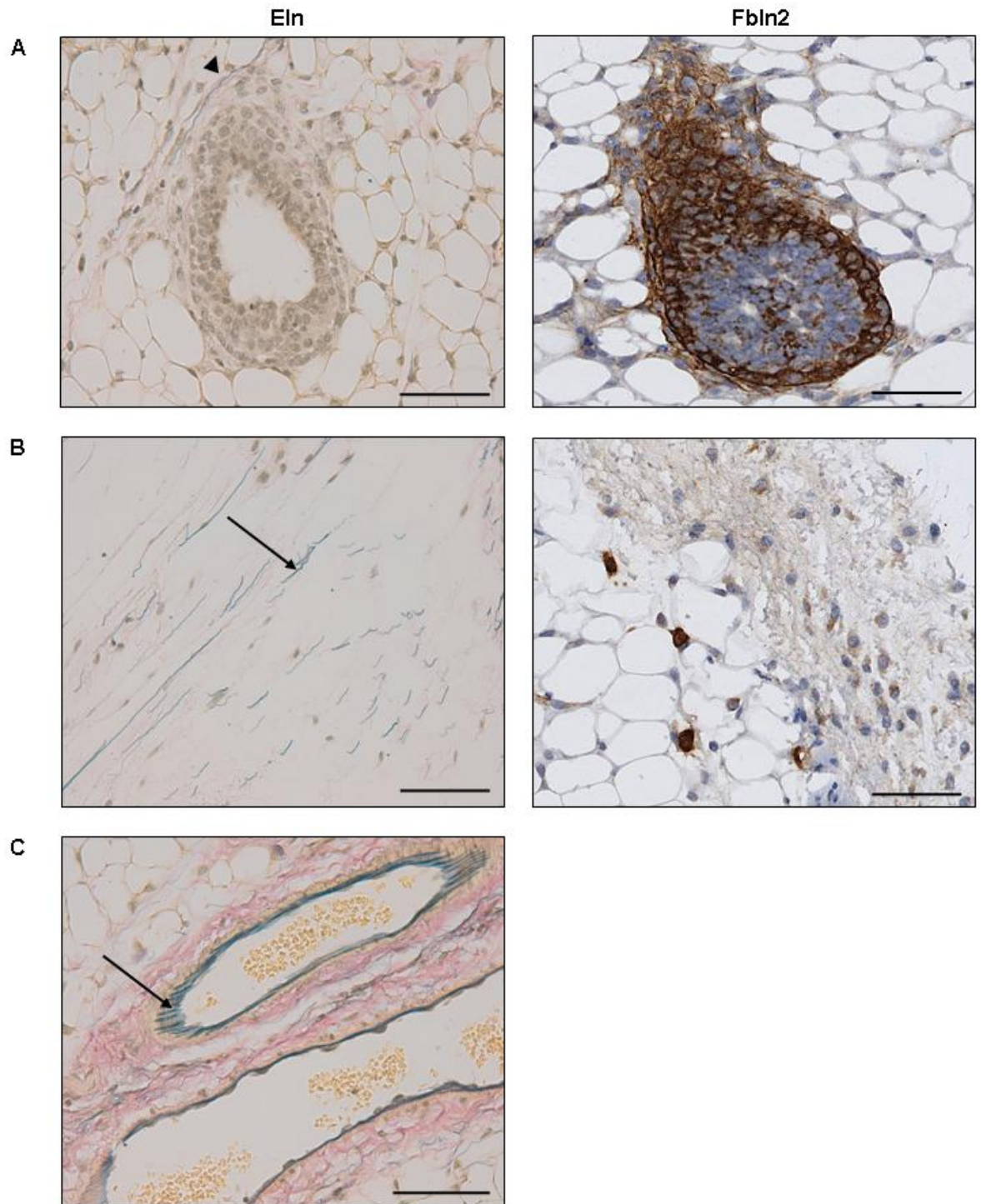


Figure 4-30 Localisation of Eln expression in pubertal mouse mammary gland using Elastica van Gieson staining.

Sections through a 6 week mammary gland showing (A) TEB (B) distal stromal capsule and (C) vein. (C) is a positive staining control. Elastin (blue) localised to the distal stromal capsule but was mostly absent from TEB epithelium and stroma. A single Eln fibre could be seen in TEB stroma (arrow head). Black arrows denote elastin fibres. Scale bars are 50 μ m. Mammary glands from at least 3 mice were used.

4.2.2.11 **Fbln2 is not essential for pre-pubertal and pubertal mouse mammary gland development.**

Since Fbln2 is highly expressed in virgin mice during pre-pubertal and pubertal mouse mammary gland development and is associated and localised to TEB it has potential to serve as a regulator of TEB structure, organisation or migration or to play a role in ductal tree morphogenesis. Thus, in order to evaluate whether the presence of Fbln2 is essential for normal ductal morphogenesis and TEB morphology, mammary wholemounts, collected from Fbln2 KO^{-/-} and WT mice, were examined to assess the impact of Fbln2 deficiency on pre-pubertal and pubertal mammary development. Both transgenic and WT mice were of the same genetic background (C57BL/6).

Total loss of Fbln2 expression in these glands was confirmed by IHC. 6 week old mouse mammary glands collected from Fbln2 KO^{-/-} and WT mice were processed, embedded in molten wax, sectioned and stained with the routinely used anti-Fbln2 antibody. No Fbln2 expression could be seen in the epithelium, its surrounding stroma or the distal stromal capsule of Fbln2 KO^{-/-} mouse mammary glands (**Figure 4-31 A**). The appearance of the section closely resembled that seen in the negative (no primary antibody) control (**Figure 4-31 B**). WT mouse mammary glands were used as a positive staining control. When stained with anti-Fbln2 antibody, a normal mouse mammary gland associated Fbln2 staining pattern was detected in the WT control. As seen in **Figure 4-31 C**, Fbln2 expression was localised to both the epithelial (cap and body cells) and stromal microenvironment of TEBs and the distal stromal capsule, thus verifying the antibody reactivity.

Wholemounts of Fbln2 KO^{-/-} and WT controls were then examined in triplicates for each time point. Analysis of the wholemounts revealed no major morphological differences between Fbln2 KO^{-/-} and WT mice. Both the length and degree of branching of the ductal tree appeared similar for Fbln2 KO^{-/-} and WT mice both at pre-puberty (3 weeks) and puberty (6 weeks) (**Figure 4-32**). Although TEBs appeared slightly smaller and more elongated in Fbln2 KO^{-/-} when compared to WT (**Figure 4-32 inserts**) further histological examination of these structures by H&E staining failed to demonstrate any significant differences

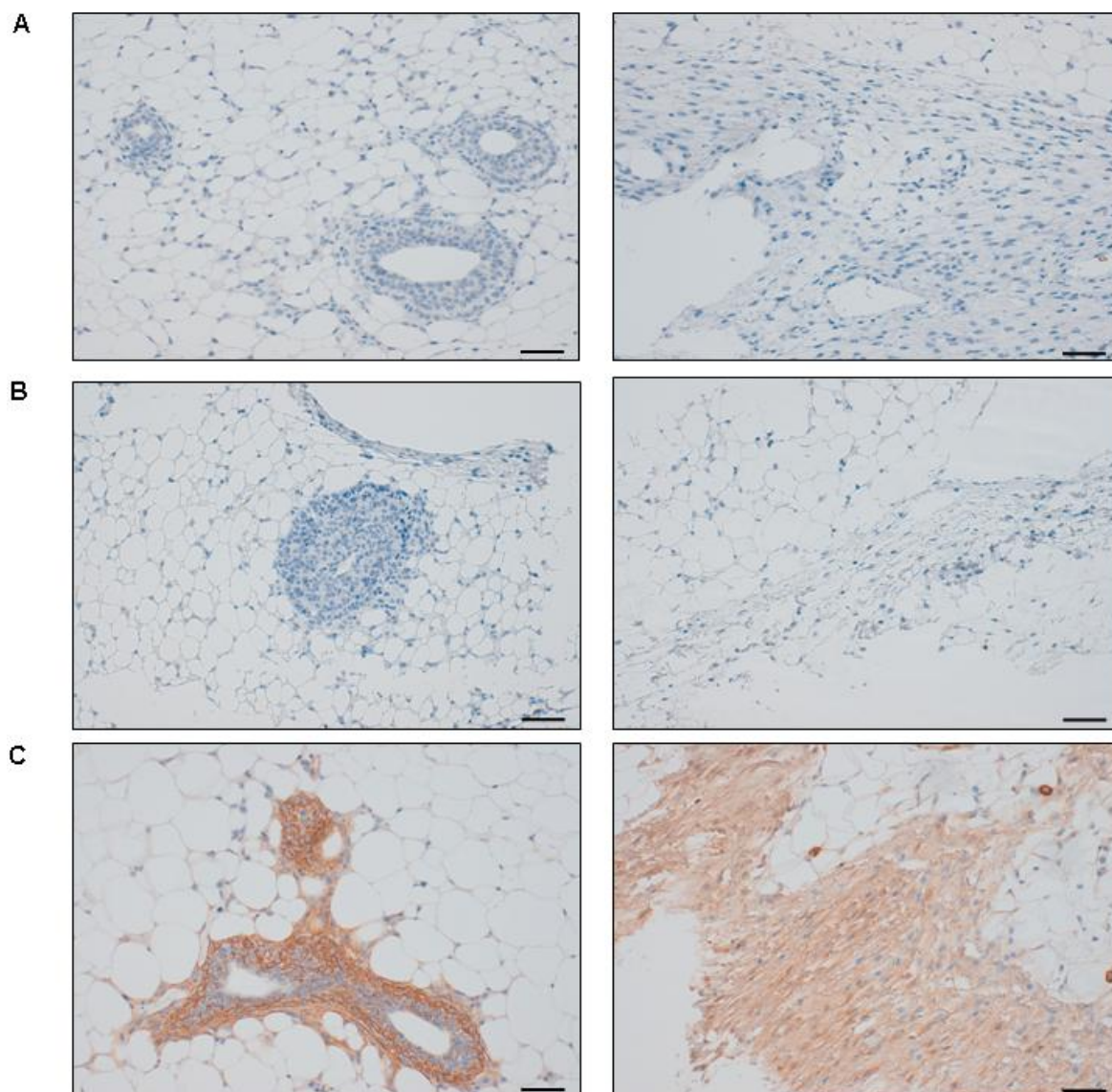


Figure 4-31 Comparison of Fbln2 expression in Fbln2 WT and Fbln2 KO^{-/-} pubertal mouse mammary glands by IHC.

Sections through a 6 week mammary glands collected from **(A)** Fbln2 KO^{-/-} and **(B) (C)** WT mice showing representative fragment of epithelium – TEB (left hand side) and stromal capsule (right hand side) stained with anti-Fbln2 antibody (brown). Nuclei were stained with haematoxylin (blue) **(A) (B)** No Fbln2 expression could be noted **(B)** is a negative (no primary antibody control) **(C)** Prominent Fbln2 staining could be seen in both the epithelium of TEB and its surrounding stroma and the stromal capsule. Scale bars are 50 μ m. 3 Fbln2 KO^{-/-} and 3 WT mice were examined.

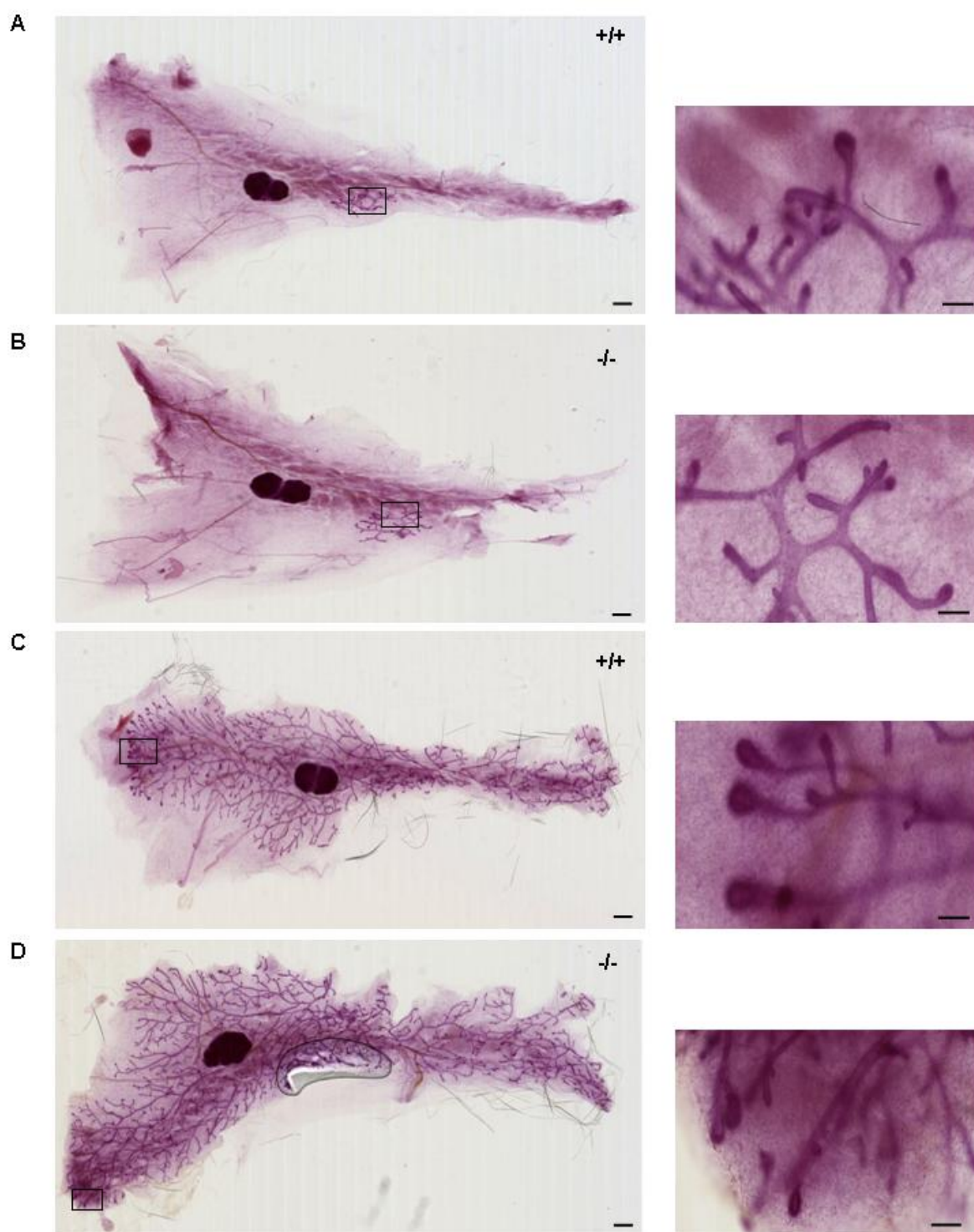


Figure 4-32 Wholemount analysis of pre-pubertal and pubertal *Fbln2* KO^{-/-} mouse mammary gland.

Representative wholemounts of 3 week **(A)** WT (+/+) and **(B)** *Fbln2* KO (-/-) and 6 week **(C)** WT (+/+) and **(D)** *Fbln2* KO (-/-) mammary glands stained with carmine alum. Inserts (on the right) show representative parts of the ductal tree and TEBs. No significant difference in the ductal outgrowth could be seen in *Fbln2* KO^{-/-} mammary glands in comparison to WT mammary glands. TEBs in the KO^{-/-} mammary glands, however, appeared smaller and more elongated than those seen in their WT counterparts. Scale bars are 1mm (wholemounts) and 200 μ m (inserts).

between the TEB from the pubertal Fbln2 KO^{-/-} and WT mammary glands (**Figure 4-33**).

Finally, based on previous reports of compensatory up-regulation of Fbln1 expression in Fbln2 KO^{-/-} aorta [266], tissue sections through the pubertal Fbln2 KO^{-/-} and WT mouse mammary glands were further stained with anti-Fbln1 antibody. The level and pattern of mammary gland associated Fbln1 expression was compared between the Fbln2 deficient and WT mouse mammary glands and it was revealed that when compared to WT mammary glands, the expression of Fbln1 in the epithelium of Fbln2 KO^{-/-} glands was significantly increased (**Figure 4-34 A and B**). Furthermore, the epithelial localisation of Fbln1 in both types of mammary glands was also different. In WT mammary glands, the expression of Fbln1 in TEBs was diffused throughout their epithelium and surrounding stroma rather than localised to specific cell types (**Figure 4-34 A**). In Fbln2 KO^{-/-} mammary glands, on the other hand, the expression of Fbln1 appeared closely associated with the epithelium of TEBs: body cells (cytoplasm and extracellular spaces), membranes, cytoplasm, extracellular spaces of cap cells and BM and their surrounding stroma (**Figure 4-34 B**), where Fbln2 preferentially localises (**Figure 4-34 C**). The observed Fbln1 staining was specific as demonstrated by the presence of minimal background staining in the negative (no primary antibody) control (**Figure 4-34 D**). The expression of Fbln1 in distal stromal capsules of Fbln2 KO^{-/-} and WT pubertal mouse mammary glands did not seem to differ (data not shown).

Collectively, these results demonstrate that in the presence of Fbln1, Fbln2 is not essential for virgin mammary gland development and suggest potential functional redundancy and compensation between Fbln1 and Fbln2 during pubertal mouse mammary gland development.

4.2.2.12 Summary

In summary, this study was carried out to examine the potential of *Upk3a* and *Fbln2* to serve as novel regulators of pubertal mouse mammary gland morphogenesis. Due to the absence of Upk3a protein detection in the pubertal mouse mammary gland all further research was focused exclusively on Fbln2 and

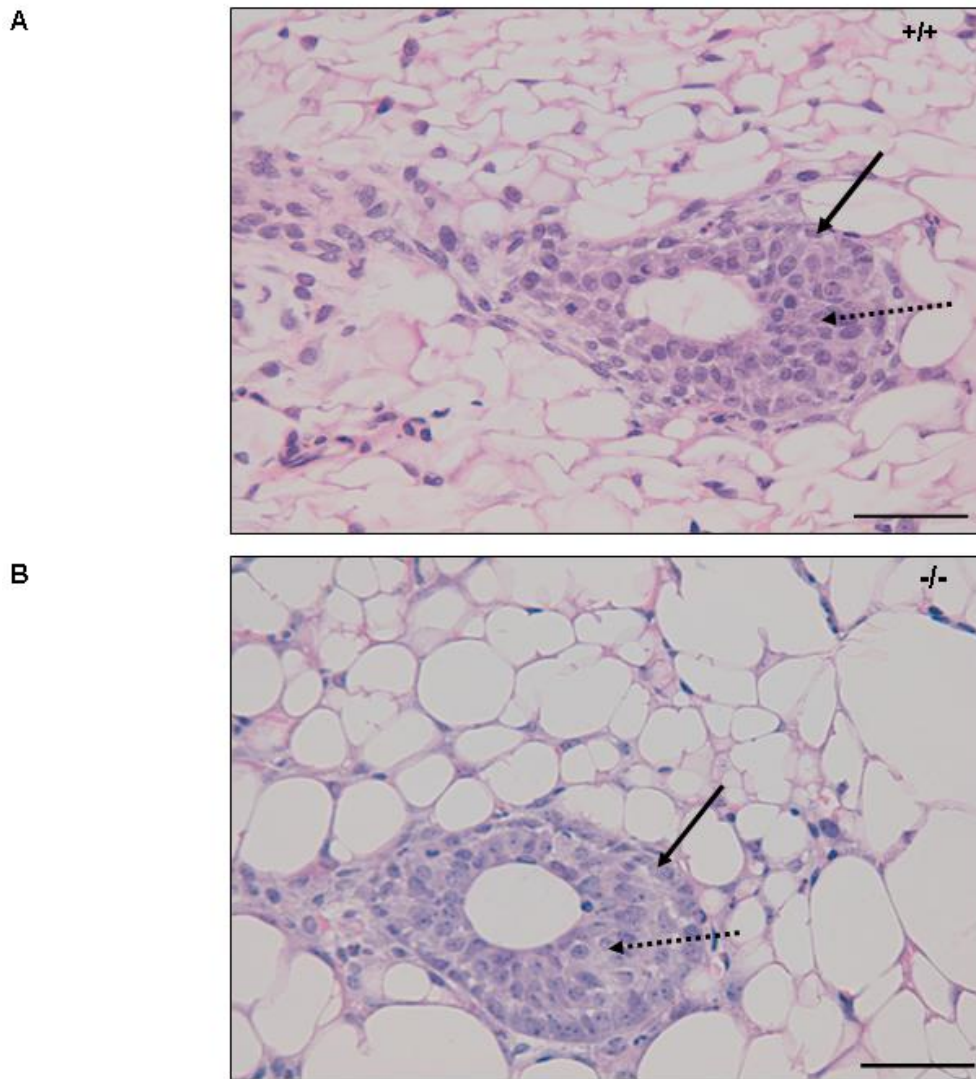


Figure 4-33 Comparison of TEB histology in WT and *Fbln2* KO^{-/-} pubertal mouse mammary glands by H&E staining.

Longitudinal sections through 6 week mammary glands collected from **(A)** WT and **(B)** *Fbln2* KO^{-/-} mice. Representative TEBs are shown. Nuclei were stained with haematoxylin while the cytoplasm was stained with eosin. No major morphological differences could be seen between the two TEBs. Cap cells are denoted by arrow. Body cells are denoted by dotted arrow. Scale bars are 50 μ m.

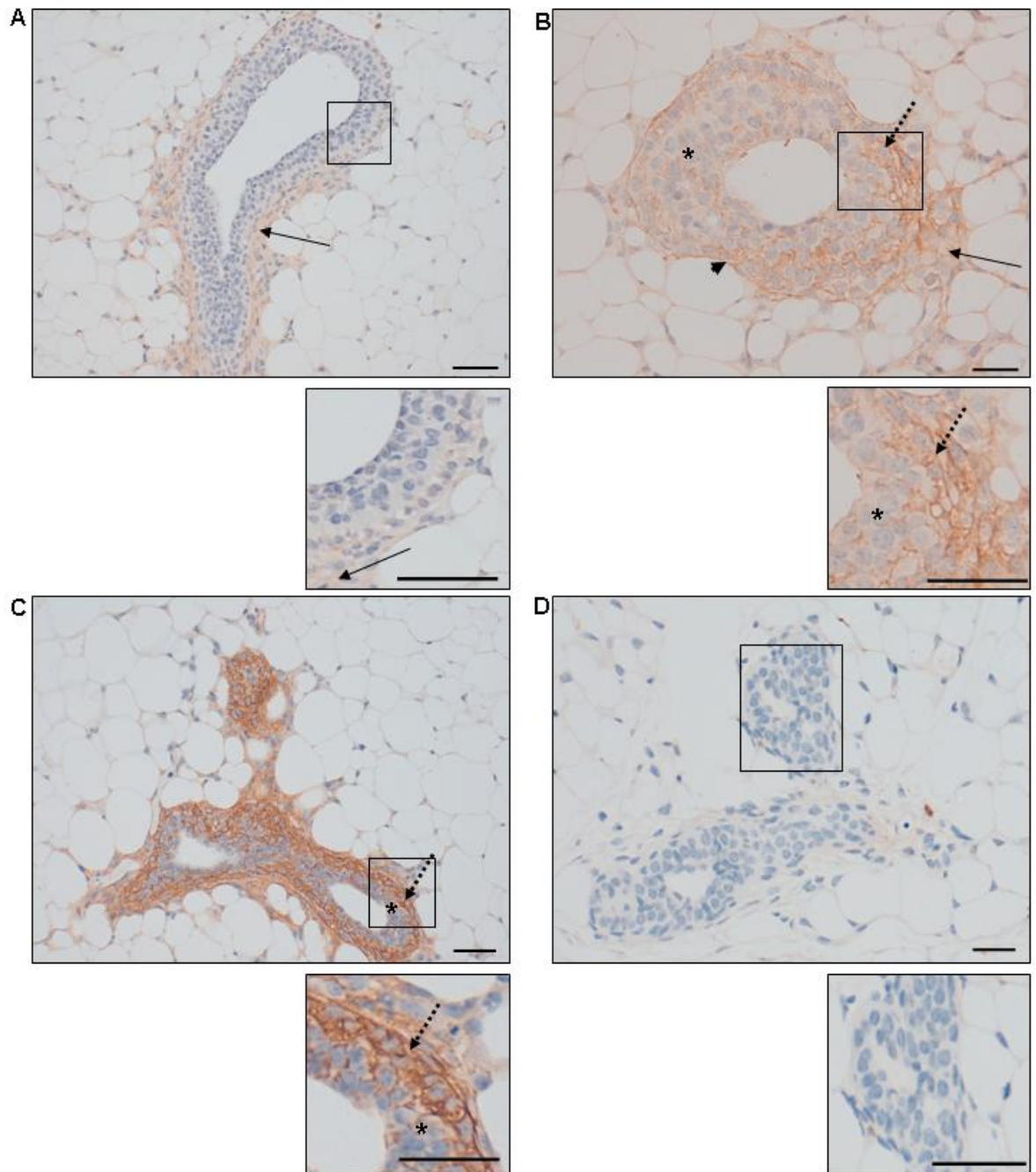


Figure 4-34 The up-regulation and spatial localisation of Fbln1 in the epithelium of Fbln2 KO^{-/-} pubertal mouse mammary glands.

Longitudinal and transverse sections through 6 week **(A) (C) (D)** WT and **(B)** Fbln2 KO^{-/-} mouse mammary glands showing representative fragments of epithelium (TEB) stained with anti-Fbln1 antibody **(A) (B)** or anti-Fbln2 **(C)** antibody. **(D)** is a negative (no primary antibody) control for Fbln1. Fbln1 in WT gland was contained in the stroma around TEB (arrow) **(A)**. In Fbln2 KO^{-/-} glands, however Fbln1 was over-expressed and localised to BM (arrow head) cap cells (dotted arrow) and cytoplasm and extracellular spaces between body cells (asterisk) **(B)**. This expression pattern was similar to that seen for Fbln2 in WT pubertal mouse mammary glands **(C)**. Scale bars are 50 μ m. Three animals were examined for each experiment.

its mammary gland associated expression, localisation and function. Fbln2 was shown to be expressed in the mouse mammary glands during pre-puberty, puberty, adulthood (very low level) and early pregnancy (24-72h). During puberty its localisation was mostly confined to the stroma and epithelium of TEBs (cap cells and some body cells) and the stromal capsule located at the edge of fat pad with only residual expression seen in the stroma and epithelium of the ducts. Preliminary experiments that aimed to develop a TEB explant culture, showed a similar pattern of Fbln2 expression in TEB outgrowths *in vitro*, with Fbln2 associating with cell membranes, cytoplasm and cellular processes. At the mRNA level, *Fbln2* was expressed in the form of two splice variants (*Fbln2 V1* and *Fbln2 V2*) with the former predominant in the TEB environment and ductal epithelium. Furthermore, the expression and localisation of Fbln2 in the mouse mammary gland appeared to be positively regulated by systemic hormones (E2 and P). The *in vitro* functional studies revealed Fbln2-mediated increase in adhesiveness of the HC11 cells to Vtn, Tn, Lama1 and Fn coated surfaces, and hence suggested the possibility of these proteins interacting with Fbln2 in the mammary gland *in vivo*. However, Fbln2 failed to co-localise with Fn *in vivo*. *In silico* analysis further revealed the over-expression of 8 out of 13 binding partners of Fbln2 in the TEB compartment (as seen for Fbln2) while 3 out of the remaining 5, even though expressed at a similar level in TEB and duct compartments, were still expressed in TEBs at a very high level. One of these binding partners was Eln which, as previously seen for Fbln2, was demonstrated to localise to distal stromal capsule of pubertal mouse mammary gland. Finally, despite the given expression pattern, Fbln2 was shown not to be necessary for ductal morphogenesis and TEB formation in pre-puberty and puberty. As suggested by the over-expression of Fbln1 in the epithelium of Fbln2 KO^{-/-} mammary glands, however, the lack of a mammary phenotype in these mice might be attributed to the possible functional redundancy and compensation between Fbln1 and Fbln2.

4.3 Discussion

Genome-wide gene expression screening, such as microarray analysis of pubertal mammary gland discussed in **Chapter 3**, is useful not only for global comparison and functional characterisation of different transcriptomes, but it can also be used to identify new genes with potential to regulate pubertal outgrowth. Several strategies, already discussed in **Chapter 3 (3.3)**, can be used to select candidate genes. The two that were used in this project include i) ranking of genes according to the highest up-regulation level and ii) candidate gene approach. It was through these two screening methods that *Upk3a* and *Fbln2* first came to the attention of our research group.

Based on the microarray analysis, the expression of both genes was associated with migrating TEBs. They were both up-regulated in the isolated epithelium of TEBs (TEB vs ducts) (**See 3.2.6.1.1**) and TEB microenvironment (Post-LN vs Pre-LN) (**See 3.2.6.1.2**). *Upk3a* was the most differentially expressed RNA in the epithelium of TEBs compared to epithelium of ducts and although the most abundant gene in TEB epithelium is not necessarily the most important in orchestrating its motility, as most of the TEB up-regulated genes are cell cycle regulators ([256] and our observations) (**See Table 3-5**), the function of *Upk3a* was unknown and it therefore seemed an obvious target for further investigation. *Fbln2*, on the other hand, despite being ranked only to position 182 and 285 within the list of genes up-regulated in the epithelial and stromal-epithelial compartment of TEB respectively, was demonstrated by literature search to be associated with biological processes known to share similarities with ductal morphogenesis. As discussed in **Chapter 3 (3.3.2.1)**, there are many molecules known to be pivotal in developmental processes such as embryogenesis (e.g. *Fgf2br* [159] [20]), branching morphogenesis of lung or kidney (e.g. *TGF- β* [379]) or axonal guidance (e.g. *Ntn1* and *Neo1* [120] [117]) that have recently also been described as crucial for mammary pubertal morphogenesis.

4.3.1 Uroplakin 3a

At the time of study (2008) fairly little was known about Upk3a. The majority of its associated research was focused on urinary bladder where Upk3a was shown to be strongly expressed and assembled as plaques (AMU) on the apical side of urothelial umbrella cells [420] [421]. The only other organs where Upk3a was localised included renal pelvis, urethra and prostatic urethra, all of which also derive from urothelium [430]. In mammary gland research, only one study mentioned Upk3a. It was a microarray study, conducted on microdissected microenvironments of TEBs and ducts to find new regulators of mouse mammary branching morphogenesis that identified *Upk3a* as one of the most highly enriched RNAs of TEB transcriptome [256] therefore confirming our results. No further investigation into its role in pubertal mammary morphogenesis, however, was carried out.

To date, the only suggested function of Upk3a is the structural stabilisation of the luminal side of terminally differentiated umbrella cells during bladder contraction and expansion [422]. Although the mechanism by which AMU stabilises the urothelial lining has not yet been elucidated it has been proposed that AMU might interact with the actin cytoskeleton of umbrella cells to regulate its dynamics [425]. Actin filaments are present and essential for the survival of most cells types. Polymerised actin filaments, in conjunction with several actin-binding/severing proteins, are critical components of the cytoskeletal scaffold which provides an internal mechanical support and maintains and regulates cellular shape. There are over 100 proteins that have been shown to regulate either the polymerisation, length, assembly, turnover or cross-linking of actin filaments. Furthermore, when interacting with myosin motor proteins, actin filaments have also been shown to provide the force for cell movement by pulling up the rear of moving cells or providing tracks for short distance movement of intracellular materials (reviewed in [466]).

Motile behaviour (migration, bifurcation and spatial positioning) and change of shape in response to systemic hormones at estrus cycle are characteristic of TEB at puberty (See 1.2.3.2.1). Furthermore, there is evidence demonstrating the importance of actin-binding proteins for sustaining the motile character of TEB

and thus promoting ductal outgrowth at puberty. Crowley *et al.* (2000) showed that lack of Gsn (Gsn KO mice), a major regulator of actin cytoskeleton formation and function, severely delays the migration and bifurcation of TEB at puberty [243]. TEB formation and ductal outgrowth is inhibited until week 9 with the epithelial tree remaining rudimentary and even when the epithelium eventually fills the fat pad, no side branching can be seen [243]. Taking into account the possible role of Upk3a in stabilising the actin cytoskeleton of urothelial umbrella cells, the high *Upk3a* mRNA expression in the epithelium of TEBs at puberty and the importance of proper regulation of actin dynamics during TEB outgrowth at puberty, it is tempting to speculate that Upk3a may stabilize the cellular actin cytoskeleton during migration and shape remodelling of TEBs at puberty.

Despite its promising potential as a new regulator of pubertal morphogenesis, *Upk3a* expression in the mammary gland could not be confirmed at the protein level (Western blot and IHC) thus preventing further investigations into its role. Such discrepancies between the mRNA and protein levels are not unusual. It has been long observed and described by many different studies that differential expression of mRNA can capture 40-50% of the variation in protein expression [467] [468] [469]. This incongruent expression between mRNA and protein is most commonly attributed to post-transcriptional regulatory mechanisms which control the stability and distribution of mRNA transcripts. The main players in this process are RNA binding proteins (RBPs) which interact with mRNA through their RNA binding motif to regulate events such as alternative splicing, mRNA processing, export, surveillance, degradation, turnover or microRNAs (miRNAs) which facilitate gene silencing. Since prominent expression of Upk3a was detected in protein extracts and tissue sections collected from bladder but none found in mouse mammary gland (**See Figure 4-3**) it is possible that post-transcriptional regulation of *Upk3a* expression differs between the two tissues. Another possibility is that *Upk3a* does undergo translation in the mammary gland but, due to the presence of different post-translational modifications (N-glycosylation or possibly phosphorylation) than those seen in the bladder, it is non-immunoreactive. In the bladder, Upk3a exists in two forms, as an immature (43 kDa) and mature (47 kDa) protein. The immature protein is synthesised in the endoplasmic reticulum of umbrella cells. It has three N-linked high mannose

oligosaccharides that are attached to an extracellular domain [418]. In order to mature, Upk3a is required to form a heterodimer with Upk1b [425]. Formation of the Upk3a/Upk1b heterodimer stabilises the Upk3a subunit and enables its exit from the endoplasmic reticulum and transit to the plasma membrane where the mature 47 kDa Upk3a protein can be seen. The molecular weight of mature protein increases which is indicative of additional post-translational modifications that occur on the way [418]. Hence, both the presence of post-translational modifications and the formation of the Upk3a/Upk1b heterodimer are prerequisites for Upk3a maturation. Since the AU1 antibody used in this project (specific mouse IgG1 monoclonal antibody that recognizes an unspecified epitope residing within the extracellular domain) stains only the apical side of umbrella cells [419], it recognises the mature form of Upk3a. It is therefore possible that either the mature form of Upk3a does not exist in mammary gland due to the failure to form a heterodimer with Upk1b or the epitope on Upk3a, which is recognised by AU1 antibody in the bladder, is masked by different post-translational modifications in the mammary gland. It is worth noting, however, that data obtained from the microarray analysis indicated that *Upk1b* is expressed in the isolated TEBs (data not shown). This suggests that unless it does not get translated, the failure to form a Upk3a/Upk1b heterodimer can not be attributed to the lack of *Upk1b* expression. As only a single anti-Upk3a antibody (AU1) was available when this study was carried out it would be of benefit, to stain mammary gland- and bladder (positive control) tissue sections with different antibodies raised against Upk3a and compare the immunoreactivity of its different epitopes and thus assess the possibility for the post-translationally modified version of Upk3a being expressed in mammary gland. However, it was decided not to pursue this line of investigation and to focus on Fbln2.

4.3.2 Fibulin 2

As for Upk3a at the time of study, little was known about the function of Fbln2 and most research concentrated on its localisation and role in the embryonic and adult cardiovascular development. Further investigation of Fbln2 expression showed its localisation in skin, hair follicles, skeletal and heart muscles and at a lower level in lung, liver, kidney, brain, spleen, testis, uterus and ovaries, suggesting it is ubiquitously expressed during adulthood [434] [435] [445] [446].

Despite being this widely expressed, however, the significance of its expression has only recently been addressed in the cardiovascular system (See below). Furthermore, although *Fbln2* has been studied in breast cancer [452] [453] [342], its role in normal mouse mammary gland has not been investigated. Currently, *in vitro* protein interaction studies and *in vivo* cardiac system investigations suggest that *Fbln2* is likely to stabilise the organisation of ECM [442] [443] [444] and promote migration of mesenchymal cells during organogenesis and tissue remodelling in response to injury [343] [342] [447] [448]. Since ECM structure, assembly and signalling are vital to tissue remodelling during ductal outgrowth at puberty and TEBs are migratory at this time point, *Fbln2* arose as a promising new potential regulator of pubertal mouse mammary gland development. The following aspects of *Fbln2* expression in the mammary gland were therefore addressed in this project:

- the localisation of *Fbln2* within pubertal mammary gland and other stages of morphogenesis (See 4.3.2.1)
- characterisation of *Fbln2* expression at puberty (See 4.3.2.2)
- hormonal regulation of *Fbln2* expression (See 4.3.2.3)
- potential functions of *Fbln2* in pubertal mouse mammary gland (See 4.3.2.4)

As a result, we demonstrated that *Fbln2* is expressed in and localised to the mouse mammary gland at pre-puberty, puberty and early pregnancy where although possibly playing a role in TEB outgrowth (puberty) and perhaps tertiary branching morphogenesis (pregnancy) it may also have a structural function. Furthermore, the functions of *Fbln2* are probably exerted by interaction with some of its known binding partners and its expression may be hormone regulated, but its loss does not produce an obvious mammary pubertal phenotype *in vivo*.

4.3.2.1 Localisation of *Fbln2* in pubertal mouse mammary gland

Our initial microarray analysis identified *Fbln2* as highly expressed in the epithelium and stroma of the TEBs and also the distal stromal capsule of the pubertal mouse mammary gland (Figure 4-7). The accompanying protein

localisation study further confirmed that Fbln2 expression is indeed not confined to a single tissue compartment.

Within mammary stroma, Fbln2 protein was strongly localised to the region of the BM and fibrous connective tissue of the ECM surrounding TEBs and the distal stromal capsule of the mammary gland (**Figure 4-7 A**) (**Figure 4-35**). When the longitudinal sections of TEB were examined it was clear that the deposition of Fbln2 in the fibrous ECM was not uniform. Fbln2 staining was more condensed around the flank and neck of TEBs rather than at their tip (**Figure 4-35**). This pattern is consistent with the general spatial localisation of interstitial fibrous connective ECM in pubertal mouse mammary gland which is denser at the neck region of TEB or around the ducts and looser at the TEB's tip [53]. The localisation of Fbln2 in the region of BM was not continuous either (**Figure 4-35**). This could be explained by the plane of sectioning or Fbln2 not being uniform throughout the whole BM of TEBs. The latter justification can be supported by the fact that the composition of BM of TEBs varies, for example the BM at their tip is composed of hyaluronate whereas the neck of TEBs contains S-GAGs [50]. Fbln2 was also found, at a very high level within the distal stromal capsule - a thin tissue layer that envelopes the edges of the mammary gland and facilitates the attachment of the excised gland to the glass slide during wholemounting (personal observation). To the best of our knowledge, the presence of this capsule in the mouse mammary gland has not been described in the literature before. In rat mammary glands, a similar structure has been described as a highly vascularised capsule of fibrillar connective tissue that determines the margins of the mammary gland and serves as a boundary for epithelial expansion [470]. Some weak Fbln2 expression was also localised to the fibrous connective tissue around ducts (**Figure 4-8 B**). The level of this expression, however, was very low and not uniform throughout the whole mammary gland. Generally, Fbln2 localisation to ductal stroma was stronger in Post-LN strips and weaker in Pre-LN strips. Since ducts form and elongate by incorporating cells that previously belonged to TEBs, the stroma around ducts which are close to TEB, is likely to share more similarities with TEB associated stroma than that seen around distal ducts, hence the level of Fbln2 expression in ductal stroma may depend on its proximity to TEBs. Although the association of Fbln2 with the stromal compartment of the mammary gland may not have been surprising, since

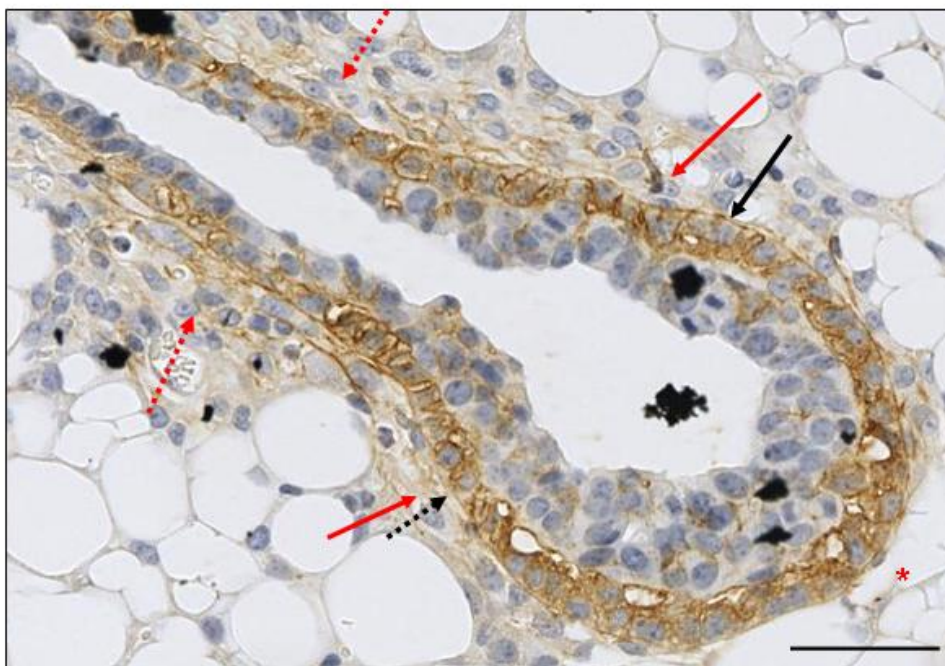


Figure 4-35 Localisation of Fbln2 expression in pubertal TEB by IHC.

Longitudinal sections through a TEB and its surrounding stroma stained with anti-Fbln2 antibody (brown). Haematoxylin was used to stain nuclei (blue). Fbln2 expression was not uniform. It could be seen in some parts of BM – black arrow while black dotted arrow denotes the area where BM is absent. Fbln2 could be also seen in fibrous ECM around the flanks (red arrows) and neck of TEB (red dotted arrows). No Fbln2 could be seen at the tip of TEB (red asterisk). Scale bar is 50 μ m.

Fbln2 has previously been localised to the ECM of other organs (BM of kidney glomeruli, internal elastic lamina of blood vessels and the stroma surrounding cornea and skeletal or heart muscles [344] [449] [434]) its localisation to the epithelium was unexpected as this has not been detected before.

Fbln2 could be detected in both cap- and body cells of TEBs, but as shown by confocal microscopy, the pattern of abundance in these cell types was not uniform. In cap cells, most protein appeared to be associated with cell membranes while a slightly weaker and more diffuse signal could be detected in what appeared to be the cytoplasm and extracellular spaces (**Figure 4-10 A**). A similarly diffuse, although more punctated pattern, was seen in body cells. Here, Fbln2 appeared to localise to extracellular spaces or cytoplasm rather than cell membranes and was not uniformly present throughout the entire mass of body cells (**Figure 4-10 B**). In the ducts, on the other hand, the pattern of Fbln2 was heterogeneous. Although predominantly negative (especially in the Pre-LN region) there were some ducts and ductules that showed a weak but similar staining pattern to that seen in TEBs. Here, however, the staining was stronger in the region of BM and ECM than the epithelium. Although confocal microscopy allowed us to localise Fbln2 to some extent, immunoelectron microscopy is needed to clarify its intracellular localisation and potential association with ECM proteins.

In pubertal mouse mammary gland, the components of BM are synthesised by both cap cells and stromal fibroblasts while the fibrous ECM is mostly secreted by fibroblasts [50] [93]. Fibroblasts may also act as a source of Fbln2 across a range of biological systems. Mouse embryonic fibroblasts (NIH3T3), human embryonic, dermal or corneal fibroblast have all been shown to express and secrete Fbln2 *in vitro* [444] [471]. Together, these results suggest that the expression of *Fbln2* in the epithelium, demonstrated by microarray analysis, is mainly associated with cap cells, while the stromal *Fbln2* may be synthesised by fibroblasts. Fbln2 is an extracellular protein and therefore after being synthesised it is probably secreted. It is most likely that fibroblasts secrete Fbln2 to BM and fibrous ECM or just fibrous ECM, while Fbln2 expressed by cap cells gets incorporated into BM. As for the epithelium localised Fbln2, while it is most probable that the *Fbln2* found in the cap cell membrane, cytoplasm and extracellular spaces is synthesised in the cap cells themselves the source of

Fbln2 expression in body cells is less clear. It is possible that body cells either synthesise and secrete *Fbln2* themselves or perhaps derive it from cap cells. To validate these hypotheses however it would be necessary to carry out *in situ* hybridisation. The secretion of *Fbln2* by cap cells towards the body cells of TEBs may result from the poor apical-basal polarity of cap cells. This may lead to *Fbln2* being non directionally secreted to the inner epithelial layers of the TEB instead of the BM, as is sometimes seen for hyaluronate and laminin [56] which could also explain the non-uniform abundance of *Fbln2*.

Our preliminary primary culture experiments on TEB clearly demonstrated that the epithelial cells in culture secrete *Fbln2*. The cytoplasmic and cell membrane associations of *Fbln2* in these cultures (**Figure 4-18**) was consistent with that seen in TEBs *in vivo* (**Figure 4-10**) while the association of *Fbln2* with cellular processes may resemble the pattern seen in TEB stroma *in vivo* (**Figure 4-8 A**). It would be beneficial, therefore, to develop this model to study regulation of *Fbln2 in vitro*.

In addition to its pubertal expression, we also detected *Fbln2* in mouse mammary glands during pre-puberty and early pregnancy. Pre-puberty is regarded as a period of around 3-4 weeks which starts at birth and lasts till the onset of puberty which is defined by three events: the vaginal opening, first oestrus and the following increase in the production and secretion of gonadotrophins and E2 [45]. Here, we reported the expression of *Fbln2* in the 2 and 3 week old mouse mammary glands by Q RT PCR (**Figure 4-12 B and C**) and showed that its spatial localisation in these glands resembled that seen at puberty, with *Fbln2* expressed in: i) the epithelial (cap cells and body cells) and stromal milieu of TEB-like structures (**Figure 4-13 A and B**) and ii) throughout the distal stromal capsule (**Figure 4-16 A**). This suggests that the expression of *Fbln2* in the pubertal mouse mammary gland instead of being novel serves a continuation of that present at pre-puberty. While given that the pre-pubertal mammary gland consists of a rudimentary ductal tree that resembles that seen at the E18.5 (reviewed in [3]) and *Fbln2* has previously been associated with cardiac- [343] and cartilage embryogenesis [440] it is further plausible that the presence of *Fbln2* at pre-puberty originates and is a continuation of that commenced during the embryonic development of mammary gland. The association of *Fbln2* with mammary embryogenesis, however, has not been

studied to date and thus IHC or *in situ* hybridisation on embryonic tissue sections, neonatal and pre-pubertal mouse mammary gland tissue sections would be needed to test this hypothesis.

While the association of *Fbln2* with pre-pubertal and pubertal mouse mammary glands appeared fairly steady (until it distinctly fades away with the onset of adulthood) the recurrence of *Fbln2* at early pregnancy was sudden and restricted to only a short time frame of around 60h, between day 2 and 4.5 of pregnancy. It is first visible at day 2, peaks at day 3 and disappears by day 4.5. In these glands *Fbln2* localised to ductal myoepithelium and stroma (**Figure 4-14**) and the distal stromal capsule (**Figure 4-16 D**). The presence of *Fbln2* in myoepithelium is consistent with myoepithelium being derived from cap cells and thus might share some of its characteristics. Stromal *Fbln2*, on the other hand, is most probably expressed by stromal fibroblasts or myoepithelial cells both of which can synthesise BM components. Although very obvious at the protein level using IHC, these changes were not apparent by Q RT PCR on the RNA level. As demonstrated in **Figure 4-12 A** the level of *Fbln2* expression at pregnancy day 3 was almost baseline. It is worth noting, however, that the RNA used for each time point was obtained from a single animal and normalised only to the amount of epithelium (*Krt18*) instead of the entire number of cells and thus might not be fully representative. Nonetheless, the expression of *Fbln2* at early pregnancy is intriguing and might provide some further clues into its function in the future.

The current knowledge of systemic and morphological events in early pregnancy is limited and only few conclusions can be made. All that is known is that early pregnancy is characterised by increased proliferation of epithelial cells [36], ducts become dilated between day 2 and 3 and epithelium starts to bud at the tips and along ducts to form either alveolar buds or tertiary side branches [48]. This could suggest a potential role of *Fbln2* during the initiation of ductal budding and perhaps that the expression of *Fbln2* is initiated in response to other genes or hormones. Some of the genes known to be active at early pregnancy include *BMP2*, *Msx2* and *Msx1* [218] but their association with *Fbln2* has not been reported to date. Furthermore, although many hormones, such as P, E2, PRL, placental lactogen, oxytocin, GH, PTH, insulin, corticosteroids, PTHrP and leptin are thought to regulate proliferation and differentiation of

mammary epithelium at pregnancy (reviewed in [36]), to the best of our knowledge the exact timing of their expression has not yet been elucidated. The two most likely candidates to stimulate *Fbln2* expression, however, are P and PRL. Prl promotes P expression and the levels of both hormones rise with the onset of pregnancy [472]. Furthermore, when primed *in vivo* with E2+P pellets, mouse mammary glands show higher *Fbln2* expression than that seen in placebo controls (**Figure 4-23**) (See 4.2.2.8). E2 is known to be particularly elevated during the second rather than the first half of gestation when the extensive lobuloalveolar growth takes place [473].

Together, the temporal and spatial expression of *Fbln2* during mouse mammary gland development suggests its association with the active stages (puberty, early pregnancy and possibly embryogenesis) and sites (TEBs at puberty and ducts at early pregnancy) of its morphogenesis.

4.3.2.2 The characteristics of *Fbln2* expression in mammary gland

Fbln2 RNA exists as one of two splice variants: *Fbln2 V1* or *Fbln2 V2*, and as shown by Grässel *et al.* (1990) the distribution of these splice variants is tissue specific [439]. It has been reported that *Fbln2 V1* is predominantly expressed in heart and NIH3T3 cells while *Fbln2 V2* is more abundant in the kidney [439]. In this study, we demonstrated that both *Fbln2 V1* and *Fbln2 V2* are expressed in mouse mammary gland at puberty (**Figure 4-19 B-D**). However, we failed to replicate the NIH3T3 *Fbln2* expression data observed by Grässel *et al.* (1990) as in our experiments, even when repeated using a number of different low passage aliquots of NIH3T3, the cells expressed both splice variants (RNA level). This discrepancy could be due to potential transformation of either of the NIH3T3 cell lines. Although neither the XRAY Excel® Array based microarray splicing analysis nor the PCR are fully quantitative, the results they generated were consistent. *Fbln2 V1* appeared to be prevalent in Post-LN strips and isolated TEBs and ducts, but no clear difference between the V1/V2 ratio could be seen in Pre-LN strips (**Figure 4-19 B-D**). These preliminary data suggest differences in *Fbln2* splice variant expression between the stroma around TEBs and that around ducts which in turn could suggest different functions of *Fbln2* in the two environments. However, this possibility still needs to be verified by repeating the experiments with a bigger array of samples or using Q RT PCR or northern

blotting for quantitative measurement of gene expression. Furthermore, it is also questionable whether the two isoforms exhibit different functions. *Fbln2 V1* and *Fbln2 V2* differ only by the RNA sequence which encodes a single EGF-like repeat which although postulated to participate in the interactions between ECM proteins [437] and stabilization of protein structure [438], when absent (human *Fbln2* expresses only the V2 isoform) does not affect protein-protein interactions [435].

Since *Fbln2 V1* and *Fbln2 V2* proteins differ only by a single EGF-like repeat their molecular weight is predicted to differ by only 5 kDa. However, the presence of a potential N-glycosylation site within the alternatively spliced domain raised the possibility that the difference in molecular weights of the two proteins was greater. Using protein extracts from NIH3T3, EpH4 and HC11 cells, which expressed *Fbln2 V1* and *Fbln2 V2*, just *Fbln2 V2* and no *Fbln2* respectively (**Figure 4-20 C**), and comparing the obtained banding pattern to that seen in protein extracts from mammary tissue strips (**Figure 4-6 C**) we showed that *Fbln2 V1* and *Fbln2 V2* can not be separated using either Bis-Tris or Tris-Acetate (better resolution for larger proteins) 1D electrophoresis and Western blotting. This suggests a small difference between their sizes which could be attributed to either the presence of small polysaccharide chain on *Fbln2 V1* or complete absence of a potential N-glycosylation at that site.

Fbln2 is known to be sensitive to proteolysis. *In vitro*, soluble *Fbln2* is cleaved by matrix metalloproteinases (stromelysin, matrilysin), circulating proteases (thrombin, plasmin and kallikrein) and granule stored proteases (leucocyte elastase, mast cell chymase), and, when immunoblotted with the routine full length anti-*Fbln2* antibody, gives rise to fragments ranging from 15-150 kDa [455]. The two bands of 150 kDa and 135 kDa that are additional to the main 195 kDa band have also been detected in protein extracts from cultured murine fibroblasts that were immunoblotted using the same anti-*Fbln2* antibody. They were suggested to result from proteolytic cleavage of the mature 195 kDa protein but no research was carried out to unravel their true nature [455]. Here, we report for the first time, that the 135 kDa and 150 kDa *Fbln2* exist *in vivo* (**Figure 4-6 C**) and add to their understanding by demonstrating that in pubertal mouse mammary gland the 135 kDa *Fbln2* peptide lacks the N-terminus (**Figure 4-21**). This finding, along with the fact that none of these bands correspond to

Fbln2 V2, and the known sensitivity of Fbln2 to proteolytic cleavage agree with the proposal of Sasaki *et al.* (1996) [455], that both of these additional peptides are products of proteolytic cleavage of mature Fbln2. Furthermore, by demonstrating that no significant differences in Fbln2 banding pattern exist between Pre- and Post-LN strip protein extracts (**Figure 4-22**) we suggest that the protease(s) responsible for Fbln2 cleavage are generic to pubertal mouse mammary gland stroma rather than specific to the migratory environment of TEB or the more static ductal milieu.

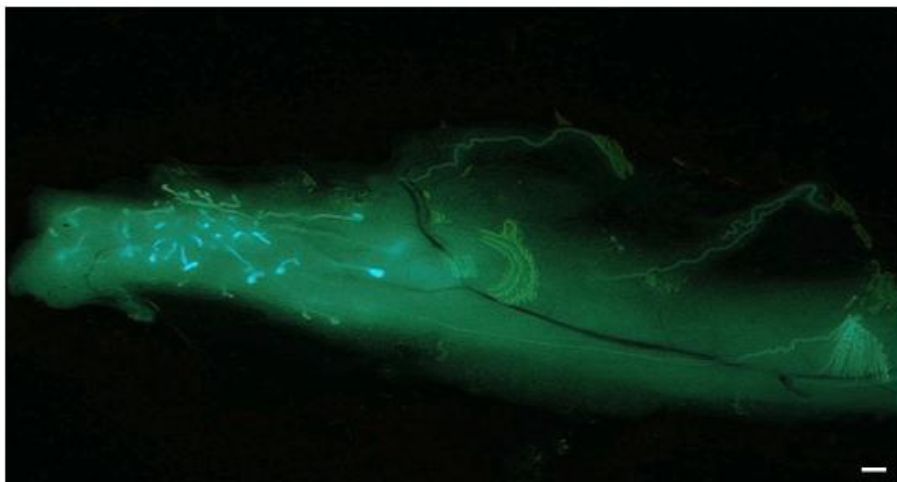
Since a similar Fbln2 binding pattern can be detected in cultured mouse fibroblasts and the fibroblasts in mammary gland are likely to synthesise stromal Fbln2, it is tempting to speculate that the proteases in question are associated with fibroblasts. Furthermore, based on the similarities between the sizes of Fbln2 fragments identified from pubertal mouse mammary gland protein extract and those generated by proteases *in vitro* [455], kallikrein and stromelysin (MMP-3) are the most likely candidates to facilitate some of Fbln2 cleavage in mammary gland. When treated with kallikrein, two types of Fbln2 products can be detected: mature undigested 195 kD protein and the 150 kDa cleavage product. In addition *Klkb1*, the gene which encodes the inactivated form of kallikrein (prekallikrein), is ubiquitously expressed throughout the body with particularly high expression in mammary gland during stromal remodelling periods, i.e. puberty and involution, where it localises to mast cells, and is critical for stromal ECM remodelling during involution [474]. Stromelysin, on the other hand, cleaves Fbln2 more effectively and only the 150 kDa band can be noted [455]. Again, the expression of stromelysin, although ubiquitous, is highly associated with pubertal mouse mammary gland where it is important for pubertal outgrowth. Mammary glands of MMP3 deficient mice (MMP3 KO^{-/-}) display a ductal tree that is thinner and characterised by a lower number of side branches than that seen in the WT controls [235]. Since Fbln2 is one of the ECM components in pubertal mouse mammary gland and since normal ECM composition and remodelling are important for ductal morphogenesis at puberty, it would be beneficial to further characterise the 135 kDa and 150 kDa Fbln2 peptides by mass spectrometry to establish their sequence. It would also be helpful to screen for other ECM remodelling proteases that are expressed in the mammary gland but are neither mammary gland specific nor expressed in front

of the advancing TEB and examine their potential to facilitate the cleavage of Fbln2. Some of these potential candidates could include MMP2, MMP9, MMP11 or MMP14 [235].

4.3.2.3 Hormonal regulation of Fbln2 expression

Our data also highlighted the possibility that Fbln2 expression in the mammary gland is regulated by systemic hormones. We demonstrated a significant increase of *Fbln2* expression in mouse mammary glands collected from 4.5 week old mice that were primed with E2 or E2+P pellets for a week (**Figure 4-23**). Although the *Fbln2* expression level was normalised to the amount of epithelium rather than the total number of cells which, as shown in **Figure 4-12 B** and **C**, could have impacted upon the level of calculated gene expression, the Q RT PCR results were consistent with the IHC data (**Figure 4.24**). Interestingly, while Fbln2 localised to the TEB and duct environments and the distal stromal capsule in both the placebo and E2+P treated glands, in E2 primed mammary glands Fbln2 expression was switched off in ductal epithelium and stroma (**Figure 4-24**). Since Fbln2 expression was seen within the ductal environment at puberty, which are regulated by E2 and P, it suggests that the observed effect of E2 on ducts might be unnatural and caused by an excessive level of E2 and thus may not reflect the Fbln2 regulation by E2 *in vivo*. This can be further substantiated by the unnatural appearance, thickness and decreased mechanical elasticity of the fat pad in these glands (**Figure 4-36 B**). The E2+P pellets used in this study consisted mostly of P and when used for the week-long priming, evoked a pregnancy-like state in the pubertal mouse mammary gland (**Figure 4-36 C**), mimicking the hormonal milieu of pregnancy where P is high and E2 levels are much less pronounced. The previously described up-regulation of Fbln2 expression during early pregnancy where P is present implies that P may play a role in promoting Fbln2 expression. This hypothesis is complicated, however, by the fact that no difference in Fbln2 expression can be seen between pre-puberty and puberty (**Figure 4-12 C**) suggesting that the levels of pubertal E2 and P do not affect Fbln2 expression *in vivo*. Collectively, it appears that while expression of Fbln2 in virgin glands is not regulated by systemic hormones (E2 and P), high levels of P characteristic of pregnancy and seen in our *in vivo* experiments, might mediate the expression of Fbln2. This hypothesis can further be supported by the identification of Fbln2 amongst the genes over-expressed in human

A



B



C

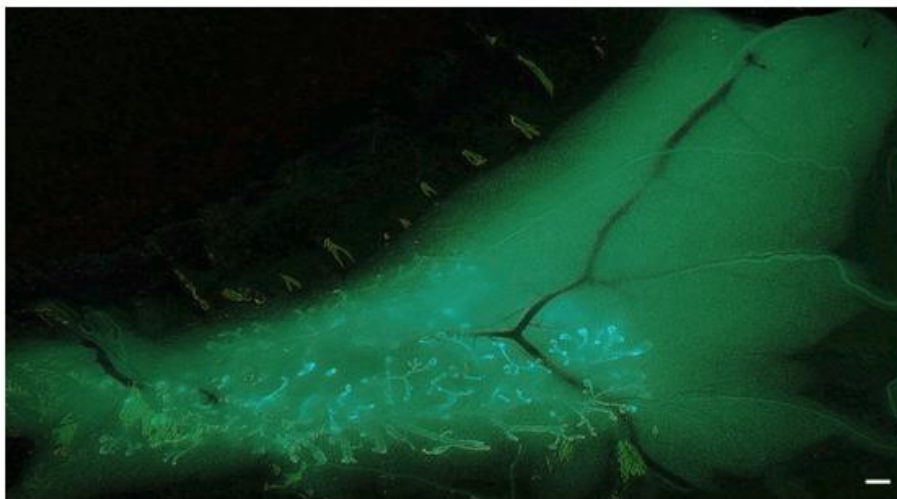


Figure 4-36 Wholemounts collected from hormone primed TG mice.

3.5 week old mice primed with (A) placebo, (B) E2 and (C) E2+P pellets for 7 days. Images were acquired using a fluorescence dissecting microscope (Stemi SV6). Scale bar is 50 μ m.

endometrial stromal short-term cell culture in response to P treatment [456]. To explore the potential role of P in mediating the expression of *Fbln2* during mammary morphogenesis in the future it would be beneficial to use the PR KO^{-/-} mice and examine the expression of *Fbln2* during different stages of mouse mammary gland development in the absence of P signalling. The *in vitro* model for TEB explant culture (See 4.2.2.5) may also facilitate the study of *Fbln2* expression in response to hormones.

4.3.2.4 Potential functions of *Fbln2* in pubertal mouse mammary gland

At puberty, *Fbln2* is mostly associated with the epithelium and stroma around TEBs which are known to be a driving force of ductal development. Thus, based on its mammary location and its to date suggested functions in different biological systems, we propose two potential functions that *Fbln2* may have in pubertal mouse mammary gland:

- Stabilising the structure of TEB
- Facilitating the motility of TEBs

4.3.2.4.1 Structural function

Numerous *in vitro* protein interaction studies and analyses of recently generated double KO^{-/-} (*Fbln2* and *Fbln5*), mice as well as the presence of multiple EGF-like repeats with Ca²⁺ binding sites, which are postulated to facilitate and regulate protein-protein and protein-cellular receptor interactions [436] [437], suggest that *Fbln2* is involved in stabilising the organisation of ECM structures, especially BM, elastic fibres and fibronectin matrix [442] [443] [444] [449]. Thus, given the partly stromal localisation of *Fbln2* in mouse mammary gland it is possible that *Fbln2* may function in a similar way in pubertal mouse mammary gland.

As demonstrated in this study, *Fbln2* localised to the BM region of TEBs where it is likely to exert its function by interacting with Lama1. Lama1 is one of the molecules that have previously been identified, by protein binding studies, to interact with *Fbln2* *in vitro* [462] [442]. It is one of the main components of BM in the mammary gland (reviewed in [91]) and, as highlighted by our microarray

study, it was highly expressed in the Post-LN strip (**Table 4-1 and 4-2**). When used to study the effect of Fbln2 over-expression on the adhesiveness of HC11 to ECM matrices, the increased adhesion of HC11 cells to Lama1 could be seen (**Figure 4-27 B**). In the mammary gland, Lama1 is crucial for normal TEB development at puberty as its deficiency results in the formation of fewer TEBs and consequently reduced ductal outgrowth when compared to WT controls [227]. Together these results suggest that Fbln2 may stabilise the supramolecular network of Lama1 in BM and therefore contribute to the machinery that maintains TEB structure and function during pubertal morphogenesis. Further co-localisation and protein binding studies, however, are required to validate this hypothesis.

The presence of Fbln2 expression in the stroma of TEBs and the distal stromal capsule of mammary gland suggest that this structural role of Fbln2 may also extend to the fibrous connective tissue of the ECM in pubertal mammary gland. The fibrous connective ECM in mammary gland consists of an extended network of cross-linked ECM components which include Fn, Col, Tn, Eln, SLRP or SPARC (reviewed in [91]). Previous evidence indicating presence of protein-protein interactions between Fn, ColVIaIII and Eln and Fbln2 in other experimental systems [442] [443] [444] [459] [460] [464] together with the identification of *Fn*, *CollVa* and *Eln* as highly expressed in the TEB environment by our microarray analysis (**Table 4-1, 4-2**) suggests that Fbln2 may be functionally associated with any of these molecules in mouse mammary gland at puberty.

As for Fn, an interaction between Fbln2 and Fn has been demonstrated both *in vitro* and *in vivo*. Fbln2 strongly binds to Fn in protein binding assays [442], co-localises with Fn in murine dermal and human embryonic fibroblasts cultures [460] and in Fn fibrils as shown by IF, and localises to Fn fibrils in human fibroblasts as shown by EM [444]. In the mammary gland, lack of Fn delays ductal outgrowth and decreases ductal branching at puberty [232] and, as demonstrated in this study, the HC11 cells over-expressing recombinant Fbln2 adhered more strongly to Fn than the controls (**Figure 4-27 B**). Although all these findings suggest Fbln2 may interact with the Fn matrix in mammary gland at puberty, no co-localisation of the two proteins in the mammary stroma could be noted (**Figure 4-29**) making it unlikely for Fbln2 and Fn to act as binding partners during TEB outgrowth *in vivo*.

In contrast potential co-localisation of Fbln2 with Eln in the mammary gland could be seen in preliminary localisation studies. Eln was demonstrated to localise mostly to the stromal capsule of pubertal mouse mammary glands. A single Eln fibre could also be seen in the stroma around TEBs (**Figure 4-30 A-B**). Eln is the second most investigated binding partner of Fbln2 after Fn. *In vivo*, it is mostly present in blood vessels, lung and skin tissue where it interacts with Fbn1 to form elastic fibres which are critical for tissue elasticity [465]. This process of elastic fibre assembly is dependent on specific protein-protein interactions between Eln and/or Fbn1 and their associated proteins. As demonstrated by Chapman *et al.* (2010) when functioning cooperatively with Fbln5, Fbln2 is likely to be one of the key players required for normal assembly of elastic fibres in internal elastic lamina of blood vessels [449]. Together these findings not only present the potential for Fbln2 and Eln interactions in the mammary gland but also provide further insights into the structure of the as yet uncharacterised stromal capsule.

Another potential Fbln2 binding partner in mouse mammary gland at puberty might be Vcan as it interacts with Fbln2 in other systems [461] [448] [344] and is up-regulated in the TEB stroma (**Table 4-1 and 4-2**), however, to date it has not been studied in mammary gland.

Taken together, the characteristic multistructural and cross linked composition of ECM in the mammary gland, the presence of Fbln2 in mammary ECM and its multifunctional binding properties, suggest that Fbln2 may serve as a global “glue” forming an intramolecular bridge which integrates into ECM using several routes to link and stabilise the structure of the mammary stroma and that in turn provides the scaffold for the associated stromal and epithelial cells. The proposed stabilising property of Fbln2 is consistent with the absence of Fbln2 expression at the tip of TEB but its deposition at its flank and neck and can further be exerted onto cap- and body cells of TEBs where the Fbln2 expression appears to be associated with cellular membranes, cytoplasm and extracellular spaces and thus may be involved in the maintenance of TEB integrity, as seen for Ntn1 and Neo1 [117].

4.3.2.4.2 *Migratory function*

The high expression of Fbln2 in both the stroma and epithelium of TEBs, which are very motile structures and serve as key drivers of ductal morphogenesis at puberty, could suggest a potential role for Fbln2 in the regulation of TEB migration and hence ductal outgrowth. To date, the role of Fbln2 in migration has only been studied in terms of single cell migration and was shown to differ depending on the experimental system. Down-regulation of Fbln2 occurred in both the breast cancer cell lines (MDA-MB-231 and BT-20) and breast tumours and, when over-expressed *in vitro*, it reduced cell motility and invasiveness of breast cancer cells [342]. It was present in murine non-neoplastic vascular lesions *in vivo* and when up-regulated it increased smooth muscle cell migration in response to injury *in vitro* [448]. Furthermore, in embryonic cardiovascular development *Fbln2* has been identified as up-regulated during EMT where it selectively localised to mesenchymal cells, i.e. migrating cells of developing cardiac valves and aortic arch vessels [441]. Our data, however, does not support these findings as it demonstrates that the over-expression of Fbln2 in non-malignant mouse mammary epithelial cells (HC11) did not alter the ability of these cells to migrate (**Figure 4-26 B**). It is worth noting, however, that the wound healing assay, which was used to study cell migration in this project, was carried out on a plastic surface. Based on the fact that Fbln2 belongs to ECM molecules and closely interacts with other ECM components it would be beneficial to validate these primary findings using additional methods which incorporate substances that mimic extracellular environment such as surfaces coated with synthetic ECM molecules or fibroblasts (2D assays). On the account of the structural complexity and varied composition of ECM *in vivo* it may further be of use to study the impact of Fbln2 expression on mammary epithelial cell migration using the 3D matrix based techniques. An example of such assay is a Matrigel coated Boyden migration chamber which uses chemoattraction to promote cell migration and heterogenic composition of Matrigel (CollIV, Lama1, proteoglycans, EMC degrading proteins and their inhibitors, growth factors and many others) to reconstitute stromal environment of mammary gland and thus can be, and in fact already has been [475], used to study the HC11 cell migration.

Although the exact mechanism is yet unknown, the migration of TEB does not appear to be based on single cells but most likely is characterised by collective cell migration - a coherent movement of a group of cells whose leading edge, in the *in vitro* cultured TEB-like organoids, is agglomerated as demonstrated by the positive E-cadherin and P-cadherin staining, and appears to migrate despite lacking cellular extensions or protrusions [105]. Although the underlying mechanism for this activity is yet to be elucidated there are several potential ways in which Fbln2 could positively regulate this mechanism of migration.

Firstly, its localisation to BM and cellular membranes of cap cells and extracellular spaces of body cells means Fbln2 may facilitate collective cell migration by maintaining the tissue integrity of TEB. It may physically strengthen the architecture of BM by binding and cross-linking it with other ECM molecules and by assisting in maintaining the adhesion between cap cells and body cells. The presence of a single RGD site within its structure supports this theory since it is indicative of adhesive properties [434] and, as shown in this study and by Sasaki *et al.* (1990), Fbln2 was able to promote adhesiveness of mammary cell lines to ECM coated surfaces (**Figure 4-27 B**) [463].

Secondly, the stroma expressed Fbln2 may not only have the structural role discussed above but, since ECM is critical for epithelial-stromal cross talk and ECM remodelling is essential for TEB migration at puberty, stromal Fbln2 may also take part in regulating pubertal outgrowth. *In vitro*, Fbln2 shows strong binding affinity to Itgb3 and Itga5, the BM associated receptors which connect the ECM with the epithelial cell cytoskeleton [463] and as demonstrated by our microarray study, were highly expressed in TEBs (**Table 4-1 and 4-2**). Fbln2 may therefore mediate signal transmission between the stroma and epithelium and hence influence the phenotype and behaviour of TEBs.

A third possibility, however, is that Fbln2 may influence TEB migration by remodelling of ECM. This property of fibulins has been long observed in *Caenorhabditis elegans* where fibulin-1 (FBL-1) which corresponds to mammalian Fbln1C is involved in directing the cellular migration of gonadal distal tip cells during gonad organogenesis *in vivo* [476] [477]. FBL-1 is expressed in the stroma around migrating cells where it appears to interact with 'Abnormal GONad Development' (GON-1), a non vertebrate homolog of ADAM metallopeptidase

with thrombospondin type 1 motif (ADAMTS). It was concluded that FBL-1 drives gonadal migration by antagonising the action of GON-1 by interacting with other ECM molecules, which are substrates for ADAMTS directed cleavage. One of these ECM molecules could be Acan which both binds Fbln1C and is known to be cleaved by ADAMTS [478]. Since Fbln1C is the closest relative to Fbln2 [434] its involvement in directing gonadal distal tip cell migration might provide insights into its potential regulatory function in mammary morphogenesis at puberty.

Finally, as the expression of Fbln2 was concentrated around the neck and flanks of TEBs, in a similar expression pattern to that described for Coll, it may play a similar role to that proposed for Coll in acting as a girdle to contain and direct the pressure generated during reshaping of TEB into ductal dimensions and thus create the force to promote their forward movement [53].

Thus, there are several ways in which the formation of the Fbln2 network in ECM or epithelium of TEBs might provide a structural backbone for mammary ductal tree development or facilitate ductal elongation in pubertal mouse mammary gland. Furthermore, it is worth adding that Fbln2 expression in the mammary myoepithelium and its surrounding stroma at early pregnancy indicates its potential in priming the ducts for tertiary branching, a process characteristic for this developmental stage, and as discussed for puberty this may be achieved by Fbln2 either i) providing a structural scaffold that maintains tissue integrity or ii) priming ductal epithelium and stroma for cellular migration via preparing the cells for collective migration, mediating epithelial-stromal cross talk or promoting/regulating ECM remodelling (See paragraphs above). Further experiments, however, are required to test these hypotheses.

Despite its specific localisation and rich array of potential functions loss of Fbln2 did not result in a mammary phenotype, but showed comparable TEB morphology (slight differences in TEB size and shape could be seen in the Fbln2 KO^{-/-} mammary glands which appeared smaller and more oval than their WT counterparts but a larger number of mouse mammary glands should be studied to substantiate this observation), length and degree of branching of the ductal tree to that seen in WT controls (Figure 4-32) (Figure 4-33). This is consistent with the results of earlier study by Sicot *et al.* (2007) which showed the dispensability of Fbln2 for general mouse development [266]. This general lack

of a phenotype in response to Fbln2 deficiency is probably due to compensation by Fbln1 expression, which in fact was not only up-regulated in TEB environment in Fbln2 KO^{-/-} mouse mammary glands when compared to WT controls (**Figure 4-34 A and B**) but also localised to cap cells and BM, places associated with Fbln2 but not Fbln1 expression in WT controls (**Figure 4-35 A, B and C**). This indicates that loss of Fbln2 triggers an increase in expression and an alteration in the localisation of Fbln1 in mammary gland. Since IHC is not quantitative, further studies should be carried out to quantify the level of Fbln1 in Fbln2 KO^{-/-} and WT mice. Fbln1 binds to most of the molecules that interact with Fbln2, such as Fn, Lama1, Nid, Col18a1, Vcan and Acan [443] [442] and therefore it is possible that the compensatory expression of Fbln1 is sufficient to rescue the Fbln2 KO^{-/-} phenotype. Further studies should be carried out to evaluate this hypothesis. It would be necessary to generate a mouse model lacking the expression of both Fbln1 and Fbln2. Since Fbln1 KO^{-/-} mice are prenatally lethal mainly due to haemorrhage (defective BM of small blood vessels) [479], however, it would be necessary to generate Fbln2 KO^{-/-} mice expressing loxP flanked Fbln1 gene and a transgene construct consisting of full-length Cre recombinase cDNA under the control of MMTV promoter. The mammary gland expressed Cre would bind to loxP sequences and splice the loxP flanked DNA and thus KO Fbln1 expression in a selective, tissue specific manner. Given the presence of the potential mechanism by which Fbln2 deficiency is immediately compensated by the Fbln1 expression it is tempting to speculate that rather than being indispensable for the pubertal mammary morphogenesis or general mouse development, as suggested before [266], it is perhaps that Fbln2 is so essential for these processes that just in case it is lost an alternative mechanism, such as compensation with Fbln1 expression, are in place. This can further be supported by the results of recently generated and studied double knockout mice for *Fbln2* and *Fbln5* genes which present a severe phenotype within the cardiovascular system (severe disorganisation of the elastic lamina in blood vessels which can not be seen in single Fbln2 or Fbln5 KO^{-/-} mouse models) suggesting that when interacting with Fbln5, Fbln2 is essential for elastic fibre formation [449]. At the time of this study the double KO mouse model was not available to us but an examination of mammary glands collected from these mice would be essential to further study the role of Fbln2 during *in vivo* mouse mammary gland development in the future.

4.3.2.5 Summary

In summary, this study is the first to demonstrate and research the expression of Fbln2 in pubertal mouse mammary gland. We propose that Fbln2 might be expressed in response to P and although its deficiency does not result in an obvious pubertal mammary phenotype, its diverse localisation throughout the mammary stroma and epithelium suggests it is likely to interact with different ECM structures at different places and thus contribute to an array of different structural and migratory functions during pubertal mammary morphogenesis and possibly pre-puberty and early pregnancy.

5 Final conclusions and future work

5.1 Final Conclusions

This thesis demonstrates the benefit of DNA microarray analysis in studying pubertal development of mouse mammary gland to either identify putative regulators ('candidate gene approach') or unravel global trends in gene expression ('pathway analysis') and thus add to the understanding of biological mechanisms that underlie the TEB driven morphogenesis and ductal branching at puberty and reveal many potential avenues for further investigations.

Using RNA obtained from isolated epithelium of TEBs, ducts and whole mouse mammary tissue strips not only did we identify gene sets associated with each of the pubertal compartments (the epithelium or stroma of TEBs, epithelium or stroma of ducts or the epithelium free distal Fat pad) but we also characterised each milieu. We are the first to identify and characterise stromal transcriptomes of TEBs and ducts and together with the detailed analysis of pubertal epithelium this thesis provides the most comprehensive comparison analysis of the functional characteristics of TEBs and ducts to date.

We focused our analysis on an individual gene level and selected *Upk3a* and *Fbln2* as potential regulators of pubertal mouse mammary morphogenesis. While our studies on *Upk3a* were limited since it could not be detected at the protein level we demonstrated strong expression of *Fbln2* in both the epithelium and stroma of TEBs and the distal stromal capsule of mouse mammary gland at puberty. In addition, we showed that *Fbln2* was expressed in TEB-like structures and distal stromal capsule in pre-pubertal mammary glands and myoepithelium, its surrounding stroma and distal stromal capsule in mammary glands during early pregnancy (day 2 - day 4.5). This suggested that *Fbln2* expression switches on at embryogenesis (embryonic expression of *Fbln2* has been demonstrated during the cardiovascular development) and continues during pre-puberty and puberty. We postulated that *Fbln2* may be expressed in response to P during puberty and early-pregnancy and that the lack of an obvious mammary phenotype in *Fbln2* KO^{-/-} mice at puberty might be attributed to the over-compensation of *Fbln2* loss by *Fbln1*. The diverse localisation of *Fbln2*

throughout the mammary stroma and epithelium suggested its potential to interact with various ECM structures at different places and thus contribute to an array of different structural and migratory functions during mammary morphogenesis.

5.2 Future directions

5.2.1 Further analysis of TEB and duct transcriptomes to study mouse mammary gland development at puberty

In this study we hypothesised that the TEB associated genes are involved in promoting and regulating the development of mouse mammary gland. We suggested many candidates with a potential to serve as these regulators from which we further researched association of two with pubertal morphogenesis (*Upk3a* and *Fbln2*). In the future, it would be beneficial, therefore, to study some of the other identified genes in more detail, to assess their role in pubertal morphogenesis (e.g. adhesion associated genes - *Emb*, *Fbn2*; EMT associated genes - *Lad1*, *Slp1*, migration associated genes or others as suggested in **Chapter 3.3**). The signals from the stroma are as important for mammary morphogenesis as these originating from the epithelium (**reviewed in 1.2.3.2**) and although not yet demonstrated for pubertal morphogenesis of mouse mammary gland, the down-regulation of genes has been proven essential in morphogenesis of other systems (HL-60 monocytic differentiation or EMT). Thus, in the future, the search for the potential regulators of pubertal mammary morphogenesis should be broadened to include the identified in this project, 579 TEB-only stroma associated genes (**See 3.2.6.2.2**) and the 186 TEB epithelium down-regulated (duct up-regulated) genes (**See 3.2.6.1.1**).

Moreover, although the ‘pathway analysis’ carried out in this study suggested the associations of TEB and duct transcriptomes with a range of different biological processes/functions, and highlighted the candidate genes associated with each one of them, this type of analysis may not be fully representative of functional processes activated *in vivo* and should only be used as a start point for further investigation (**See 3.3.3.5**). To take this analysis forward, therefore, the highlighted by IPA associations of given pathways/biological functions with

mammary gland morphogenesis should be examined at functional level. The 'Cardiovascular System Development' and 'Immune Response' are the examples of such processes. To date, only three types of innate immune system components - macrophages, eosinophils and mast cells have been documented to associate with TEBs and ducts at puberty. The 'pathway analysis' presented in this thesis, however, suggested possible association of pubertal epithelium with other immune system components (e.g. neutrophils, T lymphocytes, B lymphocytes, NKTL, phagocytes or Langerhans cells) (on the basis of their marker gene expression) (See 3.3.3.2). In the future, therefore it would be of benefit to use Q RT PCR to confirm the up-regulation of these marker genes in mouse mammary gland at puberty and IHC or IF to investigate their spatial expression. Moreover, since no active blood vessel development has been associated with mammary gland at puberty, to date, it may be of interest to follow up the link between angiogenesis and TEBs, suggested by the 'pathway analysis' and gene expression analysis. Our microarray analysis showed *VEGF* to be up-regulated in TEB epithelium, and the epithelial expression of *VEGF* during pregnancy and lactation has previously been shown to promote angiogenesis [480]. It may be that migrating TEBs express genes which take part in promoting vascular outgrowth or vascular outgrowth promotes directional migration of TEBs. It would be necessary to validate the expression *VEGF* and *VEGF* receptors (FMS-like tyrosine kinase 1 - Flt-1 and Kinase insert domain protein receptor - Flk-1) at the protein level and examine the effects of their deficiency on ductal outgrowth. Since, the *VEGF* KO^{-/-} mice are embryonically lethal [481] it would be essential to generate a mouse model that would knock out *VEGF* under the control of MMTV promoter in a cre-lox system, to enable its selective silencing at the different stages of mammary gland development. The other possibility would be to implant mouse mammary glands with the slow release *VEGF* pellets (e.g. Elvax 40P implants [52]) and examine the indirect effect of *VEGF* on local angiogenesis and TEB outgrowth.

The data generated by IPA could further be analysed to gain information about the processes already known to be associated with pubertal morphogenesis, but which underlying mechanisms are still to be elucidated, such as lumen formation in TEBs. This could be commenced by researching the association of TEB epithelium with the apoptosis/cell death-linked genes.

Finally, during the course of this project, we also compared the exon expression levels between the isolated TEBs and ducts and mouse mammary gland tissue strips to study the alternative splicing. This analysis, however, has not been addressed in this thesis due to time constraints. Since the alternative splicing of mRNA is one of the mechanisms regulating gene expression in higher Eukaryotes the comparison of splicing changes between the transcriptomes of TEBs and ducts might provide valuable information on their transcriptomics.

5.2.2 Further analysis of TEB and duct transcriptomes to study breast cancer

It has recently emerged that TEB migration might share similarities with breast cancer cell invasion. These are reflected in the rapid growth, epithelial invasion of surrounding stroma and its dependence on stromal-epithelial interactions seen in both tissues (reviewed in [100]) and the similarities in systemic and local regulation of the outgrowths. E2 and its receptor ER α are both crucial for TEB development, ductal outgrowth at puberty [126] [127] [133] (See 1.2.3.2.1) and breast cancer progression, as demonstrated by the sensitivity of some cancers to E2 and the positive impact of Tamoxifen (a synthetic molecule which binds to ER and modulates its transcriptional capabilities) on the treatment of ER+ tumours (reviewed in [482]). Both TEBs and breast cancer cells have been also suggested to migrate in similar manner and the collective cell migration (previously discussed in 4.1.3.3 and demonstrated in fully dedifferentiated breast cancers, such as lobular breast cancer) (reviewed in [388]) and EMT (previously discussed in 4.1.2.1) have been suggested as the candidate drivers. Finally, individual genes such as *ErbB2* (*Her2*), an EGF-like receptor which localises to TEBs during pubertal development and is critical for their normal morphology and ductal elongation [118] have been shown to serve as an important therapeutic target in breast cancer (reviewed in [483]).

In further studies the TEB transcriptome associated genes, identified in this thesis (425 TEB epithelium up-regulated genes (3.4.1.1.1) and 565 TEB epithelium-stroma up-regulated genes (3.4.1.1.2)), could be used to assess their expression levels in breast cancer microarray data sets, e.g. the Netherlands Cancer Institute microarray data set, comprising of 295 breast cancer patients

(NIK 295) [484], and correlate the results with outcome and metastatic potential. Preliminary work from our laboratory showed that human orthologues of mouse genes that were identified as up-regulated in isolated TEBs compared to ducts by Morris *et al.* (2006) [113] may distinguish breast cancers with good prognosis in the NIK 295 breast cancer data set [484] (unpublished data). Thus, it would be interesting to carry out further *in silico* analysis (hierarchical clustering) using our more comprehensive TEB signature to validate these results. This and other breast cancer data sets, such as a 99 breast cancer data set by Sotiriou *et al.* [485], could be used to test whether the TEB signature clusters with any of the clinical variables (e.g. presence of metastasis, cancer grade, LN status, Her2, ER, PR status). As the mitosis-associated genes constitute a large part of TEB transcriptome it would be essential that these are subtracted prior to analysis. If any associations were found, the individual genes may be identified and further studied. In addition, if carried out the 'pathway analysis' of these signatures might provide further information on the signalling pathways associated with breast cancer and its progression.

5.2.3 The use of microRNA profiling to study pubertal development of mouse mammary gland

Finally, it may be beneficial to carry out the microRNA (miRNA) expression profiling on isolated TEB and ducts and mammary gland tissue strips and compare the TEB signature with breast cancer data sets, as described above. MiRNAs are non-coding negative regulators of gene expression (reviewed in [486]). Their expression pattern is unique to different organs and processes. It can distinguish between normal and tumour tissues [487] [488] or even aid the classification of cancers based on their lineage and differentiation state. miRNA signature is more stable, reproducible and conserved between the species (~20%) than that associated with mRNA profiling [489]. Thus, when used for pubertal gene expression analysis, miRNA profiling would not only complement the mRNA results but it may also provide new insights into the mechanisms of the TEB driven ductal morphogenesis at puberty, identify new regulators or define novel signalling pathways involved. This could further define possible links between the TEB signature and breast cancer, and thus reveal new avenues for further

research on both the normal mammary gland morphogenesis and its malignant counterparts.

5.2.4 Further investigation into the role of *Upk3a* and *Fbln2* in pubertal morphogenesis of mouse mammary gland

Since only a single anti-Upk3a antibody has been tested during the course of this project, further evaluation of the expression of Upk3a in mouse mammary gland should be carried out using antibodies raised against different epitopes of the protein.

The first line for future investigation into the role of Fbln2 in pubertal morphogenesis of mouse mammary gland, on the other hand, would be to use the mouse models to study the effect of its loss on the pubertal mouse mammary gland *in vivo*. Although, the initial morphological comparison of pre-pubertal and pubertal mouse mammary glands from Fbln2 KO^{-/-} mice and their WT counterparts has already been performed during the course of this project, that study was based on a limited number of animals only (See 4.2.2.11). Although it did not demonstrate any major morphological differences in the length or the degree of branching of the ductal tree between the mammary glands, some of the TEBs in the mammary glands from pubertal Fbln2 KO^{-/-} mice appeared slightly smaller and more elongated than those seen in their WT counterparts. A more comprehensive analysis based on higher number of replicates, therefore, ought to be performed in the future to validate these results. Moreover, as we have shown that the loss of Fbln2 in Fbln2 KO^{-/-} mouse mammary glands appeared to be over-compensated by the expression of Fbln1 (also seen in Fbln2 KO^{-/-} aorta [266]) and this phenomenon may rescue the pubertal phenotype, it would be further essential to generate a double (*Fbln2* and *Fbln1*) KO. Since Fbln1 KO^{-/-} mice are prenatally lethal [479] it would be necessary, however, to generate Fbln2 KO^{-/-} mice expressing loxP flanked Fbln1 gene and a transgene construct consisting of full-length Cre recombinase cDNA under the control of MMTV promoter. The mammary gland expressed Cre would bind to loxP sequences and splice the loxP flanked DNA and thus KO Fbln1 expression in a selective tissue specific manner. Furthermore, during the write up of this thesis, the double KO^{-/-} (*Fbln2* and *Fbln5*) mouse model was generated. It showed

vascular phenotype (disorganised internal elastic lamina in blood vessels) that could not be seen in either of the single KO(s) (Fbln2 KO^{-/-} or Fbln5 KO^{-/-}) [449], but due to the time constraints of this project we could not carry out its examination. The assessment of Fbln5 expression in mouse mammary gland and its co-localisation with the mammary Fbln2, alongside with morphological examination of mammary glands, collected from these mice, therefore, would be essential to progress with studying the role of Fbln2 during *in vivo* mouse mammary gland development in the future. If present, the potential phenotype would provide further suggestions on role of Fbln2 in mouse mammary gland morphogenesis.

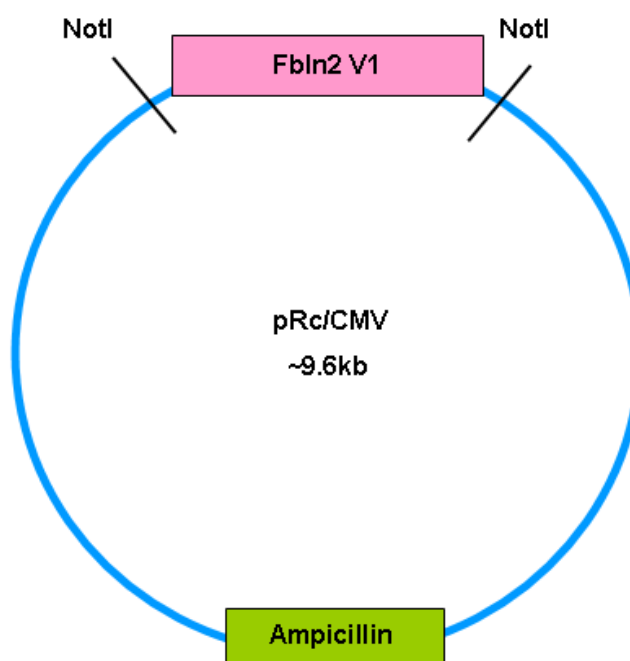
Most of the functional studies for Fbln2 in pubertal mammary gland development were based on the *in vitro* 2D cell adhesion- or wound healing assays and *in vivo* mouse models. Both systems, however, have clear disadvantages. Mouse models are expensive to produce, subject to potential over-compensation/redundancy effects and stringent regulation which often results in studies utilising low replicate numbers while the 2D *in vitro* assays fail to mimic the complex structure and composition of ECM *in vivo*. Furthermore, no cell line to date, has been generated from the pubertal mammary epithelium (mammary epithelial cell lines available to date derive from pregnant mice - HC11, EpH4 cells). Thus, no epithelial structures, with morphological similarity to TEBs *in vivo*, have been reported to form from epithelial cells in culture. Future research, therefore, should focus on the development of TEB explant culture model. Preliminary analyses showing its potential to act as a good *in vitro* model for pubertal mouse mammary gland research have been described in 4.2.2.5. Future work should address further characterisation of cells within the outgrowths to further ensure that their characteristics resemble those of TEB epithelium *in vivo* and can be maintained in culture. Moreover, given the importance of epithelial-stromal interactions during pubertal mammary morphogenesis it would be of benefit to identify the most suitable matrix for mimicking stromal environment of TEBs *in vivo*.

When successfully developed and validated this explant culture model may be used in studying the regulation of Fbln2 expression. For example, upon the positive ER and PR expression in explant cultures, this system could be used to further study the regulation of Fbln2 expression by systemic hormones.

Furthermore, the developed experimental conditions could be also used to culture the pre-pubertal TEB-like structures and mammary epithelium extracted from mammary glands at early pregnancy, both of which have been also shown to express Fbln2. These cultures could be then utilised to compare the histological characteristics of TEBs and TEB-like outgrowths (it is not yet clear if TEB-like structures are equivalent of TEBs at puberty). Furthermore, when compared, these three models might provide insights into the regulation of Fbln2 expression at different stages of mouse mammary gland morphogenesis. Similarly, the explant culture model might also be used to further characterise and compare the histology of TEBs collected from WT and Fbln2 KO mouse models. Finally, as Fbln2 may play the structural role in mammary gland by stabilising the organisation of ECM and, as shown in our study, Fbln2 enhanced the adhesiveness of HC11 cells to Lama1, Vtn and Tn it may be of benefit to further validate these findings and test the level of adhesiveness of TEB explants to each one of these matrices.

Finally, when fully developed and optimised, in the future, the TEB explant culture model may provide a relevant and accessible tool for studying the expression and regulation of any of the chosen, TEB associated genes, *in vitro*.

6 Appendices



Appendix 1 Fbln2 V1 expression vector.

Appendix 2 List of genes over-expressed in TEB and duct epithelium.

Appendix 3 List of genes over-expressed in Post- and Pre-LN mouse mammary gland tissue strips.

Appendix 4 List of genes over-expressed in the epithelium free mammary Fat pad.

Appendix 5 List of genes expressed in TEB-only and duct-only epithelium.

Appendix 6 List of genes expressed in TEB-only and duct-only stroma.

Appendix 7 List of genes associated with the identified 'Molecular and Cellular Function' categories.

Appendix 8 List of genes associated with the identified 'Physiological System Development and Function' categories.

Appendix 9 List of functional sub-group associated with 'Cellular Movement', 'Nervous System Development and Function' and 'Embryonic Development' and their associated genes.

Appendices 2-9 are provided in the **Supplementary DVD**.

Appendix 10 List of presentations prepared on the data from this thesis.

- ‘Stromal-epithelial interactions during ductal morphogenesis of mouse mammary gland’ - Oral presentation at the departmental seminar, University of Glasgow (Glasgow, UK; 2007)
- ‘Pubertal development of mouse mammary gland’ - Oral presentation at the departmental seminar, University of Glasgow (Glasgow, UK; 2008)
- ‘Epithelial and stromal transcriptome analysis of pubertal mouse mammary gland’ - Poster presentation at Breast Cancer Breakthrough Annual Meeting (Oxford, UK; 2008)
- ‘Epithelial and stromal transcriptome analysis of the pubertal mouse mammary gland and identification of Fbln2 as a novel pubertal regulator of mouse mammary gland morphogenesis’ - Poster presentation at Gordon Research Conference on Mammary Gland Biology (New Port, USA; 2009)

7 Bibliography

1. Peaker, M., *The mammary gland in mammalian evolution: a brief commentary on some of the concepts*. *J Mammary Gland Biol Neoplasia*, 2002. **7**(3): p. 347-53.
2. Bolander, F.F., Jr., *Differential characteristics of the thoracic and abdominal mammary glands from mice*. *Exp Cell Res*, 1990. **189**(1): p. 142-4.
3. Veltmaat, J.M., et al., *Mouse embryonic mammaryogenesis as a model for the molecular regulation of pattern formation*. *Differentiation*, 2003. **71**(1): p. 1-17.
4. Wu, P., et al., *Evo-Devo of amniote integuments and appendages*. *Int J Dev Biol*, 2004. **48**(2-3): p. 249-70.
5. Veltmaat, J.M., et al., *Identification of the mammary line in mouse by Wnt10b expression*. *Dev Dyn*, 2004. **229**(2): p. 349-56.
6. Balinsky, B.I., *On the prenatal growth of the mammary gland rudiment in the mouse*. *J Anat*, 1950. **84**(3): p. 227-35.
7. Sakakura, T., *Embryogenesis*. Development, Regulation and Function, ed. D.C.W. Neville M. C. 1987, New York: Plenum. 37-65.
8. Sakakura, T., Y. Sakagami, and Y. Nishizuka, *Dual origin of mesenchymal tissues participating in mouse mammary gland embryogenesis*. *Dev Biol*, 1982. **91**(1): p. 202-7.
9. Kimata, K., et al., *Participation of two different mesenchymes in the developing mouse mammary gland: synthesis of basement membrane components by fat pad precursor cells*. *J Embryol Exp Morphol*, 1985. **89**: p. 243-57.
10. Foley, J., et al., *Parathyroid hormone-related protein maintains mammary epithelial fate and triggers nipple skin differentiation during embryonic breast development*. *Development*, 2001. **128**(4): p. 513-25.
11. Cunha, G.R., *Role of mesenchymal-epithelial interactions in normal and abnormal development of the mammary gland and prostate*. *Cancer*, 1994. **74**(3 Suppl): p. 1030-44.
12. Kratochwil, K., *Organ specificity in mesenchymal induction demonstrated in the embryonic development of the mammary gland of the mouse*. *Dev Biol*, 1969. **20**(1): p. 46-71.
13. Sakakura, T., et al., *Biology of mammary fat pad in fetal mouse: capacity to support development of various fetal epithelia in vivo*. *Development*, 1987. **100**(3): p. 421-30.
14. Eblaghie, M.C., et al., *Interactions between FGF and Wnt signals and Tbx3 gene expression in mammary gland initiation in mouse embryos*. *J Anat*, 2004. **205**(1): p. 1-13.
15. van Genderen, C., et al., *Development of several organs that require inductive epithelial-mesenchymal interactions is impaired in LEF-1-deficient mice*. *Genes Dev*, 1994. **8**(22): p. 2691-703.
16. Gu, B., et al., *Pygo2 expands mammary progenitor cells by facilitating histone H3 K4 methylation*. *J Cell Biol*, 2009. **185**(5): p. 811-26.
17. Lindvall, C., et al., *The Wnt signaling receptor Lrp5 is required for mammary ductal stem cell activity and Wnt1-induced tumorigenesis*. *J Biol Chem*, 2006. **281**(46): p. 35081-7.

18. Lindvall, C., et al., *The Wnt co-receptor Lrp6 is required for normal mouse mammary gland development*. PLoS One, 2009. 4(6): p. e5813.
19. Chu, E.Y., et al., *Canonical WNT signaling promotes mammary placode development and is essential for initiation of mammary gland morphogenesis*. Development, 2004. 131(19): p. 4819-29.
20. Mailleux, A.A., et al., *Role of FGF10/FGFR2b signaling during mammary gland development in the mouse embryo*. Development, 2002. 129(1): p. 53-60.
21. Asselin-Labat, M.L., et al., *Gata-3 is an essential regulator of mammary-gland morphogenesis and luminal-cell differentiation*. Nat Cell Biol, 2007. 9(2): p. 201-9.
22. Wysolmerski, J.J., et al., *Rescue of the parathyroid hormone-related protein knockout mouse demonstrates that parathyroid hormone-related protein is essential for mammary gland development*. Development, 1998. 125(7): p. 1285-94.
23. Hens, J.R., et al., *BMP4 and PTHrP interact to stimulate ductal outgrowth during embryonic mammary development and to inhibit hair follicle induction*. Development, 2007. 134(6): p. 1221-30.
24. Heckman, B.M., et al., *Crosstalk between the p190-B RhoGAP and IGF signaling pathways is required for embryonic mammary bud development*. Dev Biol, 2007. 309(1): p. 137-49.
25. Howard, B.A. and B.A. Gusterson, *The characterization of a mouse mutant that displays abnormal mammary gland development*. Mamm Genome, 2000. 11(3): p. 234-7.
26. Satokata, I., et al., *Msx2 deficiency in mice causes pleiotropic defects in bone growth and ectodermal organ formation*. Nat Genet, 2000. 24(4): p. 391-5.
27. Andres, A.C. and R. Strange, *Apoptosis in the estrous and menstrual cycles*. J Mammary Gland Biol Neoplasia, 1999. 4(2): p. 221-8.
28. Richert, M.M., et al., *An atlas of mouse mammary gland development*. J Mammary Gland Biol Neoplasia, 2000. 5(2): p. 227-41.
29. Robinson, G.W., et al., *Mammary epithelial cells undergo secretory differentiation in cycling virgins but require pregnancy for the establishment of terminal differentiation*. Development, 1995. 121(7): p. 2079-90.
30. Lee, E.Y., et al., *Interaction of mouse mammary epithelial cells with collagen substrata: regulation of casein gene expression and secretion*. Proc Natl Acad Sci U S A, 1985. 82(5): p. 1419-23.
31. Smith, G.H., *Experimental mammary epithelial morphogenesis in an in vivo model: evidence for distinct cellular progenitors of the ductal and lobular phenotype*. Breast Cancer Res Treat, 1996. 39(1): p. 21-31.
32. Bruno, R.D. and G.H. Smith, *Functional Characterization of Stem Cell Activity in the Mouse Mammary Gland*. Stem Cell Rev, 2011. 7(2): p. 238-247.
33. Mather, I.H. and T.W. Keenan, *The cell biology of milk secretion: historical notes. Introduction*. J Mammary Gland Biol Neoplasia, 1998. 3(3): p. 227-32.
34. Conneely, O.M., B.M. Jericevic, and J.P. Lydon, *Progesterone receptors in mammary gland development and tumorigenesis*. J Mammary Gland Biol Neoplasia, 2003. 8(2): p. 205-14.
35. Ormandy, C.J., et al., *Null mutation of the prolactin receptor gene produces multiple reproductive defects in the mouse*. Genes Dev, 1997. 11(2): p. 167-78.

36. Neville, M.C., T.B. McFadden, and I. Forsyth, *Hormonal regulation of mammary differentiation and milk secretion*. J Mammary Gland Biol Neoplasia, 2002. 7(1): p. 49-66.
37. Strange, R., et al., *Apoptotic cell death and tissue remodelling during mouse mammary gland involution*. Development, 1992. 115(1): p. 49-58.
38. Stein, T., et al., *Involution of the mouse mammary gland is associated with an immune cascade and an acute-phase response, involving LBP, CD14 and STAT3*. Breast Cancer Res, 2004. 6(2): p. R75-91.
39. Pensa, S., C.J. Watson, and V. Poli, *Stat3 and the inflammation/acute phase response in involution and breast cancer*. J Mammary Gland Biol Neoplasia, 2009. 14(2): p. 121-9.
40. Stein, T., N. Salomonis, and B.A. Gusterson, *Mammary gland involution as a multi-step process*. J Mammary Gland Biol Neoplasia, 2007. 12(1): p. 25-35.
41. Lund, L.R., et al., *Two distinct phases of apoptosis in mammary gland involution: proteinase-independent and -dependent pathways*. Development, 1996. 122(1): p. 181-93.
42. Li, M., et al., *Mammary-derived signals activate programmed cell death during the first stage of mammary gland involution*. Proc Natl Acad Sci U S A, 1997. 94(7): p. 3425-30.
43. Walker, N.I., R.E. Bennett, and J.F. Kerr, *Cell death by apoptosis during involution of the lactating breast in mice and rats*. Am J Anat, 1989. 185(1): p. 19-32.
44. Monks, J., et al., *Epithelial cells remove apoptotic epithelial cells during post-lactation involution of the mouse mammary gland*. Biol Reprod, 2008. 78(4): p. 586-94.
45. Nelson, J.F., et al., *Genetic influences on the timing of puberty in mice*. Biol Reprod, 1990. 42(4): p. 649-55.
46. Nelson, J.F., et al., *A longitudinal study of estrous cyclicity in aging C57BL/6J mice: I. Cycle frequency, length and vaginal cytology*. Biol Reprod, 1982. 27(2): p. 327-39.
47. Bronson, F.H., Dagg, Ch. P., Snell G. D., *Reproduction*. 2 ed. The biology of Laboratory Mouse, ed. E.L. Green. 1975, New York: Doves Publications.
48. Cole, H.A., *The Mammary Gland of the Mouse, During the (Estrous Cycle, Pregnancy and Lactation)*. Proc. R. Soc. Lond. B Biol., 1933. 114: p. 136-160.
49. Kaye, J., Ross, M. H., Romrell, L. J., Kaye, G. I., *Histology: A text and Atlas*, ed. R.L.J. Ross M H, Kaye K. 1995, Maryland: Williams and Wilkins. 678-738.
50. Silberstein, G.B. and C.W. Daniel, *Glycosaminoglycans in the basal lamina and extracellular matrix of the developing mouse mammary duct*. Dev Biol, 1982. 90(1): p. 215-22.
51. Faulkin, L.J., Jr. and K.B. Deome, *Regulation of growth and spacing of gland elements in the mammary fat pad of the C3H mouse*. J Natl Cancer Inst, 1960. 24: p. 953-69.
52. Silberstein, G.B. and C.W. Daniel, *Elvax 40P implants: sustained, local release of bioactive molecules influencing mammary ductal development*. Dev Biol, 1982. 93(1): p. 272-8.
53. Williams, J.M. and C.W. Daniel, *Mammary ductal elongation: differentiation of myoepithelium and basal lamina during branching morphogenesis*. Dev Biol, 1983. 97(2): p. 274-90.

54. Ball, S.M., *The development of the terminal end bud in the prepubertal-pubertal mouse mammary gland*. Anat Rec, 1998. **250**(4): p. 459-64.
55. Daniel, C.W., *Regulation of cell division in aging mouse mammary epithelium*. Adv Exp Med Biol, 1975. **61**: p. 1-19.
56. Silberstein, G.B., *Postnatal mammary gland morphogenesis*. Microsc Res Tech, 2001. **52**(2): p. 155-62.
57. Daniel, C.W., P. Strickland, and Y. Friedmann, *Expression and functional role of E- and P-cadherins in mouse mammary ductal morphogenesis and growth*. Dev Biol, 1995. **169**(2): p. 511-9.
58. Daniel, C.W., Silberstein, G. B., , *Methods in Mammary Gland Biology and Breast Cancer Research*. Working with Mouse Mammary End Bud, ed. I.A. Kulwer. 2000, New York: Academic/Plenum Publishers. 155-162.
59. Daniel, C.W., et al., *The in vivo life span of normal and preneoplastic mouse mammary glands: a serial transplantation study*. Proc Natl Acad Sci U S A, 1968. **61**(1): p. 53-60.
60. Humphreys, R.C., *Programmed cell death in the terminal endbud*. J Mammary Gland Biol Neoplasia, 1999. **4**(2): p. 213-20.
61. Humphreys, R.C., et al., *Apoptosis in the terminal endbud of the murine mammary gland: a mechanism of ductal morphogenesis*. Development, 1996. **122**(12): p. 4013-22.
62. Bresciani, F., *Effect of Ovarian Hormones on Duration of DNA Synthesis in Cells of the C3h Mouse Mammary Gland*. Exp Cell Res, 1965. **38**: p. 13-32.
63. Daniel, C.W., Silberstein, G. B.,, *Postnatal Development of Rodent Mammary Gland*. The Mammary Gland. Development. Regulation and Function, ed. D.C.W. Neville M. C. 1978, New Yourk and London: Plenum Press. 3-36.
64. O'Hare, M.J., et al., *Characterization in vitro of luminal and myoepithelial cells isolated from the human mammary gland by cell sorting*. Differentiation, 1991. **46**(3): p. 209-21.
65. Mikaelian, I., et al., *Expression of terminal differentiation proteins defines stages of mouse mammary gland development*. Vet Pathol, 2006. **43**(1): p. 36-49.
66. Daniel, C.W. and K.B. Deome, *Growth of Mouse Mammary Glands in Vivo after Monolayer Culture*. Science, 1965. **149**: p. 634-6.
67. Smith, G.H. and D. Medina, *A morphologically distinct candidate for an epithelial stem cell in mouse mammary gland*. J Cell Sci, 1988. **90** (Pt 1): p. 173-83.
68. Kordon, E.C. and G.H. Smith, *An entire functional mammary gland may comprise the progeny from a single cell*. Development, 1998. **125**(10): p. 1921-30.
69. Deome, K.B., et al., *Development of mammary tumors from hyperplastic alveolar nodules transplanted into gland-free mammary fat pads of female C3H mice*. Cancer Res, 1959. **19**(5): p. 515-20.
70. Shackleton, M., et al., *Generation of a functional mammary gland from a single stem cell*. Nature, 2006. **439**(7072): p. 84-8.
71. Boulanger, C.A., et al., *Interaction with the mammary microenvironment redirects spermatogenic cell fate in vivo*. Proc Natl Acad Sci U S A, 2007. **104**(10): p. 3871-6.
72. Booth, B.W., et al., *The mammary microenvironment alters the differentiation repertoire of neural stem cells*. Proc Natl Acad Sci U S A, 2008. **105**(39): p. 14891-6.

73. Bussard, K.M., et al., *Reprogramming human cancer cells in the mouse mammary gland*. *Cancer Res*, 2010. **70**(15): p. 6336-43.
74. Jiang, S., et al., *Reconstitution of mammary epithelial morphogenesis by murine embryonic stem cells undergoing hematopoietic stem cell differentiation*. *PLoS One*, 2010. **5**(3): p. e9707.
75. Sakakura, T., Y. Nishizuka, and C.J. Dawe, *Mesenchyme-dependent morphogenesis and epithelium-specific cytodifferentiation in mouse mammary gland*. *Science*, 1976. **194**(4272): p. 1439-41.
76. Darcy, K.M., et al., *Mammary fibroblasts stimulate growth, alveolar morphogenesis, and functional differentiation of normal rat mammary epithelial cells*. *In Vitro Cell Dev Biol Anim*, 2000. **36**(9): p. 578-92.
77. Klaus, S., *Functional differentiation of white and brown adipocytes*. *Bioessays*, 1997. **19**(3): p. 215-23.
78. Girardier, L., Seydoux, J., *Neural Control of Brown Adipose Tissue*. *Brown Adipose Tissue*, ed. P. Trayhurn, Nicholls D. G.,. 1986, London: Arnold Press Ltd. 122-151.
79. Nechad, M., *Structure and development of brown adipose tissue*. *Brown Adipose Tissue*, ed. P. Trayhurn, Nicholls D. G.,. 1986, London: Arnold Press Ltd. 1-30.
80. Gouon-Evans, V. and J.W. Pollard, *Unexpected deposition of brown fat in mammary gland during postnatal development*. *Mol Endocrinol*, 2002. **16**(11): p. 2618-27.
81. Trujillo, M.E. and P.E. Scherer, *Adipose tissue-derived factors: impact on health and disease*. *Endocr Rev*, 2006. **27**(7): p. 762-78.
82. Kalluri, R. and M. Zeisberg, *Fibroblasts in cancer*. *Nat Rev Cancer*, 2006. **6**(5): p. 392-401.
83. Ingman, W.V., et al., *Macrophages promote collagen fibrillogenesis around terminal end buds of the developing mammary gland*. *Dev Dyn*, 2006. **235**(12): p. 3222-9.
84. Cinti, S., et al., *Adipocyte death defines macrophage localization and function in adipose tissue of obese mice and humans*. *J Lipid Res*, 2005. **46**(11): p. 2347-55.
85. Gouon-Evans, V., M.E. Rothenberg, and J.W. Pollard, *Postnatal mammary gland development requires macrophages and eosinophils*. *Development*, 2000. **127**(11): p. 2269-82.
86. Ryan, G.R., et al., *Rescue of the colony-stimulating factor 1 (CSF-1)-nullizygous mouse (Csf1^{op}/Csf1^{op}) phenotype with a CSF-1 transgene and identification of sites of local CSF-1 synthesis*. *Blood*, 2001. **98**(1): p. 74-84.
87. Gouon-Evans, V., E.Y. Lin, and J.W. Pollard, *Requirement of macrophages and eosinophils and their cytokines/chemokines for mammary gland development*. *Breast Cancer Res*, 2002. **4**(4): p. 155-64.
88. Garcia-Zepeda, E.A., et al., *Human eotaxin is a specific chemoattractant for eosinophil cells and provides a new mechanism to explain tissue eosinophilia*. *Nat Med*, 1996. **2**(4): p. 449-56.
89. Lilla, J.N. and Z. Werb, *Mast cells contribute to the stromal microenvironment in mammary gland branching morphogenesis*. *Dev Biol*, 2009. **337**(1): p. 124-33.
90. Metcalfe, D.D., D. Baram, and Y.A. Mekori, *Mast cells*. *Physiol Rev*, 1997. **77**(4): p. 1033-79.

91. Maller, O., H. Martinson, and P. Schedin, *Extracellular matrix composition reveals complex and dynamic stromal-epithelial interactions in the mammary gland*. *J Mammary Gland Biol Neoplasia*, 2010. **15**(3): p. 301-18.
92. Trelstad, R.L., K. Hayashi, and B.P. Toole, *Epithelial collagens and glycosaminoglycans in the embryonic cornea. Macromolecular order and morphogenesis in the basement membrane*. *J Cell Biol*, 1974. **62**(3): p. 815-30.
93. Warburton, M.J., et al., *Distribution of myoepithelial cells and basement membrane proteins in the resting, pregnant, lactating, and involuting rat mammary gland*. *J Histochem Cytochem*, 1982. **30**(7): p. 667-76.
94. Kohling, R., et al., *Nidogen and nidogen-associated basement membrane proteins and neuronal plasticity*. *Neurodegener Dis*, 2006. **3**(1-2): p. 56-61.
95. Hansen, K.C., et al., *An in-solution ultrasonication-assisted digestion method for improved extracellular matrix proteome coverage*. *Mol Cell Proteomics*, 2009. **8**(7): p. 1648-57.
96. Levental, K.R., et al., *Matrix crosslinking forces tumor progression by enhancing integrin signaling*. *Cell*, 2009. **139**(5): p. 891-906.
97. Lorand, L. and R.M. Graham, *Transglutaminases: crosslinking enzymes with pleiotropic functions*. *Nat Rev Mol Cell Biol*, 2003. **4**(2): p. 140-56.
98. Emerman, J.T., et al., *Hormonal effects on intracellular and secreted casein in cultures of mouse mammary epithelial cells on floating collagen membranes*. *Proc Natl Acad Sci U S A*, 1977. **74**(10): p. 4466-70.
99. Nunes, I., et al., *Latent transforming growth factor-beta binding protein domains involved in activation and transglutaminase-dependent cross-linking of latent transforming growth factor-beta*. *J Cell Biol*, 1997. **136**(5): p. 1151-63.
100. Lanigan, F., et al., *Molecular links between mammary gland development and breast cancer*. *Cell Mol Life Sci*, 2007. **64**(24): p. 3159-84.
101. Wipff, P.J., et al., *Myofibroblast contraction activates latent TGF-beta1 from the extracellular matrix*. *J Cell Biol*, 2007. **179**(6): p. 1311-23.
102. Hinck, L. and G.B. Silberstein, *Key stages in mammary gland development: the mammary end bud as a motile organ*. *Breast Cancer Res*, 2005. **7**(6): p. 245-51.
103. Dulbecco, R., M. Henahan, and B. Armstrong, *Cell types and morphogenesis in the mammary gland*. *Proc Natl Acad Sci U S A*, 1982. **79**(23): p. 7346-50.
104. Toole, B.P., et al., *Developmental roles of hyaluronate and chondroitin sulfate proteoglycans*. *Soc Gen Physiol Ser*, 1977. **32**: p. 139-54.
105. Ewald, A.J., et al., *Collective epithelial migration and cell rearrangements drive mammary branching morphogenesis*. *Dev Cell*, 2008. **14**(4): p. 570-81.
106. Lecaudey, V. and D. Gilmour, *Organizing moving groups during morphogenesis*. *Curr Opin Cell Biol*, 2006. **18**(1): p. 102-7.
107. Jacinto, A., et al., *Dynamic actin-based epithelial adhesion and cell matching during *Drosophila* dorsal closure*. *Curr Biol*, 2000. **10**(22): p. 1420-6.
108. Bianco, A., et al., *Two distinct modes of guidance signalling during collective migration of border cells*. *Nature*, 2007. **448**(7151): p. 362-5.
109. Gordon, J.R. and M.R. Bernfield, *The basal lamina of the postnatal mammary epithelium contains glycosaminoglycans in a precise ultrastructural organization*. *Dev Biol*, 1980. **74**(1): p. 118-35.
110. Nelson, C.M., et al., *Tissue geometry determines sites of mammary branching morphogenesis in organotypic cultures*. *Science*, 2006. **314**(5797): p. 298-300.

111. Kalluri, R. and E.G. Neilson, *Epithelial-mesenchymal transition and its implications for fibrosis*. J Clin Invest, 2003. **112**(12): p. 1776-84.
112. Affolter, M., et al., *Tube or not tube: remodeling epithelial tissues by branching morphogenesis*. Dev Cell, 2003. **4**(1): p. 11-8.
113. Morris, J.S., et al., *Involvement of axonal guidance proteins and their signaling partners in the developing mouse mammary gland*. J Cell Physiol, 2006. **206**(1): p. 16-24.
114. Wiseman, B.S. and Z. Werb, *Stromal effects on mammary gland development and breast cancer*. Science, 2002. **296**(5570): p. 1046-9.
115. Ghabrial, A., et al., *Branching morphogenesis of the Drosophila tracheal system*. Annu Rev Cell Dev Biol, 2003. **19**: p. 623-47.
116. Uv, A., R. Cantera, and C. Samakovlis, *Drosophila tracheal morphogenesis: intricate cellular solutions to basic plumbing problems*. Trends Cell Biol, 2003. **13**(6): p. 301-9.
117. Srinivasan, K., et al., *Netrin-1/neogenin interaction stabilizes multipotent progenitor cap cells during mammary gland morphogenesis*. Dev Cell, 2003. **4**(3): p. 371-82.
118. Jackson-Fisher, A.J., et al., *ErbB2 is required for ductal morphogenesis of the mammary gland*. Proc Natl Acad Sci U S A, 2004. **101**(49): p. 17138-43.
119. Jackson-Fisher, A.J., et al., *ErbB3 is required for ductal morphogenesis in the mouse mammary gland*. Breast Cancer Res, 2008. **10**(6): p. R96.
120. Kennedy, T.E., *Cellular mechanisms of netrin function: long-range and short-range actions*. Biochem Cell Biol, 2000. **78**(5): p. 569-75.
121. Miettinen, M., et al., *Estrogen metabolism as a regulator of estrogen action in the mammary gland*. J Mammary Gland Biol Neoplasia, 2000. **5**(3): p. 259-70.
122. Pasqualini, J.R. and G. Chetrite, *The anti-aromatase effect of progesterone and of its natural metabolites 20alpha- and 5alpha-dihydroprogesterone in the MCF-7aro breast cancer cell line*. Anticancer Res, 2008. **28**(4B): p. 2129-33.
123. Robinson, G.W., L. Hennighausen, and P.F. Johnson, *Side-branching in the mammary gland: the progesterone-Wnt connection*. Genes Dev, 2000. **14**(8): p. 889-94.
124. Lyons, W.R., *Hormonal synergism in mammary growth*. Proc R Soc Lond B Biol Sci, 1958. **149**(936): p. 303-25.
125. Nandi, S., *Endocrine control of mammary gland development and function in the C3H/ He Crgl mouse*. J Natl Cancer Inst, 1958. **21**(6): p. 1039-63.
126. Daniel, C.W., Silberstein, G. B., *Postnatal Development of Rodent Mammary Gland*. The Mammary Gland. Development. Regulation and Function, ed. D.C.W. Neville M. C. 1987, New York and London: Plenum Press. 3-36.
127. Silberstein, G.B., et al., *Essential role of endogenous estrogen in directly stimulating mammary growth demonstrated by implants containing pure antiestrogens*. Endocrinology, 1994. **134**(1): p. 84-90.
128. Shyamala, G. and A. Ferenczy, *Mammary fat pad may be a potential site for initiation of estrogen action in normal mouse mammary glands*. Endocrinology, 1984. **115**(3): p. 1078-81.
129. Bocchinfuso, W.P. and K.S. Korach, *Mammary gland development and tumorigenesis in estrogen receptor knockout mice*. J Mammary Gland Biol Neoplasia, 1997. **2**(4): p. 323-34.

130. Daniel, C.W., G.B. Silberstein, and P. Strickland, *Direct action of 17 beta-estradiol on mouse mammary ducts analyzed by sustained release implants and steroid autoradiography*. *Cancer Res*, 1987. **47**(22): p. 6052-7.
131. Couse, J.F. and K.S. Korach, *Estrogen receptor null mice: what have we learned and where will they lead us?* *Endocr Rev*, 1999. **20**(3): p. 358-417.
132. Cunha, G.R., et al., *Elucidation of a role for stromal steroid hormone receptors in mammary gland growth and development using tissue recombinants*. *J Mammary Gland Biol Neoplasia*, 1997. **2**(4): p. 393-402.
133. Mallepell, S., et al., *Paracrine signaling through the epithelial estrogen receptor alpha is required for proliferation and morphogenesis in the mammary gland*. *Proc Natl Acad Sci U S A*, 2006. **103**(7): p. 2196-201.
134. Grimm, S.L. and J.M. Rosen, *Stop! In the name of transforming growth factor-beta: keeping estrogen receptor-alpha-positive mammary epithelial cells from proliferating*. *Breast Cancer Res*, 2006. **8**(4): p. 106.
135. Atwood, C.S., et al., *Progesterone induces side-branching of the ductal epithelium in the mammary glands of peripubertal mice*. *J Endocrinol*, 2000. **167**(1): p. 39-52.
136. Brisken, C., et al., *A paracrine role for the epithelial progesterone receptor in mammary gland development*. *Proc Natl Acad Sci U S A*, 1998. **95**(9): p. 5076-81.
137. Humphreys, R.C., et al., *Use of PRKO mice to study the role of progesterone in mammary gland development*. *J Mammary Gland Biol Neoplasia*, 1997. **2**(4): p. 343-54.
138. Conneely, O.M., et al., *Reproductive functions of the progesterone receptor isoforms: lessons from knock-out mice*. *Mol Cell Endocrinol*, 2001. **179**(1-2): p. 97-103.
139. Bresciani, F., *Topography of DNA synthesis in the mammary gland of the C3H mouse and its control by ovarian hormones: An autoradiographic study*. *Cell and Tissue Kinetics*, 1968. **1**: p. 51-63.
140. Haslam, S.Z., *Progesterone effects on deoxyribonucleic acid synthesis in normal mouse mammary glands*. *Endocrinology*, 1988. **122**(2): p. 464-70.
141. Ruan, W., M.E. Monaco, and D.L. Kleinberg, *Progesterone stimulates mammary gland ductal morphogenesis by synergizing with and enhancing insulin-like growth factor-I action*. *Endocrinology*, 2005. **146**(3): p. 1170-8.
142. Doppler, W., B. Groner, and R.K. Ball, *Prolactin and glucocorticoid hormones synergistically induce expression of transfected rat beta-casein gene promoter constructs in a mammary epithelial cell line*. *Proc Natl Acad Sci U S A*, 1989. **86**(1): p. 104-8.
143. Kellendonk, C., et al., *Mutagenesis of the glucocorticoid receptor in mice*. *J Steroid Biochem Mol Biol*, 1999. **69**(1-6): p. 253-9.
144. Reichardt, H.M., et al., *Mammary gland development and lactation are controlled by different glucocorticoid receptor activities*. *Eur J Endocrinol*, 2001. **145**(4): p. 519-27.
145. Kingsley-Kallesen, M., et al., *The mineralocorticoid receptor may compensate for the loss of the glucocorticoid receptor at specific stages of mammary gland development*. *Mol Endocrinol*, 2002. **16**(9): p. 2008-18.
146. Ilkbahar, Y.N., et al., *Differential expression of the growth hormone receptor and growth hormone-binding protein in epithelia and stroma of the mouse mammary gland at various physiological stages*. *J Endocrinol*, 1999. **161**(1): p. 77-87.

147. Feldman, M., et al., *Evidence that the growth hormone receptor mediates differentiation and development of the mammary gland*. *Endocrinology*, 1993. **133**(4): p. 1602-8.
148. Kleinberg, D.L., *Early mammary development: growth hormone and IGF-1*. *J Mammary Gland Biol Neoplasia*, 1997. **2**(1): p. 49-57.
149. Gallego, M.I., et al., *Prolactin, growth hormone, and epidermal growth factor activate Stat5 in different compartments of mammary tissue and exert different and overlapping developmental effects*. *Dev Biol*, 2001. **229**(1): p. 163-75.
150. Wysolmerski, J.J., et al., *Overexpression of parathyroid hormone-related protein or parathyroid hormone in transgenic mice impairs branching morphogenesis during mammary gland development*. *Development*, 1995. **121**(11): p. 3539-47.
151. Dunbar, M.E., et al., *Temporally regulated overexpression of parathyroid hormone-related protein in the mammary gland reveals distinct fetal and pubertal phenotypes*. *J Endocrinol*, 2001. **171**(3): p. 403-16.
152. Zinser, G., K. Packman, and J. Welsh, *Vitamin D(3) receptor ablation alters mammary gland morphogenesis*. *Development*, 2002. **129**(13): p. 3067-76.
153. Welsh, J., et al., *Vitamin D-3 receptor as a target for breast cancer prevention*. *J Nutr*, 2003. **133**(7 Suppl): p. 2425S-2433S.
154. Hynes, N.E. and C.J. Watson, *Mammary gland growth factors: roles in normal development and in cancer*. *Cold Spring Harb Perspect Biol*, 2010. **2**(8): p. a003186.
155. Schwertfeger, K.L., *Fibroblast growth factors in development and cancer: insights from the mammary and prostate glands*. *Curr Drug Targets*, 2009. **10**(7): p. 632-44.
156. Ngan, E.S., et al., *Inducible expression of FGF-3 in mouse mammary gland*. *Proc Natl Acad Sci U S A*, 2002. **99**(17): p. 11187-92.
157. Mansour, S.L., J.M. Goddard, and M.R. Capecchi, *Mice homozygous for a targeted disruption of the proto-oncogene int-2 have developmental defects in the tail and inner ear*. *Development*, 1993. **117**(1): p. 13-28.
158. Astigiano, S., P. Damonte, and O. Barbieri, *Inhibition of ductal morphogenesis in the mammary gland of WAP -fgf4 transgenic mice*. *Anat Embryol (Berl)*, 2003. **206**(6): p. 471-8.
159. Parsa, S., et al., *Terminal end bud maintenance in mammary gland is dependent upon FGFR2b signaling*. *Dev Biol*, 2008. **317**(1): p. 121-31.
160. Lu, P., et al., *Genetic mosaic analysis reveals FGF receptor 2 function in terminal end buds during mammary gland branching morphogenesis*. *Dev Biol*, 2008. **321**(1): p. 77-87.
161. Metzger, R.J. and M.A. Krasnow, *Genetic control of branching morphogenesis*. *Science*, 1999. **284**(5420): p. 1635-9.
162. Yang, Y., et al., *Sequential requirement of hepatocyte growth factor and neuregulin in the morphogenesis and differentiation of the mammary gland*. *J Cell Biol*, 1995. **131**(1): p. 215-26.
163. Yant, J., et al., *In vivo effects of hepatocyte growth factor/scatter factor on mouse mammary gland development*. *Exp Cell Res*, 1998. **241**(2): p. 476-81.
164. Zhang, H.Z., et al., *Estrogen mediates mammary epithelial cell proliferation in serum-free culture indirectly via mammary stroma-derived hepatocyte growth factor*. *Endocrinology*, 2002. **143**(9): p. 3427-34.

165. Accornero, P., et al., *Epidermal growth factor and hepatocyte growth factor receptors collaborate to induce multiple biological responses in bovine mammary epithelial cells*. J Dairy Sci, 2009. **92**(8): p. 3667-75.
166. Kleinberg, D.L., et al., *Non-lactogenic effects of growth hormone on growth and insulin-like growth factor-I messenger ribonucleic acid of rat mammary gland*. Endocrinology, 1990. **126**(6): p. 3274-6.
167. Ruan, W., et al., *Estradiol enhances the stimulatory effect of insulin-like growth factor-I (IGF-I) on mammary development and growth hormone-induced IGF-I messenger ribonucleic acid*. Endocrinology, 1995. **136**(3): p. 1296-302.
168. Ruan, W., C.B. Newman, and D.L. Kleinberg, *Intact and amino-terminally shortened forms of insulin-like growth factor I induce mammary gland differentiation and development*. Proc Natl Acad Sci U S A, 1992. **89**(22): p. 10872-6.
169. Loladze, A.V., et al., *Epithelial-specific and stage-specific functions of insulin-like growth factor-I during postnatal mammary development*. Endocrinology, 2006. **147**(11): p. 5412-23.
170. Ruan, W. and D.L. Kleinberg, *Insulin-like growth factor I is essential for terminal end bud formation and ductal morphogenesis during mammary development*. Endocrinology, 1999. **140**(11): p. 5075-81.
171. Bonnette, S.G. and D.L. Hadsell, *Targeted disruption of the IGF-I receptor gene decreases cellular proliferation in mammary terminal end buds*. Endocrinology, 2001. **142**(11): p. 4937-45.
172. Bergers, G. and L.M. Coussens, *Extrinsic regulators of epithelial tumor progression: metalloproteinases*. Curr Opin Genet Dev, 2000. **10**(1): p. 120-7.
173. Sanderson, M.P., P.J. Dempsey, and A.J. Dunbar, *Control of ErbB signaling through metalloprotease mediated ectodomain shedding of EGF-like factors*. Growth Factors, 2006. **24**(2): p. 121-36.
174. Hynes, N.E. and H.A. Lane, *ERBB receptors and cancer: the complexity of targeted inhibitors*. Nat Rev Cancer, 2005. **5**(5): p. 341-54.
175. Coleman, S., G.B. Silberstein, and C.W. Daniel, *Ductal morphogenesis in the mouse mammary gland: evidence supporting a role for epidermal growth factor*. Dev Biol, 1988. **127**(2): p. 304-15.
176. Xie, W., et al., *Targeted expression of a dominant negative epidermal growth factor receptor in the mammary gland of transgenic mice inhibits pubertal mammary duct development*. Mol Endocrinol, 1997. **11**(12): p. 1766-81.
177. Wiesen, J.F., et al., *Signaling through the stromal epidermal growth factor receptor is necessary for mammary ductal development*. Development, 1999. **126**(2): p. 335-44.
178. Ankrapp, D.P., J.M. Bennett, and S.Z. Haslam, *Role of epidermal growth factor in the acquisition of ovarian steroid hormone responsiveness in the normal mouse mammary gland*. J Cell Physiol, 1998. **174**(2): p. 251-60.
179. Luetkeke, N.C., et al., *Targeted inactivation of the EGF and amphiregulin genes reveals distinct roles for EGF receptor ligands in mouse mammary gland development*. Development, 1999. **126**(12): p. 2739-50.
180. Kenney, N.J., et al., *Detection and location of amphiregulin and Cripto-1 expression in the developing postnatal mouse mammary gland*. Mol Reprod Dev, 1995. **41**(3): p. 277-86.
181. Ciarloni, L., S. Mallepell, and C. Briskin, *Amphiregulin is an essential mediator of estrogen receptor alpha function in mammary gland development*. Proc Natl Acad Sci U S A, 2007. **104**(13): p. 5455-60.

182. Hinkle, C.L., et al., *Selective roles for tumor necrosis factor alpha-converting enzyme/ADAM17 in the shedding of the epidermal growth factor receptor ligand family: the juxtamembrane stalk determines cleavage efficiency*. J Biol Chem, 2004. **279**(23): p. 24179-88.
183. Sternlicht, M.D., et al., *Mammary ductal morphogenesis requires paracrine activation of stromal EGFR via ADAM17-dependent shedding of epithelial amphiregulin*. Development, 2005. **132**(17): p. 3923-33.
184. Andrechek, E.R., D. White, and W.J. Muller, *Targeted disruption of ErbB2/Neu in the mammary epithelium results in impaired ductal outgrowth*. Oncogene, 2005. **24**(5): p. 932-7.
185. Muraoka-Cook, R.S., et al., *ErbB4/HER4: role in mammary gland development, differentiation and growth inhibition*. J Mammary Gland Biol Neoplasia, 2008. **13**(2): p. 235-46.
186. McNally, S. and F. Martin, *Molecular regulators of pubertal mammary gland development*. Ann Med, 2011. **43**(3): p. 212-34.
187. Tidcombe, H., et al., *Neural and mammary gland defects in ErbB4 knockout mice genetically rescued from embryonic lethality*. Proc Natl Acad Sci U S A, 2003. **100**(14): p. 8281-6.
188. Edwards, D.P., *The role of coactivators and corepressors in the biology and mechanism of action of steroid hormone receptors*. J Mammary Gland Biol Neoplasia, 2000. **5**(3): p. 307-24.
189. Xu, J., et al., *Partial hormone resistance in mice with disruption of the steroid receptor coactivator-1 (SRC-1) gene*. Science, 1998. **279**(5358): p. 1922-5.
190. Xu, J., et al., *The steroid receptor coactivator SRC-3 (p/CIP/RAC3/AIB1/ACTR/TRAM-1) is required for normal growth, puberty, female reproductive function, and mammary gland development*. Proc Natl Acad Sci U S A, 2000. **97**(12): p. 6379-84.
191. Han, S.J., et al., *Steroid receptor coactivator (SRC)-1 and SRC-3 differentially modulate tissue-specific activation functions of the progesterone receptor*. Mol Endocrinol, 2006. **20**(1): p. 45-55.
192. Mukherjee, A., et al., *Steroid receptor coactivator 2 is required for female fertility and mammary morphogenesis: insights from the mouse, relevance to the human*. Nucl Recept Signal, 2007. **5**: p. e011.
193. Howlin, J., et al., *CITED1 homozygous null mice display aberrant pubertal mammary ductal morphogenesis*. Oncogene, 2006. **25**(10): p. 1532-42.
194. McBryan, J., et al., *ERalpha-CITED1 co-regulated genes expressed during pubertal mammary gland development: implications for breast cancer prognosis*. Oncogene, 2007. **26**(44): p. 6406-19.
195. Shen, Q., et al., *The AP-1 transcription factor regulates postnatal mammary gland development*. Dev Biol, 2006. **295**(2): p. 589-603.
196. Kornberg, R.D., *Mediator and the mechanism of transcriptional activation*. Trends Biochem Sci, 2005. **30**(5): p. 235-9.
197. Jiang, P., et al., *Key roles for MED1 LxxLL motifs in pubertal mammary gland development and luminal-cell differentiation*. Proc Natl Acad Sci U S A, 2010. **107**(15): p. 6765-70.
198. Bagheri-Yarmand, R., et al., *Metastasis-associated protein 1 deregulation causes inappropriate mammary gland development and tumorigenesis*. Development, 2004. **131**(14): p. 3469-79.

199. Grimm, S.L. and J.M. Rosen, *The role of C/EBPbeta in mammary gland development and breast cancer*. J Mammary Gland Biol Neoplasia, 2003. 8(2): p. 191-204.
200. Robinson, G.W., et al., *The C/EBPbeta transcription factor regulates epithelial cell proliferation and differentiation in the mammary gland*. Genes Dev, 1998. 12(12): p. 1907-16.
201. Seagroves, T.N., et al., *C/EBPbeta, but not C/EBPalpha, is essential for ductal morphogenesis, lobuloalveolar proliferation, and functional differentiation in the mouse mammary gland*. Genes Dev, 1998. 12(12): p. 1917-28.
202. Kouros-Mehr, H., et al., *GATA-3 maintains the differentiation of the luminal cell fate in the mammary gland*. Cell, 2006. 127(5): p. 1041-55.
203. Jager, R., et al., *Loss of transcription factor AP-2gamma/TFAP2C impairs branching morphogenesis of the murine mammary gland*. Dev Dyn, 2010. 239(3): p. 1027-33.
204. Massague, J. and R.R. Gomis, *The logic of TGFbeta signaling*. FEBS Lett, 2006. 580(12): p. 2811-20.
205. Wrana, J.L., et al., *Mechanism of activation of the TGF-beta receptor*. Nature, 1994. 370(6488): p. 341-7.
206. Robinson, S.D., et al., *Regulated expression and growth inhibitory effects of transforming growth factor-beta isoforms in mouse mammary gland development*. Development, 1991. 113(3): p. 867-78.
207. Daniel, C.W. and S.D. Robinson, *Regulation of mammary growth and function by TGF-beta*. Mol Reprod Dev, 1992. 32(2): p. 145-51.
208. Silberstein, G.B., et al., *Epithelium-dependent extracellular matrix synthesis in transforming growth factor-beta 1-growth-inhibited mouse mammary gland*. J Cell Biol, 1990. 110(6): p. 2209-19.
209. Pierce, D.F., Jr., et al., *Inhibition of mammary duct development but not alveolar outgrowth during pregnancy in transgenic mice expressing active TGF-beta 1*. Genes Dev, 1993. 7(12A): p. 2308-17.
210. Joseph, H., et al., *Overexpression of a kinase-deficient transforming growth factor-beta type II receptor in mouse mammary stroma results in increased epithelial branching*. Mol Biol Cell, 1999. 10(4): p. 1221-34.
211. Ewan, K.B., et al., *Latent transforming growth factor-beta activation in mammary gland: regulation by ovarian hormones affects ductal and alveolar proliferation*. Am J Pathol, 2002. 160(6): p. 2081-93.
212. Kulkarni, A.B., et al., *Transforming growth factor beta 1 null mutation in mice causes excessive inflammatory response and early death*. Proc Natl Acad Sci U S A, 1993. 90(2): p. 770-4.
213. Ingman, W.V. and S.A. Robertson, *Mammary gland development in transforming growth factor beta1 null mutant mice: systemic and epithelial effects*. Biol Reprod, 2008. 79(4): p. 711-7.
214. Ewan, K.B., et al., *Proliferation of estrogen receptor-alpha-positive mammary epithelial cells is restrained by transforming growth factor-beta1 in adult mice*. Am J Pathol, 2005. 167(2): p. 409-17.
215. Kamalati, T., et al., *HGF/SF in mammary epithelial growth and morphogenesis: in vitro and in vivo models*. J Mammary Gland Biol Neoplasia, 1999. 4(1): p. 69-77.

216. Robinson, G.W. and L. Hennighausen, *Inhibins and activins regulate mammary epithelial cell differentiation through mesenchymal-epithelial interactions*. Development, 1997. **124**(14): p. 2701-8.
217. Kenney, N.J., H.B. Adkins, and M. Sanicola, *Nodal and Cripto-1: embryonic pattern formation genes involved in mammary gland development and tumorigenesis*. J Mammary Gland Biol Neoplasia, 2004. **9**(2): p. 133-44.
218. Phippard, D.J., et al., *Regulation of Msx-1, Msx-2, Bmp-2 and Bmp-4 during foetal and postnatal mammary gland development*. Development, 1996. **122**(9): p. 2729-37.
219. Montesano, R., R. Sarkozi, and H. Schramek, *Bone morphogenetic protein-4 strongly potentiates growth factor-induced proliferation of mammary epithelial cells*. Biochem Biophys Res Commun, 2008. **374**(1): p. 164-8.
220. Wiktor-Jedrzejczak, W., et al., *Total absence of colony-stimulating factor 1 in the macrophage-deficient osteopetrotic (op/op) mouse*. Proc Natl Acad Sci U S A, 1990. **87**(12): p. 4828-32.
221. Nagle, D.L., et al., *Physical mapping of the Tec and Gabrb1 loci reveals that the Wsh mutation on mouse chromosome 5 is associated with an inversion*. Hum Mol Genet, 1995. **4**(11): p. 2073-9.
222. Duttlinger, R., et al., *W-sash affects positive and negative elements controlling c-kit expression: ectopic c-kit expression at sites of kit-ligand expression affects melanogenesis*. Development, 1993. **118**(3): p. 705-17.
223. Couldrey, C., et al., *Adipose tissue: a vital in vivo role in mammary gland development but not differentiation*. Dev Dyn, 2002. **223**(4): p. 459-68.
224. Landskroner-Eiger, S., et al., *Morphogenesis of the developing mammary gland: Stage-dependent impact of adipocytes*. Dev Biol, 2010. **344**(2): p. 968-978.
225. Berger, J.J. and C.W. Daniel, *Stromal DNA synthesis is stimulated by young, but not serially aged, mouse mammary epithelium*. Mech Ageing Dev, 1983. **23**(3-4): p. 277-84.
226. Streuli, C.H. and G.M. Edwards, *Control of normal mammary epithelial phenotype by integrins*. J Mammary Gland Biol Neoplasia, 1998. **3**(2): p. 151-63.
227. Klinowska, T.C., et al., *Laminin and beta1 integrins are crucial for normal mammary gland development in the mouse*. Dev Biol, 1999. **215**(1): p. 13-32.
228. Paszek, M.J., et al., *Tensional homeostasis and the malignant phenotype*. Cancer Cell, 2005. **8**(3): p. 241-54.
229. Chen, J., et al., *The alpha(2) integrin subunit-deficient mouse: a multifaceted phenotype including defects of branching morphogenesis and hemostasis*. Am J Pathol, 2002. **161**(1): p. 337-44.
230. Simian, M., et al., *The interplay of matrix metalloproteinases, morphogens and growth factors is necessary for branching of mammary epithelial cells*. Development, 2001. **128**(16): p. 3117-31.
231. Sakai, T., M. Larsen, and K.M. Yamada, *Fibronectin requirement in branching morphogenesis*. Nature, 2003. **423**(6942): p. 876-81.
232. Liu, K., et al., *Conditional knockout of fibronectin abrogates mouse mammary gland lobuloalveolar differentiation*. Dev Biol, 2010. **346**(1): p. 11-24.
233. Saga, Y., et al., *Mice develop normally without tenascin*. Genes Dev, 1992. **6**(10): p. 1821-31.
234. Green, K.A. and L.R. Lund, *ECM degrading proteases and tissue remodelling in the mammary gland*. Bioessays, 2005. **27**(9): p. 894-903.

235. Wiseman, B.S., et al., *Site-specific inductive and inhibitory activities of MMP-2 and MMP-3 orchestrate mammary gland branching morphogenesis*. J Cell Biol, 2003. **162**(6): p. 1123-33.
236. Sympon, C.J., et al., *Targeted expression of stromelysin-1 in mammary gland provides evidence for a role of proteinases in branching morphogenesis and the requirement for an intact basement membrane for tissue-specific gene expression*. J Cell Biol, 1994. **125**(3): p. 681-93.
237. Witty, J.P., J.H. Wright, and L.M. Matrisian, *Matrix metalloproteinases are expressed during ductal and alveolar mammary morphogenesis, and misregulation of stromelysin-1 in transgenic mice induces unscheduled alveolar development*. Mol Biol Cell, 1995. **6**(10): p. 1287-303.
238. Lee, P.P., et al., *Functional significance of MMP-9 in tumor necrosis factor-induced proliferation and branching morphogenesis of mammary epithelial cells*. Endocrinology, 2000. **141**(10): p. 3764-73.
239. Fata, J.E., et al., *Timp-1 is important for epithelial proliferation and branching morphogenesis during mouse mammary development*. Dev Biol, 1999. **211**(2): p. 238-54.
240. Andres, A.C. and A. Ziemiecki, *Eph and ephrin signaling in mammary gland morphogenesis and cancer*. J Mammary Gland Biol Neoplasia, 2003. **8**(4): p. 475-85.
241. Nikolova, Z., et al., *Cell-type specific and estrogen dependent expression of the receptor tyrosine kinase EphB4 and its ligand ephrin-B2 during mammary gland morphogenesis*. J Cell Sci, 1998. **111** (Pt 18): p. 2741-51.
242. Munarini, N., et al., *Altered mammary epithelial development, pattern formation and involution in transgenic mice expressing the EphB4 receptor tyrosine kinase*. J Cell Sci, 2002. **115**(Pt 1): p. 25-37.
243. Crowley, M.R., et al., *The mouse mammary gland requires the actin-binding protein gelsolin for proper ductal morphogenesis*. Dev Biol, 2000. **225**(2): p. 407-23.
244. Mailleux, A.A., et al., *BIM regulates apoptosis during mammary ductal morphogenesis, and its absence reveals alternative cell death mechanisms*. Dev Cell, 2007. **12**(2): p. 221-34.
245. Ensslin, M.A. and B.D. Shur, *The EGF repeat and discoidin domain protein, SED1/MFG-E8, is required for mammary gland branching morphogenesis*. Proc Natl Acad Sci U S A, 2007. **104**(8): p. 2715-20.
246. Fathers, K.E., et al., *Crkl transgene induces atypical mammary gland development and tumorigenesis*. Am J Pathol, 2010. **176**(1): p. 446-60.
247. Gabig, M. and G. Wegrzyn, *An introduction to DNA chips: principles, technology, applications and analysis*. Acta Biochim Pol, 2001. **48**(3): p. 615-22.
248. Kuperwasser, C., et al., *Reconstruction of functionally normal and malignant human breast tissues in mice*. Proc Natl Acad Sci U S A, 2004. **101**(14): p. 4966-71.
249. Schena, M., et al., *Quantitative monitoring of gene expression patterns with a complementary DNA microarray*. Science, 1995. **270**(5235): p. 467-70.
250. Duggan, D.J., et al., *Expression profiling using cDNA microarrays*. Nat Genet, 1999. **21**(1 Suppl): p. 10-4.
251. Miller, M.B. and Y.W. Tang, *Basic concepts of microarrays and potential applications in clinical microbiology*. Clin Microbiol Rev, 2009. **22**(4): p. 611-33.

252. Cheung, V.G., et al., *Making and reading microarrays*. Nat Genet, 1999. **21**(1 Suppl): p. 15-9.
253. Dalma-Weiszhausz, D.D., et al., *The affymetrix GeneChip platform: an overview*. Methods Enzymol, 2006. **410**: p. 3-28.
254. Oliphant, A., et al., *BeadArray technology: enabling an accurate, cost-effective approach to high-throughput genotyping*. Biotechniques, 2002. **Suppl**: p. 56-8, 60-1.
255. Sosnowski, R.G., et al., *Rapid determination of single base mismatch mutations in DNA hybrids by direct electric field control*. Proc Natl Acad Sci U S A, 1997. **94**(4): p. 1119-23.
256. Kouros-Mehr, H. and Z. Werb, *Candidate regulators of mammary branching morphogenesis identified by genome-wide transcript analysis*. Dev Dyn, 2006. **235**(12): p. 3404-12.
257. Deroo, B.J., et al., *Profile of estrogen-responsive genes in an estrogen-specific mammary gland outgrowth model*. Mol Reprod Dev, 2009. **76**(8): p. 733-50.
258. Master, S.R., et al., *Functional microarray analysis of mammary organogenesis reveals a developmental role in adaptive thermogenesis*. Mol Endocrinol, 2002. **16**(6): p. 1185-203.
259. Morris, J.S., et al., *Proteomic analysis of mouse mammary terminal end buds identifies axonal growth cone proteins*. Proteomics, 2004. **4**(6): p. 1802-10.
260. Mucenski, M.L., et al., *beta-Catenin is required for specification of proximal/distal cell fate during lung morphogenesis*. J Biol Chem, 2003. **278**(41): p. 40231-8.
261. Li, C., et al., *Wnt5a participates in distal lung morphogenesis*. Dev Biol, 2002. **248**(1): p. 68-81.
262. Lewis, M.T., et al., *Defects in mouse mammary gland development caused by conditional haploinsufficiency of Patched-1*. Development, 1999. **126**(22): p. 5181-93.
263. Zhang, J. and S. Hughes, *Role of the ephrin and Eph receptor tyrosine kinase families in angiogenesis and development of the cardiovascular system*. J Pathol, 2006. **208**(4): p. 453-61.
264. Huber, M.A., N. Kraut, and H. Beug, *Molecular requirements for epithelial-mesenchymal transition during tumor progression*. Curr Opin Cell Biol, 2005. **17**(5): p. 548-58.
265. Okabe, M., et al., *'Green mice' as a source of ubiquitous green cells*. FEBS Lett, 1997. **407**(3): p. 313-9.
266. Sicot, F.X., et al., *Fibulin-2 is dispensable for mouse development and elastic fiber formation*. Mol Cell Biol, 2008. **28**(3): p. 1061-7.
267. Bolstad B, M., Comparing the effects of background, normalization and summarization of gene expression estimates. <http://stat/www.berkeley.edu/users/>, 2002.
268. Bengtsson, H., et al., *Estimation and assessment of raw copy numbers at the single locus level*. Bioinformatics, 2008. **24**(6): p. 759-67.
269. Mutch, D.M., et al., *The limit fold change model: a practical approach for selecting differentially expressed genes from microarray data*. BMC Bioinformatics, 2002. **3**: p. 17.
270. Taube, J.H., et al., *Core epithelial-to-mesenchymal transition interactome gene-expression signature is associated with claudin-low and metaplastic breast cancer subtypes*. Proc Natl Acad Sci U S A, 2010. **107**(35): p. 15449-54.

271. Tang, S., H. Han, and V.B. Bajic, *ERGDB: Estrogen Responsive Genes Database*. Nucleic Acids Res, 2004. **32**(Database issue): p. D533-6.
272. Yang, J., et al., *Twist, a master regulator of morphogenesis, plays an essential role in tumor metastasis*. Cell, 2004. **117**(7): p. 927-39.
273. Carver, E.A., et al., *The mouse snail gene encodes a key regulator of the epithelial-mesenchymal transition*. Mol Cell Biol, 2001. **21**(23): p. 8184-8.
274. Savagner, P., K.M. Yamada, and J.P. Thiery, *The zinc-finger protein slug causes desmosome dissociation, an initial and necessary step for growth factor-induced epithelial-mesenchymal transition*. J Cell Biol, 1997. **137**(6): p. 1403-19.
275. Vandewalle, C., et al., *SIP1/ZEB2 induces EMT by repressing genes of different epithelial cell-cell junctions*. Nucleic Acids Res, 2005. **33**(20): p. 6566-78.
276. Hartwell, K.A., et al., *The Spemann organizer gene, Goosecoid, promotes tumor metastasis*. Proc Natl Acad Sci U S A, 2006. **103**(50): p. 18969-74.
277. Polyak, K. and R.A. Weinberg, *Transitions between epithelial and mesenchymal states: acquisition of malignant and stem cell traits*. Nat Rev Cancer, 2009. **9**(4): p. 265-73.
278. LaGamba, D., A. Nawshad, and E.D. Hay, *Microarray analysis of gene expression during epithelial-mesenchymal transformation*. Dev Dyn, 2005. **234**(1): p. 132-42.
279. Mani, S.A., et al., *Mesenchyme Forkhead 1 (FOXC2) plays a key role in metastasis and is associated with aggressive basal-like breast cancers*. Proc Natl Acad Sci U S A, 2007. **104**(24): p. 10069-74.
280. Burdsal, C.A., C.H. Damsky, and R.A. Pedersen, *The role of E-cadherin and integrins in mesoderm differentiation and migration at the mammalian primitive streak*. Development, 1993. **118**(3): p. 829-44.
281. Piekny, A.J. and M. Glotzer, *Anillin is a scaffold protein that links RhoA, actin, and myosin during cytokinesis*. Curr Biol, 2008. **18**(1): p. 30-6.
282. Zhao, W.M. and G. Fang, *Anillin is a substrate of anaphase-promoting complex/cyclosome (APC/C) that controls spatial contractility of myosin during late cytokinesis*. J Biol Chem, 2005. **280**(39): p. 33516-24.
283. Suzuki, C., et al., *ANLN plays a critical role in human lung carcinogenesis through the activation of RHOA and by involvement in the phosphoinositide 3-kinase/AKT pathway*. Cancer Res, 2005. **65**(24): p. 11314-25.
284. Nguyen, H.G., et al., *Deregulated Aurora-B induced tetraploidy promotes tumorigenesis*. Faseb J, 2009. **23**(8): p. 2741-8.
285. Vischioni, B., et al., *Frequent overexpression of aurora B kinase, a novel drug target, in non-small cell lung carcinoma patients*. Mol Cancer Ther, 2006. **5**(11): p. 2905-13.
286. Boidot, R., et al., *The expression of BIRC5 is correlated with loss of specific chromosomal regions in breast carcinomas*. Genes Chromosomes Cancer, 2008. **47**(4): p. 299-308.
287. Monzo, M., et al., *A novel anti-apoptosis gene: Re-expression of survivin messenger RNA as a prognosis marker in non-small-cell lung cancers*. J Clin Oncol, 1999. **17**(7): p. 2100-4.
288. Alajez, N.M., et al., *MiR-218 suppresses nasopharyngeal cancer progression through downregulation of survivin and the SLIT2-ROBO1 pathway*. Cancer Res. **71**(6): p. 2381-91.

289. Jeganathan, K., et al., *Bub1 mediates cell death in response to chromosome missegregation and acts to suppress spontaneous tumorigenesis*. J Cell Biol, 2007. **179**(2): p. 255-67.
290. Williams, G.L., T.M. Roberts, and O.V. Gjoerup, *Bub1: escapades in a cellular world*. Cell Cycle, 2007. **6**(14): p. 1699-704.
291. Yu, H. and Z. Tang, *Bub1 multitasking in mitosis*. Cell Cycle, 2005. **4**(2): p. 262-5.
292. Davenport, J.W., et al., *The mouse mitotic checkpoint gene bub1b, a novel bub1 family member, is expressed in a cell cycle-dependent manner*. Genomics, 1999. **55**(1): p. 113-7.
293. Husdal, A., G. Bukholm, and I.R. Bukholm, *The prognostic value and overexpression of cyclin A is correlated with gene amplification of both cyclin A and cyclin E in breast cancer patient*. Cell Oncol, 2006. **28**(3): p. 107-16.
294. Coates, P., J. Dewar, and A.M. Thompson, *At last, a predictive and prognostic marker for radiotherapy?* Breast Cancer Res, 2010. **12**(3): p. 106.
295. Gudmundsson, K.O., et al., *Gene expression analysis of hematopoietic progenitor cells identifies Dlg7 as a potential stem cell gene*. Stem Cells, 2007. **25**(6): p. 1498-506.
296. Naim, E., et al., *Mutagenesis of the epithelial polarity gene, discs large 1, perturbs nephrogenesis in the developing mouse kidney*. Kidney Int, 2005. **68**(3): p. 955-65.
297. Laprise, P., A. Viel, and N. Rivard, *Human homolog of disc-large is required for adherens junction assembly and differentiation of human intestinal epithelial cells*. J Biol Chem, 2004. **279**(11): p. 10157-66.
298. Lin, C.Y., et al., *Inhibitory effects of estrogen receptor beta on specific hormone-responsive gene expression and association with disease outcome in primary breast cancer*. Breast Cancer Res, 2007. **9**(2): p. R25.
299. Namba, R., et al., *Molecular characterization of the transition to malignancy in a genetically engineered mouse-based model of ductal carcinoma in situ*. Mol Cancer Res, 2004. **2**(8): p. 453-63.
300. Justilien, V., et al., *Oncogenic activity of Ect2 is regulated through protein kinase C iota-mediated phosphorylation*. J Biol Chem, 2011. **286**(10): p. 8149-57.
301. Bito, H., *Dynamic control of neuronal morphogenesis by rho signaling*. J Biochem, 2003. **134**(3): p. 315-9.
302. Morita, K., K. Hirono, and M. Han, *The Caenorhabditis elegans ect-2 RhoGEF gene regulates cytokinesis and migration of epidermal P cells*. EMBO Rep, 2005. **6**(12): p. 1163-8.
303. Kudo, Y., et al., *Role of F-box protein betaTrcp1 in mammary gland development and tumorigenesis*. Mol Cell Biol, 2004. **24**(18): p. 8184-94.
304. Cox, G.A., et al., *The mouse fidgetin gene defines a new role for AAA family proteins in mammalian development*. Nat Genet, 2000. **26**(2): p. 198-202.
305. Park, S.J., et al., *Fidgetin-like 1 gene inhibited by basic fibroblast growth factor regulates the proliferation and differentiation of osteoblasts*. J Bone Miner Res, 2007. **22**(6): p. 889-96.
306. Luke-Glaser, S., et al., *The AAA-ATPase FIGL-1 controls mitotic progression, and its levels are regulated by the CUL-3MEL-26 E3 ligase in the C. elegans germ line*. J Cell Sci, 2007. **120**(Pt 18): p. 3179-87.

307. Lu, J., et al., *Genetic variants in the H2AFX promoter region are associated with risk of sporadic breast cancer in non-Hispanic white women aged <or=55 years*. *Breast Cancer Res Treat*, 2008. **110**(2): p. 357-66.
308. Uren, A.G., et al., *Survivin and the inner centromere protein INCENP show similar cell-cycle localization and gene knockout phenotype*. *Curr Biol*, 2000. **10**(21): p. 1319-28.
309. Sabo, S.L. and A.K. McAllister, *Mobility and cycling of synaptic protein-containing vesicles in axonal growth cone filopodia*. *Nat Neurosci*, 2003. **6**(12): p. 1264-9.
310. Yoon, S.Y., et al., *Monastrol, a selective inhibitor of the mitotic kinesin Eg5, induces a distinctive growth profile of dendrites and axons in primary cortical neuron cultures*. *Cell Motil Cytoskeleton*, 2005. **60**(4): p. 181-90.
311. Castillo, A., et al., *Overexpression of Eg5 causes genomic instability and tumor formation in mice*. *Cancer Res*, 2007. **67**(21): p. 10138-47.
312. Planas-Silva, M.D. and I.S. Filatova, *Estrogen-dependent regulation of Eg5 in breast cancer cells*. *Anticancer Drugs*, 2007. **18**(7): p. 773-9.
313. Nakamura, Y., et al., *Clinicopathological and biological significance of mitotic centromere-associated kinesin overexpression in human gastric cancer*. *Br J Cancer*, 2007. **97**(4): p. 543-9.
314. Borczuk, A.C. and C.A. Powell, *Expression profiling and lung cancer development*. *Proc Am Thorac Soc*, 2007. **4**(1): p. 127-32.
315. Hofmann, Y., et al., *Genomic structure of the gene for the human P1 protein (MCM3) and its exclusion as a candidate for autosomal recessive polycystic kidney disease*. *Eur J Hum Genet*, 2000. **8**(3): p. 163-6.
316. Davies, C.R., et al., *Proteomic analysis of the mouse mammary gland is a powerful tool to identify novel proteins that are differentially expressed during mammary development*. *Proteomics*, 2006. **6**(21): p. 5694-704.
317. Park, J.H., et al., *PDZ-binding kinase/T-LAK cell-originated protein kinase, a putative cancer/testis antigen with an oncogenic activity in breast cancer*. *Cancer Res*, 2006. **66**(18): p. 9186-95.
318. Tanemoto, M., et al., *PDZ binding motif-dependent localization of K⁺ channel on the basolateral side in distal tubules*. *Am J Physiol Renal Physiol*, 2004. **287**(6): p. F1148-53.
319. Mitani, A., et al., *Transcriptional coactivator with PDZ-binding motif is essential for normal alveolarization in mice*. *Am J Respir Crit Care Med*, 2009. **180**(4): p. 326-38.
320. Rizki, A., J.D. Mott, and M.J. Bissell, *Polo-like kinase 1 is involved in invasion through extracellular matrix*. *Cancer Res*, 2007. **67**(23): p. 11106-10.
321. Shimo, A., et al., *Elevated expression of protein regulator of cytokinesis 1, involved in the growth of breast cancer cells*. *Cancer Sci*, 2007. **98**(2): p. 174-81.
322. Arar, C., et al., *Structure and expression of murine mgcRacGAP: its developmental regulation suggests a role for the Rac/MgcRacGAP signalling pathway in neurogenesis*. *Biochem J*, 1999. **343 Pt 1**: p. 225-30.
323. O'Brien, R.N., et al., *Quantitative proteome analysis of pluripotent cells by iTRAQ mass tagging reveals post-transcriptional regulation of proteins required for ES cell self-renewal*. *Mol Cell Proteomics*, 2011. **9**(10): p. 2238-51.
324. Schwab, K., et al., *A catalogue of gene expression in the developing kidney*. *Kidney Int*, 2003. **64**(5): p. 1588-604.

325. Ma, X.J., et al., *Gene expression profiles of human breast cancer progression*. Proc Natl Acad Sci U S A, 2003. **100**(10): p. 5974-9.
326. Yang, C., et al., *Essential role for Rac in heregulin beta1 mitogenic signaling: a mechanism that involves epidermal growth factor receptor and is independent of ErbB4*. Mol Cell Biol, 2006. **26**(3): p. 831-42.
327. Radke, S., A. Pirkmaier, and D. Germain, *Differential expression of the F-box proteins Skp2 and Skp2B in breast cancer*. Oncogene, 2005. **24**(21): p. 3448-58.
328. Goto, A., et al., *Immunohistochemical study of Skp2 and Jab1, two key molecules in the degradation of P27, in lung adenocarcinoma*. Pathol Int, 2004. **54**(9): p. 675-81.
329. Hung, W.C., et al., *Skp2 overexpression increases the expression of MMP-2 and MMP-9 and invasion of lung cancer cells*. Cancer Lett, 2010. **288**(2): p. 156-61.
330. Boix-Perales, H., et al., *The E3 ubiquitin ligase skp2 regulates neural differentiation independent from the cell cycle*. Neural Dev, 2007. **2**: p. 27.
331. Izraeli, S., et al., *The SIL gene is required for mouse embryonic axial development and left-right specification*. Nature, 1999. **399**(6737): p. 691-4.
332. Nisman, B., et al., *Serum thymidine kinase 1 activity in breast cancer*. Cancer Biomark, 2010. **7**(2): p. 65-72.
333. Arriola, E., et al., *Genomic analysis of the HER2/TOP2A amplicon in breast cancer and breast cancer cell lines*. Lab Invest, 2008. **88**(5): p. 491-503.
334. Chang, Y.W., et al., *Rapid induction of genes associated with tissue protection and neural development in contused adult spinal cord after radial glial cell transplantation*. J Neurotrauma, 2009. **26**(7): p. 979-93.
335. Kosodo, Y., et al., *Regulation of interkinetic nuclear migration by cell cycle-coupled active and passive mechanisms in the developing brain*. Embo J, 2011. **30**(9): p. 1690-704.
336. Jin, W., et al., *UHRF1 is associated with epigenetic silencing of BRCA1 in sporadic breast cancer*. Breast Cancer Res Treat, 2010. **123**(2): p. 359-73.
337. Unoki, M., et al., *UHRF1 is a novel diagnostic marker of lung cancer*. Br J Cancer, 2010. **103**(2): p. 217-22.
338. Unoki, M., et al., *UHRF1 is a novel molecular marker for diagnosis and the prognosis of bladder cancer*. Br J Cancer, 2009. **101**(1): p. 98-105.
339. Huang, R.P., et al., *Embigin, a member of the immunoglobulin superfamily expressed in embryonic cells, enhances cell-substratum adhesion*. Dev Biol, 1993. **155**(2): p. 307-14.
340. Guenette, R.S., et al., *Embigin, a developmentally expressed member of the immunoglobulin super family, is also expressed during regression of prostate and mammary gland*. Dev Genet, 1997. **21**(4): p. 268-78.
341. Stuart, R.O., K.T. Bush, and S.K. Nigam, *Changes in gene expression patterns in the ureteric bud and metanephric mesenchyme in models of kidney development*. Kidney Int, 2003. **64**(6): p. 1997-2008.
342. Yi, C.H., et al., *Loss of fibulin-2 expression is associated with breast cancer progression*. Am J Pathol, 2007. **170**(5): p. 1535-45.
343. Zhang, H.Y., et al., *Extracellular matrix protein fibulin-2 is expressed in the embryonic endocardial cushion tissue and is a prominent component of valves in adult heart*. Dev Biol, 1995. **167**(1): p. 18-26.
344. Reinhardt, D.P., et al., *Fibrillin-1 and fibulin-2 interact and are colocalized in some tissues*. J Biol Chem, 1996. **271**(32): p. 19489-96.

345. Bax, D.V., et al., *Cell adhesion to fibrillin-1 molecules and microfibrils is mediated by alpha 5 beta 1 and alpha v beta 3 integrins*. J Biol Chem, 2003. **278**(36): p. 34605-16.
346. Yang, Q., et al., *Cloning of rat fibrillin-2 cDNA and its role in branching morphogenesis of embryonic lung*. Dev Biol, 1999. **212**(1): p. 229-42.
347. Quondamatteo, F., et al., *Fibrillin-1 and fibrillin-2 in human embryonic and early fetal development*. Matrix Biol, 2002. **21**(8): p. 637-46.
348. Schachtrup, C., et al., *Fibrinogen inhibits neurite outgrowth via beta 3 integrin-mediated phosphorylation of the EGF receptor*. Proc Natl Acad Sci U S A, 2007. **104**(28): p. 11814-9.
349. Guadiz, G., et al., *Polarized secretion of fibrinogen by lung epithelial cells*. Am J Respir Cell Mol Biol, 1997. **17**(1): p. 60-9.
350. Tabrizi, A.D., et al., *Fibrinogen and ceruloplasmin in plasma and milk from dairy cows with subclinical and clinical mastitis*. Pak J Biol Sci, 2008. **11**(4): p. 571-6.
351. Kuhn, T.B., et al., *Laminin directs growth cone navigation via two temporally and functionally distinct calcium signals*. J Neurosci, 1998. **18**(1): p. 184-94.
352. Muggerud, A.A., et al., *Frequent aberrant DNA methylation of ABCB1, FOXC1, PPP2R2B and PTEN in ductal carcinoma in situ and early invasive breast cancer*. Breast Cancer Res, 2010. **12**(1): p. R3.
353. Khialeeva, E., T.F. Lane, and E.M. Carpenter, *Disruption of reelin signaling alters mammary gland morphogenesis*. Development, 2011. **138**(4): p. 767-76.
354. Jossin, Y. and A.M. Goffinet, *Reelin does not directly influence axonal growth*. J Neurosci, 2001. **21**(23): p. RC183.
355. Du, W.W., et al., *Versican G3 promotes mouse mammary tumor cell growth, migration, and metastasis by influencing EGF receptor signaling*. PLoS One, 2010. **5**(11): p. e13828.
356. Faggian, J., et al., *Changes in versican and chondroitin sulfate proteoglycans during structural development of the lung*. Am J Physiol Regul Integr Comp Physiol, 2007. **293**(2): p. R784-92.
357. Schmalfeldt, M., et al., *Brain derived versican V2 is a potent inhibitor of axonal growth*. J Cell Sci, 2000. **113** (Pt 5): p. 807-16.
358. Roarty, K. and R. Serra, *Wnt5a is required for proper mammary gland development and TGF-beta-mediated inhibition of ductal growth*. Development, 2007. **134**(21): p. 3929-39.
359. Bodmer, D., et al., *Wnt5a mediates nerve growth factor-dependent axonal branching and growth in developing sympathetic neurons*. J Neurosci, 2009. **29**(23): p. 7569-81.
360. Caron, C., et al., *Functional characterization of ATAD2 as a new cancer/testis factor and a predictor of poor prognosis in breast and lung cancers*. Oncogene, 2010. **29**(37): p. 5171-81.
361. Shennan, D.B., et al., *L-leucine transport in human breast cancer cells (MCF-7 and MDA-MB-231): kinetics, regulation by estrogen and molecular identity of the transporter*. Biochim Biophys Acta, 2004. **1664**(2): p. 206-16.
362. Nakanishi, K., et al., *LAT1 expression in normal lung and in atypical adenomatous hyperplasia and adenocarcinoma of the lung*. Virchows Arch, 2006. **448**(2): p. 142-50.

363. Mouton-Liger, F., et al., *PCP4 (PEP19) overexpression induces premature neuronal differentiation associated with Ca(2+) /calmodulin-dependent kinase II delta activation in mouse models of down syndrome*. J Comp Neurol, 2010.
364. Thomas, S., et al., *PCP4 is highly expressed in ectoderm and particularly in neuroectoderm derivatives during mouse embryogenesis*. Gene Expr Patterns, 2003. 3(1): p. 93-7.
365. Jovanovic, I., et al., *ST2 Deletion Enhances Innate and Acquired Immunity to Murine Mammary Carcinoma*. Eur J Immunol, 2010.
366. Verri, W.A., Jr., et al., *IL-33 induces neutrophil migration in rheumatoid arthritis and is a target of anti-TNF therapy*. Ann Rheum Dis, 2010. 69(9): p. 1697-703.
367. Poirier, K., et al., *Mutations in the neuronal ss-tubulin subunit TUBB3 result in malformation of cortical development and neuronal migration defects*. Hum Mol Genet, 2010. 19(22): p. 4462-73.
368. Liu, J., D. Nethery, and J.A. Kern, *Neuregulin-1 induces branching morphogenesis in the developing lung through a P13K signal pathway*. Exp Lung Res, 2004. 30(6): p. 465-78.
369. Rentschler, S., et al., *Neuregulin-1 promotes formation of the murine cardiac conduction system*. Proc Natl Acad Sci U S A, 2002. 99(16): p. 10464-9.
370. Chua, Y.L., et al., *The NRG1 gene is frequently silenced by methylation in breast cancers and is a strong candidate for the 8p tumour suppressor gene*. Oncogene, 2009. 28(46): p. 4041-52.
371. Lopez-Bendito, G., et al., *Tangential neuronal migration controls axon guidance: a role for neuregulin-1 in thalamocortical axon navigation*. Cell, 2006. 125(1): p. 127-42.
372. Chen, J., E.M. Miller, and K.A. Gallo, *MLK3 is critical for breast cancer cell migration and promotes a malignant phenotype in mammary epithelial cells*. Oncogene, 2010. 29(31): p. 4399-411.
373. Kalluri, R. and R.A. Weinberg, *The basics of epithelial-mesenchymal transition*. J Clin Invest, 2009. 119(6): p. 1420-8.
374. Hennighausen, L. and G.W. Robinson, *Signaling pathways in mammary gland development*. Dev Cell, 2001. 1(4): p. 467-75.
375. Arendt, L.M., et al., *Stroma in breast development and disease*. Semin Cell Dev Biol, 2010. 21(1): p. 11-8.
376. Calpe-Berdiel, L., et al., *Changes in intestinal and liver global gene expression in response to a phytosterol-enriched diet*. Atherosclerosis, 2005. 181(1): p. 75-85.
377. Russo, J. and I.H. Russo, *Influence of differentiation and cell kinetics on the susceptibility of the rat mammary gland to carcinogenesis*. Cancer Res, 1980. 40(8 Pt 1): p. 2677-87.
378. Vasilyev, A., et al., *Collective cell migration drives morphogenesis of the kidney nephron*. PLoS Biol, 2009. 7(1): p. e9.
379. Gjorevski, N. and C.M. Nelson, *Branch formation during organ development*. Wiley Interdiscip Rev Syst Biol Med, 2010. 2(6): p. 734-41.
380. Watanabe, T. and F. Costantini, *Real-time analysis of ureteric bud branching morphogenesis in vitro*. Dev Biol, 2004. 271(1): p. 98-108.
381. Basson, M.A., et al., *Sprouty1 is a critical regulator of GDNF/RET-mediated kidney induction*. Dev Cell, 2005. 8(2): p. 229-39.

382. Hacohen, N., et al., *sprouty* encodes a novel antagonist of FGF signaling that patterns apical branching of the *Drosophila* airways. *Cell*, 1998. **92**(2): p. 253-63.
383. Doitsidou, M., et al., *Guidance of primordial germ cell migration by the chemokine SDF-1*. *Cell*, 2002. **111**(5): p. 647-59.
384. Halin, C., et al., *In vivo imaging of lymphocyte trafficking*. *Annu Rev Cell Dev Biol*, 2005. **21**: p. 581-603.
385. Martin, P. and S.M. Parkhurst, *Parallels between tissue repair and embryo morphogenesis*. *Development*, 2004. **131**(13): p. 3021-34.
386. Battle, E., et al., *Beta-catenin and TCF mediate cell positioning in the intestinal epithelium by controlling the expression of EphB/ephrinB*. *Cell*, 2002. **111**(2): p. 251-63.
387. Rorth, P., *Collective cell migration*. *Annu Rev Cell Dev Biol*, 2009. **25**: p. 407-29.
388. Friedl, P., Y. Hegerfeldt, and M. Tusch, *Collective cell migration in morphogenesis and cancer*. *Int J Dev Biol*, 2004. **48**(5-6): p. 441-9.
389. Christiansen, J.J. and A.K. Rajasekaran, *Reassessing epithelial to mesenchymal transition as a prerequisite for carcinoma invasion and metastasis*. *Cancer Res*, 2006. **66**(17): p. 8319-26.
390. Powers, S. and D. Mu, *Genetic similarities between organogenesis and tumorigenesis of the lung*. *Cell Cycle*, 2008. **7**(2): p. 200-4.
391. Chakravarty, G., et al., *p190-B RhoGAP regulates mammary ductal morphogenesis*. *Mol Endocrinol*, 2003. **17**(6): p. 1054-65.
392. Kanwar, Y.S., et al., *Role of membrane-type matrix metalloproteinase 1 (MT-1-MMP), MMP-2, and its inhibitor in nephrogenesis*. *Am J Physiol*, 1999. **277**(6 Pt 2): p. F934-47.
393. Lumeng, C.N., et al., *Increased inflammatory properties of adipose tissue macrophages recruited during diet-induced obesity*. *Diabetes*, 2007. **56**(1): p. 16-23.
394. Ritty, T.M., et al., *Fibrillin-1 and -2 contain heparin-binding sites important for matrix deposition and that support cell attachment*. *Biochem J*, 2003. **375**(Pt 2): p. 425-32.
395. Lu, P. and Z. Werb, *Patterning mechanisms of branched organs*. *Science*, 2008. **322**(5907): p. 1506-9.
396. Mikkola, M.L. and S.E. Millar, *The mammary bud as a skin appendage: unique and shared aspects of development*. *J Mammary Gland Biol Neoplasia*, 2006. **11**(3-4): p. 187-203.
397. Leroy, P., et al., *Down-regulation of Hox A7 is required for cell adhesion and migration on fibronectin during early HL-60 monocytic differentiation*. *J Leukoc Biol*, 2004. **75**(4): p. 680-8.
398. Pollard, J.W., *Role of colony-stimulating factor-1 in reproduction and development*. *Mol Reprod Dev*, 1997. **46**(1): p. 54-60; discussion 60-1.
399. Dai, X.M., et al., *Targeted disruption of the mouse colony-stimulating factor 1 receptor gene results in osteopetrosis, mononuclear phagocyte deficiency, increased primitive progenitor cell frequencies, and reproductive defects*. *Blood*, 2002. **99**(1): p. 111-20.
400. Palkowetz, K.H., et al., *Production of interleukin-6 and interleukin-8 by human mammary gland epithelial cells*. *J Reprod Immunol*, 1994. **26**(1): p. 57-64.

401. Krop, I.E., et al., *HIN-1, a putative cytokine highly expressed in normal but not cancerous mammary epithelial cells*. Proc Natl Acad Sci U S A, 2001. **98**(17): p. 9796-801.
402. Bourges, D., et al., *New insights into the dual recruitment of IgA+ B cells in the developing mammary gland*. Mol Immunol, 2008. **45**(12): p. 3354-62.
403. Djonov, V., A.C. Andres, and A. Ziemiecki, *Vascular remodelling during the normal and malignant life cycle of the mammary gland*. Microsc Res Tech, 2001. **52**(2): p. 182-9.
404. McLean, P., *Interrelationship of carbohydrate and fat metabolism in the involuting mammary gland*. Biochem J, 1964. **90**(2): p. 271-8.
405. Leyva-Baca, I., et al., *Identification of single nucleotide polymorphisms in the bovine CCL2, IL8, CCR2 and IL8RA genes and their association with health and production in Canadian Holsteins*. Anim Genet, 2007. **38**(3): p. 198-202.
406. Reginato, M.J., et al., *Integrins and EGFR coordinately regulate the pro-apoptotic protein Bim to prevent anoikis*. Nat Cell Biol, 2003. **5**(8): p. 733-40.
407. Lee, J.M., et al., *The epithelial-mesenchymal transition: new insights in signaling, development, and disease*. J Cell Biol, 2006. **172**(7): p. 973-81.
408. Sarrio, D., et al., *Epithelial-mesenchymal transition in breast cancer relates to the basal-like phenotype*. Cancer Res, 2008. **68**(4): p. 989-97.
409. Trimboli, A.J., et al., *Direct evidence for epithelial-mesenchymal transitions in breast cancer*. Cancer Res, 2008. **68**(3): p. 937-45.
410. Mitchell, J.M., et al., *The Prx1 homeobox gene is critical for molar tooth morphogenesis*. J Dent Res, 2006. **85**(10): p. 888-93.
411. Lewis, M.T., *Homeobox genes in mammary gland development and neoplasia*. Breast Cancer Res, 2000. **2**(3): p. 158-69.
412. Chen, C., et al., *Roles of neuropilins in neuronal development, angiogenesis, and cancers*. World J Surg, 2005. **29**(3): p. 271-5.
413. Lv, H., et al., *Ingenuity pathways analysis of urine metabonomics phenotypes toxicity of gentamicin in multiple organs*. Mol Biosyst, 2010. **6**(10): p. 2056-67.
414. Paripati, A., C. Kingsley, and G.J. Weiss, *Pathway targets to explore in the treatment of small cell and large cell lung cancers*. J Thorac Oncol, 2009. **4**(11): p. 1313-21.
415. Wognum, S., et al., *An exploratory pathways analysis of temporal changes induced by spinal cord injury in the rat bladder wall: insights on remodeling and inflammation*. PLoS One, 2009. **4**(6): p. e5852.
416. Sun, T.T., *Altered phenotype of cultured urothelial and other stratified epithelial cells: implications for wound healing*. Am J Physiol Renal Physiol, 2006. **291**(1): p. F9-21.
417. Wu, X.R., et al., *Large scale purification and immunolocalization of bovine uroplakins I, II, and III. Molecular markers of urothelial differentiation*. J Biol Chem, 1990. **265**(31): p. 19170-9.
418. Wu, X.R. and T.T. Sun, *Molecular cloning of a 47 kDa tissue-specific and differentiation-dependent urothelial cell surface glycoprotein*, in J Cell Sci. 1993. p. 31-43.
419. Liang, F.X., et al., *Organization of uroplakin subunits: transmembrane topology, pair formation and plaque composition*. Biochem J, 2001. **355**(Pt 1): p. 13-8.
420. Kong, X.T., et al., *Roles of uroplakins in plaque formation, umbrella cell enlargement, and urinary tract diseases*. J Cell Biol, 2004. **167**(6): p. 1195-204.

421. Kachar, B., et al., *Three-dimensional analysis of the 16 nm urothelial plaque particle: luminal surface exposure, preferential head-to-head interaction, and hinge formation*. *J Mol Biol*, 1999. **285**(2): p. 595-608.
422. Hu, P., et al., *Role of membrane proteins in permeability barrier function: uroplakin ablation elevates urothelial permeability*. *Am J Physiol Renal Physiol*, 2002. **283**(6): p. F1200-7.
423. Deng, F.M., et al., *Uroplakin IIIb, a urothelial differentiation marker, dimerizes with uroplakin Ib as an early step of urothelial plaque assembly*. *J Cell Biol*, 2002. **159**(4): p. 685-94.
424. Wu, X.R., J.J. Medina, and T.T. Sun, *Selective interactions of UPIa and UPIb, two members of the transmembrane 4 superfamily, with distinct single transmembrane-domained proteins in differentiated urothelial cells*. *J Biol Chem*, 1995. **270**(50): p. 29752-9.
425. Tu, L., T.T. Sun, and G. Kreibich, *Specific heterodimer formation is a prerequisite for uroplakins to exit from the endoplasmic reticulum*. *Mol Biol Cell*, 2002. **13**(12): p. 4221-30.
426. Hu, P., et al., *Ablation of uroplakin III gene results in small urothelial plaques, urothelial leakage, and vesicoureteral reflux*. *J Cell Biol*, 2000. **151**(5): p. 961-72.
427. Aboushwareb, T., et al., *Alterations in bladder function associated with urothelial defects in uroplakin II and IIIa knockout mice*. *Neurourol Urodyn*, 2009. **28**(8): p. 1028-33.
428. Matsumoto, K., et al., *Loss expression of uroplakin III is associated with clinicopathologic features of aggressive bladder cancer*. *Urology*, 2008. **72**(2): p. 444-9.
429. Lai, Y., et al., *UPK3A: A Promising Novel Urinary Marker for the Detection of Bladder Cancer*. *Urology*, 2010.
430. Moll, R., et al., *Uroplakins, specific membrane proteins of urothelial umbrella cells, as histological markers of metastatic transitional cell carcinomas*. *Am J Pathol*, 1995. **147**(5): p. 1383-97.
431. Ogawa, K., S.L. Johansson, and S.M. Cohen, *Immunohistochemical analysis of uroplakins, urothelial specific proteins, in ovarian Brenner tumors, normal tissues, and benign and neoplastic lesions of the female genital tract*. *Am J Pathol*, 1999. **155**(4): p. 1047-50.
432. Moll, R., et al., *The catalog of human cytokeratins: patterns of expression in normal epithelia, tumors and cultured cells*. *Cell*, 1982. **31**(1): p. 11-24.
433. Reedy, E.A., K.L. Colombo-Burke, and J.H. Resau, *Discrimination of cell types in primary transitional cell carcinoma by monoclonal anti-cytokeratin antibodies*. *Pathobiology*, 1990. **58**(6): p. 304-11.
434. Pan, T.C., et al., *Structure and expression of fibulin-2, a novel extracellular matrix protein with multiple EGF-like repeats and consensus motifs for calcium binding*. *J Cell Biol*, 1993. **123**(5): p. 1269-77.
435. Zhang, R.Z., et al., *Fibulin-2 (FBLN2): human cDNA sequence, mRNA expression, and mapping of the gene on human and mouse chromosomes*. *Genomics*, 1994. **22**(2): p. 425-30.
436. Rees, D.J., et al., *The role of beta-hydroxyaspartate and adjacent carboxylate residues in the first EGF domain of human factor IX*. *Embo J*, 1988. **7**(7): p. 2053-61.
437. Mayer, U., et al., *A single EGF-like motif of laminin is responsible for high affinity nidogen binding*. *Embo J*, 1993. **12**(5): p. 1879-85.

438. Baron, M., D.G. Norman, and I.D. Campbell, *Protein modules*. Trends Biochem Sci, 1991. **16**(1): p. 13-7.
439. Grassel, S., et al., *Mouse fibulin-2 gene. Complete exon-intron organization and promoter characterization*. Eur J Biochem, 1999. **263**(2): p. 471-7.
440. Zhang, H.Y., et al., *Fibulin-1 and fibulin-2 expression during organogenesis in the developing mouse embryo*. Dev Dyn, 1996. **205**(3): p. 348-64.
441. Tsuda, T., et al., *Fibulin-2 expression marks transformed mesenchymal cells in developing cardiac valves, aortic arch vessels, and coronary vessels*. Dev Dyn, 2001. **222**(1): p. 89-100.
442. Sasaki, T., et al., *Binding of mouse and human fibulin-2 to extracellular matrix ligands*. J Mol Biol, 1995. **254**(5): p. 892-9.
443. Kobayashi, N., et al., *A comparative analysis of the fibulin protein family. Biochemical characterization, binding interactions, and tissue localization*. J Biol Chem, 2007. **282**(16): p. 11805-16.
444. Sasaki, T., et al., *Expression of fibulin-2 by fibroblasts and deposition with fibronectin into a fibrillar matrix*. J Cell Sci, 1996. **109** (Pt 12): p. 2895-904.
445. Loveland, K., et al., *Developmental changes in the basement membrane of the normal and hypothyroid postnatal rat testis: segmental localization of fibulin-2 and fibronectin*. Biol Reprod, 1998. **58**(5): p. 1123-30.
446. Ng, K.M., et al., *Evidence that fibulin family members contribute to the steroid-dependent extravascular sequestration of sex hormone-binding globulin*. J Biol Chem, 2006. **281**(23): p. 15853-61.
447. Fassler, R., et al., *Differential regulation of fibulin, tenascin-C, and nidogen expression during wound healing of normal and glucocorticoid-treated mice*. Exp Cell Res, 1996. **222**(1): p. 111-6.
448. Strom, A., et al., *Fibulin-2 is present in murine vascular lesions and is important for smooth muscle cell migration*. Cardiovasc Res, 2006. **69**(3): p. 755-63.
449. Chapman, S.L., et al., *Fibulin-2 and fibulin-5 cooperatively function to form the internal elastic lamina and protect from vascular injury*. Arterioscler Thromb Vasc Biol, 2010. **30**(1): p. 68-74.
450. Hunzelmann, N., et al., *Increased deposition of fibulin-2 in solar elastosis and its colocalization with elastic fibres*. Br J Dermatol, 2001. **145**(2): p. 217-22.
451. Ramaswamy, S., et al., *A molecular signature of metastasis in primary solid tumors*. Nat Genet, 2003. **33**(1): p. 49-54.
452. Whiteaker, J.R., et al., *Integrated pipeline for mass spectrometry-based discovery and confirmation of biomarkers demonstrated in a mouse model of breast cancer*. J Proteome Res, 2007. **6**(10): p. 3962-75.
453. Hill, V.K., et al., *Identification of 5 novel genes methylated in breast and other epithelial cancers*. Mol Cancer, 2010. **9**: p. 51.
454. Gusterson, B.A. and P. Monaghan, *Keratinocyte differentiation of human buccal mucosa in vitro*. Invest Cell Pathol, 1979. **2**(3): p. 171-9.
455. Sasaki, T., et al., *Different susceptibilities of fibulin-1 and fibulin-2 to cleavage by matrix metalloproteinases and other tissue proteases*. Eur J Biochem, 1996. **240**(2): p. 427-34.
456. Okada, H., et al., *Microarray analysis of genes controlled by progesterone in human endometrial stromal cells in vitro*. Gynecol Endocrinol, 2003. **17**(4): p. 271-80.

457. Gu, Y.C., et al., *Glucocorticoids down-regulate the extracellular matrix proteins fibronectin, fibulin-1 and fibulin-2 in bone marrow stroma*. Eur J Haematol, 2001. **67**(3): p. 176-84.
458. Reichmann, E., et al., *New mammary epithelial and fibroblastic cell clones in coculture form structures competent to differentiate functionally*. J Cell Biol, 1989. **108**(3): p. 1127-38.
459. Gu, Y.C., et al., *Association of extracellular matrix proteins fibulin-1 and fibulin-2 with fibronectin in bone marrow stroma*. Br J Haematol, 2000. **109**(2): p. 305-13.
460. Raghunath, M., et al., *Confocal laser scanning analysis of the association of fibulin-2 with fibrillin-1 and fibronectin define different stages of skin regeneration*. J Invest Dermatol, 1999. **112**(1): p. 97-101.
461. Olin, A.I., et al., *The proteoglycans aggrecan and Versican form networks with fibulin-2 through their lectin domain binding*. J Biol Chem, 2001. **276**(2): p. 1253-61.
462. Utani, A., M. Nomizu, and Y. Yamada, *Fibulin-2 binds to the short arms of laminin-5 and laminin-1 via conserved amino acid sequences*. J Biol Chem, 1997. **272**(5): p. 2814-20.
463. Pfaff, M., et al., *Integrin-binding and cell-adhesion studies of fibulins reveal a particular affinity for alpha IIb beta 3*. Exp Cell Res, 1995. **219**(1): p. 87-92.
464. Sasaki, T., et al., *Tropoelastin binding to fibulins, nidogen-2 and other extracellular matrix proteins*. FEBS Lett, 1999. **460**(2): p. 280-4.
465. Rosenbloom, J., W.R. Abrams, and R. Mecham, *Extracellular matrix 4: the elastic fiber*. Faseb J, 1993. **7**(13): p. 1208-18.
466. Pollard, T.D. and J.A. Cooper, *Actin, a central player in cell shape and movement*. Science, 2009. **326**(5957): p. 1208-12.
467. Anderson, L. and J. Seilhamer, *A comparison of selected mRNA and protein abundances in human liver*. Electrophoresis, 1997. **18**(3-4): p. 533-7.
468. Griffin, T.J., et al., *Complementary profiling of gene expression at the transcriptome and proteome levels in Saccharomyces cerevisiae*. Mol Cell Proteomics, 2002. **1**(4): p. 323-33.
469. Tian, Q., et al., *Integrated genomic and proteomic analyses of gene expression in Mammalian cells*. Mol Cell Proteomics, 2004. **3**(10): p. 960-9.
470. Knight, C.H. and M. Peaker, *Development of the mammary gland*. J Reprod Fertil, 1982. **65**(2): p. 521-36.
471. Ducros, E., et al., *Expression of extracellular matrix proteins fibulin-1 and fibulin-2 by human corneal fibroblasts*. Curr Eye Res, 2007. **32**(6): p. 481-90.
472. Brisken, C., *Hormonal control of alveolar development and its implications for breast carcinogenesis*. J Mammary Gland Biol Neoplasia, 2002. **7**(1): p. 39-48.
473. Feng, Y., et al., *Estrogen receptor-alpha expression in the mammary epithelium is required for ductal and alveolar morphogenesis in mice*. Proc Natl Acad Sci U S A, 2007. **104**(37): p. 14718-23.
474. Lilla, J.N., et al., *Active plasma kallikrein localizes to mast cells and regulates epithelial cell apoptosis, adipocyte differentiation, and stromal remodeling during mammary gland involution*. J Biol Chem, 2009. **284**(20): p. 13792-803.
475. Accornero, P., et al., *Epidermal growth factor and hepatocyte growth factor cooperate to enhance cell proliferation, scatter, and invasion in murine mammary epithelial cells*. J Mol Endocrinol. **44**(2): p. 115-25.

476. Hesselson, D., et al., *GON-1 and fibulin have antagonistic roles in control of organ shape*. *Curr Biol*, 2004. **14**(22): p. 2005-10.
477. Kubota, Y., R. Kuroki, and K. Nishiwaki, *A fibulin-1 homolog interacts with an ADAM protease that controls cell migration in C. elegans*. *Curr Biol*, 2004. **14**(22): p. 2011-8.
478. Lee, N.V., et al., *Fibulin-1 acts as a cofactor for the matrix metalloprotease ADAMTS-1*. *J Biol Chem*, 2005. **280**(41): p. 34796-804.
479. Kostka, G., et al., *Perinatal lethality and endothelial cell abnormalities in several vessel compartments of fibulin-1-deficient mice*. *Mol Cell Biol*, 2001. **21**(20): p. 7025-34.
480. Hovey, R.C., et al., *Transcriptional regulation of vascular endothelial growth factor expression in epithelial and stromal cells during mouse mammary gland development*. *Mol Endocrinol*, 2001. **15**(5): p. 819-31.
481. Carmeliet, P., et al., *Abnormal blood vessel development and lethality in embryos lacking a single VEGF allele*. *Nature*, 1996. **380**(6573): p. 435-9.
482. Peng, J., S. Sengupta, and V.C. Jordan, *Potential of selective estrogen receptor modulators as treatments and preventives of breast cancer*. *Anticancer Agents Med Chem*, 2009. **9**(5): p. 481-99.
483. Mukai, H., *Treatment strategy for HER2-positive breast cancer*. *Int J Clin Oncol*, 2010. **15**(4): p. 335-40.
484. van de Vijver, M.J., et al., *A gene-expression signature as a predictor of survival in breast cancer*. *N Engl J Med*, 2002. **347**(25): p. 1999-2009.
485. Sotiriou, C., et al., *Breast cancer classification and prognosis based on gene expression profiles from a population-based study*. *Proc Natl Acad Sci U S A*, 2003. **100**(18): p. 10393-8.
486. Carthew, R.W. and E.J. Sontheimer, *Origins and Mechanisms of miRNAs and siRNAs*. *Cell*, 2009. **136**(4): p. 642-55.
487. Scholer, N., et al., *Serum microRNAs as a novel class of biomarkers: a comprehensive review of the literature*. *Exp Hematol*, 2010. **38**(12): p. 1126-30.
488. Di Leva, G. and C.M. Croce, *Roles of small RNAs in tumor formation*. *Trends Mol Med*, 2010. **16**(6): p. 257-67.
489. Lu, J., et al., *MicroRNA expression profiles classify human cancers*. *Nature*, 2005. **435**(7043): p. 834-8.

